

Abstracts

5316

ROSETTA FLYBY TARGET ASTEROID (2867) STEINS: AN ENSTATITE ACHONDRITE ANALOGUE

P. A. Abell^{1,2}, P. R. Weissman³, M. D. Hicks³, Y. J. Choi³, and S. C. Lowry³.
¹Planetary Science Institute, 1700 E. Fort Lowell, Suite 106, Tucson, AZ 85719, USA. E-mail: abell@psi.edu. ²NASA Johnson Space Center, Houston, TX 77058, USA. ³Jet Propulsion Laboratory, 4800 Oak Grove Drive, Pasadena, CA 91109, USA.

Introduction: On September 5, 2008, the European Space Agency's Rosetta spacecraft will fly by the main-belt asteroid (2867) Steins enroute to its primary target, comet 67P/Churyumov-Gerasimenko. Given that little information was known about Steins prior to its selection as a Rosetta flyby target in 2004, a ground-based observational campaign was undertaken to ensure that good constraints of the asteroid's physical characteristics were measured before the encounter.

Observations: CCD spectroscopic (~0.33 to 0.93 μm) reflectance observations of asteroid (2867) Steins were obtained to further investigate its compositional characteristics and determine the most likely meteoritic analogue. Given that the rotation period of this asteroid was previously determined to be ~6.05 h [1], two sets of spectra were collected over an ~3 h interval in order to obtain data on each hemisphere of the asteroid. An examination of the spectra demonstrates that the asteroid has a significant absorption feature located near 0.50 μm , and a red spectral slope at longer wavelengths up through 0.92 μm . In addition, previous investigators have determined that the albedo of Steins is ~0.30–0.55 [2, 3]. This suggests that it has spectral properties most consistent with the E-type asteroids, which are known for their high albedos [4].

Interpretation: Some E-type asteroids are distinguished from other E subtypes by spectral absorption features located near 0.50 μm and 0.96 μm . E(II)-type asteroids (64) Angelina and (3103) Eger have been observed to have features located near 0.50 μm [5], and both of these asteroids have high albedo values [6, 7, 8]. The preferred mineralogical interpretation is that these features are produced as a result of the presence of the calcium sulfide mineral, oldhamite (CaS) on the surface of these asteroids [9, 10]. Oldhamite is characterized by two absorption features located near 0.50 μm and 0.96 μm that are probably produced by trace amounts of a bivalent ion, such as Fe²⁺, that has been substituted into the sulfide instead of Ca²⁺. In addition, oldhamite is present only in highly reduced mineral assemblages such as aubrite (enstatite achondrite) meteorites [11, 12].

Conclusions: A comparison of laboratory spectra of aubrite ALH 78113 to the Steins data suggests that there is a plausible similarity between this meteorite and the asteroid in terms of albedo and absorption features. Hence the most likely meteoritic analogue to Steins is an aubrite with a spectrally significant amount of sulfide (e.g., CaS) present in its assemblage.

References: [1] Weissman et al. 2007. *Astronomy & Astrophysics* 466:737–742. [2] Fornasier et al. 2006. *Astronomy & Astrophysics* 449: L9–L12. [3] Lamy et al. 2006. *BAAS* 38, #59.09. [4] Barucci et al. 2005. *Astronomy & Astrophysics* 430:313–317. [5] Fornasier and Lazzarin. 2001. *Icarus* 152:127–133. [6] Tedesco et al. 1989. *Asteroids II*. pp. 151–1161. [7] Veeder et al. 1989. *The Astronomical Journal* 97:1211–1219. [8] Benner et al. 1997. *Icarus* 130:296–312. [9] Burbine et al. 2002. *Meteoritics & Planetary Science* 37:1233–1244. [10] Gaffey and Kelley. 2004. Abstract #1812. 35th LPSC. [11] Keil. 1989. *Meteoritics* 24:195–208. [12] Fogel. 1997. *Meteoritics & Planetary Science* 32:577–591.

5030

VARIETIES OF CARBON MINERALS IN ANTARCTIC CARBONACEOUS CHONDRITES BY TEM AND THEIR IMPLICATIONS

Junji Akai¹, Takayuki Aoki², and Hikaru Ohtani¹. ¹Department of Geology, Fac. Sci., Niigata University, Niigata, Japan. ²Asahi Carbon Co., Niigata, Japan.

A variety of fine-grained carbonaceous materials are contained in carbonaceous chondrite (CC) matrix. However, Antarctic meteorites have not always been examined in detail. Eight Antarctic carbonaceous chondrites Asuka-882094 (CO3), Yamato-86751 (CV3), Yamato-790992 (CO3), Yamato-81020 (CO3), Yamato-74662 (CM2), Yamato-86720 (CM2), Yamato-793321 (CM2), Belgica-7904 (CM2 or "C11"), and Allende and Murchison were systematically examined in more detail. We developed a sample separation procedure of chemical dissolution, using HF (48, nitric acid) and aqua regia, at 348 K for 30 minutes.

TEM used is JEM-2010 (JEOL) and JEM-200CX with EM-SHH4 (heating holder). Zinc powder was used for temperature calibration. Multi-slice TEM simulation (MssC) was carried out.

Nano-diamond and "carbonaceous globules" were found from seven Antarctic chondrites. Diamond grains are clearly more abundant than well-crystallized graphite in the CC. About the origin of nano-diamond, a presolar CVD formation model has been widely accepted (e.g., [1]). Although some possibility of its formation on parent body is also suggested [2], the results of this study suggest that the presolar origin is more likely than the parent-body origin. As Nakamura-Messenger et al. (2006) [3] suggested, carbonaceous globules may be primitive carbon material formed in the outermost cold regions of protoplanetary disks. The results of this study indicate that nanodiamond and carbonaceous globules are very common constituents in CC. We carried out heating and cooling experiments of carbonaceous globules in electron microscopic observation mainly to examine their thermal stability and changes. Neither graphitization nor significant changes in shape and size were observed in heating at 773 K. ED patterns show that the globule remains amorphous even after heating. This result suggests that these carbonaceous globules can survive strong thermal metamorphism. Detailed TEM observation of boundary part of the doughnut-like globules was carried out. The carbonaceous globules are similar in size to the smallest bacteria in the recent Earth environments. If much carbonaceous globules were supplied onto the Earth surface in the early stage of its evolution, we suggest the possibility that they played some role in the birth and/or early evolution of life on the Earth.

Well crystallized graphite with 2H and 3R polytypes was also found mainly from CV3 and CO3 chondrites, whereas poorly crystallized graphite was found mainly from CM2 chondrites. Characteristic carbon structures similar to tetrahedral carbon onion etc. were found from a CM2 chondrite. Finally, correspondence of carbon mineral types to petrological classification of CC is summarized. We will discuss more about the implications.

References: [1] Daulton T. et al. 1996. *Geochimica et Cosmochimica Acta* 60:4853–4872. [2] Kouchi A. et al. 2005. *The Astrophysical Journal* 626:L129–L132. [3] Nakamura-Messenger K. et al. 2006. *Science* 314:1439–1442.

5046

HIGH-PRESSURE PHASE RELATIONS OF Ca,Na-ALUMINOSILICATE, CAS PHASE, WITH IMPLICATION TO SHOCKED MARTIAN METEORITES

M. Akaogi¹, M. Haraguchi¹, M. Yaguchi¹, K. Nakanishi¹, and H. Kojitani¹.
Department of Chemistry, Gakushuin University, 1-5-1 Mejiro, Toshima-ku,
Tokyo 171-8588, Japan. E-mail: masaki.akaogi@gakushuin.ac.jp.

Introduction: Ca,Na-aluminosilicate ($\text{Ca}_{1-x}\text{Na}_x\text{Al}_{4-x}\text{Si}_{2+x}\text{O}_{11}$) named CAS phase, a high-pressure silicate with hexagonal barium-ferrite structure, was found in heavily shocked Martian meteorites by Beck et al. [1]. High pressure experiments demonstrated that the CAS phase was synthesized in high pressure mineral assemblages of anorthite [2] and oceanic sediments [3], and the CAS phase was also found as a liquidus phase in melting experiments of mid-oceanic ridge basalt [4]. We have examined high-pressure high-temperature phase relations of $\text{CaAl}_4\text{Si}_2\text{O}_{11}$ and those in the system $\text{CaAl}_4\text{Si}_2\text{O}_{11}$ - $\text{NaAl}_3\text{Si}_3\text{O}_{11}$, using a multianvil press. We have also measured enthalpies of transitions involving $\text{CaAl}_4\text{Si}_2\text{O}_{11}$ CAS phase by high temperature calorimetry techniques, and have calculated the phase relations. The obtained high-pressure phase relations have been used to estimate the P,T conditions in shock processes which occurred in some shergottites.

Results and Discussion: The experimental and calculated results indicate that $\text{CaAl}_4\text{Si}_2\text{O}_{11}$ CAS phase is stable at about 13–30 GPa at temperature above about 1200 °C. The stability field of the CAS phase is generally consistent with the experimental results in the compositions of anorthite, sediments and basalt, and would give basic constraints on the P, T conditions for the assemblages containing the natural CAS phases. Our preliminary phase relations in the system $\text{CaAl}_4\text{Si}_2\text{O}_{11}$ - $\text{NaAl}_3\text{Si}_3\text{O}_{11}$ reveal that at 1600 °C $\text{CaAl}_4\text{Si}_2\text{O}_{11}$ CAS phase dissolves $\text{NaAl}_3\text{Si}_3\text{O}_{11}$ component up to about 50–60 mol% to form the CAS solid solution at about 23 GPa. Above the pressure, NaAlSiO_4 -rich calcium ferrite coexists with the CAS solid solution with smaller amount of $\text{NaAl}_3\text{Si}_3\text{O}_{11}$ component. The synthesis of the CAS solid solution is consistent with the natural occurrence of the Ca,Na-CAS phases. In the phase relations, pressure interval where the single CAS phase is stable decreases with increasing the Na content. The phase relations suggest that the Ca,Na-CAS phases found by Beck et al. [1] in melt pockets of the shergottites were crystallized at pressure around 23 ± 5 GPa at temperature higher than 1600 °C from the melt during the shock processes.

References: [1] Beck P. et al. 2004. *Earth and Planetary Science Letters* 219:1–12. [2] Gautron L. et al. 1996. *Physics of the Earth and Planetary Interiors* 97:71–81. [3] Irifune T. et al. 1994. *Earth and Planetary Science Letters* 126:351–368. [4] Hirose K. and Fei Y. 2002. *Geochimica et Cosmochimica Acta* 66:2099–2108.

5117

WATER IN TERRESTRIAL PLANETS

F. Albarede. Ecole Normale Supérieure, 69007 Lyon, France. E-mail: albarede@ens-lyon.fr.

Mars and the Moon are dry and inactive deserts. Their interiors came to rest within one billion years of accretion. Venus, although internally very active, has a dry inferno for a surface. In contrast, the Earth is tectonically active and largely covered by a deep ocean. The strong gravity field of large planets allows for an enormous amount of gravitational energy to be released, causing the outer part of the planetary body to melt (magma ocean), thus helping retain water on the planet. The analysis of K/U and $^{87}\text{Sr}/^{86}\text{Sr}$ ratios in planetary objects further demonstrates that the inner solar system lost up to 95% of its K and Rb. Planets in such an environment cannot contain much water (~20 ppm).

The relationship between terrestrial element abundances and condensation temperatures shows that the Earth and the other terrestrial planets accreted dry. I here assume that the nebular gas is an ideal gas and use Raoult's law and the Sackur-Tetrode equation to build a simple Rayleigh distillation model accounting for nebular condensation. Using proper simplifications, the 50% condensation temperature of each element (T_{50}) can be shown to be roughly proportional to its vaporization enthalpy with a proportionality constant mildly dependent on the molar mass. This model suggests that most of the Earth's material formed at temperature in excess of 1200 K and that the terrestrial water content greatly exceeds the concentration expected in a solid phase condensing at such a high temperature. Dry planetary interiors are most easily reconciled with 3-D N-body simulations. I here investigate the consequences of a scenario in which terrestrial planets accreted bone dry and water rained down into the mantle over the planets history.

On Earth, buoyant serpentines produced by reactions between the dry terrestrial magma ocean and icy impactors received from the outer solar system isolated the magma and kept it molten for about 30 million years. Subsequent foundering of this wet surface material gradually softened the terrestrial mantle, transporting water to depth, increased the Rayleigh number, and set the scene for the onset of plate tectonics which currently lets the ocean rain into the mantle. The very same processes may have acted to remove all the water from the surface of Venus 500 Myr ago and added enough water to its mantle to make its internal dynamics active and keep the surface young. In contrast, because of the smaller radius of Mars compared to that of the Earth, not enough water could be drawn into the Martian mantle before it was lost to space and Martian plate tectonics never began.

5271

ON THE ORIGIN OF ^{22}Na IN Ne-E(L)

S. Amari. Laboratory for Space Sciences and the Physics Department, Washington University, St. Louis, MO 63130, USA. E-mail: sa@wuphys.wustl.edu.

Introduction: Ne-E(L) is carried by presolar graphite grains with a range of density (1.6–2.2 g/cm³) [1]. The ^{22}Ne in Ne-E(L) was long thought to come from the decay of ^{22}Na ($T_{1/2} = 2.6$ a). Although a dominant source of ^{22}Ne is ^{22}Na , a portion of the ^{22}Ne is ^{22}Ne produced in asymptotic giant branch (AGB) stars and proportions of ^{22}Ne from the two origins vary with density [2]. In the case of low-density graphite grains (1.65–1.72 g/cm³) from Murchison, all the ^{22}Ne originated from ^{22}Na produced in supernovae, not in novae [3]. Here we further examine the origin of ^{22}Na in higher-density separates from Murchison.

Discussion: There are two stellar sources for ^{22}Na . In type II supernovae it is produced in the O/Ne zone during hydrostatic C burning by $^{21}\text{Ne}(p,\gamma)^{22}\text{Na}$, where ^{21}Ne is produced by $^{20}\text{Ne}(n,\gamma)^{21}\text{Ne}$ and protons by $^{12}\text{C}(^{12}\text{C},p)^{23}\text{Na}$ [4, 5]. In novae, ^{22}Na is produced via $^{20}\text{Ne}(p,\gamma)^{21}\text{Na}(\beta^+\nu)^{21}\text{Ne}(p,\gamma)^{22}\text{Na}$ that requires $T \sim 4 \times 10^8$ K. Therefore, ONe novae, more massive than CO novae, can reach higher peak temperatures, have higher ^{22}Na yields [(3.1 – 65) $\times 10^{-5}$ in ONe novae; (8.5 – 34) 10^{-8} for CO novae, in mass fraction] [6].

A difficulty to explain ^{22}Na in presolar graphite by nova origin is that Ne is much more abundant than ^{22}Na in both types of novae: $^{20}\text{Ne}/^{22}\text{Na}$ ratios range from 406 to 11,300 [6]. In addition, although $^{20}\text{Ne}/^{22}\text{Ne}$ ratios expected for CO nova ejecta are low (0.07 to 0.72), those for ONe novae, which are a proficient producer of ^{22}Na , are rather high (37 to 2890) [6]. Therefore, if graphite grains contain ^{22}Na from novae, ^{22}Na must have been incorporated into the grains in an environment where Ne could be totally eliminated during the grain formation and/or in the subsequent stage.

Supernovae pose a similar situation. In the O/Ne zone in a $25M_{\text{sun}}$ star with solar metallicity, the ^{22}Na yield is estimated to be 1.89×10^{-6} (in mass fraction) and the $^{20}\text{Ne}/^{22}\text{Na}$ ratio is 1.14×10^5 [4]. However, in the case of supernovae, implanted Ne into the grain surface is likely to be removed after grains encounter the reverse shock. Infrared observations of Cassiopeia A indicate that nucleosynthetic zones are associated with characteristic dust to the zones [e.g., 7], indicating that relative velocities between the dust and the gas are relatively small. A relative velocity between grains and the gas (Ne), estimated from the amorphous rims of TiC subgrains in low-density graphite [8], is 300 km/s. Using this velocity, Ne would be implanted into 25 nm down the grain surface [3]. The layer of this thickness is very likely to be sputtered when grains travel into the hot H-rich outer zones and into the ISM (interstellar medium) after the reverse shock reaches nucleosynthetic zones, causing decoupling of the grains and the gas [9]. Whether the same scenario works for nova ejecta remains to be seen: there are no observations or theoretical work that access the interaction between the nova ejecta and the ISM yet.

References: [1] Amari S. et al. 1990. *Nature* 345:238–240. [2] Amari S. et al. 1995. *Geochimica et Cosmochimica Acta* 59:1411–1426. [3] Amari S. 2008. *The Astrophysical Journal*. Submitted. [4] Rauscher T. et al. 2002. *The Astrophysical Journal* 576:323–348. [5] Limongi M. and Chieffi A. 2003. *The Astrophysical Journal* 592:404–433. [6] José J. and Hernanz M. 1998. *The Astrophysical Journal* 494:680–690. [7] Rho J. et al. 2008. *The Astrophysical Journal* 673:271–282. [8] Croat T. K. et al. 2003. *Geochimica et Cosmochimica Acta* 67:4705–4725. [9] Nozawa T. et al. 2007. *The Astrophysical Journal* 666:955–966.

5139

MINERALOGY AND NOBLE GAS SIGNATURES OF DESERT METEORITE SHİŞR 007 (UREILITE)

K. Ando¹, T. Nakamura¹, R. Okazaki¹, D. Nakashima², Y. Kakazu¹, and F. Kitajima¹. ¹Department of Earth and Planetary Sciences, Kyushu University, Hakozaki, Fukuoka 812-8581, Japan. E-mail: k-ando@geo.kyushu-u.ac.jp. ²Laboratory for Earthquake Chemistry, University of Tokyo, Hongo, Bunkyo-ku, Tokyo 113-0033, Japan.

Carbonaceous materials are key objects to elucidate origin and formation of ureilites. We have characterized a large (1.0 \times 1.5 mm) carbonaceous material in Shişr 007 ureilite by multidiscipline techniques for mineralogy and noble gas signatures. In addition, chemical compositions and shock stages of host silicates were also determined.

Core compositions of olivine (Fo = 79) and pyroxene (En = 73) are close to the average composition of silicates in ureilites [1]. Olivine shows undulatory extinction and planar deformation fractures, corresponding to shock stage S3 [2]. Narrow (10–100 μm) reduction rims occur around olivine and pyroxene grains and contain tiny Fe metal inclusions. Compositions of olivine and pyroxene in reduction rims are enriched in Mg compared with the cores. These rims have been produced by reduction of FeO by carbon at grain boundaries during brief, shock heating at elevated temperature. There are many fragments of relict graphite in Fe-Ni-S melt in contact with the reduction rims. The presence of the Fe-Ni-S melt and the escape of melting of olivine and pyroxene suggest that temperatures were between 1200 and 1600 $^{\circ}\text{C}$ at the time of the rim formation.

The large carbonaceous material is composed of fine diamonds and graphites. It has rectangular, blade-like shape, implying that it was a large single crystal of graphite, as is observed in ALH 78019 [3]. Raman spectroscopy revealed the presence of compressed graphite that is an intermediate phase formed during graphite-diamond phase transition. Using an edged tool, the large carbonaceous material was separated into small pieces typically 200–300 μm in diameter. Individual pieces were first measured by synchrotron X-ray diffraction and the results indicated that diamond-graphite ratio varies among pieces. Then each piece was analyzed by the stepwise heating method to obtain noble gas compositions using “Pot-pie furnace” designed for μg sample analysis. A major part (80–95%) of primordial ^{36}Ar , ^{84}Kr , and ^{132}Xe was released at 1900–2100 $^{\circ}\text{C}$ fraction, indicating that a main carrier phase of noble gases is diamond. The release temperature is consistent with that achieved during the rim formation. Elemental ratios of $^{36}\text{Ar}/^{132}\text{Xe}$ and $^{84}\text{Kr}/^{132}\text{Xe}$ are 200–450 and 1.0–1.8, respectively, in the range of diamond-rich carbonaceous materials in other ureilites [e.g., 4]. Concentrations of primordial noble gases vary and do not correlate with elemental ratios and the diamond-graphite ratios. Our analyses suggest that Shişr 007 ureilite contains diamond with variable noble gas concentration and $^{36}\text{Ar}/^{132}\text{Xe}$ and $^{84}\text{Kr}/^{132}\text{Xe}$ elemental ratios.

References: [1] Mittlefehldt D. W. et al. 1998. Ureilites. In *Planetary materials*, edited by J. J. Papike. pp. 73–95. [2] Stöffler D. et al. 1991. *Geochimica et Cosmochimica Acta* 55:384–3867. [3] Goodrich C. A. et al. 2000. *Meteoritics & Planetary Science* 27:327–352. [4] Göbel R. et al. 1997. *Journal of Geophysical Research* 83:855–867.

5164

TEM OBSERVATIONS OF SYNTHESIZED FORSTERITE CRYSTALS AFTER SHOCK EXPERIMENTS

T. Aoki¹, Y. Nakamura², S. Toh³, and T. Nakamura¹. ¹Department of Earth and Planetary Sciences, Faculty of Sciences, Kyushu University, Japan. E-mail: tomotaro@geo.kyushu-u.ac.jp. ²Kyushu University Museum, Kyushu University, Japan. ³Research Laboratory for High Voltage Electron Microscopy, Kyushu University, Japan.

Introduction: The apparent strains of olivine crystals can be estimated from XRD analyses and known to be proportionally correlated to the shock pressures loaded on them [1]. In this study, microstructures of experimentally shocked forsterite crystals were observed by TEM after determining apparent strains by XRD analyses using a Gandolfi camera.

Experiments: Shock recovery experiments on synthesized forsterite crystals were carried out at the shock pressures 11.7, 20.8, 34.5, and 46.2 GPa. Double polished thin sections (PTSs) of each sample were prepared and observed under a polarizing microscope. Two or three crystals of less than 100 μm in size for each shock-recovered sample were taken out from the center of each PTS and analyzed by an XRD method using a Gandolfi camera to determine the apparent strain of crystals. One crystal for each recovered sample was fabricated to thin film by an FIB method and observed by TEM. TEM observations were carried out by using JEM-200CX at 200kV of accelerating voltage. The shapes and densities of dislocations were observed under the bright field (BF) and dark field (DF) conditions. The Burgers vectors of dislocations were determined under two DF conditions in which dislocations are out of contrast.

Results and Conclusions: The apparent strains of forsterite crystals increase with the shock pressures loaded on them. The apparent strains of selected crystals for TEM observations are 0.031(2), 0.048(4), 0.164(9) and 0.194(7)% for samples shocked to 11.7, 20.8, 34.5, and 46.2 GPa, respectively.

By TEM observations, the following textures were observed:

For 11.7 GPa Crystal: The curved dislocations are locally concentrated, while the majority of this sample shows homogeneous contrast in a BF image along [100] zone axis. This texture is thought to be a nucleation source of dislocations [2]. The Burgers vector of dislocations is *c*.

For 20.8 GPa Crystal: Straight dislocations are dominant. Many of them are directed nearly [100], while a few directed [001]. All have the same Burgers vector *c*. Most dislocations lie on a crystallographic *a-c* plane showing that the activated glide plane is (010). The dislocation density is $6.7 \times 10^8 \text{ cm}^{-2}$. The dominance of [100] edge dislocations will show the early stage of diffusion of dislocations by the fact that the velocity of edge segments is larger than the screw segments.

For 34.5 GPa Crystal: Dislocations are straight and mainly directed [001]. A few dislocations are directed [100]. All have the same Burgers vector *c*. The distribution of dislocations is heterogeneous compared with the other samples. The subgrain boundaries (dislocation array) and cracks also exist. The density of free dislocations is up to $1.3 \times 10^9 \text{ cm}^{-2}$.

For 46.2 GPa Crystal: The straight dislocations are homogeneously distributed and directed [001]. All have the same Burgers vector *c*. The subgrain boundaries and cracks also exist. The density of free dislocations is $1.3 \times 10^9 \text{ cm}^{-2}$.

References: [1] Uchizono et al. 1999. *Mineralogical Journal* 21:15–23. [2] Leroux H. 2001. *European Journal of Mineralogy* 13:253–272.

5074

ION MICROPROBE U-Pb DATING OF THE YAMATO-983885 LUNAR METEORITE

S. Arai¹, K. Terada¹, T. Arai², H. Hidaka¹, and Y. Sano³. ¹Department of Earth and Planetary Systems Science, Hiroshima University, Higashi-Hiroshima 739-8526, Japan. E-mail: optimistic-like-stars@mail.goo.ne.jp. ²Antarctic Meteorite Research Center, National Institute of Polar Research, Tokyo 173-8515, Japan. ³Center for Advanced Marine Research, Ocean Research Institute, The University of Tokyo, Nakano-ku 164-8639, Japan.

Introduction: The lunar meteorites have valuable information for understanding the evolution of the Moon's crust, since each meteorite may potentially provide a new insight into the thermal history of unexplored region of the Moon. In spite of their scientific value, chronological studies of lunar meteorites have been difficult, since most of them are complex breccias, and in some cases, their isotopic "clocks" have been disturbed by subsequent impact events. Recently, an in situ U-Pb dating method has been successfully applied to phosphate grains in the lunar basaltic meteorites [1–7] and has enabled us to unravel the lunar evolution such as ancient magmatism 4.35 Gyr ago [6] and an extremely low μ -value ($=^{238}\text{U}/^{204}\text{Pb}$) of magma sources [5, 7]. In this paper, we report an ion microprobe U-Pb dating of phosphate grains in lunar polymict breccia Yamato (Y-) 983885.

Samples: Y-983885 is a 290 g polymict regolith breccia found in Antarctica [8]. Kaiden and Kojima [8] reported a preliminary result of the petrography and oxygen isotopic composition, and verified its lunar origin. Arai et al. [9] investigated the mineralogy of thin section Y-983885.59-2 and reported that it consists of a KREEP basalt, Mg-rich troctolite/norite, a high-Al basalt, a very low-Ti (VLT) basalt, a granulite originated from ferroan anorthosite, and Si, Na-rich impact spherule. For this study, thin sections, Y-983885 57-1 and 59-6 were allocated by National Institute of Polar Research (NIPR). Based on the mineralogical studies, it was found that these thin sections also consist of a KREEP basalt, a high-Al basalt and a VLT basalt, similar to Y-983885.59-2.

Results: Tentative in situ U-Pb analyses of phosphates grains in Y-983885 57-1 were carried out using Sensitive High Resolution Ion MicroProbe (SHRIMP) at Hiroshima University, JAPAN. Although these phosphate grains are from various clasts (that is, different origins), obtained data are roughly expressed by a total Pb/U isochron line of ~ 4.0 Ga. Since the most of phosphates are likely from Mg-rich rocks and/or KREEP basalts, our preliminary data seem to be consistent with those of Apollo samples [10]. For detail discussion on the chronology of each component, further investigation will be required.

References: [1] Anand M. et al. 2003. *Geochimica et Cosmochimica Acta* 67:3499–3518. [2] Terada K. et al. 2005. *Geophysical Research Letters* 32, doi:10.1029/2005 GL023909. [3] Anand M. et al. 2006. *Geochimica et Cosmochimica Acta* 70:246–264. [4] Terada K. et al. 2006. *Meteoritics & Planetary Science* 41:A5129. [5] Terada K. et al. 2007. *Earth and Planetary Science Letters* 259:77–84. [6] Terada K. et al. 2007. *Nature* 450:849–852. [7] Terada K. et al. 2008. *Earth and Planetary Science Letters*. In press. [8] Kaiden H. and Kojima H. 2002. Abstract #1958. 33rd LPSC. [9] Arai T. et al. 2005. *Antarctic Meteorite Research* 18:17–45. [10] Nyquist L. E. et al. 2001. In *The century of space science*. pp. 1325–1376.

5326

ORIGIN OF LUNAR TROCTOLITE: IMPLICATION FOR COMPOSITION AND CRYSTALLIZATION OF MAGMA OCEAN

T. Arai¹, K. Saiki², M. Ohtake³, T. Matsunaga⁴, Y. Ogawa⁴, R. Nakamura⁵, and LISM Working Group. ¹Antarctic Meteorite Research Center, National Institute of Polar Research, Tokyo 173-8515, Japan. E-mail: tomoko@nipr.ac.jp. ²Department of Earth and Space Science, Osaka University, Osaka 560-0043, Japan. ³Planetary Science Department, Institute of Space and Astronautical Science, Japan. Aerospace Exploration Agency, Kanagawa 229-8510, Japan. ⁴Institute of National Environmental Studies, Ibaraki 305-8506, Japan. ⁵National Institute of Advanced Industrial Science and Technology, AIST Tsukuba Central 2, Ibaraki 305-8562, Japan.

Introduction: Lunar troctolites have been sampled by Apollo missions and by lunar meteorites (Dhofar 489 group). Both of them include Mg-rich olivine (Fo₈₀₋₉₀). The former is generally enriched in REE, and likely represents REE-rich, magnesian magma intruded into the anorthositic crust during the post-magma ocean magmatism [e.g., 1, 2, 3], which is probably confined to the Procellarum KREEP Terrane (PKT) of the nearside. In contrast, the latter is depleted in REE, and co-exists with magnesian anorthosite [4], thus may be generated from a primordial magma ocean. Based on Clementine ultraviolet-visible multispectral data, troctolites have been reported at some central peaks of impact craters [5, 6] and in the farside highland [7], indicating that olivine is an important mineral within the feldspathic crust.

Origin of Troctolite: As a result of low-pressure crystallization experiment [8] with a hypothetical bulk-Moon composition [9], which is nearly equal to the terrestrial mantle composition, the magma ocean (~300 km deep) first crystallizes olivine, subsequently olivine and orthopyroxene co-crystallize, and then olivine, orthopyroxene, and clinopyroxene crystallize. Finally, anorthite begins to crystallize. On the other hand, the crystallization sequence to produce troctolite should be given by olivine → plagioclase → low Ca pyroxene → high Ca pyroxene, unlike the experimental result. This infers the bulk-Moon composition should be more Al₂O₃-rich to generate troctolite than the previous assumption.

Future Studies: In order to further constrain the composition and crystallization path of the magma ocean, rock types of the global feldspathic crust should be essential. Multiband images (415, 750, 900, 950, 1000 nm for visible with spatial resolution of 20 m, and 1000, 1050, 1250, 1550 nm for near infrared with spatial resolution of 62 m) provided by Multiband Imager (MI), and visible to near infrared (500–2600 nm) continuous reflectance spectra with high spectral resolution (6–8 nm) and spatial resolution of 500 m, provided by Spectral Profiler (SP) will be utilized to investigate geologic setting and distribution of troctolites and other rock types within the feldspathic crust.

References: [1] Hess P. C. 1998. Abstract #1389. 31st LPSC. [2] Hess P. C. 2000. Abstract #1225. 29th LPSC. [3] Papike J. J. et al. 1998. *Reviews in Mineralogy*, vol. 36, 5.1–5.234. [4] Takeda H. et al. 2006. *Earth and Planetary Science Letters* 247:171–184. [5] Tompkins S. and Pieters C. M. 1999. *Meteoritics & Planetary Science* 34:25–41. [6] Pieters C. M. and Tompkins S. 1999. *Journal of Geophysical Research* 104:21935–21949. [7] Lucey P. G. 2004. *Journal of Geophysical Research* 31:L08701, doi:10.1029/2003GL019406. [8] Hodge F. N. and Kushiro I. 1974. *Geochimica et Cosmochimica Acta*, Supplement, 5:1. [9] Ganapathy R. and Anders E. 1974. *Geochimica et Cosmochimica Acta*, Supplement 5.

5230

GLOBAL LUNAR TOPOGRAPHY BY LALT (LASER ALTIMETER) ON BOARD KAGUYA

H. Araki¹, S. Sasaki², H. Noda¹, S. Tazawa², Y. Ishihara², E. Migita^{1†}, N. Kawano², I. Kamiya³, and J. Oberst⁴. ¹RISE Project, National Astronomical Observatory, 2-21-1 Osawa, Mitaka 181-8588, Japan. E-mail: arakih@miz.nao.ac.jp. ²RISE Project, National Astronomical Observatory, 2-12 Hoshigaoka, Mizusawa, Oshu 023-0861 Japan. ³Geographical Survey Institute, 1 Kitasato, Tsukuba 305-0811, Japan. ⁴German Aerospace Center (DLR), Rutherfordstrasse 2, 12489 Berlin, Germany. [†]Now at ISAS/JAXA, Sagami-hara 229-8510 Japan.

Introduction: The Laser Altimeter (LALT) on board Japanese lunar explorer KAGUYA (SELENE) is designed to map the whole lunar topography. KAGUYA was launched successfully on September 14, 2007. Health check of heater control system and low-voltage power unit in LALT was carried out on September 23 and on November 1 without laser firing. The first operation with laser shots was done on November 25 and the lunar topography was obtained successfully. We started continuous observation on December 30. So far, global lunar topography was obtained successfully.

LALT Specification: LALT uses Nd-YAG laser with wavelength 1064 nm. The width of laser pulse is 17 ns and pulse energy is typically 100 mJ with 1 Hz repetition frequency. Reflected laser signals are received by Cassegrain type reflector and detected by Si-APD (avalanche photodiode) with 10 nm band pass filter. Footprint size of the laser beam on the lunar surface is 40 m from the altitude of 100 km. The ranging distance is 50–150 km with the accuracy less than 5 m [1].

Lunar Topography: KAGUYA takes polar orbits with the mean altitude 100 km. Since LALT can detect the reflected signals day and night, global data can be acquired in half a month. So far LALT has operated more than 3 months, it has already scanned the whole surface six times. Number of data points exceeded 6.7 million as of March 31. Since the spatial resolution along the orbit is 1.5 km, we can identify features as small as 10 km, such as central peaks of craters in the produced topography map from 3 months of data. Quantitative topography of both polar regions was obtained for the first time. For example, LALT discovered a hidden small crater inside a larger crater. Clementine LIDAR could not observe the polar regions, because of its large orbital altitude.

LALT shall continue observation of the whole lunar surface by the end of 2008, when the whole lunar topography with spatial resolution as good as 2 km will be obtained. This is much better than Clementine data of a few tens of km resolution [2]. The spatial resolution at the polar regions by LALT will be better than 500 m.

References: [1] H. Araki et al. 2008. *Advances in Space Research*. In press. [2] M. T. Zuber et al. 1994. *Science* 266:1839–1844.

5322

EFFECTS OF DUST ON THERMAL INFRARED REFLECTIVITY OF IRON METEORITE CANDIDATES FOUND BY THE MARS EXPLORATION ROVERS

J. W. Ashley,^{1,2} S. W. Ruff¹, P. R. Christensen¹, and L. A. Leshin³. ¹School of Earth and Space Exploration, Mars Space Flight Facility, Arizona State University, Box 871404, Tempe, AZ 85287, USA. ²Minor Planet Research, 16662 North Aspen Drive, Fountain Hills, AZ 85268, USA. ³NASA Goddard Space Flight Center, Greenbelt, MD 20771, USA. E-mail: james.ashley@asu.edu.

Introduction: The discovery of an iron meteorite and two additional candidates on the surface of Mars at both Mars Exploration Rover (MER) locations using the Miniature Thermal Emission Spectrometer (Mini-TES) [1] demonstrates a remote sensing tool useful for their identification, which should be considered in future missions. The importance of exogenic material in general, as witness samples for Martian weathering (among other science priorities), cannot be overestimated. In the special case of irons, while wind abrasion can readily remove oxyhydroxide coatings (evidence of past water exposure) from metal surfaces, such materials may be easily preserved within cavities common to these rock types. We are therefore interested in determining the obscuring effects of dust on TIR spectra from both bare and oxidized iron meteorite substrates.

Background: Metals are highly reflective in the infrared with significantly reduced thermal emissivities [e.g., 1]. Iron meteorites stand out on Mars against the background of indigenous rocks in the way that they reflect downwelling atmospheric sky radiance. Martian dust is a problem for all remote sensing because of its ability to obscure underlying surfaces both in the TIR and visible light [e.g., 2]. Following on the results presented in [3], where oxidized surfaces were evaluated, this work focuses on the effects of dust on reflectivity of bare metal surfaces in the TIR.

Methods: Using the Nexus 670 FTIR interferometric spectrometer at ASU's Mars Space Flight Facility, TIR spectra were collected of a Meridiani Planum (MP; formerly Heat Shield Rock [4]) analog with Martian dust analog [5] loading in incremental stages to monitor spectral variations in a controlled environment. This abstract reports on the effects of dust coatings on both sandblasted, and cut and polished, samples of the Canyon Diablo IAB coarse octahedrite. An artificial, quartz-based control was placed within the spectrometer environmental chamber to simulate downwelling atmospheric sky radiance on Mars, and monitor its thermal reflectivity.

Results: Recognition of the quartz signature in the spectrum of the Canyon Diablo slab, but not the MP analog 1) confirms the highly reflective behavior of metals in the TIR, but 2) demonstrates that the reproducibility of downwelling atmospheric sky radiance is problematic in the laboratory. Natural surfaces appear to scatter the downwelling radiance, effectively attenuating the quartz signal. A maximum thickness of only 14 μm of dust was sufficient to completely obscure reflective effects evident on the undusted, polished slab surface. It therefore requires approximately one order of magnitude less dust to obscure reflectivity spectra than emissivity spectra in the TIR as presented in [2].

References: [1] Schröder C. et al. 2008. *Journal of Geophysical Research* 113:E06S22, doi:10.1029/2007JE002990. [2] Graff T. G. 2003. Master's thesis, Arizona State University. [3] Ashley J. W. et al. 2008. 39th LPSC. Abstract #2382. [4] Connolly H. C. Jr. et al. 2006. *The Meteoritical Bulletin* #90. [5] Morris R. V. et al. 2001b. *Journal of Geophysical Research* 106:5057–5083.

5120

TUNGSTEN ISOTOPIC COMPOSITIONS IN PRESOLAR SILICON CARBIDE GRAINS

J. N. Avila¹, T. R. Ireland¹, P. Holden¹, F. Gyngard², V. Bennett¹, S. Amari², and E. Zinner². ¹Research School of Earth Sciences and Planetary Science Institute, The Australian National University, Canberra ACT 0200, Australia. E-mail: janaina.avila@anu.edu.au. ²Laboratory for Space Sciences and Physics Department, Washington University, St. Louis, MO 63130, USA.

Introduction: The s-process nucleosynthesis in the Hf-Ta-W-Re-Os path has received considerable attention lately. New neutron capture cross sections for ^{174,176,177,178,179,180,182}Hf, ¹⁸⁵W, and ^{186,187,188}Os have been reported [1–4], and small anomalies in W and Os isotopes have been observed in primitive meteorites [5–7]. However, as suggested by [2, 3], model calculations for s-processes nucleosynthesis appear to underestimate ¹⁸²W and overestimate ¹⁸⁶Os, and this may have implications for the ¹⁸²Hf-¹⁸²W and ¹⁸⁷Re-¹⁸⁷Os chronometers. Tungsten isotopes are particularly important because they are affected by several branching points (¹⁸²Ta, ^{181,182}Hf, and ¹⁸⁵W), which also affect Re and Os isotopes. Here we report for the first time W isotopic measurements in presolar SiC grains in order to provide additional constraints on s-process nucleosynthesis.

Experimental: ^{182,183,184,186}W and ¹⁸⁰Hf were measured with SHRIMP RG at ANU in an aggregate of presolar SiC grains (KJB fraction) extracted from the Murchison meteorite [8]. Tungsten isotopes were measured as WO⁺ ions, which have a higher yield than the atomic species (WO⁺/W⁺ ~ 3). An O⁻ primary ion beam of 5 nA was focused to sputter an area of 20 μm in diameter. SHRIMP RG was operated at a mass resolving power of $m/\Delta m = 5000$ (at 1% peak). At this level, isobaric interferences were well resolved from the WO⁺ species. NIST silicate glasses and synthetic SiC were used to monitor instrumental mass fractionation and isobaric interferences.

Results and Discussion: The W isotopic compositions are anomalous in comparison to those observed in normal solar system materials. The SiC grains appear to be enriched in ¹⁸²W and ¹⁸⁴W relative to ¹⁸³W, as expected for s-process nucleosynthesis in AGB stars [e.g., 5]. However, an unexpected enrichment in ¹⁸⁶W is observed. The low ¹⁸⁰Hf/¹⁸³W ratios determined here imply a low contribution from radiogenic ¹⁸²W after SiC condensation, otherwise the ¹⁸²W excesses would be even higher. The observed enrichment in ¹⁸⁶W requires the activation of the ¹⁸⁵W branching point during AGB thermal pulses, when marginal activation of the ²²Ne(α, n)²⁵Mg source produces neutron densities as high as $N_n = 5 \times 10^9$ neutrons cm^{-3} [9], bypassing ¹⁸⁶Os. This result is in disagreement with ⁹⁶Zr depletions in SiC grains that indicate that the ²²Ne(α, n)²⁵Mg source was weak in their parent stars.

Production and destruction of W isotopes by cosmic rays still need to be investigated, especially for samples, such as presolar grains, exposed for a long time to galactic cosmic radiation.

References: [1] Wisshak K. et al. 2006. *Physical Review C* 73:45,807. [2] Vockenhuber C. et al. 2007. *Physical Review C* 75:15804. [3] Sonnabend K. et al. 2003. *The Astrophysical Journal* 583:506–513. [4] Mosconi M. et al. 2006. *Nuclei in the Cosmos IX*, pp. 381–387. [5] Qin L. et al. 2008. *The Astrophysical Journal* 674:1234–1241. [6] Brandon A. et al. 2005. *Science* 309:1233–1236. [7] Yokoyama T. et al. 2007. *Earth and Planetary Science Letters* 259:567–580. [8] Amari S. et al. 1994. *Geochimica et Cosmochimica Acta* 58:459–470. [9] Lugaro M. et al. 2003. *The Astrophysical Journal* 593:486–508.

5073

NOBLE GASES IN A GIBEON IRON METEORITE FRAGMENT HEAVILY SHIELDED TO COSMIC RAYS

K. Bajo¹, K. Nagao¹, and M. Honda². ¹Laboratory for Earthquake Chemistry, Graduate School of Science, University of Tokyo, Bunkyo-ku, Tokyo 113-0033, Japan. E-mail: k-bajo@eqchem.s.u-tokyo.ac.jp. ²Department of Chemistry, Nihon University, Setagaya-ku, Tokyo 156-0045, Japan.

Introduction: Gibeon iron meteorite classified as IVA has been discovered as a large number of fragments in a strewn field in Namibia, Africa. Total weight of the meteorite becomes about 21 tons [1], and its preatmospheric body was estimated to be larger than 3 m in radius (applying the model calculation from [2] for our data). The scarcity of cosmogenic noble gases may provide us with a chance to investigate primordial component in iron meteorite parent body. We will report noble gas data recently obtained for a plate-shaped sample (about 240 × 170 × 8 mm in size), which shows extraordinary low concentration of cosmogenic noble gas, e.g., ³He < 10⁻¹² cm³STP/g [3]. This belongs to a group with relatively short cosmic-ray exposure age (~10⁷ yr) [4]. Our purpose of this study is to investigate the primitive noble gas component in iron meteorite parent body.

Noble Gas Analysis: Meteorite pieces weighing 90–130 mg each, drilled out from 8 points in the sample plate, were analyzed for noble gases on a modified VG5400 (MS-III). We used a Mo crucible of which inner wall was coated with zirconium oxide to avoid melting of the crucible by forming alloy with the iron meteorite.

Results and Discussion: Measured ³He/⁴He ratios were as low as (3–5) × 10⁻⁴, which resemble isotopic ratio of “primordial helium.” Several cases can be considered for the low ³He/⁴He: 1) mixing of cosmogenic helium and radiogenic ⁴He, 2) true primordial helium, and 3) air contamination. Combination of these cases can also be considered. If ³He is totally cosmogenic, cosmogenic ³He was generated as low as (2.2 ± 0.4) × 10⁻¹³ cm³STP/g in a time spans of 10 Myr [4]. Concentrations of ⁴He were in the order of 10⁻⁹ cm³STP/g, homogeneously distribute in the sample plate. Given that the ⁴He was produced from U, Th (Th/U = 3) for 4 Gyr, concentration of uranium can be estimated as low as 0.5 ppt. Contamination of terrestrial air is improbable, because ⁴He/²⁰Ne ratios in our sample are >1.3 much larger than the atmospheric value of 0.32 and contamination generally occurs selectively in heavier noble gas.

References: [1] Buchwald V. 1975. *Handbook of iron meteorites*, vol. 2, pp. 584–593. [2] Leya I. et al. 2002. *Meteoritics & Planetary Science* 37:1015–1025. [3] Nagao K. and Honda M. 2005. 29th Symposium on Antarctic Meteorites. pp. 49–50. [4] Honda M. et al. 2007. *Meteoritics & Planetary Science* 42:A68.

5165

IMPACT GLASSES IN HOWARDITES: K-RICH LITHOLOGIES AND GRANITES ON 4 VESTA

J. A. Barrat^{1, 2}, M. Bohn^{1, 2}, Ph. Gillet³, and A. Yamaguchi⁴. ¹Université Européenne de Bretagne, France. ²UBO-IUEM, CNRS UMR 6538, place Nicolas Copernic, F-29280 Plouzané Cedex, France. E-mail: barrat@univ-brest.fr. ³CNRS UMR 5570, Université de Lyon, Ecole Normale Supérieure de Lyon, 46 Allée d'Italie, F-69364 Lyon Cedex 7, France. ⁴Antarctic Meteorite Research Center, National Institute of Polar Research, 1-9-10 Kaga, Itabashi, Tokyo 173-8515, Japan.

The howardites, are complex breccias that contain occasionally impact melt clasts, glass beads or debris, whose compositions mirror that of their source regions. Some K-rich impact glasses (up to 2 wt% K₂O) found during the course of this study, demonstrate that in addition to basalts and ultramafic cumulates, K-rich rocks are exposed on 4 Vesta's surface. Additional K-rich glasses, with a granitic composition, provide the first evidence of highly differentiated rocks on a large asteroid. They can be compared to the rare lunar granites [1] and suggest that magmas generated in a large asteroid are more diverse than previously thought.

In order to discuss the origin of glasses in HED, six glass-bearing howardites (Bununu, Kapoeta, Northwest Africa [NWA] 1664 and 1769, Yamato (Y-) 7308 and 791208) have been selected. More than fifty glassy clasts or spherules have been analyzed. Unlike glasses found in the other howardites, mafic glasses found in NWA 1664 and NWA 1769 are unusually K-rich, with K₂O concentrations ranging from 0.18 to 2.33 wt%. High-K abundances were previously noticed in glasses from NWA 1664 [2], and from the Malvern howardite [3, 4]. These K abundances are much higher than those reported for most of the HED, which contain in most cases less than 0.1 wt% K₂O. Furthermore, a silica-rich glass has been found in a fragment of a spherule from NWA 1664, and displays high K₂O abundances ranging from 4 to 6.12 wt%. The compositions correspond to a high K, low Na monzogranite. Interestingly, this glass resembles the lunar granites, but exhibits much higher Al₂O₃ abundances (about 18 wt% compared to 8.8–13 wt% in the lunar granites [1]).

The K-rich impact glasses found in howardites indicate that the rocks that outcrop on Vesta are not restricted to a series of mafic cumulates and basaltic flows, and we speculate that granites and rocks more evolved than those actually known in the HED collection will probably be observed during the surface mapping of Vesta by the Dawn spacecraft.

References: [1] Papike J. J., Ryder G., and Shearer C. K.. 1998. In *Planetary materials*, edited by Papike J. J. Reviews in Mineralogy vol. 36., 5-1. [2] Kurat G., Varela M. E., Zinner E., Maruoka T., Brandstätter F. 2003. 34th Lunar Planetary Science Conference. Abstract #1733. [3] Noonan A. F. 1974. *Meteoritics* 9:233. [4] Desnoyers C. and Jérôme J. Y. 1977. *Geochimica et Cosmochimica Acta* 41:81.

5167

STILL MORE DIVERSITY IN THE DIOGENITE PARENTAL MELTS

J. A. Barrat^{1,2}, A. Yamaguchi³, R. C. Greenwood⁴, M. Benoit², J. Cotten^{1,2}, M. Bohn^{1,2}, and I. A. Franchi⁴. ¹Université Européenne de Bretagne, France. ²UBO-IUEM, CNRS UMR 6538, place Nicolas Copernic, F-29280 Plouzané Cedex, France. E-mail: barrat@univ-brest.fr. ³Antarctic Meteorite Research Center, National Institute of Polar Research, 1-9-10 Kaga, Itabashi, Tokyo 173-8515, Japan. ⁴PSSRI, The Open University, Walton Hall, Milton Keynes MK7 6AA, UK.

We report on the major and trace element abundances of 18 diogenites (Bilanga, Johnstown, Tatahouine, Dhofar 700, NWA 4272, Asuka-881526, Asuka-881548, Asuka-881839, EETA79002, GRO 95555, LAP 02216, LAP 03569, LAP 03630, MET 00422, MET 00424, MET 00425, MET 00436, MIL 03368), and O isotopic compositions for three of them. These new analyses extend significantly the diogenite compositional range, both in respect of Mg-rich (e.g., MET 00425, MgO = 31.5 wt%) and Mg-poor varieties (e.g., Dhofar 700, MgO = 23 wt%). No strong correlations are obtained between major and trace elements, with the noticeable exception of Sc abundances, which are positively correlated with the FeO/MgO ratios. The wide ranges of siderophile and chalcophile element abundances are well explained by the presence of inhomogeneously distributed sulfide or metal grains within the analyzed chips. The behavior of incompatible elements in diogenites is more complex, as exemplified by the diversity of their REE patterns. In most cases, diogenites are light REE depleted, with a large negative Eu anomaly, but three diogenites (A-881839, MET 00425, and MET 00436) display a flat REE pattern. A leaching experiment has been undertaken on one of them, and this demonstrates that the involvement of a very limited amount of phosphate can account for their atypical REE patterns. Seven of the 13 Antarctic diogenites analyzed here (Asuka-881526–EETA 79002 group) display very similar REE patterns, and we propose that these particular samples originated from the same magmatic system, or alternatively that they formed from very similar parental melts. Another Antarctic diogenite (MET 00424) displays very low incompatible element abundances, and an extremely low $(Dy/Yb)_n$ ratio close to 0.05. The range of incompatible element abundances, and particularly the range of Dy/Yb ratios in diogenites is best explained by the diversity of their parental melts, and we confirm that some diogenites (e.g., Tatahouine and MET 00424) formed from magmas displaying significant heavy REE enrichments. The compositions of the parental melts of diogenites are difficult to constrain. We estimate that their FeO/MgO ratios range from about 1.4 to 3.5 and therefore largely overlap the values obtained for non-cumulate eucrites. Thus, the diversity of the parental melts required to explain the incompatible element features of the diogenites, and the fact that these melts were not systematically more “primitive” than the eucrites, strongly indicate that diogenites and eucrites are not cogenetic.

5097

ALTERATION OF IMPACTITES FROM THE CHESAPEAKE BAY IMPACT STRUCTURE, USA

K. Bartosova¹, D. Mader¹, R. T. Schmitt², C. Koeberl¹, and W. U. Reimold². ¹Department of Lithospheric Research, University of Vienna, Althanstrasse 14, A-1090 Vienna, Austria. E-mail: katerina.bartosova@univie.ac.at. ²Museum of Natural History, Department of Mineralogy, Humboldt University, Invalidenstrasse 43, D-10099 Berlin, Germany.

The Chesapeake Bay impact structure, 35.5 Ma old and 85 km in diameter, was drilled in 2005–06 during an ICDP-USGS drilling project. The Eyreville drill core penetrated through post-impact sediments and impactites, into fractured crystalline basement to a total depth of 1766 m [1]. The section of suevites and lithic impact breccias (SLIB) was cored at 1397–1551 m depth [2].

Detailed petrographic and chemical analyses were performed on 43 samples from the SLIB section. The suevites are most melt-rich in the upper part, where they locally grade into impact melt rocks. Below 1474 m the suevites are melt-poor and grade into polymict lithic breccias, intercalated with large blocks of cataclastic gneiss.

The impactites from the Eyreville drill core show evidence of hydrothermal alteration. Most melt particles in suevite are altered to phyllosilicate minerals and, rarely, replaced by secondary carbonate; only near the top of the section (at around 1415 m) unaltered glass particles were found. The impactites contain some secondary carbonate veins and patches and also rare secondary opaque minerals, mostly pyrite. The carbonate veins, which were found mostly in the lower parts of the section and also in the cataclastic schist below, have $\delta^{13}C$ values of -7% . The lower $\delta^{13}C$ value of the carbonate veins compared to limestone indicates hydrothermal or diagenetic origin. Smectite, a mineral typical for hydrothermal alteration, was confirmed by XRD in the suevites and was probably formed by alteration of melt. Amygdules filled with zeolites were observed in the melt-rich parts. The notable alteration of feldspar and the chloritization of mica are interpreted to be possibly of pre-impact age, as similar alteration exists in the crystalline basement rocks. The quartz grains in the impactites show abundant PDFs, which are commonly decorated with tiny fluid inclusions. The decoration of PDFs in quartz may also be a consequence of hydrothermal alteration [3]. The loss on ignition (LOI) increases with increasing depth and does not correlate with the CaO content. This suggests that the LOI is caused mostly by presence of organic matter, as well as structurally bound water in phyllosilicate minerals, and carbonates are not very significant. The increase of LOI with depth might imply increase of alteration, but can be also due to an increasing schist component with abundant mica in the SLIB interval with depth. Hydrothermal alteration was observed in samples from the STP drill core near the center of the Chesapeake Bay structure [3]. Temperatures of hydrothermal fluids reached the boiling point of seawater ($\sim 220^\circ C$ at 300 m water depth), but were lower than $550^\circ C$ [4].

References: [1] Gohn G. S. et al. 2006. *Eos* 87:349 and 355. [2] Horton J. W. et al. 2007. *Geological Society of America Abstracts with Programs* 39(6):314. [3] Horton J. W. et al. 2005. Abstract #2003. 36th Lunar and Planetary Science Conference. [4] Horton J. W. et al. 2006. *Geological Society of America Abstracts with Programs* 38(7):59.

5208

WHY IGNEOUS WOLLASTONITE IS SO RARE IN CAIs

J. R. Beckett¹, K. Thrane², and A. N. Krot³. ¹Division of Geological and Planetary Sciences, Caltech 170-25, Pasadena, CA 91125, USA. E-mail: john@gps.caltech.edu. ²Geological Institute, Copenhagen, Denmark. ³HIGP, University of Hawai'i, Honolulu, HI 96822, USA.

Introduction: Primary wollastonite (wo) thought to have crystallized from a liquid is quite rare in CAIs, having been reported in only two igneous inclusions, White Angel and KT-1 [1, 2]. Both of these CAIs exhibit significant mass fractionations in multiple elements and KT-1 is a FUN inclusion, so it is highly desirable to place as many constraints as possible on their formation. Since phase diagrams previously developed for CAIs do not involve wo [3], we use literature data on wo-saturated and wo-free phase diagrams in the system CaO-MgO-Al₂O₃-SiO₂ (CMAS) to establish a basic framework for describing crystallization of wo-bearing CAIs.

White Angel: White Angel from the Leoville CV3 chondrite is a melilite(mel)-rich (type A) CAI with ~12 vol% wo, 3% perovskite (pv), and no interior spinel (sp) [1]. The bulk composition is close to the ternary Åkermanite(Åk)-Gehlenite(Ge)-Wollastonite(Wo) so the phase diagram of [4] can be applied directly except for late stage crystallization. From the bulk composition [1], mel (~Åk₁) is the liquidus phase with fractional crystallization leading to progressively more Åk-rich mel. The onset of wo crystallization leads to a reversal in Åk. There are no data on how the addition of pv affects the phase relations but, assuming fractionation curves for mel are not strongly affected, the onset of pv crystallization will lead to a second reversal in Åk. This order of crystallization and a double reversal in melilite zoning are consistent with observations of [1] in the White Angel.

KT-1: KT-1 from the CV chondrite NWA 779 is a type B inclusion but with sp mostly restricted to a central band across the section. A fine-grained assemblage of wo + anorthite(an) + mel + diopside(di) occurs interstitial to coarse melilite grains but only in sp-free portions of the inclusion. We used literature data to construct a wo-saturated liquidus phase diagram with liquids projected from Wo onto the plane Åk-Ge-SiO₂. Compositions of one wo-bearing region, determined by defocused beam analyses, plot above the wo-saturation surface (i.e., wo is the liquidus phase) with a predicted fractional crystallization sequence of wo → an → mel → di, consistent with the observed phase assemblage of the wo-bearing regions in KT-1.

Rarity of Igneous Wollastonite in CAIs: A key observation for both White Angel and KT-1 is that sp and wo do not occur together. In White Angel, there is no interior sp. KT-1 has lots of sp but not in the wo-bearing regions. Based on phase relations in CMAS, this is not fortuitous. Sp- and wo-saturated liquidus phase fields are always separated by wo-, sp-free fields leading to mel + di + an + liquid(liq), which has a thermal minimum. As long as the CMAS phase relations are applicable, wo-saturated residual liquids cannot evolve to sp + liq and sp-saturated liquids cannot evolve to wo saturation. Since most igneous CAIs have sp on or near the liquidus, it is igneous wo that is rare. Where present, igneous wo likely implies unusual bulk (White Angel) or local melt (KT-1) compositions relative to “normal” CAIs.

References: [1] Caillet-Komorowski C. L. V. et al. 2007. *Meteoritics & Planetary Science* 42:1159–1182. [2] Thrane K. et al. 2008. Abstract# 2341. 39th Lunar and Planetary Science Conference. [3] Beckett J. R. et al. 2006. *Meteorites and the early solar system II*. pp. 399–429. [4] Osborn E. F. and Schairer J. F. 1941. *American Journal of Science* 239:715–763.

5163

CONCISE ATLAS OF THE SOLAR SYSTEM (11): COMPARISON OF THE PETROGRAPHIC TEXTURES AND EVOLUTIONARY PROCESSES IN THE PARENT BODIES

Sz. Bérczi¹, A. Gucsik², H. Hargitai¹, A. Kereszturi³, and Sz. Nagy⁴. ¹Eötvös University, Institute of Physics, H-1117 Budapest, Pázmány s. 1/a. Hungary. E-mail: berciszani@judens.elte.hu. ²Max-Planck-Institut für Chemistry, Department Geochemistry, Becherweg 27, D-55128 Mainz, Germany. ³Collegium Budapest, Institute for Advanced Study, H-1014 Budapest, Szentháromság tér 2, Hungary. ⁴Eötvös University, Department Petrology, H-1117 Budapest, Pázmány, 1/c, Hungary.

The number of the meteorites, representing a size range of PBs from asteroids through Moon to Mars are gradually increasing. In our new textbook and educational program we collected the most important rock types with their characteristic textures, arranged them in igneous units of their suggested geological settings in the PB. We used petrographic microscopic studies and the samples of several collections of: NASA Lunar Sample Set, NIPR Antarctic Meteorite Set, Hungarian meteorites, NASA meteorite educational set, Eötvös University Mineralogy database of planetary analog rocks samples. The 5 chapters of the textbook:

1. Meteorites of the Chondritic Metamorphous Evolution. First part of the chondritic PB evolution. PB heated up by short living radionuclides: results in onion-layered body (higher T in core regions, lower T at the margins of the body). Chondritic groups (initial condition) and types (T grades), the textural sequence of thermal metamorphism are represented in this section.

2. Meteorites of the Evolved, Differentiated Asteroidal Parent Body. Second part of the chondritic PB evolution: textures after the lost chondritic characteristics, textures of rocks by partial melting, migration and differentiation inside the parent chondritic body. After transitional stages of acapulcoite, lodranite, ureilitic, and mesosideritic stages: layers of differentiation appear. Two segregating materials: first the metallic/sulfide melts appear and migrate in depths, forming core (first collecting in blocks), second a low-melting point silicate (basaltic) melts migrate toward surface. Basaltic achondrites are observable on the evolved asteroidal body Vesta and on its asteroidal fragments.

3. Samples and Meteorites of the Moon. Basaltic sequence and anorthosites, breccias and soil samples all represent the interplay of inner and outer processes. Volcanic flow bodies with texturally layered igneous masses can be reconstructed from cooling rate. Example series: 74220 (orange spherule ~1000 °C/min), variolitic clast of 68501 (hundreds C/day), 12002 porphyritic tx. (large olivine grains, 20–2000 °C/h); intergranular clast in 14305 breccia (k. 100 °C/week); subophitic clast in 72275,128 breccia; 70017 poikilitic tx. (sector zoned cpx), 12005 poikilitic tx. (zoned pyroxene oikocrysts, olivine chadacrysts). Lunar meteorites reveal new types compared to Apollo samples.

4. Meteorites of the Mars. Of the ~50 distinct meteorites shergottite and nakhlite samples are shown by gradually deeper textural characteristics, modifications with depth in cumulate texture, impacts modifications, phase changes, melt pockets and veins, alteration in layered igneous masses.

5. Planetary Analog Rocks on Earth. Both larger units and “individual” examples represent rich set of textural types. Several of them: 1) Theo-flow in Canada for nakhlites, 2) basalt and peridotite inclusions for shergottites (basaltic and lherzolitic), 3) Disco-island basalts with iron nuggets inclusions to some carbon-reduced meteoritic textures, 4) komatiites and boninites with high Mg content igneous rocks.

5085

EVIDENCE FOR STRUCTURALLY CONTROLLED CONDENSATION OF SUBMICRON REFRACTORY METAL ALLOYS IN THE MURCHISON METEORITE

T. Berg¹, E. Marosits², J. Maul¹, G. Schönhense¹, U. Ott², and H. Palme³.
¹Institut für Physik, Universität Mainz, Germany. E-mail: bergt@uni-mainz.de. ²Max-Planck-Institut für Chemie, Mainz, Germany. ³Institut für Geologie und Mineralogie, Universität zu Köln, Germany.

Introduction: Alloys of refractory metals (RM: Re, W, Mo, Pt, Os, Ir, Ru, and Rh) in Ca,Al-rich inclusions of primitive meteorites are among the earliest condensates in a cooling nebular gas. Oxidation, sulfurization, and exsolution have altered the RM-metal alloys to complex opaque assemblages [1–3]. Primary single phase micrometer sized alloys with a volatility controlled RM-pattern suggest condensation in a common alloy [4]. Alternatively, [5] proposed RM condensation in three separate alloys: bcc (Fe, Ni, Pt, Rh), fcc (Fe, Ni, Ir), and hcp (Ru, Os). We report here on a population of submicron sized refractory metal nuggets (RMNs) in an acid-resistant residue of the Murchison meteorite prepared for analysis of presolar SiC grains. These RM grains provide evidence for condensation in solid alloys controlled by the crystal structure of the condensing metals.

Results and Discussion: About 500 RMNs were identified by SEM and 107 were selected for quantitative analysis by energy dispersive X-ray spectroscopy (EDS). The size distribution was found to be lognormal around a mean size of ~300 nm, indicative of cumulative growth processes expected from mechanisms like gas-solid condensation [6]. Individual grains show large variations in chemistry, with Mo, Os, Ru, and Ir accounting for more than 87% by mass. The rest is contributed by W, Pt, Rh, and some Fe and Ni. Ru is anticorrelated with Os and Ir. The grains can be understood as mixtures of an OsRuIr-component with a MoW-alloy and a PtRhFeNi component which is poorly defined, because of low abundance. The average composition of the 107 chemically analyzed grains is: (in mass%): W (4.6), Os (25.3), Ir (24.4), Mo (20.6), Ru (16.9), Pt (1.6), Rh (0.2), Fe (6.0), and Ni (0.4), indicating a smooth volatility controlled CI-normalized pattern of RM with strong depletions of the two most volatile RM, Pt and Rh. The presence of some Fe and Ni is predicted by condensation calculations. No correlation was found between the size of the grains and their composition. Effects of the chemical treatment employed in the extraction process are unlikely because of the abundant presence of W and Mo, the elements most susceptible to oxidation.

Conclusions: Size distribution and chemistry suggest formation of the RMNs by condensation in a nebular gas. The anti-correlation of Os and Ru in individual grains requires a closed system, with continuously changing Os/Ru ratios during condensation.

Acknowledgements: We thank Ch. Sudek for sample preparation.

References: [1] Palme H. and Wlotzka F. 1976. *Earth and Planetary Science Letters* 33:45–60. [2] Blum J. D. et al. 1988. *Nature* 331:405–409. [3] El Goresy A. et al. 1978. Proceedings, 9th Lunar and Planetary Science Conference. pp. 1279–1303. [4] Eisenhour D. D. and Buseck P. R. 1992. *Meteoritics* 27:217–218. [5] Sylvester et al. 1990. *Geochimica et Cosmochimica Acta* 54:3491–3508. [6] Aitchison J. and Brown J. A. C. 1969. *The lognormal distribution*. Cambridge University Press.

5298

LOW-TEMPERATURE SULFIDES IN STARDUST: TEM ANALYSIS OF A SPHALERITE/PYRRHOTITE ASSEMBLAGE FROM TRACK 10

E. L. Berger¹, L. P. Keller², D. Joswiak³, G. Matrajt³, and D. S. Lauretta¹.
¹Lunar and Planetary Laboratory, The University of Arizona, Tucson, AZ 85721, USA. E-mail: elberger@lpl.arizona.edu. ²NASA Johnson Space Center, Houston, TX 77058, USA. ³Department of Astronomy, University of Washington, Seattle, WA 98195, USA.

Introduction: Stardust achieved its mission goal of catching comet and interstellar dust particles and returning them to Earth for analysis. The particles collected span a wide range of compositions, each of which yields information about the comet's history. The refractory components in this collection reveal the large-scale distribution of high-temperature components in the early solar system. Studies of sulfides complement this information by revealing the low-T processes, as well as minor element mobilization recorded in these samples. We investigate a terminal particle from track 10, which has coexisting minerals from the Fe-Ni-S and Fe-Zn-S systems.

Results and Discussion: A microtomed section of a Stardust particle from track 10 was analyzed via TEM at JSC and at the University of Washington. The particle is polycrystalline and is predominately Ni-free pyrrhotite that shows distinct superstructure reflections in electron diffraction patterns. The particle also contains a μm -sized grain of Ni-bearing pyrrhotite $[(\text{Fe}_{0.93}\text{Ni}_{0.07})_{1-x}\text{S}]$ showing the same superstructure reflections, and a μm -sized grain of Fe-rich sphalerite (Zn,Fe)S. The sphalerite contains minor Mn (<2 at%) and shows fine-scale twinning on (111). The sphalerite and Ni-bearing pyrrhotite are not in direct contact.

The pyrrhotite superstructure reflections are only stable below ~340 °C [1]. If the grain were heated above this temperature, the superstructure reflections can be recovered only through slow cooling. The persistence of these reflections indicates that the pyrrhotite did not experience high temperatures during aerogel capture.

If sphalerite and pyrrhotite are in equilibrium, then the wt% Fe in the sphalerite constrains temperature and sulfur fugacity of their formation [2]. Using the temperature 340 °C yields a value for $\log f\text{S}_2$ of -34. However, sphalerite and pyrrhotite cannot coexist under these conditions in equilibrium [3]. We conclude that these minerals are not equilibrated.

Many of Stardust Fe-Ni sulfides contain <2 at% Ni (except pentlandite). This range matches sulfide compositions in anhydrous IDPs [4]. The increased Ni-content in a portion of this pyrrhotite, as well as the disequilibrium between the pyrrhotite and sphalerite, indicates that this grain has experienced processing, and may be more similar to hydrous IDPs or chondritic samples. One possibility is that Ni- and Zn-bearing pyrrhotite formed in the nebula. The Ni and Zn may have subsequently migrated during solid state thermal metamorphism. A second possibility is precipitation of pyrrhotite during parent body aqueous alteration followed by Ni and Zn precipitation at a later time. Either case suggests that the grain had to remain at relatively low temperatures (<340 °C) during either nebular transport to Wild 2 or parent body alteration within Wild 2.

References: [1] Li F. et al. 1996. *Journal of Solid State Chemistry* 124: 264–271. [2] Scott S. D. and Barnes H. L. 1971. *Economic Geology* 66:653–669. [3] Scott S. D. and Barnes H. L. 1972. *Geochimica et Cosmochimica Acta* 36:1275–1295. [4] Zolensky M. et al. 2006. *Science* 314:1735–1739.

5190

ODP LEG 207—A SURPRISINGLY PRISTINE K/T BOUNDARY. II—TRACE ELEMENTS

J. Berndt¹, A. Deutsch², K. Mezger¹, and P. Schulte³. ¹Institut für Mineralogie, Universität Münster, Corrensstr. 24, D-48149 Münster, Germany. ²Institut für Planetologie, Universität Münster, D-48149 Münster, Germany. E-mail: deutsca@uni-muenster.de. ³Geozentrum Nordbayern, Universität Erlangen-Nürnberg, D-91054 Erlangen, Germany.

Introduction: The ODP Leg 207 recovered apparently totally complete Cretaceous-Paleogene (K-T) sections in six boreholes at the Demerara Rise, W Atlantic [1]. An ~1.5 ppb Ir peak [1] marks the top of this 2–3 cm thick ejecta deposit, below, “glassy” (now altered) silicate and carbonate spherules, as well as minor shocked minerals in a clayey matrix form a complex spherule layer [2]. Published geochemical data for this boundary section include X-ray maps, and two INAA bulk rock analyses for a few major and some trace elements [1]. To better understand the nature of this fallout deposit, we obtained a high-resolution geochemical profile across the uppermost 5 mm of the spherule layer for (i) major elements using the JEOL JXA 8900 Superprobe (ICEM, Münster; 15 kV acceleration voltage, 5 nA sample current, 50 µm beam diameter; 97 points), and (ii) a set of trace elements using the Element2 LA-ICP-MS (Inst. f. Mineralogie; spot size 235 µm; 5 Hz, 8–9J/cm²; 37 spots) taking NIST 612 as external standard, and BHVO-2G as unknown to monitor accuracy.

Results: Major Elements: The rather friable sediments have a high porosity, a high content of clay minerals, and are immersed with resin, hence, totals of the EMP analyses range only up to 76 wt% but may be much lower. Average SiO₂ is 43 ± 3 (1σ) wt% (not normalized to 100), yet distribution is quite heterogeneous; the SiO₂ data were used as internal standard (²⁹Si) for quantification of the trace element data. Due to the presence of carbonate spherules [2], the CaO concentration also varies considerably.

Rare Earth Elements: Our results are in good agreement with data by [1] and are typical for the upper continental crust; large variations between neighboring laser spots were observed.

Ni/Cr: In the spherule layer, this elemental ratio straddle around 2.7, clearly less as the average value of 4.05 given by [3] for CM 2 carbonaceous chondrites; which is most likely the projectile type of the Chicxulub impact event [4].

PGEs: Their concentrations (analyzed masses ¹⁰³Rh, ¹⁰⁵Pd, ¹⁹⁴Pt, ¹⁹⁵Pt) increase sharply, yet discontinuously only in the upper 16 spots of the profile, peak concentrations are reached a few spots prior to the knife-sharp top of the spherule layer, followed by a drop to background values (4 spots), and a small peak in a µm-sized rip-up clast in the lowermost Danian. The respective peaks can be offset by one spot due to the obviously very small size of the PGE particles. The given PGE distribution is best explained by an increase of discrete nuggets as carrier of the “Ir anomaly” toward to top of the spherule layer.

Acknowledgements: We acknowledge the Ocean Drilling Program, J. Erbacher (BGR Hannover), the ODP 207 curators, and H. Brinkhuis (Univ. Utrecht) who made the samples available, and the DFG for funding (DE 401/13; SCHU 2248/2).

References: [1] MacLeod K. G. et al. 2007. *Geological Society of America Bulletin* 119:101–115. [2] Schulte P. and Deutsch A. 2008. *Meteoritics & Planetary Science*. This issue. [3] Tagle R. and Berlin J. 2008. *Meteoritics & Planetary Science*. In review. [4] Trinquier A. et al. 2006. *Earth and Planetary Science Letters* 241:780–788.

5304

Fe-BEARING MINERAL ABUNDANCE IN PRIMITIVE CHONDRITES BY MÖSSBAUER SPECTROSCOPY

P. A. Bland^{1,2}, F. J. Berry³, J. M. Cadogan⁴, K. T. Howard², and G. Cressey². ¹Impacts and Astronomical Research Centre (IARC), Department of Earth Science and Engineering, Imperial College London SW7 2AZ, UK. E-mail: p.a.bland@imperial.ac.uk. ²IARC, Department of Mineralogy, Natural History Museum, London SW7 5BD, UK. ³Department of Chemistry, The Open University, Milton Keynes MK7 6AA, UK. ⁴Department Physics and Astronomy, University of Manitoba, Winnipeg, MB R3T 3E1, Canada.

Introduction: Quantifying phase abundance in CCs has proved to be extremely difficult: techniques like point-counting are inapplicable due to the fine-grained nature of matrix phases.

Methodology and Results: Useful in quantifying terrestrial weathering [1–3], ⁵⁷Fe Mössbauer spectroscopy offers a partial solution [4]: relatively grain-size insensitive, it allows us to constrain the abundance of Fe-bearing phases (which in most meteorites constitute the bulk of the sample). The table shows results from bulk CCs: proportion of Fe in troilite, silicates, FeNi metal, magnetite, and a paramagnetic component (mostly Fe³⁺ bearing, but also pentlandite) as a fraction of total Fe in the bulk meteorite (ND = not detected). In appropriate cases (known bulk Fe, known Fe in the phase), these data can be converted to wt%.

Table 1.

Sample	Type	Tro	Sil	FeNi	Mag	Para
Orgueil	CI	ND	5.3	ND	45	49.8
Alais	CI	2.3	8.2	ND	33.6	56
Mighei	CM2	ND	43.7	ND	ND	56.2
Murray	CM2	ND	29.5	ND	3.5	67.1
Murch.	CM2	ND	39.1	ND	ND	60.9
Nogoya	CM2	0.8	37.9	ND	6	55.2
C. Bokk.	CM2	ND	32.7	ND	ND	67.3
Erakot	CM2	ND	40.1	ND	2.1	57.8
Kivesv.	CM2	ND	37.4	ND	ND	62.7
Al Rais	CR2	8.2	19.5	2	37.4	33
Renazzo	CR2	2.6	28.5	25.2	10.9	32.7
Kainsaz	CO3	11.7	48.3	32.9	ND	7.1
Felix	CO3	12.6	67	13.1	ND	7.4
Lance	CO3	10.4	63.2	13.3	ND	13.1
Warrant.	CO3	11.8	78.4	7.8	ND	1.9
Ormans	CO3	5.1	83.7	6.4	4.8	ND
Isna	CO3	10.4	78.3	4.7	ND	6.6
Allende	CV3 ox	11.4	87.7	ND	ND	0.9
Bali	CV3 ox	16.2	62.4	ND	18.7	2.8
Grosnaja	CV3 ox	16.9	65.4	ND	11.8	5.9
Kaba	CV3 ox	10.8	40	ND	44.1	5
Mokoia	CV3 ox	13	67.5	ND	15.6	3.8
Vigarano	CV3 red	23.6	51.2	4.9	14.7	5.5
Leoville	CV3 red	10.8	56	ND	16.4	16.7

References: [1] Bland P. A. et al. 1998. *Meteoritics & Planetary Science* 33:127–129. [2] Bland P. A. et al. 2000. *Quaternary Research* 53: 131–142. [3] Lee M. R. and Bland P. A. 2004. *Geochimica et Cosmochimica Acta* 68:893–916. [4] Bland P. A. et al. 2004. *Meteoritics & Planetary Science* 39:3–16.

5314

THE TERRESTRIAL COMPONENT OF PRIMITIVE CHONDRITE ALTERATION

P. A. Bland^{1,2}, K. T. Howard², G. Cressey², and G. K. Benedix². ¹Impacts and Astromaterials Research Centre (IARC), Department of Earth Science and Engineering, Imperial College London, SW7 2AZ, UK. E-mail: p.a.bland@imperial.ac.uk. ²IARC, Department Mineralogy, Natural History Museum, London SW7 5BD, UK.

Introduction: Studies of the terrestrial weathering of meteorites have typically focused on equilibrated ordinary chondrites [e.g., 1–3], principally because it is a simple matter to define an unweathered starting composition. By contrast, in the case of primitive chondrites, it becomes more difficult to deconvolve the effects of terrestrial and pre-terrestrial aqueous alteration. Nevertheless, it is apparent that terrestrial weathering can have a profound effect on the chemistry of these meteorites [4, 5]. Here we provide an overview of the terrestrial alteration exhibited by various primitive chondrites.

CI and CM Chondrites: It is apparent that mobilization of sulphur in the terrestrial environment (either remobilization of pre-existing sulphates, or oxidization of sulphides) is occurring in CI chondrite falls [6]. A similar process may well be occurring in the CMs. The mineralogical alteration index (MAI), designed to quantify pre-terrestrial alteration [7], shows an excellent correlation with year of fall [8]. One possible explanation is that phyllosilicate probe data for the MAI algorithm are selected based on sulphur content, and as we have seen, sulphur is readily mobilized in the terrestrial environment.

CO Chondrites: Colony and ALH 77307 are both finds, and two of the most primitive CO chondrites. An ⁵⁷Fe Mössbauer spectrum of Colony reveals that 55.3% of the Fe in the sample is present as Fe³⁺-bearing phyllosilicate. Most CO falls have <10%. The difference is likely due to terrestrial alteration.

CV Chondrites: Allende contains minor aqueous alteration products. X-ray diffraction indicates minimal alteration [9], and ⁵⁷Fe Mössbauer spectra of Allende show no paramagnetic Fe³⁺-component [10]. In contrast, the CV_{Ox(a)} Axtell shows abundant Fe³⁺-bearing phyllosilicates [11], with similar Mössbauer parameters to terrestrial weathered ordinary chondrites [1].

Ungrouped Carbonaceous Chondrites: An ⁵⁷Fe Mössbauer spectrum for Acfer 094 shows abundant Fe³⁺-bearing phyllosilicate (65.4% of total Fe). As sub- μ m matrix metals are well preserved [12], this may be attributable to weathering of amorphous matrix phases. XRD analysis of Adelaide indicates significant goethite (6.7 wt%), likely a result of terrestrial weathering.

Conclusions: Primitive chondrites have experienced terrestrial alteration. Defining the degree of alteration is clearly of value.

References: [1] Bland P. A. et al. 1998. *Meteoritics & Planetary Science* 33:127–129. [2] Bland P. A. et al. 2000. *Quaternary Research* 53: 131–142. [3] Lee M. R. and Bland P. A. 2004. *Geochimica et Cosmochimica Acta* 68:893–916. [4] Bland P. A. et al. 2005. *Proceedings of the National Academy of Science* 102:13755–13760. [5] Hammond S. J. et al. 2008. Abstract #1786. 39th Lunar and Planetary Science Conference. [6] Gounelle M. and Zolensky M. E. 2001. *Meteoritics & Planetary Science* 36: 1321–1329. [7] Browning L. B. et al. 1996. *Geochimica et Cosmochimica Acta* 60:2621–2633. [8] Benedix G. K. and Bland P. A. 2004. *Meteoritics & Planetary Science* 39:A14. [9] Bland P. A. et al. 2004. *Meteoritics & Planetary Science* 39:3–16. [10] Hoffman E. et al. 2001. Abstract #2116. 32nd Lunar and Planetary Science Conference. [11] Hoffman E. et al. 2000. *Meteoritics & Planetary Science* 35:A75–A76. [12] Bland P. A. et al. 2007. *Meteoritics & Planetary Science* 42:1417–1427.

5242

A NEW PERSPECTIVE ON THE EVOLUTION OF MARS

J. Blichert-Toft¹, A. Bouvier^{1,2}, and F. Albarède¹. ¹Ecole Normale Supérieure de Lyon, France. E-mail: jblichier@ens-lyon.fr. ²Arizona State University, Tempe, AZ, USA.

Introduction: Bouvier et al. [1, 2] interpreted the 4.1 Ga Pb-Pb ages of the enriched and intermediate shergottites (e.g., Zagami, EETA79001) as a crystallization age. This age is remarkably close to the 4.0 Ga Pb-Pb age of ALHA84001 carbonates [3]. The range of ⁸⁷Sr/⁸⁶Sr in shergottites, as best illustrated by their whole-rock isochron [2], further calls for a >4 Ga age [4]. Such old ages are in agreement with surface ages estimated by crater densities [5]. In contrast, the young internal isochron ages at 150–550 Ma obtained on shergottites by phosphate-based chronometers date recent resetting associated with shock and aqueous alteration. We have expanded our earlier Pb-Pb isotope work to include new shergottites, and since contamination has been suggested to be a potential issue [6], we also ran Pb isotopes on the non-controversial 1.3 Ga old nakhlites and Chassigny.

Samples and Procedures: We measured the Pb isotopic compositions of the basaltic NWA 480, lherzolitic RBT 04262, olivine-phyric NWA 1068, and olivine-orthopyroxene shergottite NWA 1195, plus the nakhlites Y-000593 and MIL 03346, as well as Chassigny. Mineral separates were acid-washed using 4M HF and 2.5M HCl, with a preliminary step using 1.5M HBr for whole-rocks to remove carbonates, phosphates, and terrestrial contamination, which is crucial for finds. Sample preparation, Pb separation, and mass spectrometry by MC-ICP-MS were carried out at ENS Lyon as described in [2].

Results: The new Pb isotope data on the shergottites NWA 480, NWA 1068, and RBT 04262 fall on the 4.1 Ga enriched and intermediate shergottite isochron [2], while NWA 1195 falls on the 4.33 ± 0.02 Ga internal Pb-Pb isochron of the depleted basaltic shergottite QUE 94201 [6]. In contrast, the Pb-Pb isotope data for the nakhlites Y-000593 and MIL 03346, and for Chassigny, are concordant with the ~1.3 Ga Pb-Pb internal isochron obtained on Nakhla [2] demonstrating the lack of significant contamination and confirming that these samples can be dated successfully by Pb-Pb chronometry despite their low Pb concentrations.

Discussion: The new data confirm the very tight range of formation ages at 4.1 Ga for enriched and intermediate shergottites and at 4.3 Ga for depleted shergottites. Shergottite magmatic activity therefore predates the late heavy bombardment (LHB). The Martian mantle remained hot enough to sustain strong volcanic activity, but only for the first 500 Ma of the planet's history. The 4.0 Ga old carbonates of ALH 84001 [3] represent hydrothermal activity associated with the last gasps of shergottitic magmatism. Just as for the 3.9 Ga rocks of Isua, such a short history was too short to allow mantle convection to erase the ¹⁴²Nd heterogeneities of the mantle. The rogue 1.3 Ga event associated with nakhlites and chassignites may represent the infilling by late eruptions of the major volcanoes of Tharsis or Syrtis Major of the wide craters left by the LHB. The present interpretation relieves the need for elusive widespread modern volcanic activity and re-establishes Mars as an actively convecting planet.

References: [1] Bouvier A. et al. 2005. *Earth and Planetary Science Letters* 240:221. [2] Bouvier A. et al. 2008. *Earth and Planetary Science Letters* 266:105. [3] Borg L. E. et al. 1999. *Science* 286:90. [4] Jagoutz E. 1991. *Space Science Reviews* 56:13. [5] Werner S. C. 2008. *Icarus* 195:45. [6] Gaffney A. M. et al. 2007. *Geochimica et Cosmochimica Acta* 71:5016.

5130

ISOTOPIC CHARACTERIZATION OF THE ORGANIC MATTER IN THE LITHIC CLASTS IN THE CH/CB-LIKE CHONDRITE ISHEYEVO

L. Bonal, G. R. Huss, A. N. Krot, and K. Nagashima. HIGP/SOEST, University of Hawai'i at Manoa, Honolulu, HI 96822, USA. E-mail: bonal@higp.hawaii.edu.

CB and CH carbonaceous chondrites are metal-rich meteorites with several peculiarities. First, both nebular (melting of dust in the protoplanetary disk) and asteroidal (gas-melt plume produced by planetary-scale collision) models have been proposed for the origin of their chondrules and metal [1, 2]. Second, CB and CH chondrites are characterized by a strong bulk enrichment in ^{15}N (^{15}N up to +1500‰). In the CB chondrites Bencubbin, Hammadah al Hamra 237, and QUE 94411, the similar ^{15}N -enrichment is observed in chondrules and metal grains, possibly indicating redistribution of N isotopes during shock metamorphism on the CB-parent asteroid [3]. The original carrier of ^{15}N has then not yet been identified in CB chondrites. Sugiura and Zashu [4] suggested that ^{15}N -rich carbon-silicate aggregates of interstellar origin discovered in the CH chondrite PCA 91467 could be the ultimate source of heavy N. The precursor N carrier is then likely to be organic.

The Isheyev meteorite is composed of several lithologies having mineralogical, chemical and isotopic similarities with CB and CH chondrites. Nitrogen isotopic composition of the whole-rock sample is highly enriched in ^{15}N ($\delta^{15}\text{N}$ up to 1500‰) [5]. Like in most CH and CB chondrites, there is no fine-grained matrix material interstitial to chondrules and metal grains; it occurs only as hydrated lithic clasts. Based on the petrographic, chemical, structural, and isotopic studies, Bonal et al. [6] concluded that the lithic clasts in Isheyev are not related to CI or CM chondrites. They have diverse origins and may have sampled parent bod(ies) not present in our collections.

In this context, we have initiated isotopic imaging of lithic clasts in Isheyev. The goals of our study are 1) to characterize the organic matter, which may have suffered from secondary processes under different physico-chemical conditions than those experienced by CI and CM chondrites, and 2) to test the hypothesis that the ^{15}N -rich carrier is organic matter.

The UH Cameca IMS 1280 ion microprobe is used to collect isotope-ratio images of areas of $50 \times 50 \mu\text{m}^2$ of lithic clasts from Isheyev. Initial work is being done with scanning ion imaging; direct ion imaging with SCAPS will be used when it is available. A Cs^+ primary beam focused to $\sim 1 \mu\text{m}$ is used to generate secondary negative ions of H, D, ^{12}C , ^{13}C , $^{12}\text{C}^{14}\text{N}$, $^{12}\text{C}^{15}\text{N}$, ^{18}O , and ^{28}Si . All ions, except H and D, are measured at mass resolving power (MRP) of ~ 5000 , sufficient to separate isobaric interferences, with the monocollector electron multiplier (EM). H and D are measured on a multicollector EM with the widest exit slit (MRP ~ 2000). Our preliminary results suggest that the Isheyev lithic clasts contain isotopically anomalous organic compounds.

References: [1] Weisberg M. K. et al. 1990. *Meteoritics* 25:269-279. [2] Krot A. N. et al. 2005. *Nature* 436:989. [3] Sugiura N. et al. 2000. *Meteoritics & Planetary Science* 35:987-996. [4] Sugiura N. and Zashu S. 2001. *Meteoritics & Planetary Science* 36:515-524. [5] Ivanova M. A. et al. 2006. Abstract #1100. 37th Lunar and Planetary Science Conference. [6] Bonal L. et al. 2008. Abstract #1506. 39th LPSC.

5094

IRON-ENRICHED STARDUST GRAINS IN THE METEORITES ACFER 094, QUE 99177, AND MET 00426

M. Bose, C. Floss, and F. J. Stadermann. Laboratory for Space Sciences and Physics Department, Washington University, St. Louis, MO 63130, USA. E-mail: mbose@physics.wustl.edu.

Introduction: In this study elemental compositions of the presolar grains identified in Acfer 094 are measured in the Auger Nanoprobe. Classification of the presolar silicates into olivine and pyroxene is done on the basis of the $\text{Fe} + \text{Mg}(\text{+Ca})/\text{Si}$ ratio. Fe-Mg silicates (e.g., olivine and pyroxene) are expected to have Mg-rich compositions under conditions of equilibrium condensation in the winds of evolved stars [1]. We also compare the presolar silicate grain compositions found in Acfer 094 to those in the CR chondrites QUE 99177 and MET 00426 [2].

Experimental: NanoSIMS measurements are carried out in raster ion imaging mode by scanning $<1 \text{ pA Cs}^+$ primary beam over areas of $10 \times 10 \mu\text{m}^2$ (256^2 pixels) and simultaneously collecting secondary ions of $^{12,13}\text{C}^-$ and $^{16,17,18}\text{O}^-$, as well as secondary electrons. The O-anomalous grains identified in the NanoSIMS are located with the Auger Nanoprobe and spectra are obtained at 10 kV 0.25 nA. High-resolution distribution maps of chosen elements are also obtained for most grains.

Results: We report the identification of 42 additional O-anomalous grains in $\sim 0.1\text{--}0.5 \mu\text{m}$ grain size separates from Acfer 094. Auger measurements of 36 presolar grains identify 30 silicates and 6 oxides. Among the presolar silicates measured, 4 grains have olivine-like compositions and 9 grains have pyroxene-like compositions. We found 4 grains with ferrosilite-like compositions, 1 grain with an enstatite-like composition as well as 1 forsterite-like grain. The remaining silicate grains have non-stoichiometric compositions. Among the presolar oxides, 2 grains contain only Fe and 1 grain contains only Ti in addition to O. Measurements on Ti and Fe oxide standards are needed to determine their stoichiometry.

Discussion: All 3 meteorites contain more Fe-rich pyroxenes than Mg-rich ones. Except for 1 Fe-rich olivine-like grain, the remaining olivines in the CR chondrites are Mg-rich. However, most of the silicates with non-stoichiometric compositions are Fe-rich (17 out of 28). In Acfer 094, all the grains with olivine-like compositions are Fe-rich (mg# 11-31), except for the single forsterite grain. In addition, 11 out of 15 non-stoichiometric grains are Fe-rich, including 9 silicates with only Fe (i.e., no Mg). The number of oxides containing only Fe is also high in Acfer 094. The presolar silicate compositions are in contrast to spectroscopic evidence of dust around evolved stars that have optical properties similar to crystalline Mg-rich phases such as forsterite and enstatite [3]. However, the spectra of circumstellar environments also indicate the presence of Fe-rich amorphous silicates [3]. The substantial enhancement of Fe contents in the silicate grains of the meteorites could be due to condensation of the silicate grains under non-equilibrium conditions [4] or secondary processing in the solar nebula or on the parent body [e.g., 5]. Alternately, a large fraction of the presolar silicate grains could be amorphous in nature.

References: [1] Demyk K. et al. 2000. *Astronomy & Astrophysics* 364: 170-178. [2] Floss C. and Stadermann F. J. 2008. Abstract #1280. 39th Lunar and Planetary Science Conference. [3] Molster F. J. and Waters L. B. F. M. 2003. In *Astromineralogy*. p. 121. [4] Gail H.-P. 2003. In *Astromineralogy*. p. 55. [5] Nguyen A. and Zinner E. 2004. *Science* 303:1496-1499.

5299

²⁶Al-²⁶Mg AND ²⁰⁷Pb-²⁰⁶Pb SYSTEMATICS IN AN ALLENDE INCLUSION

A. Bouvier, M. Wadhwa, and P. Janney. Arizona State University, SESE, Tempe, AZ, USA. E-mail: audrey.bouvier@asu.edu.

Introduction: The determination of high-resolution time scales of early solar system processes relies on precise, accurate, and consistent dating with long- (i.e., ²⁰⁷Pb-²⁰⁶Pb) and short-lived (e.g., ²⁶Al-²⁶Mg, ⁵³Mn-⁵³Cr) chronometers. In recent years, the precision of mass spectrometric analyses has improved dramatically, but inconsistencies remain between the different high-resolution chronometers [1]. Sources of these discrepancies may be analytical (e.g., sample preparation, mass spectrometric measurements) or due to sample characteristics (e.g., heterogeneities, closure temperatures of different isotope systems). In this study we have analyzed the Mg and Pb isotope compositions of a single inclusion from Allende to check for potential Pb isotopic fractionation during extensive acid-leaching procedures, and also to evaluate the concordance of the Al-Mg and Pb-Pb chronometers.

Analytical Methods: We made Pb and Mg isotope analyses by MC-ICPMS of acid-leached residues and their corresponding leachates, as well as of unleached fractions from a single ~1.5 g Allende inclusion which was initially characterized as a chondrule [2], but is in fact likely to be a molten CAI. For Pb and Mg analyses, the sample was split into 3 interior (~100–400 mg) and 1 rim fraction (~300 mg) and each was crushed and acid-washed using increasingly aggressive (3 to 7) leaching steps. The remaining residues (R₁₋₄ ~ 80 mg each) were then fully dissolved. For Al-Mg work, 5 interior fractions and 1 rim fraction were hand-picked or magnetically separated and were not subjected to any leaching procedures. The isotope measurements were corrected for instrumental mass bias using Tl-doping (for Pb) and sample-standard bracketing (for Pb and Mg).

Results and Discussion: Blank corrected ²⁰⁶Pb/²⁰⁴Pb ratios range from 27 to 3457 for the leachates, and from 807 to 1534 for the residues. Analyses of the NBS 981 standard (2 ppb) resulted in a typical precision of ±0.05% and ±0.3‰ (2σ SE) on the ²⁰⁷Pb/²⁰⁶Pb and ²⁰⁶Pb/²⁰⁴Pb ratios, respectively. Pb-Pb model ages for each of the residues R₁₋₃ and the most radiogenic leachate are all concordant; taken together, these yield an internal isochron age of 4567.59 ± 0.10 Ma (MSWD = 0.18) for this inclusion. This age is ~0.5 Myr older than the Pb-Pb age for the Efremovka E60 CAI [3], but ~0.9 Myr younger than the best estimate of the CV3 CAI age [4]. Mg isotope ratios in the 6 unleached fractions range from +3.72 to +4.59‰ (2 SE ~ ±0.05‰) for ^δ²⁵Mg (relative to the DSM3 standard) and radiogenic ^Δ²⁶Mg* excesses range from +0.73 to +1.01‰ (2σ SE ~ ±0.02‰). These 6 unleached fractions, with ²⁷Al/²⁴Mg ratios ranging from 2.2 to 3.1, yield an initial ²⁶Al/²⁷Al = (4.5 ± 1.1) × 10⁻⁵ (indistinguishable from the value of (4.1 ± 1.6) × 10⁻⁵ based on the 5 interior fractions). This corresponds to a Al-Mg age of 4567.1 ± 0.4 Ma relative to the E60 CAI [3], which is marginally concordant with the Pb-Pb age for this inclusion. If the D'Orbigny angrite is used as an anchor [5, 6], it translates to an Al-Mg age of 4569.2 ± 0.3 Ma for this inclusion, which is discordant with its Pb-Pb age but agrees with the CV3 CAI age of [4].

References: [1] Wadhwa M. et al. 2007. Workshop on Chronology of Meteorites and Early Solar System. Abstract #4053. [2] Bouvier A. et al. 2008. *Geochimica et Cosmochimica Acta* 72. Abstract #1981. [3] Amelin Y. et al. 2002. *Science* 297:1678. [4] Bouvier A. et al. 2007. *Geochimica et Cosmochimica Acta* 71:1583. [5] Spivak-Birndorf L. et al. 2008. *Geochimica et Cosmochimica Acta*. Submitted. [6] Amelin Y. 2008. *Geochimica et Cosmochimica Acta* 72:221.

5303

ABUNDANCES AND SIZES OF CLAST TYPES IN THE ALLENDE CV3 METEORITE: NEW RESULTS FROM MAPPING ANALYSISC. E. Brunner¹, D. S. Ebel², and M. K. Weisberg³. ¹Department of Geography and Geology, Western Kentucky University, Bowling Green, KY 42101, USA. E-mail: Chelsea.brunner@wku.edu. ²Department of Earth and Planetary Sciences, American Museum of Natural History, New York, NY 10024, USA. E-mail: debel@amnh.org. ³Department Physical Sciences, Kingsborough College, City University of New York, Brooklyn, NY 11235, USA. E-mail: mweisberg@kbcc.cuny.edu.

Introduction: The chondritic meteorites resulted from the cooling and accretion of solids in the protoplanetary disk. Large clasts include: Ca-, Al-rich inclusions (CAIs [1]), chondrules, amoeboid olivine aggregates (AOAs [2]), and dark lithic fragments (dark inclusions, DIs)[3]. Their relative abundances are primary data that pertain to the theories of their origin and relevance to planet formation [1], but have not been measured in Allende (CV3) and other CV chondrites since the point-counts reported by McSween in 1977 [4].

Procedure: Allende surfaces were mapped in X-ray emission at resolutions between 13 (slabs) and 2 (small areas) microns per pixel using electron microprobe (EMP) techniques of [5]. Element, BSE, and red-green-blue mosaics as registered layers in a drawing program were used to outline clasts by hand and determine their types [5]. Pixels were counted in output images, providing relative surface area abundances of CAIs, AOAs, chondrules (and their subtypes), and matrix, and their size distributions.

Results: We have now measured ~30 cm² of slabs at 13 μm/pxl, and small clast abundance in 12 mm² of matrix-rich areas at 2 μm/pxl, allowing correction of matrix abundance in slabs for the presence of unresolved clasts (i.e., isolated 5–10 μm olivines). We find olivine and small chondrules (<100 μm maximum dimension) to be less than 7% of what we classify as matrix at coarser scale. Matrix is 57%, chondrules 32%, CAIs 8%, opaques <1% of Allende by areal analysis. Correcting area for volume fractions assuming packed spherical clasts would increase matrix proportion by up to 10% (i.e., to 62% of the volume).

Conclusions: New methods allow counting and analyzing inclusions efficiently over large areas [e.g., 6], compared to optical point counting. In optical microscopy clasts are defined by the sharp contrast of opaque matrix framing a translucent clast. In EMP mapping boundaries are set by the differences in elemental compositions of accretionary rims around objects, which are not always consistent with those boundaries seen optically. Our findings are similar to those of McSween [4] for relative CAI/AOA/chondrule abundances, but we find more matrix than his 38%. The differences may be due to different criteria used in these procedures when assigning inclusions to individual categories.

References: [1] MacPherson G. J. et al. 2005. In *Chondrites and the protoplanetary disk*, edited by Krot A. N. et al. pp. 225–250. [2] Grossman L. and Steele I. M. 1976. *Geochimica et Cosmochimica Acta* 40:149–155. [3] Weisberg M. K. and Prinz M. 1998. *Meteoritics & Planetary Science* 33: 1087–1099. [4] McSween H. Y. Jr. 1977. *Geochimica et Cosmochimica Acta* 41:1777–1790. [5] Ebel D. S., Brunner C. E., and Weisberg M. K. 2008. 39th Lunar and Planetary Science Conference. Abstract #2121. [6] Mayne et al. 2005. 36th Lunar and Planetary Science Conference. Abstract #1791.

5315

CREATING A NEW, COMPREHENSIVE CAI REFERENCE SUITE, PART ONE: VIGARANO

E. S. Bullock and G. J. MacPherson. Department of Mineral Sciences, National Museum of Natural History, Smithsonian Institution, Washington, D.C. 20560, USA. Email: BullockE@si.edu.

Over thirty years ago, some of the first detailed studies of Allende CAIs were performed [e.g., 1, 2], when large (>1 cm sized), whole CAIs were extracted from Allende, and split for thin-sectioning and characterization, and trace element measurements. This material has proved to be invaluable, and has provided the basis for numerous subsequent isotopic studies [e.g., 3, 4] that constrain the formation and evolution of the Allende inclusions. This work often required a large amount of material, and in many cases the majority of the CAI has now been consumed and is no longer available.

Advancements in analytical techniques mean that much smaller sample volumes are required, and allow for the possibility of multiple measurements to be performed on a single CAI. This means that, for example, coordinated studies into the relationships between different isotopic systems within a single CAI can be explored. For the purpose of these investigations, a suite of large CAIs has been extracted from Vigarano, and the combined mineralogical, petrological, and isotopic characteristics can be determined. Vigarano is an ideal candidate as it has undergone less secondary mineralization than Allende, and still contains the large CAIs that are required for carrying out multiple measurements.

Once extracted from the host meteorite, the first step has been to isolate a portion of each CAI to be thin-sectioned. Full element mapping of each thin section was performed using a scanning electron microscope, so that the CAI can be characterized and preliminary bulk composition data can be obtained. So far, two fluffy Type As, two Type Bs, and an unusual compound Type B CAI have been identified.

In the future, these CAIs will become available for other investigations, including trace element studies, oxygen and magnesium isotopic systems (using high-precision SIMS and ICP-MS), absolute ages determination and measurements of intrinsic nuclear isotope anomalies. It is hoped that by having correlated studies of the different characteristics within each individual inclusion, we can better constrain the conditions under which these inclusions formed and evolved.

References: [1] Mason B. and Martin P. M. 1977. *Smithsonian Contributions to Earth Science* 19:84–95. [2] Mason B. and Taylor S. R. 1982. *Smithsonian Contributions to the Earth Sciences* 25. [3] Ireland T. R. et al. 1990. *Earth and Planetary Science Letters* 101:379–387. [4] Chaussidon M. et al. 2004. *Geochimica et Cosmochimica Acta* 70:224–245.

5309

ZINCIAN BREZINAITE AND OTHER RARE MINERALS IN TWO CUMULATE-TEXTURED AUBRITES FROM NORTHWEST AFRICA

T. E. Bunch¹, A. J. Irving², J. H. Wittke¹, and S. M. Kuehner². ¹Department of Geology, Northern Arizona University, Flagstaff, AZ, USA. E-mail: tbear1@cableone.net. ²Department of Earth and Space Sciences, University of Washington, Seattle, WA, USA.

Introduction: The fact that eight of the 20 or so known aubrites are witnessed falls probably reflects the inherent instability of these highly reduced achondrites in terrestrial weathering environments. The first bona fide aubrites to be found in Northwest Africa, NWA 4799 and NWA 5217, are relatively unweathered and contain distinctive accessory mineral phases. [We emphasize that the very large Al Haggounia paleo-meteorite from southern Morocco is NOT an aubrite, but instead an anomalous EL3 chondrite, as discussed in detail on the following website: http://www4.nau.edu/meteorite/Meteorite/Al_Haggounia.html. New analyses of kamacite in some of this material show that it contains 0.65–1.10 wt% Si, which is typical [1] for EL3 chondrites.]

Northwest Africa 4799: Numerous small pebble-like stones with minor rusty staining represent a breccia consisting of larger angular to rounded clasts (some showing igneous cumulate texture) in a matrix of smaller grains. The dominant mineral is enstatite (En_{99.5}Fs_{0.1}Wo_{0.4}) with lesser amounts of interstitial albite (some in graphic intergrowths with a silica polymorph), kamacite (Fe 92.1, Ni 4.5, Si 3.4 wt%), Ti-Cr-bearing troilite, oldhamite, niningerite, Ti-bearing daubreelite, schreibersite, and rare perryite (P-bearing Ni-Fe silicide), some of which exsolved along (111) planes of kamacite. Enstatite grains exhibit polysynthetic twinning indicating inversion from former clinoenstatite.

Northwest Africa 5217: This fine to medium-grained (<1.2 mm) unbrecciated, cumulate-textured stone with preferred orientation of euhedral to subhedral enstatite is fresher than NWA 4799, and composed predominantly of enstatite (En_{99.4}Fs_{0.2}Wo_{0.4}) with interstitial kamacite (Ni 5.8–6.6, Si 3.9–4.5 wt%), troilite (Cr 2.68, Ti 3.38 wt%), daubreelite, zincian brezinaite (S 46.0, Cr 54.1, Zn 2.1 wt%), oldhamite (S 38.7, Ca 59.2, Cr 1.4, Mn 1.2 wt%), alabandite, niningerite, caswellsilverite (S 45.3, Cr 38.4, Na 14.7, Fe 0.7 wt%), graphite, sodic plagioclase (An₁₇Or_{3.7}) and a silica polymorph. Schöllhornite (Na_{0.3}CrS₂H₂O; S 46.0, Cr 37.3, Fe 1.1 wt%) is present as a weathering product of caswellsilverite.

Discussion: The high temperature igneous cumulate characteristics of NWA 4799 and 5217 are unique among aubrites. Moreover, the complex mineralogy of NWA 5217 is remarkable and distinctive. Because these aubrites appear to be igneous cumulates and not derived from shock melts, they likely formed in a fairly large parent body rather than a small asteroid (such as main belt E asteroids and the NEO E asteroid 3103 Eger [2]).

References: [1] Keil K. 1968. *Journal of Geophysical Research* 73: 6945–6976; Zhang Y. et al. 1995. *Journal of Geophysical Research* 100: 9417–9438. [2] Clark B. et al. 2004. *Journal of Geophysical Research* 109: E02001, 11 p.

5251

PRIMITIVE INTERPLANETARY DUST FROM COMET 26P/GRIGG-SKJELLERUP (?)—DIVERSITY AND SIMILARITIES AMONG JUPITER-FAMILY COMETS

H. Busemann^{1,2}, A. N. Nguyen², L. R. Nittler², R. M. Stroud³, T. J. Zega³, A. L. D. Kilcoyne⁴, P. Hoppe⁵, and G. D. Cody². ¹PSSRI, Open University, Milton Keynes, UK. E-mail: h.busemann@open.ac.uk. ²Carnegie Institution, Washington, D.C., USA. ³Code 6366, Naval Research Laboratory, Washington, D.C., USA. ⁴ALS, Lawrence Berkeley National Laboratory, Berkeley, CA, USA. ⁵MPI für Chemie, Mainz, Germany.

Introduction: Comets are well-preserved agglomerates of the earliest solar system building blocks. Analyzing cometary dust helps in understanding the processes that led from interstellar dust accretion to the solar system. Methods used to study comets include: spectroscopy from Earth or spacecraft, e.g., Deep Impact on comet Temple 1; Stardust sample return from comet Wild 2; and analysis of interplanetary dust particles (IDP), some of which originate from comets [1–3]. IDP collection in the dust stream of comet Grigg-Skjellerup (GS-IDP) offered the opportunity to possibly sample IDPs from a known comet [4].

Origin from Grigg-Skjellerup: Our anhydrous, fine-grained porous GS-IDPs show extremely primitive characteristics: presolar grain abundances at the percent level; Raman spectra indicating very disordered organic matter (OM); and huge D and ¹⁵N enrichments suggesting interstellar OM [5, 6]. GS-IDPs also contain exotic noble gases and a new mineral phase [7, 8]. These unique features suggest that some GS-IDPs may indeed originate from Jupiter-family comet (JFC) Grigg-Skjellerup.

Results: Focused ion beam sections covering extremely D- and ¹⁵N-rich OM and presolar silicates were prepared [9] for X-ray absorption spectroscopy and transmission electron microscopy. We found, spatially associated at a sub-micron scale, GEMS (glass with embedded metal and sulfides) with low-Ni sulfides, nano-crystalline carbonates, Ca-rich pyroxene, tentatively an amphibole, amorphous and aliphatic-rich OM, and a presolar olivine spatially associated with a C nanoglobule.

Discussion: All JFCs reveal remarkable mixtures of low-T minerals and organics, as well as processed matter including refractory high-T phases and material that may indicate aqueous alteration [1, 10]. JFCs consist of well-mixed material that was probably formed and altered in various environments in the protoplanetary disk [11]. The close association of interstellar and processed matter may support a hierarchical origin of the IDPs' subgrains in multi-generations of protoplanets [12]. However, while Wild 2 dust generally resembles asteroidal material [13], GS-IDPs contain ultra-primitive assemblages. This may be due to sampling bias, or could indicate that JFCs acquired a heterogeneous mix of dust from various sources within the nebula.

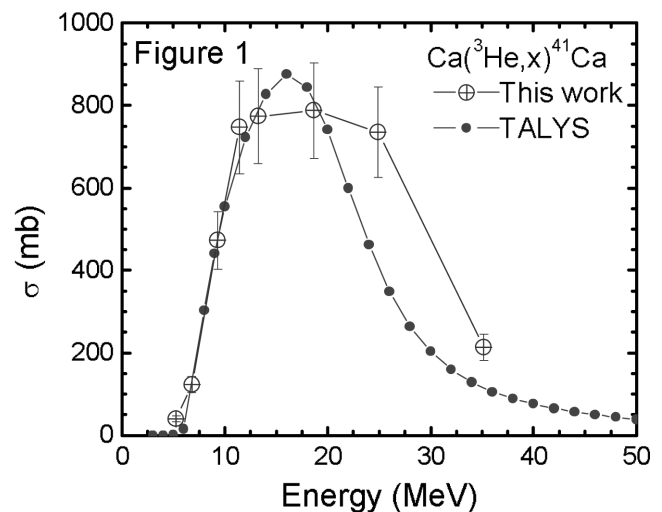
References: [1] Lisse C. M. et al. 2006. *Science* 313:635. [2] Brownlee D. et al. 2006. *Science* 314:1711. [3] Bradley J. P. 2003. *Treatise on Geochemistry*, vol. 1. p. 689. [4] Messenger S. 2002. *Meteoritics & Planetary Science* 37:1491. [5] Nguyen A. N. et al. 2007. Abstract #2332. 38th LPSC. [6] Nittler L. R. et al. 2006. Abstract #2301. 37th LPSC. [7] Palma R. L. et al. 2005. *Meteoritics & Planetary Science* 40:A120. [8] Nakamura-Messenger K. et al. 2008. Abstract #2103. 39th LPSC. [9] Zega T. J. et al. 2007. *Meteoritics & Planetary Science* 42:1373. [10] Rotundi A. et al. 2008. *Meteoritics & Planetary Science* 43. In press. [11] Zolensky M. E. et al. 2006. *Science* 314:1735. [12] Rietmeijer F. J. M. 2002. *Chemie der Erde* 62:1. [13] Ishii H. et al. 2008. *Science* 319:447.

5110

⁴¹Ca PRODUCTION IN THE SOLAR SYSTEM

M. W. Caffee¹, T. Faestermann², R. Hertenberger³, G. F. Herzog⁴, G. Korschinek², I. Leya⁵, R. C. Reedy⁶, and J. M. Sistierson⁷. ¹Department of Physics, Purdue University, W. Lafayette, IN 47907, USA. ²Fak. Physik, TU-München, D85748 Garching, Germany. ³Fak. Physik, LMU-München, D85748 Garching, Germany. ⁴Department of Chem. and Chem. Biol., Rutgers University, Piscataway, NJ 08854, USA. E-mail: herzog@rutchem.rutgers.edu. ⁵Physikal. Inst., U. Bern, CH 3012 Bern, Switzerland. ⁶Earth Planet. Sci., University of New Mexico, Albuquerque, NM 87131, USA. ⁷Francis H. Burr Proton Therapy Center, Massachusetts General Hospital, Boston, MA 02114, USA.

The X-wind hypothesis proposes that ¹H⁺ and ³He²⁺ from the early Sun produced now-extinct ²⁶Al and ⁴¹Ca. Initial model calculations with ¹H⁺ did not reproduce the isotopic footprints found in meteorites left by the decay of ²⁶Al and ⁴¹Ca. Adding ³He to the mix of nuclear-active particles improved the match for ²⁶Mg (from ²⁶Al) but overproduced ⁴¹K (from ⁴¹Ca). Uncertainties in ³He²⁺ fluxes aside, X-wind models have suffered from a lack of ³He cross section (σ) measurements. Recent measurements of cross sections for ²⁶Al [1, 2] and ³⁶Cl [2] production from Mg, Al, and Ca have reduced these uncertainties. Here we report cross sections for the reaction ^{nat}Ca(³He,x)⁴¹Ca measured using accelerator mass spectrometry and compare them with values calculated using the code TALYS (Fig. 1). These cross sections not only provide a basis for evaluating the X-wind hypothesis but also serve to validate the TALYS cross sections. With the newly measured cross sections, updated X-wind calculations of [3] give ²⁶Al/⁴¹Ca production rate ratios of 165, a factor of about 30 larger than inferred from meteoritic observations. Without a long delay between production of ²⁶Al and ⁴¹Ca and their incorporation in meteoritic material, a simple X-wind irradiation of chondritic matter does not reproduce experimental observations.



References: [1] Fitoussi et al. 2004. 35th LPSC. Abstract #1586. [2] Caffee et al. 2008. 39th LPSC. Abstract #1258. [3] Leya et al. 2003. *The Astrophysical Journal* 594:605–616.

5092

A STUDY OF Cu AND Cr DURING IRON METEORITE CRYSTALLIZATION

N. L. Chabot¹, S. A. Saslow², W. F. McDonough², and J. H. Jones³. ¹Applied Physics Laboratory, Laurel, MD, USA. E-mail: Nancy.Chabot@JHUAPL.edu. ²University of Maryland, College Park, MD, USA. ³NASA Johnson Space Center, Houston, TX, USA.

Introduction: In contrast to many other trace elements, the Cu and Cr trends observed in most magmatic iron meteorite groups have not been explained by fractional crystallization. Here, we present the results of an experimental study that determined the solid metal/liquid metal partitioning behavior for these two elements. These experimental partitioning results were then used to model elemental trends produced during fractional crystallization and compared to the Cu and Cr iron meteorite trends.

Experiments and Results: Experiments were conducted at 1 atm in evacuated silica tubes in the Fe-Ni-S system, using techniques similar to previous work [1]. Run temperatures varied from 1050 °C to 1450 °C, to produce experiments that had solid metal coexisting with liquid metal over a range of liquid metal S concentrations (3 to 30 wt%). Major and minor elements were analyzed by electron microprobe at the Carnegie Institution of Washington. Trace elements were measured using laser ablation ICP-MS microanalysis at the University of Maryland.

Both Cu and Cr exhibit similar chalcophile (S-loving) solid metal/liquid metal partition coefficients (D), whose values decrease as the S content of the metallic liquid increases. The partitioning values of Cu and Cr are similar over the entire range of S contents examined, but the Cu and Cr trends observed within an iron meteorite group [2, 3, 4] are quite different. Thus, fractional crystallization alone cannot have created both the Cu and Cr trends in these magmatic irons; another process must be responsible for the trend of at least one of these elements.

Crystallization Modeling: The D(Cu) experimental data were parameterized using a linear fit and a fit based on the free FeS domains in the metallic liquid. A simple fractional crystallization model [5] was run using different initial bulk S contents and these two parameterizations for D(Cu). The linear fit for D(Cu) produced decreasing Cu crystallization trends consistent with those observed in magmatic iron meteorite groups. Different initial S contents produced different Cu crystallization trends.

However, modeling that used the D(Cu) fit based on FeS domains did not produce any results that matched the iron meteorite trends, demonstrating that the modeling is sensitive to the choice of the mathematical expression for D(Cu). Despite the sensitivity, our work shows that the Cu trends observed in some magmatic iron meteorite groups could be formed by fractional crystallization. Our modeling work did not produce any crystallization results consistent with the steeper Cr iron meteorite trends.

References: [1] Chabot N. L. et al. 2007. *Meteoritics & Planetary Science* 42:1735–1750. [2] Wasson J. T. 1999. *Geochimica et Cosmochimica Acta* 63:2875–2889. [3] Wasson J. T. and Richardson J. W. 2001. *Geochimica et Cosmochimica Acta* 65:951–970. [4] Wasson J. T. et al. 2007. *Geochimica et Cosmochimica Acta* 71:760–781. [5] Chabot N. L. 2004. *Geochimica et Cosmochimica Acta* 68:3607–3618. [6] Supported by NASA grant NNG06G113G.

5178

EXTINCT ⁶⁰Fe IN THE EUCRITE NWA 4523

M. Chaussidon¹ and J. A. Barrat². ¹CRPG-Nancy Université-INSU/CNRS, UPR 2300, BP 20, 54501 Vandoeuvre-lès-Nancy, France. E-mail: chocho@crpg.cnrs-nancy.fr. ²CNRS UMR 6538, U.B.O-I.U.E.M., 29280 Plouzané, France. E-mail: barrat@univ-brest.fr.

Introduction: ⁶⁰Fe ($T_{1/2} = 1.49$ Ma) is a key to constrain the origin of short-lived radioactive nuclides in the early solar system (ESS) since it is the only one (among ⁷Be, ¹⁰Be, ²⁶Al, ³⁶Cl, ⁴¹Ca, and ⁵³Mn) which, because of its neutron-rich nuclei, cannot be anything else than a stellar product injected from a nearby dying star [1]. Several recent studies have confirmed the presence of ⁶⁰Fe in the ESS with a ⁶⁰Fe/⁵⁶Fe ratio of $\approx 5(\pm 5) \times 10^{-7}$ [2, 3]. However, because of Ni nucleosynthetic anomalies, the ⁶⁰Fe/⁵⁶Fe at the time of formation of Ca-Al-rich inclusions (CAIs) is difficult to constrain (and could be as high as $\approx 5 \times 10^{-6}$) [4]. In addition, the initial distribution of ⁶⁰Fe in the ESS is a matter of debate [5]. These are critical issues, especially when considering the recent determination of the high level of galactic background for ⁶⁰Fe: ⁶⁰Fe/⁵⁶Fe = 1.4×10^{-7} [6].

In order to make progress with our understanding of the distribution of ⁶⁰Fe in the ESS, we have searched for ⁶⁰Ni radiogenic excesses in the eucrite breccia NWA 4523 recently found in the Sahara. NWA 4523 contains two types of clasts embedded in a fine grained recrystallized matrix: medium grained ophitic/subophitic clasts and fine-grained clasts [7]. The medium-grained clasts (grain size between 1–2 mm) display a subophitic texture and are composed of plagioclases, pyroxenes (pigeonitic core and augitic rim), silica, ilmenite, chromite crystals, and a recrystallized mesostasis containing among others magmatic troilite crystals of 10–50 μ m.

Results and Implications: The Ni isotopic compositions and the Fe/Ni ratios were measured with the CRPG-CNRS ims 1270 ion microprobe in ≈ 15 different troilite grains. The radiogenic ⁶⁰Ni excesses were calculated from the measurement of three Ni isotopes (⁶⁰Ni, ⁶¹Ni, ⁶²Ni) at a mass resolution of ≈ 7000 . The troilite crystals have low Ni contents with ⁵⁶Fe/⁶¹Ni of $2(\pm 1) \times 10^6$ and show ⁶⁰Ni excesses positively correlated with the Fe/Ni ratio indicating a ⁶⁰Fe/⁵⁶Fe of $\approx 7 \times 10^{-7}$ at the time of isotopic closure for troilite in NWA 4523. Because sulfides are the major repository of Ni in NWA 4523, it is difficult to envisage how secondary processes could have altered the Fe/Ni ratios in a way to produce apparent high ⁶⁰Fe/⁵⁶Fe ratios. Work is in progress to look for the presence of ⁶⁰Ni excesses in the pyroxenes associated with the sulfides but peak tailing of the interferences at masses 61 and 62 make the measurement of the ⁶⁰Ni excesses difficult.

The high initial ⁶⁰Fe/⁵⁶Fe ratio found in NWA 4523 is higher than that found in ferromagnesian chondrules from ordinary chondrites [2] but similar to that reported for troilite from Semarkona [3]. It would be consistent with the upper limit of $1.6 \pm 0.5 \times 10^{-6}$ initially proposed from CAIs for the ⁶⁰Fe/⁵⁶Fe in the ESS [8].

References: [1] Lee T. et al. 1998. *The Astrophysical Journal* 506:898–912. [2] Tachibana S. and Huss G. R. 2003. *The Astrophysical Journal* 588: L41–L44. [3] Mostéfaoui S. et al. 2005. *The Astrophysical Journal* 625:271–277. [4] Quitté G. et al. 2007. *The Astrophysical Journal* 655:678–684. [5] Dauphas N. et al. 2008. Abstract #1170. 39th Lunar and Planetary Science Conference. [6] Wang W. et al. 2007. *Astronomy & Astrophysics* 469:1005–1012. [7] Barrat J. A. et al. 2007. *Geochimica et Cosmochimica Acta* 71: 4108–4124. [8] Birck J.-L. and Lugmair G. 1988. *Earth and Planetary Science Letters* 90:131–143.

5058

FIRST EVIDENCE OF HIGH-PRESSURE SILICA: STISHOVITE AND SEIFERTITE IN LUNAR METEORITE NORTHWEST AFRICA 4734

H. Chennaoui Aoudjehane^{1, 2} and A. Jambon². ¹Université Hassan II Ain Chock, Laboratoire Géosciences, BP 5366 Maârif Casablanca, Morocco. E-mail: h.chennaoui@fsac.ac.ma. ²Université Pierre et Marie Curie-Paris 6 and IGP Laboratoire MAGIE, Case 110, 4 place Jussieu, 75252 Paris, France.

Introduction: Silica is a rare phase in lunar rocks; it has been described as either quartz, cristobalite and/or tridymite [1]. Northwest Africa 4734, is an uncommon type of lunar rock, which may be launched paired with the LaPaz Icefield lunar mare basalts found in 2002–03 in Antarctica [2–6], it is a coarse grained rock of basaltic composition, exhibits a number of significant shock features, such as PDFs, extensive fracturation of pyroxene, impact melt pockets and transformation of plagioclase to maskelynite; silica is present as a minor phase.

Analytical Procedures: We studied the speciation of silica polymorphs to characterize the shock, using SEM imaging, Raman spectroscopy, CL imaging, and spectroscopy. Further details can be found in [7].

Results: According to the CL spectra [7–9], cristobalite, tridymite, high-pressure silica glass, stishovite, and seifertite, are all present. Special emphasis is made on stishovite and seifertite, which, like in shergottites, exhibit specific textural features [7]. Cathodoluminescence spectra characteristic of high-pressure silica phases: glass, stishovite, and seifertite have been recorded in addition to the original low-pressure phases. The remanence of cristobalite and tridymite underscores a significant heterogeneity of the shock supported by the rock. This is the first report of high-pressure silica phases, stishovite, and seifertite in a lunar meteorite. When compared to shergottites, plagioclase appears to be significantly less transformed to maskelynite. This probably results from the low sodium content of plagioclase, which inhibits the transformation, and not from the shock intensity.

The presence of high and low pressure silica phases, transformed from either cristobalite or tridymite, as well as plagioclase and maskelynite, indicate strong heterogeneity of shock with a peak shock intensity of about 45 GPa [10, 11, 12].

References: [1] Korotev R. L. 2005. *Chemie der Erde* (Geochemistry) 65:297–346. [2] Day et al. 2006 *Geochimica et Cosmochimica Acta* 70: 1581–1600. [3] Zeigler et al. 2005. *Meteoritics & Planetary Science* 40: 1073–1101. [4] Joy et al. 2006. *Meteoritics & Planetary Science* 41:103–1025. [5] Anand et al. 2006. *Geochimica et Cosmochimica Acta* 70:246–264. [6] Jambon et al. 2008. Submitted. [7] Chennaoui Aoudjehane H. et al. 2005. *Meteoritics & Planetary Science* 40:967–979. [8] Chennaoui Aoudjehane H. et al. 2006. Abstract #1036. 37th Lunar and Planetary Science Conference. [9] Chennaoui Aoudjehane H. et al. 2006. Abstract #1037. 37th LPSC. [10] El Goresy A. et al. 2004. *Journal of Physics and Chemistry of Solids* 65: 1597–1608. [11] Luo et al. 2003. *Journal of Geophysical Research* 108 (B9): 2421–2433. [12] Stoëffler D. et al. 1986. *Geochimica et Cosmochimica Acta* 50:889–913.

5272

OXYGEN-ISOTOPIC COMPOSITION OF MAGNETITE IN THE DOM 03238 CO3.1 CHONDRITE

B.-G. Choi¹, S. Itoh², H. Yurimoto², A. E. Rubin³, J. T. Wasson³, and J. N. Grossman⁴. ¹Department of Earth Sci. Edu. SNU, Seoul 151-748, Korea. E-mail: bchoi@snu.ac.kr. ²Department of Natural History Sci., Hokkaido University, Sapporo 060-0810, Japan. ³IGPP, UCLA, Los Angeles, CA 90095, USA. ⁴USGS, Reston, VA 20192, USA.

Magnetite is a key mineral for understanding the O-isotopic compositions of fluids in chondritic parent bodies [1]. Oxygen isotopes of magnetite in various unequilibrated chondrites that have been studied by ion microprobe show higher $\Delta^{17}\text{O}$ values than other phases in the host rocks [2–7]. Magnetite in CO chondrites has not been previously studied mainly because of its rare occurrence (typically <0.1 vol%). Dominion Range (DOM) 03238 is a unique CO chondrite having high (7.6 vol%) magnetite content [8]. It was classified as subtype 3.1 based on Cr contents in ferroan olivine [8]. We studied the occurrence of magnetite in DOM 03238 and measured their oxygen-isotopic compositions along with those of adjacent silicate minerals using the Cameca 1270 ion microprobe at Hokkaido University.

Most metal grains in both chondrules and the matrix of DOM 03238 have been replaced by magnetite. Surviving metal grains are generally Ni rich. There are many magnetite grains or magnetite-bearing assemblages that extend from chondrules into matrix; this indicates in situ formation of magnetite. Based on their occurrence, magnetite grains can be divided into two groups: (1) subhedral magnetite occurs either in chondrules or as isolated grains in the matrix and (2) irregular magnetite occurs mainly in circular or ellipsoidal opaque assemblages.

The range of O-isotopic compositions in magnetite in DOM 03238 is very similar to those of Allende and Ningqiang [2, 5, 7]. The weighted average of $\Delta^{17}\text{O}$ values is $-2.3 \pm 0.4\text{‰}$ ($n = 7$), whereas that from adjacent forsterite is -5.2 ± 1.3 ($n = 4$). The two magnetite groups differ in $\delta^{18}\text{O}$ values: $+4.0 \pm 0.8\text{‰}$ and 0.2 ± 0.8 for the first and second groups, respectively. The $\Delta^{17}\text{O}$ values are not distinguishable within analytical uncertainty: $-2.0 \pm 0.6\text{‰}$ and -2.5 ± 0.6 .

Petrological observations and O-isotopic data show that magnetite in DOM 03238 formed by alteration of pre-existing metallic phases in the parent body, a petrogenetic history similar to that of other magnetite-bearing type 3 chondrites [2–7]. Relatively high magnetite abundances require unusually large amounts of oxygen-bearing fluids (possibly H_2O); however, there is little additional evidence for aqueous alteration in this meteorite [8]. The similarity of the $\Delta^{17}\text{O}$ values (-2 to -3‰ in averages [2, 5, 7]) of magnetite in Allende (CV3), Ningqiang (C3-an) and DOM 03238 (CO3) indicates that fluids with such O-isotopic compositions were common in carbonaceous-chondrite parent bodies.

References: [1] Yurimoto H. et al. 2008. Reviews in Mineralogy and Geochemistry, vol. 68. pp. 141–168. [2] Choi B.-G. et al. 1997. *Earth and Planetary Science Letters* 146:337–349. [3] Choi B.-G. et al. 1998. *Nature* 392:577–579. [4] Choi B.-G. et al. 2000. *Meteoritics & Planetary Science* 35: 1239–1248. [5] Choi B.-G. et al. 2003. *Geochimica et Cosmochimica Acta* 67:4655–4660. [6] Greenwood J. P. et al. 2002. *Geochimica et Cosmochimica Acta* 64:3897–3911. [7] Hsu W. 2005. *Earth and Planetary Science Letters* 243:107–114. [8] Grossman J. N. and Rubin A. E. 2006. Abstract #1383. 37th Lunar and Planetary Science Conference.

5292

TWO-DIMENSIONAL TRANSPORT IN THE SOLAR NEBULA: MORE COMPLEX DISK STRUCTURES

F. J. Ciesla. Department of Geophysical Sciences, University of Chicago, Chicago, IL, USA.

Introduction: Recently it has been demonstrated that the rate and preferred direction of radial transport in viscous protoplanetary disks would be strong functions of height above the disk midplane [1]. In particular, rapid inward movement of material occurs along the surfaces of the disk, while outward transport would preferentially occur around the midplane of the nebula. Such transport offers a way of explaining the presence of high-temperature materials in comets as found by Stardust [1, 2].

Previous Work: Previously, 2-D models of transport in protoplanetary disk defined a thermal structure for the disk that was a single power law with respect to the distance from the star [1, 3, 4]. The two-dimensional flow structure of the disk was then calculated based on this thermal structure. In reality, the temperature in the inner regions of an evolving disk will largely be controlled by accretional heating associated with mass transport, where the temperature will vary with radius as $\sim r^{-3/4}$. Further out in the disk, the thermal structure is controlled by the disks ability to reprocess radiation from its central star (irradiation), where the temperature will vary with radius as $\sim r^{-1/2}$. As a result, the flows within the disk will vary with location and differ from those that assume a single power law structure of the disk.

This Study: I have improved the two-dimensional transport model used in [1] to examine more realistic disk structures. The disk still assumes a steady-state configuration, and calculates the thermal structure accounting for heating by both accretion and irradiation. The surface density of the disk is also calculated self-consistently.

As a result of the variations in thermal structure, the outward flow around the midplane in the inner disk occupies a smaller volume than in the outer disk (outward transport region does not extend as high relative to the local scale height of the disk). There is also greater velocity gradients in the inner disk with the outward flow around the midplane and inward flow along the surface of the disk being more rapid than found in the outer disk.

I am currently investigating the impact that this has on the outward transport of materials such as crystalline grains and CAIs. While significant outward transport still occurs, the vertical gradients found in [1] are greater in the inner disk than in the outer disk. Next I plan to investigate the role that opacity changes, associated with the evaporation of silicates at high temperatures or the condensation of water ice, has on the flow structure. This may serve to alter the thermal structure of the disk [e.g., 5], resulting in sharp changes in flow structure.

Acknowledgements: This work supported by funds from NASA's Discovery Data Analysis Program (Grant NNX08AG27G).

References: [1] Ciesla F. J. 2007. *Science* 318:613–615. [2] Brownlee D. 2006. *Science* 314:1711–1715. [3] Takeuchi T. and Lin D. N. C. 2002. *The Astrophysical Journal* 581:1344–1355. [4] Keller Ch. and Gail H.-P. 2004. *Astronomy & Astrophysics* 415:1177–1185. [5] Cassen P. 2001. *Meteoritics & Planetary Science* 36:671–700.

5296

MOLECULAR DISTRIBUTION OF ORGANIC MATTER AND MINERAL RELATIONSHIPS IN METEORITES AND INTERPLANETARY DUSTS. J. Clemett¹, K. Nakamura-Messenger², and D. S. McKay³. ¹ERC Inc. NASA JSC, USA. E-mail:simon.j.clemett@jsc.nasa.gov. ²Jacobs Technology, NASA JSC, USA. ³NASA JSC, USA.

Introduction: Bulk chemical analysis of carbonaceous meteorites using chromatographic and mass spectrometric techniques has revealed the presence of a wide diversity of organic species. This includes aliphatic and aromatic hydrocarbons, alcohols, aldehydes, ketones, carboxylic acids, amino acids, amines, amides, *N*-heterocycles, phosphonic acids, sulfonic acids, sugar-related compounds and a poorly defined macromolecular phase [1]. This diversity is a product of the many environments and synthetic pathways contributing to the formation and chemical evolution of meteoritic organics—from interstellar processes (ion-molecule reactions) and gas-grain chemistry in the early solar nebula (Fischer-Tropsch and Miller-Urey reactions) through to hydrothermal and shock alteration on meteorite parent bodies. Elucidating the contribution and influence such processes requires an understanding of the exact in situ spatial distribution of individual organic species and their relationships to the local host mineralogy (e.g., [2]). However technological and analytical challenges have previously severely limited such investigations.

Approach: We have applied ultrafast two-step laser mass spectrometry (μ LA-L²MS) [3] to map the molecular distribution of trace organic species ($<10^{-15}$ mol.) at μ m spatial resolution in the matrix of carbonaceous chondrites and individual interplanetary dust particles (IDPs). Samples were prepared by embedding in *N*-free epoxy potted butts. A diamond knife ultramicrotome is then used to expose a fresh surface and provide *e*⁻ transparent thin sections of the same surface for subsequent mineralogical and/or isotopic characterization. Organic molecules are non-thermally desorbed as neutral species from the exposed sample surface using a pulsed IR laser beam spatially filtered and focused to a diffraction limited ~ 5 μ m spot using a Schwarzschild reflecting objective. Desorbed neutrals are subsequently selectively photoionized using a pulsed UV and identified using a time-of-flight mass spectrometer. Spatial mapping is achieved by rastering the sample stage under the desorption laser.

Preliminary Results: Matrix containing fragments of the two carbonaceous chondrites Tagish Lake (CI1) and Bells (CM2), both known to contain ¹⁵N-rich organic globules [4], as well as two large IDP fragments (L2009O14 cluster 13 and L2036AA7*4) have been investigated. The distribution of aromatic and unsaturated hydrocarbons is heterogeneous down to the mapping resolution of the μ LA-L²MS instrument; both in terms of the absolute spatial distribution and in the relative ratio between different species including homologous alkylation series (i.e., X-H ... X-(CH₂)_n-H). There is no evidence of surface smearing of organics by the diamond microtome knife, and no interferences from the epoxy mount since such an extensively polymerized cross-linked structures cannot undergo desorption under the neutral conditions employed. The presence of organic-rich hotspots suggests specific binding of some organics to mineral phases.

References: [1] Sephton M. A. 2002. *Natural Product Reports* 19:292–311. [2] Pearson V. K. et. al 2002. *Meteoritics & Planetary Science* 37:1829–1833. [3] Clemett S. J. and Zare R. N. 1997. International Astronomical Union Symposium 178. pp. 305–320. [4] Nakamura-Messenger K. et al. 2006. *Science* 314:1439–1442.

5038

THE DENSITY AND POROSITY OF CARBONACEOUS CHONDRITES: A NEW LOOK

G. J. Consolmagno SJ¹, D. T. Britt², and R. J. Macker SJ². ¹Specola Vaticana, Vatican City State. E-mail: gjc@specola.va. ²Physics Department, University of Central Florida, Orlando, FL 32816, USA.

Introduction: We have reviewed [1] reliable meteorite density and porosity measurements. Using this “best data” set we find that carbonaceous chondrites can be divided into two density groups: anhydrous CV, CO, and CK meteorites (with hydrous, metal-rich CRs) whose densities are similar to LL chondrites; and hydrated CIs and CMs, with the lowest densities of all meteorites.

High Density Group: Five of the 8 CV/CKs measured are more than 20% porous, while the porosities of 6 of the 7 CO/CR meteorites are under 15%. All 6 low porosity CO/CR samples are finds. The one measured porosity of a CO fall (Warrenton) is 26%; it has a higher grain density than the other COs. Terrestrial weathering significantly alters the carbon isotopes in CO meteorites, as carbonates formed by the evaporation of carbonate-rich terrestrial water is taken up by the meteorite [2, 3]. Presumably this fills void spaces, thus increasing the grain volume and lowering the porosity. However, there is no distinction between the porosity of falls and finds in the CV/CK class. They show a notable spread in porosity, but the low porosity meteorites (~10%) include both a find (Leoville) and a fall (Vigarano) and similarly the high porosity CVs (>20%) are Allende, a fall, and Axtell, a find. (The three measured CKs are all >20% porosity; two are falls, one a find.) The high porosity CVs Allende and Axtell are members of the oxidized subgroup, while the low porosity CVs Leoville and Vigarano belong to the reduced subgroup [4]. The grain densities of other oxidized CVs are also significantly higher, and the bulk densities lower, than the reduced group. Reduced CVs may have been compacted in their parent body [5].

Low Density Group: Of the CMs, only Murchison and Murray have grain and bulk densities measured for the same samples, yielding >20% porosity. However, measuring porosity by point-counting voids visible in thin section [6] gives Murray a porosity of only 4%. For CIs the reported densities and porosities depend strongly on the measuring techniques used. Traditional fluid immersion methods suggest that the CI Orgueil has grain and bulk densities of ~2.2 g/cm³ and so no porosity, while the He pycnometry and bead method [1] yields a 1.6 g/cm³ bulk density, 2.4 g/cm³ grain density, and 35% porosity. This high porosity and low bulk density is also seen in the unusual C meteorite Tagish Lake, as measured by the He pycnometry/bead method.

Discussion: Most meteorites have porosities around 10% due to shock-induced microcracks [1]. Carbonaceous chondrites are the exception. Assuming they also experienced shock microcracking, they must have an additional source of porosity, likely incomplete lithification. If weathering fills the microcracks (as is seen in other meteorites) then this extra porosity must account for another 10–20% of the meteorite volume. It must be at a relatively large scale, not easily seen in thin section and impervious to infill by terrestrial weathering, but accessible to traditional density-measuring fluids like water or carbon tetrachloride.

References: [1] Consolmagno G. J. et al. 2008. *Chemie der Erde* 68:1–29. [2] Ash R. D. and Pillinger C. T. 1995. *Meteoritics* 30:85–92. [3] Greenwood R. C. and Franchi I. A. 2004. *Meteoritics & Planetary Science* 39:1823–1838. [4] Krot A. N. et al. 1995. *Meteoritics* 30:748–775. [5] MacPherson G. J. and Krot A. N. 2002. *Meteoritics & Planetary Science* 37: A91. [6] Corrigan C. M. et al. 1997. *Meteoritics* 32:509–516.

5236

SOLAR XENON IN GENESIS SILICON SAMPLES

S. A. Crowther and J. D. Gilmour. SEAES, University of Manchester, Manchester, M13 9PL, UK. E-mail: sarah.crowther@manchester.ac.uk.

The Sun is thought to have retained the original mean isotopic and elemental composition of the primordial solar nebula for the majority of elements [1]. The noble gases are major exceptions to this rule—due to their inert and volatile nature, noble gases are strongly depleted in solid matter. Xe is particularly interesting—its nine isotopes include some uniquely produced in each of the known processes of stellar nucleosynthesis that produce the heavy elements (s-, r- and p-processes), while geochemically or cosmochemically significant radioactive nuclei (e.g., ²⁴⁴Pu and ¹²⁹I) decay to produce distinct xenon isotopic signatures. Primitive meteorites are dominated by Q-Xe, a component depleted in the lighter isotopes but enriched in the heavier isotopes relative to solar Xe [2]. A more primitive component, U-Xe, has been proposed [3] which is almost identical to solar Xe in all but the two heaviest isotopes. In order to understand the relationships between these components, and determine how they derived from the solar nebula, it is important to know the solar isotopic composition of Xe accurately and precisely.

We have analyzed the Xe isotope ratios in a number of samples of FZ-Si from NASA's Genesis mission, and unflown (“blank”) samples of identical material, using the RELAX mass spectrometer in Manchester [4]. Gas was extracted by heating with a continuous wave Nd:YAG laser (1064 nm).

Initial analyses were performed by laser step-heating of the samples. This technique resulted in a number of releases of implanted gas, the largest of which have an isotopic composition consistent with accepted values for solar wind Xe [5]. The measured concentration of Xe is consistent with the exposure time. However, it is difficult to make blank corrections for Xe intrinsic to the target material by this step heating method, therefore further analyses will adopt a “one-step” method, in which all the implanted gas is extracted from the samples by a single, high temperature heating step.

FZ-Si are not ideal for these analyses—FZ-Si is produced in an Ar atmosphere, which may lead to a high background of Xe, hence future analyses will be carried out on CZ-Si samples.

References: [1] Wiens R. C. et al. 2004. *Earth and Planetary Science Letters* 222:697–712. [2] Busemann H. et al. 2000. *Meteoritics & Planetary Science* 35:949–973. [3] Pepin R. O. 2000. *Space Science Reviews* 92:371–395. [4] Crowther S. A. et al. 2008. *Journal of Analytical Atomic Spectrometry*, doi:10.1039/B802899K. [5] Wieler R. 2002. In *Reviews in Mineralogy and Geochemistry*, vol. 47. pp. 21–70.

5119

IRON ISOTOPES IN PRODUCTS OF ACID-SULFATE BASALT ALTERATION: A PROSPECTIVE STUDY FOR MARS

N. Dauphas¹ and R. V. Morris². ¹Origins Laboratory, Department of the Geophysical Sciences and Enrico Fermi Institute, The University of Chicago, Chicago, IL 60637, USA. E-mail: dauphas@uchicago.edu. ²NASA Johnson Space Center, Houston, TX 77058, USA.

Introduction: The Mars Exploration Rover Opportunity has revealed a rich mineralogy of iron-bearing phases at Meridiani Planum. The prevailing scenario for explaining this mineralogy is jarosite formation by sulfuric acid alteration of olivine-bearing basalt followed by oxidation-evaporation of the solution in an interdune environment. Jarosite was subsequently converted to hematite during a pH-raising recharge event [1, 2]. Iron isotopes in hematite/goethite concretions from the Navajo Sandstone (a possible terrestrial analogue of Mars hematite deposits, [3]) are useful tracers of Fe transport and paleo-fluid circulations [4]. Morris et al. [5, 6] identified a pattern of acid-sulfate alteration on Mauna Kea volcano (Hawai'i) as a very good terrestrial analogue for understanding the formation of hematite spherules on Mars. Possible questions that can be addressed using Fe isotopes are: did alteration occur in a closed system for Fe? If not, what was the scale and direction of the fluid flow? Are all spherules co-genetic? Did spherules grow in several pulses? What was the chemical pathway for the formation of jarosite (oxidative weathering of sulfides or acid-sulfate alteration of basalts?).

Results: We have analyzed the Fe isotopic compositions of the products of acid-sulfate alteration on Mauna Kea. Unaltered tephra have $\delta^{56}\text{Fe} \approx +0.15\text{‰}$ (relative to IRMM-014), similar to other OIBs. Jarosite-bearing tephra have more variable $\delta^{56}\text{Fe}$, from about +0.11 to +0.26‰. A hematite spherule concentrate extracted from HWMK745R [5] has heavy $\delta^{56}\text{Fe}$ (+0.42‰). Fe isotopic compositions of 15 individual hematite spherules ranging in diameter from 25 to 50 μm (33 to 261 ng Fe) were also analyzed. To our knowledge, these are the smallest natural objects ever analyzed for $\delta^{56}\text{Fe}$ by MC-ICPMS. The uncertainties of individual analyses increase as the Fe quantity decreases. All spherules, except one, appear to have identical compositions to the spherule concentrate.

Conclusions: The heavy $\delta^{56}\text{Fe}$ of jarosite-bearing tephra indicates that Fe isotopic fractionation occurred during basalt dissolution, partial oxidation, or jarosite deposition. The variable $\delta^{56}\text{Fe}$ values show that the rocks did not behave as closed systems for Fe. Electron microprobe analyses of hematite spherules revealed rims with higher (Al + Si)/Fe ratios than cores, suggesting multiple pulses of growth [5]. Hematite spherules have identical $\delta^{56}\text{Fe}$, regardless of their diameters. The sharp zonation seen in cross sections reflect changes in growth conditions rather than changes in the source of Fe. This study provides us with the opportunity to sharpen analytical tools and develop the scientific context for future sample return missions from Mars.

References: [1] McLennan S. M. et al. 2005. *Earth and Planetary Science Letters* 240:95–121. [2] Tosca N. J. et al. 2005. *Earth and Planetary Science Letters* 240:122–148. [3] Chan M. A. et al. 2004. *Nature* 429:731–734. [4] Busigny V. and Dauphas N. 2007. *Earth and Planetary Science Letters* 254:272–287. [5] Morris R. V. et al. 1996. The Geochemical Society Special Publication #5. pp. 327–336. [6] Morris R. V. 2005. *Earth and Planetary Science Letters* 240:168–178.

5325

RARE EARTH ELEMENT PRODUCTION IN ASYMPTOTIC GIANT BRANCH STARS

Andrew M. Davis¹ and Roberto Gallino². ¹Department of the Geophysical Sciences, Enrico Fermi Institute and Chicago Center for Cosmochemistry, University of Chicago, Chicago, IL 60637, USA. E-mail: a-davis@uchicago.edu. ²Dipartimento di Fisica Generale, Università di Torino, Via P. Giuria 1, 10125 Torino, Italy.

Introduction: Presolar grains provide an isotopic record of nucleosynthesis in individual stars of a variety of types, including asymptotic giant branch (AGB) stars, core collapse supernovae, and novae [1]. Silicon carbide is the most widely studied type of presolar grain and most (~90%) SiC grains have isotopic properties consistent with formation in low mass AGB stars. These stars are thought to be the primary stellar site for *s*-process nucleosynthesis. Many of the rare earth elements (REE) have elevated concentrations in presolar SiC [2]. We summarize here predictions of *s*-process nucleosynthesis calculations for low-mass AGB stars for the rare earth elements in anticipation of future measurements in individual presolar grains by resonant ionization mass spectrometry (RIMS). Analysis of REE by mass spectrometry suffers from isobaric interferences of many REE isotopes on one another, and RIMS offers the possibility of minimizing these interferences while measuring with high sensitivity.

The *s*-process in AGB stars is driven by two neutron sources: $^{13}\text{C}(\alpha, n)^{16}\text{O}$ during interpulse periods, and $^{22}\text{Ne}(\alpha, n)^{25}\text{Mg}$ during thermal pulses. Immediately after each thermal pulse, freshly synthesized *s*-process products are dredged up from the He intershell into the envelope of the star. Although the amount of ^{13}C available to produce neutrons is essentially a free parameter, but recent measurements of the isotopic compositions of Zr, Mo, and Ba suggest that most SiC grains come from AGB stars with ^{13}C pocket amounts within 50% of the standard case that explains the solar system *s*-process abundances well [3]. There are a number of *s*-only isotopes among the REE and these are all predicted to be enriched by about a factor of 10 compared to Si in the envelope of a low mass AGB star. *r*-Only or *p*-only isotopes are not produced in low mass stars, so they are expected to have solar abundances relative to Si for a solar metallicity AGB star. Isotopes with mixed *s*- and *r*- or *p*-process production will have enrichments between 1 and 10.

The REE comprise 15 elements with atomic numbers from 57 to 71. Along the *s*-process path in the REE region, there are a number of branch points that are sensitive indicators of neutron density during thermal pulses. Of the 15 REE, promethium has no long-lived or stable isotopes, praseodymium, terbium, holmium, and thulium have only one stable isotope, and, although lanthanum has two stable isotopes, one is of very low abundance. Of the remaining REE, Nd, Sm, Gd, and Dy are of greatest interest in terms of sensitivity to neutron density and potential branching effects.

References: [1] Lugaro M. 2005. *Stardust from meteorites*. World Scientific Publishing. 209 p. [2] Yin Q.-Z. et al. 2006. *The Astrophysical Journal* 647:676. [3] Barzyk J. G. et al. 2007. *Meteoritics & Planetary Science* 42:1103.

5288

NUMERICAL MODELLING OF SHOCK HEATING IN POROUS PLANETESIMAL COLLISIONS

T. M. Davison¹, G. S. Collins¹, and F. J. Ciesla². ¹Department of Earth Science and Engineering, Imperial College London, London SW7 2AZ, UK. E-mail: thomas.davison02@imperial.ac.uk. ²Department of Geophysical Sciences, The University of Chicago, 5734 S. Ellis Ave., Chicago, IL 60637, USA.

Introduction: Planetesimal impacts and collisions were fundamental processes in the early solar system. Impacts have been invoked to explain shock effects in meteorites, the compaction and lithification of the earliest planetesimals and even the presence of chondrules in the most primitive meteorites [1, 2]. In a comprehensive study, Keil et al. [3] concluded that impacts are inefficient as a source of heating and melting in planetesimals, and suggested other processes as the major source of heating, e.g., short-lived radio-nuclide decay [4] or electromagnetic induction [5]. However, their analysis focussed on the consequences of collisions between non-porous bodies of greatly differing sizes. More recent studies have modelled low velocity collisions [e.g., 6], but heating and melting in high velocity collisions between similar sized bodies, or bodies with substantial porosity has not been quantitatively investigated. In particular, the collapse of pore space during impact is known to substantially increase shock heating and lower the critical pressure for melting [3, 7, 8]. As newly accreted planetesimals are likely to have had high porosity, the collisional heating of such bodies is important to quantify.

Numerical Modelling: We quantify the efficiency of heating and melting in impacts between similar sized, km-scale, spherical dunite bodies using the iSALE hydrocode [9]. We investigate the effect of pore space closure on shock attenuation and heating with the epsilon-alpha porous compaction model [8, 9]. To compare the efficiency of heating between collision events, we measure the mass of material shock heated to a certain post-shock temperature, e.g., the solidus (incipient melting) or the liquidus (complete melting).

Results: In agreement with observations and experiments, pore space compaction has a large effect on post-shock temperature, due to extra waste heat produced by the crushing of pores. The critical velocity required to shock heat half the mass of the colliding planetesimals to post-shock temperatures above the solidus is $\sim 12 \text{ km s}^{-1}$ for non-porous bodies, but only $\sim 7.5 \text{ km s}^{-1}$ for 20% porous bodies and $\sim 5 \text{ km s}^{-1}$ for 50% porous bodies. Even at low velocity (e.g., 3 km s^{-1}), almost the entire planetesimal mass is heated by $>400 \text{ K}$ and $\sim 40\%$ is heated by $>700 \text{ K}$ after impact between two planetesimals with 50% porosity. Head-on collisions between equal sized planetesimals produce the greatest mass of material shock heated to the solidus; as the difference in size between the planetesimals increases, the total fraction of both planetesimals that is heated above the solidus decreases.

References: [1] Consolmagno G. and Britt D. T. 2004. *Planetary and Space Science* 52:1119–1128. [2] Scott E. R. D. 2002. In *Asteroids III*, edited by Bottke et al. pp. 697–709. [3] Keil K. et al. 1997. *Meteoritics & Planetary Science* 32:349–363. [4] Urey H. 1955. *Proceedings of the National Academy of Sciences* 41:127–144. [5] Sonett C. et al. 1968. *Nature* 219:924–926. [6] Benz W. 2000. *Space Science Reviews* 92:279–294. [7] Hörz F. and Schaal B. 1981. *Icarus* 46:337–353. [8] Wünnemann K. et al. 2006. *Icarus* 180:514–527. [9] Wünnemann K. et al. 2008. *Earth and Planetary Science Letters*. In press.

5276

IMPLICATIONS OF HETEROGENEOUS ACCRETION OF THE SOLAR NEBULA

Simone de Leuw¹ and John T. Wasson^{1,2}. ¹Department of Earth and Space Sciences, University of California, Los Angeles, CA 90095–1567, USA. E-mail: sdeleuw@ucla.edu. ²Institute of Geophysics and Planetary Physics, University of California, Los Angeles, CA 90095–1567, USA.

Introduction: Isotopic studies of primitive chondrites are a useful tool for understanding the cosmochemical evolution of the early solar system and for providing information about accretion scenarios of the solar nebula. The Sun and the solar nebula formed, together with other stars, from a molecular cloud. Estimated mixing times for molecular clouds are in the range of $\sim 3 \text{ Ma}$ for small molecular clouds (1 pc, $300 M_{\odot}$) [1] to $\geq 10 \text{ Ma}$ for moderate-sized molecular clouds (30 pc, $10^4 M_{\odot}$) [2]. Compared to a typical lifetime of $\sim 10 \text{ Ma}$ for moderate-sized clouds, it thus can be expected that the properties of chondritic materials reflect incomplete mixing.

Isotopic Compositions of Chondrites: Chondrites preserve the compositions of kilometer-sized planetesimals and probably the composition of solar nebula material. Previous isotopic studies raise the question of whether these isotopes were heterogeneously distributed in the solar nebula. A study by Trinquier et al. [3] showed that $\epsilon^{54}\text{Cr}$ values of inner solar system planets and planetesimals (e.g., carbonaceous chondrites, ordinary chondrites, enstatite chondrites, Mars, etc.) are different, supporting the view of heterogeneous accretion of the solar nebula. Isotopic data of $\epsilon^{54}\text{Cr}$ [3] and $\epsilon^{62}\text{Ni}$ [4, 5] also show a positive correlation; this is expected because both isotopes were synthesized in the same stellar regions by neutron-capture. Furthermore, excesses of ^{137}Ba and ^{138}Ba (formed by both s and r processes) in carbonaceous and ordinary chondrites compared to Earth favor the assumption of incomplete mixing of diverse nucleosynthetic components [6]. Other studies of Mo isotopes [7] and ^{96}Zr [8] further show that chondritic parent bodies accreted a small excess of neutron burst material as compared to Earth [6]. In addition, FUN inclusions in some carbonaceous chondrites contain excesses in heavy-element isotopes that are produced by r-processes [9]. If the solar nebula was completely mixed, these isotopic differences would not occur.

Summary: Although previous models [10] suggest that the solar system formed from a hot, well-mixed, gaseous disk, variations in isotopic compositions between bulk planetary bodies and planetesimals imply that distinct isotopic reservoirs did exist and that the material was neither completely homogenized nor sufficiently processed to erase these distinct signatures.

References: [1] Xie T. et al. 1995. *The Astrophysical Journal* 440:674. [2] Wasson J. T. 2008. Abstract #2470. 39th Lunar and Planetary Science Conference. [3] Trinquier A. et al. 2007. *The Astrophysical Journal* 655: 1179–1185. [4] Bizzarro M. et al. 2007. *Science* 316:1178–1181. [5] Regelous M. et al. 2008. *Earth and Planetary Science Letters*. Submitted. [6] Ranen M. C. and Jacobsen S. 2006. *Science* 314:809–811. [7] Yin Q. et al. 2002. *Nature* 415, 881–883. [8] Yin Q. et al. 2001. Abstract #2128. 32nd Lunar and Planetary Science Conference. [9] McCulloch M. T. and Wasserburg G. J. 1978. *The Astrophysical Journal* 22:L15–L19. [10] Cameron A. G. W. 1963. *Icarus* 1:339–342.

5096

CORE CRYSTALLIZATION AND CHEMICAL EVOLUTION OF IRON METEORITES PARENT BODIES

Renaud Deguen. LGIT, CNRS, Université J. Fourier, Maison des Géosciences, BP 53, 38041 Grenoble Cedex 9, France. E-mail: renaud.deguen@obs.ujf-grenoble.fr.

The large range in trace elements concentration measured within iron meteorite groups is usually thought to reflect fractional crystallization approaching ideal conditions, and has led to favor an Earth-like outward crystallization mode. The recognition that core crystallization in asteroid-sized bodies would in fact start at the core-mantle boundary (CMB) [1] makes the explanation of the observed chemical differentiation somewhat more problematic. We investigate here possible solidification regimes with numerical solidification models and analog experiments, and discuss the implications of our physical models in terms of the resulting chemical fractionation.

Assuming first that the iron crystals stay fixed at the CMB, a dendritic layer will grow inward, releasing S-rich liquid in between the growing dendrites. In this configuration, the interdendritic melt is stably stratified (e.g., [2]), and no large scale convection occurs in the dendritic layer. The direct consequence is that there is no chemical flux from the dendritic layer to the inner liquid domain, which therefore does not evolve chemically: no global chemical differentiation would occur. We found however that the temperature within the liquid domain eventually falls below the solidification temperature before the solidification front reaches the center of the core, allowing secondary crystallization in the deep core. While this may drive convection in the liquid domain and allow its chemical evolution, the degree of differentiation by this process is actually found to be very small.

Laboratory experiments suggest that the dendritic layer would grow until a critical thickness is reached, after which crystals will continuously fall from it. Relaxing the assumption of no crystal fall will help chemical fractionation, by removing iron rich crystals from the solidifying region, leaving behind a progressively more and more evolved liquid, and allowing further crystallization within the core. Fallen crystals will sediment and accumulate to form a partially solid inner core. The core chemical evolution would be in fact close to fractional, with deviations coming mostly from the presence of partially solidified zones: some liquid is expected to be trapped in both the loosely packed inner core and the dendritic zone below the CMB. Further crystallization of this melt will induce a secondary chemical differentiation, leveled by solid state diffusion, which may account for the scatter in element vs. element diagrams and for the distinct compositional trend measured in the Cape York meteorites shower [3].

References: [1] Haack H. and Scott E. R. D. 1992. *Journal of Geophysical Research* 97:14,727–14,734. [2] Huppert H. E. and Worster M. G. *Nature* 314:703–707. [3] Esbensen K. H. et al. 1982. *Geochimica et Cosmochimica Acta* 46:1913–1920.

5262

BEDIASITES AND IVORY COAST TEKTITES: GAS CONTENT AND COMPOSITIONAL HOMOGENEITY

A. Deutsch¹, F. Langenhorst^{2, 3}, K. Heide², and S. Luetke¹. ¹Institut für Planetologie, Universität Münster, D-48149 Münster, Germany. ²Institut für Geowissenschaften, Universität Jena, D-07749 Jena, Germany. ³Bayerisches Geoinstitut, D-95440 Bayreuth, Germany. E-mail: deutsca@uni-muenster.de.

Introduction: We have analyzed two Ivory Coast (IVC) tektites (source crater Lake Bosumtwi, Ghana) and three Bediasites (North American tektite strewn field, related to the Chesapeake Bay structure, Virginia) for major elements (electron microprobe), a set of trace element analyses (LA-ICP-MS, spot diameter 60 μm), and gas contents in order to identify precursor lithologies and to better understand formation processes.

Major and Trace Elements: Both tektite groups are remarkably homogeneous, as the whole group and single specimen too. The results of EMP line scans over Bediasites 2267, 2268, and 2269 are given below (unweighted mean).

Table 1.

wt%	2267	2268	2269
n	160	55	240
SiO ₂	76.6	77.8	75.6
TiO ₂	0.8	0.8	0.8
Al ₂ O ₃	14.1	13.3	14.9
FeO _{tot}	3.8	3.5	4.4
MnO	0.1	0.1	0.1
MgO	0.5	0.5	0.7
CaO	0.4	0.5	0.5
K ₂ O	1.8	1.9	1.9
Na ₂ O	1.3	1.4	1.4
Sum	99.4	99.8	100.1

JEOL JXA 8600 MX Superprobe (WWU Münster; 15 kV, 5 nA, 5 μm beam \emptyset ; standards—synthetic glasses)

Gas Contents: Analyses were performed with the direct coupled evolved gas analysis system (DEGAS; U. Jena), consisting of the thermogravimetry in combination with a BALZER quadrupole mass spectrometer that records 28 masses with mass numbers up to 200 (for details, see [1]). The tektite samples were stepwisely heated up to 1450 °C. Bediasites are very dry and contain between 20 and 30 ppm H₂O, about one order of magnitude less than detected by FT-IR spectroscopy [2]. In addition, traces of CO were found. IVC tektites are likewise extremely depleted in gases, too; they contain ~100 ppm H₂O, and traces of CO₂ and CO with CO/CO₂ > 1. Above 1300 °C, the glass foams and bubbles/vacuoles release H₂O, fluorine, CO₂, and CO.

Interpretation: The presence of reduced species (CO, total lack of ferric iron), and the extremely low volatile content foster the conclusion that material now forming tektites must have experienced flash heating at extreme temperatures under highly reducing conditions followed by fast quenching. This is in keeping with current models for tektite formation [3, 4]. The chemical homogeneity probably reflects more the melt/ejection process than homogeneity of the precursor materials.

Acknowledgements: This research is supported by the DFG (De 401/19, De 401/21; La 830/7, LA 830/12).

References: [1] Heide K. and Schmidt C. M. 2003. *Journal of Non-Crystalline Solids* 323:97–103. [2] Beran A. and Koeberl C. 1997. *Meteoritics & Planetary Science* 32:211–216. [3] Melosh H. J and Artemieva N. 2004. 35th Lunar and Planetary Science Conference. Abstract #1723. [4] Artemieva N. 2008. 39th Lunar and Planetary Science Conference. Abstract #1651.

5202

NEW CLUES ON COMPOSITION AND STRUCTURE OF CARBONACEOUS MATTER IN ANTARCTIC MICROMETEORITES

E. Dobrica¹, C. Engrand¹, E. Quirico², G. Montagnac³, and J. Duprat¹.
¹CNSM CNRS-Univ. Paris Sud, 91405 Orsay Campus, France. E-mail: Elena.Dobrica@cnsm.in2p3.fr. ²LPG Univ. J. Fourier CNRS-INSU 38041, Grenoble Cedex 09, France. ³LST-Lyon CNRS, 69364 Lyon Cedex 07, France.

Introduction: The carbonaceous matter of 19 Antarctic micrometeorites (AMMs) was characterized by Raman and infrared (IR) microspectroscopy. The AMMs were collected at Dome C [1] and include 6 fine-grained (Fg) (among them 3 ultracarbonaceous [UCAMMs] [2]), 8 intermediate Sc/Fg, and 5 scoriaceous particles (Sc) [3]. Two cosmic spherules (CS) were also analyzed. Raman measurements were performed with 2 Labram microspectrometers (514 nm and 244 nm excitation) [4, 5]. Micro-IR spectra were taken with a Hyperion 3000 micro-imaging system from 4000 to 950 cm⁻¹. Whole rock (WR) ordinary chondrites, and WR carbonaceous chondrites (CCs) and their extracted insoluble organic matter (IOM) were used as standards.

Results and Discussion: Sixteen out of 19 AMMs present the first-order carbon bands (G and D) in the 514 nm Raman spectrum, showing a polyaromatic structure of their carbonaceous matter. Band fitting and Principal Component Analysis of their spectra reveal no significant degree of structural order among all textural types (i.e., from Fg, UCAMMs to Sc AMMs). The 3 remaining AMMs (including one UCAMM) show odd 514 nm Raman spectra with unidentified bands. No carbon was detected in the two CSs. Thus, atmospheric entry heating has no effect on the maturation of carbonaceous matter in AMMs, even in partially melted scoriaceous AMMs. Accordingly, laboratory experiments on carbonaceous matter require long durations (>several minutes) to significantly graphitize any carbonaceous compounds [e.g., 6]. This strongly strengthens the hypothesis of very short durations (5 s < t < 120 s; [7]) of AMM pulse heating during atmospheric entry. It is however not yet possible to exclude some chemical modifications of this carbonaceous matter. While the 514 nm Raman analysis did not reveal significant differences among all types of AMMs and CC IOMs, 244 nm Raman spectra on 2 UCAMMs unambiguously show differences in their polyaromatic structures. These differences might be controlled by chemical composition variations and/or structural modifications induced by alteration processes, either in solar cavity or in the parent body. The 244 nm Raman spectra also show for the first time the presence of the nitrile (–CN) functional group in UCAMMs. Micro-IR spectra reveal the presence of aliphatic functions (e.g., –CH₃), and other functional groups typical of kerogen-like materials. A systematic survey on AMMs by micro-IR imaging reveals that all AMM but one (scoriaceous) AMMs are anhydrous. As UCAMMs-like grains are unknown in meteorites, they could constitute a family of cometary grains. The characterization of their carbonaceous matter is thus important and should be compared with Stardust samples.

References: [1] Duprat J. et al. 2007. *Advances in Space Research* 39: 605–611. [2] Dobrica E. et al. 2008. 39th LPSC. Abstract #1672. [3] Genge M. J. et al. 2008. *Meteoritics & Planetary Science*. In press. [4] Quirico E. et al. 2005. *Spectrochimica Acta Part A* 61:2368–2377. [5] Quirico E. et al. 2008. *Meteoritics & Planetary Science* 43. This issue. [6] Bény-bassez C. and Rouzaud J.-N. 1985. *Scanning Electron Microscopy* 119–132. [7] Toppani A. et al. 2001. *Meteoritics & Planetary Science* 36:1377–1396.

5231

FORMATION OF ZONED METAL GRAINS IN HAH 237

C. M. Duffy^{1,2}, P. A. Bland^{1,2}, S. S. Russell^{1,2}, A. T. Kearsley², D. J. Prior³, and E. Mariani³. ¹Impact and Astromaterials Research Centre (IARC), Imperial College London, South Kensington Campus, London SW7 2AZ, UK. E-mail: c.duffy07@imperial.ac.uk. ²Department of Mineralogy, Natural History Museum, Cromwell Road, London SW7 5BD, UK. ³Department of Earth and Ocean Science, University of Liverpool, 4 Brownlow Street, Liverpool L69 3GP, UK.

Introduction: Compositional zoning of metal grains occurs in CH and CBB meteorites: Ni and Co increase from grain rim to core while Cr content decreases from rim to core [1]. The cores of these zoned grains contain abundant refractory siderophile elements, and are depleted in volatile elements compared to CI chondrites [2, 3]. Condensation, either from the cooling solar nebula [1], or from an impact-generated vapor plume [4], combined with diffusion processes [2], are thought to be responsible for the observed profiles. Although the composition and petrography of metal in these meteorites has been explored in some detail, crystallographic data are sparse [5]. EBSD offers an effective means of quantifying crystallography at high spatial resolution, in silicates [6] and metals. EBSD has not been applied to zoned metal grains to date. We chose to explore the thermal history of individual grains using this technique.

Method: SEM-EDS analysis revealed zoned grains in a polished thin section of CB₀ HAH 237. The sample was prepared for EBSD analysis, and the same areas mapped, revealing the crystal structure of grains. Further processing generated grain boundary and texture component maps.

Results: SEM imaging of HAH 237 reveals visible elongation and deformation of grains. EBSD band contrast mapping of zoned metal grains exposes a subgrain microstructure with average diameter ~4 μm. These subgrains are regular in shape with almost circular boundaries. Misorientation angles between subgrains increase from rim to core. A band contrast map was superimposed with three texture component layers corresponding to maximum boundary angle deviations of 20°, 40°, and 60°. With no semi-transparency applied, the grain displayed an approximate radial pattern.

Discussion: Smooth and regular-sized internal subgrains are consistent with a diffusion formation process. The misorientation boundary pattern for subgrains suggests that the outer regions of the metal grain were more subjected to stress and/or deformation than the core. Such a well defined core-mantle substructure is unusual. Subgrains nearer the core are less deformed, suggesting they were protected from altering conditions. Chronologically ordering these findings suggests the following formation scenario: (i) metal condensed, (ii) underwent diffusion, and (iii) a heating event occurred which deformed the overall structure of the sample and caused local stress of the outer subgrains forming high angle boundaries near the rim. Heating event temperatures were not high enough to affect the internal substructure.

References: [1] Meibom A. et al. 1999. *Journal of Geophysical Research* 104:22,053–22,059. [2] Campbell A. et al. 2001. *Geochimica et Cosmochimica Acta* 65:163–180. [3] Campbell A. and Humayun M. 2004. *Geochimica et Cosmochimica Acta* 68:3409–3422. [4] Wasson J. and Kallemeyn G. W. 1990. *Earth and Planetary Science Letters* 101:148–161. [5] Goldstein J. et al. 2007. *Meteoritics & Planetary Science* 42:913–933. [6] Watt L. et al. 2006. *Meteoritics & Planetary Science* 41:989–1001.

5229

CHARACTERIZING PRIMITIVE CHONDRITE MATRIX: A SEM/TEM/EBSD STUDY OF ACFER 094

C. M. Duffy^{1,2}, P. A. Bland^{1,2}, S. S. Russell^{1,2}, D. J. Prior³, E. Mariani³, A. T. Kearsley², L. Howard², R. Chater⁴, M. G. Ardakani⁴, D. McPhail⁴, and B. A. Shollock⁴. ¹Impact and Astromaterials Research Centre (IARC), Imperial College London, South Kensington Campus, London SW7 2AZ, UK. E-mail: c.duffy07@imperial.ac.uk. ²Department of Mineralogy, Natural History Museum, Cromwell Road, London, SW7 5BD, UK. ³Department of Earth and Ocean Science, University of Liverpool, 4 Brownlow Street, Liverpool L69 3GP, UK. ⁴Department of Materials, Imperial College London, South Kensington Campus, London SW7 2AZ, UK.

Introduction: The matrix component of primitive solar system materials, being composed largely of sub- μm phases, has a relatively unconstrained size frequency distribution (SFD). In addition, literature on the crystallography and chemistry of matrix phases is sparse [1, 2], particularly with regard to matrix metal. Acfer 094 is an ungrouped carbonaceous chondrite, arguably one of the most mineralogically primitive [1–3]. The work we present here is part of a major project, using an array of techniques, to constrain both aspects of primitive matrix.

Methods: SEM imaging of Acfer 094 revealed a landscape of chondrules and isolated metal grains set in a fine matrix background. EBSD analysis was performed on a selection of metal grains across the entire sample with a focus on matrix metal. The crystallographic structure of the grains was determined through orientation mapping. In addition, a 10 μm TEM section of the matrix was prepared using a focused ion beam lift-out technique to investigate both the submicron matrix grains, and for TEM imaging to define a matrix SFD. TEM-EDS was employed to distinguish crystalline structures from amorphous layers and will allow element mapping at a range of resolutions to quantify the finest primitive matrix materials. Differentiation between grains and sample porosity will be achieved through contrast differences generated by tilting the section. The SFD of matrix grains will be obtained by applying image processing software to TEM images.

Results: EBSD crystallographic orientation mapping of matrix metal reveals a complicated crystal structure with several crystal orientations across a single grain. In comparison chondrule metal grains (internal chondrule; 5–15 μm , chondrule rim; ~10–30 μm) appear to have homogeneous crystal structures. TEM-EDS analysis has revealed amorphous and submicron crystalline structures within the matrix component consistent with previous findings [1, 2]. Element mapping will further constrain the primitive matrix chemical composition.

Discussion: Comparison of the crystallographic orientations between larger matrix metal (~50 μm) and chondrule metal suggests that these regions may not share a common thermal history, which has implications for formation theories and chondrule/matrix complementarity [4]. Chemical and crystallographic data on sub- μm matrix metals, and SFD results, will be presented at the conference.

References: [1] Greshake A. 1997. *Geochimica et Cosmochimica Acta* 61:437–452. [2] Bland P. A. et al. 2007. *Meteoritics & Planetary Science* 42: 1417–1427. [3] Newton J. et al. 1995. *Meteoritics* 30:47–56. [4] Bland P. A. et al. 2005. *Proceedings of the National Academy of Sciences* 102:13,755–13,760.

5287

EXPLORING OXYGEN ISOTOPE EXCHANGE IN THE SOLAR NEBULA WITH UV LASER-FLUORINATION

K. A. Dyl¹, E. D. Young², and A. N. Krot³. ¹Department of Earth and Space Sciences, UCLA, Los Angeles, CA 90095, USA. E-mail: kdyl@ucla.edu. ²Institute of Geophysics and Planetary Physics, UCLA, Los Angeles, CA 90095, USA. ³Hawai'i Institute of Geophysics and Planetology, School of Ocean and Earth Science and Technology, University of Hawai'i at Manoa, Honolulu, HI 96822, USA.

Introduction: Oxygen isotopic ratios from CAIs have been used to unravel the complex history of the solar nebula. Combining these data with the thermal and temporal histories deduced from several isotopic systems in these objects has the potential to shed light on the origins and evolution of CAIs.

Magnesium isotopic data from E44, a type B CAI from Efremovka, illustrate that this object has undergone several evaporative episodes, consistent with multiple passages through shock waves [1]. A complimentary oxygen isotopic data set would serve to further constrain or contravene the proposed thermal history for this object.

Results: Oxygen data were obtained on Efremovka matrix, E44, and a nearby chondrule using the UV-laser ablation fluorination line constructed at UCLA. Fassaite yields $\delta^{18}\text{O} = -37.7\%$ and $\delta^{17}\text{O}$ of -40.09% , anorthite $\delta^{18}\text{O}$ and $\delta^{17}\text{O}$ values range from -32.5 to -35.5% and -35.14 to -37.96% , respectively, and melilite $\delta^{18}\text{O}$ and $\delta^{17}\text{O}$ values range from -1.2 to 7.4% and -6.82 to 1.66% . Matrix points plot from 4.13 to 8.55‰ in $\delta^{18}\text{O}$ with $\Delta^{17}\text{O}$ of -1.61 to -3.98% . All CAI and matrix points lie on a line with a slope of 0.92. The difference between this line and the CCAM line is resolvable with the precision of laser-fluorination data. Measurements on a terrestrial standard indicate a precision of 0.2 to 0.3‰ in both in $\delta^{18}\text{O}$ and $\delta^{17}\text{O}$.

Using the solid-gas oxygen isotope exchange model discussed in [2], we explored the implications for E44's thermal history based upon the fluorination data.

Discussion: The oxygen isotope exchange recorded by anorthite and melilite indicates that high-temperature ($T > 1200$ K) solid-gas exchange is a plausible explanation for E44's isotopic history. This is consistent with the magnesium data obtained on this object [1]. Furthermore, the co-linear relationship between E44 and Efremovka matrix suggests that they share a common exchange medium.

Future work should be directed towards amassing a larger set of CAI and matrix oxygen data, as well as towards understanding the implications of water vapor as the exchanging gas phase (as opposed to CO) [3, 4].

References: [1] Young E. D. et al. 2005. *Science* 90:1151–1154. [2] Ryerson F. J. and McKeegan K. D. 1994. *Geochimica et Cosmochimica Acta* 58:3713–3734. [3] Yu Y. et al. 1995. *Geochimica et Cosmochimica Acta* 59: 2095–2104. [4] Boesenberg J. S. et al. 2005. *Meteoritics & Planetary Science* 40:5111.

5118

WHY DO CHONDRULES WITH VOLUMETRIC METAL/SILICATE RATIOS OF 1 TO 37% AGGREGATE TO SOLAR Fe/Si IN THE RENAZZO CR CHONDRITE?

D. S. Ebel¹ and M. K. Weisberg^{1, 2}. ¹Department of Earth and Planetary Sciences, American Museum of Natural History, New York, NY 10024, USA. E-mail: debel@amnh.org. ²Department of Physical Sciences, Kingsborough College, City University of New York, Brooklyn, NY 11235, USA.

Introduction: A first order observation is that the CR and most other chondrites have nearly identical, solar Si:Fe:Mg abundance ratios, despite very different chondrule sizes and textures, and different chondrule/matrix ratios [1]. Why are chondrules and matrix (and CAIs) complementary in always summing to near-chondritic proportions of major elements [2–5]?

The answer bears on the location and mechanism of chondrule formation in the protoplanetary disk. This “complementarity” [1] suggests that chondrule precursors and matrix originally constituted batches of material with solar Si, Fe, Mg (and Ca, Al, etc.) relative abundances, from which chondrules formed in varying amounts, and accreted with local matrix material to make chondritic meteorites. It seems unlikely that this chondritic composition could be preserved by remote formation of chondrules (e.g., near the sun), transport, and combination with matrix (e.g., at 3–5 AU). Indeed, why would the chondrules in different chondrite types have the distinctly different characteristics observed?

Results: We have measured the actual volumetric abundances of metal and total silicate in 8 chondrules representative of >100 chondrules in a 1 cm³ piece of Renazzo, using synchrotron tomography (17 micron/pixel) and image analysis [6]. Metal/silicate ratios vary widely from 1 to 37%. Modal reconstructions yield highly variable Mg/Si ratios in bulk silicates.

Discussion: The aggregate of chondrules is complementary, in the same sense as matrix and chondrules [1–5]. That is, despite their very high variability in both metal/silicate (measured in 3-D) and Mg/Si (from 2-D data) the chondrules in Renazzo have, in aggregate, just the correct abundances to combine with matrix into a chondritic whole. The chondrules are complementary individually to each other, and complementary in aggregate to the matrix. This is further evidence that local heating occurred in batches of chondritic precursor mineral dust, forming chondrules in various chondrule/matrix proportions, highly variable individual chondrule compositions, and chondrules with distinctive textures in each local region. Chondrules and local, unprocessed dust (matrix) accreted with little mixing, into parent bodies that preserve the bulk chondritic abundances present in the original local regions. This requires a widespread mechanism to heat dust aggregates in highly localized volumes out in the disk without destroying nearby presolar grains that remain in matrix [7]. Two plausible ideas consistent with accretion theory are [8, 9].

References: [1] Palme H. et al. 1992. 23rd LPSC. pp. 1021–1022. [2] Klerner S. and Palme H. 1999. 30th LPSC. Abstract #1272. [3] Kong P. and Palme H. 1999. *Geochimica et Cosmochimica Acta* 63:3673–3682. [4] Bland P. A. et al. 2005. *Proceedings of the National Academy of Sciences* 102: 13,755–13,760. [5] Hezel D. C. and Palme H. 2007. *Earth and Planetary Science Letters* 265:716–725. [6] Hertz J. et al. 2003. 34th LPSC. Abstract #1059. [7] Huss G. R. and Lewis R. S. 1995. *Geochimica et Cosmochimica Acta* 59:115–160. [8] Desch S. J. and Connolly H. C. Jr. 2002. *Meteoritics & Planetary Science* 37:183–207. [9] Joung M. K. R. et al. 2004. *The Astrophysical Journal* 606:532–541.

5013

MATHEMATICAL ESTIMATIONS FOR IMPACT CONDITIONS ON ARGYRE PLANITIA, MARS

J. C. Echaurren. Codelco Chile—North Division. Chile. E-mail: jecha001@codelco.cl.

Introduction: Argyre Planitia, named in 1973, is one of the largest impact basins on Mars with a diameter of approximately 900 km and located at 49.4°S and 42.8°W. Although workers agree that Argyre is a preserved impact crater, they disagree on the geologic processes that have subsequently operated within the basin [1]. Argyre was part of a larger surface hydrological system (the Chese Trough [Sanders 1979]) that also included two large valley networks draining the Margaritifer Sinus region northwest of Argyre. The morphometry of these systems suggest a combination of precipitation and groundwater sapping, with surface runoff for their formation (Grant and Parker 2002) [2], distributions of dust devil track has been studied in Argyre too [3]. This work is an application of mathematical models [4] for the determination of impact conditions, and for the prediction of possible hydrothermal zones generated after of the impact. All the calculations are obtained using an HP 49g.

Results Obtained with the Models: According to the models used for this basin [4], the diameter of asteroid is calculated in ~130.78 km, with both velocity and impact angle on the Martian surface of ~15.05 km/s and 72.5°, respectively. The number of rings on the crater are calculated in ~36.40 with a initial crater profundity of ~3.35 km, the melt volume is ~1.98¹⁵ m³ or ~1.98⁶ km³. The number of ejected fragments are estimated in ~8.72¹² or ~8722.2 billion of fragments, with average sizes of ~6.33 m, and a cloud of dust with diameter of ~5.68¹³ m or 56.8 billion of km. The total energy in the impact is calculated in ~1.78³² Erg (4.25⁹ megatons). Before of the erosion effects the transient crater is estimated in ~582.5 km, the hydrothermal zone (hydrothermal systems) is of ~9.35 km to 291.2 km from the nucleus of impact, i.e., a hydrothermal zone of ~281.9 km. The lifetimes estimated for this hydrothermal zone are of ~19.7 Ma to ~30.7 Ma with uncertainties of ~±1.36% to ±3.69%, i.e., from ±0.27 Ma to ±1.14 Ma. Hydrothermal temperatures from 0.25 years to 1400 years are estimated in ~366.65 °C to 10.94 °C, respectively. The fragments are ejected to ~3.11⁶ m (3108.5 km) from the impact center, with a velocity of ejection of ~4.21 km/s, ejection angle of ~20.3° and maximum height of ~287.5 km. The density of this asteroid (or comet) is calculated in ~0.386 g/cm³. The seismic shock-wave magnitude is calculated using linear interpolation in ~8.41 in the Richter scale. The maximum time of permanency for the cloud of both dust and acid in the atmosphere is ~15.1 days and 75.5 days, respectively. The temperature peak in the impact is calculated in ~4.09¹⁶ °C (~2.72⁹ times the temperature of the solar nucleus), by a space of time of ~2.4 ms. The pressure in the final crater rim is calculated in ~8.99 GPa, and the pressure to 1 km of the impact point is ~1.70 millions of GPa. The maximum density for the fragments is calculated in ~0.39 g/cm³, and the combined density for these fragments is calculated in ~0.31 g/cm³.

References: [1] Lang N. P. 2007. 38th Lunar and Planetary Science Conference. Abstract #2207. [2] Parker T. J., Grant J. A., Anderson F. S., and Banerdt W. B. 2003. Sixth International Conference on Mars. Abstract #3274. [3] Whelley P. L., Balme M. R., and Greeley R. 2003. Lunar and Planetary Science Conference. Abstract #1769. [4] Echaurren J., and Ocampo A. C. 2003. EGS-AGUEUG Joint Assembly.

5002

EVIDENCE FOR FRACTIONAL CRYSTALLIZATION OF WADSLLEYITE AND RINGWOODITE FROM INDIVIDUAL OLIVINE MELT POCKETS IN CHONDRULES ENTRAINED IN SHOCK MELT VEINS

A. El Goresy¹, M. Miyahara², E. Ohtani², T. Nagase³, M. Nishijima², Z. Washaei⁴, T. Ferroir⁵, Ph. Gillet⁵, L. Dubrovinsky¹, and A. Simionovici⁶.
¹Bayerisches Geoinstitut, Universität Bayreuth, 95447 Bayreuth, Germany. E-mail: ahmed.elgoresy@uni-bayreuth.de. ²Graduate School of Science, Tohoku University, Sendai 980-8758, Japan. ³The Tohoku University Museum, 980-8758 Sendai, Japan. ⁴Institute for Materials Research, Tohoku University, Sendai 980-8758, Japan. ⁵ENS-Lyon, 69364 Lyon, France. ⁶LGIT, Université de Grenoble, 38041 Grenoble, France.

Introduction: Ringwoodite and rare wadsleyite were reported from olivines in shock-melt veins in shocked chondrites [1–4, 7]. Ringwoodite was interpreted to have resulted from shock-induced solid-state phase transformation [1–4, 7]. This agrees with experimental results when both olivine and ringwoodite have identical compositions [e.g., 1]. Many grains however, contain chemically different ringwoodite and olivine [3, 4]. Formation of chemically different polymorphs via solid-state transformation imposes unrealistic time scales (17–500 s) to achieve encountered chemical equilibrium [3]. We investigated squeezed porphyritic olivine chondrules in shock-melt veins in the Peace River L-6 chondrite depicting concentric wadsleyite and ringwoodite intergrowths within parental olivine grains enclosed in unmelted pyroxene (CPX).

Results: Mg-rich wadsleyite (Fa_{06–10}) occupies the cores of the former olivines and is surrounded by zoned Mg-poor ringwoodite (Fa_{28–38}) belts. Wadsleyite cores and ringwoodite belts consist of polygonal crystallites (≤600 nm) of both phases, whereby wadsleyite is much more abundant in the cores than in the ringwoodite belts. ATEM study of FIB-slices reveal no zoning in wadsleyite or ringwoodite crystallites and a sharp compositional gap of Fa_{20–32} at their interfaces. Wadsleyite crystallites (Fa₁₉) surrounded by quenched feathery, poorly crystallized objects with olivine composition (Fa₂₄) at the contact to the CPX indicate that the assemblages evolved through fractional crystallization within melted individual olivines (Fa_{24–26}) in the entrained chondrules. CPX does not display evidence of melting.

Conclusions: Calculation of the duration of the shock event using mineral chemistries of wadsleyite and ringwoodite and experimentally determined solid-state diffusion parameters [5, 6] lead to unrealistic time scales (>500 s). Our results are stark evidence for fractional crystallization of both dense polymorphs from olivine melts at P ≥ 18 GPa and T ≥ 1900 °C. They also cast doubt on studies of zoned ringwoodite veins leading to time scales of ≥ 17 S [4, 7]. We present here the first evidence so far for formation of wadsleyite and ringwoodite by fractional crystallization from individual olivine melts in chondrules.

References: [1] Chen M. et al. 1996. *Science* 271:157–1573. [2] Putnis A. and Price G. D. 1979. *Nature* 280:217–218. [3] Ohtani E. et al. 2006. *Shock Waves* 16:45–52. [4] Chen et al. 2006. *Meteoritics & Planetary Science* 41:731–737. [5] Chakraborty S. et al. 1999. *Science* 283:362–365. [6] Kubo T. et al. 2004. *Physics and Chemistry of Minerals* 31:456–464. [7] Chen et al. 2007. *Earth and Planetary Science Letters* 264:277–283.

5215

MORE CLUES ABOUT THE EPICA—DOME C EXTRATERRESTRIAL EVENTS

C. Engrand¹, B. Narcisi², J.-R. Petit³, E. Dobrică¹, J. Duprat¹, J. Vaubaillon^{4,5}, and F. Colas⁴. ¹CSNSM CNRS-University, Paris Sud, 91405 Orsay Campus, France. E-mail: Cecile.Engrand@csnsm.in2p3.fr. ²ENEA, Centro Ricerche Casaccia, I-00123 Roma, Italy. ³LGGE CNRS-University J. Fourier, BP 96, 38402 Saint Martin d'Hères, France. ⁴IMCCE, Obs. Paris, 75014 Paris, France. ⁵Spitzer Science Center MC 220-6, Caltech, 1200 East California Boulevard, Pasadena, CA 91125, USA.

Introduction: Two extraterrestrial dust layers were recently discovered in two deep Antarctic ice cores (EPICA at Dome C, 75°06'S, 123°21'E [1, 2] and at Dome Fuji, 77°19'S, 39°42'E [3]). These dust layers are dated at 434 ± 6 ka (L1) and 481 ± 6 ka (L2), respectively, for the Dome C events [4], and both ice cores recorded the same two events. We have characterized the structure, mineralogy and chemical compositions of the dust from the two Dome C layers L1 and L2 by scanning electron microscopy, and by electron microprobe.

Results and Discussion: The corresponding incoming flux measured in Dome C ice core are up to 104 times the sporadic cosmic dust flux measured for micrometeorites larger than 30 μm at Dome C [1, 5]. Such high dust fluxes for the short duration recorded in the ice (less than a year) cannot be explained by an increase of the sporadic cosmic dust flux. The two events are then most probably related to impact events. The samples are not mixed with terrestrial matter, strongly suggesting that the impacts occurred on snow or ice. We confirm that the morphology, size distributions, and compositions of the samples from both layers are different [see also 2]. They correspond to two different impact events and it is not yet clear if they can be related to one another. Very large grains (>500 μm) were reported by [3] in the most recent layer of Dome Fuji ice core (i.e., L1). The largest particles in Dome C L1 sample are ~100 μm, suggesting that the impact place for L1 was closer to Dome Fuji than to Dome C.

L2 samples show in average fairly chondritic compositions for all major and minor elements except for Mn which is slightly depleted, and S which is highly depleted (S/Si ~ 0.004 CI). With the noticeable exception of Na and Ni enrichments, the L2 compositions are fairly compatible with that of cosmic spherules (CSs) [e.g., 6]. L1 samples have compositions generally slightly depleted with regard to CI, with Al, Ca, Ti, Na, and S showing larger depletions than the other elements. Although very large (S/Si ~ 0.03 CI), the average S depletion in L1 is about one order of magnitude lower than in L2. The presence of very small spherules (d < 1 μm) in L2 samples, as well as S contents lower than in L1 suggests higher entry/impact velocity for L2 than L1.

The chemical compositions of L1 or L2 do not match simple elemental depletion/enrichment mechanisms (found in CSs) expected from atmospheric entry heating. The possibility of alteration during their stay in the ice as well as interaction with the water vapour plume at high temperature after impact will have to be taken into consideration to explain the complex chemical compositions found in L1 or L2 samples.

References: [1] Narcisi B. et al. 2007. *Geophysical Research Letters* 34:L15502. [2] Engrand C. et al. 2008. 39th Lunar and Planetary Science Conference. Abstract #1554. [3] Misawa K. et al. 2008. 39th Lunar and Planetary Science Conference. Abstract #1690. [4] Parrenin F. et al. 2007. *Climate of the Past* 3:485–497. [5] Duprat J. et al. 2006. *Meteoritics & Planetary Science* 41:A48. [6] Brownlee D. E. et al. 1997. *Meteoritics & Planetary Science* 32:157–175.

5222

CATHODOLUMINESCENCE OF ANORTHITE IN TWO TYPE B CAIS FROM ALLENDE: CONTRASTING ALTERATION PATTERNS

T. J. Fagan, H. Kitou, and Y. Tasai. Department of Earth Sciences, Waseda University, Tokyo, Japan. E-mail: fagan@waseda.jp.

Introduction: Refractory Ca-Al-rich inclusions (CAIs) preserve a record of early, “primary” crystallization over a limited range of high temperatures in the solar nebula followed by poorly constrained “secondary” recrystallization/alteration events [1]. Type B CAIs from the CV3 Allende are noteworthy in this respect because they exhibit texturally distinct secondary minerals, indicating that significant thermal events post-dated primary crystallization [e.g., 2, 3]. More subtle effects of secondary processes are manifested by variable cathodoluminescence patterns of primary anorthite. In general, variable cathodoluminescence (CL) in minerals has been attributed to variations in defect structure and minor element zoning that are often difficult to detect by other means. In this study, we use CL of anorthite to identify different patterns of alteration in two CAIs—one Type B1 and one B2—from Allende.

Analytical Methods: Mineral assemblages and textures in polished thin sections of CAIs 3655A (Type B1) and 4022-1 (B2) were characterized using petrographic microscopes and a JEOL JXA-8900 electron microprobe at Waseda University. Cathodoluminescence (CL) of primary anorthite was studied using a Premier American Technologies Corporation ELM-3 Luminoscope. Covariations between CL brightness and minor element compositions of anorthite were investigated by elemental mapping and quantitative electron probe microanalysis (EPMA). Prior to EPMA, backscattered electron (BSE) images were overlain on CL images and image transparencies were adjusted using imaging software. This procedure was used to ascertain the locations of EPMA points with respect to CL-bright and CL-dark domains in anorthite. Relatively high current (50 nA) and spot size ($8 \times 9 \mu\text{m}$) were used at 15 kV for quantitative analyses in order to detect minor concentrations of Na and Mg in anorthite. Lower limits of detection under these analytical conditions are: Na_2O , 0.011 wt%; MgO , 0.012 wt%.

Results and Discussion: Primary anorthite in both CAIs exhibits blue CL with variable brightness. In CAI 3655A, CL-bright and CL-dark domains tend to have sharp, angular boundaries with simple geometries. The CL-dark domains are enriched in MgO (0.19 versus 0.11 wt%) and Na_2O (0.12 versus 0.08 wt%) compared to CL-bright domains. Primary anorthite in CAI 4022-1 exhibits patchy, irregular CL-bright and CL-dark domains with diffuse boundaries. Quantitative EPMA results do not show a simple distinction that correlates with CL in 4022-1, but elemental mapping suggests that the CL-dark domains are relatively enriched in Na_2O and MgO . The sharp boundaries, simple shapes and well-defined elemental variations of CL patterns in 3655A anorthite suggest that this CAI experienced a simpler, less extensive alteration history than 4022-1. This is consistent with Al-Mg isotopic results and subtle contrasts in textures of secondary minerals [2]. The CL-imaging combined with other data may reflect general differences in alteration histories of Type B1 and B2 CAIs.

References: [1] MacPherson G. J. In *Treatise on Geochemistry*, vol. 1, edited by Davis A. M. pp. 201–246. [2] Fagan T. J. et al. 2007. *Meteoritics & Planetary Science* 42:1221–1240. [3] Ushikubo T. et al. 2007. *Meteoritics & Planetary Science* 42:1267–1279.

5036

CHEMISTRY DURING ACCRETION OF THE EARTH. I. VOLATILES IN THE “STEAM” ATMOSPHERE

Bruce Fegley Jr. and Laura Schaefer. Planetary Chemistry Laboratory, Department of Earth and Planetary Sciences, Washington University, St. Louis, MO 63130, USA. E-mails: bfegley@wustl.edu; laura_s@wustl.edu.

Introduction: The concept of a steam atmosphere generated by impact degassing during Earth’s accretion is over 25 years old [1, 2]. Here we discuss the chemistry of H-, C-, O-, and N-bearing gases in an atmosphere formed by impact degassing of different types of chondritic material.

Methods: We use thermochemical equilibrium and kinetic calculations to model chemistry of the “steam” atmospheres produced by impact degassing of different types of accreting material. Nominal conditions are 1500 K and 100 bar total pressure. We also studied the effects of variable temperature and total pressure. Composition of the accreting material is modeled using average compositions of the Orgueil CI chondrite, the Murchison CM2 chondrite, the Allende CV3 chondrite, average ordinary (H, L, LL) chondrites, and average enstatite (EH, EL) chondrites.

Results: Our results for the nominal T (1500 K) and P (100 bar) are summarized in the table below. Impact degassing of CI and CM chondrites gives H_2O -rich “steam” atmospheres, but all other chondrites studied yield atmospheres dominated by other gases. Degassing of ordinary and EH chondritic material yields H_2 -rich atmospheres with CO and H_2O as the second and third most abundant gases. EL chondritic material gives a CO-rich atmosphere, with H_2 , CO_2 , and H_2O being the next most abundant gases. CV chondritic material gives a CO_2 -rich atmosphere with H_2O as the second most abundant gas. These results predict Earth’s “steam” atmosphere was H_2 -rich. Our results also predict spectroscopically observable gases in the atmospheres of extrasolar terrestrial planets during their accretion. We discuss the chemistry of some rock-forming elements in the “steam” atmosphere in our companion abstract [3].

Table 1. Major gases (volume%) in a “steam” atmosphere at 1500 K and 100 bar total pressure.

Gas	CI	CM	CV	H	L	LL	EH	EL
H_2	4.4	2.7	0.2	48	43	43	44	15
H_2O	69	73	18	19	17	24	17	5.7
CH_4^{a}	~0	~0	~0	0.7	0.7	0.4	0.7	0.2
CO_2	19	19	71	4.0	5.1	5.5	4.7	9.9
CO	3.2	1.8	2.5	27	32	26	31	67
N_2	0.8	0.6	~0	0.4	0.3	0.3	1.3	1.8
NH_3^{b}	~0	~0	~0	~0	~0	~0	~0	~0
H_2S	2.5	2.3	0.6	0.6	0.6	0.7	0.5	0.2
SO_2^{c}	0.1	0.4	7.4	~0	~0	~0	~0	~0
Other	0.2	0.2	1.0	0.3	0.3	0.5	0.6	0.3

^a2% 10^{-7} (CI), 2% 10^{-8} (CM), 8% 10^{-11} (CV).^b5% 10^{-6} (CI), 2% 10^{-6} (CM), 8% 10^{-9} (CV), 0.01(H), 0.01(L), 9% 10^{-5} (LL), 0.02(EH), 5% 10^{-5} (EL).^c1% 10^{-8} (H), 1% 10^{-8} (L), 3% 10^{-8} (LL), 1% 10^{-8} (EH), 1% 10^{-8} (EL).

Acknowledgments: This work is supported by the NASA Astrobiology and Origins Programs.

References: [1] Abe Y. and Matsui T. 1985. Proceedings, 15th Lunar and Planetary Science Conference. pp. C545–C559. [2] Lange M. A. and Ahrens T. J. 1982. *Icarus* 51:96–120. [3] Schaefer L. and Fegley B. 2008. *Meteoritics & Planetary Science* 43. This issue.

5077

EXTRACTING COMPOSITIONS FROM RAMAN SPECTRA OF RINGWOODITE IN THE HEAVILY SHOCKED GROVE MOUNTAINS METEORITES

L. Feng and Y. Lin. Key Laboratory of the Earth's Deep Interior, Institute of Geology and Geophysics, Chinese Academy of Sciences, Beijing 100029, China. E-mail: LinYT@mail.igcas.ac.cn.

Introduction: MicroRaman spectroscopy is a powerful tool of identifying high-pressure polymorphs of minerals found in heavily shocked meteorites. Moreover, previous measurements of Raman spectra of olivine, pyroxene and oxides demonstrated significant peak shifts related to compositions [1–4]. This feature has potential applications for simultaneous measurements of structures and compositions of extraterrestrial materials in future space exploration [5, 6]. Here we report the first discovery of Raman wavenumber shifts of ringwoodite, the spinel-structured high-pressure polymorph of olivine, resulting from Fe and Mg cation substitution. We develop calibration equations to obtain compositions of ringwoodite from Raman peak shifts.

Results: Ringwoodite studied in this work was mainly found in the heavily shocked Grove Mountains (GRV) 052049 meteorite (L6) [7]. It usually occurs as rims of olivine grains in rounded clasts entrained in shock-induced melt veins. In back-scattered electron image mode of SEM, the ringwoodite grains show different brightness even within same assemblages, suggestive of a wide range of composition. Quantitative analyses of the ringwoodite grains were carried by EPMA, leading to Fo-contents (Mg/Mg + Fe atomic ratio) ranging from 73 mol% down to 19 mol% in comparison with the homogeneous olivine ($\text{Fa}_{24.0 \pm 0.4}$) in the host meteorite. MicroRaman spectra of these grains with known Fo-contents were measured. They show two strong bands close to 790 cm^{-1} (labeled as DB1) and 840 cm^{-1} (labeled as DB2), and weak one close to 290 cm^{-1} (labeled as SB0). Other bands at 370 cm^{-1} and 600 cm^{-1} [8] are very weak.

The DB1 position of ringwoodite varies monotonically with composition, increasing from $78+1 \text{ cm}^{-1}$ to 799 cm^{-1} with the Fo-content from 19 mol% to 71 mol%. DB2 has only a small shift, and it can be affected by the coexisting olivine that has a strong band between $838\text{--}857 \text{ cm}^{-1}$ [1]. SB0 is weak but was clearly identified. Its position also varies with composition, and the peak shift range is about 15 wavenumber, increasing from 284 cm^{-1} to 299 cm^{-1} with increasing Fo-content from 19 mol% to 71 mol%. Preliminary analysis of the raw paired Raman and EPMA data derived equations of: (1) Fo mol% (DB1) = $4.483X_1 - 1258$ ($r_2 = 0.84$), and (2) Fo mol% (SB) = $2.996X_0 - 2325$ ($r_2 = 0.78$), where X_1 and X_0 refer to DB1 and SB0 positions.

Potential Applications: The monotonic relationship between Raman band shifts and composition of ringwoodite may be used to identify structure and composition of ringwoodite in future space exploration. It also provides with a possibility of online determining composition of ringwoodite growing in diamond anvil cell.

References: [1] Kuebler K. E. et al. 2006. *Geochimica et Cosmochimica Acta* 70:6201–6222. [2] Wang A. et al. 2001. *American Mineralogist* 86:790–806. [3] Wang A. et al. 2004. *Journal of Raman Spectroscopy* 35:504–514. [4] Smith D. C. 2005. *Spectrochimica Acta Part A* 61:2299–2314. [5] Haskin L. A. et al. 1997. *Journal of Geophysical Research* 102:19293–19306. [6] Hochleitner R. et al. 2004. *Journal of Raman Spectroscopy* 35:515–518. [7] Feng L. et al. 2007. *Meteoritics & Planetary Science* 42:A45. [8] McMillan P. and Akaogi M. 1987. *American Mineralogist* 72:361–364.

5066

A TESTBED FOR ADVANCED COLD CURATION OF ASTROMATERIALS

L. A. Fletcher¹, R. Bastien², and C. C. Allen¹. ¹ARES, Mail Code KT, NASA Johnson Space Center, Houston, TX 77058, USA. E-mail: lisa.a.fletcher@nasa.gov. ²Jacobs Technologies, 2224 Bay Area Boulevard, Houston, TX 77058, USA.

Introduction: The NASA Astromaterials Curation Facility at the Johnson Space Center is responsible for the curation of all astromaterial sample return collections and includes state-of-the-art processing of these samples for allocation to the scientific community. Unique challenges to traditional curation practices are being raised with planned missions to return cold samples from the Moon, Mars, comet nuclei and other icy bodies. These missions will require performing curation processes in a clean, controlled thermal environment. In anticipation of these types of unique samples, we have installed a new advanced curation laboratory to explore the feasibility of curating samples under cold, clean conditions [1]. The primary motive for this effort is to understand the potential challenges associated with processing samples cold while quantifying and minimizing organic and inorganic contamination levels.

Results and Discussion: The laboratory consists of a controlled-atmosphere, custom-designed stainless steel glovebox equipped with a $-35 \text{ }^\circ\text{C}$ freezer and $-35 \text{ }^\circ\text{C}$ cold plate for sample storage and manipulation at cold temperatures [1]. Our initial experiments have focused on measuring the thermal profile surrounding the cold plate working surface and determining sublimation rates from ice samples into the dry nitrogen purged environment of the glovebox. With the current configuration, there is a strong thermal gradient around the cold plate such that the working temperature decreases to $0 \text{ }^\circ\text{C}$ less than 1 cm above the cold plate surface. Measured sublimation rates from ultrapure water ice samples are on the order of 1% mass lost each successive 24 h period.

The cold plate is a potential source of organic contamination of samples because it may act as a “getter” for volatile organic compounds in the glovebox environment. To quantify the level of organic contamination, we are analyzing organic-free silicon witness plates exposed to the nitrogen glovebox environment using thermal desorption-gas chromatography-mass spectrometry (TD-GC-MS). These results are compared with baseline data obtained from previous organic analyses conducted inside curation gloveboxes within the Lunar, Meteorite and Genesis Curation Laboratories. We are particularly interested in the comparison of the types and abundances of organic species that adhere to the clean silicon surface when placed on the cold plate versus the warmer overall box environment. In addition to organic analyses, we are also investigating the trace metals in various locations within the glovebox environment using inductively coupled plasma–mass spectrometry (ICP-MS) of witness plates.

A series of additional experiments with simulants and astromaterial samples are planned. Now that contamination levels are better understood, efforts to reduce these levels are underway so that cold curation may be offered as a service to the community in the near future.

References: [1] Fletcher L. A. et al. 2008. 39th LPSC. Abstract # 2202.

5008

C-ANOMALOUS PHASES IN QUE 99177 AND MET 00426

Christine Floss and Frank J. Stadermann. Laboratory for Space Sciences and Physics Department, Washington University, St. Louis, MO 63130, USA. Email: floss@wustl.edu; fjs@wustl.edu.

Introduction: Carbon-rich phases (e.g., nanodiamonds, SiC, graphite) were the first forms of stardust identified in primitive meteorites [1–3] and, with the exception of nanodiamonds, are usually present in concentrations of ≤ 10 –20 ppm [e.g., 4]. We have been investigating the stardust inventories of two primitive CR chondrites, QUE 99177 and MET 00426, which have very high abundances of O-anomalous presolar grains [5, 6]. Here we report on the C-bearing presolar phases found in these two meteorites.

Experimental and Results: We used the NanoSIMS to carry out isotopic (C,O and C,N) imaging on matrix material in QUE 99177 and MET 00426 and found 34 and 35 grains with anomalous C isotopic compositions, respectively, in the two meteorites. Of the 69 grains, 43 are ^{13}C -rich with $^{12}\text{C}/^{13}\text{C}$ ratios between 5 and 82, similar to ratios observed in mainstream and type A + B SiC grains [4]. The remaining 26 grains are ^{12}C -rich, with $^{12}\text{C}/^{13}\text{C}$ ratios between 100 and 136. Nitrogen isotopes were measured in 35 of the grains. Grains that are ^{13}C -rich typically have low N abundances with normal N isotopic compositions, although two grains are ^{14}N -rich and one is ^{15}N -rich. In contrast, ^{12}C -rich grains tend to contain more N and are more likely to have anomalous N isotopic compositions (generally ^{15}N -rich).

Auger Nanoprobe elemental analyses show that the grains can be broadly divided into two subgroups: those that are very C-rich and those with lower C abundances. C-rich grains are usually dark with irregular shapes in secondary electron (SE) images, and typically have Auger spectra that are dominated by C, but also contain some N and/or O. Most of the grains with isotopically light C and heavy N fall into this category, although there are exceptions.

Grains with lower C abundances, most of which are ^{13}C -rich, are often light-colored or are difficult to distinguish from surrounding material in the SE images. Some of these have been clearly identified as SiC. In other cases, a positive identification is lacking, but elemental maps combined with isotopic characteristics also suggest SiC.

Discussion: Estimates of the abundance of SiC are ~ 20 –50 ppm in QUE 99177 and ~ 30 –110 ppm in MET 00426, higher than previous maximum estimates for primitive meteorites [7, 8]. The presence of large amounts of carbonaceous material with C (and often N) isotopic anomalies is unexpected. Similar phases have been found in IDPs [9] and primitive meteorites [10], and are usually thought to have an interstellar origin [e.g., 9]. However, the abundances found here (~ 60 –140 ppm) are unprecedented and, together with high SiC abundances, attest to the primitive nature of these meteorites.

References: [1] Lewis R. S. et al. 1987. *Nature* 326:160–162. [2] Bernatowicz T. et al. 1987. *Nature* 330:728–730. [3] Amari S. et al. 1990. *Nature* 345:238–240. [4] Zinner E. 2004. In *Treatise in Geochemistry*, vol 1., edited by A. M. Davis. pp. 17–39. [5] Floss C. and Stadermann F. J. 2007. *Meteoritics & Planetary Science* 42:A48. [6] Floss C. and Stadermann F. J. 2008. Abstract #1280. 39th Lunar and Planetary Science Conference. [7] Gao X. et al. 1996. *Meteoritics & Planetary Science* 31:A48. [8] Huss G. et al. 2003. *Geochimica et Cosmochimica Acta* 67:4823–4848. [9] Floss C. et al. *Science* 303:1355–1358. [10] Busemann H. et al. 2006. Abstract #2005. 37th Lunar and Planetary Science Conference.

5086

TRANSANTARCTIC MOUNTAIN MICROTEKTITES: NEW PETROGRAPHIC DATA, WATER CONTENT, AND Nd AND Sr ISOTOPIC COMPOSITION

L. Folco¹, M. D'Orazio², L. Ottolini³, S. Tonarini⁴, and P. Rochette⁵. ¹MNA-SI, Italy. E-mail: folco@unisi.it. ²DST, Università di Pisa, Italy. ³CNR-IGG, Pavia, Italy. ⁴CNR-IGG, Pisa, Italy. ⁵CEREGE, France.

We expand on the characterization of the recently discovered microtektites from the Transantarctic Mountains [1] by providing new petrographic data on newly identified microtektites, as well as the water content and Nd and Sr isotopic composition of a representative set of microtektites.

High Magnesium Microtektites: Of the 55 sectioned microtektites in the 300–800 μm size range analyzed to date by EMP, 52 are pale yellow transparent glass spheres with SiO_2 ranging from 64 wt% to 78 wt% and with $\text{MgO} < 5$ wt%. The other 3 microtektites are pale green transparent glass spheres with a lower SiO_2 content in the 59 to 61 wt% range and a higher MgO content in the 11 to 13 wt% range. The two compositional groups are similar to the normal and high magnesium microtektite types in the Australasian microtektite population [2, 3].

Silica-Rich Inclusions: In one of the 500 μm diameter microtektites studied by EMP, we found a rounded Si-rich, glassy inclusion 40 μm in diameter. The silica content of the inclusion ($\text{SiO}_2 = 90$ wt%) differs significantly from that of the host particle ($\text{SiO}_2 = 70$ wt%). Almost pure silica glassy inclusions, namely lechatelierite, have often been reported in microtektites [2, 4]. We interpret the newly identified inclusion as a lechatelierite-like inclusion which was partly digested during the high temperature regime of the microtektite-forming process.

Water Content: The water content of 12 microtektites obtained by means of SIMS analyses ranges from 28 to 206 ppm (avg. 85 ± 58 ppm). The lowest values were observed in the three high-magnesium microtektites (28–44 ppm). Transantarctic Mountain microtektites are thus essentially dry, like tektites [5] and unlike volcanic glasses with a similar silica content. There is no literature data on the water content of microtektites in the literature; however, a comparison with the limited literature database [5] for macroscopic tektites from the four known strewn fields (North American, Central European, Ivory Coast, and Australasian) reveals that the water content of Transantarctic Mountain microtektites is similar to that of Australasian tektites (40–300 ppm).

Sr and Nd Isotopic Composition: Two multigrain samples (10 microtektites totaling about 2.5 mg) analyzed by means of conventional TIMS gave $^{87}\text{Sr}/^{86}\text{Sr} = 0.71622 \pm 1$ (2σ) and 0.716372 ± 1 (2σ) and a $^{143}\text{Nd}/^{144}\text{Nd} = 0.51209$ ($2\sigma = 3$). Their $\epsilon_{\text{Sr}} = 166$ and 169 and their $\epsilon_{\text{Nd}} = -10.7$ clearly fall in the Australasian tektite range [6].

Conclusions: New data strengthens our previous conclusions [1] that Transantarctic Mountain microtektites are indeed microtektites and that they represent the southern extension of the Australasian tektite/microtektite strewn field.

Acknowledgements: This work was supported by PNRA.

References: [1] Folco L. et al. 2008. *Geology* 36:291–294 [2] Cassidy W. A. et al. 1969. *Journal of Geophysical Research* 74:1008–1025. [3] Glass B. P. et al. 2004. *Geochimica et Cosmochimica Acta* 68:3971–4006. [4] Koeberl C. et al. 1997. *Geochimica et Cosmochimica Acta* 61:1745–1772. [5] Beran A. and Koeberl C. 1997. *Meteoritics & Planetary Science* 32:211–216. [6] Shaw H. F. and Wassenburg G. J. 1982. *Earth and Planetary Science Letters* 60:155–177.

5194

AN ACHONDRITIC CLAST IN THE PEACE RIVER L CHONDRITE

J. M. Friedrich^{1,2} and C. D. K. Herd³. ¹Department of Chemistry, Fordham University, Bronx, NY, USA. ²Department of Earth and Planetary Sciences, American Museum of Natural History, New York, NY, USA. E-mail: friedrich@fordham.edu. ²Department of Earth and Atmospheric Sciences, University of Alberta, Edmonton, Alberta, Canada.

Introduction: We report on the mineralogy, petrology and geochemistry of an achondritic clast within the Peace River L6 chondrite to provide insights into conditions of partial melting within asteroids. The cm-scale clast is gray and fine-grained and is in sharp contact with the host chondrite. Two submillimeter veins cut across both the clast and host, indicating that the clast formed prior to the impact (shock) event(s) that produced the numerous veins present in Peace River [e.g., 1].

Methods: Electron microprobe analyses were performed at the University of Alberta on the JEOL 8600 microprobe. We performed trace element analyses on mechanically separated clast and host materials with the ThermoElectron X Series II ICPMS at Fordham University using proven methods [2].

Results and Implications: On the basis of mineral compositions, the clast and the host are indistinguishable, with olivine averaging Fo₇₅ and pyroxene Wo₁En₇₇Fs₂₂. Plagioclase ranges from Ab₇₆An₁₂Or₁₂ to Ab₈₆An₁₁Or₃. Chromite is Chr₇₃₋₇₄Usp₁₅₋₁₆Sp₁₀Mt_{<1}. In contrast, differences in the modal mineralogy between host and clast are apparent. Within the chondrite host, opaques (chromite, kamacite, taenite and troilite) comprise 6% of the rock, whereas these minerals comprise <2% of the clast. Opaques in the host consist of 21% kamacite, 8% taenite, 50% troilite, and 21% chromite. In contrast, the clast opaques consist of 9% kamacite, 6% taenite, 37% troilite, and 48% chromite.

There is a significant difference between clast and host texture. The clast is porphyritic, consisting of olivine phenocrysts 20 to 500 microns across with interstitial orthopyroxene, plagioclase, opaques and minor chlorapatite. The host has a typical L6 texture, with relict chondrules, relatively coarse interstitial plagioclase and coarse opaques.

Bulk trace element results show clast refractory siderophile abundances (W, Re, Ir, Mo, Ru, Pt) are uniformly depleted to ~20% that of the L chondrite host. Interestingly, REE are uniformly present at about 0.6 × L mean abundances, but other refractory lithophiles (Hf, Zr, Sc, Nb, V, Sr, Ba) show more variable contents (1.0–1.4 × L chondrite). Clast Te/Se ratios are reminiscent of the impact melts Shaw and Chico [3, 4], which show lower ratios than unshocked L chondrites. Moderately volatile elements such as Ga, Sb, Sn, Rb, Cs, and Zn are highly variable in the clast indicating a lack of strict volatility-controlled loss of the more thermally mobile elements.

Taken together, mineralogy, petrology and trace element chemistry strongly suggest the observed igneous nature of the clast was produced by partial melting of host chondrite-like material, followed by relatively slow crystallization.

References: [1] Chen M. and El Goresy A. 2000. *Earth and Planetary Science Letters* 179:489–502. [2] Friedrich J. M. et al. 2004. *Geochimica et Cosmochimica Acta* 68:2889–2904. [3] Taylor G. J. et al. 1979. *Geochimica et Cosmochimica Acta* 43:323–337. [4] Yolcubal I. et al. 1997. *Journal of Geophysical Research* 102:21589–21611.

5091

IMPACT-RELATED PREFERRED 3-D ORIENTATION OF METAL GRAINS IN L CHONDRITES

J. M. Friedrich^{1,2}, D. P. Wignarajah¹, S. Chaudhary¹, M. L. Rivers³, C. E. Nehru^{2,4}, and D. S. Ebel². ¹Department of Chemistry, Fordham University, 441 East Fordham Road, Bronx, NY 10458, USA. ²Department of Earth and Planetary Sciences, American Museum of Natural History, 79th Street at Central Park West, New York, NY, USA. ³Consortium for Advanced Radiation Sources, University of Chicago, Argonne, IL 60439, USA. ⁴Department of Geology, Brooklyn College, CUNY, Brooklyn, NY 11210, USA.

Introduction: Ordinary chondrites originate in the inner asteroid belt [1] and comprise about 85% of all known meteorites [2]. Information about the physical evolution of small solar system bodies can be gathered by examining ordinary chondrites. To examine the role of impacts in the evolution of asteroids, we have performed a three dimensional (3-D) petrographic study of the morphology and distribution of Fe(Ni) metal and related sulfide phases in a suite of L chondrites that experienced varying degrees of shock loading. There is already strong evidence that petrofabrics seen in chondrites are impact-related [3]. Here, we use 3-D orientation results to examine peak impact pressures necessary for foliation development in the L chondrite parent body or bodies.

Methods: We used synchrotron X-ray computed microtomography (XMT) at the GSECARS 13-BM beamline located at the Advanced Photon Source of Argonne National Laboratory to collect high-resolution tomographic data on 29 L chondrites. Volumetric (voxel) resolutions ranged from 8.4 to 18.8 μm/voxel. [4, 5] provide meteorite-specific data collection and post-processing details. To extract quantitative data from our volumetric representations, we used the BLOB3D software tool [6]. After digitally isolating each metal grain within our L chondrite volumes, we constructed a best-fit ellipsoid around them [6] to examine their degree of common orientation. To quantify the degree of orientation independent of the number of particles in our volumes, we use a normalized R (mean vector) metric [7]: the higher the R, the greater the common orientation of ellipsoid major axes within a volume.

Results and Implications: Degree of preferred orientation increases from an R of 0.7% in the case of Baszkówka (L5, S1) to 12.9% in the case of Bluff (L5, S6). Additional samples show a progressive increase in R with higher shock stage. Our results confirm that deformation resulting from uniaxial dynamic compaction is the most likely mechanism for the development of foliation in chondrites, as was concluded in [3]. By examining the evolving 3-D orientation of metal grains in L chondrites exhibiting increasing degrees of shock loading, we will show that the introduction of petrofabrics to chondrites—from the perspective of metal grains—can be accomplished with peak pressures of ~5 GPa, with shock pressure calibrations based on [8].

References: [1] Bottke W. F. et al., eds. 2002. *Asteroids III*. Tucson: The University of Arizona. [2] Grady M. M. 2000. *Catalogue of meteorites*. Oxford. [3] Gattacceca et al. 2005. *Earth and Planetary Science Letters* 234: 351–368. [4] Ebel D. S. and Rivers M. L. 2007. *Meteoritics & Planetary Science* 42:1627–1646. [5] Friedrich et al. 2008. *Planetary and Space Science*. In press. [6] Ketcham R. A. 2005. *Geosphere* 1:32–41. [7] Higgins M. D. 2006. *Quantitative textural measurements in igneous and metamorphic petrology*. Cambridge. [8] Stöffler D. et al. 1991. *Geochimica et Cosmochimica Acta* 55:3845–3867.

5182

SIMULTANEOUS ENHANCEMENT OF WATER VAPOR AND SILICATE DUST IN THE INNER SOLAR NEBULA: IMPLICATION FOR THE SMALL OXYGEN ISOTOPIC VARIATION OF CHONDRULES

T. Fukui and K. Kuramoto. Department of Cosmochemistry, Hokkaido University, Sapporo 060-0810, Japan. E-mail: ftakashi@ep.sci.hokudai.ac.jp.

Introduction: The large oxygen isotopic deviation between CAIs and chondrules [1] is possibly explained by the “water vapor enhancement model” [2]. In this model, enhancement of $^{17,18}\text{O}$ -rich water vapor relative to ^{16}O -rich CO gas gradually changes the local mean isotopic composition in the inner solar nebula from the solar (CAIs-like) composition to $^{17,18}\text{O}$ -rich (chondrules-like) one. The enhanced $^{17,18}\text{O}$ -rich H_2O , produced by the CO self-shielding in the parent molecular cloud [2] or the outer nebula [3], is supplied by sublimation of icy content in dust particles drifting from the cold outer nebula due to gas drag [4]. However, this model seems to predict large oxygen isotopic variation of chondrules, because temporal and spatial variation of the water vapor concentration would considerably remain in the chondrule formation epoch. This prediction is obviously inconsistent with observation [1]. In this study, we suggest that the cause of the discrepancy would be addressed to ignoring simultaneous enhancement of silicate dust in the inner nebula.

Enhancement of Silicate Dust: Radial transport of dust particles strongly depends on the typical size of them at each location in the disk. We assume that the size is determined at which the mutual collision velocity induced by turbulence (also the function of the size) equals the threshold collision velocity for sticking [5], which is obtained theoretically [6] and experimentally [7]. Our model suggests that dust particles get smaller after removal of their icy mantle because silicate dust is less stickier than ice-covered dust [6]. If this is the case, radial transport of silicate dust is rapidly decelerated at the ice line. This leads to enhancement of silicate dust in the inner nebula, as well as water vapor.

Results: Considering the effect of the silicate dust enhancement, we simulate the time-dependent oxygen isotopic evolution in the inner nebula. For the typical nebula and material parameters, the size of silicate dust particles is consistent with the typical chondrule size. The local mean oxygen isotopic composition in the inner nebula evolves toward $^{17,18}\text{O}$ -rich associated with enhancement of water vapor and silicate dust relative to CO gas within the first ~ 1 Myr. In this epoch, the large deviation between CAIs and chondrules would be created. During the next ~ 2 Myr, in contrast, temporal and spatial variation in the oxygen isotopic composition is small. This is explained as follows: the silicate dust particles are so small that their motion is well coupled with that of the nebula gas. Enhancement of silicate dust is thus almost same degree as that of water vapor. When the degree of enhancement is large, the local mean oxygen isotopic composition is almost determined as the average of $^{17,18}\text{O}$ -rich water vapor and solar-like silicate dust weighted by their solar abundance ratio. Chondrules would be produced in this epoch, and thus have mostly small oxygen isotopic variation.

References: [1] Clayton R. N. 1993. *Annual Review of Earth and Planetary Science* 21:115–149. [2] Yurimoto H. and Kuramoto K. 2004. *Science* 305:1763–1766. [3] Lyons J. R. and Young E. D. 2005. *Nature* 435:317–320. [4] Adachi I. et al. 1976. *Progress of Theoretical Physics* 56:1756–1771. [5] Fukui, T. et al. 2008. Abstract #1557. 39th Lunar and Planetary Science Conference. [6] Dominik C. and Tielens A. G. G. M. 1997. *The Astrophysical Journal* 480:647–673. [7] Langkowski D. et al. 2008. *The Astrophysical Journal* 675:764–776.

5330

RELATIONSHIPS AMONG UNGROUPED PRIMITIVE ACHONDRITES AND TYPE 7 ORDINARY CHONDRITES

K. G. Gardner-Vandy¹, D. S. Laurretta^{1,2}, J. S. Goreva¹, M. Killgore², and T. J. McCoy³. ¹The University of Arizona, Tucson, AZ, USA. E-mail: kgardner@lpl.arizona.edu. ²Southwest Meteorite Center, USA. ³Smithsonian Institution, USA.

Introduction: An appreciable number of meteorites exist that have been classified as either ungrouped primitive achondrites or type 7 ordinary chondrites (OCs). We are studying the genesis of the FeO-rich primitive achondrites and brachinites, and a comparison of these meteorites to the highly metamorphosed and FeO-rich OCs is needed to fully understand the metamorphism and partial melting that occurred on FeO-rich parent bodies. Here we compare the petrology and geochemistry of several of these meteorites and assess whether or not these meteorites experienced a similar metamorphic history. We also assess the validity of the type 7 designation.

Samples and Techniques: We consider four meteorites. Roberts Massif (RBT) 04239 is an ungrouped achondrite. Lewis Cliff (LEW) 88663 is an L7 [1]. LEW 88763 is an ungrouped primitive achondrite with chemical similarities to the brachinites [2–3]. Allan Hills (ALH) 84027 is tentatively classified as LL7. We obtained thin sections and bulk chips for each for analysis on the Cameca SX50 electron microprobe at LPL for mineral compositions and distribution and the Thermo Finnigan Element2 ICP-MS at LPL for bulk elemental abundances.

Results: RBT 04239 has Fe,Ni-FeS veinlets surrounding most of its grains, similar to the ungrouped primitive achondrite Divnoe, in addition to relict chondrules, and it has silicate and O-isotopic compositions in the L-chondrite range [2]. LEW 88663 has a recrystallized texture with a few relict chondrules, with L-chondrite lithophile and siderophile abundances and L-chondrite O-isotopic composition [1]. LEW 88763 has a recrystallized texture with a flat $\sim 0.9 \times$ CI-chondrite REE pattern, a silicate composition similar to the brachinites and an O-isotopic composition in line with the CR chondrites [2–3]. ALH 84027 has a recrystallized, granular texture of olivine, plagioclase, pyroxene, troilite, chromite and metal; a few poorly-defined relict chondrules are present. The average olivine composition is $\text{Fa}_{28.1}$, low-Ca pyroxene is $\text{En}_{74.4}\text{Wo}_{2.5}$, and plagioclase is $\text{An}_{10.9}\text{Ab}_{84.5}$. The composition of high-Ca pyroxene is $\text{En}_{49}\text{Wo}_{41}$ [4]. The metal grains in ALH 84027 are diverse, containing between 4 and 37 wt% Ni. The O-isotopic composition of ALH 84027 is unknown.

Discussion: Even though RBT 04239 is the only one of these four meteorites to show melt mobilization (in the form of Fe,Ni-FeS veinlets), all should be considered primitive achondrites because they have “achondritic textures but retain a chemical affinity to their chondritic precursors” [5]. All four are highly metamorphosed, RBT 04239 having experienced the initial stage of partial melting. Inconsistencies between the primitive achondrite and OC type-7 designations are likely due to multiple working definitions of the term primitive achondrite, and we hope to address this issue in the future. In addition, we do not support the use of the current, nondescript type 7 designation.

References: [1] Mittlefehldt D. W. and Lindstrom M. M. 2001. *Meteoritics & Planetary Science* 36:439–457. [2] Gardner K. G. et al. 2007. Abstract #2086. 38th LPSC. [3] Swindle T. D. et al. 1998. *Meteoritics & Planetary Science* 33:31–48. [4] Schwarz C. et al. 1985. Antarctic Meteorite Newsletter 8. [5] Weisberg M. K. et al. 2006. In *MESS II*, edited by Laurretta D. S. and McSween H. Y.

5306

SMALL-SCALE COMPOSITIONAL VARIABILITY OF THE BULK ALLENDE METEORITE

M. Gellissen¹, H. Palme¹, and J. Zipfel². ¹Institut für Geologie und Mineralogie, Universität zu Köln, Germany. E-mail: herbert.palme@uni-koeln.de. ²Forschungsinstitut und Naturmuseum Senckenberg, Frankfurt am Main, Germany.

Introduction: Carbonaceous chondrites have two major components, matrix and chondrules, with the chondrule fraction increasing from CI to CV3 from almost zero to about 50%. There is a large variability in the composition of mm-sized chondrules, and alteration of fine-grained matrix also introduces inhomogeneities on a mm to cm scale. In order to study the effect of these inhomogeneities on the bulk chemical composition at a scale of cm we determined the chemical composition of 39 individual bulk samples from a single piece of Allende, covering a large sample volume.

Samples and Analytical Procedures: We started with a 4 mm thick slice of the Allende meteorite covering an area of 22.5 cm² and with a mass of 30 grams. The slice was cut into 39 equally sized pieces with an average sample weight of 600 mg, corresponding to a cube of 6 mm length. Each individual sample was powdered. Aliquots of 120 mg were taken for XRF analyses. Analytical procedures were similar to those applied by [1].

Results: Of the 39 samples two were unusual, one sample was dominated by a CAI and another by a dark inclusion. These two samples were excluded from further considerations. The average major element composition of 37 mm sized samples is very similar to that obtained by earlier studies [2]. Si- and Mg-contents were 16.01% and 14.94% with standard deviations of 0.94% and 1.35%, barely above analytical uncertainty. Concentrations of Al 1.59 (s.d. 17%) and Ca 1.71% (s.d. 9%) are somewhat more variable. Ca and Na show similar and largely correlated variations. The concentration of Fe (total) is with 23.65% and a standard deviation of 2.6% extremely constant.

Discussion: The small standard deviations for Mg, Si, and Fe in our study and the excellent agreement with results from earlier studies [1, 2] reflect the very homogenous composition of bulk Allende even on a mm to cm-scale. Alteration effects are limited to less than 5 mm. The presence of very large chondrules, cm-sized CAIs and dark inclusions would cause larger deviations. These large objects must be rare and are not endmembers of a continuous size distribution, they are clearly exotic. Thus, large cm-sized CAIs contribute less than 10% to the bulk Al content of Allende. If smaller CAIs are responsible for the range in Al-contents, about 3% of CAIs would be required, in agreement with new estimates for CAIs in CV-chondrites (2.98% by area) by [3] and lower than the CAI estimate of [4] (3.93% by area). The bulk of Al in Allende is in chondrules and matrix and not in CAIs.

References: [1] Wolf D. and Palme H. 2001. *Earth and Planetary Science Letters* 36:559–571. [2] Klerner S. and Palme H. 1999. 30th Lunar and Planetary Science Conference. Abstract #1272. [3] Hezel D. et al. 2008. *Meteoritics & Planetary Science*. Submitted. [4] Ebel D. et al. 2008. 39th Lunar and Planetary Science Conference. Abstract #2120.

5249

BARRED OLIVINE CHONDRULE FRAGMENTS AMONG MICROMETEORITES

M. J. Genge¹ and S. Taylor². ¹Impact and Astromaterials Research Centre, Department of Earth Science and Engineering, Imperial College London, Exhibition Road, London SW7 2AZ, UK. E-mail: m.genge@imperial.ac.uk. ²U.S. Army Cold Regions Research and Engineering Laboratory, Hanover, New Hampshire 03755, USA.

Introduction: Micrometeorites (MMs) are large interplanetary dust particles that survive atmospheric entry to be recovered from the Earth's surface. Among these particles are coarse-grained MMs (cgMMs), which are dominated by pyroxene, olivine and/or glass and often have igneous textures. Minor element compositions of olivines, pyroxenes and accessory phases from these particles suggest ~70% of cgMMs are derived from an ordinary chondrite (OC)-like chondrule population [4].

The most significant difference between CgMMs and OC-chondrules is the low abundance of fragments of barred olivine materials amongst cgMMs—only a single particle being reported to date. Barred olivine chondrules are, in contrast, relatively common (~4% of chondrules) within ordinary chondrites [5]. This paper reports the discovery of new barred olivine cgMMs.

Results: Three cgMMs with BO textures (Figs. 1a and 1b) were previously misclassified among a collection of 527 MMs as radiating pyroxene (RP cgMMs; Fig. 1c) due to their fine grain-size (<5 µm). Repeat EDS analyses, however, confirm the particles consist of bars of olivine contained poikilolitically within low-Ca pyroxene.

The textures of all three particles comprise discontinuous subparallel bars of olivine within a polycrystalline pyroxene host. Two of the particles (CP94-050-214 and CP94-050-171) have olivine bars that have diverging orientations producing textures that resemble radiate pyroxenes. Barred olivine chondrules can likewise contain several domains of parallel olivine which diverge at their intersections. Particle CP94-050-056 exhibits a central region of equant olivine with parallel bars of olivine at the margins of the particle. Accessory phases in the BO particles include aluminosilicate glass and chromian spinel. Discontinuous magnetite rims are observed on two of the particles and confirm these particles are extraterrestrial.

Discussion: Interstitial pyroxene is relatively common within BO chondrules where it often occurs as dendritic crystals that poikilolitically enclose barred olivine. The absence of “typical” BO CgMMs with interstitial regions dominated by glass is problematic but may be the result of preservation factors.

Implications: The identification of BO CgMMs among MMs suggests a minimum abundance of 3% of chondrule-derived dust is similar to that of BO chondrules within ordinary chondrites. Furthermore, the abundance of RP particles is reduced to 7% of cgMMs similar to RP chondrules in ordinary chondrites. These data strongly support the interpretation of the majority of cgMMs as fragments of chondrules from an OC-like population.

Models of the delivery of asteroidal dust to Earth suggest that the majority of dust particles are derived from the dust bands associated with the Veritas, Themis, and Koronis asteroid families [3]. The Koronis asteroids are S-type asteroids and are, thus, likely to be the parent bodies of OC-like dust.

References: [1] Genge. 2006. 37th LPSC. Abstract #1759. [2] Brearley and Jones. 1998. *Min. Soc. Am.* 36. [3] Nesvorný et al. 2003. *The Astrophysical Journal* 591:486.

5057

COOLING RATES OF METEORITIC METAL—PROGRESS AND THE FUTURE

J. I. Goldstein. Department of Mechanical and Industrial Engineering, University of Massachusetts, Amherst, MA, USA. E-mail: jig0@ecs.umass.edu.

The metallographic cooling rate model simulates the growth of kamacite in taenite and the distribution of Ni in these two phases during the growth process, from ~650 °C to ~400 °C during cooling within a parent asteroidal body. The taenite profile-matching method [1] and the taenite central Ni content method [2] are applied to determine the cooling rates in this temperature range. Recent advances in the cooling rate models include the recognition of the importance of P in the growth of kamacite which controls the reaction path and the nucleation temperature, the measurement of more accurate diffusion coefficients, and the measurement of the orientation of kamacite/taenite interfaces to the plane of polish which improves the accuracy of the distance scale along the diffusion gradient. As the accuracy of the metallographic cooling rate model has improved, the measured cooling rates for a given meteorite have increased by about a factor of 100 from measurements made in the 1960s. The uncertainty in the cooling rate measurement (two standard deviations) has an apparent limitation of no better than ±30%, but is often much larger, ±100%. Measured metallographic cooling rates have been used to determine, for example, that the IVA parent body was metallic and had a radius of 150 ± 50 km [3]. At this time cooling rate variations in asteroidal parent bodies of a factor of 2.0 or less cannot be measured.

An empirical cooling rate indicator for meteoritic metal based on the size of the high-Ni particles in the cloudy zone microstructure in the taenite rims which forms at low temperatures, ~350 to 100 °C, during cooling within a parent asteroidal body, has been developed [4]. A strong inverse relationship between high-Ni particle size and metallographic cooling rate for irons, stony-irons and stony meteorites is observed. This relationship has been used to determine relative cooling rates in various meteorite groups [4, 5] although no predictive model has been developed. Recent advances, using electron microscopy of cloudy zone microstructure, has resulted in the measurement of high-Ni particles, <30 nm in size, for fast cooled meteoritic metal [6].

More and improved metallographic and cloudy zone cooling rate measurements will be made in the future. The application of the TEM will allow for measurements of micron sized Ni gradients, for example in the IVB irons. The importance of carbon in the growth of kamacite, for example in the IAB-IIICD irons, can be determined using new techniques such as the ion probe and further investigation of the effect of C on Ni diffusion in taenite. Measurement of trace element gradients in taenite may also lead to a new method for cooling rate determination. In addition a comprehensive model for the cloudy zone which forms by a spinodal transformation needs to be developed.

References: [1] Goldstein J. and Ogilvie R. E. 1965. *Geochimica et Cosmochimica Acta* 29:893–920. [2] Wood J. A. 1964. *Icarus* 3:429–459. [3] Yang J. et al. 2007. *Nature* 446:888–891. [4] Yang C. W. et al. 1997. *Meteoritics & Planetary Science* 32:423–429. [5] Yang J. et al. 2007. *Meteoritics & Planetary Science* 42:A168. [6] Goldstein J. I. et al. 2008. *Meteoritics & Planetary Science* 43. This issue.

5056

THERMAL HISTORY OF IVA IRON METEORITES FROM ELECTRON MICROSCOPY OF CLOUDY ZONE MICROSTRUCTURES

J. I. Goldstein¹, J. Yang¹, P. G. Kotula², J. R. Michael², and E. R. D. Scott³. ¹Department of Mechanical and Industrial Engineering, University of Massachusetts, Amherst, MA, USA. E-mail: jig0@ecs.umass.edu. ²Materials Characterization Department, Sandia National Labs, Albuquerque, NM, USA. ³HIGP, University of Hawai'i, Honolulu, HI, USA.

Introduction: The metallographic cooling rates of the IVA irons determined from kamacite growth modeling vary directly with Ni content by a factor of ~50 [1, 2]. Relative cooling rates can also be inferred from the sizes of high-Ni particles in the cloudy zone, which formed by a spinodal transformation at ~300 °C during cooling [3]. In order to measure high-Ni particles <30 nm in size and to avoid potential artifacts which are introduced during specimen preparation for SEM analysis, we used a transmission electron microscope (TEM) to examine the cloudy zone structure in IVA irons. Our TEM studies provide cooling rates for the IVA irons at ~300 °C and help to understand how the IVA irons formed in their parent asteroidal body. We also constrain the post-impact thermal history of moderately to heavily shocked IVA irons in which the cloudy zone has been obliterated.

Results: TEM thin sections were studied from 13 IVA irons of which 8 experienced low shock (<13 GPa) and 5 experienced medium to high shock. In ten IVAs (8 low shock and 2 medium to high shock), the high-Ni particle size in the cloudy zone varies from 10 to 32 nm as the bulk Ni content increases from 7.7 to 9.5 wt% and the metallographic cooling rates decrease from 2500 to 100 °C/Myr. The inverse correlation between high-Ni particle sizes and metallographic cooling rate for diverse meteorites shows that the IVA cooling rates at 350–200 °C vary by a factor of ~15 and are inversely correlated with bulk Ni concentration. The widths of the tetraetaenite regions correlate directly with cloudy zone particle size and with the cooling rate of the meteorite providing a third independent measurement of low temperature metal cooling rates. Cloudy zone microstructures are absent in Jamestown, Obernkirchen and Seneca Township due to moderate to high shock heating. The high Ni taenite rim is still present although in some cases grain boundaries have formed, grain boundary diffusion has taken place, and diffusion zones up to 150nm are observed at kamacite/tetraetaenite interfaces.

Discussion: The measured cooling rate range in IVA irons is incompatible with cooling in a metallic core that was insulated with a silicate mantle, but is compatible with cooling in an un-insulated metallic body of radius 150 ± 50 km [1, 2]. Our results show that measurements of high-Ni particle sizes <30 nm in fast-cooled meteorites (>100 °C/Myr) require low shock meteorites and a TEM so that high-Ni particles can be observed directly.

References: [1] Yang J. et al. 2007. *Nature* 446:888–891. [2] Yang J. et al. 2008. *Geochimica et Cosmochimica Acta*. In press. [3] Yang C. W. et al. 1997. *Meteoritics & Planetary Science* 32:423–429.

5300

NONDESTRUCTIVE 3-D CONFOCAL LASER IMAGING AND ANALYSIS OF STARDUST TRACK #82 AND DECONVOLUTION TECHNIQUES

M. Greenberg^{1,3} and D. S. Ebel^{2,4}. ¹Brandeis University, 415 South Street, Waltham, MA 02454, USA. ²Department of Earth and Planetary Sciences, American Museum of Natural History, Central Park West at 79th Street, New York, NY 10024, USA. ³E-mail: mdgreen@brandeis.edu. ⁴E-mail: debel@amnh.org.

Introduction: The Stardust mission to comet Wild 2 returned cometary and ISM particles trapped in aerogel, leaving “tracks” of melted silica aerogel on both sides of the collector [1, 2, 3]. It has been our goal to perform non-destructive 3-D textural analysis on both types of tracks. We have utilized laser scanning confocal microscopy (LCSM) as an accessible alternative to synchrotron-based techniques [4]. Here, we present greatly improved LCSM images of track #82 and analogous images of aerogel shot with basaltic glass. We also present a method of removing the axial distortion inherent in LCSM images, by means of a computational 3-D Deconvolution algorithm. LCSM images provide full 3-D maps, from which we will also present a full textural analysis of track #82.

Results: Stardust track #82 (C2092,1,82,00) is a single track in a keystone mounted on a standard “forklift” apparatus. Images were taken at the American Museum of Natural History LCSM facility. Scans of varying magnification on regions of track #82 were performed, without disturbing the keystone. The structure of the tracks is best observed via our 3-D projections, and in our movies of these 3-D projections. Earlier work demonstrated the feasibility of wet microscopy with resolution at or better than 0.04 $\mu\text{m}/\text{pixel}$ edge on stardust samples [5].

We made extensive use of a deconvolution method involving calculation of a theoretical PSF, followed by iterative deconvolution. We used a classic maximum likelihood estimation (CMLE) method to deconvolve blocks of the image stack, one at a time. We are currently working to further improve these results by experimentally determining a PSF for aerogel. We will present a full textural and particulate analysis on the deconvolved datasets, including track diameter measurements, and particulate fragment counting.

Conclusions: We have demonstrated technical improvements in using LCSM for non-destructive submicron 3-D analysis of grains and tracks in aerogel returned by the Stardust mission. Most importantly, our deconvolved image stacks allow rapid, high-resolution, nondestructive textural analysis of whole tracks, and our techniques will easily transfer to primary ISM dust analysis.

References: [1] Burchell M. J. et al. 2006. *Annual Review of Earth and Planetary Science* 34:385–418. [2] Westphal A. et al. 2004. *Meteoritics & Planetary Science* 39:1375–1386. [3] Westphal et al. 2006. 37th LPSC. Abstract #2225. [4] Ebel D. S., Mey J. L., Rivers M. L. 2007. 38th LPSC. Abstract #1977. [5] Greenberg M. et al. 2008. 39th LPSC. Abstract #1800.

5318

OXYGEN ISOTOPE VARIATION WITHIN THE PRIMITIVE ACHONDRITES

R. C. Greenwood¹, I. A. Franchi¹, J. M. Gibson¹, and G. K. Benedix². ¹Planetary and Space Sciences Research Institute, Open University, Milton Keynes MK7 6AA, UK. E-mail: r.c.greenwood@open.ac.uk. ²Impacts and Astromaterials Research Centre, Department of Mineralogy, Natural History Museum, London SW7 5BD, UK.

Introduction: Primitive achondrites exhibit near-chondritic bulk compositions and non-chondritic textures [1]. They are generally regarded as being either highly metamorphosed chondrites or partial melt residues and hence record conditions at the onset of asteroidal melting [1]. In attempting to understand early asteroid differentiation processes the composition of the precursor material remains an outstanding problem [2]. To investigate this issue we have undertaken a detailed oxygen isotope study of the primitive achondrites. Results from an earlier stage in this investigation have been reported previously [3].

Analytical Techniques: Oxygen isotope analyses were performed by infrared laser-assisted fluorination [4]. The following groups were included in this study: brachinites (n = 9), winonaites (n = 16), acapulcoites and lodranites (n = 34), various related samples (n = 7). Since many of these meteorites have experienced significant weathering most of the samples studied have been leached using a solution of ethanolamine thioglycollate [5]. This treatment removes iron oxides, hydroxides and metallic iron, but not silicate-bound iron. Replicate analyses were performed both before and after acid leaching treatment.

Results: Untreated samples, when compared to those that have been acid leached, show much greater levels of oxygen isotope variation, with major overlap between the brachinite and winonaite groups. These overlaps are clearly resolved in the acid leached samples and the level of $\delta^{18}\text{O}$ variation in acapulcoites and lodranites is significantly reduced. However, the level of $\Delta^{17}\text{O}$ variation displayed by acapulcoite and lodranite samples is largely unchanged by acid treatment and presumably reflects primary variation inherited from their chondritic precursors. Treated winonaite samples define a well-developed linear mass fractionation trend [3], whereas treated brachinite samples still show significant scatter, consistent with suggestions that they may not represent samples from a single parent body [1].

Discussion: Even when the influence of weathering is largely removed primitive achondrites display much greater oxygen isotope variation than differentiated groups. This variation is reflected in the 2σ error on the mean $\Delta^{17}\text{O}$ values, which decreases in the order acapulcoites-lodranites > brachinites > winonaites. The presence of relict chondrules in a number of acapulcoites [1] and the significant levels of primary oxygen isotope variation displayed by both acapulcoites and lodranites suggests that this group is compositionally close to that of its precursor material. In view of the evidence for early onset of partial melting in primitive achondrites [6], one outstanding question is why melting was not more extensive in these meteorites?

References: [1] Weisberg et al. 2006. In *Meteorites and the early solar system II*. pp. 19–52. [2] McCoy et al. 2006. In *Meteorites and the early solar system II*. pp. 733–745. [3] Greenwood R. C. et al. 2007. Abstract #2163. 38th Lunar and Planetary Science Conference. [4] Miller M. F. et al. 1999. *Rapid Communications in Mass Spectrometry* 13:1211–1217. [5] Cornish L. and Doyle A. 1984. *Palaeontology* 27:421–424. [6] Wadhwa et al. 2006. In *Meteorites and the early solar system II*. pp. 715–731.

5006

CHOPINITE-SARCOPSIDE SOLID SOLUTION, (Mg,Fe)₃(PO₄)₂, IN LODRANITE GRA 95209

E. S. Grew¹, M. G. Yates¹, R. J. Beane², C. Floss³, and C. Gerbi¹. ¹University of Maine, Orono, ME 04469–5790, USA. E-mail: esgrew@maine.edu. ²Bowdoin College, Brunswick, ME 04011, USA. ³Washington University, St. Louis, MO 63130, USA.

Introduction: Four phosphate minerals have the stoichiometry (M²⁺)₃(PO₄)₂. Sarcopsidite and graftonite, both Fe dominant, are found in meteorites and terrestrial rocks. Chopinite, the recently discovered Mg-dominant analogue of sarcopsidite occurring in terrestrial granulite-facies metasediments, is inferred to have formed at 800–860 °C, 6–7 kbar [1] and is a high-pressure polymorph of farringtonite [2], which has been found only in meteorites. Unidentified (Mg,Fe)₃(PO₄)₂ phases with $X_{Mg} = Mg/(Mg + Fe)$ ranging from 0.01 to 0.87, together with chladniite, CaNa₈(Ca₄Na₄)(Mg,Fe)₄₃(PO₄)₃₆, or its Fe-dominant analogue, johnsomervilleite, have been reported as minor constituents in Graves Nunatak (GRA) 95209, a lodranite containing Fe-Ni metal masses and forsterite-orthopyroxene aggregates [3, 4].

Results: To identify the unknown (Mg,Fe)₃(PO₄)₂ phases, we determined the Fe-Mg-Mn distribution between contiguous grains of (Mg,Fe)₃(PO₄)₂ and chladniite-johnsomervilleite and obtained electron backscatter diffraction patterns of the (Mg,Fe)₃(PO₄)₂ phases. Electron microprobe analyses of contiguous grains of (Mg,Fe)₃(PO₄)₂ and chladniite-johnsomervilleite in three sections of GRA 95209 give two trends for Mg-Fe, one for johnsomervilleite and chladniite with $X_{Mg} \leq 0.738$, the second for chladniite only with $X_{Mg} \geq 0.738$. The first trend is tightly constrained with a distribution coefficient, $K_D = (Mg/Fe)_{JUNK}/(Mg/Fe)_{C-J} = 0.584$, which is nearly identical to Mg-Fe distribution between terrestrial sarcopsidite and johnsomervilleite, $K_D = 0.588$ [1]. This suggests that the unknown (Mg,Fe)₃(PO₄)₂ phase is sarcopsidite (for compositions $X_{Mg} = 0.28$ –0.43) and chopinite (for compositions $X_{Mg} = 0.57$ –0.65). Mn-Fe distribution is consistent with the (Mg,Fe)₃(PO₄)₂ phases being sarcopsidite or chopinite, not graftonite, which would have contained much more Mn. The second trend in Mg-Fe gives $K_D \sim 1.51$. In this case, we infer that the unknown (Mg,Fe)₃(PO₄)₂ phase is farringtonite ($X_{Mg} = 0.80$ –0.89). Electron backscatter diffraction patterns and maps of magnesian (Mg,Fe)₃(PO₄)₂ phases confirm identification of chopinite and farringtonite.

In contrast to the phosphates, our analyses show that associated forsterite and enstatite vary little in composition, viz., $X_{Mg} = 0.93$ and 0.92–0.93, respectively, except for fayalite overgrowths on forsterite ($X_{Mg} \geq 0.2$).

Discussion: Using the experimental data for the end-member reaction [2], an isopleth calculated as in [1] at 500–1050 °C for chopinite $X_{Mg} = 0.65$, but with measured $K_D = (Mg/Fe)_{FAR}/(Mg/Fe)_{CHO} = 2.10$, gives 4–7 kbar for this chopinite-farringtonite pair, pressures far too high for any meteorite. We suggest that Fe-rich sarcopsidite initially formed by oxidation and replacement of P-rich metal; subsequent exchange with a large reservoir of Mg-rich silicates resulted in Mg enrichment of the phosphates and, consequently, Fe-rich overgrowths on forsterite. As GRA 95209 cooled, Mg-enriched sarcopsidite failed to transform into farringtonite, leaving chopinite as a metastable phase.

References: [1] Grew E. et al. 2007. *European Journal of Mineralogy* 19:229–245. [2] Brunet F. and D. Vielzeuf. 1996. *European Journal of Mineralogy* 8:349–354. [3] Floss C. 1999. *American Mineralogist* 84:1354–1359. [4] McCoy T. et al. 2006. *Geochimica et Cosmochimica Acta* 70:516–531.

5240

ORIGIN OF SCHLIREN BANDS IN CHINGA ATAXITE

V. I. Grokhovskiy¹, K. A. Uymina¹, S. A. Glazkova¹, L. E. Karkina^{1,2}, and V. M. Gundirev². ¹Ural State Technical University—UPI, Ekaterinburg 620002, Russia. E-mail: grokh@siams.com. ²Institute of Metal Physics of the Ural Division of the Russian Academy of Sciences, Ekaterinburg, Russia.

Introduction: It is well known the presence of macroscopic selective reflection bands (Schliren bands or oriented sheen) in various ataxites IVB [1, 2]. However, the origin of Schliren bands is not clear yet. There were several different suggestions such as variety of chemical and phase compositions, shock alteration, and twinning to explain Schliren bands formation, but these explanations were not evident. In the present work we suggest an origin of the Schliren bands basing on Chinga ataxite IVB multiscale study.

Experimental: Chinga ataxite IVB fragments were studied using textural X-ray diffraction (XRD), optical microscopy with image analysis (OM), scanning electron microscopy (SEM) with EDX and EBSD, atom probe microscopy (APM), and transmission electron microscopy (TEM).

Results and Discussion: It was shown that Schliren bands in Chinga ataxite IVB were parallel dark and light lines with a width in the range of 1–10 nm and the same chemical composition. XRD and TEM demonstrated the presence of α and γ phase mixture with 20 ± 5 vol% of phase for both dark and light bands. Texture of α phase was complicated in both bands and presented by six crystallographic orientations. However, the set of orientations was different for dark and light bands. The presence of retained γ phase after martensite transformation (γ_R) as well as exsolved γ phase from martensite (γ_E) was shown earlier [3, 4]. We observed that orientation of γ_R phase was the same in dark and light bands. This fact excludes twinning origin of the bands. It was further shown that planes (111) for γ_R and (011) for α were parallel. The directions [1 $\bar{1}$ 0] for γ_R and [100] for α in both dark and light bands were also parallel that was close to Nashiyama-Vasserman martensite orientation relationship. These results demonstrated that taenite decomposition in Chinga ataxite was by martensite type reaction: $\gamma_R \rightarrow \alpha_2 + \gamma_R \rightarrow \alpha' + \gamma_E + \gamma_R$. Thus, we can conclude that Schliren bands appeared due to formation of different crystallographic set of submicroscopic products during martensite transformation.

Acknowledgements: This work was supported in part by the Russian Foundation for Basic Research (grants No 06-08-00705-a and No 07-05-96061-r-ural-a).

References: [1] Axon H. J. and Smith P. L. 1972. *Mineralogical Magazine* 38:736–755. [2] Buchwald V. F. 1981. *Meteoritics* 16:298. [3] Nolze G. and Geist V. 2004. *Crystal Research and Technology* 39:343–352. [4] Goldstein J. I. and Michael J. R. 2006. *Meteoritics & Planetary Science* 41:553–570.

5228

MEASURING THE METAMORPHIC HISTORY OF UNEQUILIBRATED CHONDRITES USING SINGLE OLIVINE GRAINS

J. N. Grossman. U.S. Geological Survey, 954 National Center, Reston, VA 20192, USA. E-mail: jgrossman@usgs.gov.

Introduction: At the earliest stages of metamorphism, ordinary and carbonaceous chondrites undergo changes in mineralogy that affect: matrix, which loses S; chondrule glass, which crystallizes albite, becomes K-rich, and changes in cathodo- and thermoluminescence; metal, which changes in structure and mineralogy; and ferroan olivine, which exsolves a Cr-rich phase, likely chromite [1–3]. However, many of these materials are also sensitive to aqueous and other forms of chemical alteration on asteroids (glass, matrix, metal), or are uncommon phases in some chondrites (e.g., ferroan olivine in CV, CR, CI, EH, and EL chondrites). This makes it difficult to assess the metamorphic history of many primitive chondrites. This problem can be solved by careful characterization of individual ferroan olivine grains.

Experimental: 3–6 large (>75 μm , where possible) ferroan olivine grains, isolated or in type II chondrules, were selected from 23 chondrites, including type 3.0–3.2 ordinary and CO, CR, CM, and CV chondrites. Microprobe traverses were done across each grain with a 15 kV, 30 nA beam, ~0.5 μm steps with 1.5 s dwell-time, and spectrometers fixed on Fe, Mg, Si, Cr, and Ca. Data were reduced from working curves based on olivine standards.

Results and Discussion: Most of the olivine grains in the studied chondrites show normal, igneous FeO zoning profiles, although some isolated grains are fragments. In chondrites having the lowest petrologic type (3.00–3.03), Cr_2O_3 commonly shows zoning that correlates with FeO, although normal and reverse Cr_2O_3 zoning patterns occur in similar numbers. All grains in these meteorites have high average concentrations of Cr_2O_3 (0.4–0.5 wt% in ordinary and 0.3–0.4 wt% in carbonaceous chondrites). Cr_2O_3 varies smoothly across each grain. Slightly more metamorphosed chondrites, type 3.05–3.10, contain olivine that shows evidence for igneous zoning of Cr_2O_3 , but zoning profiles are more jagged and erratic. Average concentrations of Cr_2O_3 are similar to those in type 3.00 olivine. In petrologic type 3.15, igneous zoning of Cr_2O_3 is no longer apparent, average concentrations are lower (0.1–0.2 wt%), but zoning patterns are still quite noisy. Olivine in chondrites of types ≥ 3.2 has uniformly low Cr_2O_3 (≤ 0.1 wt%) with no trace of zoning.

Most of the ferroan olivine grains from a single chondrite show similar properties with respect to Cr_2O_3 : average concentrations and the noisiness of zoning profiles are approximately the same in each grain. The petrologic type of a chondrite can be determined with fair confidence, within 0.05, between types 3.00 and 3.2, by measuring the zoning profile of only a single olivine grain, and with high confidence by measuring several. This method can be applied to chemically altered chondrites, those with only a small amount of ferroan olivine, and individual clasts or particles in brecciated chondrites; these are all cases where other methods either fail or are difficult to apply.

References: [1] Grossman J. N. and Brearley A. J. 2005. *Meteoritics & Planetary Science* 40:87–122. [2] Kimura et al. 2008. *Meteoritics & Planetary Science* 43. In press. [3] Sears D. W. G. et al. 1990. In *Spectroscopic characterization of minerals and their surfaces*. Washington, D.C.: American Chemical Society. pp. 190–222.

5142

OUTWARD TRANSPORT OF CAIs DURING FU ORIONIS EVENTSH. Haack¹ and G. Wurm². ¹Natural History Museum of Denmark, Øster Voldgade 5-7, 1350 Copenhagen K, Denmark. E-mail: hh@snm.ku.dk. ²Institute for Planetology, University of Münster, Wilhelm-Klemm-Str. 10, D-48149 Münster, Germany.

Introduction: CAIs are believed to have formed very early and very close to the Sun. Surprisingly, they are almost exclusively found in meteorites originating from asteroids that formed last and further from the Sun than any other types of asteroids that we have sampled. CAIs carry a characteristic ⁵⁰Ti anomaly [1]. Absence of the anomaly in the Earth, Moon, and Mars and most differentiated meteorites suggest that CAIs were not abundant in the inner solar system when these objects accreted.

The mechanism that transported CAIs outward must have been very efficient and deposited the CAIs in a place where they could survive as individual particles prior to the accretion of carbonaceous chondrite parent bodies.

It has been proposed that an outward flow of gas close to the nebula midplane could be responsible for the transport of CAIs [2]. We propose an additional mechanism which could have transported CAIs outward. This process may also explain why the observed CAIs appear to have formed in a very short time and in a limited size range.

T-Tauri stars undergo FU Orionis events where enhanced accretion rates of matter to the star increase the luminosity by up to two orders of magnitude. During these events thermal radiation from the inner part of the disk becomes high enough that mm-sized particles will be levitated above the dense disk due to the photophoresis effect. We have explored how this process can lead to outward transport of particles high above the disk.

Model Results: We have calculated the movement of particles exposed to thermal radiation from two sources: the Sun and a hot disk. The total luminosity was assumed to be 100 times the current solar luminosity. The photophoresis effect on silicate spheres was determined experimentally [3]. We find that up to ~1 cm-sized particles rise from the inner edge of the dust disk to an equilibrium level where vertical photophoresis is balanced by the vertical component of the gravity from the Sun. Photophoresis from the Sun aided by a tail-wind from the gas [2] then push the particles out to several AU in about 10⁴ years. At 2–3 AU outward motion slows down and the particles begin to pile up. Since photophoresis require that the particles are only exposed to radiation from one side the lower most particles will begin to settle toward the midplane as the layer above them fills up.

Conclusions: It is possible to transport CAIs outward above the disk during FU Orionis conditions. The inferred duration of FU Orionis events are similar to the observed age variation of CAIs. The CAIs are carried high above the disk until they settle at 2–3 AU. This is consistent with the apparent absence of CAIs closer to the Sun. CAIs larger than ~1 cm cannot be levitated and thus stay close to the Sun. If this process was responsible for the transport of CAIs, the observed restricted size and age variation may therefore be a result of selection effects during transport rather than being a consequence of the way CAIs formed.

References: [1] Trinquier A. et al. 2007. Abstract #4054. Workshop Chron. Met. [2] Ciesla F. D. 2007. *Science* 318:613–615. [3] Teiser J. et al. 2008. Abstract #5080. *Meteoritics & Planetary Science* 43. This issue.

5238

MINERALOGICAL AND GEOCHEMICAL INVESTIGATIONS OF MARE BASALTS FROM THE APOLLO COLLECTION

L. J. Hallis^{1,2}, M. Anand^{1,2}, S. S. Russell¹, K. Terada³, N. Rogers², and S. Hammond². E-mail: l.hallis@nhm.ac.uk. ¹Department of Mineralogy, The Natural History Museum, Cromwell Rd., London SW7 5BD, UK. ²Department of Earth and Environmental Sciences, The Open University, Milton Keynes MK7 6AA, UK. ³Department of Earth and Planetary Systems Science, Hiroshima University, Higashi-Hiroshima 739-8526, Japan.

Introduction: The Apollo mare-basalts represent the largest and most pristine collection of lunar basaltic material on Earth. A thorough assessment of their petrological and geochemical characteristics provides key information on the evolutionary history of the Earth-Moon system. The aim of our research is to carry out systematic studies involving mineralogy, petrology, and geochemistry of a suite of mare basalts from the Apollo 11, 12, 14, 15, and 17 sites. With the aid of in situ U-Pb dating of phosphates in the Apollo basalts, the samples are being grouped within the existing lunar classification scheme(s) [1] with the aim of gaining a more precise chronology of basalt extrusions at these locations.

Methodology: Our analytical protocol includes the collection of backscatter and X-ray maps for a polished section of each sample followed by electron microprobe spot and transect analysis of individual mineral phases. LA-ICP-MS data reveals the trace element signature of minerals in each sample, while the solution ICP-MS technique is utilized for the bulk chemistry. U-Pb age dating of phosphates is currently being carried out using the SHRIMP facility at Hiroshima University [2, 3].

Results and Conclusions: Our preliminary data are consistent with previous observations that lunar basalts vary widely in terms of texture and mineralogy, which are products of complex crystallisation processes. Initial LA-ICP-MS data not only confirm the heterogeneity of REE signatures between the Apollo sites but also between individual samples from the same site. Focusing on clinopyroxene for example, the variation in La/Yb ratio throughout the sample suite ranges from 0.5 to 0.008 while Eu anomalies ($Eu^* = Eu/\sqrt{(Sm \cdot Gd)}$) range from 0.09 to 0.36. These variations were most likely produced by a combination of fractional crystallization of mare magma and their source heterogeneities. We also plan to carry out oxygen isotope measurements on these samples to further constrain the processes involved in mare-basalt petrogenesis.

References: [1] Neal A. B. and Taylor L. A. 1992. *Geochimica et Cosmochimica Acta* 56:2177–2211. [2] Terada et al. 2007. *Nature* 450:849–852. [3] Anand et al. 2003. *Geochimica et Cosmochimica Acta* 67:3499–3518.

5219

CLIMATE-BASED ANALYSIS OF MARTIAN SURFACE MORPHOLOGY

H. I. Hargitai¹, Á. Kereszturi², Sz. Berczi¹, A. Gucsik^{4,5}, and Sz. Nagy¹. ¹ELTE TTK, 1117 Budapest, Pázmány P. st 1/A. E-mail: hargitai@emc.elte.hu. ²Collegium, Budapest. ³Hungarian Astronomical Association, Hungary. ⁴Savaria University Center, Hungary. ⁵Max Planck Institute for Chemistry, Germany.

Introduction: Various groups of zonal morphological features [1] are identified on Mars. Below we outline possible connections between them, and the current zonal climatic trends [2], from the Mars Climate Diagrams Database (<http://planetologia.elte.hu/mcdd/>) [3]. We analyzed the current annual temperature curve regarding the possible role of temperature fluctuation on daily and annual basis.

Zonal Structures: *Permanent Polar Cap* (80–90° latitude): the temperature and insolation variations may produce the observed changes today.

Seasonal Cap (80–50°): changes only in the surface ice cover happens.

Polar Layered Terrain (90–70°): accumulated dust plus ice, formed by past climate changes, present effects can hardly be estimated.

Gullies (30–70°): may have formed by surface melting of snow packs recently.

Polygonal Patterned Ground (60–85°), and few close to the equator): periodic temperature changes produce contraction and expansion, as well periodic desiccation and wetting.

Fretted Terrain (30–50°): these structures are too large to be produced by the current climate.

Slope streaks (0–30°): found near the equator where dust covers the surface, and the daily temperature fluctuation is the highest.

Tropical Mountain Glaciers (0–20°): formed by ice accumulation and creep during high obliquity.

Current Climate Characteristics: 0 °C is reached every year for few sols to several Mars months, depending on latitude, between 60°N–80°S. In the southern hemisphere, the period of possible >0 °C lasts less months, but has higher peak temperatures. Freeze-thaw cycle—depending on brine characteristics—is possible each year, and occurs daily: periods of extended subzero temperatures last for the winter/continuously dark months but there is no longer period of >0 °C, and nighttime temperatures can reach only –40 °C on the warmest summer night in the southern hemisphere or during dust storms, when longer periods of stable temperature occurs on the surface.

Discussion: Based on the surface temperature, pressure, and vapor content changes, most of the above mentioned zonal structures have probably formed under different climate than today's. Beside the slope streaks and degradation structures of the permanent polar cap surface, small polygons may form actively today. The daily temperature variation around the polygonal patterned ground is 180–240 K on annual scale, and the same range on daily scale, but the later only in summer. The smallest observed polygons on MOC and HiRISE images may formed under the present climatic conditions. There are substantial differences between the climate of the two hemispheres of Mars which may have effect on the evolution of polygonal ground.

References: [1] Kreslavsky M. A. and Head J. W. 2002. *Geophysical Research Letters* 29:15. [2] Lewis S. R. et al. 1999. *Journal of Geophysical Research* 104 (E10):24,177–24,194. [3] Hargitai H., Bérczi Sz., Nagy Sz., Gucsik A., and Kereszturi Á. 2008. 39th LPSC. Abstract #1476.

5157

MINERALOGY OF VESICULAR OLIVINE IN THREE CK4-6 CHONDRITES: RELATIONSHIP TO SILICATE DARKENING

M. Hashiguchi, K. Tomeoka, and I. Ohnishi. Department of Earth and Planetary Sciences, Faculty of Science, Kobe University, Nada, Kobe 657-8501, Japan.

Introduction: A unique feature of CK chondrites is that their chondrules and matrices show silicate darkening. Most previous workers suggested that the silicate darkening resulted from shock metamorphism [e.g., 1], but the true cause has long been unknown. Recent studies of CK4 chondrites [2-4] revealed that they contain abundant unusual olivine in their matrices, and this contains numerous micron to submicron-size vesicles and inclusions of magnetite, pentlandite, and a variety of other minerals. The authors suggested that the vesicular olivine resulted from recrystallization of partially melted olivine by shock, and this is the principal cause of the silicate darkening. Here we present the results of our mineralogical and petrological investigation of LEW 86258 (CK4), EET 87507 (CK5), and EET 87860 (CK5/6). Our purpose was to examine whether vesicular olivine is the cause of the silicate darkening in these chondrites and to determine its origin and relationship to the silicate darkening.

Results: The three CK4-6 chondrites show a similar degree of strong silicate darkening in their matrices and chondrule mesostases. Backscattered electron images of highly darkened regions in the matrices of the three chondrites show that olivine with numerous vesicles (<0.1-3 μm in diameter) fills interstices of nonvesicular olivine crystals, exhibiting a complex network of veinlets. The vesicular olivine contains numerous spherical grains (<0.1-5 μm) of magnetite and pentlandite as well as grains of plagioclase, low-Ca pyroxene and diopside, although the relative abundance of these inclusions differs between the chondrites. There is a tendency that a region having a higher volume proportion of vesicular olivine to exhibit a darker and dustier appearance in transmitted light.

Discussion: Vesicular olivine occurs pervasively in the matrices in LEW 86258, EET 87507, and EET 87860. The mineralogical characteristics of the vesicular olivine in all the chondrites closely resemble those in the Kobe and Karoonda CK4 chondrites [2-4]. From these observations, we conclude that microinclusion-rich vesicular olivine is the principal cause of the silicate darkening in the LEW 86258, EET 87507, and EET 87860 chondrites.

The internal texture of the vesicular olivine resembles that of shock-induced local melts in the matrices of carbonaceous chondrites [e.g., 5]. Thus we suggest that the vesicular olivine formed from melts that were produced from fine-grained olivine in the matrix by shock. During melting, numerous small vesicles were produced in the melts, and the melts trapped numerous droplets of melted magnetite and pentlandite as well as fragmented grains of other minerals.

References: [1] Rubin A. E. 1992. *Geochimica et Cosmochimica Acta* 56:1705-1714. [2] Tomeoka K. et al. 2001. *Meteoritics & Planetary Science* 36:1535-1545. [3] Tomeoka K. et al. 2005. *Journal of Mineralogical and Petrological Sciences* 100:116?125. [4] Ohnishi I. et al. 2007. *Journal of Mineralogical and Petrological Sciences* 102:346-351. [5] Tomeoka K. et al. 1999. *Geochimica et Cosmochimica Acta* 63:3683-3703.

5267

ARGON, KRYPTON, AND XENON ABUNDANCES IN THE SOLAR WIND MEASURED IN SILICON FROM THE GENESIS MISSION

V. S. Heber¹, H. Baur¹, R. Wieler¹, R. C. Wiens², and D. S. Burnett³. ¹IGMR, NW C, ETH, 8092 Zurich, Switzerland. E-mail: heber@erdw.ethz.ch. ²LANL, Space and Atmospheric Science, Los Alamos, NM 87544, USA. ³CalTech, JPL, Pasadena, CA 91109, USA.

Introduction: Up to now solar wind (SW) abundances of Kr and Xe have been exclusively determined using SW irradiated regolith [1]. Hence, one of Genesis's major objectives is to obtain the heavy noble gas composition of the present-day SW using artificial targets exposed to the SW for 2.5 years. SW abundances will allow to study fractionation processes upon SW formation, e.g., due to the first ionization potential (FIP-effect) [2]. This is of importance to deduce solar abundances of noble gases and other elements from SW data. Solar, i.e., photospheric, abundances of noble gases are indirectly determined due to the lack of suitable lines in the spectrum. Recently, solar abundance estimates for Ne and Ar were strongly reduced whereas Kr and Xe changed only slightly [3]. This led to a dramatic decrease of the solar Ar/Kr ratio by a factor of ~3 from the earlier value [4] of 2140. If true, this change would invalidate theories of heavy noble gas fractionation in the SW identified with regolith data [1, 5]. The Kr and Xe composition in present-day SW will enable us to reassess solar abundances and fractionation theories. Thus, we concentrate here on abundances of Ar, Kr and Xe in the bulk SW.

Experimental: Kr and Xe are rare in the SW, expected abundances are 7×10^{-13} ccSTP/cm² ⁸⁴Kr and 9×10^{-13} ccSTP/cm² ¹³²Xe. Their analysis is further challenged by a possible surface contamination due to atmospheric gases. Additionally, many targets contain traces of indigenous atmospheric gases. To monitor potential atmospheric contamination, two major isotopes ^{84,86}Kr and ^{129,132}Xe will be analyzed with different abundances in the atmosphere and SW. Analyses will be carried out using CZ Si (Czochralski-pulled Si), considered to be one of the purest target materials flown on Genesis. Noble gases will be extracted from ~1 cm² by UV laser ablation (213 nm). A beam size of 200 μm , the maximum repetition rate of 20 Hz and a raster speed of 1 mm/s will allow a complete extraction of solar wind particles from this large area within ~40 min. Extraction line and mass spectrometer blanks are 8×10^{-16} ccSTP ⁸⁴Kr and 6×10^{-16} ccSTP ¹³²Xe, thus contributing only 0.1% and 0.6% to expected Kr and Xe amounts, respectively. More crucial is, however, the material blank. One first CZ Si measurement resulted in 1.13×10^{-14} ccSTP ¹³²Xe/cm² [6], corresponding to ~11% blank contribution to expected SW Xe. This value, however, may be an overestimate due to suboptimal experimental conditions [S. A. Crowter, personal communication 2008]. Daily mass spectrometer performance is controlled by a highly diluted (10^{-13} - 10^{-12} ccSTP) Kr, Xe calibration to keep the Kr and Xe memory in the mass spectrometer low. Sensitivity for Kr and Xe is 1×10^{15} and 1.3×10^{15} counts/ccSTP, respectively.

At the conference we will present the Ar/Kr and Kr/Xe composition of the bulk solar wind.

References: [1] Wieler R. and Baur H. 1995. *The Astrophysical Journal* 453:987. [2] von Steiger R. et al. 2000. *Journal of Geophysical Research* 105:27,217. [3] Asplund M. et al. 2005. ASP 336. p. 25. [4] Anders E. and Grevesse N. 1989. *Geochimica et Cosmochimica Acta* 53:197. [5] Heber V. S. et al. 2001. AIP 598. Bern, Switzerland, 387. [6] Crowter S. A. et al. 2008. 39th LPSC. Abstract #1762.

5108

THE DISCOVERY OF A LATE HOLOCENE IMPACT CRATER NEAR WHITECOURT, ALBERTA

C. D. K. Herd¹, E. L. Walton¹, D. G. Froese¹, E. P. K. Herd², and R. S. Kofman.¹ ¹Department of Earth and Atmospheric Sciences, 1-26 Earth Sciences Building, University of Alberta, Canada. E-mail: herd@ualberta.ca. ²Department of Civil and Environmental Engineering, 3-133 Markin/CNRL Natural Resources Eng. Facility, University of Alberta, Edmonton, Alberta T6G 2E3, Canada.

Introduction: Based on magnitude-frequency relations, small terrestrial craters should be more common than observed. For example, it is predicted that over 200 craters 60 m in diameter should have formed on the Earth's surface during the Holocene [1]. However, of the approximately 175 known impact craters, there are only 5 from the Holocene with diameters <100 m; it appears that a component of the Holocene impact record is missing. We report the discovery of a well-preserved late Holocene impact structure located in a forested area near the town of Whitecourt, Alberta (54°00'N, 115°36'W).

The Whitecourt Meteorite Impact Crater (WMIC): Although undetectable using visible imagery, a bare-earth model of the ground surface obtained from airborne LiDAR (Light Detection and Ranging) data clearly reveals a bowl-shape crater with a diameter of 36 m and a depth of 6 m. The target material for the crater is deglacial sediments associated with the retreat of the Laurentide Ice Sheet.

Stratigraphy and Age: The crater fill is represented by a pebble-diamict to a depth of ~2.9 m. Below this depth is a sharp transition to a well-sorted medium sand which continues, uninterrupted, to a depth of at least 5.4 m. Rare glassy fragments have been found within the diamict in the crater center; the amorphous nature of this material has been confirmed by XRD and polarizing light microscopy. The glass fragments have an amber color in transmitted light and range from <0.1 to 0.5 cm diameter. Glass has not been observed at a depth greater than ~3.1 m. We interpret the ~2.9 m transition, represented by a change in sediment from diamict to sand, to be near to the base of the transient crater. The presence of glass to a depth of 3.1 m is consistent with this interpretation.

Two radiocarbon ages of 1130 ± 25 and 1080 ± 25 ¹⁴C yr BP (UCIAMS 40058 and 40059, respectively) were obtained on charcoal from the A-horizon of a paleosol buried by impact ejecta. These data provide a concordant maximum age for the overlying ejecta of ~880–990 A.D., indicating the impact event likely occurred within the last thousand years.

Meteorites: Meteorites are embedded to depths reaching 25 cm in the surface surrounding the crater rim to a distance of 70 m. A total of 74 meteorites (IIIAB Om iron) with a combined weight of 5.4 kg have been recovered thus far. The meteorites have an angular morphology, and range in size from <1 cm to 12.5 cm in greatest dimension and in mass from 0.1 to 1196 g.

Conclusions: The WMIC represents the fall of an iron meteoroid which fragmented at low altitude, showering the immediate area with angular fragments. The main mass, with an estimated diameter of 1.1 m (after [2]), formed the crater. This study demonstrates that LiDAR may be a critical tool for searching for the missing component of young, small impact craters predicted from magnitude-frequency relations.

References: [1] Bland P. A. and Artemieva N. A. 2006. *Meteoritics & Planetary Science* 41:607–631. [2] Collins G. S. et al. 2005. *Meteoritics & Planetary Science* 40:817–840.

5234

EVOLUTION OF IMPACT EJECTION ANGLES: IMPLICATIONS FOR EARLY STAGE COUPLING

B. Hermalyn¹, P. H. Schultz¹, J. L. B. Anderson², and J. T. Heineck³. ¹Brown University, Providence, RI 02912–1846, USA. E-mail: Brendan_Hermalyn@brown.edu. ²Winona State University, Winona, MN 55987, USA. ³NASA Ames Research Center, Moffet Field, CA 94035, USA.

Introduction: Ejection angles from an impact affect the surface distribution of emplaced mass on planetary bodies. Although ejection angles are commonly assumed to remain constant throughout crater development [1], prior experimental studies indicate that the angle varies with time over the middle [2] and late stages [3] of crater formation. Here we examine the time-resolved evolution of ejection angles at early times in order to understand the progression of the cratering flow-field as it transitions from the compression to excavation stage of crater growth.

Experimental Methodology: A suite of impact experiments into quartz sand was performed at the NASA Ames Vertical Gun Range (AVGR) over an array of impact variables. Through the use of a new high-speed (1000 frames/second) Three-Dimensional Particle Imaging Velocimetry (3D-PIV) system, the velocity and ejection angle of the expanding ejecta curtain could be measured throughout the cratering process with high temporal resolution. Calculation of other ejecta characteristics, such as ejecta curtain radius, from the raw 3D-PIV images allows further insight into the physics of the excavation process.

Results and Analysis: The high degree of temporal resolution afforded in this study permits exploration of the early-stage coupling regime. The ejection angle for vertical impacts increases by ~10° in the first few milliseconds after impact before transitioning to the ballistic excavation flow stage of growth, which is characterized by ejection angles of ~50° from horizontal. This evolution occurs for both low (1 km/s) and high-speed (5 km/s) impacts, and most likely reflects the early-time migration of the flow-field center during the penetration stage. These findings are consistent with prior studies of flow-field center migration [4], but now can be applied to a much earlier stage of growth. The timing of the ejection angle augmentation and subsequent progression to the nominal ejecta-flow pattern is directly related to the shock-coupling in the impact event, and is therefore affected by impactor size, density, and velocity. Measurements of the curtain radius capture the same transition in the flow field, where an initially large curtain radius (i.e., a low ejection angle) develops into main stage ejection flow. As impact angle decreases, departures from the point-source assumption become more pronounced.

Implications: While the point-source assumption provides a useful tool for analytical approximations of the cratering flow-field, it does not capture the full complexity of crater evolution. In particular, application of such models to larger scale impacts break down at high ejection speeds (i.e., the early penetration stage). The 3D-PIV results now allow better characterization of the ejection angle, velocity, and mass flux throughout crater growth using dimensionless scaling relations keyed to different stages of excavation.

References: [1] Housen K. R. et al. 1983. *Journal of Geophysical Research* 88:2485–2499. [2] Anderson J. L. B. et al. 2003. *Journal of Geophysical Research* 108:5094. [3] Cintala M. J. et al. 1999. *Meteoritics & Planetary Science* 34:605. [4] Anderson J. L. B. and Schultz P. H. 2006. *International Journal of Impact Engineering* 33:35–44.

5327

PETROGENESIS OF Fe,Si-METALS IN BRECCIATED UREILITESJ. S. Herrin¹, D. M. Mittlefehldt¹, and J. H. Jones¹. ¹NASA/Johnson Space Center, Houston, TX, USA. E-mail: jason.s.herrin@nasa.gov.

Introduction: Ureilites are carbon-bearing ultramafic achondrites, the majority of which are unbrecciated and thought to represent samples of asteroidal mantle [e.g., 1, 2]. Approximately 15% of ureilites are polymict or dimict fragmental breccias. In these, Fe,Ni-metal containing >8 atm% Si, primarily suessite and occasional hapkeite (hereafter collectively referred to as Fe,Si-metal), have been identified [3–6].

Petrography: Fe,Si-metal is observed in three distinct petrographic occurrences. Type I: “lithology B” of dimict breccia NWA 1241 [7, 5] (and perhaps North Haig [3]) contains abundant coarse interstitial suessite of relatively uniform composition. Type II: [6] observed metals with a range of Si up to 31 atm% in shock melt veins of paired dimict ureilites FRO 90168/90228/93008 together with kamacite, phosphides, and troilite. Type III: polymict ureilites EET 83309, EET 87720, and DAG 999/1000/1023 (paired) contain metals with a range of Si up to 38 atm% as isolated clasts or adhering to mineral or lithic fragments that coexist with unrelated metals and sulfides [4]. The homogeneity and abundance of Fe,Si-metal in Type I suggests proximity to site of production. Type II is a disequilibrium assemblage wherein Fe-Si-metals were either stabilized locally at μm scales or else transported with shock melts [6]. Type III Fe,Si-metals were gardened from their original site of production and re-deposited in regolith breccias.

Petrogenesis: The texture of NWA 1241 and trace element compositions of Fe,Si-metals indicate they are indigenous to the ureilite parent body [4]. Fe,Si-metals cannot be in equilibrium with FeO-bearing silicates, so the process that produced them is clearly of short duration and likely impact-related. By contrast, Fe,Si-metals in enstatite chondrites condensed directly from reduced nebula. Fe,Si-metals in lunar breccia Dhofar 280 formed by either reduction by solar wind or condensation from vapor [8]. Surprisingly, Fe,Si-metals have not been reported from unbrecciated ureilites, suggesting that their genesis is restricted to fragmented portions of the parent body. If formed by gas-producing reaction with graphite ($\text{SiO}_2 + \text{C} \rightarrow \text{Si}^0 + \text{CO}_x$), sufficiently low $f\text{O}_2$ (buffered by $\text{CO}_2 + \text{C} \rightarrow 2\text{CO}$) could only be realized at pressures approaching zero [9, 10], much lower than the capping pressures for reduction of FeO by carbon at equivalent or higher temperatures [9, 11, 12]. This combination of high-T and low-P in a CO atmosphere is perhaps only realized in the near-surface of a carbon-rich parent body during or shortly after impact, and perhaps only experienced by detached stones.

References: [1] Warren P. H. and Kallemeyn G. W. 1992. *Icarus* 100: 110–126. [2] Goodrich C. A. et al. 2004. *Chemie der Erde* 64:283–327. [3] Keil K. and Berkley J. L. 1982. *American Mineralogist* 67:126–131. [4] Herrin J. S. et al. 2006. 38th LPSC. Abstract #2404. [5] Mittlefehldt D. W. et al. 2007. *Meteoritics & Planetary Science* 42:A109. [6] Smith C. L. et al. 2008. 39th LPSC. Abstract #1669. [7] Ikeda Y. 2006. 30th NIPR 28:835–849. [8] Anand M. et al. 2003. 34th LPSC. Abstract #1818. [9] Berkley J. L. and Jones J. H. 1982. *Journal of Geophysical Research* 87, Supp. A, 353–364. [10] French B. M. and Eugster H. P. 1965. *Journal of Geophysical Research* 70:1529–1539. [11] Walker D. and Grove T. 1993. *Meteoritics* 28: 629–636. [12] Singletary S. J. and Grove T. L. 2003. *Meteoritics & Planetary Science* 38:95–108.

5297

COMBINED Fe- AND Si-ISOTOPE MEASUREMENTS IN CV CHONDRITE CHONDRULESD. C. Hezel¹, R. Armytage², R. B. Georg², A. W. Needham¹, S. S. Russell¹, and A. N. Halliday². ¹IARC, Natural History Museum, Department of Mineralogy, Cromwell Road, SW7 5BD London, UK. E-mail: d.hezel@nhm.ac.uk. ²University of Oxford, Department of Earth Sciences, Parks Road, OX1 3PR Oxford, UK.

The Fe- [1] and Si-isotopic [2] compositions of all solar system materials analysed so far plot on a single mass-dependent fractionation line in 3-isotope space. However, individual components like chondrules and CAIs show one of the largest spreads in Fe- [1, 3–6] and Si-isotopic compositions [2, 7–8]. The Fe-isotopic compositions of chondrules spread from negative (–0.82‰) to positive (+0.32‰) $\delta^{56}\text{Fe}$ values [8], i.e., chondrules must have been enriched in light and heavy Fe-isotopes [e.g., 5, 8]. We analyzed 30 bulk chondrules from Allende, Mokoia, and Grosnaja and found that their Fe-isotopic compositions do not follow a simple trend when plotted against their bulk FeO-composition or their mass [8]. However, the spread in bulk chondrule $\delta^{56}\text{Fe}$ narrows with increasing bulk FeO or chondrule mass. A single stage process cannot produce such a spread, which rules out a single parent body process. We performed some simple modelling and found that repeated evaporation and re-condensation—as it is expected to happen in the solar nebula—can explain the observed spread. The conclusion of this modelling is that each chondrule evaporated and re-condensed different amounts of Fe. This can be due to different heating times, peak temperatures during chondrule formation, bulk FeO concentrations and different surface/volume ratios, as all chondrules have different sizes.

However, as we analyzed bulk chondrules, it is possible that the Fe-budget of a single chondrule is dominated by the occurrence of metal or sulfide. It has been demonstrated by [9] that the distribution of metal in CR chondrite chondrules is highly heterogeneous and that these chondrules have a large spread in metal abundance. We did not image the chondrules using 3-D tomography and it is therefore impossible to state whether the Fe-isotopic composition we measured is the one from the silicate, the metal/sulfide, or a combination of both. We do have bits of the chondrules that we analyzed for Fe-isotopes left over and will now attempt to measure their Si-isotopic composition. Si is not contained in metal or sulfide in significant amounts. The comparison of Fe- and Si-isotopic composition will show whether there is a possible contribution of metal or sulfide to the bulk chondrule Fe-isotopic composition. In addition we plan to conduct further bulk chondrule Fe-isotopic measurements. The Natural History Museum in London obtained a new X-ray CT scanner that allows to produce 3-D images of the chondrule before it is destroyed for isotope measurements and this technique will help to disentangle the relationship between bulk chondrule Fe-isotopic composition and metal/sulfide abundance in the chondrule.

References: [1] Zhu X. K. et al. 2001. *Nature* 412:311–313. [2] Georg R. B. et al. 2007. *Nature* 447:1102–1106. [3] Beard B. L. and Johnson C. M. 2004. Reviews in Mineralogy and Geochemistry, vol. 55. pp. 319–357. [4] Kehm K. et al. 2003. *Geochimica et Cosmochimica Acta* 67:2879–2891. [5] Mullane E. et al. 2005. *Earth and Planetary Science Letters* 239:203–218. [6] Molini-Velsko C. et al. 1986. *Geochimica et Cosmochimica Acta* 50: 2719–2726. [7] Clayton R. N. and Mayeda T. K. 1978. Proceedings, 9th Lunar and Planetary Science Conference. pp. 1267–1278. [8] Hezel D. C. et al. 2008. 39th LPSC. Abstract #1603. [9] Denton E. et al. Forthcoming. Shape, metal abundance, chemistry and origin of chondrules in the Renazzo (CR) chondrite.

5253

MODAL ABUNDANCES OF CAIS: IMPLICATIONS FOR BULK CHONDRITE ELEMENT ABUNDANCES AND FRACTIONATIONS

D. C. Hezel, A. J. Ross, S. S. Russell, and A. T. Kearsley. IARC, Natural History Museum, Department of Mineralogy, Cromwell Road, SW7 5BD London, UK. E-mail: d.hezel@nhm.ac.uk.

Introduction: Modal abundances of Ca,Al-rich inclusions (CAIs) are poorly known and reported data scatter across large ranges [1–16]. We show that this spread is the result of a Poisson distribution of the CAIs within the chondrites. We provide a new set of CAI modal abundances, considering the Poisson distribution and that we obtained for all carbonaceous chondrites except CH and CI chondrites. Beside this “classical” approach of simply counting the number of CAIs in a chondrite, we also theoretically calculate their modal abundances from (i) bulk chondrite element-concentrations and (ii) element-concentrations of individual chondrite components.

Results: We combine our own set of CAI modal abundances with reported ones and get the following results (in area%): CV: 2.98, CM: 1.21, Acfer 094: 1.12, CO: 0.99, CK/CV (Ningqiang and DaG 055): 0.77, CK: 0.2, CR: 0.12 and CB: 0.1. Our calculated CAI modal abundances are ~10–50% below these measured values. The CAI size distributions follow log-normal distributions, however, there are a few large CAIs that are not part of these distributions [17].

Conclusions: Our new CAI modal abundance data and approach to recognize them as Poisson distributed as well as our theoretical calculations show that CAI modal abundances are much smaller than previously thought. The data reduction process is crucial when obtaining CAI modal abundances. As CAIs are Poisson distributed, it is required to study larger areas (>1000, better >2000 mm²) in order to obtain modal abundances with a small error. The CAI modal abundances we provide for CC are in good agreement with their calculated Al overabundance when compared to the CI-chondritic composition. We find a correlation between this excess and CAI modal abundances and conclude that the excess Al was delivered by CAIs. Our results support the model that CAIs did not form in the same chemical reservoir as chondrules and matrix, but have later been added to this. The Al delivered by CAIs is only a minor fraction (~10%, and 25% in case of CVs) of the bulk chondrite Al and cannot have contributed much ²⁶Al to heat the chondrite parent body. Ordinary, enstatite, R- and K-chondrites have an Al deficit relative to CI chondrites in accordance with their very low, if any, CAI modal abundances. Carbonaceous chondrites also had an initial Al deficit if the contribution of Al delivered by CAIs is subtracted. Therefore all chondrites probably lost a refractory rich high-T component explaining this Al deficit. Our calculations show that CAIs contributed only minor amounts to chondrules and matrix. Most CAI size distributions contain more than one population, indicating that CAIs of one meteorite group had different origins.

References: [1] McSween H. Y. Jr. 1977. *Geochimica et Cosmochimica Acta* 41:477–491. [2] McSween H. Y. Jr. 1977. *Geochimica et Cosmochimica Acta* 41:1777–1790. [3] McSween H. Y. Jr. 1979. 10th LPSC. Abstract #810–812. [4] Simon S. B. and Haggerty S. 1979. 8th Lunar Science Conference. pp. 1119–1121. [5] Kornacki A. S. and Wood J. A. 1984. *Journal of Geophysical Research* 89:B573–B587. [6] Rubin A. E. et al. 1985. *Meteoritics* 20:175–196. [7] Kallemeyn G. W. et al. 1991. *Geochimica et Cosmochimica Acta* 55:881–892. [8] Noguchi T. 1993. Proceedings of the NIPR Symposium 6:204–233. [9] Kallemeyn G. W. et al. 1994. *Geochimica et Cosmochimica Acta* 58:2873–2888. [10] Scott E. R. D. et al. 1996. In: *Chondrules and the protoplanetary disk*. pp. 87–96. [11] Russell S. S. et al. 1998. *Geochimica et Cosmochimica Acta* 62:689–714. [12] Rubin A. E. 1998. *Meteoritics & Planetary Science* 33:385–391. [13] May C. et al. 1999. 30th LPSC. Abstract #1688. [14] Aleon J. et al. 2002. *Meteoritics & Planetary Science* 37:1729–1755. [15] Krot A. N. et al. 2002. 33rd LPSC. Abstract #1412. [16] Norton M. B. and H. Y. Jr. 2007. 38th LPSC. Abstract #1807. [17] Hezel D. C. et al. *Meteoritics & Planetary Science*. Submitted.

5153

BARIUM ISOTOPIC COMPOSITION OF CHONDRULES IN THE SAYAMA METEORITE

H. Hidaka¹ and S. Yoneda². ¹Department of Earth and Planetary Systems Science, Hiroshima University, Higashi-Hiroshima 739-8526, Japan. E-mail: hidaka@hiroshima-u.ac.jp. ²Department of Science and Engineering, National Museum of Nature and Science, Tokyo 169-0073, Japan.

Introduction: Barium is one of promising elements to address the details of nucleosynthesis and presolar grain formation of the solar system. Previous studies on the Ba isotopic compositions of carbonaceous chondrites provide useful information of the contributions of *s*-process, *r*-process and *n*-process (neutron burst) nucleosynthetic components [1–4]. In addition, ¹³⁵Ba isotopic abundance may be affected by decay from presently extinct ¹³⁵Cs isotope ($t_{1/2} = 2.3$ Ma), which can be used for Cs-Ba geochronological application. In this study, Ba isotopic composition of chondrules from the Sayama meteorite was determined to search for ¹³⁵Cs isotope in the early solar system. It is known that the Sayama meteorite (CM2) shows the extensive signature for aqueous alteration on the meteorite parent body [5, 6].

Experiments: The sample contains chondrules sized 200 to 600 μm diameter, and interestingly, most anhydrous silicates in the chondrules found in Sayama are replaced to phyllosilicates, which reveal evidence for highly aqueous alteration. 8 chondrules were collected from 0.2 g of the fragment, and leached by 1 mL of 0.1 M acetic acid (hereafter fraction#1), 0.1 M HCl (#2), 2 M HCl (#3), and aqua regia (#4), successively. The residue (#5) was finally decomposed by HF-HClO₄ with heat. Ba fraction from each leachate was chemically separated using a conventional cation exchange method [2]. The Ba fraction was divided into two portions; one for the determination of isotopic composition by TIMS, and another for the determination of elemental abundances of Cs and Ba by ICP-MS.

Results and Discussion: The Ba isotopic data of acid leachates sometimes show variable ¹³⁵Ba excesses correlated with ¹³⁷Ba excesses, suggesting the presence of independent nucleosynthetic components for *s*- and *r*-processes in the solar system. The Ba isotopic data of fractions #1 and #2 reveal negative isotopic anomalies of ¹³⁵Ba correlated with ¹³⁷Ba, suggesting enrichment of *s*-isotopes due to addition of presolar materials. These data are consistent with previous results from acid leachates of Sayama bulk sample. On the other hand, fractions #4 and #5 show isotopic excess of only ¹³⁵Ba ($\epsilon = +14.8 \pm 8.9$, and $+18.4 \pm 4.1$, respectively) possibly due to ¹³⁵Cs decay.

References: [1] Harper C. L. Jr. 1993. *Journal of Physics G* 19:S81–S94. [2] Hidaka H. et al. 2003. *Earth and Planetary Science Letters* 214:455–466. [3] Ranen M. C. and Jacobsen S. B. 2006. *Science* 314:809–812. [4] Carlson R. W. et al. 2007. *Science* 316:1175–1178. [5] Yoneda et al. 2001. Abstract #2034. 32nd Lunar and Planetary Science Conference. [6] Takaoka et al. 2001. Abstract #1645. 32nd Lunar and Planetary Science Conference.

5176

GEOLOGIC PROCESSES ON THE SURFACE OF A SMALL ASTEROID ITOKAWA

N. Hirata¹, S. Abe², M. Ishiguro³, K. Kitazato⁴, R. Nakamura⁵, H. Miyamoto⁶, H. Demura¹, M. Abe⁷, and S. Sasaki⁸. ¹The University of Aizu, Japan. E-mail: naru@u-aizu.ac.jp. ²Institute of Astronomy, National Central University, Taiwan. ³Department of Physics and Astronomy, Seoul National University, South Korea. ⁴Graduate School of Science, Kobe University, Japan. ⁵National Institute of Advanced Industrial Science and Technology, Japan. ⁶The University Museum, University of Tokyo, Japan. ⁷The Institute of Space and Astronautical, Japan Aerospace Exploration, Japan. ⁸RISE project Office, National Astronomical Observatory Japan.

Introduction: Itokawa is the smallest asteroid ever observed by a spacecraft [1]. In spite of its size, the surface of Itokawa shows a wide variety of both topographic and brightness features [1–4]. These features suggest that the asteroid underwent diverse geologic processes including impact cratering [3], seismic shaking, mass movement [4], and space weathering [5]. Recent extensive studies on Itokawa with Hayabusa observational data provide keys for comprehensive understanding on geologic processes on the surface of a small asteroid. Moreover, the understanding on surface processes will lead to gain a clear insight into an internal structure of Itokawa. It was suggested as a rubble-pile body, but actual internal structures are still unknown.

We developed a GIS-oriented software package to analyze multiple map data of an irregularly shaped body [6]. This tool can handle many kinds of data geographically associated onto a polygon shape model of an asteroid. The tool currently supports a set of scalar data associated with the polygon IDs. A slope angle map, a geopotential map, a near-infrared reflectance map [7] and a visible brightness map are now available [6].

Results and Discussions: Locations of albedo features in the visible band and near-infrared band are well consistent each other. As the surface brightness is regarded to depend on the degree of space weathering, this result means that an effect of space weathering uniformly appears on both the visible band and the near-infrared band. Comparing the shape model and the slope map, the less space weathered-regions correspond to edges/bulges of the global shape, rims of possible impact structures or steep regions. The last case was already pointed out in previous reports [2, 5]. The authors of them suggested that space-weathered regolith on steep slopes flows down by seismic shaking and the surface is kept fresh against space weathering. However, close-up views of Itokawa show that even a bulk rock surface is suffered with space weathering [4]. Accordingly, not only a removal of weathered regolith, but also some mechanism to create fresh surface are supposed to explain bright features on the steep slope. If a constituent of Itokawa is very weak, seismic shaking may break its surface. The very low density of Itokawa, which suggests a large macro porosity of the asteroid and/or a large micro porosity of its constituent, is consistent with this view. The edges/bulges are also regions where shaking power converges and creation of fresh surface may occur. These discussions imply that Itokawa is a pile of a few blocks of relatively large size and a layer of space weathered small boulders.

References: [1] Fujiwara A. et al. 2006. *Science* 312:1330–1334. [2] Saito J. et al. 2006. *Science* 312:1341–1344. [3] Hirata N. et al. 2008. *Icarus*. Submitted. [4] Miyamoto H. et al. 2007. *Science* 316:1011–1014. [5] Hiroi T. et al. 2006. *Nature* 443:56–58. [6] Hirata N. et al. 2008. 39th LPSC. Abstract #1584. [7] Kitazato K. et al. 2008. ACM abstract.

5175

MORPHOLOGICAL ANALYSES OF LARGE LUNAR CRATERS WITH LISM/KAGUYA IMAGES

N. Hirata¹, J. Haruyama², M. Ohtake², T. Matsunaga³, Y. Yokota², T. Morota², C. Honda², Y. Ogawa³, M. Torii², H. Demura¹, and N. Asada¹. ¹The University of Aizu, Ikki-machi, Aizu-Wakamatsu, Fukushima 965-8580, Japan. E-mail: naru@u-aizu.ac.jp. ²The Institute of Space and Astronautical, Japan Aerospace Exploration Agency, Japan. ³National Institute for Environmental Studies, Japan.

Introduction: Various features outside/inside of give important clues to reconstruct and understand impact cratering. Large and fresh lunar craters are best targets, because only space weathering and limited degradations by small impacts are major processes that disturb original structures of ejecta units. Lunar Imager/Spectrometer (LISM), which onboard the Kaguya lunar explorer, will provide high-resolution and multi-spectral mapping data of the Moon. Combination of high-resolution images, digital terrain models, multiband images, and spectral profiles is a complete set for geologic mapping of a crater and its surroundings. Here we introduce a preliminary report on images of the crater Jackson (D = 71 km).

Results: Jackson is a typical fresh crater on the lunar farside. Jackson has a bright ray system with a large forbidden zone in the NW sector and two minor ones in both S and SE sectors. This appearance suggests that Jackson was formed by a oblique impact of the NW-SE direction. Features outside/inside of the crater including secondary craters, ejecta blocks, melt ponds, and slumped terraces should reflected processes of a transient cavity formation and its corruption.

Impact Melt Ponds: The ponds on the ejecta blanket show a heterogeneous distribution, whereas the ponds on the terrace zone do not. There are few small ponds in the uprange (NW-N-NNE) sector. The ponds in the downrange (SE) sector and the side (S-SW) sector are large, and their number density is also high. The ponds in the side range (S-SW) seem to be larger than those in the downrange.

Impact Melt Sheet: Crater floor is mostly filled with a large sheet of impact melt. The uprange half of the floor is characterized with numerous blocky hummocks, ribbon-like pattern weaves and a networked cracks, and the rest half is more smooth. There is a good correlation between the scale of melt deposits (melt ponds and melt sheets) and their surface texture: smaller ones are more smoother.

Terrace Structure: Morphology of the terrace zone at the up/downrange contrast sharply. The uprange terrace shows a clear stepwise structure, while the downrange terrace is more chaotic. The latter one gradually transforms into hummocks on the crater floor and the central peak. Similar structure is found on famous lunar craters King [1] and Tycho. However, Tycho's corrupted terrace is found at the uprange of this crater [2].

Ejecta Blanket: Surface facies of the ejecta blanket changes gradually with distance from the rim. Regions closest (<2–3 km from the rim) to the rim show a intermingled texture of ragged and smooth surfaces. The next outer regions (<10–15 km from the rim) have fine lineations. Most lineations are concentric with the rim, but others show a cross-hatched pattern. Similar concentric lineations are also found on the surface of the terrace zone. The outermost ejecta blankets have radial ridges.

References: [1] El-Baz F. 1972. NASA SP-315. [2] Margot J. L. et al. 1999. *Journal of Geophysical Research* 104:11,875–11,882.

5283

DANGER IN INTERPRETING THE 2-MICRON BAND OF REFLECTANCE SPECTRA OF SMALL ASTEROIDS: A LESSON FROM HAYABUSA/NIRS DATA OF ITOKAWA

T. Hiroi¹, M. Abe², T. Nimura^{2,3}, K. Kitazato⁴, S. Abe⁵, Y. Takagi⁶, S. Sasaki⁷, and M. Ishiguro⁸. ¹Department of Geological Sci., Brown University, Providence, RI 02912, USA. E-mail:takahiro_hiroi@brown.edu. ²JAXA Inst. of Space and Aeronaut. Sci., Sagami-hara, Kanagawa 229-8510, Japan. ³Department of Earth and Planet. Sci., University of Tokyo, Hongo, Tokyo 113, Japan. ⁴Graduate School of Sci., Kobe University, Nada-ku, Kobe 657-8501, Japan. ⁵Inst. of Astronomy, Natl. Central Univ., 300 Jhongda Rd, Jhongli, Taoyuan 32001, Taiwan. ⁶Aichi Toho University, Meito-ku, Nagoya 465-8515, Japan. ⁷RISE Project, National Astron. Obs. Japan, Oshu City, Iwate 023-0861, Japan. ⁸Department of Physics and Astronomy, Seoul National University, Seoul 151-742, Korea.

Introduction: Visible and near-infrared reflectance spectra have been often used in interpreting the surface mineralogy of asteroids. Especially, the 1 and 2 μm absorption bands are mainly indicative of the chemical compositions and relative abundances of pyroxenes and olivine. However, the interpretation of the apparent position and relative strength of the 2 μm band has many problems, which we present here based on different observations of the asteroid 25143 Itokawa.

Distance Dependency of Itokawa's 2- μm Band: It is clear from close observations by the Near-Infrared Spectrometer (NIRS) onboard Hayabusa spacecraft in October and November 2005 that Itokawa consists of a space-weathered LL5 or 6 chondrite material [1–3]. However, Itokawa's reflectance spectra taken by the same NIRS at a farther distance in September 2005 show somewhat different properties of the 2 μm band. Because all laboratory measurements of LL chondrite samples are performed using a small, uniform sample, observations which should be compared with them are those made at higher spatial resolutions (the highest resolution of NIRS observation was in the centimeter scale). This can cause serious misinterpretation of its surface mineralogy if one blindly uses the traditional band center and strength parameters based on any ground-based observation.

Possible Causes: Itokawa (and probably many other small asteroids) has a highly diverse physical property over its surface: from large and small boulders to regolith because of its low gravity and young surface age. Therefore, when its surface is observed as a whole or with low spatial resolution, the data would contain many different physical units even if the composition may be uniform. This is very different from typical laboratory measurements of meteorites, wherein each sample is measured as a chip or powder with a centimeter-scale field of view. There is not proven validity in applying a traditional 2 μm band characterization technique to a mixture of different physical forms of the same meteorite. In addition, space weathering which exists on Itokawa [1] causes weakening of the 1 and 2 μm band in a disproportionate manner [4], thus changing their band area ratio.

Summary: In this presentation, we will try to address whether the distance dependency of Itokawa's 2 μm band could be explained by those two possible causes.

References: [1] Hiroi T. et al. 2006. *Nature* 443:56–58. [2] Ishiguro M. et al. 2007. *Meteoritics & Planetary Science* 42:1791–1800. [3] Hiroi T. et al. 2007. Abstract #1048. 38th Lunar and Planetary Science Conference. [4] Ueda Y. et al. 2002. Abstract #2023. 33rd Lunar and Planetary Science Conference.

5128

ISOTOPIC AND RARE EARTH ELEMENT STUDIES OF A FUN-LIKE FORSTERITE-BEARING INCLUSION FROM ALLENDE

H. Hiyagon¹ and A. Hashimoto². ¹Department of Earth and Planetary Science, The University of Tokyo, Japan. E-mail: hiyagon@eps.s.u-tokyo.ac.jp. ²Department of Cosmochemistry, Hokkaido University, Japan.

Introduction: So called FUN (fractionation and unknown nuclear effects) is a minor group of refractory inclusions characterized by large mass-dependent fractionation in many elements (e.g., O, Mg, Si, etc.), unknown isotopic anomalies (e.g., in ⁴⁸Ca and ⁵⁰Ti), and very low initial abundance of short-lived nuclides such as ²⁶Al [e.g., 1]. We found in Allende meteorite (CV3, oxidized) a forsterite-bearing inclusion, AL1B-F, which shows petrographic evidence of a vigorous evaporation event. Here we report ion microprobe data for O and Mg isotopes and abundances of rare earth elements (REEs) for AL1B-F. Isotopic analyses of Si, Ca, and Ti are in progress.

Petrography: In the central part of AL1B-F (2.4 mm \times 1.1 mm in size), large forsteritic olivine grains (50–100 μm in size) and some spinel grains are embedded in fassaite. The outer part is spinel-rich. Some spinel grains show zoning in Al/Mg ratios from \sim 2 up to \sim 3, and sometimes show lamellae of hibonite (and corundum in rare case), suggesting a strong evaporation event in which Mg was largely lost. Between the forsterite-rich core and spinel-rich outer part are filled with abundant secondary minerals such as nepheline, sodalite, hedenburgite, and so on.

Results: Oxygen and Mg isotopes and REE abundances were measured using a CAMECA IMS-6f ion microprobe with analytical conditions similar to those described elsewhere [e.g., 2].

Oxygen isotope data for forsterite, spinel, and fassaite are plotted far right-hand side of the CCAM line with $\delta^{18}\text{O}$ from -23 to -5 permil and $\Delta^{17}\text{O}$ of -22 to -24 permil. They form a slope \sim 0.5 line, which crosses the CCAM line at $\delta^{17,18}\text{O} \sim -47$ to -48 permil, consistent with the compositions of typical refractory inclusions. One perovskite grain shows a ¹⁶O-poor composition ($\delta^{17}\text{O} \sim 0$ and $\delta^{18}\text{O} \sim +7$ permil).

All the minerals so far measured show heavily fractionated Mg isotopes with $\Delta^{25}\text{Mg} \sim +24$ to $+29$ permil/amu for forsterite in the core, $\sim +27$ permil/amu for spinel in the core, and $\sim +37$ to $+41$ permil/amu for coexisting spinel and hibonite, respectively. So far, no excess ²⁶Mg was observed even for hibonite (²⁷Al/²⁴Mg \sim 33) within experimental uncertainty.

Fassaite in the core shows an almost flat REE pattern (50–70 \times CI) with a large depletion in Ce ($\sim 5 \times$ CI) (and smaller depletions in Eu and La). Such Ce depletion is similar to those observed in experimentally produced evaporation residue [3, 4].

All the data suggests a vigorous evaporation event occurred on AL1B-F. Further analyses on Si, Ca, and Ti isotopes are important to see if AL1B-F has a UN signature and to understand the formation condition of such rare type of inclusions in the early solar system history.

References: [1] MacPherson et al. 1995. *Meteoritics* 30:365–386. [2] Ushikubo T. et al. 2007. *Earth and Planetary Science Letters* 254. [3] Floss C. et al. 1996. *Geochimica et Cosmochimica Acta* 60:1975–1997. [4] Davis A. M. and Hashimoto A. 1995. *Meteoritics* 30:500–501.

5233

SYSTEMATIC SURVEY ON THE MAGNETIC SIGNATURE OF MARTIAN METEORITES (SNC): EXTENDING THE DATABASE

V. Hoffmann^{1, 2}, M. Funaki³, M. Torii⁴, R. Hochleitner⁵, and N. Classen.
¹Institute for Geosciences, University of Tübingen Germany. ²Faculty of Geosciences, University of München, Germany. E-mail: viktor.hoffmann@uni-tuebingen.de. ³National Institute of Polar Research, Tokyo, Japan. ⁴Department of Geosphere-Biosphere System Science, Okayama University of Science, Okayama, Japan. ⁵Museum "Reich der Kristalle," München, Germany.

Introduction: In recent years, much effort was put in the systematic investigation of the magnetic record of stony meteorites in general, and specifically of SNC [1–4 and references herein]. In this way and together with in situ studies of Martian crustal materials our knowledge about the planetary development of Mars, the potential existence of a strong dynamo field during the first 0.5–1 Gyr, the petrogenesis of Mars surface as well as the origin of the strong crustal magnetic anomalies was significantly deepened.

Magnetic Signature: The focus of our projects is a systematic survey of the magnetic signature/mineralogy, and petrofabric of Martian meteorites in order to shed light on the effects of shock, alteration/weathering (Martian and terrestrial) and consequently on the question in which way the results can be linked to the situation on Mars. The SNC magnetic database was significantly extended, and new original data of most findings of the last years could be included. The SNC magnetic signature shows a striking variability even within specific groups of SNCs. It also has to be noted that in case of the hot-desert stony meteorite findings "magnetic pollution" caused by hand-magnets is a very serious concern. Another important outcome of our projects is that the meaning of earlier paleomagnetic results obtained on SNC rocks should be reinterpreted, especially in terms of magneto-mineralogy and shock effects.

Petrofabric, Magnetic Anisotropy: The anisotropy of magnetic susceptibility is a measure of the degree of crystalline preferred orientation and shape of the magnetic recorders in a specific rock. AMS is also influenced by contributions from Fe-bearing silicates such as olivines or pyroxenes. The anisotropy ratio P (ratio of maximum/minimum principal MS) generally is quite low in case of the SNC (below $P = 1.2$ – 1.3), however it also shows significant scatter even on several chips sampled from the same SNC rock. The results are in disagreement with the high degree of shock known from many SNC meteorites.

Fe-Ni Nanophases as a New NRM Recorder: Lherzolithic shergottites show quite variable magnetic properties which contrasts with the more homogeneous magnetic signature of other shergottite groups or nakhlites. In the case of lherzolithic shergottites an obvious link between the magnetic signature (magnetic susceptibility (MS), NRM/IRM intensity) and the main mass of the respective Mars rocks was found [5]. Obviously this behavior is an effect of the high shock degree, mineral neoformation (Fe-Ni metal) and terrestrial alteration.

References: [1] Rochette P., Funaki M., Hoffmann V. et al. 2005. *Meteoritics & Planetary Science* 40:529–540. [2] Rochette P., Hoffmann V., Funaki M. 2005. 36th LPSC. Abstract #1614. [3] Hoffmann V., Funaki M. 2006. 30th Symposium on Antarctic Meteorites. pp. 22–23. [4] Funaki M., Hoffmann V., Torii M. AGU 2007. [5] Hoffmann V., Torii M., Funaki M. 2008. 39th LPSC.

5047

COSMOGENIC HISTORIES IN GIBEON AND CAMPO DEL CIELO IRON METEORITES

M. Honda¹, H. Nagai¹, K. Nagao², K. Bajo², and Y. Oura³. ¹Department of Chemistry, Nihon University, Setagaya, Tokyo, Japan. E-mail: mhonda@p07.itscom.net. ²Lab. Earthquake Chemistry, University of Tokyo, Japan. ³Department of Chemistry, Metropolitan University of Tokyo, Hachioji, Minami Osawa, Tokyo.

Introduction: The Gibeon and Campo del Cielo iron meteorites are popular large size meteorites. Their irradiation histories have been found to be different in a great extent. The Gibeon, IVA, has two different subgroups of the cosmogenic histories [1], whereas the Campo del Cielo, IA, has a typical single stage history [2] since the formation of the meteorite, in the E8 years ago. As the cosmogenic products, some typical long lived radionuclides such as ¹⁰Be, ³⁶Cl, ²⁶Al, and ⁵³Mn have been determined in their metal and troilite phases. For determinations of these nuclides recently developed accelerator mass spectrometry has been applied and their high sensitivities can be applied. For stable products light noble gases, ³He, ⁴He, ²¹Ne, ³⁶Ar, and ³⁸Ar, have been determined in the metal phases applying sensitive mass spectrometry.

Results: Because of the large size irons the contents of the products are at the lowest levels. For example, the activity levels of ¹⁰Be in Gibeon are as low as $5E^{-5}$ dpm/kg, which may inform us the depth effects of the target down to close to 2 meters. The same lower contents have been detected in the ³He contents in the second sub group members of Gibeon. The lowest levels are at E^{-12} cc/g, and the separate fresh machine can only available for the ³He without a trouble for the memory effects of the other samples.

These lowest contents of cosmogenic nuclides in Gibeon can only be attributed to the second stage short exposure records after the serious effect in space during the irradiation history. For the El Taco [3], the large fragment of Campo del Cielo, the lowest data can be determined in the deepest samples. The extents however are not extensive because of the single stage history without suffering by breaking in main body. The lowest data in the El Taco are, ³He: $0.6E^{-9}$ cc/g, ¹⁰Be: $1E^{-3}$ dpm/kg. There are no sign of serious escapes of ³He or ³H, and the contents of radionuclides and those of noble gases are variable quite smoothly with the depths.

The productions of ¹⁰Be in these two irons were observed to be parallel with those of ²⁶Al, in a wide range down to lower than 0.001 dpm/kg ¹⁰Be, simply multiplying 0.7 to ¹⁰Be data. The formula for the productions of ¹⁰Be was applied for the exposure age calculations coupling with the contents of ²¹Ne [1]. The exposure age of Gibeon group 1 is $3E^8$ years, and that of El Taco is $2E^8$ years. The average exposure age found in the group 2 of Gibeon seems to be comparable with those of H-chondrites, 8 my [4]. The ages calculated for the group 2 members are variable with ¹⁰Be, and for the lower activities in deeper locations the ages reach to the level of the group 1.

References: [1] Honda M. et al. 2007. *Meteoritics & Planetary Science* 42. Abstract #5330. [2] Schultz L. and Franke L. 2000. He, Ne and Ar in meteorites. A data collection, 2 of 2. [3] Hintenberger H. et al. 1968. *Meteorite Research* p. 895. [4] Schultz L., Weber H. W., and Begemann F. 1991. *Geochimica et Cosmochimica Acta* 55:59.

5015

A PRESOLAR SiC GRAIN FROM A SUPERNOVA WITH UNUSUAL Si-ISOTOPIC COMPOSITION

P. Hoppe¹, J. Leitner¹, and S. Amari². ¹Max-Planck-Institute for Chemistry, Particle Chemistry Department, 55128 Mainz, Germany. E-mail: hoppe@mpch-mainz.mpg.de. ²Laboratory for Space Sciences and the Physics Department, Washington University, St. Louis, MO 63130, USA.

Introduction: Silicon carbide (SiC) is the best studied presolar mineral phase and a wealth of isotopic information exists on a large number of elements [1]. Of particular importance are the SiC X grains that formed in the ejecta of Type II supernova (SNII) explosions. Recently, we reported the discovery of a presolar SiC grain with unusual Si-isotopic signature (strong enrichment in ²⁹Si, depletion in ³⁰Si) and speculated that this grain might be related to the X grain family and formed in a SNII as well [2]. Here, we will explore this possibility in more detail.

Isotope Signatures of Grain KJB2-11-17-1: Grain KJB2-11-17-1 was found during a fully automated ion imaging survey of SiC grains from Murchison separate KJB (typical grain size: 0.25–0.45 μm [3]) with the NanoSIMS at MPI for Chemistry. A total of 1280 SiC grains was identified and measured for C- and Si-isotopic compositions. Grain KJB2-11-17 has ¹²C/¹³C = 265 ± 14, ²⁹Si = +634 ± 20‰, and δ³⁰Si = -177 ± 18‰. The ²⁹Si/³⁰Si of ~2× solar is the highest ratio found so far among presolar grains. A subsequent Ca-Ti measurement gave δ⁴²Ca = -14 ± 16‰ and δ⁴⁴Ca = 40 ± 19‰. In the context of a SNII origin the small but noticeable ⁴⁴Ca excess is likely due to the decay of radioactive ⁴⁴Ti; the inferred initial ⁴⁴Ti/⁴⁸Ti is 0.018 ± 0.009.

Discussion: In order to quantitatively explore the proposed SN origin of KJB-11-17-1 we performed mixing calculation using the 15 M_⊙, 19 M_⊙, and 25 M_⊙ SNII models of [4]. The best match was obtained with the 15 M_⊙ model when matter from the SiS, ONe, HeC, HeN, and H zones was mixed in a ratio 0.19% : 2.3% : 37.3% : 22.0% : 38.2%. This gives C/O ~ 1, ¹²C/¹³C = 267, δ²⁹Si = 49‰, δ³⁰Si = -162‰, and ⁴⁴Ti/⁴⁸Ti = 0.018. This is a very good match with the KJB2-11-17-1 data except that the predicted ²⁹Si enrichment falls far short the observed value. It was suggested already previously by [5] that SN models may underestimate the ²⁹Si yield in the C- and Ne-burning (ONe, OSi) zones by about a factor of two and that the ²⁶Mg(α,n)²⁹Si reaction rate has to be roughly doubled compared to that given by [6]. Because of its very high ²⁹Si/³⁰Si ratio, which indicates relative large contributions from the ONe and/or OSi zones, grain KJB2-11-17-2 provides the opportunity to make a stringent test of this hypothesis. Taking the mixing ratio of different SN zones as given above and doubling the ²⁹Si yield in the ONe and OSi zones gives δ²⁹Si = +630‰ which is a perfect match to our data. This clearly supports the idea that current SN models underestimate the production of ²⁹Si. As pointed out by [5], this would also explain why GCE models give too low ²⁹Si/²⁸Si [7].

References: [1] Zinner E. 2003. In *Treatise on Geochemistry*, vol. 1, edited by A. Davis, H. D. Holland, K. K. Turekian. pp. 17–39. [2] Hoppe P. et al. 2008. Abstract #1025. 39th Lunar and Planetary Science Conference. [3] Amari S. et al. 1994. *Geochimica et Cosmochimica Acta* 58:459–470. [4] Rauscher T. et al. 2002. *The Astrophysical Journal* 576:323–348. [5] Travaglio C. et al. 1998. In *Nuclei in the cosmos V*, edited by N. Prantzos. pp. 567–569. [6] Fowler W. A. et al. 1975. *Annual Review of Astronomy and Astrophysics* 13:69–112. [7] Timmes F. X. and Clayton D. D. 1996. *The Astrophysical Journal* 472:723–741.

5160

MODAL MINERALOGY OF MIGHEI, NOGOYA, AND COLD BOKKEVELD CM CHONDRITES BY XRD

K. T. Howard¹, G. K. Benedix¹, P. A. Bland^{1,2}, and G. Cressey³. ¹Impacts and Astromaterials Research Centre (IARC), The Natural History Museum, Mineralogy Department, London SW7 5BD, UK. ²IARC, Department of Earth Sci. and Eng., Imperial College, London SW7 2AZ, UK. ³The Natural History Museum, Mineralogy Department, London SW7 5BD, UK. E-mail: kieren.howard@nhm.ac.uk.

Introduction: CM chondrites have a variable texture that complicates mineralogical comparisons in thin section. They contain hydrous phyllosilicate formed by aqueous alteration. The CM parent body(ies) [1–3], or the solar nebula [4] are most often suggested as the site of alteration. Defining a rocks petrogenesis is difficult without modal mineralogy data, but optical or SEM point-counting studies of CMs are hampered by fine grain size. We are therefore determining modal mineralogy of meteorites by XRD (technique described in [5] and [6]). Here we report data for Mighei(M), Nogoya (N), and Cold Bokkeveld (CB).

Results and Discussion: These meteorites have a diverse but related mineralogy controlled by the degree of aqueous alteration. For example, Mighei is composed of: olivine (15.6%); enstatite(6.6); calcite(1.1%); magnetite (3.6); cronstedtite (45%); Mg-rich serpentine (23%); and FeS (4.6%). We find that Fe-rich serpentine (cronstedtite) is a well-ordered crystalline phase. Remaining phyllosilicate is poorly crystalline and disordered (TEM indicates this is more Mg-rich serpentine [7]). The poorly crystalline structure suggests nucleation and re-nucleation during alteration, perhaps explaining the decrease in phyllosilicate grain size with increasing alteration [7].

We observe an inverse relationship in the abundance of cronstedtite and Mg-rich serpentine, reflecting the transition from Fe to more Mg-rich serpentines as aqueous alteration progresses [2, 3, 7]. There is also an inverse correlation between the modal abundance of Mg-rich serpentine and olivine + pyroxene that defines the degree of aqueous alteration. We define the alteration sequence as: (from least to most altered) M < N < CB—as in [2].

Interestingly, a positive correlation exists in the modal abundances of cronstedtite and anhydrous olivine + pyroxene. This may be interpreted to indicate a primordial or pre-accretionary origin for both phases and as evidence for aqueous alteration and phyllosilicate formation in the solar nebular [e.g., 4]. This does not rule out further aqueous alteration on the parent body as both cronstedtite and anhydrous olivine + pyroxene are altered to more Mg-rich serpentine with progressive alteration. Indeed the correlation in modal phase variations between meteorites argues strongly for parent body formation of Mg-rich serpentine.

We are extending this study to explore the modal mineralogy of other carbonaceous chondrites so as to further reveal the site(s) of aqueous alteration.

References: [1] Bunch T. E. and Chang S. 1980. *Geochimica et Cosmochimica Acta* 44:1543–1577. [2] Browning L. B. et al. 1996. *Geochimica et Cosmochimica Acta* 60:2621–2633. [3] Hanowski N. P. and Brearley A. J. 2001. *Geochimica et Cosmochimica Acta* 65:495–518. [4] Metzler K. et al. 1992. *Geochimica et Cosmochimica Acta* 56:2873–2897. [5] Cressey G. and Schofield P. F. 1996. *Powder Diffraction* 11:35–39. [6] Bland P. A. et al. 2004. *Meteoritics & Planetary Science* 39:3–16. [7] Lauretta D. S. et al. 2000. *Geochimica et Cosmochimica Acta* 64:3263–3273.

5102

A LASER PROBE $^{40}\text{Ar}/^{39}\text{Ar}$ AND INAA INVESTIGATION OF FOUR APOLLO GRANULITIC BRECCIAS

J. A. Hudgins¹, J. G. Spray¹, S. P. Kelley², R. L. Korotev³, and S. Sherlock².
¹Planetary and Space Science Centre, University of New Brunswick, Canada.
²CEPSAR, Open University, U.K. ³Department of Earth and Planetary Sciences, Washington University, St. Louis, MO, USA.

Introduction: Infrared laser probe $^{40}\text{Ar}/^{39}\text{Ar}$ geochronology, instrumental neutron activation analysis (INAA) and analytical electron microscopy have been performed on four rock tiles of Apollo granulitic breccias (60035, 77017, 78155, and 79215). Granulitic breccias are high-temperature (~1000 °C) metamorphic rocks with homogeneous mineral chemistry [1]. The mineralogy and chemistry of these rocks, as well as exhumation constraints, indicate that the source of metamorphism was shallow via juxtaposition of footwall lithologies with overlying impact melt sheets or hot ejecta blankets, potentially making them akin to basal suevite lithologies in terrestrial impact craters.

Ar-Ar Results: $^{40}\text{Ar}/^{39}\text{Ar}$ data from this study and compiled from the literature [2] indicates a range of ages from 4.2 Ga to 3.9 Ga for the granulitic breccia suite. All studied granulitic breccias were metamorphosed and cooled initially at, or prior to, 3.9 Ga. This range of ages sets limits on the extent of surface processing during the late heavy bombardment. However, the fact that all of these rocks contain high concentrations of meteoritic siderophiles provides evidence for significant impact prior to 4.0 Ga (i.e., pre-LHB). These impact events may have provided the heat responsible for high-temperature metamorphism.

Post-LHB Thermal Reprocessing: We detected partial resetting events in the finer grained granulites that occurred significantly later than 3.9 Ga. These events were low-temperature (<300 °C) and, therefore, did not alter the mineralogy or texture of these rocks, but only resulted in minor brecciation and the partial release of argon from plagioclase. Interpretation of this low-temperature overprint indicates partial thermal resetting of the argon systematics to as young as 2.3 Ga.

Conclusions: Our results increase the amount of high-precision data available for the granulitic breccias and the lunar highlands crustal samples in general. The data alludes to the survival of pre-LHB material on the lunar surface and documents the effects of contact metamorphic and impact processes during the pre-Nectarian Epoch, as well as the low-temperature partial resetting of ages by smaller event impacts after 3.9 Ga.

References: [1] Warner et al. 1977. 8th Lunar and Planetary Science Conference. pp. 2051–2066. [2] Papike et al. 1998. *Planetary materials*. Reviews in Mineralogy, vol. 36. pp. 5-1–5-234.

5324

PLANETARY ANALOG FIELD TRIPS AT HUNGARIAN SITES WITH UNIVERSITY SPACE PROBE MODELS HUNVEYOR AND HUSAR

Gy. Hudoba¹, S. Hegyi², B. Drommer², S. Józsa³, H. Hargitai³, and Sz. Bérczi³. ¹Budapest Polytechnic, H-6000 Székesfehérvár, Budai út, Hungary. ²Pécs University, Department Informatics and G. Technology, H-7624 Pécs, Ifjúság u. 6. Hungary. ³Eötvös University, Institute of Physics, H-1117 Budapest, Pázmány P. s. 1/a, Hungary. E-mail: bercziszani@ludens.elte.hu.

Introduction: Hungarian localities were visited where planetary (mainly Mars) analog studies were carried out by the educational lander Hunveyor and rover Husar at North-Balaton, Mecsek, Nógrád Mountains where igneous rocks (basalt, tephrite, phonolite) are exposed, river transported rock assemblages were delivered to a plain by floods, on Earth (Dunavarsány) and on Mars (Chryse plains). The localities are as follows:

Andesite Eruption Lava Columns: Bér, Cserhát Mountains: Although basalt lava columnar morphology is a frequent occurrence in andesite is rare. (near Bér village, Cserhát Mountains).

Phonolite of Mecsek Mountains: Venus-Venera 13 analog rock by high K content.

High-Ti Gabbro from Szarvaskő, Bükk Mountains: High-Ti basalts found by both Apollo 11 and Apollo 17 is sometimes over the 10 weight percent Ti abundance: as their counterpart rocks among Hungarian gabbros from Szarvaskő [2].

Ophiolite from Darnó Hill, Bükk Mountains: In the Darnó Hill (basalts and microgabbros) textural sequence of an ophiolite can be found. From the outer edge high cooling rate textures to the bottom of the lava layer (or to the center of a pillow lava “sphere”) the following textures represent this series: spherulitic, variolitic, intersertal, intergranular, subophitic, ophitic, poikilitic, analog to lunar cooling layered textural sequence [3].

River and Flood Transported Boulders and Gravels, Dunavarsány, South Budapest Region: Surface gravel formation at South Pest (part of Budapest) in the Plain with Pliocene-Pleistocene age, thickness of 20–100 m in this region, consisting of sediments of the terraces of Danube. Various transported rocks from the middle and upper flow of the Danube: quartzite from the Alps, (~500 km of transporting distance), andesite from the Börzsöny Mts. (~50 km transporting distance), and sedimentary rocks. This site is analogous to the Chryse Plains where Viking 1 and Pathfinder observed flood-transported boulders delivered by ancient rivers in now dry beds of Kasei and Ares [4].

Wind-Formed Sharp Pebbles: Nógrád, Börzsöny Mountains: Northwest from the Nógrád Fortress Hill there are plough fields where dreikanter (sharp pebbles) can be found from the desert period of Miocene.

Sand Dunes: Fülöpháza, Great Hungarian Plain: West from Kecskemét there are remnants of the old sand “puszta” in the Great Hungarian Plain. There moving sand dunes can be found, even today. They are counterparts of the Martian sand dunes found at every landing sites.

Szentbékálla, Hegyestű: The basaltic rocks of North-Balaton Mountains (Sátorma hill and Boncostető eruptions 3 Myr ago) contain various inclusions, especially a peridotite xenolithic series with several types being important for planetary analog studies as counterparts of Martian shergottites. Not far from Szentbékálla the Hegyestű left quarry is a beautiful basalt peak and a Mining Museum. There the basalt flow formed hexagonal columns and a landscape where broken hexagonal prisms.

5041

COMPARATIVE STUDY OF ANHYDROUS MINERALS IN MICROMETEORITES AND CARBONACEOUS CHONDRITES

N. Imae¹ and N. Iwata². ¹National Institute of Polar Research, Kaga 1-chome, Itabashi-ku, Tokyo 173-8515, Japan. E-mail: imae@nipr.ac.jp. ²Yamagata University, 1-4-12, Kojirakawa, Yamagata 990-8560, Japan.

Introduction: Micrometeorites collected from Antarctic ice are characterized in general by the bulk Mg/Si ratio of ~0.9 in wt% [1, 2]. Mafic silicates that had survived the atmospheric entry heating are mainly forsterite and enstatite. They show poikilitic textures and have small Fe-Ni metal droplets embedded in it. These evidences may suggest that the majority of micrometeorites are unequilibrated carbonaceous chondrites [1–6]. The FeO distribution in the range of 0–5 wt% and minor compositions of CaO, Al₂O₃, Cr₂O₃, MnO, and TiO₂ in forsterite and enstatite may be a useful indicator for distinguishing the type of carbonaceous chondrites. We have started to carry out the study in order to understand the origin of micrometeorites.

Experiments: Electron probe microanalyzers (JEOL JXA-8200 of National Institute of Polar Research, Japan and CAMECA SX100 in Paris VI University, France) were used for the analyses of micrometeorites from Tottuki, Antarctica [7], and unequilibrated carbonaceous chondrites, Y-81020 (CO3.0), Y980051 (CM2), A-881595 (CR2), and Tagish Lake (ungrouped). We also have used for this study previous data on micrometeorites from Cap Prud'homme, Antarctica [3–6] and unequilibrated chondrites [8, 9] for the study.

Results and Discussion: We have compared forsterite compositions from previous studies (10 micrometeorites from [1], 33 [3], and 26 [4]) with those in carbonaceous chondrites analyzed in this study. The overall compositions of unmelted olivines in micrometeorites are similar to those in CR2 [9], based on the low abundance of Fa < 1 (mol%), the most frequent Fa ~ 1–3 (mol%), and the majority of CaO content of ~0.2 wt%. Enstatite compositions in 2 micrometeorites [1], 21 [3], and 7 [6] are compared with those in carbonaceous chondrites analyzed in this study with previous data [8]. Generally the unmelted enstatite crystals found in micrometeorites are very similar to those in CR2, based on the homogeneous distribution of FeO in low Ca pyroxene which is in the range of 0–4 wt% and the minor contents of CaO 0.5–3, Al₂O₃ 0.1–2, Cr₂O₃ 0.2–2, MnO 0.1–6, and TiO₂ 0–0.45 wt%.

The results focused on coarse-grained anhydrous silicates suggest that the micrometeorites are closely related to CR meteorites.

Acknowledgments: I am grateful to E. Dobrica, C. Engrand, and J. Duprat in C.S.N.S.M. in Orsay for their fruitful discussions, and also to M. Funaki in NIPR for supplying a potted butt of the Tagish Lake chondrite.

References: [1] Imae N. et al. 2008. Abstract #1729. 39th Lunar and Planetary Science Conference. [2] Yada T. et al. 2005. *Geochimica et Cosmochimica Acta* 69:5789–5804. [3] Beckerling W. and Bischoff A. 1995. *Planetary and Space Science* 43:435–449. [4] Steele I. M. 1992. *Geochimica et Cosmochimica Acta* 56:2923–2929. [5] Engrand C. et al. 1999. *Geochimica et Cosmochimica Acta* 63:2623–2636. [6] Kurat G. et al. 1994. *Geochimica et Cosmochimica Acta* 58:3879–3904. [7] Iwata N. and Imae N. 2002. *Antarctic Meteorite Research* 15:25–37. [8] Noguchi T. 1989. *Proceedings of the NIPR Symposium on Antarctic Meteorites* 2:169–199. [9] Kallemeyn G. W. et al. 1994. *Geochimica et Cosmochimica Acta* 58:2873–2888.

5018

PECULIAR REE PATTERN IN A GRANULAR-OLIVINE INCLUSION FROM THE MURCHISON (CM2) CHONDRITE

M. Inoue¹ and N. Nakamura^{2†}. ¹Kanazawa University, Ishikawa 923-1224, Japan. E-mail: mutsuo@llrl.ku-unet.ocn.ne.jp. ²Kobe University, Kobe 657-0059, Japan. [†]Present address: NASA Johnson Space Center, Houston, TX 77058–3696, USA.

Introduction: The CM chondrites as well as CV and CO contain amounts of inclusions (e.g., chondrules and CAIs). The inclusions from CM chondrites have preserved the abundant information about the formation and evolution processes of aqueously altered meteorites [1]. The abundances of rare earth elements (REE) in various meteoritic materials are expected to be a unique tool to constrain their geochemical environments. During systematic investigation of REE abundances in CM chondrules, we have encountered a chondrule-like inclusion from the Murchison chondrites, *MC-9*, carrying a peculiar REE abundance pattern. In this study, we report analytical results of REE (La, Ce, Nd, Sm, Eu, Gd, Dy, Er, Yb, Lu), alkalis (K and Rb), alkaline earths (Ba, Sr, Ca, Mg) and Fe by isotope dilution mass spectrometry (IDMS) for the inclusion along with petrographic examinations.

Experimental Setup: The inclusion, *MC-9* (mass = ~2.8 mg) was separated from Murchison whole rock fragment by hand-picking through freeze-thaw processing. This specimen was broken into approximately two parts; One part (38 wt%) of a whole inclusion was used for preparation of a polished thin section for petrographic examinations and the rest (62 wt%) was used for analysis of IDMS.

Results and Discussion: *MC-9* exhibits homogeneous granular-olivine (Fa; 0.385) texture carrying abundant glass and phosphate inclusions and has no sign of aqueous alteration. It is notable that *MC-9* indicates smoothly light-REE enriched REE pattern together with a large negative Eu anomaly (CI-normalized La/Lu ratio = 3.0; Eu/Eu* = 0.33). This smooth REE fractionation can not be explained as due to gas/solid REE fractionation in the nebula observed in CV and CO chondrules and inclusions [2] and REE features reflecting tetrad effect in aqueously altered CM chondrules [3], but are well understood as results of liquid/solid interaction. We suggest that the observed REE pattern of *MC-9* provides a new information about formation and evolution processes of this inclusion in the early solar system and/or the CM parent bodies.

References: [1] Brearley A. J. 2006. *Meteorites and the early solar system II*, edited by Lauretta D. S. and McSween H. Y. Jr. pp. 587–624. [2] Misawa K. and Nakamura N. 1988. *Geochimica et Cosmochimica Acta* 52: 1699–1710. [3] Inoue M. et al. 2008. *Geochimica et Cosmochimica Acta*. Submitted.

5134

ISOTOPIC FRACTIONATION OF TUNGSTEN FOR METEORITICAL MATERIALS

K. Irisawa^{1,2}, T. Hirata², and M. Tanimizu³. ¹Japan Atomic Energy Agency, 2-4, Shirakatashirane, Tokai, Naka-gun, Ibaraki, 319-1195, Japan. ²Tokyo Institute of Technology, Japan. ³Kochi Institute for Core Sample Research, JAMSTEC, Japan. E-mail: irisawa.keita@jaea.go.jp.

Currently the best chronometer for metal-silicate separation is the extinct ¹⁸²Hf-¹⁸²W systematics [1–4]. In the previous studies, the Earth's core could have separated from the silicate mantle within the first 30 million years of accretion, if Earth's accretion was terminated by a giant impact involved in the formation of the Moon and accompanied by a complete metal-silicate equilibration [1–3]. In order to constrain the age of the core-mantle differentiation and of the Moon-forming giant impact in the Earth strictly, we should estimate W behavior between a metal phase and a silicate phase through the planetary formation. To determine W isotopic fractionation for chondrites, achondrites, and iron meteorites have potential interpretation of planetary core-mantle differentiation since possible scenario range from a metal-silicate differentiation which may involve a magma ocean. Moreover, the coordination number change of W could occur during a metal-silicate separation. In this study, an external correction technique using ¹⁸⁵Re/¹⁸⁷Re ratio was applied in order to detect W isotopic fractionation for various meteoritic materials.

We have measured W isotope ratios for eleven iron meteorites of various chemical groups (IAB, IIAB, IIIAB, IIICD, IVA, and IVB), six chondrites (CM2, CV3, H4, L4, and L5 groups), and an achondrite (howardite). Not only isotopic growth of ¹⁸²W/¹⁸³W ratio due to radioactive decay of ¹⁸²Hf, but also the variations in W isotopic ratios due to mass dependent isotopic fractionation (¹⁸⁴W/¹⁸³W and ¹⁸⁶W/¹⁸³W ratios) were determined by the internal and the external correction technique for mass discrimination effects of MC-ICP-MS [5]. For the radiogenic component (¹⁸²W/¹⁸³W ratio), resulting data for all meteoritic materials obtained here were consistent with the previously reported data [3, 4]. In the case of non-radiogenic components, resulting ¹⁸⁴W/¹⁸³W and ¹⁸⁶W/¹⁸³W ratios were fractionated significantly among the meteorite groups, and all the W isotope data obtained here fell close to a mass-dependent fractionation line (MFL) on three isotope diagram (plot ¹⁸⁴W/¹⁸³W against ¹⁸⁶W/¹⁸³W ratios). The ¹⁸⁴W/¹⁸³W and ¹⁸⁶W/¹⁸³W ratios for magmatic iron meteorites were identical to those for terrestrial igneous rocks. Moreover, the ¹⁸⁴W/¹⁸³W and ¹⁸⁶W/¹⁸³W ratios for chondrites were slightly heavier than those for magmatic iron meteorites and terrestrial igneous rocks. The ¹⁸⁴W/¹⁸³W and ¹⁸⁶W/¹⁸³W ratios for an achondrite showed heavier isotopic feature from those for chondrites. This suggests the presence of isotopic fractionation of W through a metal-silicate segregation at the meteorite parental planetesimals, and that W isotopic ratios for terrestrial igneous rocks could be a result of mixing with the isotopically lighter-W, possibly originating from magmatic irons or the Earth's core. If this is the case, the timing of a giant impact after the CAI formation could be significantly earlier (20–30 Myr) than that currently accepted value (30 Myr; [3]).

References: [1] Lee D.-C. and Halliday A. N. 1995. *Nature* 378:771–774. [2] Harper C. L. and Jacobsen S. B. 1996. *Geochimica et Cosmochimica Acta* 60:1131–1153. [3] Yin Q.-Z. et al. 2002. *Nature* 418:949–952. [4] Kleine et al. 2005. *Geochimica et Cosmochimica Acta* 69:5805–5818. [5] Irisawa K. and Hirata T. 2006. *Journal of Analytical Atomic Spectrometry* 21: 1387–1395.

5332

NORTHWEST AFRICA 5298: A STRONGLY SHOCKED BASALTIC SHERGOTTITE EQUILIBRATED AT QFM AND HIGH TEMPERATURE

A. J. Irving and S. M. Kuehner. Department of Earth and Space Sciences, University of Washington, Seattle, WA, USA. E-mail: irving@ess.washington.edu.

Among the 51 known unpaired Martian meteorites, at least 15 are “enriched” shergottites characterized by relatively high LIL element abundances and La/Yb ratios, high intrinsic magmatic oxygen fugacities and young crystallization ages (165–225 Ma). Petrologically these specimens range from more primitive, olivine-bearing “basalts” (such as NWA 1068/1110, NWA 4468, and RBT 04261/2) to pigeonite “basalts” (Shergotty, Zagami, NWA 3171, etc.) to more ferroan, evolved examples (Los Angeles, Dhofar 378, NWA 2800) [1]. All of these specimens plausibly are related as a series of fractionally crystallized magmatic liquids from primary olivine-saturated magmas generated by recent partial melting of a peridotitic mantle source.

Northwest Africa 5298: This moderately evolved “enriched” basaltic shergottite has more complex pyroxene zoning, more phosphates, more silica, and is more highly shocked and oxidized than most. It is composed mainly of intergrown elongated grains of zoned pyroxene (FeO/MnO = 26.3–39.4) and lath-shaped regions of vesicular, extensively devitrified plagioclase glass (~An_{51.8}Or_{1.9}), with accessory titanomagnetite (Usp₆₃Mt₃₃Sp₄Chr_{0.4}), ilmenite (Ilm_{92.5-4.3}Hem_{5.1-3.0}Gk_{0.6-1.0}Py_{1.7}), silica, Na-Fe-merrillite, Cl-apatite, pyrrhotite, fayalite, and baddeleyite. Silica forms subhedral grains (up to 0.4 mm) within plagioclase glass. Pyroxene grains are compositionally zoned from subcalcic augite cores (Fs_{23.8}Wo_{28.4}) to pigeonite mantles (Fs_{30.2}Wo_{11.7}) to ferropigeonite rims (Fs_{68.0}Wo_{15.3}), with highly irregular and curvilinear zone boundaries that may reflect dissolution/resorption of growing crystals in response to changes in fluid fugacities in evolving residual liquids or possibly subsolidus processes. Oxygen fugacities during crystallization deduced [2] from compositions of coexisting Fe-Ti oxides are essentially at QFM, T = 1012 ± 20 °C. NWA 5298 is thus more oxidized than all other known shergottites except NWA 1068 [3].

Metasomatism of the Martian Mantle? By analogy with processes operative in Earth's mantle [4], we propose that the mantle source regions for “enriched” shergottite parental magmas were metasomatized (perhaps long before their young eruption times) by hydrous and chlorine-bearing fluids or magmas, which not only added Fe and LIL elements but also ferric iron. Patterns of LIL trace element abundances and radiogenic isotope ratios also support such a model [5]. This may explain why the most primitive olivine-bearing examples (NWA 1068, NWA 4468) have Mg/(Mg + Fe) ratios (0.59) significantly lower than those (0.68) for the older depleted olivine-phyric shergottites like Yamato 980459, NWA 1195, etc.

References: [1] Barrat J.-A. et al. 2002. *Geochimica et Cosmochimica Acta* 66:3505–3518; Irving A. et al. 2007. 38th LPSC. Abstract #1526; Dalton H. et al. 2008. 38th LPSC. Abstract #2073; Lapen T. et al. 2008. 39th LPSC. Abstract #2073; Irving A. et al. 2008. *Meteoritics & Planetary Science*. In revision. Rubin A. et al. 2000. *Geology* 28:1011–1014; Bunch T. et al. 2008. 39th LPSC. Abstract #1953. [2] Ghiorsio M. and Evans B. 2008. *American Journal of Science*. In press. [3] Herd C. 2006. *American Mineralogist* 91:1616–1627. [4] Roden M. and Murthy V. 1985. *Annual Reviews of Earth and Planetary Science* 13:269–296; McGuire A. et al. 1991. *CMP* 109:252–264. [5] Treiman A. 2003. 34th LPSC. Abstract #1413.

5204

CHEMICAL CHARACTERISTICS OF NORTHWEST AFRICA 011 AND NORTHWEST AFRICA 2976

J. Isa¹, K. Shinotsuka¹, A. Yamaguchi², and M. Ebihara¹. ¹Department of Chemistry, Tokyo Metropolitan University, Hachioji, Tokyo 192-0397, Japan. E-mail: isa-junko@ed.tmu.ac.jp. ²Antarctic Meteorite Research Center, National Institute of Polar Research, Itabashi, Tokyo 173-8515, Japan.

Introduction: Northwest Africa (NWA) 011 is a basaltic achondrite. It was initially classified into non-cumulate eucrites [1], but later recognized as an anomalous achondrite based on Fe/Mn ratio and oxygen isotopic composition [2]. NWA 2976 was found in 2005 and was listed as an ungrouped achondrite, being paired with NWA 011, mainly from mineralogical observation [3]. In the previous report, we pointed that NWA 011 has high contents of siderophile elements such as Co, Ni, and Ir, and tentatively proposed that these siderophile elements were introduced by projectile through impact [2]. An alternative mechanism was suggested for the source of siderophiles, which were proposed to be indigenous to the parent body of NWA 011 [4]. Here, we present new data sets of NWA 011 and NWA 2976, and discuss the uniqueness of these meteorites in terms of chemical composition. Our discussion covers the possibility of their being paired and the source of siderophile elements (especially, platinum group elements) in both NWAs.

Chemical Analyses: Major, minor, and trace element compositions were non-destructively determined by activation analyses (PGA, INAA and IPAA). Platinum group elements (PGEs) were determined by ID-ICP-MS. We used 500 mg or more of both meteorites for PGA and aliquants of their well homogenized powderes for INAA, IPAA, and ICP-MS.

Results and Discussion: Major, minor, and trace element compositions of NWA 011 and NWA 2976 are mostly consistent with those of eucrites. There appear, however, several unique characteristics in chemical compositions of these meteorites; NWA 011/NWA 2976 meteorites contain systematically high contents of siderophile elements (40.3/42.3 ppm versus 6 ppm for Co and 167/197 ppm versus 27 ppm for Ni) and low contents of Mn (0.224/0.227% versus 0.4210%) and Cr (1120/1160 ppm versus 2360 ppm). As these meteorites also have slightly higher Fe contents than those of eucrites (16.7–18.0% versus 14%), an apparent discrepancy in Fe/Mn ratios becomes obvious between the two NWAs and eucrites (74/79 versus 30–39). These data show that the chemical composition of NWA 2976 is similar to that of NWA 011 and uniquely different from those of eucrites.

ICP-MS analysis of MWA 011 confirmed a previously reported, high Ir content [2]. Including Ir, all PGEs were observed to be highly enriched in NWA 011 compared with those in typical eucrites. CI chondrite- and Ni-normalized PGE abundance pattern for NWA 011 is rather flat, with I-PGEs (Os, Ir, Ru) being slightly enriched. Partition behaviors of PGEs between solid metal and liquid metal may exclude a possibility that the liquid metal penetrated through the silicate phase. More plausibly, the PGE-enriched material was introduced to the basaltic silicate and both phases were eventually mixed up. As far as the PGE abundance pattern is concerned, IVB iron meteorites can be the best candidate of the projectile.

References: [1] Afanasiev S. V. et al. 2000. *Meteoritics & Planetary Science* 35:A19. [2] Yamaguchi A. et al. 2002. *Science* 296:334–336. [3] The Meteoritical Bulletin No. 91. p. 421. [4] Korotchantseva E. V. 2003. 34th Lunar and Planetary Science Conference. Abstract #1575.

5213

LOCALIZED GRAVITY/TOPOGRAPHY CORRELATION SPECTRA ON THE MOON

Y. Ishihara¹, K. Matsumoto¹, S. Goossens¹, H. Araki², N. Namiki³, H. Hanada¹, T. Iwata⁴, H. Noda², and S. Sasaki¹. ¹RISE Project, National Astronomical Observatory of Japan, 2-12 Hoshigaoka, Mizusawa, Oshu 023-0861, Japan. E-mail: ishihara@miz.nao.ac.jp. ²RISE Project, National Astronomical Observatory of Japan, 2-21-1 Osawa, Mitaka 181-8588 Japan. ³Kyushu University, 6-10-1 Hakozaki, Higashi-ku, Fukuoka 812-8581, Japan. ⁴ISAS/JAXA, 3-1-1 Yoshinodai, Sagami-hara, Kanagawa 229-8510, Japan.

Introduction: The correlations between the topography and gravity anomalies provide important information on the level of isostatic compensation of the lithosphere at the geological timescale, and reflect its thermo-mechanical state. Therefore, localized correlation analysis is one of the most important studies of selenodesy. Japanese lunar exploration KAGUYA (SELENE) has two kinds of selenodesical experiments. One is RSAT/VRAD (gravity mapping) experiment and another is Laser ALTimeter (LALT; topography mapping) experiment. These two experiments enable us to conduct localized analysis for the Moon.

Data: KAGUYA mission has been yielding representation of lunar gravity and topography (shape) substantially superior in resolution and accuracy to earlier solutions. For global lunar gravity field, an accurate spherical harmonic model of gravitational potential up to 90 degrees (SGM90d) was derived from 5 month tracking (including 4-way Doppler) data [1]. For topography, LALT has obtained more than 6 million altitude measurements with 5 m, from which a spherical harmonic expansion of topography to degree and order 1439 (STM1439_grid-01) has been determined [2]. In this study, we use those new models.

Localized Spectral Analysis: We employ the spatio-spectral localization technique [3] to obtain gravity/shape correlation spectra as function of position on the Moon. In this analysis, we localize harmonic field with axisymmetric windows of constant diameter, described by L_{win} zonal harmonic coefficients. This restricts the permissible range of l in the windowed fields at both the low- ($l > L_{win}$) and high-wave number ends ($l < L_{obs} - L_{win}$; L_{obs} is the maximum degree of observation). We chose three fixed windows with $L_{win} = 5, 10, 17$ (equivalent to spatial scales 2200, 1100, and 640 km, respectively). These window sizes correspond to large-, middle-, and small-size of impact basins.

Results: For up to degree 50 with $L_{win} = 5$ scale, it is clearly shown that the near-side is contains distinct anti-correlation regions whereas the far-side is mostly occupied by high correlation region. This difference is mainly due to large mascon basins in near-side, such as mare Imbrium. For $L_{win} = 10$ and 17 scales, we can see anti-correlation regions at not only near-side but also far side. Locations of anti-correlation regions in the far-side correspond to impact basins. However, lots of far side basins are not indicated by anti-correlations. In contrast, almost all near-side basins show anti-correlations. This difference is probably due to the difference of elastic thickness between the near side and the far side during the age of impact basin formation. It provides important information on the origin of lunar dichotomy and lunar thermal history.

Acknowledgements: SHTOOLS2.3 [4] was used for calculating localized correlation.

References: [1] N. Namiki et al. 2008. *Meteoritics & Planetary Science* 43. This issue. [2] H. Araki et al. 2008. *Meteoritics & Planetary Science* 43. This issue. [3] M. Simons et al. 1997. *Geophysical Journal International* 131:24–44. [4] M. Wieczorek. 2007. <http://www.ipgp.jussieu.fr/~wieczor/SHTOOLS/SHTOOLS.html>.

5104

RESULTS FROM THE SEARCH FOR TYPICAL CP IDP SILICATES IN COMET 81P/WILD 2 DUST SAMPLES

H. A. Ishii¹, J. P. Bradley¹, Z. R. Dai¹, M. Chi^{1,2}, A. T. Kearsley³, M. J. Burchell⁴, N. D. Browning^{1,2}, and F. J. Molster⁵. ¹Institute of Geophysics and Planetary Physics, Lawrence Livermore National Lab, Livermore, CA, USA. E-mail: hope.ishii@llnl.gov. ²Department of Chem. Engineering and Materials Sci., University of California, Davis, CA, USA. ³Department of Mineralogy, Natural History Museum, London, UK. ⁴School of Physical Sciences, University of Kent, Canterbury, Kent, UK. ⁵NWO, Den Haag, The Netherlands.

Introduction: The chondritic porous subset of the interplanetary dust particles (CP IDPs), collected during high-altitude stratospheric flights, were widely expected to be the closest cousins of comet dust returned by the NASA Stardust mission to comet 81P/Wild 2 [1]. Decades of research have shown CP IDPs display characteristics consistent with cometary origins and with comet observations: mineralogy, friability, IR spectra, heating profiles, high carbon abundance, highest abundances of presolar grains. Comet Wild 2 is believed to originate beyond Neptune's orbit among Kuiper belt comets [2] and so was hoped to hold large quantities of presolar stardust grains. Results to date include presolar grain abundances similar to meteorites [3] and characteristic inner solar system materials, a CAI and igneous fragments typical of chondrules [4]. We searched Wild 2 samples specifically for two silicate materials typical of CP IDPs [5], enstatite platelets/whiskers and glass with embedded metal and sulfides (GEMS). Enstatite platelets/whiskers are readily recognizable and are uniquely [100]-elongated in CP IDPs. GEMS are abundant in CP IDPs, some shown to have presolar origins consistent with having been interstellar amorphous silicates.

Results: As reported in our recent publication [5], we identified a single enstatite whisker, but with an elongation direction characteristic of terrestrial and meteoritic enstatite instead of CP IDPs. A large abundance of objects that look, in TEM imaging, like GEMS are found in the Wild 2 sample [2]. By laboratory light gas gun shots, we demonstrated that capture of sulfides by silica aerogel at Stardust impact speed produces glass with embedded metal and sulfides and reproduces sulfide-rimmed metal beads seen in Wild 2 samples. Given the presence of melted-and-quenched pyroxenes that may have donated non-Si cations to a silicate glass, differentiating possible native GEMS from fine-grained material generated by impact is unlikely to be successful.

Conclusions: We have demonstrated that impact capture in aerogel, even at the relatively slow speeds of the Stardust mission, creates significant fine-grained intermixed material. The lack of recognizable GEMS and enstatite whiskers characteristic of the CP IDPs—in combination with prior results of inner solar system refractory objects, isotope ratios consistent with inner solar system chondrites and little refractory carbon—indicate that comet Wild 2 dust is petrogenetically more closely related to the chondritic meteorites than the CP IDPs.

Acknowledgements: We acknowledge NASA and JPL/Caltech for substrates and NASA, STFC and LLNL SEGRF grants. Portions of this work performed under U.S. DOE auspices by LLNL under contract DE-AC52-07NA27344.

References: [1] Brownlee D. E. and Joswiak D. J. 1995. 26th Lunar and Planetary Science Conference. pp.183–184. [2] Brownlee D. E. et al. 2006. *Science* 314:1711–1716. [3] Stadermann F. J. and Floss C. 2008. Abstract #1889. 39th Lunar and Planetary Science Conference. [4] Zolensky M. E. et al. 2006. *Science* 314:1735–1739. [5] Ishii H. A. et al. 2008. *Science* 319:447–450.

5100

O ISOTOPE MAPPING OF A WARK-LOVERING RIM IN A TYPE A CAI: CONSTRAINTS ON ITS FORMATION PROCESS

M. Ito and S. Messenger. ARES, NASA Johnson Space Center, 2101 NASA Parkway, Houston TX 77058, USA. E-mails: motoo.ito-1@nasa.gov; scott.r.messenger@nasa.gov.

Introduction: Wark-Lovering (WL) rims are multilayered rim sequences that surround most Ca, Al-rich inclusions (CAIs) and are composed of the same primary high-temperature minerals as CAIs, such as melilite and spinel and pyroxene [e.g., 1]. The rim minerals clearly represent a different generation formed by a separate event, but their formation processes are poorly understood [2]. Techniques for obtaining high-precision O isotopic images by ion microprobe have recently been developed, enabling the investigation of O isotopic variability within and between individual CAI minerals [3–5]. We are able to determine O isotopic ratios of minerals with ~5% precision at the ~0.4 μm spatial scale with the JSC NanoSIMS 50L [4, 5]. Here we apply this technique to investigate heterogeneous distributions of O isotopic ratios in minerals of WL rim in a CAI.

Experiment: The sample studied (7R19-1(d)) is a 3 × 3 mm Type A CAI that mainly consists of melilite, fassaite, and spinel [6]. The CAI is covered by a ~50 μm WL rim, composed of spinel, perovskite, melilite; and alteration products [6]. O isotopic maps of the CAI interior and the WL rim in the 7R19-1(d) were obtained by the JSC NanoSIMS 50L following techniques described in [4, 5]. A focused Cs⁺ primary ion beam with a diameter of ~100 nm was rastered over 20 × 20 μm. Secondary ion images of ¹⁶O⁻, ¹⁷O⁻, ¹⁸O⁻, ²⁸Si⁻, ²⁴Mg¹⁶O⁻, and ²⁷Al¹⁶O⁻ were acquired simultaneously in multidetection with EMs at a high mass resolution of ~9500. San Carlos olivine was measured as an isotopic standard. A normal incident electron gun was applied to prevent charging of the rastered area.

Results and Discussions: As expected, the O isotopic compositions of minerals in the CAI interior and the WL rim fall along the CCAM line. The O isotopic ratios in the CAI interior and the WL rim matched values determined in previous studies [6–10]. We found that spinel and melilite have δ^{17,18}O of ~-40 and ~-10‰ in the CAI interior, and spinel, perovskite, melilite, and anorthite had a δ^{17,18}O of ~-35, ~-20 to ~-10, ~-20 to 0, and ~-10 to 0‰ in the WL rim, respectively. An isotopic imaging traverse across the rim showed that the O isotopic composition varied from ¹⁶O-poor to ¹⁶O-rich to ¹⁶O-poor. This observation suggests that the accretion of the WL rim occurred as the CAI cycled between ¹⁶O-rich and ¹⁶O-poor regions of the nebula. This is consistent with a previous study which showed that the CAI formation began in a ¹⁶O-rich nebula and subsequently continued in an ¹⁶O-poor nebula [11].

References: [1] Wark and Lovering. 1977. 8th Lunar Science Conference. pp. 95–112. [2] MacPherson et al. 2005. *Chondrites and the protoplanetary disk*. ASP Conference Proceedings 341. pp. 225–250. [3] Nagashima et al. 2004. Workshop on Chondrites and the Protoplanetary Disk, 9072. [4] Ito and Messenger. 2007. 38th LPSC. Abstract #1794. [5] Ito and Messenger. 2008. *Applied Surface Science*. Accepted. [6] Ito et al. 2004. *Geochimica et Cosmochimica Acta* 68:2905–2923. [7] Hirai et al. 2002. 33rd LPSC. Abstract #1494. [8] Yoshitake et al. 2005. *Geochimica et Cosmochimica Acta* 69:2663–2674. [9] Aléon et al. 2007. *Earth and Planetary Science Letters* 263:114–127. [10] Cosarinsky et al. 2008. *Geochimica et Cosmochimica Acta* 72:1887–1913. [11] Itoh and Yurimoto. 2003. *Nature* 423:728–731.

5103

NWA 4757: METAMORPHOSED CARBONACEOUS CM CHONDRITE

M. A. Ivanova¹, C. A. Lorenz¹, L. V. Moroz^{2,3}, R. C. Greenwood⁴, I. A. Franchi⁴, and M. Schmidt⁵. ¹Vernadsky Institute, Kosygin 19, Moscow 119991, Russia. E-mail: venus2@online.ru. ²Institute of Planetology, University of Münster, Germany. ³DLR Institute of Planetary Research, Berlin, Germany. ⁴The Open University, Milton Keynes, UK. ⁵University of Heidelberg, Germany.

Introduction: Beside the Antarctic metamorphosed carbonaceous chondrites (MCCs) of the Belgica 7904 group [1] there are two non-Antarctic MCCs found in a hot desert: Dhofar 225 and Dhofar 735 [2, 3]. They differ from typical CM2 chondrites in mineralogy, oxygen isotopic compositions, H₂O content, bulk chemistry, and infrared spectra of their matrices [3, 4]. The recently discovered carbonaceous chondrite NWA 4757 has similarities with both groups of carbonaceous chondrites, MCC, and CM2. Here we report preliminary results on its petrography, mineralogy, H₂O, and C contents, oxygen isotopic compositions, and synchrotron-based infrared microspectroscopy (SIRM) to characterize the hydration states of the NWA 4757 matrix minerals.

Results: The meteorite consists of fine-grained matrix material, round objects sometimes with haloes of phyllosilicate and carbonates, and relict aggregates embedded in altered matrix. Silicates from the objects in the meteorite correspond to serpentine in composition. We analyzed the only grain of olivine found in the matrix. The minor phases are ilmenite, chromite, sulfides, kamacite, taenite, tetraenaite, phosphates, Ca,Mg-carbonates. Olivine is characterized by Fa₁₀, CaO 0.06; MnO 0.19 (wt%). Chemical composition of the matrix corresponds to serpentine, but with high analytical totals. Bulk contents (wt%) were H₂O 1.9, C 0.68. Average bulk oxygen isotopic compositions are $\delta^{18}\text{O} = +27.0\text{‰}$; $\delta^{17}\text{O} = +14.5\text{‰}$; $\Delta^{17}\text{O} = 0.48\text{‰}$. The SIRM study showed that the matrix is depleted in hydrated silicates and is dominated by Fe-rich fine-grained olivines.

Discussion: In texture and opaque mineral assemblage, NWA 4757 belongs to the CM chondrites. Bulk H₂O content is lower than that of CM2 chondrites and corresponds to MCCs. The oxygen isotopic composition of NWA 4757 is out of the range of typical CM2, and is even heavier than that of MCCs. The matrix is more homogeneous in chemical composition than that of MCCs and CM2 chondrites. Unlike matrices of typical CM2 chondrites [4], the matrix of NWA 4757 is depleted in hydrated silicates and is dominated by Fe-rich fine-grained olivines. In this respect it resembles previously studied matrices of MCCs, Dhofar 225 and Dhofar 735 [4]. Furthermore, the SIRM study also shows that several objects and halos consisting of phyllosilicates and carbonates are strongly hydrated, probably caused by terrestrial weathering. Trace element distribution will help to understand this. Based on this preliminary study, NWA 4757 belongs to the MCCs, and appears to be a mixture of dehydrated matrix material and strongly hydrated objects. If very hydrated objects and rims formed in deep space, they could survive only if the matrix had been dehydrated before their incorporation into the parent asteroid of NWA 4757.

References: [1] Ikeda Y. 1992. *Proceedings of the NIPR Symposium on Antarctic Meteorites* 5:49–73. [2] Ivanova M. A. et al. 2004. Abstract #5113. *Meteoritics & Planetary Science* 39. [3] Ivanova M. A. et al. 2005. Abstract #1054. 36th Lunar Planetary Science Conference, [4] Moroz L. V. et al. 2006. *Meteoritics & Planetary Science* 41:1219–1230.

5138

Mn-Cr SYSTEMATICS OF SECONDARY FAYALITE IN THE Y-86009 CV3 CARBONACEOUS CHONDRITE

K. Jogo¹, T. Nakamura¹, S. R. Messenger², M. Ito², and T. Miyamoto¹. ¹Department of Earth and Planetary Sciences, Kyushu University, Fukuoka, Japan. E-mail: kaori@geo.kyushu-u.ac.jp. ²ARES, NASA JSC, Houston TX, USA.

Introduction: Secondary fayalite (Fa₈₀) is one of the features characterizing Bali-like oxidized subgroup of CV3 chondrites (CV3_{OxB}) [1]. However, Vigarano meteorite, classified to reduced subgroup, contains some CV3_{OxB} clasts containing fayalite [2]. Mineralogy and Mn-Cr formation age of the fayalite in the CV3_{OxB} clasts in Vigarano are consistent with those in CV3_{OxB} chondrites [3–5], implying that all CV3_{OxB} chondrites and clasts derived from a single CV3_{OxB} asteroid. To check this scenario, we made a detailed characterization of fayalite in the CV3_{OxB} Y-86009 meteorite, and determined formation age based on Mn-Cr system using a SIMS IMS 6f at Kyushu University. Additional age determination using a NanoSIMS at NASA JSC is now in progress.

Results and Discussion: The SEM observation indicates that Y-86009 is a breccia consisting of many clasts; a clast is composed of a chondrule and a surrounding fine-grained material. The clasts are embedded in the host matrix or have direct contact with adjacent clasts, which can be recognized by boundaries in BSE image.

Fayalite grains (Fa_{85–100}) are observed in the host matrix and in several clasts. They are 5–50 μm in size and coexist with troilite and/or magnetite, suggesting that the host Y-86009 and the clasts are CV3_{OxB} materials [1]. However, the host matrix contains larger numbers of secondary minerals (e.g., fayalite, magnetite, etc.) than the fine-grained materials of the clasts, indicating that the host Y-86009 and the clasts are slightly different in lithology.

The fayalite in the clasts exists in chondrule interiors and peripheries, and in fine-grained materials. It occurs as isolated grains, or as constituents of laths (up to 20 \times 100 μm) that extended from the magnetite-sulfide nodules in the chondrule surfaces. The laths terminate near the clast boundaries, implying the preferential occurrence of the fayalite in the clasts.

Mn-Cr isotope analysis was performed on four fayalite grains (20–50 μm , Fa_{98–100} and high MnO content of 0.8 wt%) in one of the clasts. They do not show iron-magnesium zoning, indicating that the fayalite grains have not been altered after their formation. The Mn-Cr data for them define an initial ⁵³Mn/⁵⁵Mn ratio of $(2.9 \pm 0.4) \times 10^{-6}$. This ratio indicates that the fayalite in the clast in the CV3_{OxB} Y-86009 formed 4 \pm 2 Ma before angrite parent body. An absolute age was also determined to be 4562 \pm 2 Ma.

The SEM observations imply that the CV3_{OxB} clasts containing fayalite had not formed in the present structure of the Y-86009. The obtained fayalite formation age is identical within errors to that of CV3_{OxB} chondrites [3, 4] and Vigarano CV3_{OxB} clasts [5], suggesting that they formed in the same period. Therefore, the CV3_{OxB} clast in the Y-86009 could have originated from the single CV3_{OxB} asteroid where all CV3_{OxB} materials formed. Had other CV3_{OxB} clasts in the Y-86009 and the host CV3_{OxB} Y-86009 originated from the same asteroid? Additional age determination of the fayalite in them will verify it.

References: [1] Weisberg M. K. and Prinz M. 1998. *Meteoritics & Planetary Science* 33:1087–1099. [2] Krot A. N. et al. 2000. *Meteoritics & Planetary Science* 35:817–825. [3] Hutcheon I. D. et al. 1998. *Science* 282: 1865–1867. [4] Hua X. et al. 2005. *Geochimica et Cosmochimica Acta* 69: 1333–1348. [5] Jogo K. et al. 2006. *Meteoritics & Planetary Science* 41. Abstract #5242.

5221

X-RAY MICROTOMOGRAPHY OF A SULFIDE-RICH PALLASITE

D. Johnson¹, I. Rahman², and M. M. Grady^{1, 3}. ¹PSSRI Open University, Milton Keynes, MK7 6AA, UK. E-mail: D.Johnson@open.ac.uk. ²Department of Earth Science and Engineering, Imperial College London, London SW7 2AZ, UK. ³Department of Mineralogy, The Natural History Museum, London SW7 5BD, UK.

Introduction: Main Group pallasites are generally considered to have formed in an asteroidal core-mantle boundary region. It has been suggested that sulphide rich pallasites are under represented in our collections [1, 2] only two such pallasites have been identified Phillips County and Hambleton [3]. Because of the dynamic nature of the processes involved in the formation of this type of pallasite, the keys to understanding them may be as much structural as chemical. Here, we discuss the application of X-ray microtomography to the sulphide rich main group pallasite Hambleton as an attempt to further understand pallasite genesis.

Discussion: X-ray microtomography (XMT) and custom computer software were used to visualize the interior of a sample of Hambleton in three dimensions. This is a non-destructive technique used to examine the internal components of opaque solid samples. XMT was performed on a Phoenix v|tome|x “s” system, this generated a data set of several hundred two-dimensional section images (tomograms) through the specimen, with a slice thickness of approximately 60 µm. XMT maps the variation of X-ray attenuation within an object (roughly equivalent to density); strongly attenuating metals and sulfides appear as brighter pixels in slice images compared to olivine. Following the methodology of Sutton et al. [4], the two-dimensional tomographic data set was reconstructed using the custom SPIERS software suite to create a three-dimensional “virtual meteorite.” Tomograms were manually “edited” prior to reconstruction to accurately assign pixels to the major phases in the sample. Virtual models were studied on computer using stereo-capable viewing software. The samples were found to be composed of large angular olivine crystals intersected by metal and veins of FeS containing small angular fragments of olivine. The results show the sulfide distribution through the sample as thin veins and irregularly shaped sheets of FeS that are largely interconnected, filling the regions between olivine and metal.

Conclusions: X-ray microtomography is an under-utilized technique for the study of diverse samples such as pallasites. The three-dimensional textures observed in Hambleton may be explained by introduction of a large sulphide volume under pressure into a metal-olivine mixture with metal approaching solidus temperature.

References: [1] Ulf-Moller F. 1998. *Meteoritics & Planetary Science* 33:207–220, [2] Ulf-Moller F. 1998. *Meteoritics & Planetary Science* 33: 221–227. [3] Johnson D. et al. 2006. *Meteoritics & Planetary Science* 41: A88–A89. [4] Sutton M. D. et al. 2001. *Paleontologica Electronica* 4: article 2 (http://palaeo-electronica.org/2001_1/s2/issue1_01.htm).

5063

PARAMETERIZATION OF PYROXENE/LIQUID REE PARTITION COEFFICIENTS

J. H. Jones. KR, NASA/JSC, Houston, TX 77058, USA. E-mail: john.h.jones@nasa.gov.

Introduction: Rare earth elements (lanthanides; REE) have been of great importance in unraveling the petrogenesis of basaltic igneous rocks. Because of this, it is useful to have quick estimates of REE partition coefficients. Here I give a generalized method for estimating REE partition coefficients that is applicable over a wide range of pyroxene compositions—from orthopyroxenes to augites.

Rationale: McKay et al. [1] showed that REE partition coefficients were sensitive to the CaO content of the pyroxene. Because REE substitute for Ca in the pyroxene M1 site, the more Ca sites that exist, the better the chance that a REE will partition into that site. Specifically McKay et al. showed that:

$$\ln D(i) = [A(i) * W_o] - B(i) \quad (1)$$

and presented two matrices of A and B values for 8 REE—one matrix for pigeonite and one for augite. LREE changed the most with increasing W_o content, whereas HREE changed the least. However, this result was believed to only be applicable for bulk compositions near that of the Shergotty parent magma.

Further Work: Building on this theme, Jones [2] took literature and unpublished data [much of which came from McKay] and plotted $\log D(\text{REE})$ versus $\log D(\text{Ca})$. Linear trends were found that appeared to be applicable to a wide variety of bulk compositions that crystallized orthopyroxene, pigeonite, and augite [2]. Standard errors for these regressions were $\sim \pm 30\%$. As in the McKay study, LREE changed the most with $D(\text{Ca})$ and HREE changed the least. Slopes and intercepts of these regressions changed in a very regular way with REE atomic number. Both high-pressure and low-pressure D's fell on the same regression. Apparently, factors such as T and P that affect $D(\text{REE})$ change $D(\text{Ca})$ similarly.

Implications and Applications: The combined work of McKay and Jones emphasizes the importance of crystal chemistry for the partitioning of REE into pyroxene. Because the regressions of Jones are insensitive to pressure [up to 30 kbar] and temperature, it is only necessary to know the compositions of melts and pyroxenes to calculate approximate $D(\text{REE})$. Calculated D's will be compared to recently measured $D(\text{REE})$ for pyroxenes grown from a Y-980459 composition [3].

References: [1] McKay G. A. et al. 1986. *Geochimica et Cosmochimica Acta* 50:927–937. [2] Jones J. H. 1995. *A handbook of physical constants*. AGU Reference Shelf, vol. 3. pp. 73–104. [3] Blinova A. and Herd C. D. K. 2008. Goldschmidt Conference Abstracts 2008.

5263

BULK COMPOSITIONS OF CHONDRULES AND THE NATURE OF CHONDRULE PRECURSOR MATERIALS

R. H. Jones. Department of Earth and Planetary Sciences, University of New Mexico, Albuquerque, NM 87131, USA. E-mail: rjones@unm.edu.

Chondrules, by definition, have been heated at least to the point of partial melting. This heating destroyed chondrule precursor materials, which were presumably mostly fine-grained. Despite many years of effort, we are still unclear about the nature of precursor materials. Bulk compositions of chondrules can potentially provide some insights into this question, but chondrule bulk compositions are not very well defined. For the CV chondrites, existing data for chondrule bulk compositions, including chondrules from Allende [1, 2] and Vigarano [2], do not provide a definitive picture of the diversity of primary compositions [3]. Here, we use bulk compositions of a large suite of chondrules from the CV_{ox} chondrite, Mokoia [4, 5], to resolve existing discrepancies regarding CV chondrule bulk compositions, and as a basis to discuss precursor components. Bulk oxygen isotope data obtained for 20 of the chondrules [6] enable us to relate bulk chemical and isotopic properties.

The 90 Mokoia chondrules studied have masses of 0.1 to 22.5 mg. Detailed studies of the petrology of 20 of the largest chondrules show that metamorphism and secondary alteration are minimal. Chondrule densities, mean chondrule compositions, and the range of abundances for most elements, are essentially identical for different chondrule size fractions.

Among the chondrules analyzed, all major element abundances show a range of about a factor of ten. This is significantly greater than would be expected from analytical errors, matrix adhering to chondrules, or secondary alteration effects. While some of the variation might be attributable to chemical (e.g., volatilization or condensation) or physical (e.g., metal loss) processes during chondrule formation, much of it can reasonably be attributed to variations in the assembly of fine-grained precursor materials. Variations in chemistry lead to the inference that fine-grained material included: 1) a refractory component, possibly inherited from disaggregated CAIs, 2) an FeO-poor ferromagnesian component such as olivine and/or pyroxene, 3) an oxidized ferromagnesian component, and 4) a metal component. These are similar to components inferred for Allende chondrules [1]. Bulk oxygen isotopic compositions of chondrules can be explained if refractory and ferromagnesian precursor materials shared similar oxygen isotopic compositions of $\delta^{17}\text{O}$, $\delta^{18}\text{O}$ around -50% , and then significant exchange occurred between the chondrule and surrounding ^{16}O -poor gas while the chondrules were molten.

If the diversity of chondrule compositions can indeed be attributed to mixing of various dust components, it is necessary to invoke different source regions for these components, as well as a mixing mechanism that is compatible with maintaining the fundamental differences between chondrite groups.

References: [1] Rubin A. E. and Wasson J. T. 1987. *Geochimica et Cosmochimica Acta* 51:1923–1937. [2] McSween H. Y. Jr. 1977. *Geochimica et Cosmochimica Acta* 41:1777–1790. [3] Jones R. H. et al. 2005. *Chondrites and the protoplanetary disk*, edited by A. N. Krot et al. Astronomical Society of the Pacific Conference Series 341. pp. 251–285. [4] Schilk A. J. 1991. Ph.D. thesis, Oregon State University. [5] Jones R. H. and Schilk A. J. 2000. Abstract #1400. 31st Lunar and Planetary Science Conference. [6] Jones R. H. et al. 2004. *Geochimica et Cosmochimica Acta* 68:3423–3438.

5040

ACOUSTIC VELOCITY TRENDS, POROSITY, AND PORE GEOMETRY IN ORDINARY CHONDRITES: IMPLICATIONS FOR METEORITE AND METEORITE PARENT BODY ELASTIC PROPERTIES

S. F. Jones and A. R. Hildebrand. Geoscience, University of Calgary, Canada. E-mail: sfjones@ucalgary.ca.

Introduction: The study of meteorite porosity and pore geometry and its relationship to meteorite physical properties may provide proxies for parent body characteristics. Acoustic velocity, bulk density, porosity, and derived elastic moduli may help constrain collisions throughout the solar system. Significant total porosities have been reported for ordinary chondrites [1, 2], but meteorite pore geometry has not been studied in detail.

Methods: Physical properties have been documented for 80 meteorite samples, 78 from the Center for Meteorite Studies Collection at Arizona State University and 2 from the University of Calgary. Bulk density measurements were completed via an Archimedeian method [2] utilizing 1 mm glass beads as the fluid, grain densities, and derived porosities were determined using a He-pycnometer (ASU), and acoustic velocities were measured using a pulse generator, compressional and shear wave transducers and a digital oscilloscope. Pore geometries have been examined via thin section petrography for selected samples.

Discussion: Results are consistent with previous trends identified in H chondrites: acoustic velocity decreases with increasing porosity and acoustic velocity increases with meteorite darkness and bulk density [3]. These trends are also found to be true for the L chondrites as well as other chondrites (and some achondrites) examined in this study. Three pore geometries have been observed in ordinary chondrites; (1) fracture porosity (microns to hundreds of microns in diameter and microns to millimeters in length), (2) rounded to irregular equi-dimensional to ovoid pores, and (3) interstitial porosity including all irregular voids between grains and along grain contacts. The different pore geometries do not correlate with chondrite chemical groups or petrologic types, the presence of fracture porosity does not correlate solely with slow acoustic velocities, and different pore geometries may occur together in a common meteorite sample. Backscatter electron images resolve extensive microfracture networks in brecciated chondrites such as St-Robert and achondrites such as ASU 827D.1 Kapoeta. While meteorite porosity is not usually dominated by fractures, artificially fractured targets [4, 5] are also being studies to constrain fracture related effects.

Acknowledgements: Thank you to R. Hines, M. Wadhwa, L. Garvie, S. Nowak, and M. Sanborn at the Center for Meteorite Studies and A. Clarke and K. Genareau at the Volcanology Research Group at ASU. Thank you to E. Gallant, J. Wong, M. Allen, R. Stewart, and M. Bertram at the CREWES project and M. Horvath and L. Bloom in the Department of Geoscience at U of C. Project funding provided by NSERC and Alberta Ingenuity Fund.

References: [1] Britt D. T. and Consolmagno G. J. 1997. Abstract #1583. 28th Lunar and Planetary Science Conference. [2] Consolmagno G. J. and Britt D. T. 1998. *Meteoritics & Planetary Science* 33:1231–1241. [3] Hons M. 2004. B.Sc. thesis, University of Calgary. 48 p. [4] Ai H. 2006. Ph.D. thesis, California Institute of Technology. 159 p. [5] Ai H. and Ahrens T. J. 2004. *Meteoritics & Planetary Science* 39:233–246.

5020

RADIONUCLIDE STUDIES OF METEORITES FROM RAMLAT AL WAHIBAH AND OTHER OMANI DESERT LOCATIONS

A. J. T. Jull¹, M. D. Leclerc¹, D. L. Biddulph¹, L. R. McHargue¹, G. S. Burr¹, A. Al-Kathiri², E. Gnos³, and B. Hofmann⁴. ¹NSF Arizona AMS Laboratory, The University of Arizona, Tucson, AZ 85721, USA. E-mail: jull@email.arizona.edu. ²Directorate General of Commerce and Industry, Ministry of Commerce and Industry, Salalah, Oman. ³Natural History Museum Geneva, Switzerland. ⁴Naturhistorisches Museum der Burgergemeinde Bern, Bernastrasse 15, CH-3005 Bern, Switzerland.

Introduction: Meteorites appear to survive for long periods of time in arid environments, which makes the determination of their terrestrial age important to understanding compositional changes due to oxidation and weathering [1–3]. In the past, a dependence of the degree of oxidation on terrestrial age has been demonstrated [1–3]. At our laboratory, we make measurements of ¹⁴C and ¹⁴C/¹⁰Be. The ratio of ¹⁴C/¹⁰Be can be used to get better precision on terrestrial ages. Recently, we have also developed the capability to do ¹²⁹I measurements on meteorites, which has the potential to be useful as an exposure-age chronometer.

Oman Meteorites: In 2005–2007, new samples have been recovered from the areas Ramlat al Wahibah (RaW), Ramlat as Sahmah (RaS), and Sayh al Uhaymir (SaU). We have determined the ¹⁴C terrestrial ages for a new suite of samples from these sites, and of all available LL samples. The results indicate that weathering is generally dependent on terrestrial age, as noted earlier [3–5]. The terrestrial age distribution from RaW shows a bimodal behavior, with a suite of younger dates consistent with infall and older dates >25 kyr, suggesting some removal or sorting process at this location, which is geologically different from all other Oman find sites (fossil dunes). Previously, Al-Kathiri et al. [3] have summarized the terrestrial ages of 53 meteorites from Oman, which showed an approximately exponential distribution of ages, but with a deficiency of ages <10 kyr.

¹²⁹I Studies: We have developed a new method using ¹²⁹I which we believe will allow us to assess exposure ages of the meteorites (in conjunction with ¹⁰Be), as well as possible contamination of the weathering products of meteorites by oceanic I. In this initial study, we have applied ¹²⁹I to SaU 033 and the only meteorite from Qarat al Milh (QaM 001), which gives approximate exposure ages of 8.4 and ~3 Myr, respectively, based on production rates for L chondrites given by Schnabel et al. [6].

Acknowledgements: This work was supported in part by the NASA Cosmochemistry program, grant no. NNG06GC23G.

References: [1] P. A. Bland et al. 1996. *Monthly Notices of the Royal Astronomical Society* 238:551. [2] P. A. Bland et al. 2000. *Quaternary Research* 53:131. [3] A. Al-Kathiri et al. 2005. *Meteoritics & Planetary Science* 40:1215. [4] F. Wlotzka et al. 1995. Lunar and Planetary Institute Technical Report 95-02. 72 p. [5] A. J. T. Jull. 2006. Terrestrial ages of meteorites. In *Meteorites in the early solar system II*, edited by D. Lauretta et al. Tucson: The University of Arizona Press. pp. 889–905. [6] C. Schnabel et al. 2004. *Meteoritics & Planetary Science* 39:453–466.

5136

OXYGEN ISOTOPE RATIOS AND RARE EARTH ELEMENT ABUNDANCE OF THE SILICA-RICH CHONDRULE RIMS IN THE SAHARA 00182 CARBONACEOUS CHONDRITE

Y. Kakazu¹, T. Nakamura¹, R. Okazaki¹, and I. Ohnishi². ¹Department of Earth and Planetary Sciences, Kyushu University, Fukuoka, Japan. E-mail: kakazu@geo.kyushu-u.ac.jp. ²Department of Earth and Planetary Sciences, Kobe University, Kobe, Japan.

CR carbonaceous chondrites are primitive meteorites that largely escaped thermal metamorphism. Sahara 00182 carbonaceous chondrite has a mineralogical affinity to CR [1] but shows oxygen isotope ratios similar to CV [2]. The meteorite contains silica-rich rims that are one of important features of CR chondrites [3]. The origin and formation of silica-rich rims are not fully understood, because with a solar Mg/Si-ratio (1.07) only olivine and pyroxene but no free silica phase are stable during equilibrium condensation [4, 5]. Rather, silica-rich rims are thought to have formed during short-period chondrule heating events [3]. In order to elucidate origin and mechanism of formation for silica-rich rims, we have performed synchrotron X-ray diffraction (S-XRD), oxygen isotope and REE analyses.

Silica-rich rims consist of silica, low- and high-Ca pyroxene and glass [6]. S-XRD shows that silica polymorphs are tridymite and cristobalite. The silica shows euhedral and lath-shaped texture, indicating that they crystallized from a melt. Oxygen isotope ratios of the silica distribute roughly along the CCAM line with a range of $\delta^{18}\text{O}$ from -7 to $+5\%$, while those of the inner chondrules make a cluster around -7% in $\delta^{18}\text{O}$. The results suggest that oxygen isotopes in the silica phases are mixtures of two components: ¹⁶O-poor and ¹⁶O-rich. The ¹⁶O-rich material comes from the inner chondrule, while ¹⁶O-poor oxygen is inherited from precursor material of the silica-rich rims that formed in the ¹⁶O-poor solar nebula. The bulk REE abundance of the silica-rich rims is close to the solar abundance. Microscopic observation revealed that Ca-rich glass comprises 20 vol% in the silica-rich rims. Ca-rich glass contain high concentrations of REEs (2–10 times CI). We infer that the precursor material of silica-rich rims contains REEs in the solar abundance, and REEs were concentrated into melt during crystallization of pyroxene and silica.

We suggest that the following model for silica-rich rim formation (1) rapid condensation of silica-normative materials with ¹⁶O-poor oxygen composition and REEs in the solar abundance. (2) Melting of peripheries of the chondrules by a brief high-temperature heating process. (3) Crystallization of silica and pyroxene, then Ca- and REE- rich glass formed.

References: [1] Smith et al. 2004. *Meteoritics & Planetary Science* 39: 2009–2032. [2] Grossman J. N. and Zipfel J. 2001. *Meteoritics & Planetary Science* 36:A293–A322. [3] Krot et al. 2004. *Meteoritics & Planetary Science* 39:1931–1955. [4] Ebel and Grossman. 2000. *Geochimica et Cosmochimica Acta* 64:339–366. [5] Palme and Jones. 2003. *Meteorites, comets and planets*. In Holland H. D. and Turekian K. K., editors. Treatise on Geochemistry, vol. 1. Oxford: Elsevier-Pergamon. [6] Kakazu et al. 2007. Abstract #1695. 38th LPSC.

5254

THE PARTITIONING OF CR AND V BETWEEN PYROXENE-MELT IN MARTIAN BASALT QUE 94201

J. M. Karner¹, J. J. Papike¹, G. McKay², S. R. Sutton³, C. K. Shearer¹, P. Burger¹, and L. Le⁴. ¹Institute of Meteoritics, University of New Mexico, Albuquerque, NM 87131, USA. E-mail: jkarner@unm.edu. ²Mail Code ST, NASA JSC, Houston, TX, 77058. ³Department of Geophysical Sciences, University of Chicago, Chicago, IL 60637, USA. ⁴ESC Group, JE23, Houston, TX, 77058, USA.

Introduction: Studies on the partitioning of Cr and V between pyroxene-melt in both natural QUE 94201 and in synthetic charges of the QUE composition have provided clues to the 1) fO_2 of the natural sample, 2) behavior of V and Cr in both augite and pigeonite, and 3) valence state of these elements in pyroxene and melt under constrained fO_2 conditions.

Estimates of fO_2 for QUE 94201: Partitioning of Cr and V between pigeonite cores and bulk composition shows that QUE 94201 crystallized at an fO_2 between IW+0.2 and IW+0.9 [1]. These estimates are based on calibration curves for DCr , DV , and DCr/DV (pyroxene/melt) derived from experimental charges that were synthesized at fO_2 conditions of IW-1, IW, and IW+1. Our fO_2 estimate is robust because 1) the fO_2 is measured in the earliest crystallizing pyroxenes 2) the calibration curves are based on the same bulk composition as the natural sample, and 3) that bulk composition represents a melt from the Martian mantle, so an accurate DCr and DV are measured.

Valence State Partitioning of Cr Between Pyroxene-Melt: DCr augite/melt is approximately double that of DCr pigeonite/melt in synthetic Martian basaltic samples equilibrated at the same fO_2 [2]. This increase is not related to changing fO_2 and the valence of Cr, but rather to the increased availability of elements for coupled substitution with the Cr^{3+} ion, namely Na and Al. The availability of Al and Na to partition into pyroxene is due to delayed nucleation of plagioclase for the QUE 94201 Martian basalt composition. Direct valence determination by XANES shows that Cr^{3+} is dominant in pyroxene at IW-1, IW, and IW+1. Trivalent Cr is apparently much more compatible in the pyroxene structure than divalent Cr, and thus an increasing DCr for both augite/melt and pigeonite/melt with increasing fO_2 is a function of the increased activity of Cr^{3+} in the crystallizing melt.

Valence State Partitioning of V Between Pyroxene-Melt: DV augite/melt is greater than DV pigeonite/melt in samples equilibrated under the same fO_2 conditions [3]. This increase is due to the increased availability of elements for coupled substitution with the V^{3+} or V^{4+} ions, namely Al and Na. For this bulk composition, both Al and Na are higher in concentration in augite compared with pigeonite; therefore more V can enter augite than pigeonite. Valence state determination by XANES shows that the V^{3+} and V^{4+} are the main V species in the melt at fO_2 conditions of IW-1 to IW+3.5, whereas pyroxene grains at IW-1, IW, and IW+1 contain mostly V^{3+} . This confirms the idea that V^{3+} is more compatible in pyroxene than V^{4+} . The XANES data also indicates that a small percent of V^{2+} may exist in melt and pyroxene at IW-1. The similar valence of V in glass and pyroxene at IW-1 suggests that V^{2+} and V^{3+} have similar compatibilities in pyroxene.

References: [1] Karner et al. 2007. *American Mineralogist* 92:1238. [2] Karner et al. 2007. *American Mineralogist* 92:2002. [3] Karner et al. Forthcoming. *Meteoritics & Planetary Science*.

5170

ELEMENTAL MAPPING OF THE MOON BY THE SELENE GRS OBSERVATION

Y. Karouji¹, N. Hasebe¹, E. Shibamura², M.-N. Kobayashi³, O. Okudaira¹, N. Yamashita¹, S. Kobayashi¹, M. Hareyama¹, T. Miyachi¹, S. Kodaira¹, S. Komatsu¹, K. Hayatsu¹, K. Iwabuchi¹, S. Nemoto¹, Y. Takeda¹, K. Tsukada¹, H. Nagaoka¹, M. Ebihara⁴, T. Hihara⁴, T. Arai⁵, T. Sugihara⁶, H. Takeda⁷, C. d'Uston⁸, O. Gasnault⁸, B. Diez⁸, O. Forni⁸, S. Maurice⁸, R. C. Reedy⁹, and K. J. Kim¹⁰. ¹Waseda University, Japan. E-mail: karouji@aoni.waseda.jp. ²Saitama Prefectural University, Japan. ³Nippon Medical School, Japan. ⁴Tokyo Metropolitan University, Japan. ⁵NIPR, Japan. ⁶JAMSTEC, Japan. ⁷Chiba Institute of Technology, Japan. ⁸CESR, France. ⁹University of New Mexico, USA. ¹⁰KIGAM, Korea.

Introduction: Determining the distribution of major and important trace elements on the lunar surface is essential in the lunar science. Gamma-ray spectroscopy (GRS) is suited for measuring elemental composition on the lunar surface. The Japanese lunar mission SELENE consists of a main orbiter KAGUYA, and two small daughter satellites (Relay Satellite and VRAD Satellite), successfully launched from Tanegashima Space Center on September 14, 2007. The main orbiter carries a GRS with a large germanium semiconductor detector as a main detector and bismuth germinate and plastic scintillators as an active shielding [1]. With the highest energy resolution, the GRS provides the concentrations of the major elements and natural radioactive elements of the material of the lunar surface. Here, the initial results available from SELENE GRS obtained during the period from December 14, 2007 to February 17, 2008 are discussed.

Initial Observation of SELENE GRS: Gamma rays emitted from lunar surface were measured by GRS on the SELENE at around 100 km in altitude. SELENE GRS observes gamma-ray peaks of elements: potassium, thorium, uranium, oxygen, magnesium, aluminum, silicon, calcium, titanium, and iron. We have acquired the global measurements of gamma-ray spectrum from the lunar surface and determined elemental compositions. Individual net area of the gamma-ray peaks is related to the concentration of elements. Typical peaks are attributed to natural radioisotopes of K, Th, and U, and major elements such as O, Al, and Si produced through the inelastic scattering interaction of fast neutrons and capture reaction of thermal neutron. The uniquely identified peaks by the Ge detector are essential in the complex mixed gamma-ray field to derive elemental abundances with high precision.

Clear peaks emitted from natural radioisotopes of ^{40}K and daughters of ^{232}Th and ^{238}U are seen in each energy spectrum of gamma rays from the whole Moon. The intensities of ^{40}K , ^{208}Tl (^{232}Th chain) and ^{214}Bi (^{238}U chain) gamma rays were distinguishable among each regions (30 degree pixel) on the lunar surface, without corrections for cosmic ray variations and asymmetric response of the GRS instrument. The area where gamma-ray intensity of K is highest among those of other regions is consistent with the position of the KREEP-rich terrane [2].

References: [1] Hasebe N. et al. 2008. *Earth, Planets and Space* 60: 299–312. [2] Lawrence D. J. et al. 1998. *Science* 281:1484–1489.

5232

MULTIMINERAL INCLUSIONS IN THE MORASKO COARSE OCTAHEDRITE

Ł. Karwowski¹ and A. Muszyński². ¹Faculty of Earth Sciences, University of Silesia, ul. Będzińska 60, 41-200 Sosnowiec, Poland. E-mail: lkarwows@wnoz.us.edu.pl. ²Institute of Geology, Adam Mickiewicz University, ul. Maków Polnych 16, 60-606 Poznań, Poland. E-mail: ammu@amu.edu.pl.

Introduction: The Morasko (IAB-MG) iron is known since 1914. New specimens were found recently including the 164 kg mass found in 2006. The specimens contain irregularly scattered, mostly oval inclusions composed mainly of troilite and graphite, often rimmed with schreibersite and cohenite. Many accessory minerals were found in the inclusions including sphalerite, whitlockite [1], altaite, daubreelite, kosmochlore [2].

Analytical Methods: 20 recent finds of Morasko were cut in half, sliced and 50 part slices containing inclusions were examined with optical microscope. Then detailed examination was carried out with the CAMECA SX 100 microprobe.

Results and Discussion: Troilite is associated with pyrrhoite and daubreelite, which forms elongated grains in troilite or grains intergrown with troilite and graphite usually in outer parts of inclusions. There are two varieties of sphalerite: Fe- and Mn-rich (19–20 at% and 0.3–4.0 at%, respectively) and Fe-poor. Rare in the schreibersite rims is djerfisherite usually adjoining troilite. Altaite (PbTe) is situated usually in the discontinuity zone between troilite and the schreibersite rim, composed of cataclased mixture of troilite and graphite with tiny grains of schreibersite. Altaite was found too in tiny grains in kamacite together with schreibersite and sphalerite. Chromites are associated with phosphates: buchwaldite, brianite and phases: Na_2MgPO_4 and $\text{Na}(\text{Ca}_{0.75}\text{Mg}_{0.25})\text{PO}_4$. Rutile containing Cr–0.24 at%, Nb–0.27–0.29 at% and Fe–0.13–0.19 at% appears in form of grains poikilically enclosing graphite. Kosmochlore is the most common pyroxene. Enstatites occur separately from kosmochlore, sometimes they are contacting with feldspar or phosphates. They sometimes contain numerous small inclusions of troilite or silica. The most interesting are Cr-rich Na-Ca pyroxenes we call kosmochlore-augite [3]. Sometimes grains of K-feldspar are associated with pyroxenes. Olivines are very scarce in form of tiny isolated grains in troilite. Silica (unidentified) appears quite often together with chromite and pyroxenes. The origin of pyroxenes seems to be more complex than is suggested by [4]. In our opinion two types of silicate melts occurred during pyroxene formation. The melts were rich in Na, K, Ca, Cr, Fe, and phosphate ions. From the first one, chemically close to aubrites, crystallized two enstatites, silica and olivine. The second one gave rise to kosmochlore. When fractionated (rich in Ca, Na, and Cr), it reacted with previously formed enstatites leading to kosmochlore-augite.

References: [1] Dominik B. 1976. *Prace Mineralogiczne PAN* 47:7–53. [2] Muszyński A. et al. 2001. *Polskie Towarzystwo Mineralogiczne—Prace Specjalne* 18:134–137. [3] Karwowski Ł. and Muszyński A. 2006. *Mineralogia Polonica* 29:140–143. [4] Benedix G. K. et al. 2000. *Meteoritics & Planetary Science* 35:1127–1141.

5209

THE KAGUYA (SELENE) MISSION: PRESENT STATUS AND LUNAR SCIENCE

M. Kato, Y. Takizawa, S. Sasaki, and Selene Project Team. Japan Aerospace Exploration Agency, Japan. E-mail: kato@planeta.sci.isas.jaxa.jp.

Lunar orbiter Kaguya (Selene) was successfully launched from Tanegashima Space Center TNSC on September 14, 2007. The Kaguya project started in 1999 JFY as a joint mission of ISAS and NASDA, which were merged into the space agency JAXA in 2003. On October 4, Kaguya was inserted into large elliptical orbit circulating the Moon after passing the phasing orbit rounding the Earth 2.5 times. After lowering the apolune altitudes, Kaguya has reached the nominal observation orbit with 100 km circular and polar on October 18. On the way to nominal orbit two subsatellites Okina (Rstar) and Ouna (Vstar) were released into the elliptical orbits of 100 km perilune, and 2400 km and 800 km apolune, respectively. After the checkout of bus system the extension of four sounder antennas with 15 m length and the 12 m mast for magnetometer, and deployment of plasma imager were successfully carried out to start checkout of science instruments.

Nominal observation term for ten months was started on December 21, 2007 after performance test in the checkout term for about 1.5 months. Six lunar days of observation are already passing till now, and science data of each instrument are being acquired to study lunar science.

5184

OPTIMIZING OF THE PHOTOMETRIC FUNCTION BY USING STATISTICAL PROCESSING OF CLEMENTINE UVVIS IMAGES

S. Kawabe and K. Saiki. Department of Earth and Space Science, Graduate School of Science, Osaka University, 1-1 Machikaneyama, Toyonaka 560-0043, Osaka, Japan. E-mail: kawabe@astroboy.ess.sci.osaka-u.ac.jp.

Introduction: The surface brightness of the Moon depends on viewing geometry which is specified by the position of the Sun, the Moon, and a spacecraft. The Clementine UV-VIS images are normalized to the reflectance expected at an incident angle and phase angle of 30 degrees and an emission angle of 0 degrees. The spectral feature of the surface materials depend on their physical properties (such as the size distribution of the regolith, packing, etc.) and chemical properties (lithologies). Clementine's photometric correction parameters are not adjusted depending on these properties [1]. Even in some lithologically homogeneous regions, the reflectance changes with phase angle and it means that Clementine's photometric correction parameters are not perfect.

Analyzing Method: Using Clementine UV-VIS images, we classified the lunar surface according to abundance of FeO derived by Lucey's algorithm [2] and obtained histograms of the reflectance for every phase angle in the low-FeO (<10 wt%) region. We checked phase angle dependence of the mode of reflectance in the low-FeO region on both near and far side of the Moon separately. Next, we optimized parameters of phase function to reduce phase angle dependence of the mode of reflectance. And using optimized parameters, we recalculated the abundance of FeO.

Results: In the low-FeO region on the far side of the Moon, the mode of the reflectance is almost constant, and has no phase angle dependence. In this area, Clementine's photometric correction parameters work well. On the near side, however, the mode of reflectance has phase angle dependence and increases with phase angle. On the near side, the mode of FeO content recalculated by using optimized parameters is 5.1 wt%. This result is smaller than 5.9 wt% using Clementine's photometric correction parameters.

Discussion: Spectroscopic behavior of the surface materials in the highland on the near side of the Moon is different from that on the far side. However, recalculated FeO content on the near side is close in value to 4.1 wt%; the mode of FeO content on the far side. The previous study [3] suggested that FeO content of highland on the near side of the Moon is different from that on the far side. Our result indicates that within the highland, the surface materials on the near side of the Moon are lithologically similar to that on the far side. On the other hand, spectroscopic behavior of the surface materials indicates the difference of physical properties between the near side and the far side.

References: [1] McEwen A. S. et al. 1998. Abstract #1466. 29th LPSC. [2] Lucey P. G. and Blewett D. T. 2000. *Journal of Geophysical Research* 105:20,297–20,305. [3] Lucey P. G. 1996. *Journal of Geophysical Research* 103:3679–3699.

5147

SHOCK PRESSURE ESTIMATION FOR MARTIAN METEORITE (DHOFA 019) BY RAMAN SPECTROSCOPY AND CATHODOLUMINESCENCE

M. Kayama¹, T. Nakazato¹, H. Nishido¹, K. Ninagawa², A. Gucsik³, and Sz. Bérczi⁴. ¹Research Institute of Natural Sciences, Okayama University of Science, 1-1 Ridaicho, Okayama 700-005, Japan. E-mail: kayama0127@gmail.com. ²Department of Applied Physics, Okayama University of Science 1-1 Ridaicho, Okayama 700-005, Japan. ³Max Planck Institute for Chemistry, Department of Geochemistry, Mainz, Germany. ⁴Eötvös University, Institute of Physics, Dept. G. Physics, Cosmic Materials Space R. Group, H-1117 Budapest, Hungary.

Introduction: Dhofar 019 classified as an olivine-bearing basaltic shergottite consists of subhedral grain (0.2–0.5 mm) of pyroxene (pigeonite and augite), olivine, and feldspar mostly converted to maskelynite and minor K-feldspar, merrillite, chromite, ilmenite, and pyrrhotite, associated with terrestrial secondary phases. An estimation of shock pressure for this meteorite has been an important subject under discussion, whereas it was qualitatively presumed in the range of 30–35 GPa judging from the formation of maskelynite (An_{36–68}) [1, 2]. In this study, we evaluate the shock pressure by quantitative comparison with experimentally shocked plagioclase using cathodoluminescence (CL) and microRaman spectroscopy.

Samples and Methods: Two polished thin sections of Dhofar 019 meteorite were employed for CL and Raman measurements. Experimentally shocked plagioclase (Ab₄₀) at 20, 30, and 40 GPa were used as a reference sample for known shock pressure. CL measurements were carried on in the range from 300 to 800 nm using a SEM-CL system, which is comprised of a secondary electron microscope (JEOL: JSM-5410) combined with a grating monochromator (OXFORD: Mono CL2). The Laser Raman spectroscopy is carried out using a NRS-2100 (JASCO CO.) with an Ar laser of 514.5 nm wavelength. The sample excitation and Raman scatter collection was performed using a 100× optical lens on the Raman microscope.

Results and Discussion: CL spectra of maskelynite in Dhofar 019 exhibit two broad band peaks at around 400 and 600 nm, which can be assigned to self-trapped exciton (STE) and Mn²⁺ impurity center, respectively. Similar blue emission at around 400 nm is observed in plagioclase shocked at 40 GPa, whereas it has not been recognized in the plagioclase at 0, 20, and 30 GPa. The wavelength of the peak in yellow region shifts from 560 nm for unshocked plagioclase to 630 nm for maskelynite and shocked plagioclase at 20, 30, and 40 GPa. Maskelynite in Dhofar 019 and experimentally shocked plagioclase at 40 GPa show a weak and broad Raman spectral peak at around 450 cm⁻¹, which can be assigned to T-O-T symmetrical stretching vibration, suggesting the alteration of the crystal field related to Mn²⁺ activator. However, lower shocked plagioclase at 20 and 30 GPa indicate their high crystallinity without any change of framework configuration by Raman spectral analysis. These facts imply that shock pressure induced on this meteorite is relatively high at approximately 40 GPa.

Acknowledgements: This work is carried out in part under the Visiting Researcher's Program of the Reactor Institute, Kyoto University.

References: [1] Badjukov D. D et al. 2001. Abstract #2195. 32nd LPSC. [2] Taylor L. A. et al. 2002. *Meteoritics & Planetary Science* 37: 1107–1128.

5034

THERMAL STABILITIES OF ORGANIC MATTER IN CARBONACEOUS CHONDRITES USING IN SITU HEATING MICRO FTIR ANALYSES

Y. Kebukawa¹, S. Nakashima¹, and M. E. Zolensky². ¹Department of Earth and Space Science, Osaka University, 1-1 Machikaneyama, Toyonaka, Osaka 560-0043, Japan. E-mail: yoko.soleil@ess.sci.osaka-u.ac.jp. ²Astromaterials Research and Exploration Science, KT, NASA Johnson Space Center, Houston, TX 77058, USA.

Primitive carbonaceous chondrites (CC) are known to contain up to a few wt% organic carbon. The largest fraction of the organic matter (70–99%) consists of insoluble organic matter (IOM) [1]. The IOM is considered to be at least partially interstellar in origin. For the CM chondrites, graphitization of organic matter correlates to parent-body thermal alteration subsequent to the aqueous processing [2]. Heating experiments of CC have been conducted using Fourier transform infrared spectroscopy (FTIR) [3–5]; these authors discussed thermal changes in infrared spectra, mainly 3000–2800 cm⁻¹ due to aliphatic C-H, and ~1700 cm⁻¹ due to C=O. Since there is no kinetic study of thermal stability of these organic features, we report here results of a preliminary kinetic study which show a decrease in aliphatic C-H peaks under in situ heating micro FTIR experiments.

Matrix powder from a freshly broken surface of the Murchison meteorite was pressed on a KBr plate. The samples were set onto a heating stage (LINKAM FTIR 600) and placed into the micro FTIR (JASCO FT-IR-620+IRT30) with a MCT detector. The samples were heated isothermally at a variety of temperatures around 200 °C, because labile portions of organic matter decompose around 200–300 °C. During the heating, sample spectra were collected at every 120 s for several hours.

The spectral changes with time were analyzed using the Arrhenius equation with the reaction rate α , the pre-exponential factor A , the temperature T , and the activation energy E_α :

$$\frac{d\alpha}{dt} = A \exp\left(-\frac{E_\alpha}{RT}\right) f(\alpha)$$

$f(\alpha)$ is a function depending on the reaction mechanism. Preliminary data suggest that the observed decrease of aliphatic C-H could be rate-limited by diffusion, or by a combination of the two first order reactions. These results will be compared with kinetic data for simulated IOM (humic substances) with or without minerals, and used to constrain temperature-time conditions of parent body processes.

Acknowledgments: This research was supported by Research Fellowships of the Japan Society for the Promotion of Science for Young Scientists to YK.

References: [1] Pizzarello S. et al. 2006. In *Meteorites and the early solar system II*, edited by Lauretta D. S., Leshin L. A., and McSween H. Y. Jr. Tucson, Arizona: The University of Arizona Press. pp. 625–651. [2] Kitajima F. et al. 2002. *Geochimica et Cosmochimica Acta* 66:163–172. [3] Wdowiak T. J. et al. 1988. *The Astrophysical Journal* 328:L75–L79. [4] Flynn G. J. et al. 2001. Abstract #1593. 32nd LPSC. [5] Nakamura K. et al. 2003. Abstract #1432. 34th LPSC.

5295

MID- AND FAR-INFRARED SPECTRA OF ANHYDROUS INTERPLANETARY DUST PARTICLES

L. P. Keller¹ and G. J. Flynn². ¹Code KR, NASA Johnson Space Center, Houston, TX 77058, USA. E-mail: Lindsay.P.Keller@nasa.gov. ²Department of Physics, SUNY Plattsburgh, NY 12901, USA.

Introduction: IR spectroscopy is the primary means of mineralogical analysis of materials outside our solar system. The identity and properties of interstellar and circumstellar grains are inferred from spectral comparisons between astronomical observations and laboratory data from natural and synthetic materials. The overall objective of this study was to relate laboratory infrared (IR) spectra of primitive interplanetary dust particles (IDPs) to astronomical IR measurements of comets, asteroids and extrasolar objects (e.g., disks around young stars, outflows from evolved stars). The astronomical measurements provide a broad context for interpreting the IDP studies, while the laboratory measurements on IDPs provide an element of “ground truth” for the astronomical observations [1, 2].

Results and Discussion: We obtained mid-IR spectra from 31 individuals anhydrous IDPs using IR microscopes on synchrotron beamlines at Brookhaven National Lab. The IDP spectrum shows small peaks at positions that correspond to the strong peaks in enstatite and forsterite that are superimposed on a broad glassy silicate feature. The similarity between the comet and the average anhydrous IDP spectrum is remarkable. For 12 of the IDPs we also obtained IR spectra in the far-IR (15–50 μm)—the comparison to the Hale-Bopp data is still excellent over the wavelength range although pyroxene appears more abundant in the average IDP spectrum. The average anhydrous IDP spectrum is very similar to spectra of several Oort cloud comets that have high crystalline-to-amorphous silicate ratios [4] but is very different from spectra from the matrices of primitive chondritic meteorites.

References: [1] Sandford S. A. et al. 1985. *The Astrophysical Journal* 291:838. [2] Bradley J. P. et al. 1992. *The Astrophysical Journal* 394:643. [3] Hanner M. S. et al. 1997. *EMP* 79:247. [4] Wooden D. E. et al. 2004. *The Astrophysical Journal* 612:L77.

5227

RELICT AMORPHOUS SILICATES IN STARDUST SAMPLES

L. P. Keller and S. Messenger. Robert M. Walker Laboratory for Space Science, ARES, NASA Johnson Space Center, Houston, TX 77058, USA. E-mail: Lindsay.P.Keller@nasa.gov.

Introduction: Cometary grains impacting the Stardust aerogel collector experienced wide ranges in thermal alteration and mixing with aerogel during capture. Fine grained materials appear to have experienced the most severe alteration. Although amorphous silicates are common in Comet Wild 2 samples, their original nature is clouded by variable thermal alteration and intimate association with ubiquitous molten/compressed aerogel. Electron microscopy observations show that most of these grains contain abundant nanophase FeNi metal and FeNi sulfides inclusions dispersed in an amorphous silicate matrix. This structure is characteristic of the most common amorphous silicates in interplanetary dust particles (IDPs): GEMS grains (glass with embedded metal and sulfides), but they differ in several respects [1–3]. Few data exist on the bulk elemental compositions of the amorphous grains in Wild 2 samples [2–4]. Here we present results of nanometer-scale quantitative compositional mapping of Stardust amorphous silicate grains using the JSC JEOL 2500SE scanning-transmission electron microscope. Our objective is to gain insight into the nature of the precursor cometary materials that impacted the collector and the degree of their preservation.

Results and Discussion: We obtained quantitative X-ray maps of “melt” particles from four different tracks (C2044 track 41, C2054 track 35, FC3 track 2, and Arianna track 7). Our results show that the silicate matrices of these particles are compositionally heterogeneous on a sub- μm scale. The Mg maps are particularly illuminating, showing $\sim 0.1\text{--}0.25\ \mu\text{m}$ Mg-rich domains enclosed within melted/compressed aerogel. The average bulk element/Si (at.) ratios of 20 such domains are Mg/Si = 0.42, Al/Si = 0.05, S/Si = 0.19, and Fe/Si = 0.21. Disregarding Si, the average Mg/Fe and Fe/S ratios for the Mg-rich domains are chondritic. Interestingly, the compositional range of the Mg-rich domains overlaps that of GEMS grains in anhydrous IDPs [5], although they are somewhat enriched in Si compared to GEMS probably due to contributions from melted aerogel. The Mg-rich domains in Stardust melt particles and GEMS grains in IDPs both contain nanophase metal and sulfide inclusions, but the metal/sulfide inclusions in Wild 2 samples reflect melting and re-equilibration during capture.

Conclusions: The amorphous silicates in Wild 2 samples appear to span a broad range of compositions, but chemical imaging reveals relict Mg-rich domains partially preserved within molten aerogel. The sizes and compositions of the Mg-rich domains are consistent with them being cometary GEMS grains that have been variably modified or mixed with aerogel. GEMS grains have not been reported from meteorite samples and are an abundant component of anhydrous IDPs. This observation suggests that comet Wild 2 bears a closer resemblance to anhydrous IDPs than to any of the chondritic meteorite classes.

References: [1] Chi M. et al. 2007. Abstract #1766. 38th LPSC. [2] Keller L. P. et al. 2006. *Science* 314:1728. [3] Ishii H. et al. 2008. *Science* 319:447. [4] Leroux H. et al. 2008. Abstract #1292. 39th LPSC. [5] Keller L. P. and Messenger S. 2004. Abstract #1985. 35th LPSC.

5273

ANALYSES OF NEAR-IR SPECTRA FOR THREE ASTEROIDS IN THE HUNGARIA REGION

M. S. Kelley¹, V. Reddy², and M. J. Gaffey³. ¹Planetary Science Division, NASA Headquarters, USA. E-mail: Michael.S.Kelley@nasa.gov. ²Department of Earth System Science and Policy, University of North Dakota, USA. ³Department of Space Studies, University of North Dakota, USA.

Introduction: Approximately 60% of all E-class asteroids reside in this region of the inner main belt. Gaffey et al. [1] found a probable genetic link between the E-class NEA 3103 Eger and the aubrites, and pointed out that the aphelion of Eger is situated in the midst of the Hungaria family. Kelley and Gaffey [2] showed additional evidence for a genetic link between 434 Hungaria, 3103 Eger, and the aubrites. The crustal material of the aubrite parent body has not been found in meteorite collections. Also, crustal material of an E-class parent body has not been identified in asteroid spectral databases. Fragments of this material may exist within the X- or S-class, or unclassified asteroids in this region. These objects should elucidate the compositional and thermal evolution of the Hungaria parent body.

Observations and Data Reduction: Near-IR spectroscopic observations of asteroids studied here were carried out using the SpeX medium-resolution spectrograph [3] at the NASA Infrared Telescope Facility on Mauna Kea, Hawai‘i. All spectra were reduced and analyzed using IRAF software and the SpecPR program [4]. Spectral parameters (e.g., 1 and 2 μm band centers, and band area ratios) [5] were calculated using SpecPR.

Results: The spectrum of (3940) Larion is somewhat noisy near the 1.4 and 1.9 μm telluric water vapor absorptions due to less than perfect weather during the observations. However, a broad, weak absorption feature appears to be present at $\sim 1.2\text{--}1.6\ \mu\text{m}$. The cause of this feature is still being determined.

Asteroid (4483) Petofi was previously assigned a taxonomic designation of X [6]. The new NIR spectrum shows iron-bearing silicate absorption features near 1 and 2 μm . Our analyses show it to be either an S(III) or S(IV) subclass [7] with an olivine abundance of 80%. Petofi is a member of the Hungaria dynamical group, but its olivine abundance and pyroxene chemistry rule out a common origin with the Hungaria parent body.

Asteroid (3169) Ostro exhibits a weak, but well-defined, broad absorption feature near 1 μm . The visible-region spectrum [8] of Ostro exhibits an absorption feature near 0.5 μm . The combination of these features place the asteroid in the E[II] subclass [9].

Acknowledgements: Portions of this work were supported by NASA PAST grant NNG05GF90G, and NEOO grants NNG04GI17G, and NNX07AL29G. The authors are visiting astronomers at the NASA Infrared Telescope Facility.

References: [1] Gaffey M. J., Reed K. L., and Kelley M. S. 1992. *Icarus* 100:95–109. [2] Kelley M. S. and Gaffey M. J. 2002. *Meteoritics & Planetary Science* 37:1815–1827. [3] Rayner J. T. et al. 2003. *Publ. ASP* 115: 362–382. [4] Clark R. N. 1980. *Publ. ASP* 92:221–224. [5] Cloutis E. A. et al. 1986. *Journal of Geophysical Research* 91:11,641–11,653. [6] Lazzaro D. et al. 2004. *Icarus* 172:179–220. [7] Gaffey M. J. et al. 1993. *Icarus* 106: 573–602. [8] Bus S. J. and Binzel R. P. 2002. *Icarus* 158:106–145. [9] Gaffey M. J. and Kelley M. S. 2004. Abstract #1812. 35th LPSC.

5068

FLUOROPHLOGOPITE IN THE EH CHONDRITE Y-82189

M. Kimura¹, Y. Lin², C. Floss³, A. Suzuki⁴, T. Mikouchi⁵, and M. Ebihara⁶.
¹Ibaraki University, Japan. E-mail: makotoki@mx.ibaraki.ac.jp. ²Institute of Geology and Geophysics, Chinese Academy of Sciences, China. ³Washington University, USA. ⁴Tohoku University, Japan. ⁵University of Tokyo, Japan. ⁶Tokyo Metropolitan University, Japan.

Introduction: Enstatite chondrites commonly include many unusual minerals, such as niningerite and perryite, reflecting highly reducing conditions, and occasionally also contain fluorrichterite [e.g., 1, 2]. Lin and Kimura [3] first reported another F-bearing phase, fluorophlogopite, from the EH chondrite Y-82189. This phase was also reported from the enstatite meteorite NWA 1235 [4]. Here we report the mineralogical and chemical features of fluorophlogopite in Y-82189 and discuss the implications of its presence for the genesis of this enstatite chondrite.

Petrography and Mineral Chemistry: Y-82189 is an EH melt rock, consisting predominantly of euhedral enstatite grains [3]. It also contains several grains of subhedral fluorophlogopite, 10–30 μm in size, which occur among enstatite, coexisting with albite and quartz [5]. It contains 45.1–46.5 wt% SiO₂, 9.4–10.4 wt% Al₂O₃, 0.2–1.2 wt% FeO, 27.4–28.8 wt% MgO, 0.6–1.4 wt% Na₂O, 9.1–9.9 wt% K₂O, and 8.9–9.4 wt% F, with an average chemical formula of (K_{0.85}Na_{0.11})_{0.96}(Mg_{2.93}Fe_{0.03})_{2.96}(Si_{13.18}Al_{0.80})_{3.98}O₁₀F_{1.99}. The phlogopite contains virtually no OH and Cl. The Raman peaks at 1093, 685, 368, 319, and 202 cm⁻¹, are consistent with those of phlogopite [6]. Moreover, the spectra showed no peak in the OH region at ~3600–3800 cm⁻¹, consistent with the presence of F rather than OH.

Trace Elements: Concentrations of REE and other trace elements were determined using SIMS. The phlogopite shows subchondritic, flat REE patterns, except for Eu, which is below detection. Ba and Zr concentrations are enriched compared to CI values. The Ba enrichment is due to similar partitioning behavior as K. High Zr concentrations may reflect preferential partitioning into phlogopite rather than enstatite and plagioclase [7].

Discussion: Low concentrations of FeO in the phlogopite show that it crystallized under highly reducing conditions. Our observations suggest that phlogopite, like enstatite, crystallized from a melt, which is consistent with the flat REE patterns [6]. This also supports the origin of Y-82189 as an EH melt rock [3]. On the other hand, the source of F is problematic. Floss et al. [8] found fluorooedenite in a winonaite, and suggested that a possible source of F was fluorapatite. However, apatite has never been reported from any pristine EH chondrites. More likely phlogopite formed from other pre-existing phases with trace amounts of F.

References: [1] Douglas J. A. V. and Plant A. G. 1968. *Meteoritics* 4: 166. [2] Rubin A. E. 1983. *Earth and Planetary Science Letters* 64:201–212. [3] Lin Y. and Kimura M. 1998. *Meteoritics & Planetary Science* 33:501–511. [4] Lorenz C. et al. 2003. Abstract #1211. 34th LPSC. [5] Kimura M. et al. 2005. *Meteoritics & Planetary Science* 40:855–868. [6] McKeown D. A. et al. 1999. *American Mineralogist* 84:1041–1048. [7] Fujimaki H. et al. 1984. Proceedings, 14th LPSC. B662–B672. [8] Floss C. et al. 2007. *American Mineralogist* 92: 460–467.

5069

CHARACTERIZATION OF PYROXENE HIGHLY ENRICHED IN Ca-TSCHERMAK COMPONENT IN THE CH CHONDRITE ALH 85085

M. Kimura¹, T. Mikouchi², A. Suzuki³, M. Miyahara³, E. Ohtani³, and A. El Goresy⁴.
¹Ibaraki University, Japan. E-mail: makotoki@mx.ibaraki.ac.jp. ²University of Tokyo, Japan. ³Tohoku University, Japan. ⁴Bayerisches Geoinstitut, Universität Bayreuth, Germany.

Introduction: Aluminian diopside is commonly encountered in refractory inclusions in many carbonaceous chondrites. Especially it often contains >40 wt% Al₂O₃, showing extreme enrichment in hypothetical Ca-tschermak component (CaTs) [1–5]. Although such pyroxene is mineralogically significant, it was not subjected to further detailed characterization because of its tiny grain size. Here we report the important mineralogical features of such pyroxene in ALH 85085 (CH) previously documented by Kimura et al. [1], by using EPMA, laser microRaman and electron backscatter diffraction (EBSD).

Petrography and Mineral Chemistry: ALH 85085 contains abundant refractory inclusions [1]. A spherical inclusion (#186), ~15 μm in size, consists of grossite in its center and surrounding pyroxene [1]. The pyroxene contains 28.8–29.9% SiO₂, 40.3–42.4 Al₂O₃, 1.0–1.2 FeO, 1.4–2.0 MgO, and 25.1–26.2 CaO. The chemical formula is Ca_{1.01}Mg_{0.09}Fe_{0.03}Al_{0.88}(Al_{0.92}Si_{1.08})O₆ in average, which indicates 88% CaTs component. A small area of this pyroxene contains 8.7–10.3% TiO₂.

Identification of the Pyroxene: We identified the exact nature of this pyroxene by Raman and EBSD. It always shows Raman peaks at 959, 675, 369, and 334 cm⁻¹, consistent with those of pure CaTs [6]. However, these bands are inconsistent with those of hexagonal CaAl₂SiO₆ phase first synthesized by [7]. The EBSD patterns of this pyroxene well agree with those of diopside and pure CaTs.

Discussion: From the results obtained by EPMA, Raman and EBSD, we unambiguously exclude the possibility that this is the hexagonal CaAl₂SiO₆ phase, or other Ca-Al-silicate and fine-grained breakdown product of pyroxene. The pyroxene studied here has CaTs component much higher than 50 mol%. Therefore, our study identifies for the first time such phase as CaTs-pyroxene.

CaTs is one of the most important hypothetical components of pyroxene. Here we suggest that this component is no more hypothetical, but a really existing natural mineral. However, CaTs is only stable under high-pressure conditions [8]. No obvious evidence for impact in this inclusion and ALH 85085 may exclude the crystallization under high-pressure conditions. Alternatively, we suggest the metastable crystallization of this pyroxene from liquid under low nebular pressure condition [1–3].

References: [1] Kimura M. et al. 1993. *Geochimica et Cosmochimica Acta* 57:2329–2359. [2] Simon S. B. et al. 1998. *Meteoritics & Planetary Science* 33:411–424. [3] Krot A. N. et al. 1999. Abstract #2018. 30th LPSC. [4] Petaev M. I. et al. 2001. Abstract #1445. 32nd LPSC. [5] Simon S. B. et al. 2001. *Meteoritics & Planetary Science* 36:331–350. [6] Sharma S. K. et al. 1983. *American Mineralogist* 68:1113–1125. [7] Kirkpatrick R. J. and Steele I. M. 1973. *American Mineralogist* 58: 945–946. [8] Hays J. F. 1966. *American Mineralogist* 51:1524–1529.

5168

CRYSTALLINITY OF Mg-BEARING SILICATE GRAINS DUE TO CONDENSATION OR THERMAL EVOLUTION

Y. Kimura¹, C. Kaito², and J. A. Nuth III³. ¹Hokkaido University, Japan. E-mail: ykimura@lowtem.hokudai.ac.jp. ²Ritsumeikan University, Japan. ³Code 691, NASA's GSFC, USA.

Introduction: It has been realized that a fraction of silicates are crystalline in comets [1–3] and interplanetary dust particles (IDPs) [4]. Crystalline silicates have also been identified in comet Wild 2 Stardust samples [5]. Since the fraction of crystalline interstellar silicates along a sight line to the galactic center is $0.2 \pm 0.2\%$, i.e., almost completely amorphous [6], only a part of the interstellar silicate must be crystallized by thermal annealing or other processes in protoplanetary nebula.

During the formation of silicate grains, whether a silicate grain becomes crystalline or amorphous depends sensitively on its formation conditions. Generally, we believe that crystalline forsterite grains are formed at a slower cooling rate ($< \sim 700$ K/s: [7]) or by later annealing (~ 1000 K) of previously condensed amorphous grains. In the case of smoke experiments, since the cooling rate is very fast on the order of 10^4 K/s, the particles are generally amorphous. Indeed, the silicate smoke particles condensed from Mg-SiO-H₂-O₂ flowing gas are amorphous [8]. Therefore, heating source is required to form crystalline silicate grains. Generally, it has been considered that central protosun is the heating source to crystallize the amorphous silicate grains. During a thermal annealing, the amorphous silicates gradually crystallized in the hot inner solar nebula over time and then were transported outward and incorporated into comets [9–10].

Experimental Demonstration: During the condensation of forsterite particles in laboratory, it was found that partially crystallized forsterite particles are directly produced caused by oxidation energy of magnesium through condensation from the vapor phase and the crystallinity is a result of the balance between the heat generated by oxidation of magnesium and the heat dissipated by radiation. Namely, partially crystalline silicates can be produced accompanying with the higher oxidation energy after evaporation of aggregates composed of silicates and ices during energetic shocks. Thus, the partial pressure of oxygen and the time scale during condensation are important factors on the formation of silicate grains.

In this report, crystallinity of Mg-bearing silicate grains in protostellar system will be discussed based on the two experimental demonstrations: direct formation of magnesium-bearing silicate grain analogs by the gas evaporation method and the thermal evolution of amorphous Mg-bearing silicate grain analogs observed using differential scanning calorimetry.

References: [1] Campins H. and Ryan E. V. 1989. *The Astrophysical Journal* 341:1059–1066. [2] Ryan E. V. and Campins H. 1991. *The Astrophysical Journal* 101:695–705. [3] Crovisier J. et al. 1997. *Science* 275: 1904–1907. [4] Sandford S. A. and Walker R. M. 1985. *The Astrophysical Journal* 291:838–851. [5] Brownlee D. et al. 2006. *Science* 314:1711–1716. [6] Kemper F. et al. 2004. *The Astrophysical Journal* 609:826–837. [7] Tangeman J. A. et al. 2001. *Geophysical Research Letters* 28:2517–2520. [8] Hallenbeck S. L. et al. 1998. *Icarus* 131:198–209. [9] Shu F. H. 1996. *Science* 271:1545–1552. [10] Boss A. P. 2004. *The Astrophysical Journal* 616:1265–1277.

5026

NORTHWEST AFRICA 1232—A CO₃ CARBONACEOUS CHONDRITE WITH TWO LITHOLOGIES

Miho Kiriishi and Kazushige Tomeoka. Department of Earth and Planetary Sciences, Faculty of Science, Kobe University, Nada, Kobe 657-8501, Japan. E-mail: miho@stu.kobe-u.ac.jp.

Introduction: Northwest Africa (NWA) 1232 has recently been classified as a CO₃ carbonaceous chondrite. A striking feature of NWA 1232 is that it consists of two different lithologies (A and B). NWA 1232 may therefore be a polymict breccia, and if so, this meteorite may provide new insight into the carbonaceous chondrite parent body and its formation history. We present the results of our mineralogical and petrographic study of NWA 1232. Our goal was to determine the chemical and petrologic types of the two lithologies and how these are related to each other.

Results: Both lithologies A and B contain well-defined chondrules set in a fine-grained matrix. The modal abundances and the average diameters of chondrules in lithologies A and B are consistent with those of the CO type carbonaceous chondrites [1].

Lithology A: Olivine phenocrysts in type I chondrules are mostly Mg-rich (Fa_{4–13}). In some chondrules, plagioclase in mesostasis contains minor amounts of nepheline as thin lamellar intergrowths. In the CAIs, in addition to primary minerals such as melilite, spinel, and anorthite, nepheline has been formed by replacing melilite and anorthite. Olivine grains in the matrix are Fe-rich and heterogeneous (Fa_{41–59}).

Lithology B: Type I chondrules have texture and mineralogy generally similar to those in lithology A. However, olivine phenocrysts are more Fe-rich (Fa_{20–40}) than those in lithology A. Mesostases have been more extensively replaced by nepheline than those in lithology A. The size and texture of CAIs in lithology B are also similar to those in lithology A. However, melilite is absent, and anorthite is rare. Nepheline is much more abundant. The matrix in lithology B consists of minerals similar to those in lithology A. However, olivine grains are relatively more Fe-poor and homogeneous (Fa_{38–44}) than those in lithology A.

Discussion: Both lithologies A and B can be classified as type CO₃. However, olivine in lithology B chondrules is more enriched in Fe than in lithology A, whereas olivine in lithology B matrix is more depleted in Fe than in lithology A. Chondrules and CAIs in lithology B show a higher degree of nephelinization than those in lithology A. Previous studies suggested that nephelinization in these objects is correlated with thermal metamorphism of their host chondrites [2–4]. We therefore conclude that these differences are related to the difference in degree of thermal metamorphism.

These two lithologies probably represent rocks that have been thermally metamorphosed at different locations within a single CO parent body and later mixed to form the present combined rock during a brecciation process. Our results thus suggest that the CO parent body has undergone a heterogeneous distribution of its metamorphic condition, and a brecciation process has subsequently occurred in the parent body. The results further suggest that the CO₃ chondrites of different subtypes from 3.0 to 3.8 [5] constituted the same, single parent body.

References: [1] Brearley A. J. and Jones R. H. 1998. *Planetary materials*, pp. 3-1–3-398. [2] Kojima T. et al. 1995. *Proceedings of the NIPR Symposium on Antarctic Meteorites* 8:79–96. [3] Russell S. S. et al. 1998. *Geochimica et Cosmochimica Acta* 62:689–714. [4] Tomeoka K. and Itoh D. 2004. *Meteoritics & Planetary Science* 39:1359–1373. [5] Chizmadia L. J. et al. 2002. *Meteoritics & Planetary Science* 37:1781–1796.

5282

HETEROGENEOUS OXYGEN ISOTOPE RATIOS OF OLIVINE IN CHONDRULES FROM Y-793408 (H3.2) CHONDRITE

N. T. Kita¹, T. Ushikubo¹, M. Kimura², L. E. Nyquist³, and J. W. Valley¹.
¹University of Wisconsin-Madison, Wisconsin, USA. E-mail: noriko@geology.wisc.edu. ²Ibaraki University, Japan. ³NASA Johnson Space Center, USA.

Introduction: Oxygen isotope ratios in chondrules in primitive meteorites generally show a range of ¹⁶O enrichment [1]. Based on ¹⁶O-rich relict olivine grains in chondrules, it has been suggested that the variation resulted from a reaction between ¹⁶O-poor nebula gas with molten chondrules [e.g., 2]. It is expected that $\Delta^{17}\text{O} (= \delta^{17}\text{O} - 0.52 \times \delta^{18}\text{O})$ in different phases in a chondrule would increase with a crystallization sequence, such as olivine < low Ca pyroxene < high-Ca pyroxene. However, SIMS oxygen isotope analyses of Ca-pyroxene in chondrules from Semarkona (LL3.0) do not show measurable difference (<1‰) between co-existing olivine and low Ca pyroxene [3, 4]. These data are not consistent with extensive oxygen isotopic exchange with ¹⁶O-poor nebula gas during chondrule melting.

Chondrules from Y-793408 (H3.2): We have reported high-precision oxygen three isotope analyses of 56 chondrules from Y-793408 (H3.2), one of the least equilibrated H chondrites [5, 6]. Compared to the previous study on LL 3.0–3.1 chondrites [3], chondrules in Y-793408 show wider variation in $\Delta^{17}\text{O}$. 13 chondrules show internal heterogeneity in $\Delta^{17}\text{O}$ ($\geq 1\%$) along a slope 1 line, with lowest $\delta^{18}\text{O}$ down to -13% . They include all types of porphyritic chondrules. In most cases, the lowest $\Delta^{17}\text{O}$ is observed from Mg-rich olivine often enriched in Al and Cr, and depleted in Mn, sharing a similar tendency with the refractory forsterite [7]. At the same time, all type I chondrules also contain olivine with high $\Delta^{17}\text{O}$ above 1‰ with maximum $\sim 1.8\%$. This is significantly higher than bulk H chondrites ($\Delta^{17}\text{O} \sim 0.7\%$). The $\Delta^{17}\text{O}$ values in pyroxene analyzed from 10 chondrules do not show significant internal variation with values similar to or lower than the highest $\Delta^{17}\text{O}$ of olivine in the same chondrules.

Discussion: A wide range of $\Delta^{17}\text{O}$ among olivine grains in a single chondrule indicates that they are partial melting residues during chondrules melting events and did not exchange oxygen isotope ratios. These results suggest that solid precursors of UOC chondrules might be depleted in ¹⁶O prior to chondrule forming events. Mixing of ¹⁶O-rich refractory precursors would result in the observed heterogeneous oxygen isotope ratios in these chondrules. In several chondrules, $\Delta^{17}\text{O}$ values in low Ca pyroxene grains are similar to those of average olivine grains, consistent with pyroxene being crystallized from a melt in which oxygen isotope ratios were homogenized. Therefore, it is likely that oxygen isotope ratios of chondrule melt are inherited from those of solid precursors, but may not be a result of isotope exchange with nebula gas.

References: [1] Clayton R. N. 1993. *Annual Review of Earth and Planetary Sciences* 21:115–149. [2] Krot A. N. et al. 2006. *Chemie der Erde* 66:249–276. [3] Kita N. T. et al. 2006. Abstract #1496. 37th LPSC. [4] Kita N. T. et al. 2007. Abstract #1791. 38th LPSC. [5] Kimura M. et al. 2002. *Meteoritics & Planetary Science* 37:1417–1434. [6] Kita N. T. et al. 2008. Abstract #2059. 39th LPSC. [7] Pack et al. 2004. *Geochimica et Cosmochimica Acta* 68:1135–1157.

5289

A MICRORAMAN STUDY ON THE THERMAL HISTORY OF SEVERAL CHONDRITIC AND TERRESTRIAL CARBONACEOUS MATTERS

F. Kitajima and T. Nakamura. Kyushu University, Japan. E-mail: kitajima@geo.kyushu-u.ac.jp.

Introduction: Chondritic insoluble organic matter converts gradually to graphitic matter during thermal metamorphism. Raman spectroscopy is a useful tool to evaluate the structural ordering of the matter, and it suggests to what extent thermal metamorphism has proceeded. In this investigation, we examined the maturity level of the carbonaceous matter in several carbonaceous chondrites, together with terrestrial coals (vitrinites) and Archean carbonaceous matter.

Samples: 13 CM chondrites, Ivuna (CI), Allende (CV), Ornans (CO), NWA 801 (CR), Tagish Lake, Coolidge were analyzed. Vitrinites were collected from the Cretaceous Shimanto belt, Japan. Archean samples are black cherts from Western Australia (3.2 Ga) and South Africa (3.3–3.2 Ga) [1]. The estimated peak metamorphic temperature of the Archean samples range from 300 to 400 °C.

Experimental: Raman spectra were obtained using JEOL JRS-SYSTEM 2000 Raman spectrometer. An excitation wavelength of 514.5 nm was used on an argon ion laser. The laser beam was focused by a microscope equipped with a X50 objective, leading to a spot diameter of 2 μm. The power at the sample surface was 1.0 mW. Curve fitting was carried out using pseudo-Voigt function, after subtraction of fluorescence background.

Results and Discussion: Raman spectra of the carbonaceous matter in the chondrites that suffered thermal metamorphism show a distinguishable feature from those of the unheated chondrites. The CM chondrites experienced extended thermal metamorphism (A-881334, Y-86695, Y-82054, B-7904, Y-86789), Y-793321 (CM, weakly heated), Coolidge, Allende (CV), and Ornans (CO) showed well-developed G- and D-bands even if laser power was reduced to 0.1 mW. On the other hand, unheated CM chondrites (Y-791198, Cold Bokkeveld, Sayama, Boriskino, Murray, Murchison), Tagish Lake, Ivuna (CI), NWA 801 (CR), and A-881458 (CM, very weakly heated) showed weak G- and D-bands on the slope of a fluorescence background, and reducing the laser power to 0.1 mW, the D-bands disappeared. This property can be non-destructive tool to distinguish strongly heated chondrites from unheated chondrites. The G-band position of the chondritic carbonaceous matter shifts up with increasing metamorphic grade, and the FWHM-G (Full width at half maximum of G-band) decreases as observed in the IDPs [2, 3]. The G-band position of the vitrinites shows an almost linear correlation to the FWHM-G [1]. Chondritic and Archean data plot off the line described by the vitrinites, suggesting a difference in precursor. The estimated peak metamorphic temperatures of the strongly heated CMs are higher than those of the Archean samples, however, the CMs show less matured Raman spectra than those of the Archean samples. It may suggest relatively short duration time of the metamorphism of the CMs.

References: [1] Kitajima F. et al. 2007. Abstract G120-010. Abstracts of the Japan GeoScience Union Meeting 2007. [2] Quirico E. et al. 2005. *Planetary and Space Science* 53:1443–1448. [3] Sandford S. A. et al. 2006. *Science* 314:1720–1724.

5313

IMPACTOR TYPE OF THE LATE EOCENE AGE IMPACT CRATERS ON EARTH: CONSTRAINTS FROM IMPACTITE STUDIES AT THE CHESAPEAKE BAY IMPACT STRUCTURE

C. Koeberl. Department of Lithospheric Research, University of Vienna, Althanstrasse 14, A-1090 Vienna, Austria. E-mail: katerina.bartosova@univie.ac.at.

There are currently at least five impact craters known that are of late Eocene age, a relatively large number within a short time span. These impact craters are accompanied by tektites and clinopyroxene-bearing spherules (microkrystites) in upper Eocene marine deposits, some containing an iridium anomaly. Specifically, upper Eocene marine sediments around the world contain evidence for at least two closely spaced impactoclastic layers—i.e., layers containing impact debris, such as tektites and microtektites and shocked minerals and rock fragments. The Chesapeake Bay impact is thought to be responsible for the younger of the two impact layers. It is now commonly assumed that the older global upper Eocene microkrystite layer originated from the Popigai impact event.

Enhanced levels of ^3He were found to coincide with the two upper Eocene impactoclastic layers [1]. This isotope is a proxy for the influx of extraterrestrial dust and is interpreted as indicating that, during the late Eocene, there was a time of enhanced collision activity in the inner solar system, probably resulting in a higher impact rate than usual. An open question is whether or not the two large impact events (Chesapeake Bay and Popigai) and the smaller ones were all produced by parts of the same asteroid (or comet) after a collision event in the inner solar system.

The melt rocks of the Popigai impact structure show enrichments in characteristic siderophile trace elements, the ratios of which point toward an ordinary chondrite projectile, possible of the L chondrite type (e.g., [2]). These authors also indicate a chondritic projectile for the late Eocene Wanapitei impact structure. Therefore, identification of the projectile involved in the late Eocene Chesapeake Bay impact structure (CBIS) may provide more information about the nature of the late Eocene impactors and whether they are related to a comet or asteroid shower.

At the Chesapeake Bay impact structure (age 35.5 Ma, diameter 85 km) the situation is less clear cut than at Popigai. In 2005–06, an ICDP-USGS drilling project obtained the Eyreville drill core, which penetrated through post-impact sediments and impactites, into fractured crystalline basement to a total depth of 1766 m; suevites and lithic impact breccias are at 1397–1551 m depth [3]. Even samples, including 7 suevites, were analyzed for their PGE composition by [4], but only very low PGE abundances (e.g., Ir from 0.03 to 0.09 ppb) and fractionated (non-chondritic) PGE abundance patterns were found, which does not constitute evidence for a distinct extraterrestrial component. Thus only a small but measurable Os isotopic anomaly [5] indicates a meteoritic component in Chesapeake Bay impactites. The question if Chesapeake Bay and Popigai formed from projectiles of the same origin remains open at this time.

References: [1] Farley et al. 1998. *Science* 280:1250. [2] Tagle and Claeys. 2005. *Geochimica et Cosmochimica Acta* 69:2877. [3] Gohn et al. 2006. *Eos* 87:349, 355. [4] McDonald et al. Forthcoming. GSA SP (Chesapeake volume). [5] Lee et al. 2006. *Meteoritics & Planetary Science* 41:819.

5109

A GEOLOGIC OVERVIEW OF THE LATE HOLOCENE WHITECOURT METEORITE IMPACT CRATER

R. S. Kofman¹, C. D. K. Herd¹, E. L. Walton¹, D. G. Froese¹, and E. P. K. Herd². ¹Department of Earth and Atmospheric Sciences, 1-26 Earth Sciences Building, Canada. E-mail: rkofman@ualberta.ca. ²Department of Civil and Environmental Engineering, 3-133 Markin/CNRL Natural Resources Eng. Facility. University of Alberta, Edmonton, Alberta T6G 2E3, Canada.

Introduction: Small impact events resulting in simple impact structures <100 m in diameter are common features recorded on the solid surfaces in our solar system. Such structures are rare in Earth's impact cratering record; most are typically heavily modified by subsequent erosion or are often found in remote locations. The recently discovered Whitecourt meteorite impact crater (WMIC) provides significant contrast in that it is both well preserved and easily accessible. The level of preservation, age (<1.13 ka) and associated meteorite fragments [1] suggest that this site will provide considerable data for the improvement of current models for similar structures.

Structure: The WMIC target surface consists of gently sloping materials resulting in the southwest crater rim being 4 m higher than the northeast rim. The crater is 36 m in diameter and has a depth of 6 m as measured from a cross section oriented parallel to the hill slope. The crater shape is similar to other Barringer type (simple) structures.

The subsurface stratigraphy is presently constrained by a single borehole 5.4 m deep located at the center of the crater. The local water table is below this depth. The stratigraphy consists of a 10 cm thick organic-rich silty soil sharply overlying a pebble diamict. The diamict includes clasts up to 10 cm in diameter in the upper 50 cm decreasing to 5 cm to a depth of ~2.9 m. At ~2.9 m there is a sharp transition to medium bedded sand, which continues uninterrupted to the base of the borehole. Rare fragments of amber-colored glass have been identified using XRD and polarizing light microscopy in samples from ~2.9 m within the diamict. A soil pit located 11.5 m east of the crater rim reveals a buried charcoal-rich soil horizon sharply overlain by a 20 cm thick pebble diamict.

Conclusions: The sharp contact observed at 2.9 m is interpreted as being very near to the base of the transient crater. The presence of glass above this boundary and its abrupt disappearance immediately below the 2.9 m boundary support the expected rapid dissipation of energy in unconsolidated material. The soil pit reveals the classic overturned topography found along impact crater rims. The current model, based on only seven simple structures ranging from 400 to 3800 m in diameter, overestimates the true depth of the WMIC [2].

Further Investigations: A detailed field investigation is currently underway which includes magnetic, seismic refraction tomography, and auger/soil pit surveys. The purpose of the magnetic survey is to determine if any of the main impactor mass remains embedded in the crater floor. The refraction tomography survey will elucidate any seismic velocity disturbances in the subsurface material caused by the impact. Additional soil pits and boreholes will further constrain the crater morphology and stratigraphy, and determine the distribution of the ejecta blanket.

References: [1] Herd C. D. K. et al. 2008. This issue. [2] Grieve R. and Theriault A. 2004. *Meteoritics & Planetary Science* 39:199–216.

5127

CRYSTALLIZATION RELATIONSHIP OF YAMATO-980459 AND QUE 94201 DEPLETED SHERGOTTITES

E. Koizumi^{1, 2}, T. Mikouchi², G. McKay³, and M. Miyamoto². ¹Remote Sensing Technology Center of Japan, Roppongi Tokyo 106-0032, Japan. E-mail: koizumi_eisuke@restec.or.jp. ²Department of Earth and Planet. Sci., University of Tokyo, Hongo, Tokyo 113-0033, Japan. ³Mail Code KR, NASA Johnson Space Center, Houston, TX 77058, USA.

Introduction: Although the number of Martian meteorites are drastically increasing thanks to the recent recovery of many meteorites from hot and cold deserts, most of them are cumulate rocks, which makes it difficult to estimate their source melt compositions. Yamato-980459 (Y-98) and QUE 94201 (QUE) are mineralogically distinct samples of the “depleted” shergottites, that have no evidence for assimilation with the Martian crustal material [1]. In this study, we investigated the formation sequence and relationship of these two meteorites mainly with the crystallization experiments and the computational calculations.

Yamato 980459: Y-98 is an olivine-phyric shergottite that consists of olivine megacrysts with the groundmass composed of olivine, pyroxene and glassy mesostasis, and no plagioclase. The core compositions of olivine (Fo₈₆) and pyroxene (En₈₁Fs₁₇Wo₂) are the most mafic compositions among Martian meteorites found so far [2]. The equilibrium calculation using MELTS and crystallization experiment with the bulk composition of Y-98 indicated that Y-98 crystallized from the source melt having the bulk composition of Y-98 in a closed system. This mafic depleted shergottite crystallized at cooling rate of 1 °C/hr according to the Mg-Fe diffusion calculation considering fractional crystallization on olivine megacryst of Y-98 as well as the results from dynamic crystallization experiments.

QUE 94201: QUE is a basaltic shergottite that mainly consists of coarse-grained pyroxene and maskelynite. QUE is one of the most Fe-rich Martian meteorites [3]. Crystallization experiments revealed that the major mineral phases (pyroxene and plagioclase) crystallized from the source melt whose composition was similar to the bulk composition of QUE, and unique chemical zoning of pyroxene could be reproduced. The results from the cooling experiments at various cooling rates gave the upper limit of cooling rate (0.5 °C/hr) for the QUE crystallization.

Relationship Between Y-98 and QUE: Although Y-98 and QUE show different mineralogical features, the ages and REE patterns of these meteorites are similar [4]. The result of the MELTS calculation suggested that the similar composition to the bulk composition of QUE could be produced as the residual melt from the Y-98 melt at 1160 °C. The temperature of 1160 °C was the estimated liquidus temperature of the QUE bulk composition from crystallization experiments, indicating that QUE could be derived from the melt of Y-98, and Y-98 seems to retain the information of primitive reservoir of depleted shergottites that may have been formed from the Martian magma ocean. Therefore, the melt of Y-98 seems to be the first sample that has a direct relationship with the Martian mantle.

References: [1] Borg L. E. and Draper D. S. 2003. *Meteoritics & Planetary Science* 38:1713–1731. [2] Mikouchi T. et al. 2003. *Proceedings of the NIPR Symposium on Antarctic Meteorites* pp. 82–83. [3] Mikouchi T. et al. 1998. *Meteoritics & Planetary Science* 33:181–189. [4] Shirai N. and Ebihara M. 2004. *Antarctic Meteorite Research* 17:55–67.

5214

HYDROUS AND ANHYDROUS ALTERATION OF UNSUBGROUPED CV CHONDRITE Y-86751

M. Komatsu¹, T. Mikouchi², and M. Miyamoto². ¹The University Museum, University of Tokyo, Japan. E-mail: mutsumi@um.u-tokyo.ac.jp. ²Department of Earth and Planetary Science, University of Tokyo, Japan.

Introduction: The CV chondrites are subdivided into the reduced (CV_{red}) and two oxidized subgroups, Allende-like (CV_{oxA}) and Bali-like (CV_{oxB}) [e.g., 1]. It has been suggested that CV_{oxA} experienced mainly anhydrous alteration [2], and CV_{oxB} experienced hydrous alteration [3]. The reduced CV chondrites experienced alteration similar to that of CV_{oxA}, but of a small degree [4]. Although the presence of subgroups are believed to be due to their complex alteration history and each subgroup may represent different lithological varieties of the same asteroidal body [5], the relationship between these alterations remains unclear.

Results and Discussion: We have studied one thin section of Y-86751, 47,1, ungrouped CV3 chondrite. Chondrules, CAIs, and AOAs in Y-86751 exhibit the alteration characteristic similar to CV_{oxA}, including the formation of secondary olivine zonation, replacement of primary melilite or anorthite by nepheline, whereas the composition and modal abundance of metal-sulfide nodules are similar to those from CV_{red}. The grain sizes of matrix olivines from both lithologies are intermediate between CV_{red} and CV_{oxA}.

Y-86751 contains two lithological units. Lithology A (lith. A) is distinguishable having more Mg-rich and Si-poor matrix than lithology B (lith. B). Olivine phenocrysts in most chondrules from lith. A show compositional zoning from magnesian cores to ferroan rims, and enstatite grains coexisting with the zoned olivine are replaced by olivine at the grain boundaries. Chondrule olivines in lith. A are typically more ferrous than those from lith. B. The matrix in lith. A is coarser-grained than those in lith. B. These observations suggest that lith. A experienced higher degree of alteration than lith. B.

There is another important difference between two lithologies. In both types, metal-sulfide nodules (kamacite, taenite, FeS, pentlandite in some cases) occur in chondrules, AOAs, or as isolated nodules in matrix. Magnetite is commonly observed around Fe, Ni-metal grains in lith. B, on the other hand, ferrous olivine surrounds Fe, Ni-metal grains in lith. A. The proposed sequence of secondary ferrous olivine formation is as follows [6]: (i) magnetite formed by oxidation of Fe, Ni-metal, (ii) magnetite reacted with SiO₂ through aqueous solution, and (iii) replacement of magnesian olivine. It is likely that metal-sulfide nodules in lith. A experienced three stages of reactions (i) to (iii), while those in lith. B experienced two stages of reactions (i) and (ii).

Based on the observation, we infer that Y-86751 was originally similar to CV_{red}, and then experienced a small degree of hydrous and anhydrous alteration. Because phyllosilicates are not common in both lithologies, it is likely the alteration sequence took place in the presence of small amount of aqueous solutions that was largely consumed during the alteration. The coexistence of two lithologies may suggest that the alteration occurred in a local scale, in an asteroidal setting.

References: [1] Weisberg M. K. and Prinz M. 1998. *Meteoritics & Planetary Science* 33:1087–1111. [2] Kimura M. and Ikeda T. 1997. *Antarctic Meteorite Research* 10:191–202. [3] Keller L. P. et al. *Geochimica et Cosmochimica Acta* 58:5589–5598. [4] Krot A. N. et al. 2004. *Chemie der Erde* 64:185–282. [5] Krot A. N. et al. 1998. *Meteoritics & Planetary Science* 33:1065–1085. [6] Krot A. N. et al. 2004. *Antarctic Meteorite Research* 17: 153–171.

5152

LARGE SAMARIUM ISOTOPIC SHIFT OF THE NORTON COUNTY METEORITE BY NEUTRON CAPTURE EFFECT

T. Kondo¹, H. Hidaka¹, and S. Yoneda². ¹Department of Earth and Planetary Systems Science, Hiroshima University, Higashi-Hiroshima 739-8526, Japan. E-mail: m080360@hiroshima-u.ac.jp. ²Department of Science and Engineering, National Museum of Nature and Science, Tokyo 169-0073, Japan.

Introduction: The exposure history of meteorites has been characterized by several cosmogenic nuclides. Sm and Gd isotopic shifts by neutron capture reactions also provide useful information to understand the exposure records of meteorites, because ¹⁴⁹Sm and ¹⁵⁷Gd have very large thermal neutron capture cross sections [1, 2]. Most of aubrites show brecciated-textures and sometimes contain unique inclusions having unknown origins [3]. In previous works of Sm and Gd isotopic studies of one of aubrites, Pesyanoe, the neutron fluences of four different phases taken from a small fragment show significant variation up to 30% relative to the matrix portion, suggesting the existence of preirradiation components in the matrix [2]. In this study, in order to find a possibility of the early irradiation record on the other aubritic species than Pesyanoe, Sm isotopic compositions of light-colored fragment taken from Norton County was determined.

Sample and Experiments: Norton County is a brecciated aubrite, and has a long cosmic-ray exposure age (111 Ma). In this study, the whole rock and handpicked material of the light-colored phase were prepared. Each sample weighing about 0.2 g was decomposed by HF-HClO₄. The samples was then taken to dryness and redissolved in 1 mL of 2M HCl. The solution was divided into two portions: the main portion for Sm isotopic measurement and the rest for the determination of REE abundances. Sm was separated by conventional cation exchange methods [2]. A micro-mass VG54-30 thermal ionization mass spectrometer equipped with seven Faraday cup collectors was used for the isotopic measurement of Sm. ICP-MS (VG Plasma Quad III) was used for the determination of REE contents in two samples.

Results and Discussion: The neutron fluence of $(3.40 \pm 0.01) \times 10^{16}$ n/cm² estimated from Sm isotopic composition of the whole rock of Norton County used in this study is 2.3 to 2.9 times higher than those reported before [2]. The difference can be explained by the difference of depths in the parent body. On the other hand, the neutron fluence of the light-colored phase is 5.5 times larger than that of the whole rock. This cannot be simply explained by the difference of depth.

The REE pattern of the whole rock sample shows slightly negative anomalies of Ce, Eu, and Yb, that has been previously reported in the early condensation materials such as hibonite in Murchison [4]. The REE data also support the existence of preirradiation materials in the Norton County meteorite.

References: [1] Eugster O. et al. 1970. *Earth and Planetary Science Letters* 7:436–440. [2] Hidaka H. et al. 2007. *Geochimica et Cosmochimica Acta* 71:1074–1086. [3] Müller O. and Zähringer J. 1966. *Earth and Planetary Science Letters* 1:25–29. [4] Ireland T. R. et al. 1988. *Geochimica et Cosmochimica Acta* 52:2841–2854.

5161

⁴⁰Ar-³⁹Ar DATING OF NEW EUCRITE DHOFAR 1439 REVEALS A RECENT IMPACT EVENT ON THE EUCRITE PARENT BODY

E. V. Korochantseva^{1, 2}, A. I. Buikin^{1, 2}, C. A. Lorenz², J. Hopp¹, and M. Trieloff¹. ¹Mineralogisches Institut, Ruprecht-Karls-Universität Heidelberg, Im Neuenheimer Feld 236, D-69120 Heidelberg, Germany. E-mail: trieloff@min.uni-heidelberg.de. ²Vernadsky Institute of Geochemistry, Kosygin St. 19, 119991 Moscow, Russia.

Introduction: Dhofar 1439, a single stone weighing 5132 g, was discovered in the Oman desert in 2003. The minor weathered meteorite is composed of cm-sized light-colored lithic clasts (~40 vol%) set within a dark devitrified melt matrix. Based on mineralogical and petrological observations Dhofar 1439 is a monomict eucrite melt breccia. To reveal the thermal history of this rock we performed high-resolution ⁴⁰Ar-³⁹Ar stepwise heating analyses on clast material, plagioclase separate and two portions of melt: dark-brown with empty gas pores—melt with fluidal texture—and black, well-mixed melt.

Results and Discussion: The age spectrum of clast material corrected for air-like argon in the low temperature extractions shows stepwise increasing apparent ages, indicating partial degassing <1 Ga ago. The gradually increasing apparent ages from 3.47 up to 3.61 Ga over 19–100% of the ³⁹Ar release indicate slow cooling after an impact event that completely reset the K-Ar system of this rock ~3.6 Ga ago, i.e., just after the Late Heavy Bombardment, similar to other HED meteorites [1–3]. The plagioclase age spectrum is similar to clast material.

Melt matrix is less retentive of Ar than clast material. For the dark-brown melt with vesicles, we identified and corrected for two different (diffusively separated) trapped argon components resulting in an age plateau of 289 ± 52 Ma (1–90% ³⁹Ar release). Over the last 10% of the ³⁹Ar release the apparent ages increase with extraction temperature up to 3 Ga due to the presence of relict ⁴⁰Ar in more retentive high temperature sites. Two distinct reservoirs of trapped argon were previously reported for impact metamorphosed L chondrites [4]. Judging from Ar degassing patterns, an association with shock metamorphosed feldspathic phases or alterations is more likely than with pyroxene or olivine [3–8].

Young impact ages (<1.3 Ga) are typical for ordinary chondrites and uncommon for HED meteorites [1–5, 9]. Meanwhile two other eucritic melt breccias, Palo Blanco Creek and ALHA81011, also show young melting event(s): 1 Ga [10] and 350 Ma [5], respectively. Our new data confirm and specify a large-scale recent melting event on the HED parent body.

References: [1] Bogard D. D. 1995. *Meteoritics* 30:244–268. [2] Kunz J. et al. 1995. *Planetary and Space Science* 43:527–543. [3] Korochantseva E. K. et al. 2005. *Meteoritics & Planetary Science* 40:1433–1454 [4] Korochantseva E. V. et al. 2007. *Meteoritics & Planetary Science* 42:113–130. [5] Kunz J. et al. 1997. *Meteoritics & Planetary Science* 32:647. [6] Trieloff M. et al. 1997. *Geochimica et Cosmochimica Acta* 61:5065–5088. [7] Hopp J. and Trieloff M. 2005. *Earth and Planetary Science Letters* 240:573–588. [8] Trieloff M. et al. 2005. *Geochimica et Cosmochimica Acta* 69:1253–1264. [9] Kring D. A. and Swindle T. D. 2008. Abstract #1305. 39th LPSC. [10] Dickinson T. et al. 1984. *Meteoritics & Planetary Science* 19: 219–220.

5095

PHYSICAL PROPERTIES OF HIGH-POROSITY DUST AGGREGATES

M. Krause¹, J. Blum¹, and M. Trieloff². ¹Institut für Geophysik und extraterrestrische Physik, TU Braunschweig, Germany. ²Mineralogisches Institut, Universität Heidelberg, Germany.

Introduction: Although extensive laboratory investigations have been performed in the past years [1], many questions concerning the first stage of planet formation, i.e., the growth from protoplanetary dust to planetesimals [2], remain unsolved. To better understand the processes and physical properties affecting the sticking efficiency of colliding protoplanetary dust, we investigated the impact behavior of high-porosity dust aggregates. Additionally, we present a non-invasive method to measure the thermal conductivity of protoplanetary dust analogs.

Compression Behavior: The analyzed high-porosity dust samples, consisting of micron-sized spherical SiO₂ monomers, were produced by random ballistic deposition and have a volume filling factor of $\Phi = 0.15$ [3]. We determined the dynamical compaction behavior by dropping a single mm-sized glass bead under vacuum conditions into the dust sample using X-ray microtomography. The example shown in the figure (sphere diameter ≈ 1 mm, height of fall ≈ 77 mm) clearly displays the compressed area underneath the intruded sphere, which has an increased volume filling factor of $\Phi \approx 0.23$. Our measurements with different sphere sizes and sintering stages of the dust sample provide the following qualitative conclusions. The compressed volume, the depth of intrusion, the compressed volume normalized by the sphere volume, and the depth of intrusion per sphere size decrease with increasing sintering temperature. With increasing sphere size the compressed volume, the depth of intrusion, and the volume filling factor increase, whereas the compressed volume per sphere volume and the depth of intrusion per sphere size decrease. Further measurements, comprising a systematic parameter study, will be performed to constrain these tendencies quantitatively.

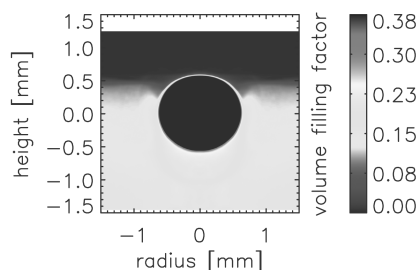


Fig. 1.

Thermal Conductivity: The measurement of the thermal conductivity of protoplanetary dust analogs may reveal the influence of the radioactive decay heat of short lived nuclides, like e.g., ²⁶Al, on the ability to melt or sinter highly porous protoplanetary bodies. Besides this, we expect considerable changes in the collision behavior due to these processes. We invented a non-invasive method for the determination of the thermal conductivity of very loose dusty bodies by measuring the temporal and spatial temperature distribution of a dust sample heated by a laser-illuminated black glass sphere placed on its surface. Temperature measurements are done non-invasively with an IR camera. As we expect thermal conductivity values lower than that of air (≈ 0.002 W/(m K)), these measurements are performed under high-vacuum conditions. The experimental results will be compared with numerical simulations.

References: [1] Blum J. and Wurm G. F. Forthcoming. *Annual Review of Astronomy and Astrophysics* 46:21. [2] Weidenschilling S. J. and Cuzzi J. 1993. In *Protostars and planets III*, edited by Levy E. and Lunine J. I. Tucson, Arizona: The University Arizona Press. 369 p. [3] Blum J. and Schräpler R. 2004. *Physical Review Letters* 93:115503.

5113

OXYGEN ISOTOPE COMPOSITIONS OF CHONDRULES FROM THE CH/CB-LIKE CHONDRITE ISHEYEVO AND CB CHONDRITES MAC 02675 AND QUE 94627

Alexander N. Krot¹ and Kazuhide Nagashima. HIGP/SOEST, University of Hawai'i at Manoa, HI, USA. ¹E-mail: sasha@higp.hawaii.edu.

It has been previously suggested [1, 2] that CH chondrites and CH/CB-like chondrite Isheyevu contain several generations of chondrules formed by different mechanisms: (i) Fe-Mg and Al-rich porphyritic chondrules resulted from melting of precursors in the solar nebula, and (ii) magnesian cryptocrystalline (CC) and skeletal chondrules, similar to those from CB chondrites, formed in an impact generated plume of melt and gas. Based on the presence inside the Al-rich and Fe-Mg porphyritic (Type I and Type II) chondrules of relict CAIs, which are mineralogically (grossite- and hibonite-rich) and isotopically (¹⁶O-rich and ²⁶Al-poor) similar only to those from Isheyevu and CHs, Krot et al. [3] concluded that porphyritic chondrules from Isheyevu and CHs belong to a unique population of objects originated at a different time or in a different nebular region than chondrules from other carbonaceous chondrites. To test these hypotheses, we measured in situ O-isotopic compositions of Fe-Mg porphyritic (Type I and Type II), and ferrous and magnesian CC chondrules from Isheyevu and magnesian CC chondrules from MAC 02675 and QUE 94627 (CB_b) using the UH Cameca ims-1280. On a three-isotope oxygen diagram, all these chondrules plot along slope-1 line. Data for 19 magnesian CC chondrules from Isheyevu and 18 magnesian CC chondrules from CB_b chondrites have nearly identical compositions: $\Delta^{17}\text{O} = -2.2 \pm 0.9\%$ and $-2.3 \pm 0.6\%$ ($\text{avr} \pm 2\sigma$), respectively. In contrast, $\Delta^{17}\text{O}$ values for 11 Type I and 9 Type II chondrules range from -5% to $+4\%$ and from -17% to $+3\%$, respectively. Most Type Is and Type IIs are isotopically uniform. Contrary to typical chondrules from carbonaceous chondrites, 7 out of 11 Type I chondrules from Isheyevu plot on or above the TF line; 7 out of 9 Type IIs plot on or below the TF line. Type II chondrule #141 is isotopically heterogeneous: $\Delta^{17}\text{O}$ ranges from 17% to 7% . The only two ferrous CC chondrules analyzed plot above the TF line ($\Delta^{17}\text{O} = 1.3 \pm 1.0\%$). We conclude that: (i) O-isotopic compositions of the Isheyevu and CB_b magnesian CC chondrules are consistent with their single-stage formation in an impact-generated plume, possibly as gas-liquid condensates [2], and (ii) Ferromagnesian and Al-rich porphyritic chondrules from CH/CB and CH chondrites belong to a unique population of objects, suggesting formation either in a different nebular region or at a different time than chondrules from other carbonaceous chondrites.

References: [1] Wasson J. T. and Kallemeyn G. W. 1990. *Earth and Planetary Science Letters* 101:148–161. [2] Krot A. N. et al. 2008. *Chemie der Erde* 67:283–300. [3] Krot A. N. et al. 2007. *Meteoritics & Planetary Science* 42:A90.

5180

FORMATION OF JADEITE FROM PLAGIOCLASE: CONSTRAINTS ON THE P-T-t CONDITIONS OF SHOCKED METEORITES

T. Kubo¹, M. Kimura², M. Nishi¹, A. Tominaga¹, T. Kato¹, T. Kikegawa³, K. Funakoshi⁴, and M. Miyahara⁵. ¹Department of Earth and Planetary Sciences, Kyushu University, Fukuoka 812-8581, Japan. E-mail: kubotomo@geo.kyushu-u.ac.jp. ²Institute of Astrophysics and Planetary Science, Ibaraki University, Mito 310-8512, Japan. ³Photon Factory, High Energy Accelerator Research Organization, Tsukuba 305-0801, Japan. ⁴Japan Synchrotron Radiation Research Institute, Hyogo 679-5198, Japan. ⁵Institute of Mineralogy, Petrology, and Economic Geology, Tohoku University, Sendai 980-8578, Japan.

Introduction: It is well known that sodic plagioclase decomposes into jadeite and silica phase (coesite or stishovite) at high pressures. However in shocked meteorites, only jadeite has been found without silica phase even in the grain having a chemical composition of plagioclase. We have conducted in situ X-ray diffraction experiments on this decomposition reaction using Kawai-type high-pressure apparatus and synchrotron radiation, and found differences in nucleation kinetics between jadeite and silica phase. P-T-t conditions for the presence of jadeite and no silica phase have been constrained based on the experimental kinetic data.

Results and Discussion: The starting material is natural albite ($\text{Ab}_{98.0}\text{An}_{0.4}\text{Or}_{1.6}$). Fully amorphization was not observed during compressions up to 27 GPa at room temperature, but occurred by heating at high pressures. The amorphization pressure decreases with increasing temperature. For example, we have observed that albite becomes amorphous at 23 GPa and 1173 K. This amorphization pressure is much lower than those reported in previous shock experiments and DAC studies at room T.

Crystallization kinetics of high-pressure assemblages from amorphous albite was examined by time-resolved X-ray diffraction measurements every 10 s using energy dispersive method. We observed that jadeite first appears from amorphous albite and nucleation of stishovite is significantly delayed. Pressure and temperature dependences on the crystallization rate of jadeite and stishovite were determined to estimate P-T-t kinetic boundaries among amorphous albite, jadeite (no stishovite), and jadeite + stishovite.

Extrapolations of kinetic data obtained to the time scale of 1 s indicate that only jadeite is present between 1473–1973 K at around 20 GPa. Stishovite also appears at higher T, and both jadeite and stishovite are not formed at lower T. In the time scale of 10 s, these kinetic boundaries shift to lower T by 200–400 K. Thus, the presence of jadeite without silica phase found in shocked meteorites can be explained due to the difference in crystallization kinetics from amorphous albite. This can be an important constraint on the P-T-t conditions of shock events.

Reaction microstructures of recovered samples were observed by SEM, which were compared to those of shocked meteorites. Preliminary results suggest that the grain size of reaction products in shocked meteorites is much smaller than that in the experiments probably due to differences in P-T-t conditions.

5235

AIO(OH) IS A MAJOR CONSTITUENT OF THE CAI “BLUE MOON” FROM THE RENAZZO (CV3) CHONDRITE

G. Kurat¹, M. E. Varela², and E. Zinner³. ¹Department of Lithospheric Sciences, University of Vienna, Vienna, Austria. E-mail: gero.kurat@univie.ac.at. ²CASLEO/CONICET, San Juan, Argentina. ³Laboratory of Space Sciences and Department Physics, Washington University, St. Louis, MO, USA.

Water- and (OH)-bearing phases in Ca-Al-rich inclusions (CAIs) are known from CM chondrites [e.g., 1] as well as from micrometeorites and IDPs [e.g., 2–6]. They are widely believed to be parent body alteration products of former non-hydrous phases and comprise typically Fe, Mg phyllosilicates, which take the place of, e.g., diopside, that commonly covers spinel + melilite + perovskite intergrowths [7]. Here we report on the first occurrence of AIO(OH) as a major constituent in a CAI.

Blue Moon is a large (~3 mm), bright blue colored CAI from a Renazzo sample of the NHM in Vienna. It has an irregular, elongated shape and consists of complex intergrowths of refractory minerals of varying grain sizes, forming two distinct lithologies, which differ in texture and mineral abundances. The principal units appear to be AIO(OH) (up to ~100 µm) enveloped by hibonite laths (up to ~50 µm long) embedded in spinel, which form an amoeboid, fluffy network that is incompletely rimmed by gehlenite and embedded in anorthite (± gehlenite ± spinel ± diopside ± forsterite). Wollastonite, nepheline, and calcite are rare interstitial phases.

AIO(OH) commonly encloses small elongated, rounded perovskites. AIO(OH) is optically isotropic and Raman-amorphous [8] and fairly pure with (EMP analysis) 85 wt% Al_2O_3 and low Na_2O (~0.1), SiO_2 (~0.5), CaO (~0.5), and TiO_2 (~0.1 wt%) contents. Hibonite contains some TiO_2 (1–4 wt%); spinel, diopside, and forsterite are very poor in FeO (0.1, 0.1, and 0.4 wt%, respectively) and anorthite is free of Na. Refractory trace element (RTE) contents (as determined by SIMS) are ~200–350 × CI in perovskite, 3–20 × CI in all other phases, except AIO(OH) and calcite (~1–2 × CI). Ubiquitous are negative abundance anomalies of Yb, Eu, and Ce in most phases, except AIO(OH), and calcite, which have only an Yb deficiency. AIO(OH) contains excess ^{26}Mg with an initial $^{26}\text{Al}/^{27}\text{Al}$ of $(5.24 \pm 0.14) \times 10^{-5}$.

Because AIO(OH) cannot be a primary phase condensed from solar nebula gas it had to have a precursor that was Al-rich and RTE-poor, perhaps AlN , or Al_4C_3 , or ? Such a phase, however, will need a gas that was more reducing than the solar nebula [e.g., 9]. The abundant negative abundance anomalies of Yb and Eu point into the same direction. However, the small but also common Ce(-) anomaly (not present in perovskite!) demonstrates the highly refractory nature of the assembly for condensation conditions close to those predicted for the solar nebula [9].

Acknowledgements: Supported by FWF (Austria) and NASA.

References: [1] MacPherson G. J. et al. 1983. *Geochimica et Cosmochimica Acta* 47:823. [2] Lindstrom D. J. and Klöck A. O. 1992. *Meteoritics* 27:243. [3] Kurat G. et al. 1994. Abstract #763. 25th LPSC. [4] Hoppe P. et al. 1995. Abstract #623. 26th LPSC. [5] Zolensky M. E. 1987. *Science* 237:1466. [6] McKeegan K. D. 1987. *Science* 237:1468. [7] Kurat G. 1970. *Earth and Planetary Science Letters* 9:225. [8] Wopenka B. 2005. Personal communication. [9] Lodders K. and Fegley B. Jr. 1993. *Earth and Planetary Science Letters* 117:125.

5177

TRANSMISSION ELECTRON MICROSCOPY OF OLIVINE IN THE LAR 06319 OLIVINE-PHYRIC SHERGOTTITE

T. Kurihara, T. Mikouchi, K. Saruwatari, J. Kameda, and M. Miyamoto. Department of Earth and Planetary Science, Graduate School of Science, University of Tokyo, Hongo, Bunkyo-ku, Tokyo 113-0033, Japan. E-mail: kurihar@eps.s.u-tokyo.ac.jp.

Introduction: Some Martian meteorites (especially, NWA 2737 chassignite) are known to contain brown-colored olivine. Recent TEM studies revealed that nanoparticles of Fe-Ni metal in olivine are responsible for the brown color of olivine in NWA 2737, which was probably formed by reduction of olivine due to heavy shock events [1, 2]. Our TEM study demonstrated broad existence of Fe-rich nano-particles (Fe-Ni metal and magnetite) in olivine among Iherzolitic shergottites (ALH 77005, LEW 88516, and Y-000097) [3]. It is quite natural to expect the same story in other shergottites with brown colored olivine. In this abstract, we report TEM observation of olivine in LAR 06319, a new olivine-phyric shergottite from Antarctica, to look for Fe-rich nanoparticles.

Olivine Mineralogy: Olivine in LAR 06319 reaches 1–2 mm in size and shows extensive chemical zoning (Fo_{75-45}). The olivine grains in the thin section display brown to dark color similar to NWA 2737 olivine. Another remarkable feature of olivine in LAR 06319 is the presence of abundant tiny dark inclusions usually a few micrometers in size. These inclusions are widely distributed in olivine grains and not related to the color of olivine. The FE-SEM (Hitachi S-4500) observation revealed that these inclusions were symplectite exsolution composed of submicron intergrowth of augite and chromite.

TEM Observation: We prepared TEM samples by crashing a small rock chip of LAR 06319 into powder by hand (~100 μ m in size) to look for nano-particles in olivine. The TEM observation was performed by JEOL JEM 2010 TEM equipped with EDS. Careful observation by TEM showed that nanoparticles were present in LAR 06319 olivine. The diameter of nanoparticles is 5–20 nm. The electron diffraction patterns show that they are Fe metal. The EDS analysis shows that these particles are enriched in Fe supporting the result by electron diffraction analysis. No obvious secondary phases were found around the nanoparticles. These nanoparticles are very similar to those in olivines from other Martian meteorites with brown-colored olivine, in their size, texture, and compositions.

Conclusions: Fe metal nanoparticles in LAR 06319 olivine can account for the dark color of their host olivine. The formation of nanoparticles yields minimum shock pressure of 40 GPa according to the result from shock experiments [4]. This shock pressure is consistent with the presence of maskelynite and shock melt vein in LAR 06319. We plan to analyze other olivine-phyric shergottites such as Dar al Gani 476 and Dhofar 019 for comparison.

References: [1] Van de Moortele B. et al. 2007. *Earth and Planetary Science Letters* 262:37–49. [2] Treiman A. H. et al. *Journal of Geophysical Research* 112:E04002. [3] Kurihara T. et al. 2008. Abstract #2478. 39th LPSC. [4] Kurihara T. et al. 2008. Abstract #2505. 39th LPSC.

5174

THE ^{26}Al CONCENTRATION IN 53 ANTARCTIC METEORITES

H. Kusuno¹, T. Fukuoka¹, H. Kojima², and H. Matsuzaki³. ¹Department of Environment Systems, Faculty of Geo-Environmental Science, Ritsso University, Japan. E-mail: 089w00002@ris.ac.jp. ²Antarctic Meteorite Research Center, National Institute of Polar Research, Japan. ³School of Engineering, the University of Tokyo, Japan.

Introduction: The terrestrial age of Antarctic meteorite brings us useful information for the frequency of meteorites fall, mechanism of accumulation of meteorites on ice and the age of ice. ^{26}Al ($T_{1/2} = 7.16 \times 10^5$ y) is one of useful tool for the dating of terrestrial age of meteorites. ^{26}Al concentrations in meteorites were measured by extremely low background γ -ray counting system analysis (Institute of Cosmic Ray Research, the University of Tokyo) and Accelerator mass spectrometry (AMS) analysis (Micro Analysis Laboratory, the University of Tokyo).

Analytical Procedure for AMS: HF treatment was carried out in a teflon beaker for 10 mg of powdered sample with 3 mg of Al carrier. Purified Al was precipitated as $\text{Al}(\text{OH})_3$ by NH_4OH . $\text{Al}(\text{OH})_3$ precipitation in Pt crucible was heated at 900 °C to get Al_2O_3 . ^{26}Al concentration was determined by AMS analysis using Al_2O_3 sample mixed with Ag metal.

Results and Discussion: We determined ^{26}Al concentration in 50 of HED meteorites and 3 of chondrites from the Mt. Yamato and the Mt. Asuka region in Antarctica. Concentration of ^{26}Al in HED meteorites had a range from 54 to 100 [dpm/kg]. Our results of HED meteorites are similar to those of previous works [1] and [2]. ^{26}Al concentration in chondrites had a range from 14 to 39 [dpm/kg]. These results are also similar to those of previous works [3] and [4].

The results with previous works suggest that ^{26}Al concentrations of HED meteorites were higher than those of chondrites. This seems the terrestrial ages of HED meteorites were younger than chondrites. However, this discrepancy may explain the difference of the ^{26}Al production rate in space for these meteorites. Namely the ^{26}Al production rate relates to the major chemical composition such as Si, Al, Fe, Ca, etc. So we examined the ^{26}Al concentration in 8 falls of HED meteorites and in 9 falls of chondrites. The range of ^{26}Al concentrations for falls meteorites similar to those for Antarctic meteorites.

References: [1] Aylmer D. et al. 1988. *Geochimica et Cosmochimica Acta* 52:1691–1698. [2] Welten K. C. et al. 1997. *Meteoritics* 32:891–902. [3] Evans J. et al. 1992. *Smithsonian Contributions to the Earth Sciences* 30: 45–56. [4] Nishiizumi K. 1987. *Nuclear Tracks and Radiation Measurements* 13:209–273.

5019

¹⁴C TERRESTRIAL AGES OF METEORITES FROM THE ATACAMA DESERT (CHILE)

M. D. Leclerc¹, E. M. Valenzuela², and A. J. T. Jull¹. ¹NSF-Arizona AMS Laboratory, University of Arizona, Tucson, AZ 85721, USA. E-mail: leclerc@email.arizona.edu. ²Dep. de Geologia, Universidad de Chile, Santiago, Chile.

Introduction: The terrestrial age is an important parameter in understanding the current degree of weathering [1, 2] and compositional changes in a desert meteorite [3]. Substantial numbers of meteorites are found in arid environments and can survive for at least 50,000 yr [4–6]. A few meteorites of much older age have been reported from Arabia and there are some meteorites over 250,000 yr old from these locations [5, 7].

Atacama Desert: The Atacama is a semiarid to hyperarid desert [8] located in northern Chile between the Andes and the Pacific Ocean. It is one of the oldest desert of the world [9], and has the lowest rainfall records, some as little as 1 mm/yr.

Meteorites Studied: We studied 34 ordinary chondrites and 1 carbonaceous chondrite from various locations within the Atacama Desert: 17 meteorites were found in the Coastal Range within and near the Pampa de Mejillones [8] and 18 come from diverse locations of the central part of the desert.

Trends in Terrestrial Ages: At our laboratory, we make measurements of ¹⁴C and ¹⁴C/¹⁰Be. In this study, we have applied ¹⁴C measurements to the terrestrial-age distribution of the meteorites. The terrestrial ages measured span a range from recent falls to >35 kyr. The age distribution for the Atacama Desert appears to define a modified simple exponential decay process, as has been discussed earlier [5, 6]. We will compare the age distributions with those of other sites such as Arabia, Western Australia and North American deserts. Furthermore, we will study the proportions of L and H chondrites according their terrestrial ages as it was shown that, in hot deserts, meteorites with higher iron content weather faster [1].

We will also discuss improvements to our methodology at Arizona and the application of terrestrial-age measurements to meteorites from desert environments and their significance for understanding of climatic effects.

References: [1] Bland P. A. et al. 1996. *Monthly Notices of the Royal Astronomical Society* 238:551. [2] Bland P. A. et al. 2000. *Quaternary Research* 53:131. [3] Al-Kathiri A. et al. 2005. *Meteoritics & Planetary Science* 40:1215. [4] Wlotzka F. et al. 1995. Lunar and Planetary Institute Technical Report #95-02. 72 p. [5] Jull A. J. T. 2006. Terrestrial ages of meteorites. In *Meteorites in the early solar system II*, edited by Lauretta D. et al. Tucson, Arizona: The University of Arizona Press. [6] Jull A. J. T. et al. 1998. *Geological Society of London Special Publication* 140:75. [7] Welten K. C. et al. 2003. *Meteoritics & Planetary Science* 38:499. [8] Muñoz C. et al. 2007. *Journal of Arid Environments* 71:188. [9] Dunai et al. 2005. *Geology* 33:321.

5141

¹⁸²Hf-¹⁸²W CHRONOMETRY AND THE EVOLUTION OF ACAPULCOITE-LODRANITE PARENT BODY

D.-C. Lee. Institute of Earth Sciences, Academia Sinica, Taipei, Taiwan, ROC. E-mail: dclee@earth.sinica.edu.tw.

Acapulcoites and lodranites are two small groups of achondrites that share the same oxygen isotopic compositions [1], and, therefore, are regarded to have come from the same parent body. Compared to the other more evolved achondrites, such as eucrites, angrites, and ureilites, acapulcoite-lodranite clan appears to be less evolved [2], suggesting that the acapulcoite-lodranite parent body had not experienced global melting events as the differentiated asteroids. Acapulcoites and lodranites have different petrographic features, as well as mineral and bulk chemical compositions [2, 3], suggesting that they did not share a common petrogenetic origin.

Three samples (NWA 725, GRA 95209, and NWA 2235) from the acapulcoite-lodranite clan have been studied with the short-lived chronometer ¹⁸²Hf-¹⁸²W system [4], in order to better constrain the early evolution history in the acapulcoite-lodranite parent body. Different from the more evolved achondrites originated from differentiated asteroids, e.g., eucrites and angrites, bulk rock acapulcoite and lodranite are characterized with distinct ¹⁸²W deficits relative to the terrestrial W, as well as to the undifferentiated chondrites, ϵ_w varies from -2.7 to -2.4. This suggests that live-¹⁸²Hf was present during the formation of acapulcoites and lodranites, and their parent body probably had never experienced a global melting event [4]. Internal isochron has also been determined for each samples, however, the uncertainties associated to the isochron for each sample are quite substantial. Consequently, the bulk isochron regressed through the mineral separates of all three samples has provided currently the best estimate for the timing of metamorphism in the acapulcoite-lodranite parent body, 5 (+6/-5) myrs after the start of the solar system. The formation of acapulcoite-lodranite clan appears to have post-dated the metal-silicate segregation in differentiated asteroids, consistent with a slower accretion rate for the acapulcoite-lodranite parent body, or it had never accreted to a critical mass for metal-silicate segregation to occur naturally.

In order to better constrain if acapulcoites and lodranites shared the same petrogenetic origin, as well as the formation age of acapulcoites, two acapulcoites, NWA 2714 and Dhofar 125, plus a new fraction of NWA 725, are currently being analyzed for the short-lived ¹⁸²Hf-¹⁸²W isotope system, and the results will be presented in the meeting.

References: [1] Clayton R. N. and Mayeda T. K. 1996. *Geochimica et Cosmochimica Acta* 60:1999–2017. [2] Mittlefehldt D. W. et al. 1998. *Reviews in Mineralogy*, vol. 36. [3] McCoy T. J. et al. 2006. *Geochimica et Cosmochimica Acta* 70:516–531. [4] Lee D.-C. Forthcoming. *Meteoritics & Planetary Science*.

5275

SIDEROPHILE ELEMENT DISTRIBUTION IN METAL-SULFIDE NODULES FROM EH3 SAHARA 97072

S. W. Lehner¹, P. R. Buseck¹, W. F. McDonough², and R. D. Ash². ¹Arizona State University, SESE, Tempe, AZ 85287-1404, USA. E-mail: slehner@asu.edu. ²University of Maryland, Department of Geology, College Park, MD 20742, USA.

Introduction: It is generally agreed that the enstatite chondrites formed in a highly reducing part of the inner nebula, but questions remain regarding the nature of this environment. Trace-element distributions in metal-sulfide nodules (MSN) could advance our understanding of this region. The distribution of trace [or minor] siderophile elements can provide insight into the history of their host phases since they partition differently into melt-derived phases than into phases resulting from volatility-controlled nebular evaporation and condensation. Sahara 97072 (paired with Sahara 97096) contains complex, layered MSN that were proposed as pre-accretionary nebular objects [1]. We measured siderophile element distributions to test this hypothesis.

Methods: We used a magnetic-sector Finnegan Element 2—New Wave UP213 Laser Ablation inductively-coupled plasma mass spectrometry (LA-ICPMS) to gather data on the trace element distributions in kamacite, perryite [(FeNi)₅(SiP)₂], and schreibersite in MSN from EH3 Sahara 97072. Regions of interest were chosen on the basis of SEM energy dispersive spectroscopy element maps, electron microprobe analyses, and petrographic microscope observations. Then mineral phases >~15 to 30 μm diameter were analyzed using LA-ICPMS.

Results: Preliminary analyses of Fe, Co, Ni, Cu, Ga, Pd, Ru, and Ir in kamacite, schreibersite, and perryite, within MSN indicate the kamacite is enriched in the volatile elements Ga and Au normalized to Ni and relative to CI by a factor of 1.8. The kamacite Pd/Ir ratio is also higher than CI, whereas Ru and Ir are slightly depleted by the same amount and correlated. These results are similar to earlier INAA analyses [2–5]. Perryite, with up to 72 wt% Ni, is enriched in Cu and Pd relative to kamacite. Schreibersite averages about 14 wt% Ni and contains slightly less Ru and Pd than kamacite, whereas other elements are below detection limits. Subtle Ni and siderophile-element zoning occurs in the kamacite mantle surrounding MSN cores. The Co/Ni ratios of kamacite average 2 times, but range up to 3 times, solar. However, the weighted average Co/Ni ratio of kamacite, perryite, and schreibersite or kamacite and perryite alone is near to but less than solar, possibly indicating exsolution from a single phase.

Conclusions: The schreibersite could be an early condensate. The perryite composition and the subtle Ni and siderophile-element zoning in the kamacite may be explained by the redistribution of Si, Ni, Cu, and Pd during pre-accretionary heating and sulfurization events.

References: [1] Weisberg M. K. and Prinz M. 1998. Sahara 97096: A highly primitive EH3 chondrite with layered sulfide-metal-rich chondrules. 29th LPSC. [2] Hertogen J. et al. 1983. Enstatite chondrites: Trace element clues to their origin. *Geochimica et Cosmochimica Acta* 47:2241–2255. [3] Horan M. F. et al. 2003. Highly siderophile elements in chondrites. *Chemical Geology* 196:5–20. [4] Kallemeyn G. W. and Wasson J. T. 1986. Compositions of enstatite (EH3, EH4,5, and EL6) chondrites: Implications regarding their formation. *Geochimica et Cosmochimica Acta* 50:2153–2164. [5] Weeks K. S. and Sears D. W. G. 1985. Chemical and physical studies of type 3 chondrites—V: The enstatite chondrites. *Geochimica et Cosmochimica Acta* 49:1525–1536.

5053

NANOSIMS SEARCH FOR PRESOLAR GRAINS IN MATTER FROM COMET 81P/WILD 2 AND THE CR CHONDRITE NWA 852

J. Leitner¹, P. Hoppe¹, J. Huth¹, and J. Zipfel². ¹Max Planck Institute for Chemistry, 55128 Mainz, Germany. E-mail: leitner@mpch-mainz.mpg.de. ²Forschungsinstitut und Natur-museum Senckenberg, 60325 Frankfurt, Germany.

Introduction: Primitive solar system materials contain varying amounts of presolar dust grains that formed in the winds of evolved stars or in the ejecta of stellar explosions [1]. Presolar silicates and oxides are among the most abundant types of these grains [2–6]. Although they belong to the most primitive chondrite groups, first studies of CR chondrites indicated only low presolar dust abundances. Recent investigations, however, revealed much higher abundances of presolar dust in individual meteorites of this group [7, 8]. Comets are believed to have formed in the cold, outer regions of the protosolar cloud, representing the most primitive matter in the solar system. NASA's Stardust mission collected dust from the coma of comet 81P/Wild 2 and successfully returned it to Earth in 2006 [9]. Preliminary examination revealed the dust to be an unequilibrated mixture of heterogeneous material of mainly solar system isotopic composition. To date, only three ¹⁷O-rich presolar grains were found [10, 11]. Here, we present first results of our investigation of the presolar silicate/oxide grain inventory of Wild 2 foil crater residues and matrix of the CR2 chondrite NWA 852.

Samples and Experimental: In this ongoing study, impact residues in 18 small craters (∅ 520–1760 nm) on Stardust Al foil C2037N, found in a SEM high-resolution survey, were investigated, as well as fine-grained matrix on a thin section of NWA 852. A ~100 nm primary Cs⁺ beam was rastered over the sample areas in the NanoSIMS 50, and ¹⁶O⁻, ¹⁷O⁻, ¹⁸O⁻, ²⁸Si⁻, and ²⁷Al¹⁶O⁻ ion images were acquired in multi-collection mode.

Results and Discussion: The 18 investigated craters so far (total area: 25 μm², some 3 pg of cometary matter) contain no presolar silicate/oxide grains. All residues are isotopically normal within 2σ, with δ¹⁷O and δ¹⁸O values from -66 ± 42 to +164 ± 94‰ and from -32 ± 30 to +24 ± 35‰, respectively. In 8 fine-grained matrix areas analyzed in NWA 852, all 10 × 10 μm² in size, we found one presolar silicate grain. The 300 nm-sized grain has ¹⁷O/¹⁶O = (5.98 ± 0.31) × 10⁻⁴ (i.e., 1.55× solar) and solar ¹⁸O/¹⁶O. It belongs to group 1, most likely originating in low-mass AGB stars [12]. This grain represents an abundance of ~90 ppm in NWA 852, slightly below the abundances inferred for the CR chondrites QUE 99177 and MET 00426 [7, 8].

References: [1] Hoppe P. and Zinner E. 2000. *Journal of Geophysical Research* 105:10,371–10,385. [2] Nguyen A. and Zinner E. 2004. *Science* 303:1496–1499. [3] Mostefaoui S. and Hoppe P. 2004. *The Astrophysical Journal* 613:L149–L152. [4] Messenger S. et al. 2003. *Science* 300:105–108. [5] Nguyen A. et al. 2007. *The Astrophysical Journal* 656:1223–1240. [6] Vollmer C. et al. Forthcoming. *The Astrophysical Journal*. [7] Floss C. and Stadermann F. J. 2007. *Meteoritics & Planetary Science* 42:A48. [8] Floss C. and Stadermann F. J. 2008. Abstract #1280. 39th LPSC. [9] Brownlee D. et al. 2006. *Science* 314:1711–1716. [10] McKeegan K. et al. 2006. *Science* 314:1720–1724. [11] Stadermann F. J. and Floss C. 2008. Abstract #1889. 39th LPSC. [12] Nittler L. R. et al. 1997. *The Astrophysical Journal* 483: 475–495.

5076

GROVE MOUNTAINS (GRV) 020090: A HIGHLY FRACTIONATED LHERZOLITIC SHERGOTTITE

Y. Lin¹, T. Liu¹, W. Shen¹, L. Xu², and B. Miao³. ¹Key Laboratory of the Earth's Deep Interior, Institute of Geology and Geophysics, Chinese Academy of Sciences, Beijing, China. E-mail: LinYT@mail.igcas.ac.cn. ²National Astronomical Observatories, CAS, Beijing, China. ³Key Laboratory of Geological Engineering Center of Guangxi Province, Guilin University of Technology, China.

Introduction: Lherzolitic shergottites are a small group of Martian meteorites, with only six of this group were reported. The first five, i.e., ALHA77005, Y-793605, LEW 88516, GRV 99027, and NWA 1950 share similar petrology and geochemistry, probably ejected from a same igneous unit on the Mars [e.g., 1–5]. GRV 020090 was classified as the sixth rock [6]. It may be unique, with a low abundance of olivine and high FeO-contents of Mg, Fe-silicates. In this work, we continue the study of GRV 020090, in order to clarify its petrogenesis.

Petrography: GRV 020090 consists of poikilitic and interstitial parts as other lherzolitic shergottites, but pyroxene oikocrysts contain much less olivine. Common presence of baddeleyite (up to 4 $\mu\text{m} \times 10 \mu\text{m}$) in association with ilmenite is characteristic of GRV 020090. Another unique feature is coexistence of three distinct phases of feldspars that have been converted to maskelynite. Orthoclase and silica-excess feldspar usually occur at rims of the major plagioclase.

Mineral Chemistry: The Fa-content of olivine shows a bimodal distribution, with a peak at Fa₃₃ for the grains in poikilitic part and another one at Fa₄₁ for those in the interstitial region. The interstitial pigeonite is also enriched in FeO-content (Fs_{26–34}). Chromite in the interstitial part usually coexists with ilmenite, and is TiO₂-rich (13.5–19.1 wt%) in comparison with the euhedral grains in the pyroxene oikocrysts (0.71–2.82 wt% TiO₂). Compositional ranges of feldspars are An_{24–57}Ab_{41–68}Or_{1–9} for the major plagioclase, An_{1–7}Ab_{36–51}Or_{43–63} for orthoclase, and An_{37–62}Ab_{33–55}Or_{4–9} (based on only Na, K, Ca atomic ratios) with [Si₄O₈] up to 38 mol% for silica-excess feldspar (here [] is vacancy). Excess of silica up to 52 mol% [Si₄O₈] was also found in orthoclase.

Discussion: (Na⁺, K⁺) + Al³⁺ can be substituted with [] + Si⁴⁺ or Ca²⁺ + 2Al³⁺ with [] + 2Si⁴⁺, and presence of [Si₄O₈] was reported in plagioclase in lunar rocks [7]. The excess of silica of feldspars in GRV 020090 correlates negatively with the albite-content of K-poor plagioclase or KAlSi₃O₈-content of orthoclase, suggesting of presence of [Si₄O₈]. The high contents of [Si₄O₈] of feldspars, FeO-contents of Mg, Fe-silicates, TiO₂-contents of the interstitial chromite, and the common occurrences of orthoclase and baddeleyite suggest that GRV 020090 crystallized from a melt probably produced by low-degree partial melting, and it may sample a unique igneous unit on the Mars.

Acknowledgements: The meteorite was supplied by the Polar Research Institute of China. This study was supported by the Knowledge Innovation Program (kzcx2-yw-110) of the Chinese Academy of Sciences.

References: [1] Lin Y. et al. 2005. *Meteoritics & Planetary Science* 40: 1599–1619. [2] Gillet Ph. et al. 2005. *Meteoritics & Planetary Science* 40: 1175. [3] McSween H. Y. Jr. et al. 1979. *Science* 204:1201–1203. [4] Harvey R. P. et al. 1993. *Geochimica et Cosmochimica Acta* 57:4769–4783. [5] Ikeda Y. 1997. *Antarctic Meteorite Research* 10:13–40. [6] Miao B. et al. 2004. *Acta Geologica Sinica* 78:1034–1041. [7] Beatty D. W. and Albee A. L. 1980. *American Mineralogist* 65:63–74.

5258

SULFUR IN THE ORGUEIL CI CHONDRITE

K. Lodders. Department of Earth and Planetary Science, Washington University, Saint Louis, MO 63130, USA. E-mail: lodders@wustl.edu.

Sulfur in CI chondrites occurs in at least 7 reservoirs: (1) Most S is “(Fe,Ni)S” in phyllosilicates, extractable with (NH₄)₂S_x but not easily released as H₂S when treated by HCl. Sulfur in (2) pyrrhotite and (3) pentlandite is released as H₂S when treated with HCl. (4) Sulfur in water soluble sulfates. Minor S is in (5) elemental S, (6) hyposulfites and (7) organic compounds. The distribution of S among these phases changed since the meteorite fell and may affect the determination of total amount of S.

Oxidation of sulfides produces sulfate efflorescence on the outside and salt deposits in phyllosilicate veins of the Orgueil meteorite [1]. If sulfates are terrestrial weathering products, the sulfate content should be a function of the meteorite's residence time on Earth. In 1834, Berzelius describes his sample from the 1806 Alais CI chondrite fall: “Its color is black with a touch of gray, with dense, fine, white dots or incrustations. This is not reported in the older descriptions; only in the Dictionnaire des sciences naturelles, XXX, p. 339, it is noted that this meteorite tends to cover itself with some efflorescence, which the authors give as iron vitriol.” He shows that Fe-sulfate was a misidentification; FeSO₄ is never found in any significant quantities in water extracts or in crystalline form. FeSO₄ oxidizes to limonite: FeSO₄ × 7H₂O + 1/4 O₂ = Fe(OH)SO₄ + 6.5 H₂O and Fe(OH)SO₄ + 2 H₂O = Fe(OH)₃ + H₂SO₄; also providing H₂SO₄ to leach Mg out of phyllosilicates for making the MgSO₄ efflorescence.

Three analyses reported ~2 months after the Orgueil fall give S in sulfate form as 1.1 ± 0.3 wt% and total S in all forms as 6.3 ± 0.6 wt% [3–5]. The amount of S in sulfates (~17.5% of all S measured) represents the upper limit to the pre-terrestrial sulfate content in Orgueil. Five recent analyses [6–10] yield 2.4 ± 0.3 wt% S in sulfate form, which is ~45% of all S measured in recent bulk analyses of Orgueil (5.3 ± 0.2% [10–12]). The recent bulk S appears 1 wt% lower than the average of the 3 earlier analyses, which may indicate loss of S through efflorescence formation. In that case, redistribution of S during terrestrial alteration within Orgueil was not isochemical with respect to elemental composition, and use of larger samples, suggested to obtain representative average bulk compositions [13], cannot improve the analytical situation. However, the atomic S/Si ratios (0.40–0.52) in the older analyses are close to the recommended photospheric value of 0.46 [15], which suggests higher absolute element concentrations in the older analyses because of lower H₂O contents of the samples. There is no obvious reason to question that the solar S abundance derived from recent Orgueil analysis is too low.

References: [1] Gounelle M. and Zolensky M. 2001. *Meteoritics & Planetary Science* 36:1321. [2] Berzelius J. J. 1834. *Annual Review of Physical Chemistry* 33:113–148. [3] Pisani F. 1864. *Comp. Rend. Paris* 59: 132–135. [4] Cloez S. 1864. *Comp. Rend. Paris* 59:37–40. [5] Filhol E. and Mellies. 1864. *Mem. Acad. Imp. Sci.* 6:379–382. [6] DuFresne E. R. and Anders E. 1962. *Geochimica et Cosmochimica Acta* 26:1085–1114. [7] Bostrom K. and Fredriksson K. 1966. *Smithson. Misc. Coll.* 151:1–39. [8] Kaplan I. R. and Hulston J. R. 1966. *Geochimica et Cosmochimica Acta* 30: 479–496. [9] Fredriksson K. and Kerridge J. F. 1988. *Meteoritics* 23:35–44. [10] Burgess R. et al. 1991. *Meteoritics* 26:55–64. [11] Wiik H. B. 1956. *Geochimica et Cosmochimica Acta* 9:279–289. [12] Mason B. 1962. *Space Science Reviews* 1:621–646. [13] Dreibus G. et al. 1995. *Meteoritics* 30:439–445. [14] Morlok et al. 2006. *Geochimica et Cosmochimica Acta* 70:5371–5394. [15] Lodders K. 2003. *The Astrophysical Journal* 591:1220–1246.

5320

OXYGEN ISOTOPE FRACTIONATION DURING CO SELF-SHIELDING: DEPENDENCE ON THE FUV SOURCE STARJ. R. Lyons¹. ¹Institute of Geophysics and Planetary Physics, UCLA, Los Angeles, CA, USA. Email: jimlyons@ucla.edu.

Introduction: Self-shielding during CO photolysis is central to Clayton's prediction [1] of the oxygen isotope composition of the Sun. In the far-UV (FUV) (91–110 nm) CO has an absorption spectrum comprised of ~3 dozen electronic bands, most of which contain sharp rovibronic lines. Self-shielding results in large abundance-dependent fractionation in oxygen isotopes, and yields O atoms that are eventually incorporated into H₂O with $\delta^{17}\text{O}$ and $\delta^{18}\text{O}$ values of +1000 ‰. Photochemical models of the solar nebula [2] and parent molecular cloud [3, 4] have demonstrated that the CO self-shielding process is viable. With confirmation of the underlying prediction of CO self-shielding from preliminary analyses of Genesis results [5], we can now use the CAI oxygen isotope data to constrain the UV radiation field experienced by the solar nebula or parent cloud, thereby defining the solar system birth environment.

FUV Source Stars: The FUV radiation needed to drive CO photodissociation could have come from a massive O or B star that was part of the solar system's birth cluster, and therefore was in close proximity to the protosun [2]. If this scenario is correct, the required flux of FUV radiation constrains the size of the massive star, and therefore the size of the cluster in which the protosun formed [6]. It was concluded that the solar system formed in a cluster of ~200 stars with the massive star at a distance of ~1 parsec (yielding a radiation field $G_0 \sim 10^3$) [2]. Alternatively, young low-mass stars have enhanced FUV flux relative to the modern Sun, and may be able to drive sufficient CO photodissociation in the surface region of the solar nebula [7]. The key to distinguishing between these two UV sources is in the spectral details of their emitted fluxes. Massive O or B stars have temperatures ~20,000 to 50,000 K, with peak blackbody radiation at 150 to 60 nm, respectively, which bounds the FUV region. By contrast, low-mass protostars have an FUV spectrum that consists of continuum plus several strong emission lines (e.g., O VI, C III) produced as a result of mass accretion events onto the young star [8], resulting in a distinctly non-blackbody FUV spectrum. The latter spectrum will yield different isotope fractionation during CO self-shielding than will the more blackbody-like FUV spectrum of a massive star.

By computing optical depths for H₂ as a function of wavelength, together with synthetic spectra for each FUV band of CO and its isotopologues, isotopic fractionation during CO photodissociation is accounted for. I will present results for several important CO bands, along with implications for the FUV source.

References: [1] Clayton R. N. 2002. *Nature* 415:860–861. [2] Lyons J. R. and Young E. D. 2005. *Nature* 435:317–320. [3] Yurimoto H. and Kuramoto K. 2004. *Science* 305:1763–1766. [4] Lee J.-E., Bergin E. A., and Lyons J. R. Forthcoming. *Meteoritics & Planetary Science*. [5] McKeegan K. D. et al. 2008. Abstract #2020. 39th LPSC. [6] Adams F. C. et al. 2004. *The Astrophysical Journal* 611:360–379. [7] Young E. D. 2007. *Earth and Planetary Science Letters* 262:468–483. [8] Herczeg G. et al. 2004. *The Astrophysical Journal* 607:369–383.

5027

CHONDRULES AND RIMS IN THE LEAST AQUEOUSLY ALTERED CM CHONDRITE QUE 97990: IS THIS METEORITE A PRIMARY ACCRETIONARY ROCK?

M. Maeda and K. Tomeoka. Department of Earth and Planetary Sciences, Faculty of Science, Kobe University, Nada, Kobe 657-8501, Japan. E-mail: 055s460s@stu.kobe-u.ac.jp.

Introduction: The Yamato-791198 CM chondrite has been described by Metzler et al. [1] as “a primary accretionary rock, obviously unaltered by secondary parent body processes such as aqueous alteration or brecciation.” Recently, however, Rubin et al. [2] reported that QUE 97990 is the least aqueously altered of the CM chondrites that they studied, including 791198. If this is the case, QUE 97990 would potentially provide more primitive information regarding the formation of CM chondrites. Here we present the results of our mineralogical and petrological investigation of the QUE 97990 and Y-791198 CM chondrites. Our goal was to unravel the formation process of chondrule rims in the CM chondrites and the early aqueous alteration history of these meteorites.

Results and Discussion: QUE 97990 consists largely of an agglomerate of rimmed chondrules and PCP, having a general resemblance to Y-791198.

Chondrule mesostases in QUE 97990 have largely been altered to Mg-Fe serpentine. In many mesostases, however, arrays of parallel, thin lath-shaped crystallites of high-Ca pyroxene, which are primary quenched products, remain unaltered. Such high-Ca pyroxene crystallites are extremely rare in CM chondrites. On the other hand, chondrule mesostases in Y-791198 have also been altered to Mg-Fe serpentine, but quenched crystallites are absent. These characteristics can be ascribed to that Y-791198 has been affected by a higher degree of aqueous alteration than QUE 97990.

Rims surrounding chondrules in both QUE 97990 and Y-791198 consist mainly of Mg-Fe serpentine. Chondrules in QUE 97990 commonly show topographic depressions (embayments) on their surfaces. In many of the embayments, the rims are distinctly Fe-rich compared to other portions and contain grains of Fe-Ni metal, PCP, and Fe-Ni sulfide, some of which reside partly in both the chondrule and the rim. The Fe-Ni metal grains have been partially replaced by PCP. These observations suggest that the embayments containing Fe-Ni metal, PCP, and Fe-Ni sulfide were formed by replacing opaque nodules in their host chondrules. These characteristics resemble those observed in the phyllosilicate-rich chondrule rims in the Vigarano CV3 chondrite [3]. On the other hand, chondrules in Y-791198 also show embayments on their surfaces. However, Fe-Ni metal, PCP, and Fe-Ni sulfide are rare, which is probably explained by that these opaque minerals have been more extensively replaced by phyllosilicates than those in QUE 97990.

The results of our study are consistent with that the degree of aqueous alteration in QUE 97990 is lower than that in Y-791198 [2]. Nonetheless, our observations reveal abundant evidence suggesting that QUE 97990 has experienced a significant degree of aqueous alteration.

References: [1] Metzler K. et al. 1992. *Geochimica et Cosmochimica Acta* 56:2873–2897. [2] Rubin A. E. et al. 2007. *Geochimica et Cosmochimica Acta* 71:2361–2382. [3] Tomeoka K. and Tanimura I. 2000. *Geochimica et Cosmochimica Acta* 64:1971–1988.

5135

CORRELATED MEASUREMENTS OF OXYGEN AND MAGNESIUM ISOTOPES IN CR CAIs: CONSTRAINTS ON THE DURATION OF CAI FORMATION AND EVOLUTION OF OXYGEN ISOTOPES IN THE INNER SOLAR NEBULA

K. Makide¹, K. Nagashima¹, A. N. Krot¹, G. R. Huss¹, I. D. Hutcheon², and A. Bischoff³. ¹HIGP, University of Hawai'i at Manoa, HI, USA. ²Lawrence Livermore National Laboratory, USA. ³Institut für Planetologie, Münster, Germany.

Correlated O- and Mg-isotope measurements of CAIs can be used to constrain the initial abundance of ²⁶Al in the early Solar System, as well as the duration of CAI formation and the evolution of O isotopes in the inner solar nebula. Most previous studies were performed on CAIs from CV chondrites, which experienced multi-stage thermal processing and alteration in the solar nebula and on the CV asteroid. These processes resulted in significant disturbance of O- and Mg-isotope systematics of the CV CAIs [e.g., 1–4]. Here we report O- and Mg-isotope compositions of 23 mineralogically pristine CAIs from CR chondrites measured with the UH Cameca ims-1280 ion microprobe using analytical procedures described in [5, 6].

Based on the major mineralogy, 165 CAIs discovered in 45 polished sections of 15 CR chondrites are classified into three major types: spinel ± melilite ± pyroxene (80%), grossite ± hibonite-bearing (8%), and anorthite-rich (12%); 8 of the CR CAIs are associated with chondrule materials. Most CR CAIs measured have uniformly ¹⁶O-rich ($\Delta^{17}\text{O} \leq -21\%$) compositions similar to the inferred composition of the Sun [7] and show no evidence for post-crystallization isotopic exchange. The inferred (²⁶Al/²⁷Al)₀ values of the ¹⁶O-rich CAIs range from $(4.2 \pm 0.7) \times 10^{-5}$ to $(5.5 \pm 0.5) \times 10^{-5}$, consistent with the canonical value of $\sim 5 \times 10^{-5}$ [8, 9], and suggest a short duration (<0.4 Myr) of CR CAI formation. Our data do not support the supra-canonical (²⁶Al/²⁷Al)₀ value of $(5.8-7) \times 10^{-5}$ inferred from whole-rock and mineral isochrons of CAIs from CV chondrites [10-12]. Two of the ¹⁶O-rich igneous CR CAIs have no resolvable excess of $\delta^{26}\text{Mg}$; one of these inclusions has resolvable deficit in $\delta^{26}\text{Mg}$ and highly fractionated O-and Mg-isotope compositions. This is the first FUN CAI from CR chondrites. We suggest that the ²⁶Al-poor/free, ¹⁶O-rich CAIs formed prior to injection and homogenization of ²⁶Al in the early Solar System [13]. Three of eight CAIs associated with chondrule material were measured for O and Mg isotopes. These CAIs experienced melting and O-isotope exchange with an ¹⁶O-poor ($\Delta^{17}\text{O} > -5\%$) gas during chondrule formation. The inferred (²⁶Al/²⁷Al)₀ of these CAIs ($<0.7 \times 10^{-5}$) suggest melting >2 Myr after crystallization of CAIs having the canonical ²⁶Al/²⁷Al ratio and indicate evolution of O-isotope compositions of the inner solar nebula on a similar time scale, consistent with [14].

References: [1] Podosek F. A. et al. 1991. *Geochimica et Cosmochimica Acta* 55:1083. [2] Clayton R. N. 1993. *Annual Review of Earth and Planetary Sciences* 21:115. [3] Fagan T. J. et al. 2004. *Meteoritics & Planetary Science* 39:1257. [4] Ito M. et al. 2004. *Geochimica et Cosmochimica Acta* 68:2905. [5] Makide K. et al. 2007. Workshop on the Chronology of Meteorites and the Early Solar System, 108. [6] Makide K. et al. 2008. Abstract #2407. 39th LPSC. [7] Hashizume K. and Chaussidon M. 2005. *Nature* 434:619. [8] MacPherson G. J. et al. 1995. *Meteoritics & Planetary Science* 30:365. [9] Jacobsen B. et al. Forthcoming. *Earth and Planetary Science Letters*. [10] Thrane K. et al. 2006. *The Astrophysical Journal* 646:L159. [11] Bizzarro M. et al. 2004. *Nature* 431: 275. [12] Young E. et al. 2005. *Science* 308:223. [13] Sahijpal S. and Goswami J. N. 1998. *The Astrophysical Journal* 509:L137. [14] Krot A. N. et al. 2005. *The Astrophysical Journal* 622:1333.

5003

MANITO STONE: NATIVE CREE BELIEFS OF THE IRON CREEK ALBERTA, CANADA IRON METEORITE

A. A. Mardon. Antarctic Institute of Canada, P.O. Box 1223, MPO, Edmonton, Alberta, Canada. E-mail: aamardon@yahoo.ca.

Introduction: Meteorites were held in special reverence in many pre-industrial societies. This abstract outlines the contemporary record of the instance of the worship of this meteorite and the legend of how it was tied to the destruction of the Cree people of Western Canada. It is currently located in the Royal Alberta Provincial Museum and originally fell and was located near Edmonton, Alberta very near the small community of Sedgewick.

Historical Account from 1872: "In the farmyard of the mission house lay a curious block of metal it was of immense weight; It was rugged deeply indented, and polished on the outer edges of the indentations by the wear and friction of many years. Its history was a curious one. Longer than any man could say, it had laid on the summit of a hill far out in the Southern prairies. It had been a medicine-stone of surpassing virtue among the Indians over a vast territory. No tribe or portion of a tribe would pass in the vicinity without paying a visit to this great medicine: it was said to be increasing yearly in weight. Old men remembered having heard old men say that they had once lifted it easily from the ground. Now, no single man could carry it. And it was no wonder that this metallic stone should be a Manito-stone and an object of intense veneration to the Indian: it had come down from heaven: it did not belong to the earth, but had descended out of the sky: it was, in fact, an aerolite. Not very long before my visit this curious stone had been removed from the hill upon which it had so long rested and brought to the Mission of Victoria by some person from that place. When the Indians found that it had been taken away, they were loud in the expression of their regret. The old medicine-men declared that its removal would lead to great misfortunes, and that war, disease, and dearth of buffalo would afflict the tribes of the Saskatchewan. This was not a prophecy made after the occurrence of the plague of smallpox, for in a magazine published by the Wesleyan Society in Canada there appears a letter from the missionary, setting forth the predictions of the medicine-men a year prior to my visit. The letter concludes with an expression of thanks that their evil prognostications had not been attended with success. But a few months later brought all the three evils upon the Indians, and never, probably, since the first trader had reached the country had so many afflictions of war, famine and plague fallen upon the Crees and the Blackfeet as during the year which succeeded the useless removal of their Manito-stone from the lone hill-top upon which the skies had cast it." [1]

Conclusions: Many different societies without contact with each other held meteorites in special reverence even in some cases worship the meteorites. Other native American societies held meteorites in special reverence including the special place it was held by the Inuit. It being until contact with the Europeans their only source of Iron. The legend of its removal is also similar to the worship of Kaaba in Mecca. Many pre-industrial societies knew that meteorites came from the skies and were unique and not of this world. Its place in the sacra emphasizes the importance they were held with.

References: [1] Butler W. F. 1872. *The great lone land*. London. 304 p. [2] White R. 1984. *Canadian meteorites: A catalogue of meteorites found in Canada*. Provincial Museum of Alberta, Edmonton, 27–28.

5024

COMET REFERENCES BY THE VENERABLE BEDE IN *HISTORIA ECCLESIASTICA* OBSERVED IN 678 C.E. AND 729 C.E.

C. A. Mardon¹, A. A. Mardon², and E. G. Mardon³. ¹Newman Theological College, Canada. E-mail: ccmardon@yahoo.ca. ²Antarctic Institute of Canada. E-mail: aamardon@yahoo.ca. ³Antarctic Institute of Canada.

Introduction: The Venerable Bede, born around 672 C.E. was an early Medieval monk that spent his life in a monastery in Jarrow, Northumbria, England and is remembered today as one of the great figures of his age as an Anglo-Saxon theologian, historian and chronologist who is best known for his *Ecclesiastical history of the Anglo-Saxon people*, completed shortly before his death in 735 C.E. His chronology was translated from the original Medieval Latin by the Order of King Alfred the Great into Anglo-Saxon. The modern English text used for this abstract was translated by Sherrley-Price in 1955.[1]

In 731–732 C.E., Bede completed his *Historia ecclesiastica* and divided this lengthy work into five books. In the last book, written in his old age, he mentions three different cometary references. This poster will discuss the three comets that Bede includes in his chronicle.

Cometary References: In the month of August, 678, in the eighth year of Egfrids's reign, there appeared a star known as comet, which remained visible for three months, rising in the morning and emitting what seemed to be a tall column of bright beams.[2]

In the year 729, two comets appeared around the sun striking terror into all who saw them. One comet rose early and preceded the sun while the other followed the setting of the sun at evening, seeming to portend awful calamity to the east and west alike. Sine one comet was the precursor of the day and the other of the night, they indicated that mankind was menaced by evil at both times they appeared in the month of January and remained visible for about a fortnight, pointing their fiery torches northward.[3]

Research Support: Was supported by the Antarctic Institute of Canada. Dedicated to J. B. Hunter, C.M.

References: [1] Bede. 732. Translated Sherrley-Price 1955. *Ecclesiastical history of the English people*. Penguin: 1991, 224, 327. [2] Bede. 732. Translated Sherrley-Price. 1955. *Ecclesiastical history of the English people*. Penguin: 1991, 224. [3] Bede. 732. Translated Sherrley-Price. 1955. *Ecclesiastical history of the English people*. Penguin: 1991, 327.

5005

INVESTIGATING NOBLE GASES IN PRE-ANNEALED METEORITIC NANODIAMONDS

E. Marosits and U. Ott. Max-Planck-Institut für Chemie, Abteilung Geochemie, Becherweg 27, D-55128 Mainz, Germany. E-mail: marosits@mpch-mainz.mpg.de.

Introduction: Nanodiamonds are the most abundant among the noble gas-carrying presolar grains [1]. They have an almost solar ¹²C/¹³C ratio [2], but at the same time they also carry several characteristic noble gas components (~normal P3; anomalous HL and probably ~normal, minor P6) [3]. The observation that these are released at different temperatures when the grains are heated indicates that they could have different origins.

Experimental: We investigated the noble gas release of pre-annealed and chemically treated meteoritic nanodiamond samples. For this we isolated nanodiamonds from acid dissolution residues of the CM2 Murchison following the procedure of [4]. We annealed the diamonds in vacuum at different temperatures (600, 800, 1000 °C). This was followed by treatment of the annealed samples with perchloric acid for several days in an attempt to remove heating products (onions and amorphous carbon [5]). We measured the weight loss and the noble gases remaining in the samples.

Results and Discussion: Weight Loss: The weight loss due to heating followed by chemical treatment increased as expected with the heating temperature (600 °C: ~27%, 800 °C: ~38%, 1000 °C: ~52%).

Noble Gases: The release of Kr and Xe was measured for the treated samples in 3 pyrolysis steps, at 600 °C, 1000 °C, and 1800 °C. For comparison with the original sample we calculated the difference between the (heated + treated) samples and the gases remaining in the original sample after heating to the equivalent temperature only.

For the 600 °C pre-heated sample additional loss due to chemical treatment is in the range 15–18% both for Kr and Xe. This indicates that at least some of the noble gases are retained during transformation of diamond into onion/amorphous carbon, which can be (partially) removed by acid treatment [5]. While no distinction is found between the P3 and HL components in this respect for the sample pre-heated at 600 °C, the situation differs for the 1000 °C pre-heated sample; where P3 losses are more severe than those of HL.

A further noteworthy observation is that the concentration of Xe-HL is virtually identical in the original and all three annealed samples.

Acknowledgments: We thank S. Hermann for the noble gas measurements and Ch. Sudek for valuable help with the chemical treatment.

References: [1] Huss G. R. et al. 2003. *Geochimica et Cosmochimica Acta* 67:4823–4848. [2] Russel S. S. et al. 1996. *Meteoritics & Planetary Science* 31:343–355. [3] Huss G. R. and Lewis R. S. 1994. *Meteoritics* 29: 791–810. [4] Amari S. et al. 1994. *Geochimica et Cosmochimica Acta* 58: 459–470. [5] Marosits E. et al. 2008. Abstract #1252. 39th LPSC.

5195

AMINO ACID COMPOSITION OF PRIMITIVE CR2 CHONDRITES

Z. Martins¹, C. M. O'D. Alexander², G. E. Orzechowska³, J. E. Elsila⁴, D. P. Glavin⁴, J. P. Dworkin⁴, M. A. Sephton¹, and P. Ehrenfreund⁵. ¹Department of Earth Science and Engineering, Imperial College, London, UK. E-mail: z.martins@imperial.ac.uk. ²Department Terrestrial Magnetism, Carnegie Institution of Washington, Washington, D.C., USA. ³JPL, California Institute of Technology, Pasadena, CA, USA. ⁴NASA Goddard Space Flight Center, Greenbelt, MD, USA. ⁵Space Policy Institute, Elliott School of International Affairs, Washington, D.C., USA.

Introduction: It is thought that the soluble organic material of CR2 chondrites is more primitive than in any other chondrite and, therefore, closer to the original material accreted by chondrites [1]. Our present work focuses on the distribution and isotopic composition of amino acids present in primitive CR chondrites in order to provide important clues about the mechanisms of formation of these compounds, the conditions of the early solar system and the effect of parent body processing.

Methods: The amino acid contents of the Antarctic CR2s MET 00426, QUE 99177, EET 92062, and GRA 06100 were analyzed using an established amino acid procedure [1, 2]. In addition, compound-specific carbon isotopic measurements of individual α -amino acids present in the MET 00426 meteorite were achieved by gas chromatography-combustion-isotope ratio mass spectrometry (GC-C-IRMS). GC-C-IRMS measurements of the amino acid content of the QUE 99177, EET 92062, and GRA 06100 meteorites are currently being carried out.

Results: Our results show that the CR2 chondrites MET 00426 and QUE 99177 have amino acid abundances (185 and 80 ppm, respectively) and distributions that are similar to the ones previously detected in the CR2 EET 92042 and GRA 95229 [1]. The highly enriched $\delta^{13}\text{C}$ values (+4 to +32‰) of the α -amino acids present in the MET 00426, and the racemic amino acid enantiomeric ratios (D/L~1) for all the Antarctic CR2 chondrites, indicate that primitive indigenous organic matter is preserved in them.

Our data supports the hypothesis [1, 2] that the relative abundances (glycine = 1) of α -AIB and β -alanine depend on the degree of aqueous alteration in the CR parent body. In particular, the least aqueous altered CR2 chondrites MET 00426 and QUE 99177 [3, 4] have relative abundances of α -AIB that are higher than the mildly aqueous altered CR2s GRA 95229 and EET 92042, and much higher than the CR1 GRO 95577. On the other hand, the relative abundances of β -alanine are much lower (~0.1) in these four Antarctic CR2 chondrites than in the GRO 95577 meteorite (~0.9).

Conclusions: The high amino acid content observed in a variety of CR2 chondrites suggests that their soluble organic material is more primitive than any other chondrite. The analysis of the amino acid content of CR meteorites may help to reveal the processes that formed abundant prebiotic organic material in the early solar system. In particular, the relative amino acid abundances of α -AIB and β -alanine may be used to assess the degree of aqueous alteration.

References: [1] Martins Z. et al. 2007. *Meteoritics & Planetary Science* 42:2125–2136. [2] Glavin et al. 2006 *Meteoritics & Planetary Science* 41:889–902. [3] Abreu N. M. and Brearley A. J. 2005. *Meteoritics & Planetary Science* 40:A13. [4] Abreu N. M. and Brearley A. J. 2008. Abstract #1391. 39th LPSC.

5281

NITROGEN ISOTOPES IN THE RECENT SOLAR WIND: FURTHER ANALYSIS OF GOLD-PLATED CONCENTRATOR FRAME FROM GENESIS

B. Marty¹, L. Zimmermann¹, P. G. Burnard¹, D. L. Burnett², J. H. Allton³, R. C. Wiens⁴, V. S. Heber⁵, R. Wieler⁵, P. Bochsler⁶, S. Sestak⁶, and I. A. Franchi⁶. ¹CRPG, Nancy Université, CNRS, France. E-mail: bmarty@crpg.cnrs-nancy.fr. ²Department of Geological Sciences, California Institute of Technology, Pasadena, CA 91125, USA. ³Johnson Space Center, 2101 NASA Parkway, Houston, TX 77058, USA. ⁴Los Alamos National Laboratory, Space and Atmospheric Science, Los Alamos, NM 87544, USA. ⁵Isotope Geology and Mineral Resources, ETH Zürich, Switzerland. ⁶Planetary and Space Sciences Research Institute, Open University, Milton Keynes MK7 6AA, UK.

Introduction: Nitrogen, the fifth most abundant element in the universe, displays the largest (after H) stable isotope variations in the solar system materials (excluding pre-solar grains). Recently several studies concluded that protosolar nebula N was depleted by ~400%, from (i) the combined ion probe analysis of H and N isotopes in lunar soil grains ($\delta^{15}\text{N} \leq 240\%$, [1]), (ii) the analysis of the Jupiter atmosphere by either infrared spectroscopy [2] or in situ by the Galileo probe [3] and (iii) $\delta^{15}\text{N}$ of ~400‰ for osbornite (TiN) embedded in a CAI [4]. The Genesis mission sampled solar wind ions during 27 months in space by passive implantation of SW ions in targets made of pure material. Despite a hard landing of the sample capsule, target material could be recovered and analyzed. Nitrogen and helium, neon and argon were extracted under very high vacuum at CRPG Nancy, France, by UV laser (wl : 193 nm) ablation of targets with a spot size of $\sim 50 \times 150 \mu\text{m}$ rastered over surfaces up to 1 cm². The N extraction efficiency was checked with test targets implanted with known ¹⁵N fluence. Layers of gold could be removed sequentially by modulating the power of the laser beam or the number of pulses per area, with a depth resolution of a few nm. Noble gases abundances and isotopic ratios, analyzed together with N in each extraction step, were used as tracers of SW occurrence, of terrestrial contamination, and of elemental and isotopic fractionation. We have analyzed gold-over-sapphire target fragments and have focused recently our effort on target material exposed in the Genesis SW ion concentrator and more enriched in SW ions. Data obtained so far are heavily affected by terrestrial contamination. Nevertheless, we could not find evidence for a light N component in any of the samples analyzed so far and data point to a SW N isotope composition within the range of inner planetary and meteoritic values. We are in the process of analyzing another gold-plated fragment of the concentrator frame (the so-called "12 o'clock arm"), and results will be presented at the conference.

References: [1] Hashizume K. et al. 2000. *Science* 290:1142–1145. [2] Fouchet T. et al. 2000. *Icarus* 143:223–243. [3] Owen T. et al. 2001. *The Astrophysical Journal* 553:L77–L79. [4] Meibom A. et al. 2007. *The Astrophysical Journal* 656: L33–L36.

5183

A HERCYNITE-RICH INCLUSION IN THE VIGARANO CV3 CHONDRITE

S. Maruyama, T. Kunihiro, and E. Nakamura. The Pheasant Memorial Laboratory, Institute for the Study of the Earth's Interior, Okayama University, Japan. E-mail: maruyama@misasa.okayama-u.ac.jp.

An unusual hercynite-rich inclusion was found in the Vigarano CV3 chondrite. Pure and coarse-grained hercynite crystals occupy more than 50 vol% of the inclusion, and it contains small amount of melilite (1 vol%) and Mg-bearing spinel. Moreover, there is calcium monoaluminate CaAl_2O_4 , which has been found only in a refractory inclusion of a CH chondrite [1, 2], in the core of this inclusion. However, it consists of grossite, corundum, and perovskite, which are common in normal refractory inclusions. Therefore, it obviously has a close relationship with normal refractory inclusions.

The crystallization sequence of the hercynite-rich inclusion is consistent with equilibrium condensation sequence in the solar nebular gas, except for corundum. It is possible that corundum was produced by a reaction between grossite and FeO-bearing fluids during aqueous alteration on the parent body. The oxygen isotopic compositions of the minerals lie along the mass-dependent terrestrial fractionation line rather than the mass-independent fractionation line obtained from normal CAIs in carbonaceous chondrites. Hercynite and calcium monoaluminate is the lightest phases in this inclusion ($\delta^{17}\text{O} \sim -12\text{‰}$, $\delta^{18}\text{O} \sim -20\text{‰}$), heavier than spinels in normal refractory inclusions. The hercynite-rich inclusion is indicative of unusual nebular conditions where it formed.

References: [1] Ivanova M. A. et al. 2001. Abstract #1957. 32nd LPSC. [2] Ivanova M. A. et al. 2002. *Meteoritics & Planetary Science* 39: 1337–1344.

5082

SODIUM SOLUBILITY IN MOLTEN SYNTHETIC CHONDRULES

R. Mathieu¹, G. Libourel^{1, 2}, and E. Deloule¹. ¹CRPG-Nancy Université-INSU-CNRS, UPR2300, BP 20, 54501 Vandoeuvre-lès-Nancy, France. ²ENSG-Nancy Université, 54500 Vandoeuvre-lès-Nancy, France. E-mail: rmathieu@crpg.cnrs-nancy.fr.

The fact that alkali contents in chondrule mesostases vary by almost three orders of magnitude is still poorly understood [1, 2]. Variable degrees of evaporation, direct condensation from gaseous nebular environments [3] or low temperature alteration in the parent body are some of the possible explanations. In the lack of thermodynamic properties of alkali metals (mainly Na and K) in molten silicates, we have developed, to go further on chondrule formation, a new device that allows to measure the Na solubility in molten silicates under a known Na partial pressure (P_{Na}) at high temperature and fixed oxygen fugacity (P_{O_2}). Our method, mimicking condensation of Na into chondrule melts under nebular conditions, consists in equilibrating in a closed system at high temperature molten silicates with alkali vapor established by a $\text{Na}_2\text{O-xSiO}_2$ binary melt. The sodium evaporates from the source according to:



bathing the samples in alkali vapor, which dissolves in the molten silicate samples in agreement with:



At equilibrium conditions, the alkali metal oxide activity in molten samples is fixed by the source according to:



With the above design, sodium solubility have been investigated at 1400 °C and 1 atm total pressure in molten silicates belonging to the $\text{CaO-MgO-Al}_2\text{O}_3\text{-SiO}_2$ system (130 samples) and covering a large range of compositions ($0 < \text{CaO}$ and $\text{MgO} < 40$; $0 < \text{Al}_2\text{O}_3 < 45$; $0 < \text{SiO}_2 < 85$; in wt%) with bulk polymerization (NBO/T) varying from 0 to 3. Different $\text{Na}_2\text{O-xSiO}_2$ sources [4–6] were used to impose Na partial pressures in the range of 10^{-4} atm to 10^{-6} atm. At equilibrium, the solubility of sodium: S_{Na} ($\text{mole.g}^{-1}.\text{atm}^{-1}$) and the sodium oxide activity coefficient: $\gamma_{\text{NaO}_{1/2}}^{(\text{sample})}$ are calculated. From this set of experiments, it is possible to derive simple equations of Na solubility and sodium oxide activity coefficient as function of melt composition that shed light on how melt composition (and melt structure, i.e., Q species) controls sodium solubility in molten silicates. Applications to chondrule formation will be then discussed.

References: [1] Hewins et al. 2005. *Astronomical Society of the Pacific Conference Series*, vol. 341, pp. 286–317. [2] Grossmann and Alexander. 2008. Abstract #2084. 39th LPSC. [3] Georges P. et al. 2000. *Meteoritics & Planetary Science* 35:1183. [4] Yamagushi S. et al. 1983. *Journal of the Japanese Institute of Metals* 45:736.B. [5] Piacente V. and Matousek J. 1973. *Silikaty* 4:26. [6] Rego D. N. et al. 1988. *Metallurgical and Materials Transactions B* 19B:655.

5151

NOBLE GAS STUDY OF THE SARATOV CHONDRITE (L4)

J. Matsuda¹, H. Tsukamoto¹, C. Miyakawa¹, and S. Amari². ¹Department of Earth and Space Science, Graduate School of Science, Osaka University, Toyonaka, Osaka 560-0043, Japan. E-mail: matsuda@ess.sci.osaka-u.ac.jp. ²Laboratory for Space Sciences and the Physics Department, Washington University, St. Louis, MO 63130, USA.

Introduction: A noble gas component that is highly enriched in the heavy noble gases is carried by Q, which comprises a very small portion of primitive meteorites. Phase Q is most likely carbonaceous material, but a precise nature has not been determined. It has been known that Q and presolar diamond are closely associated. Although Q and presolar diamond, carrying Xe-HL, decrease with increasing petrologic subtype among L3 ordinary chondrites, Q is more resistant to thermal metamorphism than presolar diamond [1]. This implies that Q becomes more abundant relative to diamond in meteorites of higher petrologic type, allowing us to analyze Q gases in detail. Here we report high-precision noble gas data of bulk and an HF-HCl residue of the Saratov chondrite (L4).

Sample and Experimental: We prepared an HF-HCl residue using a chemical procedure commonly used to concentrate Q. The HF-HCl residue comprises 0.76% of the bulk meteorite. Elemental and isotopic abundances of the noble gases in the HF-HCl residue and bulk Saratov were measured with the VG5400 sector-type mass spectrometer at Osaka University, using stepwise heating at 600, 800, 1000, 1200, 1400, and 1600 °C.

Results and Discussion: Argon, Kr, and Xe concentrations in the HF-HCl residue are two orders of magnitude higher than those in the bulk sample, while He and Ne concentrations are comparable in both samples. However, the residue contains only portions of the heavy noble gases in meteorites; 38% for Ar, 58% for Kr, and 48% for Xe. A substantial portion of the heavy noble gases in meteorites may reside in minerals dissolved with HF and/or HCl. It has also been observed that HF-HCl residues from LL chondrites contain just portions of bulk meteorites [2].

Argon, Kr, and Xe concentrations in the HF-HCl residue are low compared with those of L3 ordinary chondrites [1], suggesting that Q gases were partially lost during thermal metamorphism. Helium and Ne in the bulk Saratov are mainly of cosmogenic origin.

Xenon isotopic ratios of the HF-HCl residue indicate that there is no HL component in Saratov. Neon isotopic ratios in the HF-HCl residue show an interesting feature; all data points in a Ne three-isotope plot lie on a straight line connecting the cosmogenic component and a composition between Ne-Q and Ne-A2 (²⁰Ne/²²Ne = 9.6). This may indicate that Ne isotopic composition of Q has been altered by thermal metamorphism. Neon isotopic compositions that are slightly different from those observed in carbonaceous chondrites are also seen in the residues of Julesburg (L3.6) and Abee (EH4) [1]. Huss et al. [1] discussed the possibility that Q acquired Ne from presolar diamond during thermal metamorphism. However, no correlation between Ne isotopic ratios and metamorphic grade was observed in the residues analyzed with closed-system stepped etching technique [3]. Further investigation is needed.

References: [1] Huss G. R. et al. 1996. *Geochimica et Cosmochimica Acta* 60:3311–3340. [2] Alaerts L. et al. 1979. *Geochimica et Cosmochimica Acta* 43:1399–1415. [3] Busemann H. et al. 2000. *Meteoritics & Planetary Science* 35:949–973.

5154

NOBLE GAS STUDY OF UNGROUPED ACHONDRITE GRA 06129

S. Matsuda¹, D. Nakashima¹, T. Mikouchi², and K. Nagao¹. ¹Laboratory for Earthquake Chemistry, University of Tokyo, Bunkyo-ku, Tokyo 113-0033, Japan. E-mail: matsuda@eqchem.s.u-tokyo.ac.jp. ²Department of Earth and Planetary Science, University of Tokyo, Bunkyo-ku, Tokyo 113-0033, Japan.

Introduction: GRA 06128 and 06129 paired achondrites display an unusual mineralogical feature distinct from any known meteorites. They are characterized by a high abundance of Na-rich plagioclase [1]. Zeigler et al. [1] suggest that the two meteorites are chemically similar to brachinites. We measured noble gases in GRA 06129 by total melting and stepwise heating to understand the formation history of this meteorite and to compare the noble gas compositions with those in brachinites.

Results and Discussion: The samples show high ⁴⁰Ar/³⁶Ar ratios ~10,000 and high concentrations of ⁴⁰Ar ($1.7\text{--}2.0 \times 10^{-4}$ cm³STP/g. K-Ar ages are estimated as 4.3–4.5 Ga from the ⁴⁰Ar concentrations and K content of 0.25 wt% [2]. Interestingly, the high ⁴⁰Ar/³⁶Ar ratios and high concentrations of ⁴⁰Ar are observed constantly in the 1000, 1300, and 1800 °C fractions, although radiogenic ⁴⁰Ar in most meteorites is generally released at low temperatures (<1000 °C). Kr isotopic compositions show excesses of ^{80,82}Kr derived from neutron capture on ^{79,81}Br, in addition to spallogenic Kr and atmospheric contamination. Moreover, isotopic ratios of Xe exhibit ¹²⁹Xe excess. Thus, Kr and Xe isotopic ratios are indicative of the presence of volatile elements such as Br and I, consistent with the petrologic observation [2]. Detection of ¹²⁹Xe excess (2.2×10^{-11} cm³STP/g) suggests early formation of GRA 06129 before ¹²⁹I extinction.

Like GRA 06129, the two brachinites, Brachina and Eagles Nest, show ¹²⁹Xe excesses, however, the excesses are higher ($7.8\text{--}35 \times 10^{-11}$ cm³STP/g; [3, 4]) than that in GRA 06129. Brachinites contain Ar-rich trapped noble gases [3, 4]. On the other hand, trapped noble gases are not seen in GRA 06129.

He isotopic ratios appear to be mixtures of cosmogenic He and radiogenic ⁴He. Ne isotopic compositions are mostly cosmogenic, and demonstrate contribution of Ne produced via Na-spallation [5]. This is consistent with the results that the meteorite is composed mainly of Na-rich plagioclase [1]. Cosmic-ray exposure ages (T₃ and T₂₁) are calculated from concentrations of ³He ($4.0\text{--}6.9 \times 10^{-9}$ cm³STP/g and ²¹Ne ($7.8\text{--}8.2 \times 10^{-9}$ cm³STP/g. Production rates for ³He (1.5×10^{-8} cm³STP/g/Ma) and ²¹Ne (2.7×10^{-9} cm³STP/g/Ma) are calculated using the formulae for eucrites [6], the assumed average shielding parameter (²²Ne/²¹Ne = 1.11), and the chemical composition [2]. The ²¹Ne production rate from Na is included in the calculation using the production rate ratio P²¹_{Na}/P²¹_{Mg} = 0.67 [7]. T₃ and T₂₁ are estimated as 0.27–0.46 Ma and 2.9–3.0 Ma. The shorter T₃ than T₂₁ would be caused by ³He loss induced by solar heating.

References: [1] Zeigler R. A. et al. 2008. Abstract #2456. 39th LPSC. [2] Arai T. et al. 2008. Abstract #2465. 39th LPSC. [3] Ott U. et al. 1985. *Meteoritics* 20:69–78. [4] Swindle T. D. et al. 1998. *Meteoritics & Planetary Science* 33:31–48. [5] Vogel N. et al. 2004. *Meteoritics & Planetary Science* 39:767–778. [6] Eugster O. and Michel Th. 1995. *Geochimica et Cosmochimica Acta* 59:951–970. [7] Huneke T. C. et al. 1972. *Geochimica et Cosmochimica Acta* 36:269–301.

5007

MICROMETEORITE CONSTRAINTS ON THE SOURCES OF THE SPORADIC METEOROID CLOUD

M. Maurette. CSNSM, Bat.104, 91405 Orsay-Campus, France. E-mail: maurette@csnsm.in2p3.fr.

Introduction: Complex modelings allow characterizing the sporadic meteoroid background cloud from assemblages of data [1]. The comparison of Antarctic micrometeorites (AMMs) with particles from comet Wild 2 (W2s) returned by Stardust help supporting a recent “best-fit” model of this cloud [1].

Antarctica Micrometeorites: Their Relationships with Meteorites and W2s: Over 20,000 unmelted AMMs were first recovered from the blue ice fields of Cap-Pudhomme, in 4 size fractions (25–50 μm ; 50–100 μm ; 100–200 μm ; 400 μm), in which AMMs are very similar [2]. About 99% of them are related to the hydrous carbonaceous chondrites (HCCs). However, in AMMs, the pyroxene to olivine ratio (~ 1) is about 10 times larger and saponite (and not serpentine) is the dominant hydrous silicate. The least weathered collection of AMMs was made at Dome C, in central Antarctica [3]. It contains very friable AMMs looking like fluffy IDPs, which were destroyed in previous collects.

Enggrand et al. [4] next noted striking similarities between the sulfides (only preserved at Dome C), anhydrous silicates and refractory inclusions observed in both AMMs and W2s. We also reported strong evidence for saponite in W2s [5]. Consequently, about 99% of the AMMs with sizes $\geq 30 \mu\text{m}$ (mass $\geq 4 \times 10^{-8}$ g), would be cometary dust particles.

The Abrupt Drop of “Big” Asteroidal Meteoroids in the Ecliptic Plane: The best-fit model [1] indicates that “big” meteoroids are confined near the ecliptic plane and that the cumulative flux of meteoroids from asteroids drops down abruptly at about 10^{-5} g (see Figs. 5 and 8 in Ref. 1). Therefore, the remaining big meteoroids would originate from Jupiter family comets. This key conclusion is well supported by the “big” cometary AMMs. The finding that AMMs in the 25–50 μm size fraction are very similar to the larger ones [2] further suggests that the abrupt asteroidal drop might be shifted to $\sim 0.5 \times 10^{-8}$ g.

A Geometrical Correction for the Flat Surface Snow Detector at Dome C: In January 2002, ~ 500 AMMs with sizes $\geq 30 \mu\text{m}$ were recovered from 10 tons of snow at Dome C, which are equivalent to a flat surface detector of 100 m^2 , exposed for one year to the micrometeorite flux. This snow detector yielded an average value of the micrometeorite mass flux, $\Phi \sim 5300$ tons/y [3]. But most of the big meteoroids are concentrated in the ecliptic plane, and the snow flat detector spins around the tilted rotation axis of the Earth (obliquity, $\epsilon = 23.5^\circ$). Consequently, its efficiency of detection for the big micrometeorites is about $\sin \epsilon \sim 0.40$, and Φ has to be increased up to $\sim 13,000$ tons/yr. This value looks rather similar to the meteoroid mass flux near the Earth ($\sim 15,000$ tons/yr, see Ref. 1). However, a large fraction (at least 50%) of this incoming meteoroid flux is destroyed upon atmospheric entry. Therefore, the assessment of the meteoroid mass flux still poses problem.

References: [1] Dikarev V. et al. 2004. *Earth, Moon, and Planets* 95: 109–122. [2] Gounelle et al. 2005. *Meteoritics & Planetary Science* 40:917–932. [3] Duprat et al. 2006. *Meteoritics & Planetary Science* 40:A9. [4] Enggrand et al. 2007. Abstract #1668. 39th LPSC. [5] Maurette et al. 2007. *Geochimica et Cosmochimica Acta* 71: A639.

5107

“SPECTROLOGY” OF THE UNBRECCIATED EUCRITES: THE LINK BETWEEN PETROLOGY AND SPECTRA

R. G. Mayne¹, T. J. McCoy¹, J. M. Sunshine², and H. Y. McSween Jr.³.
¹Smithsonian Institution, Washington, D.C. 20560–0119, USA. ²University of Maryland, College Park, MD 20742, USA. ³University of Tennessee, Knoxville, TN 37996–1410, USA.

Introduction: The proposed connection between the howardite, eucrite, and diogenite meteorites (HEDs) and asteroid 4 Vesta is a primary reason that Vesta was chosen as a target for the Dawn mission. The instrumentation onboard will provide information about Vesta’s surface morphology and composition, providing a geologic context for the HEDs [1]. More importantly, Dawn should provide us with a better understanding of the processes that form a large, differentiated asteroid.

Mineralogical information from Dawn will be derived primarily from the VIR (visible-infrared) spectrometer [1]; however, this requires an understanding of the relationship between the spectra and petrology of basaltic to pyroxenitic meteorites. This study quantifies the petrologic information that can be extracted from the VISNIR (visible-near infrared) spectra (0.3–2.5 μm) of the unbrecciated eucrites by analyzing the spectra of petrologically well-characterized HEDs.

Linking Spectra and Petrology: VISNIR spectra were collected and then analyzed using the Modified Gaussian Model [2, 3]. The features in each spectrum (i.e., spectral contrast, band centers, widths, and strengths) were compared to detailed petrologic data collected earlier in this study to see if any relationship between the two could be established. Relative abundances of high and low-Ca pyroxene (HCP and LCP) were predicted to within 15% of the actual values and four primary spectral features that serve as petrologic indicators were identified:

1. Position of band 1 and band 2 centers, reflecting pyroxene composition and relative abundances of HCP and LCP [4, 5]. The basaltic eucrites have longer band centers than the cumulates, reflecting primarily their higher modal abundance of HCP.
2. The strength of the 1.2 μm band is directly related to the amount of Fe^{2+} in pyroxene and the modal abundance of HCP relative to LCP and not to the presence of plagioclase. The basaltic eucrites have both higher HCP contents and more Fe-rich pyroxenes relative to their cumulate counterparts and consequently have a stronger 1.2 μm band.
3. Strength of the 0.6 μm band. This can be attributed to Cr^{3+} in pyroxene, which is preserved in early-crystallizing, fast-cooling eucrites that have not undergone later high-degree metamorphic reequilibration.
4. Reduced spectral contrast is seen in eucrites with a higher modal abundance of metals and sulfides, as well as those with widespread fine-grained opaque minerals.

Implications: Information on not only the mineralogy, but also the magmatic history (e.g., fast-cooling versus slow-cooling, early crystallization from melt versus late, highly metamorphosed and equilibrated eucrites versus unequilibrated) can be obtained from the spectra of the unbrecciated eucrites. Therefore, the information returned by Dawn can be used to not only extract information about the mineralogy of the surface units, but also to map the processes that formed them.

References: [1] Russell C. T. et al. 2006. *Advances in Space Research* 38:2043–2048. [2] Sunshine J. M. et al. 1990. *Journal of Geophysical Research* 95:6955–6966. [3] Sunshine J. M. and Pieters C. M. 1993. *Journal of Geophysical Research* 98:9075–9087. [4] Adams J. B. 1974. *Journal of Geophysical Research* 79:4829–4836. [5] Burns R. G. 1993. In *Mineralogical applications of crystal field theory*.

5293

IRON OXIDES IN FERRAR DOLERITE WEATHERING PRODUCTS (MARTIAN SOIL ANALOGS)

A. C. McAdam¹, E. J. Hoffman², A. Coleman Jr.², T. G. Sharp¹, and R. P. Harvey³. ¹School of Earth and Space Exploration, Arizona State University, Tempe, AZ 85287, USA. E-mail: amcadam@asu.edu. ²Physics Department, Morgan State University, Baltimore, MD 21251, USA. E-mail: eugene.hoffman@morgan.edu. ³Department of Geological Sciences, Case Western Reserve University, 10900 Euclid Avenue, Cleveland, OH 44106, USA.

Introduction: The Ferrar Dolerite from the Antarctic serves as an analog to basaltic Martian crust [1]. The rock sample and dolerite-derived soils investigated here were collected near Lewis Cliff in the Transantarctic Mountains. One soil sample (Station A) has been previously described [2–4]; the magnetic properties of an Antarctic Ferrar rock sample from a different location have also been investigated [5].

Experimental: Samples of crushed parent rock and soils from Station A and Station B were sieved to <20 µm and subjected to X-ray diffraction (XRD) and ⁵⁷Fe Mössbauer spectroscopy (MS) at room temperature and at 12.5 K. XRD was performed with a Cu source, making Fe phases hard to detect.

Results and Discussion: As Table 1 shows, clay minerals in the soils are also present in the parent rock, possibly a result of deuteric alteration. Nanoparticulate oxides (MS sextets at 12.5 K), more prominent in the soils, apparently derive from clays (paramagnetic Fe³⁺ doublets), pyroxenes and other primary minerals. Another Ferrar Dolerite rock sample, by contrast, shows far less oxidative alteration [5].

Table 1. Results of powder diffractometry and MS at 12.5 K. The Mössbauer spectra at room temperature showed essentially no sextets, so 12.5 K spectra indicate nanoparticulate iron oxides.

	Parent rock	Station A	Station B
Minerals by XRD (wt% with ±5–10% uncertainty)			
Feldspar	44	19	37
Clay minerals (smectite, chlorite, illite)	19	15	30
Gypsum	0	34	6
Pyroxene	20	10	7
Quartz	8	2	8
Zeolites	8	5	9
Bassanite (CaSO ₄ × 0.5H ₂ O)	0	15	2
Amphibole	1	0	1
Oxidized phases by Mössbauer spectroscopy at 12.5 K			
% area in paramagnetic Fe ³⁺ doublets	61.3	55.8	44.4
% area in magnetic sextets	3.7	15.2	13.3
% area total, doublets + sextets	65.0	71.0	57.7

References: [1] Harvey R. P. 2001. Abstract #4012. Field Trip and Workshop on the Martian Highlands and Mojave Desert Analogs. [2] McAdam A. C. et al. 2003. Abstract #3203. 6th International Conference on Mars. [3] McAdam A. C. et al. 2004. Abstract #8050. 2nd Conference on Early Mars. [4] McAdam A. C. et al. 2005. Abstract #2041. 36th LPSC. [5] Chevrier V. et al. 2006. *Earth and Planetary Science Letters* 244:501–514.

5278

HOW DO HIGH-Ni IRONS FORM?

T. J. McCoy¹, C. M. Corrigan¹, J. Yang², and J. I. Goldstein². ¹Department of Mineral Sciences, Smithsonian Institution, Washington, D.C. 20560–0119, USA. ²University of Massachusetts, Amherst, MA 01003, USA.

Introduction: Iron meteorites preserve diverse chemical compositions and metallographic textures, reflecting igneous history and subsequent cooling. Four processes—condensation, oxidation, fractional crystallization, and impact—have been invoked to explain the range of iron meteorite compositions. We focus on the chemical fingerprint produced by these processes and how they interacted to form a range of high-Ni irons.

Processes: *Condensation:* Incomplete condensation could produce high-Ni metal (≤19 wt% Ni), which subsequently melts to form high-Ni cores. Enriched in Ni and refractory siderophiles, it is depleted in volatile siderophiles (Ga, Ge) [1].

Oxidation: Oxidation produces high-Ni concentrations, by converting Fe⁰ to oxidized iron [1], as well as depletions in readily-oxidized elements (e.g., W, Cr, P), probably by reaction between chondritic metal and water during heating and melting.

Fractional Crystallization: Fractional crystallization produces higher Ni irons and distinct compositional trends that can be modeled using experimental partition coefficients. [2]

Impact: Impact might produce partial melting or reduction of chondritic precursors [3, 4] during melting or devolatilization.

Products: High-Ni irons include a broad array of types:

Milton-South Byron Trio: Enriched in Ni, with moderate Ga and Ge concentrations, and depletions in W, Mo, Fe, and P, the composition primarily reflects oxidation rather than condensation, with evidence for fractional crystallization [5].

IVB-Tishomingo: The Ni-rich IVB irons (~16–18 wt% Ni) and Tishomingo (~33 wt% Ni) are depleted in volatile siderophiles and readily oxidized elements. Both likely formed via incomplete condensation followed by oxidation (more extensive in the case of Tishomingo) and fractional crystallization (particularly for the IVB irons) [6] on two separate parent bodies.

IVA: While incomplete condensation might explain the high-Ni (8–12 wt%) and volatile depletion, impact must have occurred during the formation of IVA irons [3, 7, 8]. [7, 8] explain a correlation between Ni and cooling rate through fractional crystallization of a core stripped of its mantle and devolatilized by impact. Localized devolatilization on the IVA parent body might also produce some ungrouped iron meteorites [9].

IAB: The highest-Ni irons (≤60 wt% Ni) occur in group IAB, where oxidation likely played a minimal role and impact must have played a significant role [4]. One must either invoke selective impact melting perhaps with crystal segregation [4] or fractional crystallization [10], although partitioning in complex C-P-S-rich melts is inadequately known to model such a process.

Conclusions: Recent work has increased our ability to fingerprint some of the processes in the formation of high-Ni irons (e.g., oxidation), although much remains to fully understand the roles of fractional crystallization and impact in IVA and IAB.

References: [1] Kelly and Larimer. 1977. *Geochimica et Cosmochimica Acta* 41:93. [2] Walker et al. 2008. *Geochimica et Cosmochimica Acta* 72:2198. [3] Wasson et al. 2006. *Geochimica et Cosmochimica Acta* 70:3149. [4] Choi et al. 1995. *Geochimica et Cosmochimica Acta* 59:593. [5] Reynolds et al. 2006. *Meteoritics & Planetary Science* 41:A147. [6] Corrigan et al. 2005. Abstract #2062. 36th LPSC. [7] Yang et al. 2007. *Nature* 446:888. [8] Yang et al. Forthcoming. *Geochimica et Cosmochimica Acta*. [9] McCoy et al. 2007. *Meteoritics & Planetary Science* 42:A102. [10] Kracher. 1982. *Geophysical Research Letters* 9:412.

5311

COMPLEX NANOSTRATIGRAPHY OF VOLCANIC SURFACE COATINGS ON APOLLO 15 GREEN PYROCLASTIC GLASS BEADS

D. S. McKay,¹ S. J. Wentworth², K. L. Thomas-Keptra², and S. J. Clemett².
¹NASA-Johnson Space Center, Houston, TX 77058, USA. E-mail: David.S.McKay@nasa.gov. ²ESC Group, Mail Code JE23, NASA-JSC, Houston, TX 77058, USA.

Introduction: The most common pyroclastic glasses in the Apollo collections are the Apollo 15 green and Apollo 17 orange (and black) beads formed as a result of fire-fountain eruptions during the same time period as most mare basalt volcanism. The green and orange/black mare-composition glass spherules have distinctive sublimate deposits formed from the eruptive vapor during cooling of the volcanic plumes. These surface coatings are in no way related to space-weathering rims on maturing lunar soil grains. Earlier SEM and chemical studies of the volcanic surface features [e.g., 1–3] demonstrated that both major types of pyroclastic glass have similar coatings comprised of submicrometer-scale “micromounds” and even tiny crystals of various soluble salts.

Purpose and Samples: We have begun a detailed new study of volcanic glass surface coatings in order to constrain the nature and distribution of the surface coatings, to help define the conditions and history of lunar pyroclastic volcanism, and characteristics of the deep lunar interior. Today's technology permits much higher resolution and higher precision investigations than were possible in the past. We are using high-resolution field-emission TEM (FE-TEM) and EDS X-ray mapping, along with field-emission SEM (FE-SEM) and EDS. Initial results reported here are for FE-TEM imaging and X-ray mapping of ultramicrotomed cross-sections normal to the surfaces of Apollo 15 green spherules we selected from our existing sample allocations. Studies of freshly opened pristine samples are also planned along with equivalent studies of the Apollo 17 orange/black glasses and, eventually, less common types of lunar pyroclastic glass.

Results and Summary: FE-TEM X-ray maps demonstrate that the green glasses have Si-deficient layered surface deposits, ~20–150 nm thick. Such layers have not been previously documented. These layers form a complex nanostratigraphy: the innermost layer typically consists of amorphous material rich in Fe and minor S while the outer layer seems to be primarily Fe (no detectable S). In places the innermost layer also contains significant Zn which appears to be partially correlated with S. It is clear that volcanic surface deposits are still present in the non-pristine samples (exposed to air ~30 years ago), and that they contain complex textures and chemistries. The documented layering is heterogeneous at the nanometer scale. The composition, stratigraphic sequence, and structure of the vapor-deposited nanolayers may contain information on the eruption sequence, the plume and deposit time-temperature regime, and the composition and source of the volatile species. Other phases, including euhedral individual crystals documented previously [1, 2], have not yet been identified; pristine samples never exposed to Houston air may be needed to find them.

References: [1] McKay et al. 1975. Proceedings, 4th LSC. pp. 225–238. [2] Clanton et al. 1978. Proceedings, 9th LSC. pp. 1945–1957. [3] Meyer et al. 1975. Proceedings, 6th LSC. pp. 1673–1699.

5149

ISOTOPIC COMPOSITIONS AND SYSTEMATICS OF EARLY SOLAR SYSTEM AND PRESOLAR MATERIALS: AN EVALUATION OF MATRIX EFFECTS AND MASS INTERFERENCES

S. J. McKibbin, J. N. Avila, T. R. Ireland, P. Holden, and H. St. C. O'Neill. Research School of Earth Sciences and Planetary Science Institute, Australian National University, Canberra ACT 0200, Australia. E-mails: seann.mckibbin@anu.edu.au; janaina.avila@anu.edu.au.

Introduction: The precision and accuracy of SIMS data is extremely dependent on the selection of suitable calibration standards. It is well recognised that SIMS analysis ideally requires standards that are compositionally and structurally similar to the analytical target (here referred to as matrix-matched) [1, 2], but it is common for this to go unaddressed. In order to analyse early solar system [3] and presolar materials using SHRIMP-RG, matrix-matched mineral standards have been used to monitor instrumental mass fractionation, determine elemental yields and delineate possible mass interferences.

Cr Isotopes in Silicates: Measurements of Cr isotopic ratios in mafic silicate minerals indicate that instrument-induced mass-fractionation is strongly dependent on the crystal lattice. Olivine-structure minerals return $^{53}\text{Cr}^+ / ^{52}\text{Cr}^+$ ratios that are typically fractionated by 10–30% in favor of the light isotope. Fractionation is even more pronounced in pyroxenes, with the $^{53}\text{Cr}^+ / ^{52}\text{Cr}^+$ 40–50% enriched in the light isotope.

Inter-element ratios such as $^{55}\text{Mn} / ^{52}\text{Cr}$ are invariably fractionated by many tens of percent during sputtering of olivine, and this is extremely dependent on the bulk major oxide matrix composition (Mg, Fe, and Ca content). Correction factors have been calculated by measurement of $^{55}\text{Mn} / ^{52}\text{Cr}^+$ in synthetic olivine [(Mg,Fe)₂SiO₄; Mg# ~60], high-Ca fayalite and low-Ca kirschsteinite [(Fe,Ca)₂SiO₄] using SIMS followed by LA-ICP-MS. The measured $^{55}\text{Mn} / ^{52}\text{Cr}^+$ decreases with decreasing Fe-content; for high-Ca fayalite the two techniques give similar results, but for olivine the SIMS ratio is 40% lower than the LA-ICP-MS result. Downhole ion yields also change during sputtering depending on matrix composition. Olivine gives increasing Cr⁺ and decreasing Mn⁺ within each spot over several minutes, resulting in decreasing $^{55}\text{Mn} / ^{52}\text{Cr}^+$ with time. High-Ca fayalite and low-Ca kirschsteinite show either no net change or the opposite trend. Notably, we have not observed any effect on the $^{53}\text{Cr}^+ / ^{52}\text{Cr}^+$ ratio due to Mg, Fe, and Ca content of olivine-structure minerals.

Ba Isotopes in Silicon Carbide: Experiments involving measurement of Ba isotopes in SiC grains indicate the presence of molecular interferences on all Ba isotopes. However, the interferences observed in SiC are not present in silicates, as evidenced by the analysis of several NIST glasses and USGS basaltic reference materials. Contributions from interferences are particularly large for ¹³⁴Ba and ¹³⁶Ba. SHRIMP RG was operated at mass resolving power of $m/\Delta m = 9000$ (at 1% peak), which was not enough to resolve the molecular interferences. These interferences were suppressed with the use of energy filtering which reduced the intensity of the secondary ion beam, resulting in isotope ratios with lower precision but improved accuracy.

References: [1] Shimizu N. and Hart S. R. 1987. *Annual Review of Earth and Planetary Sciences* 10:483–526. [2] Ireland T. R. 1995. *Advances in Analytical Geochemistry* 2:1–118. [3] McKibbin S. J. 2008. This issue.

5132

A NEW ION-PROBE DETERMINATION OF $^{53}\text{Mn}/^{55}\text{Mn}$ IN D'ORBIGNY AND SAHARA 99555 USING MATRIX-MATCHED STANDARDS

S. J. McKibbin, T. R. Ireland, Y. Amelin, H. St. C. O'Neill, and P. Holden. Research School of Earth Sciences, Australian National University, Australia. E-mail: seann.mckibbin@anu.edu.au.

Introduction: The developing chronology for the angrite meteorites shows that their parent body had a prolonged thermal history. New results show that the angrite meteorite series exhibit a spread of Pb-Pb ages as large as 7 Ma [1], but the time intervals measured with U-Pb do not match time intervals recorded by existing Mn-Cr ages [2]. When compared to Lewis Cliff 86010 (LEW), the older Pb-Pb ages of D'Orbigny and Sahara 99555 (SAH) imply that their $^{53}\text{Mn}/^{55}\text{Mn}$ ratio should be around 3.8×10^{-6} , but so far the highest reported value is only $3.24 \pm 0.04 \times 10^{-6}$ [3]. The discrepancy between these isotopic systems warrants investigation at the scale of mineral separates and, where possible, within individual crystals. We have determined new $^{53}\text{Mn}/^{55}\text{Mn}$ isochrons for the D'Orbigny and SAH meteorites using sensitive high-mass resolution ion micro-probe reverse geometry (SHRIMP-RG) which enables measurement of large surpluses of radiogenic ^{53}Cr ($^{53}\text{Cr}^*$) in major and accessory minerals and in crystal rims which have very low Cr concentrations.

Methods: $^{53}\text{Cr}/^{52}\text{Cr}$ and $^{55}\text{Mn}/^{52}\text{Cr}$ were measured in situ in olivine, high-Ca fayalite and low-Ca kirschsteinite in chips of D'Orbigny and SAH. Suitable areas $\sim 20 \mu\text{m}$ in diameter were sputtered using a 2 nA O^- primary ion beam, with mass resolution $m/\Delta m \sim 6000$ (10% peak height) to resolve molecular interferences. Three compositionally matched synthetic mineral standards were used to monitor instrumental mass-fractionation and to determine Mn-Cr relative sensitivity factors. This is necessary because the relative sensitivity for these elements changes considerably as a function of the bulk matrix composition [4].

Results: $^{53}\text{Cr}/^{52}\text{Cr}$ and $^{55}\text{Mn}/^{52}\text{Cr}$ are well correlated in Fe-Ca olivine, allowing isochrons to be calculated. Both D'Orbigny and SAH have $^{53}\text{Mn}/^{55}\text{Mn}$ of approximately 3.5×10^{-6} , accurate to about 10%. This value is higher than a previous ion probe determination [5] and one thermal ionization mass spectrometry study [TIMS; 6], but agrees with the TIMS result of [3].

Discussion: The discrepancy between our result and those of [5] is likely due to changes in ionization potential for Mn and Cr in different sputtered matrices. Understanding the effects of using a glass versus a mineral standard for determining relative sensitivity is crucial to interpreting ion-probe Mn-Cr ages and is being investigated.

The Mn-Cr age difference between formation of D'Orbigny and SAH on one hand, and LEW on the other, is about 5.5 Ma. This interval agrees with the highest previous TIMS determination of [3] and is close to the Pb-Pb age difference of 6 Ma [1]. The latter suggests that isotopic closure for both Cr and Pb diffusion occurred at nearly the same time within each sample.

References: [1] Amelin Y. and Irving A. J. 2007. Workshop on the Chronology of Meteorites and the Early Solar System. pp. 20–21. [2] Wadhwa M. et al. 2007. Workshop on the Chronology of Meteorites and the Early Solar System. pp. 173–174. [3] Glavin D. P. et al. 2004. *Meteoritics & Planetary Science* 39:693–700. [4] McKibbin S. J. et al. 2008. This issue. [5] Sugiura N. et al. 2005. *Earth, Planets and Space* 57:E13–E16. [6] Nyquist L. E. et al. 2003. Abstract #1388. 34th LPSC.

5329

EVOLUTION OF CHEMICAL AND ISOTOPIC COMPOSITIONS OF FORSTERITE-RICH MELTS DURING EVAPORATION

R. A. Mendybaev^{1,2}, F. M. Richter^{1,2}, R. B. Georg³, and A. M. Davis^{1,2,4}. ¹Chicago Center for Cosmochemistry, USA. ²Department of the Geophysical Sciences, USA. E-mail: ramendyb@uchicago.edu. ⁴Enrico Fermi Institute, University of Chicago. USA. ³Department of Earth Sciences, University of Oxford, UK.

Introduction: The CAIs Vigarano 1623-5 and Allende C1 are the FUN inclusions that are most enriched in heavy Mg and Si, with $\delta^{25}\text{Mg}$ and $\delta^{30}\text{Si}$ reaching $\sim 31\%$ and $\sim 14\%$ [1] and have identical nucleosynthetic isotope anomalies in many elements [2]. On the other hand, mineral and chemical compositions of these two inclusions are distinctly different: Vig1623-5 is forsterite-rich and contains $\sim 35 \text{ wt}\%$ MgO and SiO_2 , while chemical and mineralogical compositions of C1 is indistinguishable from regular Type B CAIs. Recently we reproduced chemical and Mg-isotopic compositions of Vig1623-5 by evaporating essentially forsteritic melt (FUN1, forsterite plus $\sim 3 \text{ wt}\%$ Al_2O_3 and $\sim 2.5 \text{ wt}\%$ CaO) in a vacuum at $1900 \text{ }^\circ\text{C}$ [3]. We present here results of new experiments in which evaporation of forsterite-enriched melt resulted in the residuals with their chemical composition close to that of C1. We also expect that the enrichment factors of heavy Mg and Si-isotopes in these residuals to be close to those observed in C1.

Results and Discussion: Experimental conditions and protocol used in this study were the same as in [3]. As a starting material (FUN2) we used a composition close to that of Vig1623-5. Similar to the experiments with FUN1 melt, evaporation of FUN2 at $1900 \text{ }^\circ\text{C}$ in vacuum resulted in a loss of MgO and SiO_2 with essentially the same rates ($\sim 4 \times 10^{-2} \text{ mg min}^{-1} \text{ mm}^{-2}$) as from FUN1, despite substantially different compositions of FUN1 and FUN2. As a result of the same evaporation kinetics, the evaporation trajectory of FUN2 in a SiO_2 versus MgO plot forms a continuous trend established by evaporation of FUN1 which extends toward the compositions of normal Type B CAIs. Evaporation kinetics and composition of evaporation residues suggest that the weight loss in both cases is due to the evaporation of Mg_2SiO_4 which is the dominant component of both starting materials. The residues from 30–35 minute-long evaporations of FUN2 contain $\sim 11\text{--}13 \text{ wt}\%$ MgO (fraction of Mg lost, F_{Mg} , is $\sim 80\text{--}85\%$) and $25\text{--}27 \text{ wt}\%$ SiO_2 ($F_{\text{Si}} \sim 65\text{--}70\%$) which is typical for Type B CAIs. Corresponding to these F_{Mg} and F_{Si} , $\delta^{25}\text{Mg}$ and $\delta^{29}\text{Si}$ values of these residues are expected to be within the range of $26.5\text{--}32\%$ and $8.5\text{--}12.5\%$, respectively. These estimates are based on our previously determined values of $\alpha_{\text{Mg}} = 0.9861$ and $\alpha_{\text{Si}} = 0.9900$ for CAIB melt [4] and $\alpha_{\text{Mg}} = 0.9838$ and $\alpha_{\text{Si}} = 0.9925$ for molten Mg_2SiO_4 [5]. These estimated values of $\delta^{25}\text{Mg}$ and $\delta^{29}\text{Si}$ are close to $\delta^{25}\text{Mg} = 30\%$ and $\delta^{29}\text{Si} = 14\%$ measured in C1 FUN CAI. The measured Mg- and Si-isotopic compositions of the residues will be presented during the meeting.

The results presented above allow us to suggest that both forsterite-rich and “normal” FUN CAIs could have been formed by high temperature evaporation of forsterite-bearing precursors.

References: [1] Clayton R. N. et al. 1988. *Philosophical Transactions of the Royal Society of London A* 325:483–501. [2] Loss R. D. et al. 1994. *The Astrophysical Journal* 436:L193. [3] Mendybaev R. A. et al. 2008. Abstract #2345. 39th LPSC. [4] Richter et al. 2007. *Geochimica et Cosmochimica Acta* 71:5544. [5] Davis et al. 1990. *Nature* 347:655.

5308

OXYGEN ISOTOPIC COMPOSITIONS OF WILD 2 SILICATES

S. Messenger¹, M. Ito¹, D. J. Joswiak², L. P. Keller¹, R. M. Stroud³, K. Nakamura-Messenger^{1,4}, G. Matrajt², and D. E. Brownlee². ¹Robert M. Walker Laboratory for Space Science, ARES, NASA/JSC, Houston, TX, USA. E-mail: scott.r.messenger@nasa.gov. ²University of Washington, Department of Astronomy, Seattle, WA, USA. ³Materials Science and Technology Division, Naval Research Laboratory, Code 6366, 4555 Overlook Avenue SW, Washington D.C., USA. ⁴ESCG, NASA/JSC Houston, TX, USA.

Introduction: Comet 81P/Wild 2 Stardust samples have both similarities and differences with carbonaceous chondrite meteorites and anhydrous interplanetary dust particles. Oxygen isotopic measurements show that presolar grains are present but rare, that the average composition is near terrestrial values, and that CAIs are present [1]. These results indicate that much of cometary material formed at high T and cycled over vast distances early in solar system history. In order to elucidate the relationships between cometary and meteoritic components we are pursuing a systematic coordinated mineralogical and isotopic study of Stardust samples. Here we report O isotopic measurement of silicate minerals from 4 tracks. The samples were embedded in epoxy or acrylic and 70 nm thick sections were obtained for TEM investigation. Following the TEM study, the samples were analyzed for O isotopic compositions by isotopic imaging with the JSC NanoSIMS 50L ion microprobe.

Results: The samples included an 8 μm forsterite (Fo_{98}) terminal particle (C2067 Track 112,1), a 1 μm forsterite (Fo_{98}) grain from track 10,84 (Arrina), and two 1 μm enstatite grains (Track 80,1,6, Tule) and (Track Fc 13b,1). Adjacent sections of the latter enstatite grain contained organic materials and are enriched in D/H [1, 2]. The small forsterite and enstatite grains had terrestrial O isotopic compositions within error ($\delta^{17}\text{O} = 10 \pm 11$, $\delta^{18}\text{O} = -9 \pm 5$; $\delta^{17}\text{O} = -16 \pm 18$, $\delta^{18}\text{O} = 0 \pm 5$; $\delta^{17}\text{O} = 16 \pm 12$, $\delta^{18}\text{O} = 13 \pm 8$, 1σ), respectively. These values are similar to values we previously found for enstatite, fayalite, and tridymite grains from tracks Ada and Febo [3]. In contrast, forsterite grain T112,1 was significantly ¹⁶O-rich ($\delta^{17}\text{O} = -65 \pm 4$, $\delta^{18}\text{O} = -59 \pm 3$). Isotopic images of T112,1 have homogeneous O isotopic composition.

Discussion: O isotopic compositions of Wild 2 samples are generally near terrestrial values. Notable exceptions are the CAI-like particle Inti ($\delta^{17}\text{O} = \delta^{18}\text{O} = -40\%$) [1] and a fine-grained olivine/pyroxene particle Gozen-Sama whose O isotopic composition is heterogeneous and falls along the CCAM line with $\delta^{17}\text{O}$ and $\delta^{18}\text{O}$ values ranging from ~ 0 to -45% [4]. T112,1 is somewhat more ¹⁶O-rich in comparison with these samples, falling near the endpoint of the CCAM trend line. The isotopic, mineralogical, and chemical compositions of T112,1 are similar to components of some AOAs and a unique chondrule [5, 6]. The large ¹⁶O enrichment and Mg-rich composition is consistent with this grain having condensed from a high T gas, possibly together with refractory inclusions in meteorites.

References: [1] McKeegan K. D. et al. 2006 *Science* 314:1724. [2] Sanford S. A. et al. 2006. *Science* 314:1720. [3] Matrajt G. et al. 2006. *Meteoritics & Planetary Science* 43:1. [4] Nakamura T. et al. 2008. Abstract #1695. 39th LPSC. [5] Imai H. and Yurimoto H. 2003. *Geochimica et Cosmochimica Acta* 67:765. [6] Kobayashi S. et al. 2003. *Geochemical Journal* 37:663.

5060

GROVE MOUNTAINS (GRV) 052382—LIKELY A MOST HEAVILY SHOCKED UREILITE

B. Miao^{1,2}, Y. Lin², D. Wang³, S. Hu², W. Shen², X. Wang¹. ¹Key Laboratory of Geological Engineering Center of Guangxi Province, Guilin University of Technology, Guilin 541004, China. E-mail: miaobk@glute.edu.cn. ²Key Laboratory of the Earth's Deep Interior, Institute of Geology and Geophysics, CAS, Beijing, China. ³Guangzhou Institute of Geochemistry, CAS, China.

Introduction: Ureilites are achondrites featured by abundant carbon polymorphs [1]. They share igneous and primitive features, then igneous cumulates [2] and partial melting [3] models were proposed. The common occurrence of diamond is consistent with shock-induced melting [4]. However, most of ureilites exhibit weak shock-induced features [1]. Recently, 6 new samples of ureilites were found from GRV meteorite collection [5], and one of them, GRV 052382, was very heavily shocked. Here we report petrography and mineralogical chemistry of GRV 052382, which may shed light on petrogenesis of ureilites.

Petrology: GRV 052382 is a monomict ureilite (1.86 g) found in a moraine in Grove Mountains, Antarctica. It consists mainly of olivine (75 vol%), pigeonite (5 vol%), and carbonaceous matrix (20 vol%). Outlines of the original coarse-grained olivine (0.5–1.5 mm) are preserved, but the interiors were converted to fine-grained assemblages, consisting predominantly of small euhedral grains of olivine (10–20 μm) with minor interstitial glass. Compositions of the small euhedral grains of olivine probably inherited from the previous grains, with the Fa-contents decreasing from 21.8 mol% at the interiors to 12.2 mol% along the margins of the assemblages. Pigeonite (0.4–0.9 mm) is rounded in shapes, and show patch-like compositional heterogeneity ($\text{En}_{76.4-82.6}\text{Wo}_{4.6-9.8}\text{Fs}_{10.9-13.8}$), probably suggestive of decomposition. The carbonaceous matrix is composed of fine-grained MgO-rich silicates and various carbon polymorphs, including irregular-shaped graphite (0.2–0.4 mm) and diamond (1–3 μm). Small grains of Ni-poor metal (probably produced by reduction of Fe,Mg-silicates) are common, and those along the reduction zone of olivine contain high Si content (5.02–6.43 wt%). This is one of highest Si contents of Fe-Ni metal reported in meteorites.

Discussion: The recrystallization texture of olivine indicates that GRV 052382 experienced a very strong shock event, with a shock stage analogue to S6 of ordinary chondrites [6]. This is probably a most severely shocked ureilite. The shock event postdated crystallization of the meteorite from a melt and the reduction reaction, because the secondary olivine inherits the zoning feature of the previous large grains. In addition, the zoning features suggest that the secondary olivine was not crystallized from melts, although there is glass interstitial to the secondary olivine.

Acknowledgements: The sample was supplied by the Polar Research Institute of China. This study was supported by the Knowledge Innovation Program (kzcx2-yw-110) of the Chinese Academy of Sciences, and the National Natural Science Foundation of China (no. 40673055 and 40473037).

References: [1] Goodrich C. A. 1992. *Meteoritics* 27:327–353. [2] Berkley J. L. et al. 1980. *Geochimica et Cosmochimica Acta* 44:1579–1597. [3] Singletary S. J. and Grove T. L. 2003. *Meteoritics & Planetary Science* 38:95–108. [4] Bischoff A. et al. 1999. Abstract #1100. 30th LPSC. [5] Miao B. et al. 2008. *Progress in Natural Science* 18:431–439. [6] Stöffler D. et al. 1991. *Geochimica et Cosmochimica Acta* 55:3845–3867.

5012

DISTRIBUTIONS OF THE TERRESTRIAL METEORITE CRATERS: A REVIEW

K. Mihályi¹ and A. Gucsik^{2, 3}. ¹University of Debrecen, Department of Physical Geography and Geoinformatics, H-4010 Debrecen, Hungary, Pb. 9. E-mail: k.mihalyi@freemail.hu. ²Max Planck Institute for Chemistry, Department of Geochemistry, Joh.-J.-Becherweg 27, Mainz D-55128, Germany. ³Department of Physical Geography, Savaria University Center, H-9700 Szombathely, Károlyi Gáspár tér 4, Hungary.

Based on Earth Impact Database (2008) [1] data, 174 confirmed impact craters are known on Earth currently. They are situated randomly at different surfaces—leastwise for the first sight, but after particular investigations it can be recognized that the impact structures are concentrated on older surfaces and became relatively rare on younger ones. In the case of the Earth's surface this distribution is complicated by the effects of wide range of erosion types and endogenic processes (e.g., metamorphism, tectonic movements, magmatic infillings, etc.). But even here, it can be recognized, that the largest meteorite crater density and the oldest forms can be found on the old cratons (shields) of North Europe, North America and Australia. In the first two cases (North Europe, and North America), probably because of the ice-dominated exhumation under the last ice age (pleistocene): the covering sediment layers and the sedimentary infillings of the crater basins were removed by moving ice. Impact craters in these two regions were formed before the pleistocene and they are relatively small (most of them under 20 km in diameter). Impact craters became rare in the tropical regions because of the rich vegetation cover and the fast landscape destruction. Ocean floors are other poorly cratered regions. In depths of thousands of meters, smaller meteorites or asteroids can't impact into the floor-surface because of the drag of the water. Other reasons: the young ages of the seafloors (not older than 200 million years), according to the plate tectonics; the rapid sedimentation and the relatively poorly explored topography of ocean basins. There is a third region too, where meteorite craters are missing: these are the inland ice sheets and the Antarctica: on the relatively young, moving, melting-refreezing and rapid-changing ice surfaces, where impact craters were deformed and eroded rapidly [2].

Distribution graphs and diagrams can divide the continents into two groups [2, 3]: North-America (especially for the Canadian-shield) and Europe (Baltic-shield) are in one group, as pleistocene glaciated continents. The other group of continents consists of Africa, Asia, South America and Australia, as pleistocene unglaciated continents. These two groups can be identified by distributions by diameters as well as distributions by age, at the different levels of diameter ranges and age intervals (eras, eons, epochs). The graphs and diagrams suggest some further questions: is there any crater exhumation on the rock surfaces, under recent ice masses? Can any impact signs be recognized on the surfaces of ice masses?

References: [1] Earth Impact Database (EID) website: <http://www.unb.ca/passc/ImpactDatabase/index.html>. [2] Mihályi K. 2007. Mater's thesis, University of Debrecen, Department of Physical Geography and Geoinformatics. [3] Mihályi K. Forthcoming. Hydrogeological features of terrestrial meteorite craters. *Acta Geographica Debrecina*.

5181

PETROGENESIS AND CRYSTALLIZATION HISTORY OF QUENCHED ANGRITES

T. Mikouchi¹, G. McKay², and J. Jones². ¹Department of Earth and Planetary Science, University of Tokyo, Hongo, Tokyo 113-0033, Japan. E-mail: mikouchi@eps.s.u-tokyo.ac.jp. ²Mail Code KR, NASA Johnson Space Center, Houston, TX 77058, USA.

Introduction: Angrites constitute an enigmatic achondrite group characterized by unique mineralogies and old crystallization ages [e.g., 1]. By distinct textures, they can be divided into two subgroups, “quenched” and “slowly cooled” samples. Because Mn-Cr chronology shows that quenched samples are ~5 Ma older than slowly-cooled ones [e.g., 2], quenched samples possibly represent primary igneous activity on the angrite parent body.

Petrogenesis: Quenched angrites show fine-grained ophitic to porphyritic textures, but some samples contain large (reaching several mm) olivine xenocrysts out of Fe/Mg equilibrium with the Fe-rich groundmass. There are strong correlations among major element contents in quenched angrites that can be well explained by olivine control [3]. Because olivine xenocrysts are absent or rare in Sahara 99555, D'Orbigny and NWA 1296, their bulk compositions may represent an angrite magma composition that is not contaminated by the xenocryst component. In fact, their bulk compositions are nearly identical [4, 5]. These compositions are close to experimental partial melts of Allende CV3 chondrite at 1200 °C and $\log f_{O_2} = IW + 1 \sim 2$ [6]. At this condition, the degree of partial melting is ~15% and the solid residua are dominated by olivine. The calculated calcium and REE abundances of 15~20% partial melting of Allende match with those of Sahara 99555 and D'Orbigny.

Crystallization: The Fe-Mg and Ca chemical zoning of olivine xenocrysts adjacent to the groundmass is useful to estimate cooling rates of quenched angrites. The cooling rate calculation of xenocryst-bearing quenched angrites gave 7–13 °C/hr [7]. The crystallization experiments using the Asuka-881371 groundmass composition with ~1 mm fragments of San Carlos olivine (Fo₈₉) well reproduced textures and mineral compositions of quenched angrites when cooled at 10–50 °C/hr [7], which is consistent with the result of the cooling rate calculation. Thus, quenched angrites formed by rapid cooling of magmas entraining magnesian olivine xenocrysts of locally different abundances. Minor differences in groundmass compositions may be attributed to locally different melt compositions in the same magma due to different degrees of dissolved olivine xenocryst component.

Conclusions: A possible parent melt composition for quenched angrites could be derived from the partial melts of carbonaceous chondrites. Then, these melts experienced rapid cooling, forming quenched angrites with addition of olivine xenocrysts in some samples.

References: [1] Mittlefehldt D. W. et al. 1998. *Reviews in Mineralogy*, vol. 36. pp. 4–131. [2] Shukolyukov A. and Lugmair G. W. 2008. Abstract #2094. 39th LPSC. [3] Mikouchi T. et al. 2004. Abstract #1504. 35th LPSC. [4] Mittlefehldt D. W. et al. 2002. *Meteoritics & Planetary Science* 37:345–369. [5] Jambon A. et al. 2005. *Meteoritics & Planetary Science* 40:361–375. [6] Jurewicz A. J. G. et al. 1993. *Geochimica et Cosmochimica Acta* 57: 2123–2139. [7] Mikouchi T. et al. 2001. *Meteoritics & Planetary Science* 36: A134–A135.

5260

MARTIAN METASOMATIC AND/OR ALTERATION COMPONENTS PRESERVED IN MASKELYNITIZED PLAGIOCLASE IN SHERGOTTITES?

K. Misawa¹, J. Park², C.-Y. Shih³, Y. Reese⁴, D. D. Bogard², and L. E. Nyquist². ¹Antarctic Meteorite Research Center, NIPR, Tokyo 173-8515, Japan. E-mail: misawa@nipr.ac.jp. ²NASA-JSC, Houston, TX 77058, USA. ³ESCG/Jacobs Sverdrup, Houston, TX 77058, USA. ⁴ESCG/Muñiz Engineering, Houston, TX 77058, USA.

Introduction: Because of the key role of plagioclase in Rb-Sr isotopic systematics of shergottites, it is important to understand the mobility of alkali and alkaline earth elements in plagioclase during metasomatism and alteration on the Martian surface. In the context of impact melt glass veins, it is suggested that enrichments of plagiophile elements (aluminum, calcium and sodium) and sulfur in EET 79001 Lithology C are due to mixing of plagioclase with a Martian soil component [1].

Results and Discussion: During the course of isotopic studies of Yamato 00 lherzolitic shergottites, a large enrichment of strontium, 346 ppm, was observed in the acid-washed plagioclase sample, Plag(r)_{Y000097} [2]. The strontium isotopic composition of Plag(r)_{Y000097} is comparatively radiogenic, with the result that the data point deviates upward from the Rb-Sr isochron. The strontium content of maskelynitized plagioclase in GRV 99027 determined by ion microprobe is 136 ppm [3], which is comparable to that of acid-leached plagioclase fractions from Y-793605, ALH 77005, and LEW 88516 [4, 5]. Adhering phase(s), phosphates and/or impact melt, with maskelynitized plagioclase is a possible cause of the strontium enrichment observed in Plag(r)_{Y000097}. The strontium concentration of GRV 99027 merrillite measured by ion microprobe is ~150 ppm [3] and is comparable to that of maskelynitized plagioclase in other lherzolitic shergottites. The samarium and neodymium concentrations of Plag(r)_{Y000097} are not much different from those of plagioclase in ALH 77005 and LEW 88516 [2, 5]. This fact suggests that the Plag(r)_{Y000097} fraction does not contain REE-rich phases such as impact-melt glasses or phosphates. One of the possible interpretations of the strontium enrichment is that a more evolved component in metasomatic fluids or in secondary alteration products such as Ca-sulfates with very high strontium abundance may have been added and/or adsorbed onto plagioclase either prior to or during impact on the Martian surface. Owing to intense shock loading, plagioclase plus extraneous phases may have become compacted and transformed into maskelynite. If this is the case, we can expect an enrichment of barium in maskelynitized plagioclase in Y-000097.

The strontium-rich component may not necessarily involve Martian atmospheric noble gases; there is little to no evidence for Martian atmospheric ⁴⁰Ar, krypton, or xenon in Y-000097 [2, 6], whereas a whole-rock sample of ALH 77005 contains shock-implanted ⁴⁰Ar from the Martian atmosphere [7].

References: [1] Rao M. N. et al. 1999. *Geophysical Research Letters* 26:3265–3268. [2] Misawa K. et al. Forthcoming. *Polar Science*. [3] Lin Y. et al. 2005. *Meteoritics & Planetary Science* 40:1599–1619. [4] Morikawa N. et al. 2001. *Antarctic Meteorite Research* 14:47–60. [5] Borg L. E. et al. 2001. *Geochimica et Cosmochimica Acta* 66:2037–2053. [6] Nagao K. et al. Forthcoming. *Polar Science*. [7] Bogard D. D. and Garrison D. H. 1999. *Meteoritics & Planetary Science* 34:451–473.

5072

Fe-Ni AND Al-Mg ISOTOPE SYSTEMATICS IN CHONDRULES FROM SEMARKONA (LL3.0) AND LEW 86314 (L3.0)

R. K. Mishra and J. N. Goswami. Physical Research Laboratory, Ahmedabad 380009, India. E-mail: ritesh@prl.res.in.

Introduction: The short-lived nuclide ⁶⁰Fe is an unique product of stellar nucleosynthesis. A robust value for the initial abundance of ⁶⁰Fe in the solar system allows us to infer its possible stellar source and contribution from this source to the inventory of the other co-injected short-lived nuclides. The lack of Fe-rich phases in CAIs led to studies of sulfide in UOC matrix and both sulfide and silicates in UOC chondrule to infer initial ⁶⁰Fe/⁵⁶Fe at the time of their formation [1–3]. Based on an independent estimate of the time of formation of the chondrules, relative to CAIs, from a study of ²⁶Al records, one can infer the solar system initial ⁶⁰Fe/⁵⁶Fe. However, such an approach will not work if the recent suggestion [4] that injection of ²⁶Al preceded that of ⁶⁰Fe (from the same stellar source) by more than a million year is valid. We have initiated a combined study of Al-Mg and Fe-Ni isotope systematics in a set of UOC chondrules to address these issues.

Samples: The analyzed chondrules are from two UOCs, Semarkona (LL3.0) and LEW 86314 (L3.0), belonging to the lowest petrologic grade. We have selected five chondrules, three from Semarkona and two from LEW 86314, for this study; data for ²⁶Al in three of these chondrules have been reported earlier [5, 6]. The Al-Mg and Fe-Ni isotope systematics in these chondrules were studied using a Cameca ims-4f ion microprobe following procedures described earlier [5, 7]. Data from multiple analyses on a given spot were combined, as long as the Al/Mg and Fe/Ni ratios are nearly the same, to improve precision of the measured isotope ratios.

Results and Discussion: The data for four chondrules yielded initial ⁶⁰Fe/⁵⁶Fe ratios ranging from $\sim 5 \times 10^{-7}$ to 3.8×10^{-7} ; the corresponding range of initial ²⁶Al/²⁷Al is $\sim 1.6 \times 10^{-5}$ to 1.1×10^{-5} . The Al-Mg isotope data were obtained primarily in glassy mesostasis, while the Fe-Ni isotope data are based on analysis of silicate phases. In one of these chondrules, a radial chondrule with low Al/Mg ratio in mesostasis, we could not obtain meaningful initial ²⁶Al/²⁷Al. The fifth chondrule, hosting the lowest initial ²⁶Al/²⁷Al [$(5.5 \pm 0.32) \times 10^{-6}$; (2 σ)], yielded an upper limit of 3×10^{-7} for initial ⁶⁰Fe/⁵⁶Fe. Our data suggest a very good correlation between the initial ⁶⁰Fe/⁵⁶Fe and initial ²⁶Al/²⁷Al in the analyzed chondrules if we infer their time of formation based on the canonical solar system initial ²⁶Al/²⁷Al value of 5×10^{-5} . This correlation argues for simultaneous injection of these nuclides from a common stellar source and yields a solar system initial ⁶⁰Fe/⁵⁶Fe value of $\sim 9 \times 10^{-7}$. Our results raise questions on the validity of the proposed late injection of ⁶⁰Fe relative to ²⁶Al into the early solar system [4].

References: [1] Tachibana S. and Huss G. R. 2003. *The Astrophysical Journal Letters* 588:41–44. [2] Mostefaoui S. et al. 2005. *The Astrophysical Journal* 625:271–277. [3] Tachibana S. et al. 2006. *The Astrophysical Journal Letters* 639:87–90. [4] Bizzarro M. et al. 2007. *Science* 316:1178–1181. [5] Rudraswami N. G. and Goswami J. N. 2007. *Earth and Planetary Science Letters* 257:231–244. [6] Rudraswami et al. Forthcoming. *Earth and Planetary Science Letters*. [7] Goswami J. N., Mishra R., and Rudraswami N. G. 2007. Abstract #1943. 38th LPSC.

5307

PETROLOGY AND GEOCHEMISTRY OF MARTIAN METEORITES LAR 06319, RBT 04261, AND RBT 04262

David W. Mittlefehldt and Jason S. Herrin. NASA/Johnson Space Center, USA. E-mail: david.w.mittlefehldt@nasa.gov.

We have begun petrologic and geochemical study of three recently discovered Martian meteorites, two of which are paired. Here we present our preliminary petrologic data on them, and compare them to other Martian meteorites. Our geochemical studies are just beginning.

The paired stones RBT 04261 and RBT 04262 have already been described [1, 2], and we will only discuss them briefly. As described [1], these stones have coarse-grained poikilitic areas essentially devoid of maskelynite, and medium-grained equigranular regions containing maskelynite. The poikilitic areas consist of low-Ca pyroxene grains enclosing olivine, chromite and ilmenite. They are texturally very similar to the light phase of ALHA77005 and some xenoliths in EETA79001 lithology A. Melt inclusions are common, especially in olivine. These inclusions are rich in late-stage phases such as alkali-rich aluminosilicate glass, Si-rich glass and phosphates, and commonly contain sulfides. In one inclusion we found two grains that may be titanite (molar Si:Ca:Ti of $\sim 1.0 : \sim 1.1 : \sim 0.9$), but the small size precluded quality analyses.

LAR 06319 is an olivine-phyric basalt consisting of euhedral to subhedral brownish olivine phenocrysts up to ~ 2 mm in size set in a medium-grained subophitic basalt consisting of generally euhedral prismatic to tabular pyroxene grains up to 1 mm long, mostly euhedral plagioclase laths ~ 0.2 mm long (now maskelynite) and subhedral to anhedral brownish olivine grains up to 0.5 mm in size (hereafter matrix olivine). Oxide phases include chromite and ilmenite. Olivine phenocryst cores have mg#s up to 76–75 with rims as ferroan as mg# 54. Matrix olivine cores are mg# 61–43. Phenocryst and matrix olivine hosts abundant melt inclusions, and again these are rich in the late-stage phases alkali-rich aluminosilicate glass and phosphates, and possibly rutile (two grains too small for clean analyses). As in RBT, melt inclusion in LAR contain sulfides. Pyroxene cores are either low-Ca or augite, and the most magnesian are mg# 75–74, $Wo_{3.6-4.5}$, and mg# 68–67, Wo_{26-29} . Pigeonite and subcalcic augite overgrow the cores. The most ferroan rims are pigeonite and subcalcic augite with compositions as ferroan as mg# 35, Wo_8 and mg# 32, Wo_{20} .

Olivine phenocryst core compositions of LAR 06319 are similar to the most magnesian olivines we find in DaG 476, but pyroxene cores in the latter are more magnesian; mg# 83, $Wo_{1.6}$ and mg# 77–76, Wo_{34-35} for low-Ca pyroxene and augite. Literature data on DaG 476 (and pairs) extend olivine compositions to higher mg#s [3]. The most magnesian olivine phenocrysts in Dhofar 019 are like those in LAR 06319, but pyroxene cores in the former are more ferroan; mg# <70 for pigeonite and <60 for augite [4]. Olivine core compositions in SaU 005 (mg# 74) are also similar to those in LAR 06319, but magnesian low-Ca pyroxenes (mg# 75) are pigeonites with $Wo_{.8}$ [3]. Thus, although LAR 06319 shows some similarities to other olivine-phyric Martian basalts, it is distinctly different.

References: [1] Mikouchi T. et al. 2008. Abstract #2403. 39th LPSC. [2] Anand M. et al. 2008. Abstract #2173. 39th LPSC. [3] Goodrich C. A. 2003. *Geochimica et Cosmochimica Acta* 67:3735–3771. [4] Taylor L. A. et al. 2002. *Meteoritics & Planetary Science* 37:1107–1128.

5148

DYNAMIC CRYSTALLIZATION SIMULATION OF BARRED OLIVINE TEXTURESH. Miura¹, E. Yokoyama², K. Tsukamoto¹, and K. Nagashima³. ¹Tohoku University, Japan. E-mail: miurah@ganko.tohoku.ac.jp. ²Gakushuin University, Japan. ³Osaka University, Japan.

Introduction: Chondrules are abundant in most of chondritic meteorites falling onto the Earth. They are believed to have been formed from molten silicate droplets 4.6 billion years ago in our early solar system [1]. Some of them have interesting crystalline textures with rim and bars. The rim has a thin shell-like morphology surrounding a chondrule. The bars are planar crystals parallel each other observed inside the rim. The remarkable features are that the rim connects with bars and the crystal orientation of the rim is the same as adjoining bars [2]. Such texture has not been reproduced in the laboratory experiments except a few examples [3, 4], therefore, the formation mechanism is unclear.

We notice that the Mullins-Sekerka instability at the interface between the previously formed rim and the inside supercooled melt results into the formation of bars, based on the linear stability analysis [5]. We carry out the numerical simulation of the crystallization of a supercooled silicate melt (dynamic crystallization simulation) by using a phase-field model [6].

Model: For simplicity, we consider a droplet of one component in our model, so we solve the equations for evolutions of crystals, which are described by a phase field, and the temperature, but do not of chemical zoning. Initially, we assume that the rim is formed at the droplet surface. Since the rim is heated up to about the melting temperature by the release of the latent heat of crystallization, the temperature gradient from the hotter rim to the cooler inside is generated.

Numerical Results: The interface between the rim and the inside supercooled melt is unstable during the solidification. Our simulation shows that the instability grows nonlinearly and parallel planar crystals are formed. This morphology is similar to that observed in some natural samples of chondrules. The formation timescale and width of bars depend on the supercooling $dT (= T_m - T)$, where T_m is the melting temperature and T is the droplet temperature. However, when the supercooling dT exceeds the hypercooling limit (~ 425 °C for forsterite [7]), the barred olivine texture is not reproduced.

Conclusions: Our dynamic crystallization simulation shows that the barred olivine textures were formed from a supercooled melt with the supercooling of about $dT < 400$ °C due to the Mullins-Sekerka instability. In contrast, the barred olivine textures cannot be formed when the supercooling exceeds the hypercooling limit. The dynamic crystallization simulation can be a very powerful tool to elucidate the formation mechanism of chondrule textures by comparing with the dynamic crystallization experiments.

References: [1] Amelin T. et al. 2002. *Science* 297:1678–1683. [2] Lofgren G. and Lanier A. B. 1990. *Geochimica et Cosmochimica Acta* 54: 3537–3551. [3] Tsuchiyama A. et al. 2004. *Geochimica et Cosmochimica Acta* 68:653–672. [4] Tsukamoto K. et al. 2001. Abstract #1846. 32nd LPSC. [5] Mullins W. W. and Sekerka R. F. 1964. *Journal of Applied Physics* 35: 444–451. [6] Wang S.-L. et al. 1993. *Physica D* 69:189–200. [7] Nagashima K. et al. 2006. *Journal of Crystal Growth* 293:193–197.

5203

FORMATION OF SPHERULE-CHAINED TEXTURE BY SHOCKED KUGA METEORITE IN AIR

Y. Miura. Div. Earth Sci., Graduate School of Sci. and Eng., Yamaguchi University, Yoshida 1677-1, Yamaguchi 753-8512, Japan. E-mail: yasmiura@yamaguchi-u.ac.jp.

Introduction: Spherule texture can be formed in impact reaction during meteoritic impact in air. There are no reports on spherule-chained texture with iron oxides in composition and microtexture with 100 nm order [1]. The purpose of the present study is to elucidate spherule-chained texture with micro-texture of 100 nm in order found in the Kuga iron meteorite, Iwakuni, Yamaguchi, Japan.

Complex Textures in the Kuga Meteorite: The Kuga iron meteorite found in Kuga, Iwakuni, Yamaguchi, Japan shows spherule-chained texture with Fe, Ni-rich composition with 10 μm in size, where each spherule contained long microtexture in 100 nm in size (Fig. 1) [1, 2]. The complex texture can be found only in fusion crust probably formed by vapor-melting process in air. The FE-ASEM analyses by an in situ observation indicate that the matrix of the spherule-chained texture with Fe, Ni, O-rich composition is carbon-rich composition probably formed impact reactions in air.

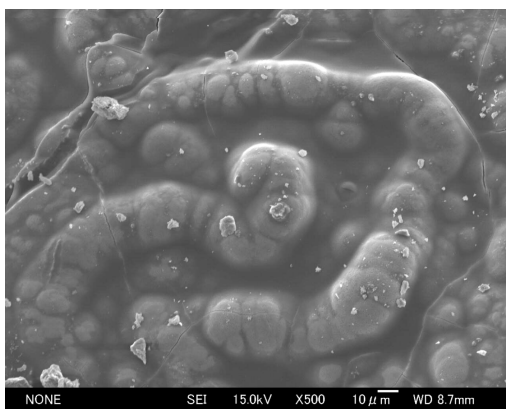


Fig. 1. Electron micrograph (FE-SEM) of Fe-Ni-Cl rich spherules with spherule-chained shapes in the Kuga meteorite found in Kuga, Yamaguchi, Japan taken by author [1, 2].

Comparison with the Kuga and Martian Meteorite: Remnant of life in ocean can be found by mineralized fossil, which can be found in deep interior of the Earth and the Martian meteorite ALH 84001 shows bacteria-like chained texture of magnetite in composition (in 100 nm order) around carbonate spherules formed by water reaction on the Mars [3]. Similarity of bacteria-like texture of the ALH 84001 compared with the Kuga meteorites are composition of Fe-rich, C-bearing, chained texture of small size probably replaced by Fe and O-rich composition in air. Big difference of these textures is no carbonates minerals in the Kuga meteorite [1–3].

Summary: Spherule-chained texture with Fe, Ni, and Cl has been obtained at fusion crust of the Kuga iron meteorite found in Japan, where the Kuga iron meteorite is different with the Martian meteorite ALH 84001 with several steps of formation including carbonate formation.

References: [1] Miura Y. Forthcoming. CD#ST-A014. Asia Oceania GeoSciences Society. [2] Miura Y. Forthcoming. 31st Japan GeoScience Union Meeting. [3] McKay D. S. et al. 1996. *Science* 273:924–930.

5189

ROSETTES TEXTURES WITH METEORITIC ELEMENTS IN SOME JAPANESE METEORITES

Y. Miura. Division of Earth Sciences, Graduate School of Science and Engineering, Yamaguchi University, Yamaguchi 753-8512, Japan. E-mail: yasmiura@yamaguchi-u.ac.jp.

Introduction: Formation of flake (rosettes) textures is discussed by weathering or impact effects [1, 2]. The purpose of the present paper is to elucidate its texture with sporadic distribution at some Japanese meteorites of the Nio, Kuga, and Mihonoseki meteorites, as well as the Carancas chondrite and artificial synthesis of glass [2].

Samples Used in This Study: Three meteorites of the Nio, Kuga, Mihonoseki (in Japan) are used in this study, as well as support data of an artificial slag glass, where similar flake (“rosettes”) texture has been taken by the FE-ASEM in Yamaguchi, Japan operated by author.

The Nio Chondritic Meteorite: Meteoritic spherules and fragments formed at explosion in atmosphere by the Nio meteoritic shower found at the fallen sites of Niho, Yamaguchi, Japan (i.e., few contamination of melted fragments from the ground) reveal sporadic distribution of many Fe rosettes texture with chlorine, where all sources of Fe, Ni, Cl, and O are originated from the meteorite due to explosion in atmosphere before impact to the ground. Its texture is similar with the Carancas chondrite [2].

The Kuga Iron Meteorite: The Kuga iron meteorite found in Kuga, Iwakuni, Yamaguchi, Japan has “fusion-crust” (i.e., melted layer during passing to atmosphere before impact to the ground) which includes Fe-Ni-Cl-bearing rosettes texture formed from meteorite melting in atmosphere.

The Mihonoseki Chondritic Meteorite: The Mihonoseki chondritic meteorite has been found in the ground after passing through wooden house in Mihonoseki, Shimane, Japan. Minor fragments found in the ground are used to observe texture by the FE-ASEM in this study. Sporadic distribution of the texture with 1?m in size can be found in this sample.

Artificial Formation of Fe-Cl Rosettes Texture: Artificial slag cement in composition formed at high temperature shows Fe-Cl-bearing rosettes-texture obtained by the FE-ASEM analyses.

Formation of Rosettes Texture with Fe and Cl: The rosettes (flake) textures of three Japanese meteorites with meteoritic Fe, Ni, Cl-bearing composition reveal sporadic distribution in this study. The detailed comparison of chemistry and texture indicates that the rosettes texture with sporadic distribution is considered to be formed by dynamic impact reaction [2].

References: [1] Frondel J. W. 1975. *Lunar mineralogy*. New York: John Wiley & Sons. pp. 84–87. [2] Miura Y. 2008. Abstract #2027. 39th LPSC.

5191

NOBLE GAS STUDIES OF EUCRITES, DIOGENITES, AND SOME OTHER ACHONDRITES

Y. N. Miura. Earthquake Research Institute, University of Tokyo, Yayoi, Bunkyo-ku, Tokyo 113-0032, Japan.

Introduction: Cosmogenic, radiogenic, and fission-derived noble gases provide us important knowledge for cosmic-ray irradiation, impacts on parent bodies, early thermal histories and so on. For detailed discussion based on these components, both measurements and data reduction (e.g., decomposition of measured values into each component) have to be carefully done. Here, I evaluate procedure of data reduction for achondrites, and report obtained characteristic features such as cosmogenic noble gas compositions, ^{244}Pu -Xe age distribution and presence of radiogenic ^{129}Xe .

Samples and Analyses: The samples studied here include 30 eucrites, 12 diogenites, a basaltic achondrite (Northwest Africa 011), an angrite (Northwest Africa 1670) and an anomalous CR clan (or primitive achondrite, Tafassasset), among which several data were published before [1, 2]. Noble gases were measured with a mass spectrometer (modified-VG5400) at LEC, University of Tokyo [3, 4]. For gas extraction, total melting or stepwise heating was applied.

Results and Discussion: $^{124-130}\text{Xe}$ is mixtures of trapped (usually terrestrial atmospheric) and cosmogenic Xe. The compositions of cosmogenic Xe in most cases are consistent with those calculated from cosmogenic Xe spectra of Ba and REE targets [5] and Ba/LREE compositions [6, 7]. Some samples such as Asuka-87272 (eucrite) and NWA 011 show slightly Ba-enhanced spectra. ^{128}Xe derived from neutron capture on iodine is not found in all the samples (only Ibitira might have a small amount of excess ^{128}Xe), possibly indicating that thin regolith-like layer covers the eucrite surfaces. This may explain equilibrated textures [8] and/or younger ages (e.g., ~50–100 Ma after Angra dos Reis by ^{244}Pu -Xe ages) observed in many eucrites.

Four eucrites (Ibitira, Juvinas, Pecora Escarpment 82502, and Pecora Escarpment 91007) clearly show excess ^{129}Xe likely derived from extinct ^{129}I . Among the measured eucrites, these have old ^{244}Pu -Xe ages (within ~20 Ma after ADOR). Eucrites with old ^{244}Pu -Xe ages tend to retain radiogenic ^{129}Xe . However, radiogenic ^{129}Xe amounts are not correlated well with ^{244}Pu -Xe ages, and there are eucrites having old ^{244}Pu -Xe ages without radiogenic ^{129}Xe . This is mainly attributed to different contents of iodine among eucrites due to chemical fractionation.

Fission components are dominant at heavy Xe isotopes in several eucrites. Subtracting cosmogenic and ^{238}U -derived fission Xe, ^{244}Pu -derived fission Xe spectra are calculated to be $^{131}\text{Xe} : ^{132}\text{Xe} : ^{134}\text{Xe} : ^{136}\text{Xe} = 0.20 (6) : 0.87 (3) : 0.920 (9) : =1$, the average of ten data with small errors.

References: [1] Miura Y. N. et al. 1998. *Geochimica et Cosmochimica Acta* 62:2369–2387. [2] Yamaguchi A. et al. 2002. *Science* 296:334–336. [3] Nagao K. et al. 1999. *Antarctic Meteorite Research* 12:81–93. [4] Miura Y. N. et al. 2007. *Geochimica et Cosmochimica Acta* 71:251–270. [5] Hohenberg C. M. et al. 1981. *Geochimica et Cosmochimica Acta* 45:1909–1915. [6] Miura Y. N. et al. Forthcoming. [7] Koblitz J. 2005. *MetBase* 7.1 and references therein. [8] Yamaguchi A. et al. 1996. *Icarus* 124:97–112.

5017

FURTHER EVIDENCE FOR UBIQUITOUS FRACTIONAL CRYSTALLIZATION OF WADSLLEYITE AND RINGWOODITE FROM OLIVINE MELTM. Miyahara¹, M. Kimura², E. Ohtani¹, A. El Goresy³, S. Ozawa¹, T. Nagase⁴, and M. Nishijima⁵. ¹Graduate School of Science, Tohoku University, Sendai 980-8758, Japan. E-mail: miyahara@ganko.tohoku.ac.jp. ²Faculty of Science, Ibaraki University, Mito, 310-8512, Japan. ³Bayerisches Geoinstitut, Universität Bayreuth, 95447 Bayreuth, Germany. ⁴The Tohoku University Museum, Sendai 980-8758, Japan. ⁵Institute for Materials Research, Tohoku University, Sendai 980-8758, Japan.

Introduction: El Goresy et al. [1] and Miyahara et al. [2] found a novel wadsleyite-ringwoodite assemblage in a shock-melt vein (SMV) of Peace River (L6) chondrite. Both wadsleyite and ringwoodite display granoblastic-like texture. The wadsleyite-ringwoodite interface denoted a compositional gap of up to 32 mole% fayalite (Fa). The assemblage was interpreted to have formed through fractional crystallization of olivine melt generated by a shock event. We here present further evidence that such fractional crystallization mechanism is not unique to Peace River only but is indeed pervasive in the SMVs of L6 chondrites. We scrutinized several SMVs in Allan Hills 78003 (L6) and Yamato-74445 (L6) chondrites using FE-SEM and EPMA because previous studies showed that they contained wadsleyite and ringwoodite in their SMVs [3, 4]. We also conducted FIB-TEM/STEM microanatomy of important parts to obtain additional evidences disclosing details of the mechanism of fractional crystallization of wadsleyite and ringwoodite.

Results and Discussion: We found diverse wadsleyite-ringwoodite assemblages (~50 by ~30 μm) and unzoned olivine crystals (Fa_{24-25}) with ringwoodite veins in the SMVs of Allan Hills 78003. The assemblages are elongated parallel to walls of SMVs. There is unambiguous dichotomy in the chemical compositions of wadsleyite and ringwoodite; wadsleyite is depleted in Fe (Fa_{11-13}) whereas, ringwoodite is rich in Fe (Fa_{30-32}). We also found very similar wadsleyite-ringwoodite assemblages in the SMVs of Yamato-74445. We maintain that these wadsleyite-ringwoodite assemblages were also formed by fractional crystallization from olivine melt. In some cases, wadsleyite grains in the assemblages are idiomorphic with preferred orientation and allotriomorphic ringwoodite grains in their interstices, indicating that ringwoodite crystallized subsequent to wadsleyite from olivine melt. In most cases, the assemblages have wadsleyite rim (width <10 μm). Poorly crystallized materials are present between idiomorphic wadsleyite grains of the rim. A few idiomorphic majorite-pyrope_{ss} grains were encountered within the wadsleyite rim. These textures imply that olivine melt partially mixed with chondritic melt.

Conclusions: We strongly suggest that liquidus wadsleyite-ringwoodite assemblages are ubiquitous in the SMVs of L6 chondrites and were not noticed in earlier studies. We found here additional supporting evidence for fractional crystallization of wadsleyite and ringwoodite from olivine melt.

References: [1] El Goresy A. et al. 2007. Abstract #5024. *Meteoritics & Planetary Science* 42:A40. [2] Miyahara M. et al. Forthcoming. *Proceedings of the National Academy of Sciences*. [3] Ohtani E. et al. 2006. *Shock Wave* 16:45–52. [4] Ozawa S. et al. 2007. AGU 2007 Fall meeting, MR43B-1234.

5031

A MODEL TO CALCULATE THE COOLING RATE BY Fe-Mg DIFFUSIONAL CALCULATION DURING OLIVINE CRYSTAL GROWTH

M. Miyamoto¹, T. Mikouchi¹, and R. H. Jones². ¹Space and Planetary Science, University of Tokyo, Hongo, Tokyo 113-0033, Japan. ²Department of Earth and Planetary Sciences, University of New Mexico, Albuquerque, NM 87131, USA. E-mail: miyamoto@eps.s.u-tokyo.ac.jp.

Introduction: We developed a new model to calculate the cooling rate (or burial depth) by using the Fe-Mg chemical zoning profile of olivine considering diffusional modification during crystal growth [1], because chemical zoning provides information on thermal history of minerals. Although dynamic crystallization experiments are useful for estimating the cooling rate [e.g., 2], experimental results only show the possibility of the cooling rate. It is, therefore, important to determine the cooling rate of actual olivines in rocks.

Calculation Procedures and Verification: The olivine crystal grows as temperature decreases. Fe-Mg zoning forms by closed-system fractional crystallization as the olivine crystal grows. Fe-Mg diffusion takes place in the growing olivine crystal. By simulating the above processes, we compute the zoning profile and determine the cooling rate (or burial depth) to obtain the best-fit profile to the observed one. We used the Fe-Mg interdiffusion coefficient of olivine reported by Misener [3] with oxygen-fugacity variation extrapolated by Miyamoto et al. [4].

We have successfully verified our model by using experimentally produced Fe-Mg zoning of olivine for analogs of Semarkona (LL3.00) chondrules [5] and those of Martian and lunar meteorites [6]. These results mean that our model can be of use for a wide variation of chemical compositions

Results and Discussion: We applied this model to calculating the cooling rate (or burial depth) for olivines of type II porphyritic olivine chondrules in Semarkona and for olivines in Martian and lunar meteorites. For example, the calculated cooling rates for Semarkona olivines show a wide range from 0.8 °C/hr to 2400 °C/hr, and are different among chondrules. This result suggests that each chondrule formed in different environmental conditions and assembled in Semarkona after chondrule formation. Calculated cooling rates are broadly consistent with those determined in dynamic crystallization experiments (10–2000 °C/hr) [2]. The lower limit of the calculated cooling rate, 0.8 °C/hr, is about one order magnitude slower than experimental results (10 °C/hr). Our model can be applied to estimating the cooling rate of olivines in terrestrial rocks as well as extraterrestrial materials.

Acknowledgments: We thank Dr. G. MacPherson for the Semarkona thin section.

References: [1] Miyamoto M. et al. 1999. Abstract #1323. 30th LPSC. [2] Hewins R. H. 1988. In *Meteorites and the early solar system*. Tucson, Arizona: The University of Arizona Press. pp. 660-679. [3] Misener D. J. 1974. In *Geochemical transport and kinetics*. Carnegie Institute, Washington Publication #634. pp. 117–129. [4] Miyamoto M. et al. 2002. *Antarctic Meteorite Research* 15:143–151. [5] Jones R. H. and Lofgren G. E. 1993. *Meteoritics* 28:213–221. [6] Miyamoto M. et al. 2006. Abstract #1538. 37th LPSC.

5319

NWA 5134: A NEW EUCRITE FROM SAHARAWI REGION

V. Moggi-Cecchi¹, G. Pratesi², M. Di Martino³, I. A. Franchi⁴, and R. C. Greenwood⁴. ¹Museo di Scienze Planetarie, Provincia di Prato, Via Galcianese, 20/h, I-59100 Prato, Italy. E-mail: v.moggi@pratoricerche.it. ²Dipartimento di Scienze della Terra, Università di Firenze, Via La Pira, 4, I-50121, Florence, Italy. E-mail: g.pratesi@unifi.it. ³INAF-Osservatorio Astronomico di Torino, Via Osservatorio 20, I-10025 Pino Torinese, Italy. ⁴Planetary and Space Sciences Research Institute, Open University, Walton Hall, Milton Keynes MK7 6AA, UK.

Introduction: Two stones with a total weight of 61.6 g were purchased in 2004 in a Saharawi village near Tindouf, Algeria by the astronomer Mario Di Martino during a scientific expedition studying impact craters. The main mass, now weighing 49.4 g, displays an achondritic fine grained texture with a predominant light gray color and several dark grey clasts. A small portion of a black fusion crust is visible on one side. Another small specimen, weighing 10.2 g, is currently on deposit at the Museo del Cielo e della Terra of San Giovanni in Persiceto, Italy. A total of 12 g and one thin section is on deposit at Museo di Scienze Planetarie, Prato (inventory number MSP 5061). M. Di Martino holds the main mass.

Description: Thin section examination shows NWA 5134 to be an achondritic polymict breccia displaying mineral clasts of various kinds set into a fine-grained matrix of pigeonite, exsolved low-Ca pyroxene and plagioclase (Fig. 1a). The large clasts are predominantly plagioclase, pigeonite, and exsolved low-Ca clinopyroxene. Silica is present as a minor phase, exsolved pyroxene grains show alternating fine to very fine low-Ca pyroxene and augite lamellae (10 and 2 µm, respectively, Fig. 1b). Among opaque phases troilite, ilmenite, and an Al-Ti-chromite have been observed. The section presents a moderate degree of shock and low degree of weathering. EMPA analyses performed at the IGG-CNR of Florence show that plagioclase has an anorthitic composition (An_{90.9}), while pyroxene shows wide variations, ranging from pigeonite (Fs_{32.7-39.1}Wo_{6.3-7.2}) in unexsolved crystals to exsolved augite-low-Ca pyroxene assemblages displaying augite lamellae (Fs_{30.6}Wo_{10.5}) associated with low-Ca pyroxene (Fs_{37.6}Wo_{1.8}). Oxygen isotopes analyses performed at the Open University confirmed the classification as belonging to the HED group (δ¹⁷O = 1.71‰, δ¹⁸O = 3.71‰, Δ¹⁷O = -0.22‰).

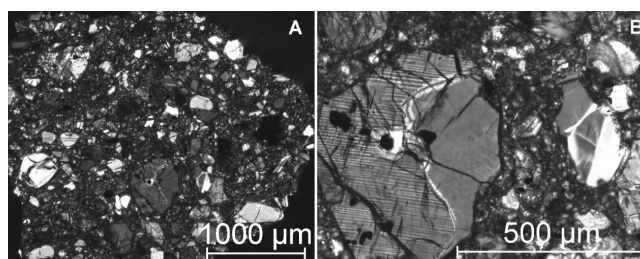


Fig. 1. Photomicrographs of a thin section of NWA 5134. a) General view showing the achondritic texture. b) Blowup of (a) displaying the exsolution lamellae in pyroxene (both transmitted light, crossed polars).

Conclusions: According to minerochemical and isotopic data, the specimen shows strong affinities with recently classified polymict eucrites like NWA 4271, 4391, 4396, 4397, 4825, and 4883 [1, 2] thus suggesting a probable pairing among these samples and NWA 5134.

References: [1] Connolly et al. 2007. *Meteoritics & Planetary Science* 42:1653. [2] Connolly et al. Forthcoming. *Meteoritics & Planetary Science*.

5099

ALTERATION IN CR CHONDRITES: AN ANALOGUE FOR THE LONG TERM STORAGE OF NUCLEAR WASTE

A. Morlok^{1, 2} and G. Libourel^{1, 3}. ¹CRPG-Nancy Université-INSU-CNRS, UPR2300, BP 20, 54501 Vandoeuvre-lès-Nancy, France. ²ANDRA-DS/CM, 1/7 rue Jean Monnet, 92298 Châtenay-Malabry, France. ³ENSG-Nancy Université, 54500 Vandoeuvre-lès-Nancy, France. E-mail: amorlok@crpg.cnrs-nancy.fr.

Introduction: As part of a study to study the corrosion of nuclear waste glass over a longer (>10⁵ years) time frame, we use aqueous alteration features in CR chondrites as analogue. CR chondrites were selected because there are samples available in all stages of aqueous alteration, from type 3 to 1 [1–3]. This allows the study of even very long term effects of corrosion (>10⁷ years, [4]) of metal and glass. They also contain abundant components (metal, glass) useful as analogues for the nuclear waste glass material in steel containments. In our study, we mainly focus on three interfaces:

- mesostasis/FeNi metal as analogue for the contact between the nuclear glass and the container,
- FeNi metal/matrix, for steel containment in clay environment, and
- mesostasis/phyllosilicates for glass/alteration products.

Samples and Techniques: To cover the whole range of alteration processes expected, we selected a series of CR chondrites. Renazzo, Al Rais (both CR2) and GRO 95577 (CR1) will be the focus of the study.

Samples were mapped using an SEM in BSE mode. Based on these maps, we selected interesting alteration structures for quantitative elemental mapping and point analyses using an EMPA at Nancy University. We will present an overview of changes in chemical composition and mineralogy of the interfaces at different stages of alteration.

Discussion: Al Rais turns out to show abundant features of varying degrees of alteration even in one sample, indicating many microchemical environments. Renazzo is on the whole less altered, and shows less variance.

Alteration at the glass/metal interface around metal grains in mesostasis is already widespread in Renazzo.

In Al Rais, heavily corroded metal grains in chondrules are also common.

The clay/metal interface in Al Rais usually shows incipient alteration, and often already layered corrosion rims around larger metal grains in the fine-grained matrix of Renazzo and Al Rais.

Also, structures in the fine-grained matrix in Al Rais give insight in the later stages of alteration: Fe and S enriched areas around a chondrule indicate sulfide precipitation from dissolved species.

Furthermore, abundant fine-grained intergrowths of iron-oxides and carbonate seem to have isomorphically replaced silicates in remnants of completely altered chondrules. Carbonates were also observed around chondrules in earlier studies [1].

Future work will include detailed mineralogical studies (e.g., TEM), as well as isotopic analyses to trace the elemental dispersion during alteration processes.

References: [1] Weisberg et al. 1993. *Geochimica et Cosmochimica Acta* 57:1567–1586. [2] Abreu. 2007. Ph.D. thesis. [3] Weisberg M. K. and Huber H. 2007. *Meteoritics & Planetary Science* 42:9. [4] Hutcheon et al. 1999. Abstract #1722. 30th LPSC.

5098

ALTERATION OF METAL IN CR2 CHONDRITES: AN ANALOGUE FOR LONG-TERM CORROSION PROCESSES

A. Morlok^{1, 2} and G. Libourel^{1, 3}. ¹CRPG-Nancy Université-INSU-CNRS, UPR2300, BP 20, 54501 Vandoeuvre-lès-Nancy, France. ²ANDRA-DS/CM, 1/7 rue Jean Monnet, 92298 Châtenay-Malabry, France. ³ENSG-Nancy Université, 54500 Vandoeuvre-lès-Nancy, France. E-mail: amorlok@crpg.cnrs-nancy.fr.

Introduction: The long term storage of nuclear waste provides a big challenge for material science. The material has to be stored safely for a time frame of at least 10⁴–10⁵ years—something difficult to simulate in a laboratory environment. In France, the nuclides are stored in a boro-silica glass, which is contained in steel containers, which are stored in a clay-rich geological repository. To gain insight in the long term behaviour of this materials at the metal-glass-clay interface, CR chondrites provide a good analogue. Glassy chondrule mesostasis are similar to the nuclear waste glasses. Abundant larger metal grains help to estimate corrosion processes of the steel container. These components are embedded in a phyllosilicate-rich matrix [1]. CR chondrites also show alteration over the whole range from type 3 to 1, thus allowing the investigation of all steps in alteration of the materials [2, 3]. The physico-chemical environment of the parent body during the alteration (Table 1) is sufficiently similar to that expected in the storage facility [4].

Table 1. Comparison environments. Sources: [1–4].

	CR chondrites	Storage facility
T°C	50–150	40–90
fO ₂	>10 ⁻⁵⁵ –10 ⁻⁷⁰	>10 ⁻⁵⁵ –10 ⁻⁷⁰
W/R	0.4–1.1	0.1–0.6
Mineralogy	Serpentine, saponite, calcite, magnetite, maghemite, pyrrhotite, pentlandite	Serpentine, smectite, siderite, magnetite

Samples and Techniques: Samples of Renazzo and Al Rais CR2 were selected for their advanced degree of alteration. In a first step, we obtained BSE maps of important areas of the samples, followed by quantitative elemental mapping using an EMPA at Nancy University.

Discussion: In one part of this project, alteration of metal grains inside the matrix of CR2 chondrites is used to investigate the corrosion of the steel container. Preliminary results from big metal grains (>400 μm) in Renazzo and Al Rais show multi-layered reaction rims. These rims are fine-grained mixtures, probable dominating phases were identified based on element ratios. The grain in Renazzo, which is altered to a lower degree than Al Rais, has a sequence of layers dominated by FeNi metal/sulfide/iron oxide/carbonate/sulfide/matrix or FeNi/sulfide/carbonate/matrix.

The grain in Al Rais has a different sequence: layers on one side are dominated by FeNi/iron oxide/ sulfide /phosphate carbonate/sulfide/matrix. The rim on the other half is mainly sulfide.

Acknowledgements: Renazzo was provided by the Musée d'Histoire Naturelle, Paris, Al Rais BM1971,289 by the Natural History Museum, London).

References: [1] Weisberg et al. 1993. *Geochimica et Cosmochimica Acta* 57:1567–1586. [2] Abreu. 2007. Ph.D. thesis. [3] Weisberg M. K. and Huber H. 2007. *Meteoritics & Planetary Science* 42:9. [4] Zolensky M. et al. 1993. *Geochimica et Cosmochimica Acta* 57:3123–3148.

5062

ROOM- AND LOW-TEMPERATURE MÖSSBAUER SPECTROSCOPY FOR ORDINARY CHONDRITES FROM THE SAN JUAN STREW FIELD AT THE ATACAMA DESERT (CHILE)

P. Munayco¹, E. M. Valenzuela², R. B. Scorzelli¹, J. B. de Campos³, R. R. Avillez⁴, P. Rochette⁵, J. Gattacceca⁵, C. Suavet⁵, M. Denise⁶, and D. Morata². ¹Centro Brasileiro de Pesquisas Físicas (CBPF/MCT), RJ, Brazil. E-mail: scorza@cbpf.br. ²Dep. de Geologia, Universidad de Chile, Santiago, Chile. ³Instituto Nacional de Tecnologia (INT/MCT), RJ, Brazil. ⁴Departamento de Ciência dos Materiais e Metalurgia, PUC/Rio, RJ, Brazil. ⁵CEREGE CNRS Université Aix-Marseille, France. ⁶MNHN Paris, France. E-mail: mpablo@cbpf.br.

Introduction: We report the quantitative results obtained by Mössbauer spectroscopy (MS) run at room temperature (RT) and at 4,2K (LT) for 9 new meteorites from the strewnfield of San Juan, located in the central part of the Atacama Desert (AD), northern Chile. Results for another recovery site were presented before [1, 2], and this study helps in the understanding of the weathering processes at different accumulation areas of the AD.

Samples: The meteorites are ordinary chondrites (OC), from which 7 are type H, 1 is type L and 1 is a LL, that were found during the last 2007 expedition. Preliminary classification was done at CEREGE, and petrographic and microprobe classification at the Musée National d'Histoire Naturelle, Paris, confirming that the samples were not paired. We also include 2 other samples from the same area, studied before.

Methodology: As recently fallen equilibrated OC contain iron only as Fe⁰ (kamacite and taenite) and Fe²⁺ (olivines, pyroxenes, and troilite), the abundance of ferric iron is directly related to the level of terrestrial weathering [3]. As MS is extremely sensitive to changes in Fe valence state, the technique, complemented by XRD, allows the recognition and quantification of all the Fe-bearing phases. The percentage of these phases was obtained for the primary minerals: olivine, pyroxene, troilite, and Fe-Ni metal, and for the ferric alteration products which gives the percentage of oxidation of the samples. The subspectra arising from the presence of Fe³⁺ are generally fitted with a paramagnetic doublet and a magnetic sextet(s). The doublet can be associated with the paramagnetic phases: akaganéite, lepidocrocite, and/or small-particle goethite, while the sextet(s) are due to the magnetically ordered phases: magnetite, maghemite, hematite, and large-particle goethite.

Results: From the MS absorption areas of these oxides, the terrestrial oxidation of the San Juan samples was found to range from ~10% to ~57%. The amounts of silicates as well as the opaque phases (troilite and Fe-Ni) were found to decrease in a constant rate with increasing oxidation level. A histogram of percentage oxidation versus frequency shows a peak at ~55%, the highest peak ever found for other hot desert meteorites populations, commonly around values of ~45% [4], possibly indicating a very old and stable accumulation surface.

References: [1] Valenzuela E. M. et al. 2006. Abstract #5203. *Meteoritics & Planetary Science* 41:A179. [2] Valenzuela E. M. et al. 2007. Abstract #5099. *Meteoritics & Planetary Science* 42:A152. [3] Bland P. A. et al. 2002. *Hyperfine Interactions* 142:481. [4] Bland P. A. et al. 1998. *Geochimica et Cosmochimica Acta* 62:3169.

5155

COMPREHENSIVE STUDIES OF THE HIROSHIMA H CHONDRITE

S. Murakami¹, K. Kato¹, N. Fujikawa¹, K. Terada², S. Yoneda³, S. Arai², H. Hidaka², A. Okada⁴, K. Nagao⁵, J. Park⁶, N. Ebisawa⁵, and M. Kusakabe⁷. ¹Hiroshima Children's Museum, 5-83 Motomachi, Naka-ku, Hiroshima City 730-0011, Japan. E-mail: murakami@pyonta.city.hiroshima.jp. ²Department of Earth and Planetary System Sciences, Hiroshima University, Higashi-Hiroshima 739-8526, Japan. E-mail: terada@sci.hiroshima-u.ac.jp. ³National Museum of Nature and Science, Shinjuku-ku, Tokyo 169-0073, Japan. ⁴RIKEN, Wako, Saitama 351-0198, Japan. ⁵Laboratory for Earthquake Chemistry, Graduate School of Science, University of Tokyo, Hongo, Bunkyo-ku, Tokyo 113-0033, Japan. ⁶ARES, code KR, NASA, Johnson Space Center, Houston, TX 77058, USA. ⁷Korea Polar Research Institute, Incheon, Korea.

Introduction: The Hiroshima meteorite penetrated the roof of the Distribution Center of EVERTH Co. Ltd., Hiroshima, Japan, and was discovered on Tuesday, February 4. First information was reported to Hiroshima Children's Museum, and this was identified as a meteorite by Yoneda at the National *Science* Museum [1]. Its size and mass are 5.8 cm × 10.5 cm × 4.6 cm and 414 g, respectively. Date of the fall has not been specified but Saturday, February 1 is most likely because several people in Hiroshima observed a fireball around 22:30 on February 1 [2]. In this paper, we report the results of comprehensive studies of this "fall" meteorite.

Results: The first characterization of the Hiroshima meteorite was carried out at the National *Science* Museum and RIKEN. This meteorite mainly consists of olivine of Fa_{17.0-18.7} and pyroxene of Fs_{15.7-18.6} with CaO 1.0-1.7 wt%, whereas clinopyroxenes are rare. Cosmogenic nuclides such as ²⁶Al, ²²Na, ⁵⁴Mn, ⁴⁶Sc, ⁵⁶Co, ⁷Be, ⁵¹Cr, and ⁴⁸V are detected by gamma ray analysis [3].

Noble gases in Hiroshima meteorites were investigated at Laboratory for Earthquake Chemistry, University of Tokyo. The ²¹Ne cosmic exposure age is ~90 Ma and estimated K-Ar ages are 4.55 ± 0.23 Ga for stepwise heating method, and 4.24 ± 0.23 Ga for total melting method [4]. Trapped heavy noble gas concentrations of ³⁶Ar, ⁸⁴Kr, and ¹³²Xe are 27.82, 0.267, and 0.147 in 10⁻⁹ cm³ STP/g, respectively [4].

Oxygen isotope analyses was performed at Institute for Study of the Earth's Interior, Okayama University, showing that the Δ¹⁷O is ~0.65.

In situ U-Pb dating of phosphates in Hiroshima meteorites was carried out using sensitive high-resolution ion microprobe (SHRIMP) at Hiroshima University. In situ analyses of five phosphate grains resulted in a total Pb/U isochron age of 4.54 ± 0.07 Ga in ²³⁸U/²⁰⁶Pb-²⁰⁷Pb/²⁰⁶Pb-²⁰⁴Pb/²⁰⁶Pb 3-D space (95% confidence limit).

All of these geochemical data suggest that the Hiroshima meteorite is a typical H5 chondrite.

Acknowledgements: We thank EVERTH Co. Ltd. for providing us with the Hiroshima meteorite sample.

References: [1] Russell S. S. et al. 2003. The Meteoritical Bulletin, no. 87. *Meteoritics & Planetary Science* 38:A189-A248. [2] Japan Fireball Network (JN), website: <http://www3.cnet.ne.jp/c-shimo>. In Japanese. [3] Yoneda S. et al. 2003. Abstracts of the 50th Annual Meeting of the Geochemical Society of Japan. 1P40. In Japanese. [4] Park J. et al. 2003. *Geochimica et Cosmochimica Acta* 67:A374.

5033

SOLAR GASES IN KAVARPURA IRON METEORITE

S. V. S. Murty¹, R. R. Mahajan¹, Suruchi Goel¹, Krishnan Dutt², and P. S. Dhote². ¹Physical Research Laboratory, Ahmedabad, India. ²Geological Survey of India, Jaipur, India.

Introduction: Solar wind (SW) noble gases have been usually found in stone meteorites that are regolith breccias [1]. So far very few stony irons [2] and only Washington County iron meteorite [3] have been found to contain SW noble gases, though several irons have been reported to host primordial noble gases either in the metal [4] or in the inclusions [5]. Kavarpura iron meteorite fell in India on August 29, 2006. Based on Ni, Ir, Ga, and Ge contents and the presence of non-metallic inclusions, it has been classified as IIE-Anom. Two adjacent pieces of Kavarpura have been analyzed for noble gases by stepwise heating.

Results: Large amounts of He, Ne, and Ar are present in Kavarpura and are found to be a mixture of trapped and cosmogenic components, while Kr and Xe are close to blank levels, due to small amounts of samples used. The highest measured ²⁰Ne/²²Ne ratio is 12.47 and in Ne three-isotope plot the data fall along the SW-cosmogenic mixing line. Using the cosmogenic He, Ne and Ar systematics of iron meteorites [6], we have calculated the trapped and cosmogenic gas amounts in the two samples 1 and 2 of Kavarpura, and they are (in 10⁻⁸ ccSTP/g units), respectively ²⁰Ne_t: 209 and 58; ²¹Ne_c: 6.2 and 6.1. The elemental ratios in both samples are indistinguishable with (⁴He/²⁰Ne)_t ~ 500; (²⁰Ne/³⁶Ar)_t ~ 20; (³He/²¹Ne)_c ~ 50 and (³⁸Ar/²¹Ne)_c ~ 4.3. The peak release of trapped gases occurred at 800 °C, while that of cosmogenic gases occurred at 1600 °C. The two adjacent samples differ by about a factor of four in their trapped SW component, clearly suggesting that the trapped gases are likely present in some inclusions that are inhomogeneously distributed and not hosted in the metal phase. Using (³⁸Ar/²¹Ne)_c as shielding parameter [6], we calculated the production rate of P₂₁ and an exposure age of 272 Ma.

Discussion: BSE images of a polished surface of Kavarpura have revealed the presence of inclusions of up to several hundred microns in size. EDX spectra have shown the presence of C (in some), Si, Cr, Mg, Al, and Ca in most of these inclusions. Peak release of SW gases at 800 °C and cosmogenic gases at 1600 °C (from the principal target phase, metal) suggest that the SW gases are not volume correlated in the metal; they are either hosted in a non-metallic phase with low thermal stability (if volume correlated) or the surface sited SW gases in this host phase are not disturbed during the formation of the parent body of Kavarpura. A nonmagmatic origin has been proposed for IIE irons [7]. The survival and low temperature release of SW gases from Kavarpura imposes severe constraints on the formation conditions of its parent body. Formation of IIE irons in a local melt pool by the impact of a body into a regolith and survival of the SW bearing inclusions without any appreciable noble gas elemental fractionation are required to explain the Kavarpura data. This requires intact survival of volatiles in the inclusions trapped in IIE irons.

References: [1] Wieler R. 1998. *Space Science Reviews* 85:303–314. [2] Mathew K. J. and Begemann F. 1997. *Journal of Geophysical Research* E102:11,015–11,026. [3] Becker R. H. and Pepin R. O. 1984. *Earth and Planetary Science Letters* 70:1–10. [4] Voshage H. 1982. *Earth and Planetary Science Letters* 61:32–40. [5] Mathew K. J. and Begemann F. 1995. *Geochimica et Cosmochimica Acta* 59:4729–4746. [6] Voshage H. 1984. *Earth and Planetary Science Letters* 71:181–194. [7] Wasson J. T. and Wang J. 1986. *Geochimica et Cosmochimica Acta* 50:725–732.

5274

GENETIC RELATIONSHIPS AMONG TYPES OF CAIs AND CHONDRULES

H. Nagahara and K. Ozawa. Department of Earth Planet. Sci., The University of Tokyo, Japan. E-mail: hiroko@eps.s.u-tokyo.ac.jp.

Introduction: Despite numerous petrologic, isotopic, and chronological work on CAIs and chondrules, genetic relationships among types of CAIs and chondrules including the diversity of chemical composition of types have not been well understood yet. Important observation include: Most CAIs and chondrules possess evidence for multiple heating/melting events: chondrules often have relicts of CAIs but not vice versa: there are systematic chronological difference between CAIs and chondrules and between type I and type II chondrules.

Compositional Variations: Bulk chemical compositions of types A, B, and C CAIs, AOAs, type I, II, and Al-rich chondrules are examined on (Al₂O₃ + CaO) – MgO – SiO₂ (–FeO) ternary diagram(s). Equilibrium and kinetic condensation calculations are made with the same method as [2]. As pointed out previous workers, types A and B CAIs form a compositional trend, whereas type C CAIs are on another trend from type A CAIs toward SiO₂-rich composition, where some Al-rich chondrules are a little richer in MgO + SiO₂. We have previously shown that type I and II chondrules have a constant MgO + SiO₂ components, of which compositions are explained by kinetic condensation of liquid [2].

Nebular Processes: Types A and B CAIs are on the path of equilibrium condensation from gas with the solar composition. The gas from which about half of type A and B CAIs were extracted then condensed either solid at low pressures as AOA or liquid of type I chondrules at higher pressures. Precursor of Type II chondrules were rapid condensates of gas from which type I chondrule precursors were condensed.

Remelting and Compositional Modification: All the condensates were subjected to heating after 1–2 Ma; where considerable amounts of Mg and Si were evaporated to form a gas probably due to shock events, as shown by Al-rich chondrules in Semarkona [3]. Type C CAIs were formed from type A CAIs through condensation of Si- and Mg-components, which resulted in melting due to low solidus temperature of their compositions. The difference in the degree of condensation of Mg/Si resulted in variation of compositions of Al-rich chondrules. Type I chondrules were also melted in the same regions as Al-rich chondrules. Types A and B CAIs could be heated to melt or not melt, but they have suffered evaporation. Thus, almost all materials were reheated (and either melted or not melted) and recondensed Mg- and Si-components in the same region, but type II chondrules were exception, which were reheated to melt but neither evaporation nor condensation took place, which was possible by melting in a region with very high dust/gas ratios.

References: [1] Kurahashi E. 2005. 15th Goldschmidt Conference. [2] Nagahara H. et al. 2005. ASP Conference Series, vol. 341. pp. 456–468. [3] Nagahara H. et al. 2008. *Geochimica et Cosmochimica Acta* 72:1442–1465.

5200

NOBLE GASES AND COSMIC-RAY EXPOSURE AGES OF TWO MARTIAN SHERGOTTITES, RBT 04262 AND LAR 06319, RECOVERED IN ANTARCTICA

K. Nagao¹ and J. Park². ¹Laboratory for Earthquake Chemistry, Graduate School of Science, University of Tokyo, Bunkyo-ku, Tokyo 113-0033, Japan. E-mail: nagao@eqchem.s.u-tokyo.ac.jp. ²ARES, code KR, NASA, Johnson Space Center, Houston, TX 77058, USA.

Introduction: Paired Martian meteorites Robert Massif (RBT) 04261/04262, weighing 78.8 g and 204.6 g, respectively, are classified as olivine-phyric shergottites [1]. Mineralogical, petrological, geochemical studies have been reported [2–5]. Lu-Hf age of RBT 04262 was 255 ± 21 Ma [6]. Mineral separates of this meteorite show high concentrations of Xe and $^{129}\text{Xe}/^{132}\text{Xe}$ ratios with a small ^{129}Xe -excess, up to $^{129}\text{Xe}/^{132}\text{Xe} = 1.04$ [7]. In contrast, only limited information about the Larkman Nunatak (LAR) 06319 olivine-phyric shergottite (78.6 g) is available [8]. We report noble gas isotopic compositions of these shergottites. Noble gases were extracted by total melting at 1800 °C and stepwise heating (400–1800 °C) and measured on a modified VG5400(MS-II) at the University of Tokyo. Though stepwise heating experiment on LAR 06319 has not been finished, results will be presented at the meeting.

Results and Discussion: Both meteorites show similar noble gas isotopic compositions, e.g., isotopic ratios of Kr and Xe are very close to the terrestrial atmospheric values, no significant ^{129}Xe excess which is regarded as a signature of Martian atmosphere, and cosmogenic Ne is dominant and their $^{21}\text{Ne}/^{22}\text{Ne}$ ratios are rather low (<0.73). The Xe isotopic compositions in BRT 04262 obtained by us are consistent with those by Cartwright et al. [7].

Average cosmic-ray exposure age of 2.1 Ma was calculated for RBT 04262 based on the concentrations of cosmogenic ^3He , ^{21}Ne , and ^{38}Ar , production rates by [9] and elemental compositions [3]. The age is in the range for olivine-phyric shergottites [10]. If these production rates are applied to LAR 06319, about 50% longer exposure age (3.3 Ma) is obtained. The age belongs to those for basaltic shergottites [10]. K-Ar age for RBT 04262 was calculated as 880 and 820 Ma using the ^{40}Ar concentrations by stepwise heating and total melting methods, respectively, and K_2O concentration of 0.08 wt% [3]. The ages are much longer than the Lu-Hf age [6], which may be due to Martian atmosphere with high $^{40}\text{Ar}/^{36}\text{Ar}$ ratio trapped in this meteorite. U/Th- ^4He ages ranging in 60–86 Ma for RBT 04262 were calculated from the radiogenic ^4He concentrations (cosmogenic ^4He was subtracted from total ^4He concentrations) and concentrations of U and Th [3]. The ages are much shorter than the Lu-Hf [6] and K-Ar ages, which might have been caused by diffusion loss of He from the meteorite.

Acknowledgments: We thank Shih C.-Y. for preparation of the meteorite samples.

References: [1] McCoy T. and Reynolds V. 2007. Antarctic Meteorite Newsletter 30(1). [2] Greenwood J. P. 2008. Abstract #2011. 39th LPSC. [3] Anand M. et al. 2008. Abstract #2173. 39th LPSC. [4] Dalton H. A. et al. 2008. Abstract #2308. 39th LPSC. [5] Mikouchi T. et al. 2008. Abstract #2403. 39th LPSC. [6] Lapen T. J. 2008. Abstract #2073. 39th LPSC. [7] Cartwright J. A. et al. 2008. Abstract #2000. 39th LPSC. [8] McCoy T. et al. 2007. Antarctic Meteorite Newsletter 30(2). [9] Eugster O. and Michel Th. 1995. *Geochimica et Cosmochimica Acta* 59:177–199. [10] Okazaki R. and Nagao K. 2004. *Antarctic Meteorite Research* 17:68–83.

5246

MOST FERROAN FELDSPATHIC LUNAR METEORITE NWA 2200

H. Nagaoka¹, Y. Karouji¹, T. Arai², K. Shinotsuka³, M. Ebihara³, and N. Hasebe¹. ¹Research Institute for Science and Engineering, Waseda University, Tokyo 169-8555, Japan. E-mail: karouji@aoni.waseda.jp. ²Antarctic Meteorite Research Center, National Institute of Polar Research, Tokyo 173-8515, Japan. ³Department of Chemistry, Tokyo Metropolitan University, Tokyo 192-0397, Japan.

Introduction: Northwest Africa (NWA) 2200 is a feldspathic lunar meteorite (552 g) which was found in the Atlas Mountains, Morocco in August 2004 [1]. Kuehner et al. [2] reported that NWA 2200 is a polymict glassy impact-melt breccia with ferroan anorthosite (FAN) affinity based on petrological investigation. We examined bulk chemistry and mineralogy of NWA 2200 in order to characterize this meteorite in comparison with other feldspathic lunar meteorites and Apollo samples.

Mineralogy: Two polished thin sections were studied. NWA 2200 is composed of diverse mixtures of glassy clasts and lithic clasts embedded in a dark glassy matrix. Most lithic clasts display either fine-grained ophytic/dendritic texture, or granulitic texture. These clasts are dominated by plagioclase with minor olivine and pyroxenes. A relatively large, granulitic clast (1×0.75 mm in size) consists of plagioclase and olivine (~15 vol%) with smaller volume of orthopyroxene and augite. Fragments olivine and pyroxene ($<200 \mu\text{m}$) are widely distributed, though they are volumetrically minor. Plagioclase compositions (An_{96-97}) are consistent across the thin sections. Olivine compositions are mostly Fo_{54-57} with one Mg-rich grain (Fo_{74-75}). Pyroxenes are slightly more Mg-rich ($\text{Mg}\#_{66-70}$ for augite and $\text{Mg}\#_{60-64}$ for orthopyroxene) than olivines. Pyroxenes generally exhibit exsolution lamellae of submicron to a few μm in thickness. Pyroxene fragments with chemical zoning are Mg-rich ($\text{Mg}\#_{63-73}$) unlike those in mare basalts. The highly feldspathic nature and the presence of calcic plagioclase and relatively Fe-rich olivine/pyroxene indicate a derivation from FAN-suite rocks.

Bulk Chemistry: Measured major-element composition (in wt%) is: $\text{SiO}_2 = 42 \pm 2$, $\text{TiO}_2 = 0.18 \pm 0.01$, $\text{Al}_2\text{O}_3 = 30.0 \pm 0.4$, $\text{FeO} = 4.8 \pm 0.3$, $\text{MgO} = 3.5 \pm 0.6$, $\text{MnO} = 0.055 \pm 0.002$, $\text{CaO} = 17 \pm 1$, $\text{Na}_2\text{O} = 0.33 \pm 0.03$, and trace element (in $\mu\text{g/g}$) is: $\text{Sm} = 1.0 \pm 0.2$ (Errors are due to counting statistics [1σ]). Most elements were determined by neutron-induced prompt gamma-ray analysis (PGA). Our data about sodium and samarium of NWA 2200 are nearly consistent with those of Korotev et al. [3] ($\text{Na}_2\text{O} = 0.330$ wt%, $\text{Sm} = 1.09$ ppm). However, the iron content is slightly (~1 wt%) higher than that of Korotev et al. [3] ($\text{FeO} = 3.95$ wt%). While the chemical composition is within the range of known feldspathic lunar meteorites, the $\text{Mg}\#$ (56) is the lowest among them (57–80). Concentrations of Al_2O_3 , MgO , and FeO is consistent with those of Apollo FAN rocks ($\text{Al}_2\text{O}_3 = 28.0$ – 35.6 wt%, $\text{MgO} = 0.25$ – 5.11 wt%, and $\text{FeO} = 0.21$ – 5.89 wt%) [e.g., 4]. These chemical composition and mineralogy suggest that NWA 2200 is originated from FAN lithologies, in line with the previous study [2], and that it may represent the ferroan portion within the range of the FAN suite.

References: [1] Connolly et al. 2006. *Meteoritics & Planetary Science* 41:1383. [2] Kuehner et al. 2005. *Meteoritics & Planetary Science* 40:A88. [3] Korotev et al. 2008. Abstract #1209. 39th LPSC. [4] Heiken et al. 1991. *Lunar sourcebook*. Cambridge: Cambridge University Press.

5171

INFLUENCE OF THE SPECULAR REFLECTION ON SPECTROSCOPIC IDENTIFICATION OF THE LITHOLOGY OF LUNAR CENTRAL PEAKS

K. Nagasawa, S. Kawabe, and K. Saiki. Department of Earth and Space Science, Graduate School of Science, Osaka University, Osaka, Japan. E-mail: nagasawa@astroboy.ess.sci.osaka-u.ac.jp.

Introduction: Lunar surface is covered by mineral soils. The comparison between spectroscopic observation of the lunar surface from satellites and spectroscopic measurement of mineral powders at laboratory derives a global estimate of lunar lithologies. On the other hand, central peaks are believed to have exposed rock material from deep crust and their surface might not be covered with regolith materials. However, central peak's lithologies have been discussed based on laboratory spectra of mineral powders [1]. This study was performed in order to examine whether reflectance spectra of rocks change against emission angle or not.

Experiments: Three samples with different roughness, 16 mm × 16 mm × 4 mm in dimension, were made using Hawai'i basalt. All samples had been polished to have mirror surface. One of them named B2 was polished with #1000 sandpaper, another named B3 was polished with #80 sandpaper, and the remaining one named B1 was left smooth. The atomic force microscope (AFM) measurements were conducted to characterize their surface roughness.

Variable-viewing-geometry device which can change incident and emission angle of illumination was developed. The device is equipped with a cooling CCD Camera (Apogee ALTA U260), a Liquid Crystal Tunable Filter (VariSpec SNIR), and a Lens (Nikkor 50 mm). Samples were measured with 650, 750, 900, 950, and 1000 nm in wavelength and with 0, 10, 20, 25, 30, 35, 40, 50, 60 degrees in emission angle (incident angle was fixed to 30 degrees).

Results: The results of reflectance measurements show that the light with shorter wavelength is less reflected around specular reflection angle. Iron-bearing silicate minerals such as pyroxene and olivine have characteristic Fe²⁺ electronic transition absorption bands around 1 μm. In spectroscopic classification of lunar lithologies, the depth of absorption is diagnostic of the amount of mafic mineral. Despite this, all basalt samples look as if having no absorption band from 20 to 40 degrees in emission angle. In any other emission angle (0, 10, 50, 60 degrees), Fe²⁺ absorption bands were identified.

Discussion: Sunny side of the central peaks could have a slope near specular reflection angle. In Clementine UVVIS images we found some central peaks (e.g., Bettinus Crater) whose sunny side is more anorthositic than shadow side. Moreover the sunny side looks Fe-poor in FeO map [2]. It may suggest that the optical properties of such central peaks are much similar to rock surface rather than powder materials. Using topographic data of Terrain Camera onboard Selene (Kaguya), we could point out the area of misclassification of rock types. Such kind of filtering is useful for us to select the landing site of our next lunar probe Selene-2 planned to launch around 2015.

References: [1] Tompkins S. and Pieters C. M. 1999. *Meteoritics & Planetary Science* 34:25–41. [2] Lucey P. G. et al. 2000. *Journal of Geophysical Research* 105:20,297–20,305.

5133

RELICT CAI WITH HIGHLY FRACTIONATED OXYGEN ISOTOPES INSIDE A TYPE I CHONDRULE

K. Nagashima¹, A. N. Krot, and G. R. Huss. HIGP/SOEST, University of Hawai'i at Manoa, USA. ¹E-mail: kazu@higp.hawaii.edu.

FUN CAIs and platy hibonite crystals (PLACs) with highly fractionated O are very rare igneous objects, which also have no or small excess of ²⁶Mg (²⁶Mg*) due to decay of ²⁶Al [e.g., 1–3]. The only ²⁶Al-rich CAIs with highly fractionated O are forsterite-bearing CAI TE [4] and hibonite-rich CAI Kz1-2 [5]. Here we describe a compound object, ACF209-UH1#1, composed of a relict CAI with highly fractionated O inside a Type I chondrule from the CR chondrite Acfer 209. The CAI portion, 200 × 300 μm², has an igneous, concentric zoned texture and consists of grossite with perovskite inclusions, hibonite, and spinel. Spinel grains near the CAI-chondrule boundary appear to be corroded by chondrule melt and contain variable Cr contents. The host chondrule, ~500 μm in diameter, is composed of olivine, Al-rich, and Al-poor low-Ca pyroxenes, anorthitic plagioclase, and Fe,Ni-metal. Oxygen and Mg isotopes of ACF209-UH1#1 were measured in situ using the UH Cameca ims-1280 [3, 6, 7]. Data for chondrule olivine, low-Ca pyroxenes, and plagioclase are uniformly ¹⁶O-depleted ($\Delta^{17}\text{O} \sim -2.5\text{‰}$) and cluster slightly above CCAM line. CAI minerals are ¹⁶O-depleted and fractionated to varying degrees. Hibonite is the most fractionated ($\delta^{18}\text{O} = +73\text{‰}$) and ¹⁶O-depleted ($\Delta^{17}\text{O} = -0.5\text{‰}$). Data for grossite ($\delta^{18}\text{O} = +27\text{‰}$ and $+34\text{‰}$; $\Delta^{17}\text{O} = -7\text{‰}$ and -9‰) and spinel ($\delta^{18}\text{O} = +2\text{‰}$ to $+63\text{‰}$, $\Delta^{17}\text{O} = -8\text{‰}$ to -3‰) are less fractionated and define a linear array with slope of ~0.6, different from mass-dependent fractionation line. Data for Cr-bearing spinels near the CAI edge plot close to the chondrule minerals. We infer that this array recorded incomplete O-isotope exchange between highly fractionated CAI minerals and unfractionated chondrule melt. Oxygen compositions of the relict CAI indicate that it experienced significant evaporative loss from melt prior to incorporation into the host chondrule.

Chondrule anorthite shows no resolvable ²⁶Mg*, (²⁶Al/²⁷Al)₀ < 6 × 10⁻⁶. Spinel, hibonite, and grossite show very small intrinsic Mg-isotope fractionation and no resolvable ²⁶Mg*, (²⁶Al/²⁷Al)₀ < 4 × 10⁻⁷. The lack of ²⁶Mg* in CAI minerals could be due to either the absence of ²⁶Al in the original CAI, or Mg isotope exchange between the relict CAI minerals and/or the host chondrule melt. The preservation of ²⁶Mg excesses and deficits in relict hibonite inside chondrules [8] and rare occurrences of ²⁶Al-rich CAIs with highly fractionated O (TE, Kz1-2) support the former.

References: [1] Lee T. et al. 1980. *Geophysical Research Letters* 7: 493. [2] Ireland T. R. et al. 1992. *Geochimica et Cosmochimica Acta* 56: 2503. [3] Krot A. N. et al. 2008. Abstract #2162. 39th LPSC. [4] El Goresy A. et al. 1991. 22nd LPSC. p. 345. [5] Ushikubo T. et al. 2006. *Earth and Planetary Science Letters* 254:115. [6] Nagashima K. et al. 2008. Abstract #2224. 39th LPSC. [7] Makide K. et al. 2008. Abstract #2407. 39th LPSC. [8] Krot A. N. et al. 2006. *The Astrophysical Journal* 639:1227.

5028

CATHODOLUMINESCENCE CHARACTERIZATION OF SHOCKED K-FELDSPAR FROM BOSUMTWI METEORITE CRATER

Sz. Nagy¹, T. Okumura², and A. Gucsik³. ¹Eötvös University, Dept. Petrology and Geochemistry, H-1117 Budapest, Pázmány Péter sétány 1/c, Hungary. E-mail: ringwoodit@yahoo.com. ²Open Research Center, Okayama University of Science, 1-1 Ridai-cho, Okayama 700-0005, Japan. ³Max Planck Institute for Chemistry, P.O. Box 3060, D-55020 Mainz, Germany.

Introduction: The Bosumtwi crater in Ghana, West Africa, is centered at 06°30'N, 01°25'W. The 1.07 Myr old impact structure is situated in the Ashanti region, about 32 km east of Kumashi, the regional capital. The Bosumtwi impact structure is arguably the youngest and best-preserved terrestrial impact structure larger than 6 km in diameter [1]. The crater has a pronounced rim, with a rim to rim diameter of about 10.5 km. The structure forms a hydrologically closed basin [2]. The country rocks, mainly meta-graywacke, shale, and phyllite of the Early Birimian Supergroup and some granites of similar age, are characterized by two generations of alteration. Suedeite, which occurs in restricted locations to the north and to the south-southwest of the crater rim, contains melt fragments, diaplectic quartz glass, ballen quartz, and clasts derived from the full variety of target rocks [3]. No planar deformation features (PDFs) in quartz were found in the country rock samples. The Bosumtwi granites have tonalitic to quartz-dioritic compositions [3]. Here, we characterize shocked K-feldspar samples by means of cathodoluminescence (CL) microscopy and spectroscopy.

Samples and Methods: The samples employed here are K-feldspar specimens from syenite from a sampling location of Bosumtwi impact crater. They were prepared as polished thin sections coated with 20 nm thickness carbon. CL imaging and spectral analysis were performed in a SEM-CL system comprising a secondary electron microscope with a grating-type monochromator. Operating condition is set at an acceleration voltage of 15 kV with a beam current of 1.5 nA. The scanning electron microscope-cathodoluminescence (SEM-CL) measurements were carried out at Okayama University of Science, Okayama, Japan.

Results and Discussion: In the OM-image shows well characterized shock features in K-feldspar grains. In general, the edges of the planar fractures (PFs) are ending in wedge shape. The surface of some K-feldspar exhibits slightly kink banding effect. The investigation exhibited shear faults in K-feldspar grains, and abundant planar deformation features (PDFs) lamellae. The characteristic cathodoluminescence spectral features of shocked K-feldspar samples are emission bands at 450 (Al-O⁻-Al center), 500 (Si-O-...M²⁺), and 680 nm (Fe³⁺). In the SEM-CL images, PDFs, and microtwinning patterns are also discernible, indicating that this sample was subjected under the high shock pressure regime (around 15 GPa).

Consequently, cathodoluminescence microscopy and spectroscopy should be a powerful technique to characterize shock-induced microdeformations such as PDFs and microtwinning in minerals from the Lake Bosumtwi impact structure.

References: [1] Scholz et al. 2002. *Geology* 30:939–942. [2] Koeberl et al. 2007. *Meteoritics & Planetary Science* 42:483–511. [3] Karikari et al. 2007. *Meteoritics & Planetary Science* 42:513–540.

5243

SHAPES OF COSMIC SPHERULES: WHAT DO THEY TELL US?

T. Nakamoto¹, M. Doi¹, T. Nakamura², and Y. Yamauchi². ¹Department of Earth and Planetary Sci., Tokyo Institute of Technology, Tokyo 152-8551, Japan. E-mail: nakamoto@geo.titech.ac.jp. ²Department of Earth and Planetary Sci., Kyushu University, Fukuoka 812-8581, Japan.

Introduction: Cosmic spherules are products of dust-particle heating in the Earth's atmosphere: dust particles are heated by the gas friction and melted, and re-solidified to form spherules. Tsuchiyama et al. [1] have examined 3-D shapes of cosmic spherules and found that they have spherical, prolate and oblate shapes. Since the spherules melt in the Earth's atmosphere, the mechanism that forms such shapes should be related to the atmosphere. In this work, we examined some mechanisms that may form observed shapes of cosmic spherules, and found that some mechanisms may work well but they cannot explain the degree of deformation.

3-D Shapes of Cosmic Spherules: We examined more than 500 cosmic spherules collected from Antarctica. We measured three axial radii of once molten stony cosmic spherules in a radius range from 40 μm to 120 μm . We have found that there are spherical, oblate, and prolate shapes in the cosmic spherule. When those shapes are approximated by triaxial ellipsoids, we can define the degree of deformation. Some of the spherules have the degree of deformation as large as 0.4 (0 means a perfect sphere and 1 means a thick less needle or a disk), though many of them have 0.1 or less.

After the measurement of sizes, each spherule was polished to have flat surface and analyzed for major element concentrations using an electron microprobe analyzer.

A Model: We have developed a model to describe the motion of dust particles in the atmosphere (this part is similar to the one by Love and Brownlee [2]) and evaluate the gas ram pressure on the molten particle. Using the obtained ram pressure, we calculate the hydrodynamic motion of molten material in the particle and estimate the shape of the particle at the moment of the re-solidification [3, 4]. If the particle has a spin (rotation), the particle is expected to become prolate or oblate shape, depending on the direction of the rotation axis and the rotation rate.

Results and Discussions: The current model can successfully explain the formation of both prolate and oblate shapes. However, the model cannot reproduce the observed degree of deformation: the predicted degree of deformation is 0.1 or less. We examined the effects of different surface tension and viscosity, but we concluded that they were not able to explain the observed deformation. Thus, the discrepancy between the measured deformation and the model prediction is left unsolved. Some unknown mechanisms may play a role.

References: [1] Tsuchiyama A. et al. 2004. *WCPD* 9033–9034. [2] Love S. G. and Brownlee D. E. 1991. *Icarus* 89:26–43. [3] Sekiya M. et al. 2003. *Progress of Theoretical Physics* 109:717–728. [4] Miura H. et al. 2007. 38th LPSC. pp. 1505–1506.

5124

MINERALOGICAL AND STABLE ISOTOPE SIGNATURES OF EL-QUSS ABU SAID CM2 CARBONACEOUS CHONDRITE: PRISTINE MATERIAL FROM OUTER ASTEROID BELT

T. Nakamura¹, T. Noguchi², R. Okazaki¹, K. Jogo¹, and K. Ohtsuka³.
¹Department of Earth and Planetary Sciences, Kyushu University, Fukuoka 812-8581, Japan. E-mail: tomoki@geo.kyushu-u.ac.jp. ²Department of Materials and Biological Sciences, Ibaraki University, Mito, Ibaraki 310-8512, Japan. ³Tokyo Meteor Network, Setagaya, Tokyo 155-0032, Japan.

The parent asteroids of CM chondrites formed from ice and small solid particles having been present beyond the snowline. However, the initial mineralogical and isotopic properties of the solid particles have changed during post-accretionary aqueous alteration. The initial dust characteristics of CM chondrites are important for the understanding of material continuum between outer asteroid and Kuiper belt regions [e.g., 1]. We have characterized mineralogy and isotope signatures of El-Quss Abu Said CM2 chondrite [2] and found that it is a pristine material from the outer asteroid belt.

El-Quss Abu Said shows texture of typical CM2 chondrites. Type IA chondrules are abundant, but many type IIAB chondrules remain unaltered with olivine up to Fo₇₀. Limited areas of mesostasis glass in chondrules escape alteration, suggestive of weak aqueous alteration. 16 type I and 15 type II chondrules were analyzed using SIMS at Kyushu University. Oxygen isotope compositions distribute on the slope = 1 line between -10 and +10 permil in $\delta^{18}\text{O}$ and has a tendency that the type I has $\delta^{18}\text{O}$ lower than the type II. Four CAIs were analyzed and the oxygen composition varies from -45 and -20 permil in $\delta^{18}\text{O}$, but each CAI shows a narrow compositional range, suggesting that the composition was not disturbed during aqueous alteration.

Transmission electron microscope observation of matrix showed that it contains many primary anhydrous silicates that escaped alteration. The silicates are mostly Mg-rich olivine and low-Ca pyroxene up to a few hundreds nm in size. Two enstatite whiskers with length of approximately 500 nm were discovered: they elongated to a-axis with many (100) stacking disorder. The morphology and crystallographic features indicate they are condensation from products a nebula gas. The major element abundances of matrix primary silicates are also interesting. Many FeO-poor olivines are enriched in MnO, whose concentrations are comparable to or even higher than FeO: they are LIME olivine found in anhydrous IDPs [3]. These mineralogical properties of matrix indicate that it preserves the records of primitive nebular dust. This is also suggested from isotope signatures: (1) the oxygen composition of matrix falls on the slope = 1 line and (2) Ar-rich noble gases remain, although they are easily escaped during alteration [4].

References: [1] Ishii H. A. et al. 2008. *Science* 319:447–450. [2] Grossman J. N. 2000. *The Meteoritical Bulletin*, no. 84. *Meteoritics & Planetary Science* 35:A199. [3] Klöck et al. 1989. *Nature* 339:126–128. [4] Yamamoto et al. 2006. *Meteoritics & Planetary Science* 41:541–551.

5083

NOBLE GAS ANALYSES OF INDIVIDUAL CHONDRULES FROM THE ALLENDE CV3 CHONDRITE

Y. Nakamura, K. Bajor, D. Nakashima, and K. Nagao. Laboratory for Earthquake Chemistry, Graduate School of Science, University of Tokyo, Bunkyo-ku, Tokyo 113-0033, Japan. E-mail: nakamura@eqchem.s.u-tokyo.ac.jp.

Introduction: Previous study discovered that some chondrules in an enstatite chondrite contain high concentrations of Ar-rich gases so called trapped noble gases [1]. They suggest that the subsolar gases may reflect implantation of high energetic particles into the chondrule precursors and support X-wind model. However, other previous studies on chondrules have shown that trapped noble gas concentrations of the most chondrules are low to zero [2–5]. For the investigation of trapped noble gases, stepwise heating method is useful for decomposition of various components with different origins. Here we present the results of noble gas analyses of individual chondrules with stepwise heating extraction.

Experimental: A fragment of the Allende CV3 chondrite, approximately 7 g, was crushed by freeze-thaw method. We picked up some chondrules and treated with HNO₃ in an ultrasonic bath in order to remove surrounding matrix. After we selected some chondrules without matrix, noble gases were extracted by heating stepwisely, and measured with the modified VG5400 mass spectrometer at the University of Tokyo. We will report results obtained with a miniature furnace designed for small samples.

Results and Discussion: The concentrations of noble gases in the chondrules are in the range of those in the previous studies [2–5], suggesting that the surrounding matrix is mostly removed by the HNO₃ treatment. The isotopic ratios show that noble gases in the individual chondrules are dominated by cosmogenic, radiogenic, and terrestrial components. He isotopic ratios can be explained by a mixture of cosmogenic He and radiogenic ⁴He. The low ²¹Ne/²²Ne ratios (~0.7) observed in the low temperature fractions may be indicative of Na-spallation Ne. The ³⁸Ar/³⁶Ar ratios for some chondrules are lower than that for terrestrial air, which is attributed to neutron capture on ³⁵Cl. Additionally, samples show excesses of ^{79,81}Br-derived ^{80,82}Kr, ¹²⁷I-derived ¹²⁸Xe, and ¹²⁹Xe derived from ¹²⁹I decay. Xe isotopic ratios show fissionogenic component derived from ²³⁸U or ²⁴⁴Pu.

The cosmic-ray exposure ages of individual chondrules and Allende bulk are roughly the same within uncertainties, suggesting no pre-compaction irradiation to the chondrules.

Noble gas signatures of the Allende chondrules are different from those of the enstatite chondrite chondrules [1]. This may suggest two different processes of chondrules. 1) Degassing occurred during formation of chondrules from the precursors with trapped noble gases. 2) Precursors had degassed before chondrule formation. Thus, it is inferred that the chondrules from Allende had gone through different formation processes from the chondrules in the enstatite chondrite [1].

References: [1] Okazaki R. et al. 2001. *Nature* 412:795–798. [2] Swindle T. et al. 1983. *Geochimica et Cosmochimica Acta* 47:2157–2177. [3] Kim J. S. and Marti K. 1994. *Meteoritics* 29:482. [4] Miura Y. N. and Nagao K. 1997. 22nd Symposium on Antarctic Meteorites. pp. 118–120. [5] Vogel N. et al. 2004. *Meteoritics & Planetary Science* 39:117–135.

5247

MINERALOGY OF INTERPLANETARY DUST PARTICLES FROM THE COMET GRIGG-SKJELLERUP DUST STREAM COLLECTIONS

K. Nakamura-Messenger¹, L. P. Keller¹, S. Messenger¹, S. J. Clemett¹, M. E. Zolensky¹, R. L. Palma^{2,3}, R. O. Pepin³, and S. Wirick⁴. ¹NASA/JSC, USA. E-mail: keiko.nakamura-1@nasa.gov. ²Minnesota State University, Minnesota, USA. ³University of Minnesota, Minnesota, USA. ⁴State University, New York at Stony Brook, USA.

Introduction: Comet 26P/Grigg-Skjellerup was identified as a source of an Earth-crossing dust stream with low Earth-encounter velocities, with peak anticipated fluxes during April 2003 and 2004 [1]. In response to this prediction, NASA performed dedicated stratospheric dust collections using high altitude aircraft to target potential interplanetary dust particles (IDPs) from this comet stream. Low noble gas abundances [2], high abundances of large deuterium enrichments [3] and presolar grains [4] in IDPs from this collection are consistent with an origin from the comet Grigg-Skjellerup [1]. Here we report a mineralogical study of 6 IDPs from 4 different clusters from the Grigg-Skjellerup collections, L2054 and L2055, using a JEOL 2500SE field-emission scanning TEM (FE-STEM).

Results: All cluster IDPs we observed in this study are very porous fine grained aggregates. We did not observe well developed magnetite rims on the surfaces of the mineral grains, suggesting that these samples were not strongly heated during atmospheric entry. Solar flare tracks were not detected in any mineral grains, either, consistent with a short space exposure time. L2055I3 of cluster#7 (4 μm) shows typical characteristics of anhydrous IDPs, except that it was found to contain a new mineral (stoichiometric MnSi) [5]. Major components of I3 include GEMS (glass with embedded metal and sulfides) grains, and 20–200 nm sized enstatite, forsterite and sulfides bound together by carbonaceous material. Enstatite and forsterite grains contain up to 5 wt% of MnO, typical of LIME (low-Fe Mn-enriched) olivines and pyroxenes in other IDPs [6]. A related fragment, L2055L1 from the same cluster#7 (9 μm) only consists of GEMS grain aggregates embedded in carbonaceous material. L2054I2 cluster#2 (8 μm), on the contrary, is dominated by crystalline grains and only a few GEMS grains are observed. L2054O2 from cluster #2 is a 10 μm IDP and 85% of its volume is carbonaceous material containing few mineral grains. L2054L2 (3 μm) and L2054I4 (7 μm) both from cluster #4 are as porous as typical anhydrous IDPs but consist of Al oxides.

Although the mineralogy of these Grigg-Skjellerup IDPs is similar to components of anhydrous IDPs, they show a remarkable mineralogical diversity. More importantly, these IDPs are devoid of solar flare tracks, yet do not appear to have been strongly heated, consistent with short space exposure ages expected for particles from the Grigg-Skjellerup dust stream.

References: [1] Messenger S. 2002. *Meteoritics & Planetary Science* 37:1491. [2] Palma R. L. et al. 2005. Abstract #5012. *Meteoritics & Planetary Science* 40:A120. [3] Nittler L. R. et al. 2006. Abstract #2301. 37th LPSC. [4] Nguyen A. N. et al. 2007. Abstract #2332. 38th LPSC. [5] Nakamura-Messenger K. 2008. Abstract #2103. 39th LPSC. [6] Klöck W. et al. 1989. *Nature* 339:126.

5032

IN SITU OBSERVATION OF DIAMONDS IN UREILITES BY RAMAN SPECTROSCOPY

Y. Nakamuta. Kyushu University Museum, Kyushu University, Japan. E-mail: nakamuta@museum.kyushu-u.ac.jp.

Introduction: Ureilites are unique in containing relatively large amounts of C occurring as graphite or diamond [1]. The mode of occurrence and X-ray properties of carbon minerals in ureilites show that diamond in ureilites formed by high-pressure conversion of graphite that crystallized during igneous or metamorphic processes on an ureilite parent body or bodies [2]. Under an optical microscope ureilites show that they have been shocked at variable degrees and the appearance of diamonds in them varies in a wide range. In this study, each diamond grain showing different appearance was analyzed by Raman spectroscopy together with graphite coexisting with them.

Samples and Experiments: Polished thin sections of eight Antarctic ureilites, Y-74123, A-77257, Y-8448, A-881931, Y-74659, Y-74130, Y-792663, and Y-74154 and Goalpara ureilite were observed under an optical microscope. The sizes of C-rich grains are about 1–2 μm in length and 0.1–0.05 μm in width. In each grain, diamond crystals can be observed in high relief under an optical microscope of high magnification.

MicroRaman spectra were recorded with a Jobin-Yvon T64000 triple-grating spectrometer equipped with confocal optics and a nitrogen-cooled CCD detector. A microscope was used to focus the 514.5 nm Ar excitation laser beam to a 1 μm spot. Accumulations lasting 120 to 600 s were made. The laser power on the sample was 2 mW.

Results: In relatively weakly shocked ureilites, i.e., Y-74123, A-77257, Y-8448, and A-881931, diamonds occur as small granular grains of about a few micrometer or less in size in graphite. They show sharp Raman spectra at around 1332 cm^{-1} on the background which rise toward the high wave number side.

In highly shocked ureilites, i.e., Y-74130, Y-792663, Y-74154, and Goalpara, a bulky hard material of about few tens of micrometers in size is found which shows a very broad Raman band spreading over the positions between 1650 and 1200 cm^{-1} with two broad peaks at around 1600 and 1330 cm^{-1} . X-ray powder diffraction pattern taken by a Gandolfi camera shows that this material is an intimate mixture of lonsdaleite-like mineral and graphite. Small granular grains which show sharp Raman spectra of diamond are also found. However, they are restricted in their distribution to the area near metal veinlets in a C-rich grain. The result reveals that metal played an important role in the formation of well crystallized diamonds in ureilites as suggested by [3].

References: [1] Goodrich C. A. 1992. *Meteoritics* 27:327–352. [2] Nakamuta Y. and Aoki Y. 2000. *Meteoritics & Planetary Science* 35:487–493. [3] Nakamuta Y. and Aoki Y. 2001. *Meteoritics & Planetary Science* 36:A146.

5079

NOBLE GASES IN INDIVIDUAL GLASSY SPHERULES FROM THE SAU 290 CH3 CHONDRITE

D. Nakashima and K. Nagao. Laboratory for Earthquake Chemistry, Graduate School of Science, University of Tokyo, Hongo, Bunkyo-ku, Tokyo 113-0033, Japan. E-mail: naka@eqchem.s.u-tokyo.ac.jp.

Introduction: Numerous glassy spherules (50–200 μm) were found in the SaU 290 CH3 chondrite. The spherules are considered to be chondrules. Since SaU 290 is the solar-gas bearing meteorite [1], it could be possible that the spherules have been exposed to solar winds and cosmic-rays on the parent body. Here we report the results of noble gas analyses of the individual glassy spherules.

Noble Gas Analysis: More than 300 of glassy spherules were picked up from the crushed samples of SaU 290 (~1.5 g). Most of them are transparent, some are opaque under an optical microscope. Four opaque spherules and thirteen transparent spherules (100–150 μm ; 2.6–10.4 μg) were selected for noble gas analysis. SEM-EDX shows that the spherules have low-Ca pyroxene like chemical compositions (Fe poor). Noble gases in the individual spherules were extracted by a Nd-YAG laser system, and the purified noble gases were analyzed with the “MS-III” noble gas mass spectrometer at the University of Tokyo.

Results and Discussion: Concentrations of ^4He and ^{20}Ne are one or two orders of magnitude lower than those of the bulk sample [1]. Isotopic ratios of He and Ne show no clear evidence for solar wind implantation, suggesting that the spherules may have not been exposed to solar winds or may have lost the implanted solar noble gases due to later parent body processes. The ^3He concentrations are almost constant ($2.3 \pm 0.4 \times 10^{-8} \text{ cm}^3/\text{g}$ on average; 2σ) except for a spherule ($4.8 \pm 0.6 \times 10^{-8} \text{ cm}^3/\text{g}$; 2σ). Assuming that He in the spherules consists of cosmogenic He and radiogenic ^4He , the ^3He is essentially entirely cosmogenic. Considering the production rate of cosmogenic ^3He is independent from the target element chemistry, the cosmogenic ^3He excess is indicative of parent body exposure. Since SaU 290 is the solar-gas-bearing meteorite, the constituent materials should have been exposed to solar winds and cosmic rays in various depths on the parent body. The spherule with cosmogenic ^3He excess would have been located at the active zone of cosmic rays for longer duration than the other spherules. It could be also possible that the spherules with lower ^3He concentrations had experienced partial loss of He during transit to the Earth and/or on the parent body. Since all the spherules we studied are from the small sample (~1.5 g), it is unlikely that the only one spherule with ^3He excess avoided the He partial loss during transit to the Earth. The latter case is more likely, which leads to cosmic ray irradiation to the spherules on the parent body.

The most spherules contain lower concentrations of ^{40}Ar than that in the bulk sample ($1.0 \times 10^{-5} \text{ cm}^3/\text{g}$; [1]), which could be attributed to low K contents and/or ^{40}Ar diffusive loss due to later parent body processes. Only two spherules show high concentrations of ^{40}Ar ($2.4\text{--}3.5 \times 10^{-4} \text{ cm}^3/\text{g}$) as well as high $^{40}\text{Ar}/^{36}\text{Ar}$ ratios (6000–9300). Assuming the gas retention age is 4.5 Ga, the two spherules should contain 0.3–0.45 wt% of K.

References: [1] Park J. et al. 2005. 29th Symposium on Antarctic Meteorites. pp. 69–70.

5078

NOBLE GASES IN ANGRITES NWA 2999/4931, NWA 4590, AND NWA 4801: EXPOSURE AGES AND EVIDENCE OF FISSIOGENIC Xe

D. Nakashima¹, K. Nagao¹, and A. J. Irving². ¹Laboratory for Earthquake Chemistry, University of Tokyo, Hongo, Bunkyo-ku, Tokyo, Japan. E-mail: naka@eqchem.s.u-tokyo.ac.jp. ²Department of Earth and Space Sciences, University of Washington, Seattle, WA, USA.

Introduction: NWA 2999 (and petrologically similar NWA 4931), NWA 4590, and NWA 4801 are classified as angrites based on their mineral compositions and oxygen isotopic compositions [1]. The very ancient formation ages of the angrites (4562–4558 Ma; [2]) would allow us to expect the presence of decay products of now extinct nuclides such as ^{244}Pu and ^{129}I . Here we report results of noble gas analyses of the four angrites.

Results and Discussion: Isotopic ratios of He, Ne, and Ar are dominated by the spallogenic component and radiogenic ^4He and ^{40}Ar . Solar-like noble gases, as found in D’Orbigny glass [3], were not observed. The ^{40}Ar concentrations ($0.5\text{--}3.5 \times 10^{-6} \text{ cm}^3/\text{g}$) are lower than those in chondrites ($>10^{-5} \text{ cm}^3/\text{g}$), suggesting the low K contents and/or later parent body processes. Kr appears to be a mixture of spallogenic Kr and a terrestrial Kr contaminant. Xe is dominated by spallogenic Xe, fissionogenic Xe, and a terrestrial Xe contaminant. The spallation-corrected $^{129}\text{Xe}/^{132}\text{Xe}$ ratios show no ^{129}Xe excess derived from ^{129}I . Heavy isotopes of spallation-corrected Xe appear to be the mixtures of atmospheric Xe and ^{244}Pu -Xe [4]. This indicates that fissionogenic Xe is mostly derived from ^{244}Pu , which reflects a relatively short interval between the end of nucleosynthesis and formation of these four angrites. NWA 2999 and NWA 4931 have lower fissionogenic ^{136}Xe concentrations ($1.8\text{--}2.6 \times 10^{-12} \text{ cm}^3/\text{g}$) than those in the other two ($1.0\text{--}2.5 \times 10^{-11} \text{ cm}^3/\text{g}$), suggesting that the former two angrites are relatively younger (with respect to ^{136}Xe gas retention age), if the abundance of the reference isotope such as ^{238}U or ^{150}Nd is comparable among the four specimens.

The ^{81}Kr -Kr cosmic-ray exposure ages (CRE ages; $\pm 1\sigma$) are $73.4 \pm 6.6 \text{ Ma}$, $26.4 \pm 1.2 \text{ Ma}$, $31.6 \pm 1.5 \text{ Ma}$, and $69.6 \pm 11.2 \text{ Ma}$ for NWA 2999, NWA 4590, NWA 4801, and NWA 4931. The indistinguishable ^{81}Kr CRE ages of NWA 2999 and NWA 4931, along with the strong petrologic similarities of these specimens, indicates that they are paired. Previously a ^{10}Be exposure age of $0.6 \pm 0.1 \text{ Ma}$ was obtained for the angrite LEW 87051 [5], and reported noble gas CRE ages for other angrites are 5.3, 6.1, 11, 15, 17.6, and 55.5 Ma [3, 6]. The observed large and fairly uniform spread in CRE ages among 10 analyzed angrites (0.6 to 71 Ma) implies that the angrite parent body is large enough to have been struck and sampled episodically for a very long time.

References: [1] Kuehner S. et al. 2006. Abstract #1344. 37th LPSC. Kuehner S. and Irving A. 2007. Abstract #1522. 38th LPSC; Irving A. and Kuehner S. 2007. Workshop on the Chronology of Meteorites and the Early Solar System. pp. 74–75. [2] Amelin Y. and Irving A. 2007. Workshop on the Chronology of Meteorites and the Early Solar System pp. 20–21. [3] Busemann H. et al. 2006. *Geochimica et Cosmochimica Acta* 70:5403–5425. [4] Lewis R. 1975. *Geochimica et Cosmochimica Acta* 39:417–432. [5] Nishiizumi K. et al. 1996. *Meteoritics & Planetary Science* 31:A99–100. [6] Lugmair G. and Marti K. 1977. *Earth and Planetary Science Letters* 35:273–284; Eugster O. et al. 1991. *Geochimica et Cosmochimica Acta* 55:2957–2964; Weigel A. et al. 1997. *Geochimica et Cosmochimica Acta* 61:239–248; Miura Y. N. et al. 2004. 28th Symposium on Antarctic Meteorites. pp. 50–51.

5010

EVALUATION OF DEHYDRATION MECHANISM DURING HEATING OF HYDROUS ASTEROIDS BASED ON EXPERIMENTALLY HEATED CM CHONDRITES

A. Nakato¹, T. Nakamura¹, F. Kitajima¹, and T. Noguchi². ¹Department of Earth and Planetary Sciences, Kyushu University, Fukuoka, Japan. E-mail: aiko@geo.kyushu-u.ac.jp. ²Department of Materials and Biological Sciences, Ibaraki University, Ibaraki, Japan.

Based on the evidence derived from spectroscopic observation and meteorite analysis, some C type asteroids were heated and dehydrated at a certain period after aqueous alteration [e.g., 1]. On the other hand, many hydrous carbonaceous chondrites show evidence of dehydration due to high-temperature heating in the parent asteroids [e.g., 2]. In order to reproduce processes having occurred during the heating, we experimentally heated Murchison CM chondrite and compared the experimental products with Belgica (B-) 7904 CM chondrite, a meteorite from a dehydrated asteroid, in respect to characteristic properties with different reaction rates to form. The heating experiments were performed at 600 °C for 1 hr (600 °C/1 hr), 600 °C/96 hr, 900 °C/1 hr, 900 °C/96 hr under controlled oxygen partial pressures. The products were characterized by various analytical methods.

Based on synchrotron XRD analysis, all the four products show decomposition of serpentine and tochilinite. The combination and crystallinity of secondary minerals in B-7904 are similar to those in the product of 900 °C/1 hr, rather than 900 °C/96 hr that contains abundant secondary pyroxene. Crystallinity of secondary olivine are estimated from full width at half maxima (FWHM) of (031) and (120) olivine reflections. B-7904 has FWHM intermediate between 900 °C/1 hr and 900 °C/96 hr products. The degree of dehydration is also measured by increase of totals in EPMA analysis. B-7904 is well dehydrated and its total is comparable to those of 600 °C/96 hr, 900 °C/1 hr and 900 °C/96 hr products. Primary olivine grains at outer edges of chondrules in B-7904 ubiquitously show narrow Fe-Mg zoning. The product heated at 900 °C/96 hr best reproduces the zoning profile of B-7904. Calculated Fe-Mg diffusion constant is close to the value (2×10^{-17} m²/s for Fo₈₆ at 900 °C) reported in a previous experimental study [3]. Thermal evolution of amorphous carbonaceous material was estimated by using Raman spectroscopy. All Raman spectra of B-7904, Murchison and the products show the D1, D2, and G bands. Based on the intensity of the D1 band, the maturation grade of B-7904 is similar to that of 900 °C/1 hr and 900 °C/96 hr products. In addition, the presence or absence of some temperature-sensitive minerals [2] in B-7904 is used to constrain the temperature to be higher than 700 °C but lower than 890 °C.

Based on these results, the ranges of temperature and time for heating of B-7904 are estimated: from 10 to 10³ days at 700 °C to 1 to 10² hours at 890 °C. The obtained durations are much shorter than those expected for internal heating that keeps maximum temperature over million years. Therefore, it is unlikely that the short-lived radionuclide ²⁶Al is a heat source for dehydration of B-7904. Instead short-duration local heating, arose from impacts or solar radiation, is more promising heat source.

References: [1] Hiroi T. et al. 1993. *Science* 261:1016–1018. [2] Kimura M. and Ikeda Y. 1992. *Proceedings of the NIPR Symposium on Antarctic Meteorites* 5:74–119. [3] Misener D. J. 1974. In *Geochemical transport and kinetics*, edited by Hofmann A. W. et al. Washington, D.C.: Carnegie Institution of Washington. pp. 117–129.

5150

MARTIAN ORIGIN OF CALCITE IN DHOFAR 019

T. Nakazato¹, M. Kayama¹, H. Nishido¹, K. Ninagawa², A. Gucsik³, and Sz. Bérczi⁴. ¹Research Institute of Natural Sciences, Okayama University of Science, 1-1 Ridaicho, Okayama 700-005, Japan. E-mail: nakazato@rins.ous.ac.jp. ²Department of Applied Physics, Okayama University of Science, 1-1 Ridaicho, Okayama 700-005, Japan. ³Max Planck Institute for Chemistry, Department of Geochemistry, Mainz, Germany. ⁴Eötvös University, Institute of Physics, Dept. G. Physics, Cosmic Materials Space R. Group, H-1117 Budapest, Hungary.

Introduction: Dhofar 019 found in Oman is classified as an olivine bearing basaltic shergottite. It consists of subhedral grain of pyroxene (pigeonite and augite), olivine, and feldspar mostly converted to maskelynite and minor phases, with terrestrial secondary phases. Calcite occurs in it as a small grain coexisted with merrillite and olivine, and interstitial filling in olivine crack. Although carbonates have been recognized in several Martian meteorites such as ALH 84001 [1], most of the minerals have been interpreted as a weathering product after the fall on the Earth. The calcite in Dhofar 019 meteorite has been referred to as a secondary mineral [2], whereas it has not been investigated in detail. In this study, cathodoluminescence (CL) and Raman spectroscopy clarify the origin of Dhofar 019 calcite as Martian.

Samples and Methods: Two polished thin sections of Dhofar 019 meteorite were employed for CL and Raman measurements. Color CL images were obtained by Luminoscope ELM-3R (Nuclide) at accelerating voltage of 15 kV and beam current of 0.5 mA. The CL spectral measurements were carried out using a cathodoluminescence scanning microscopy (SEM-CL), SEM (JEOL: JSM-5400) combined with a grating monochromator (OXFORD: MonoCL2), in the range from 300 to 800 nm at accelerating voltage of 15 kV and beam current of 1.0 nA. The Laser Raman spectroscopy are carried out using a NRS-2100 (JASCO CO.) with an Ar laser of 514.5 nm wave length. The sample excitation and Raman scatter collection was performed using a 100× optical lens on the Raman microscope.

Results and Discussion: The calcite has a dull orange emission with homogeneous feature in color CL images. CL spectra of the calcite have two broad peaks at around 420 nm related to defect center and at around 620 nm assigned to Mn²⁺ impurity center. CL of terrestrial calcite generally has a pronounced red to orange emission due to Mn²⁺ activator without blue emission. This fact indicates that the calcite in Dhofar has a high density of the defect in its lattice, suggesting different genetic condition from terrestrial calcite. The calcite in Dhofar 019 gives very weak Raman peaks at around 142 cm⁻¹, 264 cm⁻¹, and 1085 cm⁻¹, whereas Raman spectra of terrestrial calcite exhibit pronounced peaks at around 154 cm⁻¹, 281 cm⁻¹, and 1089 cm⁻¹ with unambiguous peak shift by comparison with the calcite in Dhofar 019. Shock pressure of this meteorite has been estimated at approximately 40 GPa on the basis of formation condition of the observed shocked plagioclase. These facts imply that the calcite in Dhofar 019 is of Martian origin.

Acknowledgements: This work is carried out in part under the Viting Researcher's Program of the Reactor Institute, Kyoto University.

References: [1] McKay D. et al. 1996. *Science* 273:924–930. [2] <http://curator.jsc.nasa.gov/atmet/mmc/index.cfm>.

5193

LUNAR FAR SIDE GRAVITY FROM THE KAGUYA (SELENE) MISSION AND DICHOTOMY OF THE MOON

N. Namiki¹, H. Hanada², T. Iwata³, and RSAT and VRAD teams. ¹Earth Planet. Sci., Kyushu University, Japan. E-mail: geo.kyushu-u.ac.jp. ^{2,3}JAXA, Japan.

Introduction: Current lunar gravity field models include large uncertainties on the far side of the Moon. This is because synchronous rotation of the Moon inhibits a direct link between a ground tracking station and a spacecraft over the far side. In order to compensate for the lack of tracking data on the far side, all previous workers [e.g., 1] advocated an a priori constraint [4] in processing tracking data to produce the global lunar gravity field.

RSAT Experiment: In order to track a spacecraft over the lunar far side, we developed a satellite-to-satellite Doppler tracking sub-system (RSAT) on KAGUYA (SELENE) [2]. Main function of RSAT is to relay Doppler tracking signals between the main orbiter (MAIN) over the far side and ground-based antenna. When MAIN is orbiting over the far side of the Moon, tracking signal in S band transmitted from Usuda Deep Space Center of JAXA is relayed by RSAT-1 on Rstar to RSAT-2 on MAIN. Then RSAT-2 returns the tracking signal to RSAT-1, and RSAT-1 translates the S band signal into X band to downlink a coherent Doppler signal to UDSC. We call this tracking system four-way Doppler measurement. RSAT realizes the first direct observation of the gravity field over the far side of the moon [5, 6].

SELENE Gravity Model: Most recent lunar gravity field model from KAGUYA (SGM90d) enables global gravity anomaly mapping of the Moon up to degree as high as . Gravity anomaly of SGM90d on near side is almost identical with that of Lunar Prospector, however, gravity anomaly map on far side reveals dramatic improvement. Gravity signatures over farside basins, such as Korolev, Mare Moscovice, Mendeleev, Apollo, that used to be recognized as linear features are now identified as circular anomaly. Presently equatorial area have been better covered by four-way Doppler than at high latitude, however, entire far side will be covered by the end of nominal mission [5, 6].

Lunar Dichotomy: New gravity model reveals a marked difference of gravity signatures between nearside and farside. It has been well known that nearside gravity anomaly is dominated by mascons, that is, positive gravity anomaly indicating mantle uplift beneath basins [7]. In contrast, farside gravity field is characterized by rings of negative free-air anomaly over basins and large craters. Bouguer gravity anomaly map shows that such negative anomaly can be mostly attributed to topographic depression of basin, and that contribution of Moho variation is minor. Thus SGM90d suggests that elastic thickness of lithosphere was thin on near side while was thick on far side 3.9 Gy ago, and propose an important constraint on the origin of dichotomy.

References: [1] Konopliv A. S. et al. 2001. *Icarus* 150:1–18. [2] Namiki N. et al. 1999. *ASR* 23:1817–1820. [3] Iwata T. et al. 2004. International Association of Geodesy Symposia, vol. 128. pp. 157–162. [4] Hayashi et al. 1994. *Proceedings of the IEEE* 82:646–657. [5] Goossens S. and Matsumoto K. 2007. *ASR* 40:43–50. [6] Matsumoto K. et al. 2007. *ASR*, doi:10.1016/j.asr.2007.03.066. [7] Wieczorek M. A. and Phillip R. J. 1997. *Journal of Geophysical Research* 102:10,993–10,943.

5279

GAMMA IRRADIATION EFFECTS ON MARTIAN ANALOGUES

A. W. Needham¹, C. L. Smith¹, M. A. Sephton², Z. Martins², and S. S. Russell¹. ¹IARC, Department of Mineralogy, The Natural History Museum, London, UK. ²IARC, Department of Earth Science and Engineering, Imperial College, London, UK.

Introduction: The search for life on Mars is a primary focus of sample return missions planned for the coming decades. The chance of finding extant life in returned samples is small, but non-zero. Mars sample return missions will be designated COSPAR category IV_{b-c}. Sterilization of Martian material is essential prior to removing samples from biocontainment. Gamma irradiation with doses exceeding 30 Mrad may provide a suitable method of biological sterilization due to the limited alteration it produces in the host sample [1]. The present study aims to quantify the potential irradiation-induced alteration of petrological, chemical and isotopic properties in a range of Martian analogue material.

Methods: A ⁶⁰Co radiation source will be used to expose the samples to ≥30 Mrad. Sections of irradiated and unirradiated samples will be analysed by a broad range of techniques, including: field emission SEM, XRD, optical and IR microscopy, Raman spectroscopy, ICP-MS, light stable isotope analyses (C, N, O), and analyses of organic compounds and bacteria will also be undertaken.

Samples: Previous studies have demonstrated several effects of gamma irradiation [1]. Various rocks and minerals were demonstrated to respond differently to intense gamma irradiation. To further our knowledge of irradiation effects it is therefore important to study a diverse range of physical and chemical properties across a range of Mars-like lithologies. Such investigations are essential and should form a major part of planning for future Mars sample return missions.

Data from recent Mars missions suggest the presence of evaporite and sulphate minerals such as jarosite [2, 3], as well as the typical weathered basaltic soils. Samples of basalt, Mars soil simulant, jarosite, halite, and illite will be analysed. Additional samples will also be analyzed in order to quantify the irradiation effects in organic compounds. These samples will include both synthetically doped and naturally organic rich samples, such as Kimmeridge clay and CM2 Murchison.

References: [1] Allen C. C. et al. 1999. *Journal of Geophysical Research* 104. [2] Gendrin et al. A. 2005. *Science* 307:1587. [3] Klingelhöfer G. et al. 2004. *Science* 306:1740.

5277

AN ABUNDANT MIX OF PRESOLAR MATTER IN THE HIGHLY PRIMITIVE CR CHONDRITE QUE 99177

A. N. Nguyen, C. M. O'D. Alexander, and L. R. Nittler. Department of Terrestrial Magnetism, Carnegie Institution of Washington, Washington, D.C. 20015, USA. E-mail: nguyen@dtm.ciw.edu.

Introduction: Presolar silicate grains are preserved in interplanetary dust particles and meteorites that have escaped extensive aqueous alteration [1–4]. The primitive natures of the chondrites Acfer 094 (unique) and ALHA77307 (CO3) are exemplified by their large abundance of presolar silicate grains [3]. Here we studied the CR chondrite QUE 99177, which has been shown to be one of the most primitive of its class [4, 5], and compare the presolar grain abundances with those of the aforementioned meteorites.

Experimental: A thin section of QUE 99177 was analyzed by raster ion imaging in the Carnegie NanoSIMS 50L. Negative secondary ions of ^{12}C , ^{13}C , ^{16}O , ^{17}O , ^{18}O , ^{28}Si , and ^{30}Si were measured for a total area of 21,100 μm^2 . The average isotopic compositions of the matrix material were used as standards. A few regions containing anomalous carbonaceous material were re-measured for ^{12}C , ^{13}C , $^{14}\text{N}^{12}\text{C}$, $^{15}\text{N}^{12}\text{C}$, ^{28}Si , ^{29}Si , and ^{30}Si .

Results and Discussion: We identified 39 anomalous O-rich grains, and all but 7 appear to be silicates according to the NanoSIMS $^{28}\text{Si}^{16}\text{O}$ -ratios. Additional analyses, using Auger spectroscopy for instance, are needed to make unambiguous identifications. Most of these grains have O isotopic compositions consistent with Group 1 presolar oxides [6]. Four grains are enriched in ^{17}O and ^{18}O and fall in the Group 4 classification. Grains having similar isotopic compositions have been suggested to originate in SN explosions [7]. The Si isotopic compositions of all the presolar silicate and oxide grains are normal within error. One ~500 nm grain having CAI-like O isotopic composition ($\delta^{17}\text{O} = -70\text{‰}$, $\delta^{18}\text{O} = -80\text{‰}$) was determined by SEM-EDX to be a Cr-bearing spinel.

C isotopic analysis revealed 28 regions with depletions in ^{13}C (as much as -25‰), and 5 with enrichments in ^{13}C (up to 24%). One grain with $\delta^{13}\text{C} > 10,000\text{‰}$ is likely a presolar graphite. Preliminary analysis of N isotopes indicates that QUE 99177 contains abundant organic material having $\delta^{15}\text{N}$ ranging up to 2000‰. We will continue to characterize the N isotopic composition of the anomalous C-rich material and of other organic material. 12 mainstream SiC grains and one SiC type X were also identified.

The matrix-normalized abundance of presolar silicates in QUE 99177 is 130 ppm (lower than reported by [2]) and of presolar oxides is 40 ppm (higher than reported by [2]). These abundances are comparable to those reported for Acfer 094 and ALHA77307 [3]. The abundance of presolar SiC is high (50 ppm), in agreement with recent data for CR chondrites [8].

References: [1] Messenger S. et al. 2003. *Science* 300:105–108. [2] Floss C. et al. 2006. *Geochimica et Cosmochimica Acta* 70:2371–2399. [3] Nguyen A. N. et al. 2007. *The Astrophysical Journal* 656:1223–1240. [4] Floss C. et al. 2008. Abstract #1280. 39th LPSC. [5] Abreu N. M. and Brearley A. J. 2006. Abstract #2395. 37th LPSC. [6] Nittler L. R. et al. 1997. *The Astrophysical Journal* 483:4715–495. [7] Nittler L. R. et al. Forthcoming. *The Astrophysical Journal*. [8] Davidson J. et al. 2008. Abstract #1184. 39th LPSC.

5166

THERMOLUMINESCENCE STUDY IN THE JAPANESE ANTARCTIC METEORITES COLLECTION: YAMATO-98 UNEQUILIBRATED ORDINARY CHONDRITES

K. Ninagawa¹, H. Matsui¹, N. Imae², and H. Kojima². ¹Department of Applied Physics, Okayama University of Science, Okayama 700-005, Japan. E-mail: ninagawa@dap.ous.ac.jp. ²National Institute of Polar Research, Tokyo 173-8515, Japan.

Introduction: Induced TL (thermoluminescence), the response of a luminescent phosphor to a laboratory dose of radiation, reflects the mineralogy and structure of the phosphor, and provides valuable information on the metamorphic and thermal history of meteorites. Especially the sensitivity of the induced TL is used to determine petrologic subtype of unequilibrated ordinary chondrites [1]. Natural TL, the luminescence of a sample that has received no irradiation in the laboratory, reflects the thermal history of the meteorite in space and on Earth. Natural TL data thus provide insights into such topics as the orbits of meteoroids, the effects of shock heating, and the terrestrial history of meteorites [2]. Natural TL properties are usually applied to find paired fragments [3–5].

This time we measured induced and natural TL properties of twenty-four Yamato unequilibrated ordinary chondrites (LL3: 4, L3: 4, H3: 16) from Japanese Antarctic meteorite collection. Sampling positions of these chondrites were measured by GPS.

Primitive Ordinary Chondrites: Most of the chondrites had TL sensitivities over 0.1 (Dhajala = 1), corresponding to petrologic subtype 3.5–3.9. One chondrite, Y-983183 (LL3) was revealed to be a primitive ordinary chondrite, petrologic subtype 3.0. It is particularly significant in understanding the nature of primitive material in the solar system.

Pairing: Natural and induced TL properties were also applied to find paired fragments, and we found 21 TL potential paired fragments. A group of H3 comprises a chain of 7 paired fragments, Y-980052, Y-980053, Y-980054, Y-980072, Y-980074, Y-980075, and Y-980078. They were sampled at the same position, 35.336°E, 72.152°S. They all could be paired. Another group of H3 is composed of two fragments, Y-980129 and Y-983420. However, their sampling positions were far from each other, 35.170°E, 72.432°S and 35.942°E, 71.654°S, respectively.

Acknowledgements: This work was carried out in part under the Visiting Researcher's Program of the Research Reactor Institute, Kyoto University.

References: [1] Sears D. W. G. et al. 1991. Proceedings, 21st Lunar and Planetary Science Conference. pp. 493–512. [2] Benoit P. H. et al. 1991. *Icarus* 94:311–325. [3] Ninagawa K. et al. 1998. *Antarctic Meteorite Research* 11:1–17. [4] Ninagawa K. et al. 2002. *Antarctic Meteorite Research* 15:114–121. [5] K. Ninagawa et al. 2005. *Antarctic Meteorite Research* 18:1–16.

5291

LARGE METEORITIC IMPACT ON ANTARCTIC ICE SHEET 434 KYR AGO—MICROMETEORITES FOUND IN THE DOME FUJI ICE CORE

K. Nishiizumi¹, M. W. Caffee², M. Kohno³, K. Misawa³, and T. Tomiyama³.
¹Space Sciences Laboratory, University of California, Berkeley, CA 94720–7450, USA. E-mail: kuni@ssl.berkeley.edu. ²Department of Physics, Purdue University, West Lafayette, IN 47907, USA. ³National Institute of Polar Research, Itabashi, Tokyo, Japan.

Introduction: Two distinct highly concentrated particles layers are found in the Dome Fuji (77°19'S, 39°42'E) and the EPICA-Dome C (75°06'S, 123°21'E) ice cores, Antarctica [1, 2]. The two layers are 434 kyr and 481 kyr old, respectively, based on the ice core dating. These two ice cores are separated by ~2000 km. Analyses of mineralogy, petrology, and bulk chemical composition indicate that these particles may be extraterrestrial [1, 2].

Cosmogenic Radionuclides: Five large particles were hand picked from the upper layer of the Dome Fuji ice core at the depth of 2641 m. Cosmogenic ¹⁰Be ($t_{1/2} = 1.36$ Myr), ²⁶Al (0.705 Myr), and ³⁶Cl (0.30 Myr) in individual particles (30–70 μg) were measured by AMS at Purdue University. Four out of the five particles contain 2.5–4.2 dpm/kg of ¹⁰Be [3]. None of the particles contain ²⁶Al ($\leq 1 \times 10^4$ atom) or ³⁶Cl ($\leq 1.4 \times 10^4$ atom), levels indistinguishable from the chemistry blank.

Discussion: In previous work, we favored a the hypothesis that ¹⁰Be detected in the Dome Fuji particles was produced in space, however we could not exclude the possibility of terrestrial ¹⁰Be contamination [3]. However, the observed activity ratios of ²⁶Al/¹⁰Be in these particles are <0.2; the production rate ratio in space is ~3. The lack of cosmogenic ²⁶Al indicates that ¹⁰Be was inherited from the Antarctic ice by impact on Antarctic ice sheet. Since major elemental abundances relative to CI chondrites are 0.6–1.5 (except some volatile elements) [1], an impact on a continent or in the ocean is excluded. Assuming the ¹⁰Be concentration of the ice sheet was $(0.5\text{--}2) \times 10^5$ atom/g at 434 kyr ago, the observed ¹⁰Be concentration in 4 particles accounted for by less than a few g of melted ice. This implies that the mass of melted ice was more than 10^4 times that of the particles. Oxygen isotopic compositions of olivine in two particles from this dust layer fall along the terrestrial fractionation line and reach up to $\delta^{18}\text{O} = -47\%$ [1]. The light oxygen isotopes might be indicative of exchange with ice at the impact site.

Impact on the Ice: Based on the existing evidence we favor a scenario in which a large chondritic object, >100 m in diameter, impacted on the Antarctic ice sheet 434 kyr ago. The projectile interacted with ice and trapped ¹⁰Be (and possibly ³⁶Cl) from the ice. The ¹⁰Be was concentrated by evaporating melted ice, while the void spaces and quenched texture of the particles were produced by impact heating. Some volatile elements, noble gases, and terrestrial ³⁶Cl contamination in the ejected particles were lost by heating. Since the ejecta was not contaminated with bedrock, the impact site must have been inland where the ice is thick. We further speculate that the projectile size was not a ~km sized object. It might be possible to find the site by techniques such as ice penetrating radar but there are currently no other ice cores available that reach older than 434 kyr.

References: [1] Misawa K. et al. 2008. Abstract #1690. 39th LPSC. [2] Narcisi B. et al. 2007. *Geophysical Research Letters* 34:L155022. [3] Nishiizumi K. et al. 2008. Abstract #2231. 39th LPSC.

5207

IRREVERSIBLE CHANGES IN ANISOTROPY OF MAGNETIC SUSCEPTIBILITY: STUDY OF BASALTS FROM LUNAR CRATER AND EXPERIMENTALLY IMPACTED BASALTIC ANDESITE

I. Nishioka and M. Funaki.

Magnetic data provide valuable information on buried impact craters. An understanding of how stress waves change magnetic properties of rock is critical for correct interpretation of magnetic data, especially in case that rock samples are not available. Effects of relatively weak shock for those of rocks in crater wall have been poorly studied. We investigated shock effects on magnetic properties through studies of experimentally impacted basaltic andesite, and basalt from Lonar crater in India.

An initial peak pressure of 5 GPa was generated in a block of basaltic andesite containing Ti-rich titanomagnetite with the impact of a cylindrical projectile. Effects of decaying stress waves on magnetic properties were subsequently quantified. Natural remanent magnetization (NRM) was partially but significantly demagnetized at peak pressures higher than 1 GPa. High-coercivity part of NRM, even higher than 80 mT, was partially demagnetized. At higher pressure (3–5 GPa), low-field magnetic susceptibility was significantly reduced and coercivity was increased, probably due to increased internal stress. Different patterns of change in AMS were observed at different distance from the impacted surface. In high-pressure range (>3 GPa), the anisotropy degree was increased, the minimum susceptibility was oriented toward the shock direction, and the average susceptibility was decreased. This feature is consistent with the result of a previous shock experiment. The initial orientations of AMS were however significantly changed at around 0.4–1 GPa; The maximum susceptibility was induced parallel to the shock direction, and superposed on the initial AMS.

Basalt samples were collected from flows in the crater wall, ejecta clasts, and flow outside the rim of Lonar crater. Irreversible thermomagnetic curves and the maximum Curie temperature of 500–560 °C indicated presence of Ti-poor titanomagnetite and its oxidized phase as the main magnetic minerals in Lonar basalts. The result of AMS measurement of both inside and outside samples showed relatively weak anisotropy degree ($P < 1.03$), which is similar to that of basalt from outside the crater rim. The samples from the crater wall showed predominantly oblate shape of AMS ellipsoid, with tightly clustered vertical distribution of the minimum principal axes. Substantial, but not strict, parallelism between the maximum principal axes and the radial direction from the crater center was observed only for the samples from the lower part of the crater wall. This fact and the result of the shock experiment indicate that radially expanding stress waves reoriented the initial AMS.

5333

HYDROTHERMAL EXPERIMENTS OF SYNTHETIC AMORPHOUS SILICATES WITH CI CHONDRITIC COMPOSITION IN THE SYSTEMS WITH AND WITHOUT FeO

R. Noguchi, K. Murata, A. Tsuchiyama, H. Isobe, H. Chihara, T. Nakamura, and T. Noguchi. Department of Earth and Space Science, Osaka University. E-mail: noguchi@astroboy.ess.sci.osaka-u.ac.jp.

Introduction: In order to investigate the aqueous alteration process in carbonaceous chondrites, many hydrothermal experiments have been performed using mineral grains, such as olivine and enstatite, or chondrites themselves as the starting materials. (e.g., [1]). In contrast, interstellar silicates, which are considered to be the most primitive material in the solar nebula, are amorphous based on infrared astronomical observations [2]. In addition, unique carbonaceous chondrites, such as Acfer 094, contain primitive amorphous silicates in the matrix [3]. Therefore, it is important to investigate the aqueous alteration of amorphous silicates. In this study, in order to understand the aqueous alteration process and its conditions on the chondrite parent bodies, we have carried out hydrothermal alteration experiments of synthetic amorphous silicates with the CI chondritic composition.

Experimental: Two types of starting materials were synthesized by sol-gel method. The first is FeO-free amorphous silicate with the CI chondritic composition ($\text{Na}_2\text{O-MgO-Al}_2\text{O}_3\text{-SiO}_2\text{-CaO-NiO}$). This amorphous silicate was heated at 750 °C for 20 hr for preparing a mixture of amorphous and crystalline silicates (forsterite), which was also used as starting materials. A mixture of the starting material and pure water was put in an inner reaction vessel of Teflon with an outer stainless steel jacket (SUS-316). The vessel was heated in an electric furnace at 100–200 °C for 24–336 hr. Run products were analyzed using X-ray diffraction, field-emission scanning electron microscopy equipped with energy-dispersive X-ray spectroscopy and infrared spectroscopy. Some results have been already reported in [4]. Saponite was formed first from amorphous silicates, then serpentine was formed by consuming saponite and forsterite. Calcite was formed at 200 °C. A mineral assemblage of serpentine, calcite and a minor amount of forsterite at 200 °C for 504 hr resembles that of CM chondrites.

The other starting material is FeO-bearing amorphous silicate with the CI chondritic composition ($\text{Na}_2\text{O-MgO-Al}_2\text{O}_3\text{-SiO}_2\text{-CaO-FeO-NiO}$; a part of Fe was excluded as FeS). In this type of experiments, we used a double-tube of Ag-Pd alloy (inner tube) and Au (outer tube) as a reaction vessel. A mixture of starting material (amorphous silicates, amorphous silicates with metallic iron or amorphous silicates with iron sulfide) was put in the outer tube with pure water or 1N ammonia water. Wüstite and magnetite powders were put in the inner tube to buffer the oxygen partial pressure in the vessel. The charge was heated in an electric furnace at 300 °C for 5 and 30 days. Serpentine, magnetite, and calcite were formed in this FeO-bearing system. This mineral assemblage is also similar to that of CM chondrites as in the case of Fe-free system.

References: [1] Ohnishi I. and Tomeoka K. 2006. *Meteoritics & Planetary Science* 42:49–61. [2] Kemper F. et al. 2004. *The Astrophysical Journal* 609:826–837. [3] Greshake A. 1997. *Geochimica et Cosmochimica Acta* 61:437–452. [4] Noguchi R. et al. 2007. The Japanese Society for Planetary Science, Fall meeting, 76.

5129

DISCOVERY OF ANTARCTIC MICROMETEORITES CONTAINING GEMS AND ENSTATITE WHISKERS

T. Noguchi¹, N. Ohashi¹, S. Nishida¹, T. Nakamura², T. Aoki², S. Toh³, T. Stephan⁴, and N. Iwata⁵. ¹College of Science, Ibaraki University, Japan. E-mail: tngc@mx.ibaraki.ac.jp. ²Department of Earth and Planetary Science, Faculty of Science, Kyushu University, Japan. ³HVEM Laboratory, Kyushu University, Japan. ⁴Department of the Geophysical Sciences, University of Chicago, USA. ⁵Department of Earth and Environmental Science, Iwate University, Japan.

Introduction: About a half of interplanetary dust particles (IDPs) collected in the stratosphere is quite porous and has chondritic compositions and anhydrous mineralogy. It has been thought that at least a part of them were derived from comets [1]. Such chondritic porous IDPs (CP IDPs) are characterized by the presence of GEMS (glass with embedded metal and sulfides) and enstatite whisker [1, 2]. However, CP IDPs have not been discovered among Antarctic micrometeorites (AMMs) to date. Discovery of AMMs containing these components are quite important to testify that CP IDPs could reach the surface of the earth in the past. Here we report the first discovery of AMMs that contain GEMS and enstatite whiskers.

Samples and Methods: We have been identified >3000 AMMs among fine-grained particles collected at Tottuki Point, Antarctica, in 2000. Synchrotron radiation X-ray diffraction was performed to obtain bulk mineralogy of each AMM. We selected three porous AMMs, To440020, TT54C394, and T5BB2066, containing primary pyroxene. A TEM sample of a rod-shaped object (0.2 μm × 2 μm) on the surface of To440020 was prepared by focused ion beam (FIB) technique. Ultrathin sections of all samples and a highly carbonaceous AMM (TT54B397) investigated by [3] were prepared for detailed TEM study.

Results and Discussion: Selected area electron diffraction patterns and TEM photographs of the rod-shaped object display that it is a unit-scale mixture of clino- and ortho-enstatite with many stacking disorders parallel to (100) and elongated along a-axis. The features are common to those of enstatite whiskers in CP IDPs. We also identified enstatite whiskers from the interiors of To440020 and TT54C394. All the AMMs contain 100 to 400 nm across spheroidal objects, containing Fe-Ni metal and Fe-bearing sulfide. Their chemical composition overlaps with those of GEMS in CP IDPs. In addition, they have features uncommon among CP IDPs. To440020 and TT54C394 contain organic globules found among hydrated carbonaceous chondrites [4, 5]. TT54C394 and T5BB2066 contain Mg-bearing Fe oxide, which was probably Mg-rich siderite before entering earth's atmosphere. Mg-rich siderite is common among carbonaceous chondrites such as Tagish Lake [6]. It is obvious that the AMMs are past CP IDPs containing GEMS and enstatite whiskers. They can also serve to understand parent body processes of very primitive small bodies.

References: [1] Bradley J. P. 2004. *Treatise on Geochemistry*, vol. 1. Amsterdam: Elsevier. 689 p. [2] Ishii H. A. 2008. *Science* 319:447–450. [3] Yada T. et al. Forthcoming. *Meteoritics & Planetary Science*. [4] Nakamura K. et al. 2002. *International Journal of Astrobiology* 1:179–189. [5] Garvie L. A. J. and Buseck P. R. 2004. *Earth and Planetary Science Letters* 224:431–439. [6] Zolensky M. E. et al. 2002. *Meteoritics & Planetary Science* 37:373–361.

5269

RECONSTRUCTION OF AN IMPACT EVENT IN CARANCAS, SOUTH OF PERU, BY GPR STUDIES ON A SMALL CRATER

H. Núñez del Prado, W. Pari, M. Ramirez, J. Machare, and L. Macedo.

The identification and description of the subsurface impact structures beneath the crater of Carancas by using a GPR (ground penetrating radar) system (EKKO PRO) was one of the main achievements within the general study of the impact event of Carancas carried out by the INGEMMET staff and co-workers.

The GPR prospection method is based on the changes in the propagation velocity of an electromagnetic wavefront passing through the sediment.

The main goal of this study was the reconstruction of the buried and surface characteristics of the crater and the consequent identification of probable remnants of chondritic material. Furthermore, the identification of geometrical features within the crater as a whole enable us to propose the impact azimuth and angle.

The prospection study by GPR was carried out on the October 27, 2007; 6 transects (A, B, C, D, E, and F) were planned to pass approximately through the center of the geoform, thus producing a network of intersected profile lines. Two frequencies were used: 100 and 200 MHz, reaching a maximum depth of up to 10 m. The radargrammes obtained were processed and edited in order to carry out the structural interpretation. Two main guide layers were identified in radar profiles, associated with two different lithologic groups: a) a poorly-consolidated surface soil of limonite and clay on a layer b) constituted of fine and coarse sand, and consolidated blocks with a large percentage of clay matrix (autochthonous soil) overlying the deepest identified material which presents a very high conductivity because of its content of water (low amplitude and dispersion layer).

The recognition of these three layers allowed us to visualize the deformation up to a depth of 7 m just beneath the impact point, showing a maximum amplitude over 12 m on the surface.

To summarize, the analysis of these stratigraphic deformation units showed:

- A deformation (folding) zone with very clear limits ranging 13 m as an approximate mean width.
- A wedge-like shape of the main zone of deformation (b and c materials).
- Outside this latter zone, some layers are moderately deformed following the outer walls of the transitional “wedge.” Deformation also consists on an upward bending linear layer offset to an opposite direction from the theoretical impact direction.
- In some radar profiles, it is possible to observe a little uplift (interlayer between a and b materials) containing upward bending arches.

No hyperbolic segments showing the presence of rare bodies as meteoritic remnants exist. On the surface, the contour of the crater figures a horseshoe shape with the overture to the S/SE. Combining all the structural data from the GPR study, we conclude that the impact was oblique (20–30°) with a direction NW-SE.

5321

EQUILIBRATION OF THE OXYGEN ISOTOPES IN THE EARTH-MOON SYSTEM

Joseph A. Nuth III. Astrochemistry Laboratory, Code 691, Solar System Exploration Division, NASA's Goddard Space Flight Center, Greenbelt MD 20771, USA. E-mail: Joseph.A.Nuth@NASA.gov.

Introduction: Oxygen isotopes can be used to distinguish material that comes from individual asteroids and planets. Each body appears to have a specific isotopic signature. Signatures from many meteorite parent bodies such as carbonaceous chondrites, ordinary chondrites, etc. cluster around common isotopic values, though none are identical. The Earth and Moon have identical oxygen isotopic compositions, a situation typically attributed to the breakup of a common parent body when looking at meteorites. If the Earth's moon formed from the fragments of a gigantic collision between two independently accreted, planetary-scale bodies, how did the isotopic composition of the resultant system equilibrate to yield the same signature in both?

We have previously shown that the size of the feeding zones for the accretion of planetesimals depend on both size of the body and the total mass of the nebula. For reasonable values of nebular mass (up to 50 times the Hayashi Minimum Mass Nebula) and planetesimals that have grown to roughly one kilometer in diameter, all contain significant quantities of ice ranging from 5 to 35%.

Consequence of Wet Planetesimals: Most planetesimals that are accreted into planets growing via runaway accretion will bring substantial quantities of water into the protoplanet. The later stage of the accretion process will generate considerable thermal energy due to the accreting planetesimals that will melt the initially accreted ice and generate a large flux of hot, liquid water through the planet. If the planet is large enough to hold an atmosphere and hydrosphere, this will be thoroughly equilibrated with the oxygen of the planetary interior.

A second consequence of wet planetesimals will be that the protoEarth must accrete considerably more initial mass (including the ice) in order to accrete sufficient rocky mass to account for the current mass of the planet.

Oxygen Isotopes in the Earth-Moon System: If both the protoEarth and the “Mars-size impactor” were both equilibrated bodies containing significant reservoirs of liquid water prior to impact, the energy of the collision would vaporize any oceans on the surfaces of the bodies while simultaneously equilibrating the isotopic composition of both bodies in the debris cloud surrounding the Earth. Depending on the accretional loss of water during the initial accretion of both bodies, there could be several tenths of an Earth mass of water vapor in this cloud. Although most of this water would be lost from the system due to the high temperature of the debris disk, this same high temperature would ensure the equilibration of the silicates in the cloud. If the oceans of the larger protoEarth dominate the contribution to this disk, then the cloud will be equilibrated with the Earth before it coalesces into the Moon.

5223

EARLY PARTIAL MELTING OF THE GRA 06128/9 PB FROM Sm-Nd AND Rb-Sr ISOTOPIC STUDIES

L. E. Nyquist¹, C.-Y. Shih², Y. D. Reese³, and A. H. Treiman⁴. ¹NASA Johnson Space Center, Houston, TX 77058, USA. E-mail: laurence.e.nyquist@nasa.gov. ²ESCG Jacobs-Sverdrup, Houston, TX 77058, USA. ³Mail Code JE-23, ESCG/Muniz Engineering, Houston, TX 77058, USA. ⁴Lunar and Planetary Institute, Houston, TX 77058, USA.

Introduction: Consortium studies of GRA 06128/9 (GRA) [1–5] conclude that it represents a partial melt of a parent body of approximately chondritic composition. Arai et al. [2] suggested that carbonaceous chondrites are more suitable precursors than ordinary chondrites. $\Delta^{17}\text{O} \sim -0.21$ for GRA excludes ordinary and most carbonaceous chondrite parent bodies, and links it to the brachinite achondrites, possibly as a flotation cumulate [5]. Min-pet and textural studies show that GRA was metamorphosed at high temperature estimated variously as ~ 700 °C [1], up to ~ 845 °C [4], and 670 ± 50 °C by pyroxene thermometry to $\sim 900 \pm 50$ °C by spinel-olivine thermometry [3].

¹⁴⁷Sm-¹⁴³Nd Isochron: Whole rock and whole rock leachate (~phosphate) analyses yield nearly identical Sm-Nd isotopic data. Combined with those data, whole rock and pyroxene residues after leaching define the crystallization age as 4.545 ± 0.087 Ga. Initial $\epsilon_{\text{Nd,CHUR}}$ [6] and $\epsilon_{\text{Nd,HEDR}}$ [7, 8] are $+1.07 \pm 0.40$ and $+0.24 \pm 0.40$, respectively. A plagioclase separate with the whole rocks and leachates gives an apparent age of ~ 3.5 Ga, an upper limit to the time of metamorphism.

¹⁴⁶Sm-¹⁴²Nd Isochron: Whole rock and whole rock leachate analyses define initial $^{146}\text{Sm}/^{144}\text{Sm} = 0.0068 \pm 0.0016$ and $\epsilon(^{142}\text{Nd})_{\text{Earth}} = -0.30 \pm 0.12$ at $(^{147}\text{Sm}/^{144}\text{Nd})_{\text{CHUR}} = 0.1967$ [6]. One plagioclase and one whole rock residue analysis fail to give useful data. The ^{146}Sm - ^{142}Nd age relative to $^{146}\text{Sm}/^{144}\text{Sm} = 0.0057 \pm 0.0005$ at 4.542 Ga ago [8] is 4.57 ± 0.03 Ga.

⁸⁷Rb-⁸⁷Sr Data: Whole rock, whole rock leachate, and whole rock residue data for GRA 06128 show that the leachate is contaminated with a high $^{87}\text{Sr}/^{86}\text{Sr}$ (~ 0.713) phase. A 4.54 Ga reference isochron (Sm-Nd age) passed through the 06128 whole rock residue datum gives initial $^{87}\text{Sr}/^{86}\text{Sr}$ (I_{Sr}) ~ 0.69924 .

Discussion: A bulk sample of Brachina has Sr, Nd, and Sm abundances $\sim 4\times$ and Rb abundances $\sim 3\times$ lower than GRA. An “andesitic” plagioclase/diopside silicate inclusion from the Caddo County IAB iron [9] has feldspar of composition $\text{Ab}_{80-84}\text{An}_{12-16}\text{Or}_3$ [11] similar to that for GRA. It has similar Rb and Sr abundances as GRA, and Sm and Nd abundances $\sim 2\times$ higher [10]. $I_{\text{Sr}} = 0.69915 \pm 10$ for the 4.52 ± 0.05 Ga Caddo County inclusion [10], within error limits of I_{Sr} for GRA. It, too, likely formed by partial melting within its parent body [9].

References: [1] Treiman A. H. et al. 2008. Abstract #2214. 39th LPSC. [2] Arai T. et al. 2008. Abstract #2465. 39th LPSC. [3] Shearer C. K. et al. 2008. Abstract #1825. 39th LPSC. [4] Ash R. D. et al. 2008. Abstract #2271. 39th LPSC. [5] Zeigler R. A. et al. 2008. Abstract #2456. 39th LPSC. [6] Jacobsen S. B. and Wasserburg G. J. 1984. *Earth and Planetary Science Letters* 67:137–150. [7] Nyquist L. et al. 2006. *Geochimica et Cosmochimica Acta* 70:5990–6015. [8] Nyquist L. E. et al. 2008. Abstract #1437. 39th LPSC. [9] Takeda H. et al. 2000. *Geochimica et Cosmochimica Acta* 64:1311–1327. [10] Liu Y. Z. et al. 2003. Abstract #1983. 34th LPSC. [11] Takeda H. et al. 2002. *Meteoritics & Planetary Science* 37:A139.

5143

INCORPORATION OF HYDROUS OXYGEN INTO INSOLUBLE ORGANIC MATTER (IOM) OF MURCHISON

Yasuhiro Oba¹ and Hiroshi Naraoka². ¹Institute of Low-Temperature Science, Hokkaido University, Japan. E-mail: oba@neko.lowtem.hokudai.ac.jp. ²Department of Earth and Planetary Sciences, Kyushu University, Japan.

Introduction: Meteoritic insoluble organic matter (IOM) has been considered as a source of solvent-extractable organic compounds through aqueous alteration on meteorite parent bodies [1]. Experimentally, various carboxylic acids are generated by hydrous pyrolysis of IOM from the Murchison [2] and Murray [3] meteorites, suggesting that some solvent-extractable carboxylic acids could be formed during hydrous activity on the meteorite parent bodies. The generated acids are closely related to the chemical structure of IOM containing relatively abundant carboxyl carbon [4]. During the release of pyrolysis products, incorporation of H (chemical reduction) or OH (chemical oxidation) into IOM could occur. In this study, we will report variations in oxygen contents of the Murchison IOM during hydrous pyrolysis, as well as the changes in the carboxyl (-COOR; R=H or alkyl group) amount, in order to consider the chemical reaction processes.

Samples and Analytical Procedures: The purified IOM from Murchison and its hydrous pyrolysis residues were used in this study. The detailed procedure for the hydrous pyrolysis of the IOM was reported previously [2]. Briefly, IOM was heated with H₂O under vacuum at 270–330 °C for 72 hr. Oxygen concentration of samples was determined as CO by pyrolysis at 1450 °C in the presence of graphite using a high temperature EA. Carboxyl content was determined as CO₂ by pyrolysis at 750 °C [5].

Results and Discussion: The oxygen/carbon (O/C) ratio of IOM increases from 0.22 (original) to 0.48 for the hydrous pyrolysis residue at 270 °C, and 0.28 for that at 300 °C, which suggests O incorporation into IOM during hydrous pyrolysis. For the residue at 330 °C, however, the O/C decreases to 0.10. These observations suggest that the Murchison IOM is subjected to chemical oxidation at up to ~ 300 °C, followed by decarboxylation at higher temperature.

The carboxyl amount decreases from 2.4 (original) to 0.9 mmol/gC at 270 °C, in spite of the increase in O/C ratio. Under this process, the original carboxyl group is lost from IOM by decarboxylation, while new O-containing groups such as -OH are produced. Through the progressive chemical oxidation, the carboxyl amount increases again to 1.6 mmol/gC with continuous decarboxylation at 300 °C. Finally, further O-addition stops (O/C = 0.10) due to consumption of active sites (e.g., methylene carbon) with minor amounts of carboxyls (0.6 mmol/gC) at 330 °C. Under these reactions, IOM can release carboxylic acids, being consistent with abundant acetic acid production during hydrous pyrolysis [2].

References: [1] Cronin J. R. and Chang S. 1993. In *Chemistry of life's origins*, edited by Greenburg J. M. and Pirronello V. pp. 209–258. [2] Oba Y. and Naraoka H. 2006. *Meteoritics & Planetary Science* 41:1175–1181. [3] Yabuta H. et al. 2007. *Meteoritics & Planetary Science* 42:37–48. [4] Cody G. D. et al. 2002. *Geochimica et Cosmochimica Acta* 66:1851–1865. [5] Oba Y. and Naraoka H. 2006. *Rapid Communications in Mass Spectrometry* 20:3649–3653.

5156

FINDING OF HIGH-TEMPERATURE ORTHOPYROXENE IN A CHONDRITE

S. Ohi¹, H. Ito¹, A. Miyake¹, N. Shimobayashi¹, T. Noguchi², and M. Kitamura¹. ¹Department of Geology and Mineralogy, Division of Earth and Planetary Sciences, Graduate School of Science, Kyoto University, Kyoto 606-8502, Japan. E-mail: shugo-ohi@kueps.kyoto-u.ac.jp. ²Department of Materials and Biological Sciences, Ibaraki University, Bunkyo 2-1-1, Mito 310-8512, Japan.

Introduction: Texture and chemical composition of pyroxene, one of the main constituents of chondrules, have been studied extensively, because they give information about the formation conditions of chondrules. On the other hand, for thirty years there has been controversy about the phase relations of the Mg₂Si₂O₆-CaMgSi₂O₆ system [e.g., 1–4]. The contentious point is that although Ca-bearing orthopyroxene (Ca-Opx) and orthoenstatite (Oen) have the same space group (*Pbca*), they occupy distinctly separate positions in a phase diagram [1, 4]. Recently, we report an isosymmetric phase transition of Ca-Opx from low-temperature form (LT-Opx) to high-temperature form (HT-Opx) at around 1170 °C, identified in in situ high-temperature synchrotron X-ray powder diffraction experiments (Ohi et al., Forthcoming). The study provides direct evidence that HT-Opx is thermodynamically distinct from Oen. The P-T condition of the stability field of HT-Opx suggests the possible origin of the pyroxene in chondrules in unequilibrated chondrites. Here we report the finding of HT-Opx in a chondrule of Y-86751 (CV3).

Results and Discussion: A chondrule in Y-86751 (CV3) includes HT-Opx (70 μm × 20 μm). The chondrule is porphyritic and includes olivine, pyroxene and troilite grains among interstitial glass. The crystal system of the pyroxenes was determined under an optical microscope and EBSD of a SEM. The compositions of minerals were obtained by EDX analysis of a SEM.

Two grains of pyroxene in the chondrule consist of three different polymorphs as the zoning from the core of clinoenstatite to the rim of diopside through Ca-bearing Opx. Clinoenstatite has the average composition of En₉₈Fs₁Wo₁ and shows the polysynthetic twinning, indicating that the transformation from protoenstatite during cooling. Diopside in the rim has the average composition of En₆₄Fs₁Wo₃₅. Ca-bearing Opx in the mantle of the grains has the space group of *Pbca* and the average composition of En₉₅Fs₁Wo₄. This result indicates that Ca-bearing Opx grew as HT-Opx and transformed to LT-Opx during cooling. Coexistence of protoenstatite and HT-Opx suggests the temperature about 1400 ± 30 °C by phase diagram in En-Di system [4].

Noguchi (1989) [5] reported that the four kinds of pyroxenes in chondrules; protoenstatite (Wo < 2), orthopyroxene (Wo 2–5), pigeonite (Wo 5–15) and augite (Wo > 25) based on only the composition, although the orthopyroxene has not been identified as Ca-bearing Opx. The orthopyroxene is considered to be Ca-bearing Opx, implying the common occurrence of the pyroxene in chondrules.

References: [1] Longhi J. and Boudreau A. E. 1980. *American Mineralogist* 65:563–573. [2] Jenner G. A. and Green D. H. 1983. *Mineralogical Magazine* 47:153–160. [3] Biggar G. M. 1985. *Mineralogical Magazine* 49:49–58. [4] Carlson W. D. 1988. *American Mineralogist* 73:232–241. [5] Noguchi T. 1989. *Proceedings of the NIPR Symposium on Antarctic Meteorites* 2:169–199.

5197

PRELIMINARY RESULTS OF THE MULTIBAND IMAGER AND SPECTRAL PROFILER

M. Ohtake¹, T. Matsunaga², J. Haruyama¹, Y. Yokota¹, T. Morota¹, C. Honda¹, M. Torii¹, Y. Ogawa², and the LISM Team. ¹Planetary Science Department, Japan Aerospace Exploration Agency, Japan. E-mail: ohtake.makiko@jaxa.jp. ²National Institute for Environmental Studies, Japan.

Introduction: The Lunar Imager/SpectroMeter (LISM) is an instrument developed for the SELENE (KAGUYA) mission. SELENE was launched by an H-IIA Launch Vehicle on September 14, 2007. LISM consists of three subsystems, the Terrain Camera (TC), the Multiband Imager (MI), and the Spectral Profiler (SP).

The MI is a high-resolution multiband imaging camera and it acquires push-broom imaging data by using selected lines of area arrays. The spectral band assignments are 415, 750, 900, 950, and 1000 nm for the visible spectrum and 1000, 1050, 1250, and 1550 nm for the near infrared spectrum. The spatial resolution of visible bands is 20 m, and that of near infrared bands is 62 m from the 100 km SELENE orbital altitude. We will observe the global high resolution mineral distribution of the lunar surface in nine band images acquired by MI [1].

The SP is a visible-near infrared spectrometer. SP will obtain continuous reflectance spectra of the lunar surface with broad spectral coverage (500–2600 nm), high spectral resolution (6–8 nm), and high spatial resolution (500 m) [2].

Objectives: One of the important scientific goals of MI and SP is to investigate small but scientifically very important areas such as crater central peaks and crater walls. Investigations of such small areas will help answer current questions such as the existence, chemical composition, and source of olivine at the central peaks of some craters [3].

In-Flight Performance: MI successfully took its first lunar images on November 3, 2007. To check LISM-MI hardware functions, all possible observation parameters, such as exposure, compression table and nominal/SP support mode, were used and were confirmed to be normal. In-flight performance of SP are now being evaluated using the “first light” data as well as other data acquired during the initial checkout period. “Dark” and its noise level are being investigated for every pixel of three detectors using data acquired during nighttime. So far no new dead/damaged pixels have been found. The radiometric sensitivity and spectral location of each pixel is being monitored using internal calibration lamp data. It is confirmed that overall difference of sensitivity between in-flight and pre-flight data is small. Derived MI images and MI and SP spectra demonstrate advantage of MI’s high spatial resolution and SP’s high S/N ratio and continuous reflectance spectra to understand surface mineral distribution of the moon. Latest results from our researches will be presented at the conference.

References: [1] Ohtake M. et al. 2008. *Earth, Planets and Space* 59:1–8. [2] Matsunaga T. et al. 1999. *Journal of Remote Sensing Society of Japan* 19:152–169. [3] Tompkins S. and Pieters C. M. 1999. *Meteoritics & Planetary Science* 34:25–41.

5055

APOLLO ASTEROID 1999 YC: ANOTHER LARGE MEMBER OF THE PGC?

K. Ohtsuka¹, H. Arakida², T. Ito³, M. Yoshikawa⁴, and D. J. Asher⁵. ¹Tokyo Meteor Network, 1-27-5 Daisawa, Setagaya-ku, Tokyo 155-0032, Japan. E-mail: ohtsuka@jb3.so-net.ne.jp. ²Waseda University, Shinjuku-ku, Tokyo 169-8050, Japan. ³National Astronomical Observatory, Mitaka, Tokyo 181-8588, Japan. ⁴ISAS/JAXA, Sagami-hara, Kanagawa 229-8510, Japan. ⁵Armagh Observatory, College Hill, Armagh BT61 9DG, UK.

Introduction: (3200) Phaethon and (155140) 2005 UD are near-sun Apollo asteroids and (km-sized) large members of the Phaethon-Geminid stream complex (PGC) [1], thus genetically related to each other [2–4]. Both Apollos are classified as thermally metamorphosed C-types, i.e., F- or B-type [3, 4] having bluish reflectance spectra, presumably due to a solar heating effect since the subsolar points on the surface of both objects reach T_{eq} of >700 K. Their surface (meteoritic) analogues would be related to the dehydrated CI/CM chondrites [5]. The F- and B-type asteroids are rare, $\sim 5\%$, among all the Apollos [3]. The Geminid meteor stream, belonging to the PGC, also underwent a thermal history which caused the observed Na-depletion [6]. In order to explore the PGC's formation, here we surveyed the "JPL asteroid orbit database" to determine whether any further large members of the PGC can be identified.

Results: The method for our survey is the same as in [2], numerically integrating back and forward the orbital motion for 20,000 yr by applying the KS regularized Adams method. As a result, we found a candidate, Apollo asteroid 1999 YC. The variations for three criteria ($\bar{\omega}$ and two integrals of motion Θ and K) [1] of 1999 YC are compared to those of the other PGC members, where $\bar{\omega}$ is longitude of perihelion, $\Theta = (1 - e^2) \cos^2 i \sim \text{const.}$ and $K = e^2 (0.4 - \sin^2 i \sin^2 \bar{\omega}) \sim \text{const.}$, and the orbital parameters, e , i , and $\bar{\omega}$, are eccentricity, inclination, and argument of perihelion, respectively. The orbital behaviour of 1999 YC is dominated by the Lidov-Kozai mechanism during the integrated interval, as is that of the other PGC objects, Θ being almost constant at around ~ 0.20 . Besides, its critical argument librates in the (weak) 7:1 mean motion resonance with Jupiter from JDT $1.8e+06$ to $5.3e+06$, during which 1999 YC avoids close encounters with the terrestrial planets. Correspondingly, the semimajor axis (a) of ~ 1.42 AU is also constant over the integrated timescale and comparable to that of the Geminids, although considerably larger than Phaethon and 2005 UD which both have $a \sim 1.27$ AU. This means large differences in the orbital energy.

Discussion: Based on the three criteria $\bar{\omega}$, Θ , and K , 1999 YC seems to be another large member of the PGC. However, whereas the difference in a between Phaethon-Geminids is explained in terms of the Geminids, having masses of gram-order, being ejected from Phaethon at perihelion and then accelerated by >0.2 km s⁻¹, such an ejection mechanism is not acceptable for 1999 YC because of the large energy required for a km-sized body. Instead, we hypothesize that 1999 YC may have undergone a grazing encounter with a terrestrial planet long ago, allowing the necessary transfer of orbital energy. This would be an a priori rare event, but if it occurred then 1999 YC would simultaneously be subject to planetary tides. Physical observations for 1999 YC, such as colorimetry (rare F- or B-type Apollo?) and light-curve measurements (tidally distorted?), may make clear whether it has a PGC origin.

References: [1] Babadzhanyan P. B. and Oubrov Yu. V. 1992. *Celestial Mechanics and Dynamical Astronomy* 54:111–127. [2] Ohtsuka K. et al. 2006. *Astronomy and Astrophysics* 450:L25–L28. [3] Jewitt D. and Hsieh H. 2006. *The Astronomical Journal* 132:1624–1629. [4] Kinoshita D. et al. 2007. *Astronomy and Astrophysics* 466:1153–1158. [5] Nakamura T. 2005. *Journal of Mineralogical and Petrological Sciences* 100:260–272. [6] Kasuga T. et al. 2005. *Astronomy and Astrophysics* 438:L17–L20.

5126

EXPERIMENTAL REPRODUCTION OF VOIDS IN CHONDRULES UNDER LOW PRESSURE LIKE PREMITIVE SOLAR NEBULA

M. Oka, M. Uesugi, and A. Tsuchiyama. Department of Earth and Space Science, Graduate School of Science of Osaka University, 1-1 Machikaneyama-cho, Toyonaka-shi, Osaka, Japan. E-mail: oka@astroboy.ess.sci.osaka-u.ac.jp.

Introduction: 3-D observation of chondrules shows that voids are commonly present in chondrules although their amounts are small (up to 3 vol%) [1]. If the voids were formed in chondrule formation process, we can obtain information of chondrule formation, such as ambient pressure, heating temperature, and heating time, by investigating the origin of them. Nakashima et al. [2] performed experimental reproduction of voids in chondrules by heating dust ball of mineral grains at 1 atm. They observed many voids but could not reproduce low porosities of natural chondrules. One of the possible origins for the voids in chondrules is interstitial gas among mineral grains in a precursor dust ball, which became voids by melting. If this is the case, the inconsistency between the natural chondrules and experimental products in [2] should be due to the difference of ambient gas pressures between them.

In this study, we performed a new heating experiment under low pressures, which are expected in the primitive solar nebula, to reproduce voids in chondrules.

Methods: An FeO-rich analog composition with a low liquidus temperature (~ 1200 °C) to natural chondrules was used as a starting material (FeO ~ 50 wt%). They were prepared from a mixture of mineral grains of olivine, clinopyroxene, orthopyroxene, and plagioclase. We heated them at 1040–1400 °C for 30 s–40 min at 10^{-3} atm, in a mixing gas of H₂ and CO₂ (H₂ 15 ml/min, CO₂ 15 ml/min). We observed run products using X-ray CT, and obtained the porosity of run products, connectivity, number density of voids by image analysis.

Results and Discussion: Voids were present in run products heated at more than 1080 °C. Many of the run products had higher porosities than natural chondrules as in the case of 1 atm experiments [2]. The porosity does not decrease monotonously, but the void formation occurred intermittently like bubbling. This result shows that the origin of voids in the experiments is not the interstitial gas among mineral grains. Moreover, the voids still existed in the run products even if we removed H₂O by heating at 400 °C for 1 hour, or Na by taking out plagioclase from the starting materials. This may suggest that voids are formed by vaporization of major elements, such as Fe or Si. The low porosities of natural chondrules might be due to low degrees of vaporization of the major elements. We will obtain more restrictions on the heating conditions of chondrules by obtaining conditions which can suppress vaporization of the major elements at low pressures.

References: [1] Tsuchiyama A. et al. 2003. Abstract #1271. 34th LPSC. [2] Nakashima R. et al. 2005. Fall Meeting of the Japanese Society for Planetary Sciences, 104.

5023

MINERALOGY, CHEMISTRY, AND ISOTOPE COMPOSITIONS OF COARSE-GRAINED ANTARCTIC MICROMETEORITES

R. Okazaki and T. Nakamura. Department of Earth and Planetary Sciences, Kyushu University, Fukuoka, Japan. E-mail: okazaki@geo.kyushu-u.ac.jp.

Coarse-grained micrometeorites (cg-MMs) consist mainly of olivine and/or pyroxene. Recently, crystalline dust particles are found in Stardust samples and show similarities with chondrites, IDPs, and cg-MMs [1–3]. Comparison of Stardust samples with cg-MMs is important to understand the material evolution in the solar system. For this purpose, we have performed multidiscipline analyses on cg-MMs. Samples are recovered from the Kuwagata and Tottuki NIPR collections (50–100 μm fraction). Synchrotron X-ray diffraction patterns were obtained for four Antarctic MMs (AMMs) at KEK in Japan. Interior texture and mineral chemistries were investigated with SEM and EPMA. Oxygen isotopes and REEs were determined with a Cameca 6f. Noble gases were extracted stepwise at 800 and 1800 °C using a furnace (named “Pot Pie”) and determined with a modified MM5400 (named “Jack and the Beanstalk”).

Ten cg-AMMs are identified in addition to our previous study [4]. All but one AMM contain solar ^4He and ^{20}Ne ($10\text{--}1800$ and $0.4\text{--}42 \times 10^{-6} \text{ cm}^3\text{STP/g}$, respectively), indicating that they were liberated as small particles to space. It is noteworthy that one AMM has unusual, AOA-like features. The AMM is composed of olivine (Fo_{99-96}) and a Ca, Al-rich phase. Olivine has higher Cr_2O_3 (0.37–0.47 wt%), MnO (1.0–1.5 wt%) and CaO (0.2–1.0 wt%). Its oxygen composition plots on the CCAM line with $\delta^{18}\text{O}$ of -40% , and the bulk REE abundance is $10\times$ CI with negative Eu anomaly. These features suggest a close link to AOAs [5].

Chondritic texture are seen in three AMMs that consist of FeO-poor (<3 wt%) olivine and/or pyroxene and FeO-rich material. Chemical compositions of the FeO-rich material are identical to those of chondrite matrix [6], while those of olivine and pyroxene are similar to those of type I chondrules [7]. The olivine and pyroxene are enriched in ^{16}O (up to -20% in $\delta^{18}\text{O}$), while the FeO-rich material is depleted in ^{16}O , similar to the CM-chondrite matrix composition [8]. These features resemble those of CM-chondrites and suggest asteroidal origin.

Three cg-AMMs are composed of porphyritic olivine/pyroxene with FeO of 10–15 wt% and MnO of 0.5 wt%. Their mineral chemistry resembles those of type II chondrules [7]. Two cg-AMMs are ^{16}O -poor along the TF line ($\delta^{18}\text{O}$ of 5–20%), while one AMM consisting of pyroxene ($\text{Wo}_4\text{En}_{87}$) is ^{16}O -rich (slightly above the CCAM line with $\delta^{18}\text{O}$ of $-4\text{--}0\%$). It is plausible that these AMMs are chondrule fragments.

References: [1] Brownlee D. et al. 2006. *Science* 314:1711–1716. [2] Flynn P. B. et al. 2006. *Science* 314:1731–1735. [3] Zolensky M. E. et al. 2006. *Science* 314:1735–1739. [4] Okazaki R. and Nakamura T. 2007. *Antarctic Meteorites* 31:83–84. [5] Krot A. N. et al. 2004. *Chemie der Erde* 64:185–239. [6] McSween H. Y. Jr. and Richardson S. M. 1977. *Geochimica et Cosmochimica Acta* 41:1145–1161. [7] Hutchison R. 2006. In *Meteorites*. Cambridge: Cambridge University Press. 506 p. [8] Rowe M. W. et al. 1994. *Geochimica et Cosmochimica Acta* 58:5341–5347.

5198

CATHODOLUMINESCENCE CHARACTERIZATION OF “BALLEN QUARTZ” IN IMPACTITEST. Okumura¹, A. Guccsik², H. Nishido³, K. Ninagawa⁴, M. Schmieder⁵, and E. Buchner⁵. ¹Open Research Center, Okayama University of Science, 1-1 Ridai-cho, Okayama 700-0005, Japan. E-mail: okumura@rins.ous.ac.jp. ²Max Planck Institute for Chemistry, P.O. Box 3060, D-55020 Mainz, Germany. ³Research Institute of Natural Sciences, Okayama University of Science, 1-1 Ridai-cho, Okayama 700-0005, Japan. ⁴Department of Applied Physics, Okayama University of Science, 1-1 Ridai-cho, Okayama 700-0005, Japan. ⁵Institute of Planetology, University of Stuttgart, Herdweg 51, D-70174, Stuttgart, Germany.

Introduction: “Ballen quartz” observed in impactites is characterized by bubble-wall texture under a petrological microscope. It has been known to be formed as a reversion product from lechatelierite or diaplectic quartz glass at a shock pressure from ~ 30 to ~ 55 GPa [1, 2]. However, its formation mechanism has not been understood well. In this study, we characterize ballen quartz by means of cathodoluminescence (CL) microscopy and spectroscopy.

Samples and Methods: The samples were selected from ballen quartz found in terrestrial impact craters; Dellen, Mien (both Sweden), Lappajärvi (Finland), Terny (Ukraine), and Ries (Germany). Their polished thin sections coated with 20 nm thickness carbon were employed for CL imaging and spectral analysis using a SEM-CL system comprising a secondary electron microscope combined with a grating-type monochromator. The measurements were carried on at an acceleration voltage of 15 kV with a beam current of 1.5 nA.

Results and Discussion: The Ballen quartz shows fairly weak CL with homogeneous feature in its grain. Most of all samples exhibit a broad band peak at around 650 nm, which might be assigned to a nonbridging oxygen hole center (NBOHC) recognized in amorphous and crystalline SiO_2 [3]. The CL spectral profiles are almost same among the samples, suggesting the resemblance of the crystal field around luminescence centers inferred from similar formation mechanism of ballen quartz. The sample from Lappajärvi crater has another band peak at around 450 nm, presumably attributed to a radiative recombination of the self-trapped exciton (STE) or an oxygen deficient center (ODC) [4]. Micro-XRD analysis shows that this part is composed of cristobalite and α -quartz. This indicates that ballen quartz might be formed in the quenching process from relatively high temperature. Furthermore, microRaman spectral analysis will be performed on the samples to identify minor crystal phase and to estimate quartz crystallinity.

Consequently, the facts obtained from CL result imply that the post-shock superheating effect could play a key role in the formation of ballen quartz texture.

References: [1] Carstens H. 1975. *Contributions to Mineralogy and Petrology* 50:145–155. [2] Bischoff A. and Stöffler D. 1984. *Journal of Geophysical Research* 89:B645–B656. [3] Stevens Kalceff M. A. and Phillips M. R. 1995. *Physical Review B* 52:3122–3134. [4] Stevens Kalceff M. A. 1998. *Physical Review B* 57:5674–5683.

5206

MICROINFRARED SPECTROSCOPY OF INSOLUBLE ORGANIC MATTER EXTRACTED FROM PRIMITIVE CHONDRITES

F. R. Orthous-Daunay, E. Quirico, O. Brissaud, and B. Schmitt. E-mail: forthous@ujf-grenoble.fr. ¹LPG Université Joseph Fourier, CNRS/INSU, BP 53 38041 Grenoble Cedex 9, France.

Introduction: Most of the organic matter in primitive chondrites consists in insoluble organic matter (IOM). Its polyaromatic substructure and isotopic compositions (D and ¹⁵N) are consistent with a presolar origin [1]. Similar polyaromatic compounds have been reported in stratospheric IDPs [2], Stardust grains and Antarctic micrometeorites [3]. The search of such compounds in both interstellar medium and comets using ground-based or spacecraft observations (e.g., Rosetta) is a major issue. This requires to determine the optical properties of IOMs and to understand the relation between their spectroscopic variations and their geological history. To date, it has been established that large isotopic, compositional and structural [4, 5] variations of IOMs depend on post-accretion processes, and possibly heterogeneity in the accreted precursors. In this study, we present a systematic infrared study of series of IOMs extracted from chondrites.

Methods and Results: We measured mid-infrared spectra (4000–650 cm⁻¹) with a Hyperion 3000 micro-imaging spectrometer (Bruker). IOMs were extracted with an original-designed method based on HCl/HF demineralization. The mechanical steps of phase segregation or centrifugation have been replaced by a continuous filtration process. 10–100 µg of initial whole chondrite rock and one single day suffice to obtain IOM material suitable for analyses. The IOM was then prepared as tens-of-micrometers-sized samples and were flattened between two windows (ZnS or KBr). Absorption spectra were acquired both by transmission through an original heated vacuum device or by attenuated total reflection with a Bruker Si crystal that improves spatial resolution for imagery.

Vibration bands from metamorphosed chondrites IOMs are not detectable, consistently with their high maturity. In contrast, IOMs from unmetamorphosed carbonaceous chondrites have typical spectra of kerogen-like compounds [6, 7]. They are similar to those of coals or type III kerogens. That way, we were able to use the standard modes assignment for terrestrial carbonaceous materials [8]. By combining different bands parameters, we will present a structural classification of IOMs extracted from CI, CM, CR groups and ungrouped C2 Tagish Lake.

References: [1] Robert F. and Epstein S. 1982. *Geochimica et Cosmochimica Acta* 42:81–95. [2] Quirico E. et al. 2005. *Planetary and Space Science* 43:1443–1448. [3] Dobrika E. et al. This issue. [4] Bonal L. et al. 2006. *Geochimica et Cosmochimica Acta* 70:1849–1863. [5] Cody G. D. and Alexander C. M. O'D. 2005. *Geochimica et Cosmochimica Acta* 69:1085–1097. [6] Wdowiak T. J. et al. 1988. *The Astrophysical Journal* 328: L75–L79. [7] Gardinier A. et al. 2000. *Earth and Planetary Science Letters* 184:9–21. [8] Painter P. C. et al. 1981. *Applied Spectroscopy* 35:461–514.

5022

NOBLE GAS RETENTIVITY OF CARBON ALLOTROPES AND KEROGEN: FEASIBILITY OF KEROGEN AS PHASE Q

T. Osawa¹, N. Hirao², N. Takeda³, and Y. Baba². ¹Neutron Imaging and Activation Analysis Group, Quantum Beam Science Directorate, Japan Atomic Energy Agency (JAEA), Tokai-mura, Naka-Gun, Ibaraki 319-1195, Japan. E-mail: osawa.takahito@jaea.go.jp. ²Surface Chemistry Research Group, Synchrotron Radiation Research Unit, Quantum Beam Science Directorate, Japan Atomic Energy Agency (JAEA), Tokai-mura, Naka-gun, Ibaraki 319-1195, Japan. ³JAPEX Research Center, Japan Petroleum Exploration Co. Ltd. Hamada 1-2-1, Mihama-ku, Chiba 261-0025, Japan.

Heavy noble gases in primitive meteorites are mainly hosted by an enigmatic phase referred to as phase Q, which is a residue left after treatment of bulk meteorites by hydrochloric acid and hydrofluoric acid [1–3]. Extremely large amounts of heavy noble gases are concentrated in a carbonaceous phase analogous to terrestrial type III kerogen [4–7]. Although the trapping mechanism of noble gases in the phase is still unclear, phase Q must have very high noble gas retentivity because extremely large amounts of heavy noble gases are tightly retained in a minor fraction, about 1%, of the total mass of the whole meteorite. To verify that kerogen is a carrier phase of Q-noble gases, X-ray absorption spectroscopy (XAS) and X-ray photoelectron spectroscopy (XPS) using synchrotron radiation were carried out for type II and III kerogens (coals, collected in Hokkaido, north Japan) and carbon allotropes (highly oriented pyrolytic graphite [HOPG], carbon nanotube, fullerene mixture, and chemical vapor deposition [CVD] diamond) which had been bombarded by 3 keV Ar, Kr, and Xe ions, and noble gas retentivities of the materials were compared. The experiments were performed at the BL-27A station of the Photon Factory in the High Energy Accelerator Research Organization (KEK-PF). Ar concentrations were estimated from two methods: the peak area of Ar1s in XPS and the jump ratio of Ar K-edge appearing at ~3200 eV in XAS. Kr and Xe concentrations were estimated by the peak areas of Kr3p3/2 and Xe3d5/2 in XPS. The concentrations were used as indexes of the relative retentivity of noble gases. Our investigation shows that the surface concentrations of carbon allotropes (0.40–0.79 atom%) are much higher than those of kerogens (0.04–0.08 atom%). Ar retentivity of pyridine-treated kerogens was the same as non-treated ones, indicating that the existence of bitumen does not affect Ar retentivity. This unexpected result clearly shows that the terrestrial kerogens are inferior to other carbon materials in noble gas retentivity, and thus, phase Q might not be similar to terrestrial kerogen, especially coals tested in this work. If heavy noble gases are really concentrated in carbonaceous components of primitive chondrites, phase Q may have a more orderly structure than terrestrial kerogen because the greatest difference between terrestrial kerogen and carbon allotropes is orderliness of molecular structure.

References: [1] Lewis et al. 1975. *Science* 190:1251–1262. [2] Ott et al. 1981. *Geochimica et Cosmochimica Acta* 45:1751–1788. [3] Huss et al. 1996. *Geochimica et Cosmochimica Acta* 60:3311–3340. [4] Hayatsu et al. 1983. *Meteoritics* 18:310. [5] Murae. 1994. *Proceedings of the NIPR Symposium of Antarctic Meteorites* 7:262–274. [6] Gardinier et al. 2000. *Earth and Planetary Science Letters* 184:9–21. [7] Remusat et al. 2003. Abstract #1230. 34th LPSC.

5196

RE-EXAMINATION OF CHINGA METEORITE USING MÖSSBAUER SPECTROSCOPY WITH HIGH-VELOCITY RESOLUTION: PRELIMINARY RESULTS
M. I. Oshtrakh¹, N. V. Abramova¹, V. I. Grokhovsky¹, and V. A. Semionkin².

¹Faculty of Physical Techniques and Devices for Quality Control, Ural State Technical University, UPI, Ekaterinburg 620002, Russian Federation. E-mail: oshtrakh@mail.ut-net.ru. ²Faculty of Experimental Physics, Ural State Technical University, UPI, Ekaterinburg 620002, Russian Federation.

Introduction: Iron meteorite Chinga was classified as ataxite (IVB) with about 16.8 wt% of Ni. Previous Mössbauer study of Chinga meteorite [1] showed the presence of three phases such as α_2 -Fe(Ni, Co) (martensite with about 19.6 at% of Ni), α -Fe(Ni, Co) (kamacite with about 4.8 at% of Ni) and γ -FeNi (tetrataenite with 50 at% of Ni). Recently new possibilities of Mössbauer spectroscopy with high velocity resolution in meteorites studies were showed [2–4]. Therefore, reexamination of Chinga meteorite using this technique was started.

Experimental: Metal of Chinga meteorite was prepared as powder and measured at room temperature using high stable, precision and sensitive Mössbauer spectrometer SM-2201 (see [2–4]) in 4096 channels.

Results and Discussion: High-velocity resolution Mössbauer spectrum of Chinga meteorite (4096 channels) is shown in Fig. 1. The best fit demonstrated more than three sextets as in previous study [1]. New results may be explained as the presence of martensite α_2 -Fe(Ni, Co) with different Ni content (sextets 1 and 2 with $H_{\text{eff}} = 354$ and 344 kOe), kamacite α -Fe(Ni, Co) (sextet 3 with $H_{\text{eff}} = 335$ kOe), taenite γ -Fe(Ni, Co) with different Ni content (sextets 4 and 5 with $H_{\text{eff}} = 326$ and 313 kOe) and tetrataenite γ -FeNi (sextet 6 with $H_{\text{eff}} = 295$ kOe).

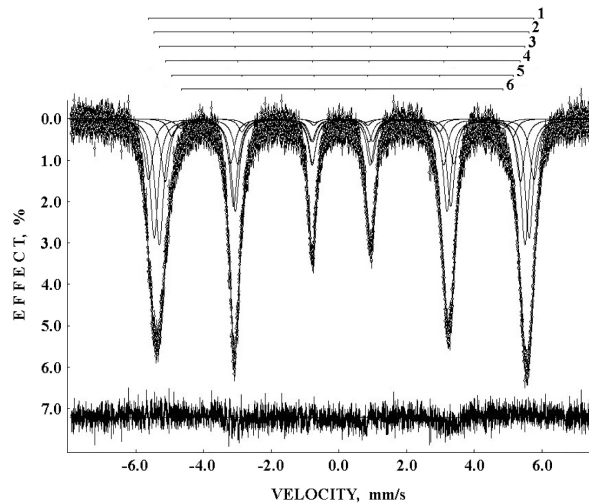


Fig. 1. Mössbauer spectrum of Chinga meteorite with high velocity resolution.

Acknowledgements: This work was supported in part by the Russian Foundation for Basic Research (grants No 06-08-00705-a and No 07-05-96061-r-ural-a).

References: [1] Oshtrakh M. I. et al. 2004. *Hyperfine Interactions* 158: 365–370. [2] Zhiganova E. V. et al. 2007. *Physica Status Solidi A* 204:1185–1191. [3] Petrova E. V. et al. Forthcoming. *Journal of Physics and Chemistry of Solids*. [4] Oshtrakh M. I. et al. Forthcoming. *Meteoritics & Planetary Science*.

5244

SUBSURFACE CHEMISTRY OF THE IMBRIUM BASIN INFERRED FROM CLEMENTINE UVVIS SPECTROSCOPY

Hisashi Otake. Japan Aerospace Exploration Agency, 2-1-1 Sengen, Tsukuba, Ibaraki 305-8505, Japan. E-mail: ootake.hisashi@jaxa.jp.

Since ejecta around an impact crater is excavated from a depth, its mineralogy and chemistry will provide us with information of the pre-impact subsurface composition.

The depth from which crater ejecta were excavated was obtained from laboratory experiments, field studies, and a simplified quantitative model (Z-model and the scaling law of ejection velocity).

From these studies, it is believed that surface material of an ejecta blanket between 1.1 and 1.5 radii from the crater was excavated from a depth of 0.13 to 0.15 radii.

Combining the surface and subsurface basalt distributions with crater-counting ages for the mare basalt [1], we obtained the following results:

1. The averages of TiO₂ and FeO increased with time from the Imbrian to the Eratosthenian periods.
2. Volcanic activities in Mare Imbrium drastically decreased and basalts changed from low-Ti to high-Ti content around the transition of the Imbrian to Eratosthenian period.
3. Basalts with less than 3 wt% TiO₂ erupted by turns mainly in the Imbrian period.

References: [1] Hiesinger H., Jaumann R., Neukum G., and Head J. W. 2000. *Journal of Geophysical Research* 29:239–275.

5089

TRAPPING OF COSMIC RAY HELIUM BY INTERSTELLAR DIAMOND

U. Ott¹ and G. R. Huss². ¹Max-Planck-Institut für Chemie, J.-J.-Becher-Weg 27, D-55128 Mainz, Germany. E-mail: ott@mpch-mainz.mpg.de. ²HIGP, University of Hawai'i at Manoa, Honolulu, HI 96822, USA.

Introduction: Nanodiamond was the first of the pre-solar phases to be recognized in primitive meteorites, but progress in understanding them has been much slower than in cases of other pre-solar ("stardust") grains. Major problems are the small size of the nanodiamonds, which does not allow for single grain analysis, and the fact that the most diagnostic isotopic features are carried by trace noble gases, which are only present in a minority of the diamonds (e.g., [1]). In fact, at present it is unclear whether all diamonds are of pre-solar origin or just a small fraction.

Implantation Experiments: Some progress regarding the origin and trapping of the noble gases has been made thanks to ion implantation experiments using terrestrial artificial nanodiamond as an analogue material [2, 3]. Taking these experiments at face value and using them to interpret meteoritic nanodiamonds, it follows that the bi-modal release and isotopic difference between low-T and high-T releases can be largely explained by release of a single component (P3) to which Kr- and Xe-HL have been added [4, 5]. Variations in ³⁸Ar/³⁶Ar and ²⁰Ne/²²Ne can be accounted for without calling for a major contribution from a nucleosynthetic component.

²¹Ne and ³He: The rare isotopes ²¹Ne and ³He show excesses relative to fractionated P3, a fact that naturally brings cosmogenic contributions to mind. There are three problems associated with this, however: a) cosmogenic ²¹Ne is not produced from carbon; b) nanodiamonds are so small that cosmogenic nuclides produced within them are lost due to recoil. Only if produced in a larger entity (≥tens of μm), with which the nanodiamonds are associated, can cosmogenic products be trapped [5]; c) the observed high ratio of excess ³He to excess ²¹Ne of >40 [5].

Cosmic Ray Trapping: Galactic cosmic rays arriving at the top of the atmosphere are rich in ³He (³He/²¹Ne ~300 [6–8]). In interstellar space, cosmogenic production of ³He in grains by (high energy) protons cannot be avoided, although the ³He may be lost. Similarly, trapping of GCR ³He cannot be avoided after it has been slowed down sufficiently. For a preliminary estimate of the efficiency of ³He trapping by nanodiamonds dispersed in an interstellar cloud presenting an obstacle <0.02 g/cm² to cosmic rays, we have used the mean interstellar proton flux and energy spectrum of [9] with the requisite abundance of ³He (³He/H ~ 0.02; [7]). Under these conditions trapping of GCR ³He is more efficient than production in carbon following [9]. Assuming all the nanodiamonds to be pre-solar, a CRT (cosmic ray trapping) age is suggested to be in the range 25–100 Ma.

References: [1] Nittler L. R. 2003. *Earth and Planetary Science Letters* 209:259–273. [2] Verchovsky A. B. et al. 2000. Goldschmidt Conference. Abstract #1050. [3] Koscheev A. P. et al. 2001. *Nature* 412:615–617. [4] Huss G. R. et al. 2000. *Meteoritics & Planetary Science* 35:A79–A80. [5] Huss G. R. et al. Forthcoming. *Meteoritics & Planetary Science*. [6] Lund N. 1984. *Advances in Space Research* 4:5–14. [7] Wang J. Z. et al. 2002. *The Astrophysical Journal* 564:244–259. [8] Israel M. H. et al. 2005. *Nuclear Physics A* 758:201c–208c. [9] Reedy R. C. 1989. 20th LPSC. pp. 888–889.

5088

NOBLE GASES IN THE CARANCAS (PUNO, PERU) METEORITE

U. Ott¹, L. Franke¹, and Th. Grau². ¹Abteilung Geochemie, Max-Planck-Institut für Chemie, Joh.-J.-Becher-Weg 27, D-55128 Mainz, Germany. E-mail: ott@mpch-mainz.mpg.de. ²D-16321 Bernau b. Berlin, Germany.

Introduction: The Carancas meteorite fell on September 15, 2007, in Carancas, Lake Titicaca region, in southern Peru, forming a spectacular nearly 15 m (diameter) crater [1]. It is probably an H4–5 ordinary chondrite and its mass and diameter have been estimated as ~1.1 m and 3 tons, respectively [1].

Experimental: We analyzed for their noble gas content several specimens collected shortly after the fall. One of them (APE-H) was taken from the dust layer around the crater rim and is expected to be a mixture from various portions of the impactor. Analyses were performed using standard procedures [2].

Radiogenic and Solar Wind Gases: Helium and neon contain radiogenic and cosmogenic components plus implanted solar wind. Except for one case (APE-C) with a very small amount, solar Ne is clearly observable in all samples. Concentrations of trapped ²⁰Ne range from ~1 to ~50 × 10⁻⁸ cc/g. The APE-H sample has an abundance of ~20 × 10⁻⁸ cc/g, which is close to the mean of the others, as expected. He-Ne abundance systematics suggests solar Ne with a ⁴He/²⁰Ne ratio of ~160 to have been added to ~1100 × 10⁻⁸ cc/g of radiogenic ⁴He (corresponding to a U/Th-He gas retention age of ~3100 Ma, assuming average H chondrite U and Th abundances [3]). Nominal K-Ar ages assuming average H chondrite K abundance [3] range between ~4100 and ~4600 Ma.

Cosmic Ray Exposure: Cosmic ray exposure ages have been calculated following [4] with the modified ³⁸Ar production rate of [5] and assuming average H chondrite chemistry [3]. Nominal ³He ages range from 6.5 to 8.0 Ma, ²¹Ne and ³⁸Ar ages between 8.4 and 10.1 and between 7.2 and 12.4 Ma. There are systematic uncertainties because, with abundant solar Ne present, the shielding parameter (²²Ne/²¹Ne)_{cos} is not well determined in several cases and because for large meteoroids the empirical shielding correction becomes unreliable [6]. Specimen APE-C with little solar Ne has a rather well determined (²²Ne/²¹Ne)_{cos} ratio of 1.07, consistent with the estimated large size and similar to what has been measured in the large H chondrite Jilin [7]. Its mean age from ³He, ²¹Ne, and ³⁸Ar is 8.4 Ma, so Carancas may belong to the ~7–8 Ma exposure age peak for H chondrites [8, 5].

Planetary Gases and Radiogenic ¹²⁹Xe: Trapped argon, krypton, and xenon are mostly of the planetary type. Concentrations (³⁶Ar between ~1 and ~3 × 10⁻⁸ cc/g) are more consistent with an H5 classification than type H4 [9]. Excesses of ¹²⁹Xe from ¹²⁹I decay amount to between 2 and 12 × 10⁻¹¹ cc/g.

References: [1] Tancredi G. et al. 2008. Abstract #1216. 39th LPSC. [2] Schelhaas N. et al. 1990. *Geochimica et Cosmochimica Acta* 54:2869–2882. [3] Wasson J. T. and Kallemeyn G. W. 1988. *Philosophical Transactions of the Royal Society London A* 325:535–544. [4] Eugster O. 1988. *Geochimica et Cosmochimica Acta* 52:1649–1662. [5] Schultz L. et al. 1991. *Geochimica et Cosmochimica Acta* 55:59–66. [6] Masarik J. et al. 2001. *Meteoritics & Planetary Science* 36:643–650. [7] Begemann F. et al. 1985. *Earth and Planetary Science Letters* 72:247–262. [8] Eugster O. 2003. *Chemie der Erde* 63:3–30. [9] Marti K. 1967. *Earth and Planetary Science Letters* 22:193–196.

5090

METEORITE FINDS FROM SOUTHERN TUNISIA

N. Ouazaa¹, N. Perchiazzi², S. Kassaa¹, A. Zeoli³, M. Ghanmi¹, and L. Folco³. ¹Département du Géologie, Faculté de Sciences de Tunis, Campus Universitaire, 1060 Tunis, Tunisia. E-mail: nejia_ouazaa@yahoo.fr. ²Dipartimento di Scienze della Terra, Università di Pisa, Via S. Maria 53, 56126 Pisa, Italy. ³Museo Nazionale dell'Antartide, Università di Siena, Via Laterina 8, 53100 Siena, Italy.

From April 5 to April 11, 2008, we undertook a reconnaissance campaign in southern Tunisia to assess the potential for yielding high concentrations of meteorites.

We explored some areas of the eastern sector of southern Tunisia 120 km due south of the town Rémada, close to the Bir Zar Tunisian-Lybian frontier post. This is a rocky desert (reg) region due east of the Grand Erg Oriental, which is dominated by plateaus and mesas consisting of upper Cretaceous sedimentary rock sequences. Local logistic support was provided by Compagnie Général de Géophysic-Veritas (CGG-VERITAS).

Search traverses were conducted using four-wheel drive vehicles and on foot. Although search conditions were difficult during most of the expedition due to the fairly strong April sandstorms, nine meteorites totaling 1.3 kg were found (mass range: 5–630 g). Two meteorites were found in the Es-Soud area (~31°29'N, 9°51'E), whereas the other seven were found in the Makhrouga area (~31°54'N, 10°11'E).

Meteorites show variable degrees of terrestrial weathering, ranging from minor to severe, suggesting different resident times on Earth. In situ classification and pairing, based on magnetic susceptibility measurements with a hand-held meter (SM30) following [1, 2], revealed that the nine meteorite specimens are nine distinct meteorites likely belonging to the ordinary chondrite group. We hope to present the petrographic classification of these meteorites at the 71st Meteoritical Society annual meeting and subsequently announce their discovery in the Meteoritical Bulletin, possibly using their present field name, Bir Zar, as an official name. Specimens were split and are now maintained by the Faculté de Sciences de Tunis, Département de Géologie, and the Museo Nazionale dell'Antartide in Siena.

In conclusion, the nine meteorites found during our reconnaissance expedition document that the rocky deserts in southern Tunisia are suitable terrains for systematic searches for meteorites. We are planning a second search campaign in autumn 2008.

Acknowledgements: The idea for this meteorite search expedition stemmed from the meeting of the Tunisian and Italian parties at the Desert Meteorites Workshop held in Casablanca in August 2006, organized by H. Chennaoui, and sponsored by the Meteoritical Society. NP, LF and AZ are supported by PNRA, Pisa University and Siena University.

References: [1] Folco L. et al. 2006. *Meteoritics & Planetary Science* 41:343–353. [2] Rochette P. et al. 2003. *Meteoritics & Planetary Science* 38: 251–268.

5042

PRESSURE-TEMPERATURE CONDITIONS AND U-Pb AGES OF SHOCK MELT VEINS IN L6 CHONDRITES

S. Ozawa¹, E. Ohtani¹, A. Suzuki¹, M. Miyahara¹, K. Terada², and M. Kimura³. ¹Graduate School of Science, Tohoku University, Sendai 980-8578, Japan. E-mail: ozawasin@ganko.tohoku.ac.jp ²Earth and Planetary Systems Science, Hiroshima University, Higashi-Hiroshima 739-8526, Japan. ³Faculty of Science, Ibaraki University, Mito 310-8512, Japan.

Introduction: Collision events of planetary materials are fundamental processes of planet formation and evolution. Shocked meteorites have recorded such impact events in the solar system as some features of shock metamorphism. In recent studies, many high pressure minerals have been found in shock melt veins or melt pockets of meteorites and shock conditions such as pressure, temperature and shock duration have been estimated [1–3]. In this study, mineralogy of shock melt veins in two L6 chondrites (Sahara 98222 and Yamato-74445) was investigated using a microRaman spectrometer and a FE-SEM to estimate the pressure and temperature conditions during the shock events. Moreover, U-Pb dating of phosphates in and around the shock melt vein of Sahara 98222 was conducted with SHRIMP II to reveal when the impact event happened.

Results and Discussion: In the shock melt veins of Sahara 98222, wadsleyite, jadeite, and tuite (high-pressure polymorph of whitlockite) were found as solid-state transformation products. Shock melt vein of Yamato-74445 contains ringwoodite (+wadsleyite), majorite, akimotoite, and lingunite formed by solid-state phase transition. Based on mineralogy of shock melt veins and phase diagrams of constituent minerals, pressure-temperature conditions of shock events recorded in these meteorites were estimated as follows: 13–15 GPa, >1900 °C for Sahara 98222 and 23–24 GPa, >2100 °C for Yamato-74445 [4–7]. U-Pb dating of phosphates in and around the shock melt vein of Sahara 98222 was conducted using a SHRIMP II. Sahara 98222 contains apatite and whitlockite as phosphate minerals and all whitlockite grains entrained in shock melt veins are completely transformed into high-pressure polymorph, tuite. In situ analyses of eleven phosphate grains resulted in a total Pb/U isochron age of 4467 ± 22 Ma in $^{238}\text{U}/^{206}\text{Pb}$ - $^{207}\text{Pb}/^{206}\text{Pb}$ - $^{204}\text{Pb}/^{206}\text{Pb}$ 3-D space (95% confidence limit). Previously reported ages of unshocked chondrites are basically older than 4500 Ma and our results are slightly younger than 4500 Ma, even the experimental uncertainty were considered [8, 9]. It suggests that Sahara 98222 recorded a shock event occurred at the very early stage of the solar system, when planetary formation was going on.

References: [1] Ohtani E. et al. 2004. *Earth and Planetary Science Letters* 227:505–515. [2] Beck P. et al. 2005. *Nature* 435:1071–1074. [3] Xie Z. et al. 2006. *Geochimica et Cosmochimica Acta* 70:504–515. [4] Akaogi M. et al. 1989. *Journal of Geophysical Research* 94:15,671–15,685. [5] Ohtani E. et al. 1991. *Earth and Planetary Science Letters* 102:158–166. [6] Agee C. B. et al. 1995. *Journal of Geophysical Research* 100:17,725–17,740. [7] Zhang J. and Herzberg C. 1994. *Journal of Geophysical Research* 99:17,729–17,742. [8] Göpel C. et al. 1994. *Earth and Planetary Science Letters* 121:153–171. [9] Rotenberg E. and Amelin Y. 2003. 34th LPSC. pp. 1902.

5302

³⁹Ar-⁴⁰Ar AGES OF THE NAKHLITES: A SYNTHESIS

J. Park^{1,2}, D. H. Garrison^{1,3}, and D. D. Bogard¹. ¹ARES code KR, NASA Johnson Space Center, Houston, TX 77058, USA. ²NASA Postdoctoral Program, TX, USA. ³ESCG/Barrios Technology.

Introduction: Radiometric ages, including Ar-Ar data, of all nakhlites are similar at 1.2–1.4 Ga (e.g., [1, 2]). This is not the case for shergottites with the presence of Martian atmosphere and inherited radiogenic ⁴⁰Ar from magma [3, 4]. A total of seven nakhlites have been found (Nakhla, Lafayette, Governador Valadares, Northwest Africa [NWA] 817, NWA 998, and the paired group Yamato- [Y-] 000593/749/802 and Miller Range [MIL] 03346). Including this study, Ar-Ar measurements have been conducted on five of these specimens at NASA-JSC.

Ar-Ar Ages of Nakhlites: For MIL 03346, measurements were made on a whole rock sample (WR), as well as plagioclase (Plag) and pyroxene separates (Pyx). Ar-Ar ages of MIL 03346-WR, -Plag, and -Pyx are 1396 ± 100 Ma [5], 1413 ± 88 Ma [6], and 1404 ± 182 Ma, respectively, based on Ar-Ar spectra. Isochron slopes for WR and Plag are 1434 ± 96 Ma and 1368 ± 83 Ma, respectively. The preferred MIL 03346 age is 1368 ± 83 Ma obtained from the Plag isochron. This Ar-Ar age for MIL agrees with the Sm-Nd age of 1.36 ± 0.03 Ga [7]. Ar-Ar ages spectra of Y-000593-WR, -Plag, and -Pyx are 1405 ± 106 Ma [8], 1397 ± 91 Ma [6], and 1416 ± 116 Ma, respectively. The preferred Ar-Ar age of Y-000593 is 1397 ± 91 Ma from Plag spectrum, which overlaps within the uncertainties with the Sm-Nd age of 1.31 ± 0.03 Ga [9]. The analyzed Ar-Ar age of NWA 998-Plag is 1334 ± 12 Ma [8] derived from its age spectrum. The Ar-Ar age of Nakhla measured as 1356 ± 21 Ma [8] agrees with Ar-Ar ages of Nakhla reported by others as 1.3 Ga [10] and 1332 ± 10 Ma [11]. For reference, the Ar-Ar ages of Lafayette are 1330 ± 33 Ma [10, 12] and 1322 ± 10 Ma [11], and the Ar-Ar age of Governador Valadares is 1320 ± 40 Ma [13]. The Ar-Ar age of NWA 817 has yet to be reported.

K-⁴⁰Ar Isochron Age of Six Nakhlites: We plot the isochron of total ⁴⁰Ar versus total K for the six nakhlites for which data is available, including whole rock and mineral separates. The combined data set from NASA-JSC and Lafayette [10] adheres well to the line of the unweighed isochron age of 1325 ± 18 Ma (2σ). Unlike shergottites, the Ar-Ar ages and K-Ar isochrons of nakhlites are not strongly affected by excess ⁴⁰Ar in low-temperature extractions due to their older radiometric ages of 1.2–1.4 Ga, and perhaps lower initial excess ⁴⁰Ar.

Comments: The authors would like to dedicate this abstract to Gordon A. McKay, who really loved his work and friends.

References: [1] Nyquist L. E. et al. 2001. *Space Science Reviews* 96: 105–164. [2] Borg L. and Drake M. J. 2005. *Journal of Geophysical Research* 110:E12S03. [3] Bogard D. D. and Johnson P. 1983. *Science* 221: 651–654. [4] Bogard D. D. and Park J. Forthcoming. *Meteoritics & Planetary Science*. [5] Bogard D. D. and Garrison D. H. 2006. Abstract #1108. 37th LPSC. [6] Park J. et al. 2007. Abstract #1114. 38th LPSC. [7] Shih C.-Y. et al. 2006. #1701. 37th LPSC. [8] Garrison D. H. and Bogard D. D. 2005. Abstract #1137. 36th LPSC. [9] Misawa K. et al. 2005. *Antarctic Meteorite Research* 18:133–151. [10] Podosek F. A. 1973. *Earth and Planetary Science Letters* 19:135–144. [11] Swindle T. D. and Olson E. K. 2004. *Meteoritics & Planetary Science* 39:755–766. [12] Podosek F. A. and Huneke J. C. 1973. *Geochimica et Cosmochimica Acta* 37:667–684. [13] Bogard D. D. and Husain L. 1977. *Geophysical Research Letters* 4:69–71.

5239

CARBON AND NITROGEN COSMOCHEMISTRY OF THE CO3 GROUP

V. K. Pearson, R. C. Greenwood, A. B. Verchovsky, D. C. Turner, and I. Gilmour. Planetary and Space Sciences Research Institute, Open University, Milton Keynes MK7 6AA, UK. E-mail: v.k.pearson@open.ac.uk.

Introduction: Previous studies have determined that thermal alteration played a major role on the CO3 parent body, resulting in a metamorphic sequence through the group [1, 2]. However, the alteration of C and N components in the CO3 parent body may not be as straightforward as a single metamorphic sequence. [3–5] have reported mineralogical evidence for minor aqueous alteration in Kainsaz and Warrenton, and traces of carbonates have been inferred in Lance, Kainsaz, and Felix [6]. The apparent “anomalous” specimen, Ornans [7, 8] displays an apparent higher metamorphic grade according to its light element geochemistry than that perceived by its petrography. We have previously reported preliminary studies of the CO3 chondrites in relation to their carbon and nitrogen cosmochemistries [9, 10]. Here we present the results of further high-resolution studies on the newly fallen Moss CO3 and its status within the CO3 group.

Experimental: High-resolution C and N stepped combustion (and pyrolysis) mass spectrometry was undertaken [11] on ~2 mg of the Moss meteorite and compared with similar analyses reported by [12]. Carbon and nitrogen elemental abundances and isotopic compositions will be measured using an elemental analyzer (Europa ANCA-SL) coupled to a continuous-flow mass spectrometer (Europa GEO 20-20) [13]. Organic characterization was undertaken using a Pegasus GCxGC-TOFMS [16].

Results: The total carbon yield of Moss from stepped combustion was 0.21 wt% (comparable to Ornans (0.24 wt% [12] but lower than other CO3 falls) with a total integrated δ¹³C value of –10.4‰ (heavier than all other CO3s). This may imply the presence of isotopically heavy carbonates in Moss as seen in other carbonaceous chondrites. A broad C release at 500 °C typical of carbonates [6] is not accompanied by a characteristically heavy δ¹³C value and when compared with stepped pyrolysis, the results are therefore not typical of the presence of extraterrestrial carbonates in Moss. The retention of ¹³C-rich components in Moss compared with other CO3s may be an indicator of heterogeneous secondary alteration on the CO3 parent body and will be investigated through further work on elemental C and organic phases. Simultaneous nitrogen analysis liberated 8 ppm N (lower than other CO3 falls) with a total integrated δ¹⁵N of –43.14‰ (lighter than other CO3 falls). Further work is intended to establish if these isotopic anomalies are related to the secondary loss of ¹⁵N-rich entities or the presence of exotic components not seen in other CO3s.

References: [1] Scott and Jones. 1990. *Geochimica et Cosmochimica Acta* 54:2485–2502. [2] Chizmadia et al. 2002. *Meteoritics & Planetary Science* 37:1781–1796. [3] Kerridge. 1964. *Annals of the New York Academy of Sciences* 119:41–53. [4] Keller and Buseck. 1990. *Geochimica et Cosmochimica Acta* 54:1155–1163. [5] Brearley and Jones. 1998. Chondritic meteorites. In *Planetary materials*. [6] Grady et al. 1988. 19th LPSC. pp. 409–411. [7] McSween. 1977. *Geochimica et Cosmochimica Acta* 41:477–491. [8] Greenwood and Franchi. 2004. *Meteoritics & Planetary Science* 39: 1823–1838. [9] Greenwood et al. 2006. Abstract #2267. 38th LPSC. [10] Pearson et al. 2006. Abstract #1846. 38th LPSC. [11] Verchovsky et al. 1997. *Meteoritics & Planetary Science* 32:A131. [12] Newton. 1994. Ph.D. thesis, Open University. [13] Pearson et al. 2006. *Meteoritics & Planetary Science* 41:1891–1918. [14] Pearson et al. 2006. Abstract #5090. 38th LPSC.

5186

INTERPRETATION OF REMOTE SENSING DATA WITH SH-MATRIX METHOD

D. V. Petrov and Yu. G. Shkuratov. Kharkov Astronomical Observatory, 35 Sumskaya Street. Kharkov 61022, Ukraine. E-mail: petrov@astron.kharkov.ua.

Introduction: The *T*-matrix method is widely used for calculations of scattering properties of non-spherical particles [1]. In the *T*-matrix method, the incident and scattered electric fields are expanded in a series of vector spherical wave functions, and then a relation between the expansion coefficients of these fields is established by means of a transition matrix (or *T* matrix). *T*-matrix elements depend on the optical and geometrical parameters of the scatterers and do not depend on the illumination/observation geometry, so the *T*-matrix approach allows for the separation of the influence of illumination/observation parameters and inner properties of a scattering object such as its size, shape parameters, and refractive index. Our modification of the *T*-matrix approach (specifically we use here Extended Boundary Condition Method) consists of a further development, namely, we separate the contributions of the different inner parameters of the scattering object [2–5].

Sh-Matrix Method: We developed a modification of the *T*-matrix method, which allows us to effectively study scattering properties of particles having irregular shapes. This method allows us to calculate a scattered field in any point of space, and any characteristic of scattered light; that is why this method is very useful. Principal new features: the possibility of calculation of scattering properties of particles without any limitations (such as symmetry axis requirement) on the shape and the possibility of analytical averaging of particle scattering properties over ensemble of particles with different sizes and refractive indices. These new features of modified *T*-matrix method make this method much faster than the analogous methods and suggest that this method seems to be most promising for investigations in many branches of science, for example, in space studies of the Moon, planets, and small bodies of the solar system by remote sensing methods—for investigation of scattering properties of remote objects. This method of scattering calculation allow us to interpret the scattered light data, and based on this data, to estimate information about remote planets, such as sizes and refractive indices of particles ensemble, cover the surfaces of the Moon, planets, and small bodies of the solar system.

References: [1] Mishchenko M. I., Travis L. D., Mackowski D. W. 1996. *T*-matrix computations of light scattering by nonspherical particles: A review. *Journal of Quantitative Spectroscopy and Radiative Transfer* 55: 535–575. [2] Petrov D., Synelnyk E., Shkuratov Yu., and Videen G. 2006. The *T*-matrix technique for calculations of scattering properties of ensembles of randomly oriented particles with different size. *Journal of Quantitative Spectroscopy and Radiative Transfer* 102:85–110. [3] Petrov D. V., Shkuratov Yu. G., and Videen G. 2007. Analytical light-scattering solution for Chebyshev particles. *Journal of the Optical Society of America A* 24: 1103–1119. [4] Petrov D., Shkuratov Yu., Zubko E., and Videen G. 2007. Sh-matrices method as applied to scattering by particles with layered structure. *Journal of Quantitative Spectroscopy and Radiative Transfer* 106: 437–454. [5] Petrov D., Videen G., Shkuratov Yu., and Kaydash M. 2007. Analytic *T*-matrix solution of light scattering from capsule and bi-sphere particles: Applications to spore detection. *Journal of Quantitative Spectroscopy and Radiative Transfer* 108:81–105.

5051

THE MARTIAN SURFACE REVISITED BY MEX/OMEGA AND IMPLICATIONS FOR THE FORMATION OF SHERGOTTITES

F. Poulet¹, V. Sautter², N. Mangold³, J.-P. Bibring¹, J.-M. Bardintzeff³, B. Platevoet³, Y. Langevin¹, and B. Gondet¹. ¹Institut d'Astrophysique Spatiale, Université Paris-Sud, 91405 Orsay Cedex, France. E-mail: francois.poulet@ias.u-psud.fr. ²Museum National d'Histoire Naturelle, Paris, France. ³IDES, Université Paris-Sud, 91405 Orsay Cedex, France.

Using classical methods of spectral identification (spectral parameter, Modified Gaussian Model, linear mixing), the VIS/NIR imaging spectrometer OMEGA aboard ESA/Mars Express has provided a consensus on the identification and spatial distribution of several classes of mafic minerals [1, 2]. The Noachian crust is enriched in low-Ca pyroxene, with respect to more recent lavas flows in which high-Ca pyroxene dominates, whereas olivine is present without hydrated phases in dunes and eroded layers corresponding to ancient lava flows or melt ejectas.

The objective of this work is to: 1) quantify the modal mineralogy of different low-albedo regions using OMEGA data, 2) compare the derived modal and elemental compositions with those derived from previous analyses based on thermal measurements, 3) constrain the evolution of the Martian upper crust, and 4) identify the relationship with the range of mineral assemblages of the so-called SNC Martian meteorites.

The modal mineralogy of several low-albedo regions of Mars is derived by using a spectral model based on the Shkuratov radiative transfer model [3]. The derived mineralogy was classified by the relative abundances of plagioclase, olivine, low-calcium pyroxene (LCP), and high-calcium pyroxene (HCP) on ternary diagrams. For all the studied low-albedo regions, both HCP and LCP are modeled above the detection limits, with HCP being the dominant pyroxene. The neutral components (plagioclase) and pyroxene abundances are consistent with those measured by MGS/TES. By contrast, the notable difference between this work and the different TES deconvolutions is the larger abundance of LCP found in our work. Region-to-region differences in modal mineralogy exist for the low-albedo olivine-free regions. The variations of LCP abundance show a compositional trend from the oldest terrains exhibiting larger abundance (LCP-rich outcrops, Nili Fossae highlands) to the youngest ones (Syrtris lavas).

This LCP/HCP ratio decrease through time correlates with HCP-rich mineralogy of SNC young volcanics assemblages. Such an evolution translates to CaO increase and Al₂O₃ and mg# decreases, which could evidence a decreasing degree of partial melting from Noachian to Hesperian and Amazonian younger volcanics. The basaltic shergottites are LCP-rich compared to nakhlites. The old ages found recently by [4] of about 4.1 Gy for basaltic shergottites would better fit our analysis. This would explain at the same time that the young lava flows are different from shergottites, whereas ancient crustal rocks are much closer to their composition.

References: [1] Mustard J. F. et al. 2005. *Science* 307:1594–1597. [2] Poulet F. et al. 2007. *Journal of Geophysical Research* 112:E08S02. [3] Shkuratov Y. et al. 1999. *Icarus* 137:235–246. [4] Bouvier et al. 2005. *Earth and Planetary Science Letters* 240:221–233.

5116

BRAZILIAN METEORITE PATOS DE MINAS (OCTAHEDRITE)

F. N. Pucheta and F. S. L. Cassino.

During a recent reorganization of the meteorite collection of the Museu de Ciência e Técnica da Escola de Minas da Universidade Federal de Ouro Preto, MG, Brazil, a fragment with 851 g of an iron meteorite was found without any classification and of unknown origin. At the same time, in 2002, a mass of about 200 kg of an iron meteorite was found by Paulo Garcia in the country side of Presidente Olegário, next to Patos de Minas city, MG, Brazil. An endpiece of about 1000 g of Paulo Garcia find was sent to the attention of Prof. M. E. Zucolotto of the Brazilian National Museum and another one with 170 g to the MCT/EM to be identified. The analysis performed at National Museum showed that the 1000 g endpiece structure was identical with that of Patos de Minas (octahedrite), found in 1925 next to the same location, from which the National Museum has a sample with 18 g in its collection donated by the MCT. In this work we show that the iron of the 851 g found unclassified at MCT collection is probably the whole section from which was cut the sample of 18 g of the NM, and, consequently, that it is part of Patos de Minas (octahedrite). These conclusions trace out the history of the known fragments of Patos de Minas (octahedrite) existing in Brazilian collections: 851 g + 170 g in the MCT collection and 18 g + 1000 g in the NM collection.

5226

UV RAMAN SPECTROSCOPY AS A POWERFUL TOOL FOR INVESTIGATING INSOLUBLE ORGANIC MATTER OF CHONDRITES AND COMETARY DUST

E. Quirico¹, G. Montagnac², and B. Reynard². ¹Laboratoire de Planétologie de Grenoble Université Joseph Fourier, CNRS/INSU BP53, 38041 Grenoble Cedex 9, France. E-mail: eric.quirico@obs.ujf-grenoble.fr. ²LST Ecole Normale Supérieure-CNRS 46, allée d'Italie, 69364 Lyon Cedex 7, France.

Introduction: The characterization of carbonaceous matter in micrometric grains (IDPs, AMMs, Stardust grains) is a big issue as most analytical techniques are insensitive to such low amounts of material. Raman spectroscopy has been proposed as a useful tool for characterizing natural carbonaceous matter, in particular for metamorphism issues. However, this technique apparently presents limitations for the characterization of insoluble organic matter (IOM) extracted from unmetamorphosed chondrites, and more generally immature kerogens. First, many of these compounds induce a fluorescence background, which makes difficult or even impossible the interpretation of the Raman spectrum. Secondly, for such disordered compounds, spectra acquired with a single visible wavelength provide little information, and it would be more useful to take advantage of the dispersive character of the first-order carbon bands [1]. We present the first study of natural kerogen-like compounds by UV Raman spectroscopy. We show this technique is suitable 1) to distinguish structural differences among various samples as chondritic IOMs, coals, and stratospheric IDPs, and 2) to identify specific functional groups like cyanides. The implementation of this technique to study AMMs is presented in this volume [2].

Methods and Results: We studied series of IOMs extracted from chondrites (CI, CM, CR, ungrouped C2), two IDPs, and coals. Measurements were carried out using a JOBIN-YVON LabRaman microRaman spectrometer, equipped with a X40 objective and using a 244 nm wavelength. Particular care was devoted to minimize beam damage (thermal/photolysis alteration). The spot size on the sample was around 4–5 μm . The 244 nm Raman spectra of all samples do exhibit a very intense and narrow G band and a weak D band. These spectra present some similarities with those of hydrogenated amorphous carbon, and point to highly disordered compounds with a significant sp^3/sp^2 ratio. Interestingly, coal and IOMs spectra have slight but significant spectral differences, which are quantified either by bands fitting or principal components analysis (PCA). They definitely evidence the polyaromatic structure are dissimilar, consistently with independent analytical measurements [3, 4]. In one chondrite, Alais (CI1), we report the first identification of the cyanide (-CN) functional group. In the case of two stratospheric IDPs, significant spectral differences were observed in the intensity of the D band, when compared with chondritic IOMs. These results confirmed the systematic trend derived from 514 nm measurements by [5], and point to differences in IOMs in dust and chondrites. Recent analyses of two ultra-carbonaceous AMMs seem to confirm this observation [2]. We will present in detail the implementation of this technique and provide extensive details on these new results.

References: [1] Ferrari A. C. et al. 2001. *Physical Review B* 63:121405. [2] Dobrika et al. 2008. This volume. [3] Gardinier A. et al. 2000. *Earth and Planetary Sciences* 184:9–21. [4] Cody and Alexander. *Geochimica et Cosmochimica Acta* 69:1085–1097. [5] Quirico et al. 2005. *Planetary and Space Science* 53:1443–1448.

5257

COMPOSITION OF BAPTISTINA ASTEROID FAMILY: IMPLICATIONS FOR K-T IMPACTOR LINK

V. Reddy¹, M. S. Kelley², J. P. Emery³, M. J. Gaffey⁴, W. F. Bottke⁵, M. Schaal⁶, A. P. Cramer⁷, and D. Takir⁴. ¹Department of ESSP, University of North Dakota (UND), Grand Forks, ND, USA. ²NASA Headquarters, Washington, D.C., USA. ³Carl Sagan Center, Mountain View, CA, USA. ⁴Department of Space Studies, UND, USA. ⁵Department of Space Studies, SWRI, Boulder, CO, USA. ⁶Department of Physics, UND, USA. ⁷Department of Geology, Georgia Southern University, Statesboro, GA, USA.

Introduction: Catastrophic impacts have channeled the course of evolution of life on planet Earth. The most recent event took place 65 Myr ago when an ~10 km object impacted off the present-day Yucatán Peninsula, Mexico, resulting in a mass extinction event [1–4]. The identification of a source region for the K-T impactor in the main asteroid belt was recently addressed.

It has been suggested that the K-T impactor originated from the break-up of the parent body of 298 Baptistina 160 Myr ago forming the Baptistina asteroid family (BAF) [5]. A key line of evidence linking 298 and the K-T impactor was their similar composition (CM2 carbonaceous chondrites) [5]. The composition of 298 was assumed from its taxonomic classification of C or X [6], which was based on a visible spectrum. That spectrum shows a 0.9 μm feature suggesting an S-type rather than a C- or X-type. The lack of albedo data made it difficult to confirm its taxonomy.

Observation/Data Reduction: In order to better constrain the composition and albedo of BAF members, an observation campaign was launched in February–March 2008 using the NASA IRTF. Members of the BAF were observed using SpeX on February 28 and March 21 and 22 UT in prism (0.7–2.5 μm) and LXD (1.9–4.2 μm) modes. The prism data were reduced using IRAF and SpecPR; the LXD data using IDL routine developed by Emery.

Analysis: The average spectrum of 298 Baptistina from March 21 (0° rotational phase) and 22 (180° rotational phase) shows a well resolved Band I feature at $1.0 \pm 0.01 \mu\text{m}$ with a depth of $7 \pm 1\%$ and a weaker (depth $2 \pm 1\%$) Band II feature at $2.0 \pm 0.2 \mu\text{m}$. Based on the absorption features and the band parameters, the mineralogy of 298 includes olivine and traces of orthopyroxene. The LXD data show a rise in reflectance beyond 3.0 μm due to thermal emission. Using the standard thermal model, the estimated albedo is $\sim 14^{+2}_{-3}\%$. Based on the mineralogy and the albedo, it is evident that 298 Baptistina is not a CM2 assemblage. The spectrum of BAF member 1365 Henyey also shows deep silicate features (Band I center: $1.01 \pm 0.01 \mu\text{m}$, depth: $15 \pm 1\%$, Band II center: $2.0 \pm 0.1 \mu\text{m}$, depth $4 \pm 1\%$), suggesting an olivine and OPX dominated S-type taxonomic classification rather than C- or X-type. While these results weaken the link between the BAF and the K-T impactor, Baptistina's dynamical location does not exclude the possibility of it being a) the remnant core of the original parent body, b) the impactor that destroyed the parent body, or c) an interloper from other families. Spectral analyses of other BAF members are currently underway to solve the mystery.

Acknowledgments: This research was supported by NASA NEOO Program Grants NNG04GI17G and NNX07AL29G, and by NASA PAST Grant NNG05GF90G.

References: [1] Alvarez et al. 1980. *Science* 208:1095–1108. [2] Dressler et al. 1994. GSA Special Paper #293. 348 p. [3] Sharpton V. L. 1995. *Eos* 76:534. [4] Steuber et al. 2002. *Geology* 30:999–1002. [5] Bottke et al. 2007. *Nature* 449:48–53. [6] Lazarro et al. 2004. *Icarus* 172:179–220.

5252

COSMOGENIC ARGON ISOTOPES: CROSS SECTIONS AND PRODUCTION RATES

R. C. Reedy. Institute of Meteoritics, MSC03-2050, University of New Mexico, Albuquerque, NM 87131, USA. E-mail: rreedy@unm.edu.

Introduction: The two minor isotopes of argon, ³⁶Ar and ³⁸Ar, are often recognizable as having been made by cosmic rays and used to study the cosmic-ray exposure record of an object in space. These isotopes can be measured while doing Ar-Ar dating and then used as cosmogenic nuclides.

Many of the production rates used for these isotopes of Ar were calculated a long time ago [e.g., 1]. Some cross sections were updated in 1992 [2]. Production rates for the production of Ar isotopes from Fe and Ni have been reported [e.g., 3]. However, there is a need for new and improved production rates for Ar isotopes, especially the targets Ca and K.

To get good production rates, the best cross sections are needed. All cross sections measured for making Ar isotopes were compiled and evaluated, as has been done recently for other cosmogenic nuclides [e.g., 4].

Cross Sections: There are a few cross sections [e.g., 5] for making ³⁸Ar from ³⁹K with neutrons having 14–15 MeV of energy. No other cross sections for making Ar isotopes with energetic neutrons were found. Most measured cross sections are for incident protons, as is the cases for most nuclides [e.g., 4].

Most cross sections for making Ar isotopes were measured long ago and used in previous work [1, 2]. Many cross sections for making of Ar isotopes have been measured very recently using Fe and Ni targets [6]. A few cross sections have been measured using high-energy beams of ions of ⁴⁰Ca [7] and ⁵⁶Fe [e.g., 8] on targets of H with in-beam identification of the products.

These new cross sections for proton-induced reactions are generally consistent with the older ones and allowed improved sets of cross sections as a function of energy to be generated. There are several sets of data for reactions with Ca, Fe, and Ni, but only one set for Ti. There are no cross sections for making Ar isotopes from proton reactions with K.

Production Rates: Neutrons are the dominate particle for the galactic-cosmic-ray production of cosmogenic nuclides, including Ar. Only for Fe and Ni is proton-production fairly significant. In developing the neutron cross sections used in [1] for making ³⁶Ar and ³⁸Ar from Ca, the proton-induced cross sections were modified considerably. These adjusted cross sections were used as the bases for the latest set of cross sections. Changes to these cross sections using the newer cross sections were mainly at the higher energies. For Fe and Ni, the newer cross sections were mainly used in getting the final set of cross sections. For elements with very few cross sections, especially K and Ti, the calculated production rates have greater uncertainties.

References: [1] Hohenberg C. M. et al. 1978. Proceedings, 9th LPSC. pp. 2311–2344. [2] Reedy R. C. 1992. 23rd LPSC. pp. 1133–1134. [3] Leya I. et al. 2001. *Meteoritics & Planetary Science* 36:1547–1561. [4] Reedy R. C. 2008. Abstract #1907. 39th LPSC. [5] Foland K. A. et al. 1987. *Nuclear Science and Engineering* 95:128–134. [6] Ammon K. et al. 2008. *Nuclear Instruments and Methods in Physics Research Section B* 266:2–12. [7] Chen C. X. et al. 1997. *Physical Review C* 56:1536–1543. [8] Villagrasa-Canton C. et al. 2007. *Physical Review C* 75:044603.

5250

LABORATORY EXPERIMENTS ON THE KINETICS OF THERMAL ANNEALING OF DUST IN PROTO-PLANETARY DISKS

Bianca Reinhard¹, Dominique Lattard¹, Michael Burchard¹, Mario Trieloff¹, Ralf Dohmen², Markus Klevenz³, and Annemarie Pucci³. ¹Mineralogisches Institut, Universität Heidelberg, Im Neuenheimer Feld 236, 69120 Heidelberg, Germany. ²Institut für Geologie, Mineralogie und Geophysik, Ruhr-Universität Bochum, Universitätsstr. 150, 44780 Bochum, Germany. ³Kirchhoff Institut für Physik, Universität Heidelberg, Im Neuenheimer Feld 227, 69120 Heidelberg, Germany.

Since the Infrared Space Observatory (ISO) mission we know that interstellar dust particles are partly crystalline. One of the main processes leading to the crystallization of amorphous cosmic dust is thermal annealing. In this project, we investigate the kinetics of this process by measuring the time scale and the activation energy of crystallization for different dust compositions (olivine, ortho- and clinopyroxene). This data is needed for a consistent astrophysical modeling of the radial abundances of dust and of its chemical composition at various evolutionary stages.

The contradictory results of previous studies were probably related to the use of distinct, not comparable starting materials (e.g., gels and smokes), from which some were chemically inhomogeneous and/or contained crystal seeds. Moreover, the experimental sequences and the definition of the degree of crystallinity were vastly different.

We have embarked on a new strategy by using amorphous thin films deposited on a germanium-wafer via pulsed laser deposition (PLD). With this method we obtain a chemically well-defined amorphous thin film of stoichiometric composition with a constant and accurate adjustable thickness. We have developed a simple annealing sequence in an upright furnace, with short heating periods and the possibility to quench the sample. Before and after annealing the sample is characterized not only by IR spectroscopy but also by Raman spectroscopy, atomic force microscopy (AFM), and scanning electron microscopy (SEM) analysis.

The IR spectra of the first annealed samples on the Mg₂SiO₄ composition showed the development of characteristic forsterite peaks. Observation with SEM and AFM revealed a dewetting of the thin film from the surface of the carrier material.

Experimental series with different annealing times and temperatures are on the way.

5255

ARE SHERGOTTITES SULFIDE-SATURATED?

K. Righter¹ and L. R. Danielson². ¹Mailcode KT, NASA-JSC, 2101 NASA Parkway, Houston, TX 77058, USA. E-mail: kevin.righter-1@nasa.gov. ²Mailcode KR, NASA-JSC, 2101 NASA Parkway, Houston, TX 77058, USA.

Introduction: Shergottites have high S contents (1300 to 4600 ppm; [1]), but it is unclear if they are sulfide-saturated or under-saturated. Resolution of sulfide saturation depends on temperature, pressure, oxygen fugacity (FeO), and magma composition [2]. Expressions derived from experimental studies allow prediction of S contents, though so far they are not calibrated for shergottitic liquids [3–5]. We have initiated an experimental study to test current S saturation models for shergottitic liquids, and to make new calibrations if necessary. This issue has fundamental implications for determining the long term S budget of the Martian surface and atmosphere (from mantle degassing), as well as evolution of the highly siderophile elements (HSE) Au, Pd, Pt, Re, Rh, Ru, Ir, and Os, since concentrations of the latter are controlled by sulfide stability.

Experiments: Mixtures of shergottitic bulk compositions and FeS in alumina capsules, with an oxygen buffer in a separate alumina capsule, are sealed into silica tubes and equilibrated in Deltech furnaces for 48–72 hr [6]. These experiments are quenched and sectioned for analysis by electron microprobe for major elements and S. Two shergottite compositions—one evolved and a second more primitive—are currently being studied so that effects of melt compositional variation can be evaluated.

Calculations: The S content of a silicate melt in equilibrium with sulfide liquid is known to be a function of T, P, fO₂, and bulk composition [2]. Recent calibrations have included the effects of all of these variables. We use several recent studies [3–5] to compare predicted S contents to those measured in our shergottitic quench glass. Initial comparisons are good, with expressions recovering S contents of FeO-rich liquids at the IW buffer. More experiments are required to explore melt compositional ranges in Al₂O₃, FeO, and MgO appropriate to shergottites.

Conclusions: Preliminary assessments indicate that most shergottites may be sulfide undersaturated, whereas a few appear to be sulfide-saturated. The two groups also have distinctly different HSE absolute concentrations, showing that sulfide-saturated shergottites contain much lower HSE contents than the S saturated. Because shergottite parent melts are likely generated at higher pressures [7, 8], and sulfide saturation has a negative pressure dependence, melts from the Martian mantle may initially be saturated, become undersaturated during ascent, and then become saturated again upon subsequent differentiation in the crust. The importance of olivine, chromite, and sulfide fractionation, as well as the stabilization and destabilization of sulfide during fractionation, will be emphasized with various shergottite [9, 10] and terrestrial examples.

References: [1] Meyer C. Jr. 2008. <http://curator.jsc.nasa.gov/antmet/mmc/index.cfm>. [2] Wallace P. J. and Carmichael I. S. E. 1992. *Geochimica et Cosmochimica Acta* 56:1863–1874. [3] Li C. and Ripley E. M. 2005. *Mineralium Deposita* 40:218–230. [4] Liu Y. et al. 2007. *Geochimica et Cosmochimica Acta* 71:1783–1799. [5] Holzheid A. and Grove T. L. 2002. *American Mineralogist* 87:227–237. [6] Righter K. et al. 2006. *Chemical Geology* 227:1–25. [7] Monders A. G. 2007. *Meteoritics & Planetary Science* 42:131–148. [8] Musselwhite D. S. et al. 2006. *Meteoritics & Planetary Science* 41:1271–1290. [9] Puchtel I. et al. 2008. Abstract #1650. 39th LPSC. [10] Jones J. H. et al. 2003. *Chemical Geology* 196:21–41.

5328

PARTITIONING OF Hf BETWEEN CHROMITE AND SILICATE MELTS: IMPLICATIONS FOR Lu-Hf ISOTOPIC SYSTEMATICS OF MARTIAN METEORITE ALH 84001

M. Righter¹, T. J. Lapen¹, K. Righter², and A. Brandon². ¹Department of Geosciences, University of Houston, Houston, TX 77204-5007, USA. E-mail: mrighter@uh.edu. ²NASA Johnson Space Center, Houston, TX 77058, USA.

Introduction: The differentiation history of Martian meteorites is still debated. The crystallization ages of shergottites are currently not agreed on [e.g., 1, 2]. ALH 84001 is known as the Martian meteorite which has the oldest crystallization age of 4.5 Gyr [e.g., 3, 4], but this meteorite has suffered several impact events during its history and shows large uncertainty on the age.

One of our coauthors recently reported Lu-Hf age and isotope systematics of the olivine-phyric shergottite RBT-04242 [5]. Mineral isochron data showed chromite could have high Hf concentration with a low Lu/Hf ratio, and yields a tighter constraint on source composition. If it is true, chromite is a very important phase for Lu-Hf systematics, especially to obtain initial Hf isotopic composition of source material.

To answer this question, we determined Hf partitioning between chromite and basaltic melt using the experiments of Righter et al. (2006) [6, 7] on natural basalts. We also measured Hf concentration in ALH 84001 chromites to test the idea that chromite can concentrate Hf.

Experimental: A Hawai'ian ankaramite was used to study spinel-melt equilibrium. All samples were doped with 1% Cr₂O₃ to promote spinel growth. Experimental details are described in the papers of Righter et al. (2006) [6, 7].

Analytical: Run products and ALH 84001 chromite were analyzed using a Cameca SX-100 electron microprobe at NASA-JSC for major elements and a CETAC LSX-213 laser ablation system coupled to a Varian 810-MS ICP-MS at University of Houston for REE and Hf concentration. Spinel-silicate partition coefficients, D (ppm in spinel/ppm in glass), were determined on 2 sets of experiments.

Results and Discussion: Concentrations of Hf in the experimental chromites ranged from 43.4 ppb and 124.5 ppb, corresponding to D(Hf) of 0.022 and 0.028 which is lower than literature values (0.078 and 0.092) [8]. The range of D(Hf) values might indicate a crystal chemical control since chromite can have Ti, Al, and Fe³⁺ components.

Hafnium concentration of chromites in ALH 84001 are 132–298 ppb. Lutetium concentration is under detection limit (0.8 ppb), yielding maximum ¹⁷⁶Lu/¹⁷⁷Hf ratios of 0.0008.

Given the available data, it appears that Hf concentration in chromite can be quite variable.

References: [1] Bouvier A. et al. 2008. *Earth and Planetary Science Letters* 266:105–124. [2] Nyquist L. E. et al. 2001. *Chronology and Evolution of Mars* 96:105–164. [3] Jagoutz E. et al. 1994. *Meteoritics & Planetary Science* 29:478–479. [4] Nyquist L. E. et al. 1995. 26th LPSC. pp. 1065–1066. [5] Lapen T. L. et al. 2008. Abstract #2073. 39th LPSC. [6] Righter K. et al. 2006. *Chemical Geology* 227:1–25. [7] Righter K. et al. 2006. *American Mineralogist* 91:1643–1656. [8] McKay et al. 1986. *Journal of Geophysical Research* 91:D229–D237.

5224

METAMORPHIC GRADES OF ENSTATITE CHONDRITES AS REVEALED BY CARBONACEOUS MATTER

C. Robin¹, E. Quirico¹, M. Bourot-Denise², and G. Montagnac³. ¹Laboratoire de Planétologie de Grenoble Université Joseph Fourier, CNRS/INSU BP53, 38041 Grenoble Cedex 9, France. E-mail: eric.quirico@obs.ujf-grenoble.fr. ²LEME MNHN 61, rue Buffon, 75231 Paris, France. ³LST Ecole Normale Supérieure-CNRS 46, allée d'Italie, 69364 Lyon Cedex 7, France.

Introduction: Enstatite chondrites (ECs) have a poor silicate mineralogy and very scarce matrix area, rendering difficult an accurate determination of their metamorphism grade. Following our previous works on ordinary and carbonaceous chondrites [1], we have determined the metamorphism grade of 7 ECs by studying the maturity of matrix carbonaceous matter by Raman spectroscopy. The following series of ECs was studied: ALH 84206, SAH 97096, ALH 84170, ALH 85119, MAC 88184, MAC 88136, and Parsa. They were all provided by the JSC NASA center, except Parsa, provided by Museum National d'Histoire Naturelle (Paris).

Methods and Results: Raman measurements were mostly performed on thin films or polished sections. The lack of polishing artifact was checked by crossed-measurements with whole rocks for some chondrites. Raman measurements were carried out with a LabRaman JOBIN-YVON Raman microspectrometer, using a 514 nm excitation and a X50 long distance working objective.

Tiny zones of matrix were localized by optical microscopy, and were found present in all objects. Most of them were carbon-rich and could be studied by Raman spectroscopy. Their texture was also studied by scanning electron microscopy at Paris VI University, and was used as a metamorphism grade indicator. Opaque minerals assemblages were studied by optical microscopy at Museum National d'Histoire Naturelle, and were used as a highly sensitive and qualitative metamorphic indicator (e.g., [1] and references therein).

The Raman spectra of CM trapped in matrix inclusions exhibit the G and D first-order carbon bands. Bands fitting and principal component analysis reveal spectral variations in the G and D bands which point to different maturation grades of CM. Those variations were found correlated with indications from both opaque petrography and matrix texture, evidencing CM maturity is mostly controlled by thermal metamorphism, as in ordinary and carbonaceous chondrites.

Using carbonaceous and ordinary chondrites previously investigated, an interclassification has been proposed. The lowest petrologic type was found around ~3.4 (ALH 84206, SAH 97096) and the highest 3.8/3.9 (MAC 88136). These new petrologic types have been used for discussing previous classifications and thermometric approaches [2, 3], as well as heterogeneity of organic precursors accreted by ECs with respect to ordinary and carbonaceous chondrites.

References: [1] Bonal et al. 2007. *Geochimica et Cosmochimica Acta* 71:1605–1623. [2] Zhang et al. 1995. *Journal of Geophysical Research* 100: 9417–9438. [3] Zhang et al. 1996. *Meteoritics & Planetary Science* 31:647–655.

5044

MAGNETIC PROPERTIES OF LUNAR MATERIALS: COMPARISON BETWEEN METEORITES AND SAMPLE RETURN

P. Rochette¹, J. Gattacceca¹, A. Ivanov², M. Nazarov², and N. Bezaeva^{1,3}.
¹CEREGE (CNRS/Aix-Marseille Université), Aix en Provence, France.
²Vernadsky Institute, Science Academy, Moscow, Russia. ³Faculty of Physics, M.V. Lomonosov Moscow State University, Moscow, Russia.

Our natural satellite is the only body in the solar system from which samples are available through two completely different processes: sampling by man-made spacecrafts, i.e., “sample return,” and natural sampling by impact and transport to the Earth, i.e., meteorites.

While the samples returned by the Apollo 11 to 17 missions from 1969 to 1972 (380 kg of soils and rocks) and by the Luna 16, 20, and 24 missions from 1970 to 1976 (320 g of soils and minute rock fragments) has been the subject of considerable work in the years following missions, only two lunar meteorites have studied previously for their magnetic properties: Yamato-791197 and ALH 81005 [1, 2]. We will present a comprehensive magnetic study of lunar meteorites (on 33 unpaired meteorites), and compare it to published data on the Apollo [3] and Luna missions [4, 5], as well as new data from the Luna 16 and 20 surface soil samples, and from the Luna 24 two meters long core. We concentrate on magnetic susceptibility (χ in nm³/kg) and saturation remanence (M_{rs} in mA·m²/kg), which reflects the amount and grain size of metallic iron. In Luna soils, χ decreases with increasing depth and grain size, due to the predominance of metal nanoparticles due to regolithization processes (amount of metal up to a few%). Meteorites, Luna, and Apollo samples share the same wide range of susceptibility ($1.9 < \log \chi < 4.6$) and remanence ($-1 < M_{rs} < 2.5$), although meteorites have on average lower metal content due to a lower regolithic component. Most mare basalts appear nearly paramagnetic (metal content $\ll 0.1\%$) and more magnetic rocks are found within the highland or impact reprocessed materials. Meteorites provide a better sampling of the anorthosite highland lithology, very rare in sample return collection. This lithology provides the least magnetic material ever sampled in the solar system ($\log \chi < 2.5$). The unpaired meteorite GRA 06128 shows close similarities with lunar highlands lithology, but shows exceptionally high coercivity. In meteorites, metal amount appears well correlated with Ni and Ir amount, i.e., with the meteoritic contamination. Metal production is interpreted as the combined effect of meteoritic contamination and iron silicates reduction by regolithic processes (e.g., solar wind and microimpacts).

Acknowledgements: This work was supported by CNRS PICS program.

References: [1] Nagata T. and Funaki M. 1986. *Memoirs of NIPR* 41: 152–164. [2] Morris R. V. 1983. *Geophysical Research Letters* 10:807–808. [3] Fuller M. and Cisowski S. M. 1987. In *Geomagnetism*, vol. 2, edited by Jacobs J. A. London: Academic Press. pp. 307–455. [4] Pillinger et al. 1978. In *Mare Crisium: The view from Luna*. pp. 217–228. [5] Stepheson A. et al. 1978. In *Mare Crisium: The view from Luna*. pp. 701–709.

5217

EXPOSURE AGES OF CHONDRULES IN ALLENDE AND MURCHISON

A. S. G. Roth, H. Baur, V. S. Heber, E. Reusser, and R. Wieler. ETH Zürich, Isotope Geology & Mineral Resources, NW C84, CH-8092 Zürich, Switzerland. E-mail: rotha@student.ethz.ch.

Introduction: Whether meteorites retain a record of irradiation by energetic particles in the early Solar System prior to parent body compaction remains an outstanding question. Hohenberg and coworkers [1] reported large excesses of cosmogenic neon in olivine grains with solar flare tracks in CM chondrites. Previous attempts to deduce pre-compaction exposures of chondrules yielded equivocal results, however [2]. Here we present ³He and ²¹Ne exposure ages of 13 chondrules from Allende (CV3) and 14 chondrules from Murchison (CM2) with individually determined major element concentrations. Murchison was chosen for its very low recent exposure age of ~1 Ma, which should facilitate the detection of precompaction exposure events.

Results: Spheroids were hand-picked after freeze-thaw disaggregation of small meteorite chips to assure constant shielding. Chondrules were then individually abraded to remove possible gas-rich rims. Samples were finally split into fragments. The largest one was used for He and Ne analysis by IR-laser extraction. Major element concentrations on ~20 broad spots in up to 3 smaller fragments per chondrule were measured by electron microprobe. Mg concentrations in a given chondrule were reproducible to within 15%.

Production rates of ³He and ²¹Ne were determined with elemental production rates from [3] for a meteoroid radius of 32 cm and a shielding depth of 4–6 cm. Stated exposure ages thus assume present-day GCR flux. All exposure ages of Allende chondrules fall in a very narrow range (1 σ) of 3.2 ± 0.3 Ma (²¹Ne) and 4.4 ± 0.2 Ma (³He). The age spread is 2–3 times lower than the spread in ³He_{cos} and ²¹Ne_{cos} concentrations, proving the reliability of the production rate determination. The difference between nominal ³He and ²¹Ne ages is of no concern here and may be due to the rather arbitrary assumption of the shielding parameters. Most Murchison chondrules have exposure ages of 0.8 ± 0.1 Ma (²¹Ne) and 1.2 ± 0.2 Ma (³He). One chondrule with low nominal ages of ~0.4 Ma may have lost He and Ne. However, one Murchison chondrule yields nominal exposure ages of 6.0 ± 0.4 Ma (³He) and 4.7 ± 0.4 Ma (²¹Ne).

Discussion: With one exception, all studied chondrules show a remarkably narrow range of cosmic ray exposure ages. Their cosmic ray record is thus plausibly explained by their recent meteoroid exposure alone. This is also supported by the basic agreement of the noble gas ages reported here with radionuclide-based exposure ages of Allende and Murchison. Any pre-compaction exposure of chondrules would correspond to less than a few hundred thousand years irradiation at present day GCR flux. However, one out of fourteen Murchison chondrules definitely shows a precompaction exposure record, corresponding to 4–5 Ma irradiation at present-day GCR intensity. Whether this He and Ne excess is related to gas excesses found in olivines from Murchison [1], which may be due to an early intense solar radiation, or whether the data may constrain lifetimes of chondrules in the solar nebula needs further investigation.

References: [1] Hohenberg C. M. et. al. 1990. *Geochimica et Cosmochimica Acta* 54:2133–2140. [2] Eugster O. et al. 2007. *Meteoritics & Planetary Science* 42:1351–1371. [3] Leya I. et al. 2000. *Meteoritics & Planetary Science* 35:259–286.

5050

CHEMICAL COMPOSITION OF Ca,Al-RICH INCLUSIONS IN RUMURUTI (R) CHONDRITES

S. S. Rout and A. Bischoff. Institut fuer Planetologie, Westfaelische Wilhelms-Universitaet Muenster, Wilhelm-Klemm-Strasse 10, 48149 Muenster, Germany. E-mail: suryarout@uni-muenster.de.

Introduction: Ca,Al-rich inclusions (CAIs) in the Rumuruti chondrite are a distinct group of inclusions [1–3]. We studied 20 R chondrites and found 101 CAIs, which can be subdivided into four different groups: (a) simple concentric spinel-rich inclusions (42); (b) fassaite-rich spherules (3); (c) complex spinel-rich CAIs (53); and (d) complex diopside-rich inclusions (3). In contrast to CAIs in many other C chondrites, these refractory inclusions do not contain melilite and grossite [4, 5]. The bulk compositions of the inclusions presented here were determined by defocused-beam analysis using a JEOL 8900 electron microprobe operated at 15 kV and a probe current of 15 nA.

Results: Simple concentric and complex spinel-rich CAIs show high Al_2O_3 concentrations (13–71 wt%). Generally, Al_2O_3 increases with decreasing CaO and trends away from the cosmic Ca/Al line (Fig. 1), similar to what has previously been observed for fine-grained CAIs in ordinary chondrites [6, 7]. The highest Al_2O_3 concentrations were found in the hibonite-bearing, spinel-rich CAIs. The fassaite-rich spherules and the complex diopside-rich inclusions on the other hand plot close to the cosmic Ca/Al line having Al_2O_3 and CaO concentrations of 11–34 wt% and 12–24 wt%, respectively.

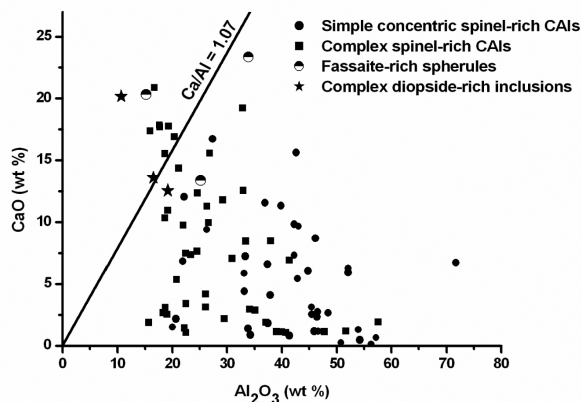


Fig. 1. CaO versus Al_2O_3 plot for the CAIs in R chondrites.

Most of the CAIs are heavily altered due to parent body and nebular alteration processes. This is indicated by high FeO (up to 34 wt%), Na_2O (up to 12.5 wt%), K_2O (up to 2.3 wt%), and ZnO (up to 2.9 wt%).

References: [1] Rout S. S. and Bischoff A. 2007. *Geochimica et Cosmochimica Acta* 71:A855. [2] Rout S. S. and Bischoff A. Forthcoming. *Meteoritics & Planetary Science*. [3] Rout S. S. and Bischoff A. 2008. Abstract #1255. 39th LPSC. [4] Brearley A. J. and Jones R. H. 1998. In *Planetary materials*, edited by Papike J. J. Washington, D.C.: Mineralogical Society of America. pp. 3-01–3-398. [5] Weber D. and Bischoff A. 1994. *Geochimica et Cosmochimica Acta* 58:3855–3877. [6] Bischoff A. and Keil K. 1983. Special Publication #22. Albuquerque, NM: Institute of Meteoritics, University of New Mexico. pp. 1–33. [7] Bischoff A. and Keil K. 1984. *Geochimica et Cosmochimica Acta* 48:693–709.

5011

STUDY ON IMPACT MATERIALS AROUND THE BARRINGER METEOR CRATER BY ED-SEM AND MICRO-PIXE TECHNIQUES

P. Rózsa¹, I. Uzonyi², Gy. Szöör¹, P. Pelicon³, J. Simčič³, Cs. Cserhádi⁴, L. Daróczi⁴, A. Gucsik⁵, Gy. Szabó², and Á. Z. Kiss². ¹Department of Mineralogy and Geology, University of Debrecen, H-4032 Debrecen, Egyetem tér 1., Hungary. E-mail: rozsap@puma.unideb.hu. ²Institute of Nuclear Research of the Hungarian Academy of Sciences, H-4026 Debrecen, Bem tér 18/C, Hungary. ³Jožef Stefan Institute, Microanalytical Center, Jamova 39, p.p. 3000, SI-1001 Ljubljana, Slovenia. ⁴Department of Solid State Physics, University of Debrecen, H-4026 Debrecen, Bem tér 18., Hungary. ⁵Max Planck Institute for Chemistry, Department of Geochemistry, D-55128, Joh.-J.-Becherweg 27, Mainz, Germany.

The one of the most famous and well-preserved simple meteorite craters is the Barringer Meteor Crater (Arizona, USA). It has been studied extensively from mineralogical, geochemical, and cosmo-chemical points of view for many decades. In recent years, we have been focusing to the elemental characterization of various impact materials collected in its near environment [1–3]. Besides metallic spherules, very fine (200–300 μ m) magnetic Fe-rich grains of irregular shape were collected around the crater for this study.

The combined application of an energy dispersive scanning electron microscope (ED-SEM) and a scanning nuclear microprobe (SNM) is a powerful technique for the complex characterization of such materials. SEM provides the fine textural information and concentration of the major elements. SNM with proton-induced X-ray emission (PIXE) method serves for the determination of both the major constituents and the important minor and trace elements such as the PGEs: Ru, Rh, Pd, Os, Ir, Pt. In this study, analytical data will be presented for S-Fe-Ni-Cu systems providing basic information on the composition of the parent meteorite and physical-chemical processes during the impact event.

The results presented in elemental maps show extreme heterogeneous composition of the samples. Beside the dominant S-Fe-Ni system, Fe-Ni-Cu-S phases can also be found within a single grain. Moreover, composition may change on a tenth micrometer scale; therefore the data do not correspond to exact mineral composition.

Consequently, based on the analytical data, the impact origin of the particles seems to be obvious; however, the extremely heterogeneous elemental compositional pattern may reflect a quite complex genesis of the grains.

References: [1] Szöör Gy et al. 2001. *Nuclear Instruments and Methods in Physics Research B* 181:557–562. [2] Uzonyi I. et al. 2004. *Spectrochimica Acta B* 59:1717–1723. [3] Szöör Gy et al. 2005. *Acta Geologica Hungarica* 48:419–434.

5101

CLASTIC MATRIX IN THE Y-691 EH3 CHONDRITE

A. E. Rubin¹, C. D. Griset², B.-G. Choi^{1,3}, and J. T. Wasson¹. ¹Institute of Geophysics, UCLA, Los Angeles, CA 90095, USA. E-mail: aerubin@ucla.edu. ²Physics Department, Caltech, Pasadena, CA 91125, USA. ³Department Earth Sci. Ed., SNU, Seoul, 152-748, Republic of Korea.

Fine-grained primitive matrix material in type 3 enstatite chondrites [1–3] has previously been characterized only superficially. Kimura [1] identified matrix material in Y-691 (EH3), one of the most primitive enstatite chondrites; Ebata et al. [3] reported presolar silicate and carbonaceous grains in Y-691 that presumably reside in the fine-grained matrix. Our modal analysis indicates that Y-691 contains ~5 vol% clastic matrix (including ~2 vol% fine-grained material that we infer to be nebular) present as 15–400 μm patches. This modal value is much lower than the 14 ± 5 vol% matrix abundance reported in EH3 Qingzhen [2]; the discrepancy has not yet been resolved. Matrix patches in Y-691 consist (in vol%) of (1) ~50% relatively coarse (2–20 μm) fragments and polycrystalline assemblages of kamacite, schreibersite, perryite, troilite (some grains with daubréelite exsolution lamellae), niningerite, oldhamite, and caswellsilverite, (2) ~10% relatively coarse silicate grains including enstatite, albitic plagioclase, silica, and diopside, and (3) an inferred fine nebular component (~40%) comprised of submicrometer-size grains.

The O-isotopic composition of clastic matrix in Y-691 is indistinguishable from that of olivine and pyroxene grains in adjacent chondrules; both sets of objects lie on the TF line [4]. These results imply that the principal components of Y-691 originated from (or equilibrated with) the same O-isotope reservoirs.

We carried out electron microprobe analysis of five $50 \times 50 \mu\text{m}$ size matrix patches using a 3 μm wide beam. A total of 49 points were analyzed in each patch; many points had variant compositions (mainly due to beam overlap on coarse clastic grains) and were discarded (including 37–53% of the points in each of four patches and 76% in the fifth patch). Bulk compositions of the patches are similar, but resolvable in concentrations (wt%) of alkalis: patch H13, $n = 29$: $1.21 \pm 0.19\%$ Na, $0.25 \pm 0.03\%$ K; patch K11, $n = 23$: $0.80 \pm 0.15\%$ Na, $0.18 \pm 0.03\%$ K (uncertainties are 95% confidence limits). Larger compositional differences were observed among matrix patches in CR2 LAP 02342 [5].

It seems likely that a substantial fraction of matrix material in primitive chondrites was produced in the nebula from condensed, partly amorphous, volatile species evaporated from chondrules during heating [6]. Porous clumps of this fine-grained nebular material formed matrix patches after accreting with other primitive components and being compacted by parent-body impact events. Compositional variations in matrix patches reflect heterogeneities among the porous fine-grained clumps.

There are differences among chondrite groups in the abundance of matrix: e.g., 10–15 vol% in type 3 OC; ~35 vol% in CO3, R3, and reduced CV3 chondrites. We attribute these differences to regional/temporal variations in chondrule-matrix recycling and to the settling efficiency of fine-grained materials to the nebular midplane prior to planetesimal formation.

References: [1] Kimura M. 1988. *Proceedings of the NIPR Symposium on Antarctic Meteorites* 1:51–64. [2] Huss G. R. and Lewis R. S. 1995. *Geochimica et Cosmochimica Acta* 59:115–160. [3] Ebata S. et al. 2006. Abstract #1619. 37th LPSC. [4] Choi B.-G. et al. 2008. Abstract #1006. 39th LPSC. [5] Wasson J. T. and Rubin A. E. Forthcoming. *Geochimica et Cosmochimica Acta*. [6] Wasson J. T. Forthcoming. *Icarus*.

5310

TRACE-ELEMENT ANALYSES OF PYROXENE AND PLAGIOCLASE IN THREE HED METEORITES

A. Ruzicka and T. J. Schepker. Cascadia Meteorite Laboratory, Department of Geology, Portland State University, 1721 SW Broadway, Portland, OR 97207, USA. E-mail: ruzickaa@pdx.edu.

Introduction: We obtained trace-element compositions of pyroxene (px) and plagioclase (plag) in HED meteorites using the technique of LA-ICP-MS. HED meteorites of different classes and metamorphic grades were analyzed: Pasamonte, an unequilibrated (weakly metamorphosed) main group eucrite that contains zoned pigeonite and augite grains; Juvinas, an equilibrated (metamorphosed) main group eucrite that contains inverted pigeonite; and a new howardite from Northwest Africa (NWA 4848) that contains pyroxene with a wide dispersion of major-element compositions, ranging from Mg-diogenite ($\text{Wo}_{0.7}\text{En}_{7.8}$), to Fe-diogenite ($\text{Wo}_{3.1}\text{En}_{57.9}$), to pigeonite ($\text{Wo}_8\text{En}_{5.6}$), to augite ($\text{Wo}_{3.1}\text{En}_{14}$). Our data permit a preliminary assessment of the role that igneous and metamorphic processes played for these three contrasting sample types.

Pasamonte: We confirm earlier suggestions that mineral trace-element compositions in Pasamonte mainly record igneous processes [1, 2]. For incompatible elements, we measured a factor of ~10 \times variation in px and a factor of ~1.5–2.5 \times variation in plag. A noteworthy feature is the different behavior in px of Al compared to other elements, with Al content first dropping as crystallization progresses (i.e., as incompatible elements such as Y increase), then rising. We interpret this to indicate the rapid onset of plagioclase crystallization during pigeonite crystallization. Pasamonte appears to sample one evolving magma type.

Juvinas: Juvinas shows the effects of metamorphic redistribution [1, 2], but mainly for px [2] and only for some elements, notably those that concentrate in plag (Al, Sr) and chromite (Cr, V). We suggest that these elements diffused out of px and into the other phases during subsolidus metamorphism. Low but relatively constant values of Ti/Y and Zr/Y in Juvinas px compared to Pasamonte px suggests that Ti and Zr had been previously depleted in the magma by ilmenite crystallization.

NWA 4848: Not unexpectedly, the trace-element composition of px in the howardite extends over a much larger range than in Pasamonte and Juvinas although compositions overlap the other meteorites. Abundances of incompatible elements (e.g., Ti, Y) in px vary by over 3 orders of magnitude, being lowest in Mg-diogenite and highest in augite, whereas Ba content in plag varies by 1 order of magnitude. Pyroxene appears to have crystallized from multiple magmatic systems. However, none of the px compositions in the howardite match for all elements those found in Pasamonte.

Conclusions: Our data suggest that studies of mineral trace-element compositions in HED meteorites can provide important information. For example, it appears that a magmatic signature in Juvinas px was incompletely erased by metamorphism, and that the signature of co-crystallizing or prior-crystallizing phases can be identified in Pasamonte and Juvinas. Analysis of clasts in howardites can yield a more comprehensive understanding of the diversity of igneous rock types and their genetic relationships than otherwise possible. Further work is needed to more definitively assess the genetic relationship of diogenites and eucrites.

References: [1] Pun A. and Papike J. J. 1996. *American Mineralogist* 81:1438–1451. [2] Hsu W. and Crozaz G. 1996. *Geochimica et Cosmochimica Acta* 60:4571–4591.

5334

STUDY OF CHEMICAL EVOLUTION OF LAVA FLOWS IN MARE SERENITATIS USING HYPER SPECTRAL DATA

K. Saiki and H. Okuno. Department of Earth and Space Science, Graduate School of Science, Osaka University, Osaka, Japan. E-mail: ksaiki@ess.sci.osaka-u.ac.jp.

Introduction: Mg-number ($Mg\# = \text{atomic Mg}/(\text{Mg} + \text{Fe})$) serves as an important petrologic discriminator when analyzing and understanding lunar rocks. Mg-number variation shifts the wavelength of the absorption spectra of ferrous iron with their peaks at around 1000 nm and 2000 nm. The shift had, however, not been detected by remote sensing because it is limited to a very small spectral range. In order to detect this slight shift, ground-based observations of the moon were carried out and the absorption-peak map of Mare Serenitatis has been made [1]. Using this map, we tried to interpret the chemical evolution process of some characteristic lava flows in Mare Serenitatis.

Methods: The spectral data of the lunar surface was obtained by Advanced Lunar Imaging Spectrometer (ALIS) [2]. ALIS is a hyper-spectral telescope using a prism-grating-prism device. The location of the observation was Science City at the peak of Mt. Haleakala, Maui, Hawai'i, USA. The obtained image cubes of the moon were processed by the following steps; (1) dark and flat field correction, (2) normalization of all mare spectra with the same standard highland spectrum, and (3) baseline correction with line which starts at 693 nm and ends at 1059 nm. Comparing the resultant spectra, we detected the slight shift of the absorption spectra of ferrous iron and absorption-peak map of Mare Serenitatis was made. FeO and TiO₂ maps of Mare Serenitatis were made from Clementine UVVIS image cubes using Lucey's algorithm [3]. Lava flow units were identified based on Kodamas's geological map [4].

Results: In two lava flow units on Mare Serenitatis, notable shifts of the absorption spectra of ferrous iron at around 1000 nm were detected. One is in Sr4 and another is in Sr5 lava of Kodamas's classification [4]. The northern part of Sr4 and the western part of Sr5 have the absorption peak with shorter wavelength and the southern part of Sr4 and the eastern part of Sr5 have the peak with longer wavelength. FeO content of Sr4 lava changes from 15 to 17 wt% from north to south, while there is no obvious change in FeO content within Sr5. TiO₂ contents are almost constant within these lava flows.

Discussion: If two areas with shorter wavelength of absorption peak locating Sr4 and Sr5 have Mg-rich lithology, it leads two interpretations. One is that the shift is caused by the difference of the degree of partial melting of parent rock. The lavas of high Mg# areas may be higher degree partial melt in the latter stage. Another is that the variation is caused by the difference of the degree of magma differentiation after eruption. Mg# would be expected to decrease along the flow line as pyroxene and olivine with higher Mg# crystallized and were removed from the melt. The latter case may have advantage in maintaining FeO content. In both cases, the high Mg# area indicates the presence of a vent.

References: [1] Okuno H. et al. 2008. *Earth, Planets and Space* 60: 425–431. [2] Saiki K. et al. 2004. Abstract #1483. 35th LPSC. [3] Lucey P. G. and Blewett D. T. 2000. *Journal of Geophysical Research* 105:20,297–20,305. [4] Kodama S. and Yamaguchi Y. 2003. *Meteoritics & Planetary Science* 38:1461–1484.

5140

POSSIBLE MINERALOGICAL VARIATION OF D-TYPE ASTEROIDS DEDUCED FROM NEW TYPE HYDROUS MICROMETEORITES COLLECTED FROM ANTARCTIC SNOW

K. Sakamoto¹, T. Nakamura¹, T. Noguchi², and A. Tsuchiyama³. ¹Department of Earth and Planetary Science, Kyushu University, Fukuoka 812-8581, Japan. E-mail: kanako@geo.kyushu-u.ac.jp. ²Department of Materials and Biological Sciences, Ibaraki University, Mito 310-8581, Japan. ³Department of Earth and Space Science, Graduate School of Science, Osaka University, Toyonaka 560-0043, Japan.

Introduction: Micrometeorites (MMs) from Antarctic surface snow are preserved intact mineralogical and chemical characteristics due to very low alteration degrees compared with samples from Antarctic blue ice fields, and have an undepleted CI elemental abundance pattern [1]. We found unique hydrous micrometeorites (SK series) that contain saponite and serpentine [2]. The phyllosilicate mineralogy is most similar to that of Orgueil CI chondrite and Tagish Lake carbonate-poor lithology (TL-CP) among groups of carbonaceous chondrites. Therefore, the mineralogy of SK series was compared in detail with that of the two meteorites based mainly of TEM observation.

Results and Discussion: SK series contain phyllosilicates, and abundant pyrrhotites and Fe-Mg carbonates. Magnetite occurs as framboidal aggregates only in one SK series MM. Saponite tends to be higher in abundance than serpentine. Fine-grained phyllosilicates are almost saponite, while coarse-grained ones are enriched in both Mg and serpentine. Most of the sulfides in SK series are pyrrhotites with Ni content typically less than 5 atomic%. Carbonates often occur as hollow aggregates. At present, it is not clear that their centers are really hollow or filled by organic material.

In a Mg-Fe-Si ternary diagram, the compositions of phyllosilicates in SK series are plotted slightly below the saponite solid solution, similar to those in TL-CP, meanwhile those in Orgueil are plotted in a range between saponite and serpentine solid solutions. In TL-CP, Ni content in pyrrhotite is more variable than those in SK series. Our synchrotron diffraction analysis indicated that carbonate in SK series is dominated by Fe-Mg carbonate, while Ca-Mg carbonate is a major phase of TL-CP and Orgueil.

Electron-probe analysis of a polished surface of three SK series MMs showed that major element abundances differ from CI. SK series show large depletions in Ca and Ni and an enrichment in K. On the other hand, TL-CP shows Ca and Ni depletion, but no K enrichment.

The mineralogical characteristics of SK series are most similar to TL-CP, but differ in K abundance and carbonate and pyrrhotite mineralogy. The results suggest that SK series came from a hydrous asteroid with mineralogy slightly different than TL-CP. The reflectance spectrum studies indicated that TL came from D-type asteroids [4]. Therefore, the presence of SK series indicates mineralogical variation of D-type asteroids.

References: [1] Duprat J. et al. 2007. *Advances in Space Research* 39: 605–611. [2] Sakamoto K. et al. 2008. Abstract #1577. 39th LPSC. [3] Zolensky M. E. et al. 2002. *Meteoritics & Planetary Science* 37:737–761. [4] Hiroi T. et al. 2001. *Science* 293:2234–2236.

5093

DO CAIs HAVE A GIANT IMPACT ORIGIN?

Ian Sanders. Department of Geology, Trinity College, Dublin, Ireland.
E-mail: isanders@tcd.ie.

Introduction: Calcium-aluminium-rich inclusions (CAIs) are rare refractory oxide grains found in many classes of primitive meteorite. As the oldest dated objects in such meteorites, their age of 4567 Myr [1] is commonly taken to be the age of the solar system. They evidently formed in a very hot gas of solar composition, either by condensation or as evaporative residues. But where they formed is unclear. Many believe the hot gas was located close to the infant Sun, perhaps at the irradiated inner edge of the accretion disk [2]. If so, the CAIs subsequently traveled several AU outward because they are now entombed in asteroids. Here I ask whether instead most CAIs formed in or near the asteroid belt, with the hot “solar” gas being generated locally by a giant impact between very early (accreted, say, 300 kyr pre-CAIs) pre-heated, Moon-sized planetary embryos. This idea may seem outrageous, but the following evidence suggests that it is not implausible:

Brief Formation Time: Bulk CAIs in CV chondrites plot on a tight Al-Mg isochron, suggesting they formed in <20,000 years [3], and perhaps, therefore, in an instantaneous event.

Planetary Accretion and Melting Before CAIs: $\epsilon^{182}\text{W}$ in some iron meteorites is more negative than the initial $\epsilon^{182}\text{W}$ in CAIs, even allowing for cosmic ray effects [4, 5]. Although the two $\epsilon^{182}\text{W}$ values overlap within error, the data imply that these irons are from cores of planetary bodies that accreted and became molten probably before CAIs were made.

Early Giant Impacts: Cooling rates for IVA irons suggest that their parent body was created following an early giant hit-and-run impact [6]. Strong depletion of volatile elements in these irons, and also in HED meteorites has also been attributed to early giant impacts [7]. Accretion modeling predicts Moon-sized planetary embryos possibly within 100 kyr of in-fall [8].

^{26}Al Superheating: ^{26}Al was a short-lived, widespread, potent heat source [3]. It would rapidly have heated early formed Moon-sized bodies well above the normal melting point because pressure raises the solidus. The stored heat would have aided vaporization following catastrophic decompression.

Impact-Generated CAIs: Chondrules in CB meteorites evidently formed in a giant impact about 5 Myr after the beginning [9]. Unusual CAIs in related metal-rich chondrites have small ^{26}Mg excesses [10] consistent with their formation at the same 5 Myr time, and thus, perhaps, in the same event.

Oxygen Isotopes: If the above CAIs were made at 5 Myr, then their ^{16}O enrichment probably resulted from local fractionation of oxygen in the impact vapor plume. Thus high ^{16}O in normal CAIs may have a similar origin. Extremely enriched ^{18}O in so called PCPs in the pristine chondrite, Acfer 094 [11] may be a rare survivor of the complementary mass-independently fractionated oxygen from CAI formation.

References: [1] Amelin Y. 2006. Abstract #1970. 37th LPSC. [2] Shu F. H. et al. 2001. *The Astrophysical Journal* 548:1029–1050. [3] Thrane K. et al. 2006. *The Astrophysical Journal* 646:L159–L162. [4] Markowski A. 2006. *Earth and Planetary Science Letters* 242:1–15. [5] Kleine T. 2007. Abstract #5258. *Meteoritics & Planetary Science* 42:A84. [6] Yang J. et al. 2007. *Nature* 446:888–891. [7] Halliday A. N. and Porcelli D. 2001. *Earth and Planetary Science Letters* 545–559. [8] Chambers J. E. 2005. *Bulletin of the American Astronomical Society* 37:674. [9] Krot A. N. et al. 2005. *Nature* 436:989–992. [10] Krot A. N. et al. 2008. *The Astrophysical Journal* 672: 713–721. [11] Sakamoto N. et al. 2007. *Science* 317:231–233.

5245

DIFFERENCE OF SPACE WEATHERING DEGREE ON ASTEROIDS OF VARIOUS SIZES

S. Sasaki¹ and T. Hiroi². ¹RISE Project, National Astronomical Observatory of Japan, 2-12 Hoshigaoka, Mizusawa, Oshu, Iwate 023-0861, Japan. E-mail: sho@miz.nao.ac.jp. ²Department of Geological Science, Brown University, Providence, RI 02912, USA.

Introduction—Space Weathering: The surface of airless silicate bodies in the solar system show darkening of overall reflectance, spectral reddening, and attenuation of absorption bands in time. Space weathering is considered to be responsible for these optical signatures. According to the space weathering, the surface of airless silicate bodies show darkening, spectral reddening, and weakening of absorption bands in time. Formation of nanophase metallic iron particles in soil coatings would be responsible for the process [1]. Those nanoparticles were confirmed in lunar soils as well as meteorite sample [2, 3] and they would derive from the deposition of ferrous silicate vapor, which was formed by high-velocity dust impacts as well as sputtering by solar wind. Nano-Fe particles were also confirmed by laboratory simulation using pulse laser shots [4].

Regolith or Not: Spacecraft observation of large (>10 km) S-type asteroids shows regolith-covered weathered surface as expected. Spectral slopes of near-Earth asteroids suggest that the transition from Q-type (ordinary chondrite-like) objects to S-type objects occurs around the size range 0.1 to 5 km [5]. It was considered that the presence of regolith on larger bodies should enhance the space weathering and that smaller regolith-free bodies would not have weathered surface.

However, observation of 550 m Itokawa by Hayabusa suggested that the rocky small asteroids should be weathered although they lack regolith [6]. High-resolution (a few cm) image on a darker terrain of Itokawa shows various size of dark boulders without fine regolith. Some large boulders have brighter scratches and dots on the surface. These can be explained by impact of small meteoroids on the rock surface coated with a very thin weathered layer.

Pulse laser irradiation simulating space weathering on meteorites revealed the surface of ordinary chondrite pieces can have darkened/reddened coating [7]. The irradiation experiments also show that rocky surface is less likely to be weathered than particulate surface. However, surface mixing probably caused by impacts would have weakened the weathering on the particulate surface. This effect should be taken into account for regolith-covered larger bodies such as Eros, Ida, and, of course, the Moon.

References: [1] Hapke B. et al. 1975. *The Moon* 13:339–353. [2] Keller L. P. and McKay D. S. 1993. *Science* 261:1305–1307. [3] Noble S. K., Pieters C. M., and Keller L. P. 2004. Abstract #1301. 35th LPSC. [4] Sasaki S. et al. 2001. *Nature* 410:555–557. [5] Binzel R. P. et al. 2004. *Icarus* 170:259–294. [6] Saito J. et al. 2006. *Science* 312:1341–1344. [7] Sasaki S. et al. 2006. Abstract #1705. 37th LPSC.

5037

CHEMISTRY DURING ACCRETION OF THE EARTH. II. ROCK-FORMING ELEMENTS IN THE "STEAM" ATMOSPHERE

Laura Schaefer¹ and Bruce Fegley Jr.² Planetary Chemistry Laboratory, Department of Earth and Planetary Sciences, Washington University, St. Louis, MO 63130, USA. ¹E-mail: laura_s@wustl.edu. ²E-mail: bfegley@wustl.edu.

Introduction: It has long been thought that impacting of rocky planetesimals during Earth's accretion led to the formation of a "steam" atmosphere [1, 2]. In our companion abstract [3], we discussed the composition of volatile elements in "steam" atmospheres produced by different types of planetesimals. Here we discuss our results for the rocky elements S, P, Cl, F, Na, and K.

Methods: We use thermochemical equilibrium and, where relevant, thermochemical kinetic calculations to model the chemistry of the "steam" atmosphere produced by impact volatilization of different types of accreting material. Our nominal conditions are 1500 K temperature and 100 bar total pressure. We also studied the effects of variable temperature and total pressure. The composition of the accreting material is modeled using average compositions of the Orgueil CI chondrite, the Murchison CM2 chondrite, the Allende CV3 chondrite, average ordinary (H, L, LL) chondrites, and average enstatite (EH, EL) chondrites.

Results: Sulfur: Sulfur is much more volatile in CI chondrites than in any other chondrite studied. At 100 bar pressure and 2500 K, nearly 90% of sulfur is in the gas phase for CI chondrites, primarily as SO₂. In contrast, other chondrites had no more than 4% of total sulfur in the gas phase, primarily as H₂S in the ordinary and enstatite chondrites and SO₂ in the CV chondrites.

Phosphorus: Phosphorus is fairly volatile, with essentially all phosphorus in the gas phase at temperatures greater than 2000 K for all chondrites except Allende (CV), which had only ~20% of phosphorus in the gas at 2500 K. The major P-bearing gas is P₄O₆, except in CI chondrites, which had more PO and PO₂ at high temperatures.

Chlorine and Fluorine: Chlorine is volatile in all chondrites at temperatures greater than ~1000 K, although more so for the CI chondrite than all others. All chlorine was in the gas at 1500 K for CI chondrites but was in condensed phases at higher temperatures for other chondrites. All chlorine was in the gas by 2000 K for all chondrites. Fluorine is less volatile in all chondrites. Again fluorine was found to be more volatile in CI chondrites than in other chondrites, although to a lesser degree than Cl. Fluorine was considerably less volatile in CV chondrites than in all other chondrites, with only ~20% in the gas at 2500 K, versus 100% for all other chondrites. At high temperatures the major gases for all chondrites were NaCl, KCl, HF, NaF, and KF.

Sodium and Potassium: Potassium was much more volatile than sodium, with 100% of potassium in the gas phase at 2500 K for CI, CV, and EH chondrites. Potassium was less volatile in H and EL chondrites, with 70% and 50% in the gas phase, respectively. Sodium was most volatile in CI chondrites, which lost ~90% to the gas phase at high temperature, versus ~5% for all other chondrite types.

Acknowledgments: This work is supported by the NASA Astrobiology and Origins Programs.

References: [1] Abe Y. and Matsui T. 1985. *Proceedings, 15th LPSC*. pp. C545-C559. [2] Lange M. A. and Ahrens T. J. 1982. *Icarus* 51:96-120. [3] Fegley B. Jr. and Schaefer L. 2008. *Meteoritics & Planetary Science*. This issue.

5001

THE INFLUENCE OF IMPACTORS ON THE CHEMICAL COMPOSITION OF EARTH AND MARS

G. Schmidt. Max Planck Institute of Chemistry, Mainz, Germany. E-mail: schmidtgerhard@aol.com.

A key issue for understanding the origin and the influence of impactors on the chemical composition of planets is the knowledge of the relative abundances of highly siderophile elements (HSE: Os, Ir, Ru, Pt, Rh, Pd) in the Earth's primitive upper mantle (PUM) and the continental upper crust (UCC). The past twelve years we have measured HSE in many mantle suites of the Earth by neutron activation. Estimates of Rh/Ir, Ru/Ir, Pd/Ir, and Pt/Os derived from PUM indicates modestly suprachondritic compositions [1]. The Os, Ir, Ru, Pt, and Pd pattern on PUM perfectly match the IVA iron meteorite Charlotte recently measured by Walker et al. [2]. The question arises if HSE in PUM are added to the accreting Earth by a late bombardment of iron meteorites or some unsampled inner solar system materials from formation regions closer to the sun (Mercury-Venus region), as it is supposed for enstatite chondrites and not sampled through meteorite collections?

The HSE and Ni systematics of the UCC closely resembles IIIAB iron meteorites (many impact craters on Earth are produced by this type of iron meteorite projectiles, e.g., [3] and references therein), pallasites, and the evolved suite of Martian meteorites (Fig. 1), possibly representing the elemental pattern of the Martian crust [4]. Probably Martian crust and Earth crust preserves an imprint of similar materials. About 160 impacting asteroids (M-type objects?) with radii of 10 km would yield the total abundances of HSE and Ni in the UCC [5]. In fact the first meteorite of any type ever identified on another planet by NASA's Mars Exploration Rover Opportunity was an iron meteorite.

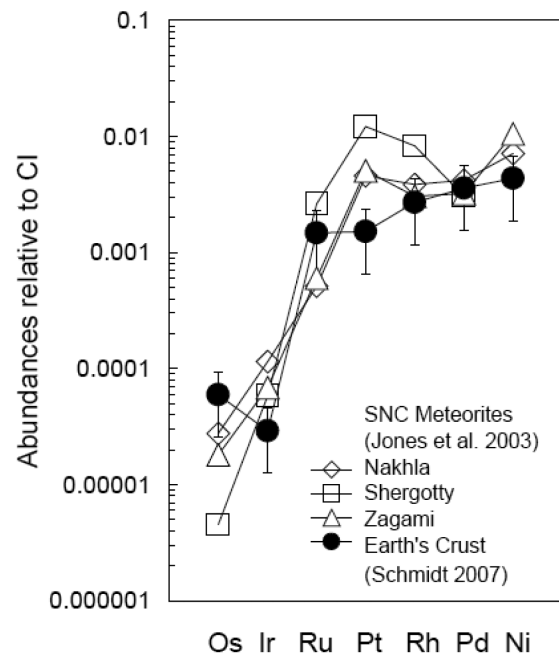


Fig. 1.

References: [1] Schmidt G. 2004. *Meteoritics & Planetary Science* 39: 1995-2007. [2] Walker R. J. et al. 2005. Abstract #1313. 36th LPSC. [3] Schmidt G. et al. 1997. *Geochimica et Cosmochimica Acta* 61:2977. [4] Jones J. H. et al. 2003. *Chemical Geology* 196:21-41. [5] Schmidt G. Forthcoming. *Meteoritics & Planetary Science*.

5268

THE CADMIUM ISOTOPE COMPOSITION OF CHONDRITES AND EUCRITES

M. Schönbachler^{1,2}, R. G. A. Baker¹, H. Williams³, A. N. Halliday³, and M. Rehkämper². ¹SEAES, The University of Manchester M13 9PL, UK. E-mail: m.schonbachler@manchester.ac.uk. ²IARC, Imperial College, London SW7 2AZ, UK. ³Department of Earth Sciences, University of Oxford, Oxford OX1 4BH, UK.

Introduction: Cadmium is a highly volatile element that is significantly depleted in most chondrites and inner Solar System bodies relative to CI chondrites. In unequilibrated ordinary chondrites and slightly metamorphosed CO chondrites, this depletion is accompanied by large Cd isotope variations in the permil range [1, 2]. These effects are thought to result from condensation/evaporation processes that took place on the parent bodies of those meteorites [1]. In contrast, CI, CM, and the CV3 chondrite Allende have identical Cd isotope compositions to the Earth within the previously reported analytical uncertainty of ± 4 epsilon for $^{114}\text{Cd}/^{110}\text{Cd}$ [1]. This is important in regard to short-lived chronometers e.g., Pb-Tl and Pd-Ag, whose two daughter isotopes could suffer from stable isotope fractionation. Such effects would limit their dating capabilities. To further investigate this topic, we developed a ^{111}Cd - ^{113}Cd double spike method by MC-ICPMS. The external reproducibility of this procedure is 0.6 epsilon for $^{114}\text{Cd}/^{110}\text{Cd}$ obtained from standards solutions analyzed over one day. All data were measured relative to the standard Alfa Cd Zurich [3], which is identical to JMC Cd employed by [1].

Results and Discussion: We report new double spike Cd data for various carbonaceous chondrites (CI, CM, CO, CR, and CV), eucrites, and terrestrial samples. The new Cd isotope data for Orgueil (CI), Murchison (CM), and Allende (CV) reproduce the values reported by [1]. In addition, we analyzed the CM chondrite Cold Bokkeveld and two CR2 chondrites and taken together, CI, CM, CR, and the CV chondrite Allende do not show significant Cd isotope variations and yield an average epsilon $^{114}\text{Cd}/^{110}\text{Cd} = 3.9 \pm 0.9$. This is identical to seawater (3.2 ± 1.0 ; [3]) but slightly higher than MORB (1.9 ± 0.2 ; this study) and terrestrial peridotites/komatiites (-0.6 ± 0.6 ; this study). The Cd isotope compositions of eucrites have a relatively large analytical uncertainty (± 4 epsilon) due to their low Cd content. They fall within the range defined by terrestrial samples and primitive carbonaceous chondrites. Only Juvinas shows a tendency to lighter Cd composition, which is not well resolved at present. Therefore, eucrites did not experience large Cd isotope fractionation, although Cd is depleted by a factor of ~ 600 relative to CI chondrites. This implies that processes such as volatile depletion in the solar nebula, accretion, core formation, and fractional crystallization did not cause significant mass-dependent isotope fractionation as expected, e.g., from processes involving kinetic Rayleigh evaporation/condensation. However, our data for CO and the oxidized CV chondrite Leoville confirm that thermal metamorphism on their corresponding parent body apparently lead to large Cd fractionation in the permil range [1, 2]. For Leoville, our data suggests an even heavier isotopic composition (epsilon $^{114}\text{Cd}/^{110}\text{Cd} = 31 \pm 3$) than obtained by [1] (epsilon $^{114}\text{Cd}/^{110}\text{Cd} = 18 \pm 4$), which indicates that the anomalous Cd might be distributed inhomogeneously within Leoville.

References: [1] Wombacher F. et al. 2008. *Geochimica et Cosmochimica Acta* 72:646–667. [2] Rosman K. J. R. and De Laeter J. R. 1988. *Earth and Planetary Science Letters* 89:163–169. [3] Ripperger S. and Rehkämper M. 2007. *Geochimica et Cosmochimica Acta* 71:631–642.

5185

ODP LEG207—A SURPRISINGLY PRISTINE K-T BOUNDARY. I—SEDIMENTOLOGY, MINERALOGY, Sr-Nd ISOTOPE SYSTEMATICS

P. Schulte¹ and A. Deutsch². ¹Geozentrum Nordbayern, Universität Erlangen-Nürnberg, D-91054 Erlangen, Germany. ²Institut für Planetologie, Universität Münster, D-48149 Münster, Germany. E-mail: deutsca@uni-muenster.de.

Introduction: Six cores from ODP Leg 207, Demerara Rise, tropical W Atlantic, recovered a 2–3 cm thick Chicxulub ejecta deposit marking the Cretaceous-Paleogene (K-T) boundary. The stunning feature of this sedimentary sequence is its uniformity over an area of ~ 30 km², and the total absence of bioturbation. Our high-resolution study reveals the remarkable complex composition and distinct microstratigraphy of the spherule deposit.

The Spherule Layer: The slightly graded K-T boundary layer consists predominantly of spherules fining upward from ≤ 1 to ≥ 0.4 mm in diameter. Texture of the spherules ranges from hollow over vesicle-rich to massive; some show in situ collapse. They are generally altered to aluminian dioctahedral Na-rich smectite, occasionally distinct globules rich in Fe and Mg, and pseudomorphs after quench crystals are present. Spherules are more Fe-Mg-enriched in the uppermost few mm of the layer, which contain abundant calcite and dolomite spherules, as well as shocked quartz and feldspar grains. Among others, we have discovered specific sponge-like, porous carbonate spherules whose textures resemble experimentally degassed calcites [1]. Some of the carbonate spherules are rimmed by now-altered silicate melts, indicating strong thermal overprint during ejection; others are polycrystalline with equilibrium textures, or consist of loosely accreted, μm -sized calcite and dolomite crystallites.

Sr-Nd Isotope Data: The altered glass spherules and the clayey matrix (site 1259B) display strongly negative $\epsilon_{\text{Nd}}^{T=65}$ Ma values with consistent $T_{\text{Nd}}^{\text{DM}}$ ages of ~ 1.9 Ga—much older than any model age reported so far for target or melt lithologies from Chicxulub (cf. [2]). The Sr-Nd isotope data for the ODP 207 samples are very different from those for spherules in other K-T ejecta deposits, obviously reflecting the uptake of Nd from the contemporaneous ocean water during alteration of the glass.

Interpretation: Overall characteristics (grading, excellent preservation of delicate textures) indicate that the K-T spherule bed drilled by ODP Leg 207 is an air-fall deposit with settling in quiet, ~ 2000 m deep water, followed only by minor soft-sediment deformation-drilling disturbance. The microstratigraphy is unlike to most other distal marine K-T boundary records that are affected by turbidity currents or/and bioturbation. In contrast, the ODP 207 K-T record strongly resembles the dual-layer K-T boundary in the terrestrial Western Interior that also yields a thick basal spherule layer overlain by clay enriched in iridium, shocked minerals, and Fe-Mg-rich spherules. We emphasize that we provide the first evidence of shocked carbonates and dolomites in Chicxulub ejecta deposits.

Acknowledgements: The Ocean Drilling Program (ODP) provided the samples, and the DFG funding for this research (SCHU 2248/2; DE 401/13). We acknowledge ODP, J. Erbacher (BGR Hannover), the ODP 207 curators, and H. Brinkhuis (University of Utrecht), who made the samples available.

References: [1] Agrinier P. et al. 2001. *Geochimica et Cosmochimica Acta* 65:2615–2632. [2] Kettrup B. and Deutsch A. 2003. *Meteoritics & Planetary Science* 38:1079–1092. [3] Berndt J. et al. 2008. *Meteoritics & Planetary Science*. This issue.

5111

THERMAL EVOLUTION OF PRIMITIVE ACHONDRITE PARENT BODIES

T. Schulz¹, C. Münker^{1, 2}, H. Palme², and K. Mezger³. ¹Mineralogisch-Petrologisches Institut Universität Bonn, Poppelsdorfer Schloss, D-53115 Bonn, Germany. ²Institut für Geologie und Mineralogie, Universität zu Köln, Zulpicherstr. 49b, D-50674 Köln, Germany. ³Zentrallabor für Geochronologie, Institut für Mineralogie, Universität Münster, Corrensstr. 24, D-48149 Münster, Germany.

Introduction: Acapulcoites and winonaites belong to the group of "primitive achondrites." They were heated to significantly higher temperatures than type 6 ordinary chondrites (~900 °C), often exceeding the silicate solidus (~1100 °C), although evidence for silicate differentiation is absent in most cases. These achondritic meteorites should have formed earlier than ordinary chondrites, at a time when more ²⁶Al was available to generate the very high temperatures. Due to the presence of abundant metal in both types of meteorites, their equilibration can be dated with the Hf-W chronometer. This chronometer was applied to the two acapulcoites Monument Draw and Dhofar 125 and the resulting ages are compared with published age constraints for chondrites and winonaites [1].

Results: Non- and weakly magnetic fractions of all analyzed acapulcoite separates from the two samples define a combined Hf-W isochron with an initial ¹⁸²W/¹⁸⁴W of $-3.1 \pm 0.3 \epsilon$ -units and a slope corresponding to an age of 4.6 ± 1.4 Myr after CAIs (using ¹⁸²Hf/¹⁸⁰Hf = $(1.01 \pm 0.05) \times 10^{-4}$ for Allende CAIs [2]). A Hf-W isochron for similar mineral fractions for winonaites yielded a much younger age of 14.5 ± 2.8 yr [1]. A comparison of the Hf-W age with published Pb-Pb and Ar-Ar ages of the acapulcoites implies cooling rates of about 100°/Myr between the closure temperatures of the Hf-W and Ar-Ar systems. This is faster than cooling rates for the H5 and H6 ordinary chondrites [3]. The winonaites and IAB meteorites yield cooling rates from 5 to 100°/Myr for the same temperature interval.

Discussion: The Hf-W age for acapulcoites is similar to maximum ages of ~4–5 Myr after CAI formation obtained for other differentiated meteorites (D'Orbigny angrite 4.3 ± 1.3 Myr [4]; eucrites 4.3 ± 1.4 Myr [5]; and IAB silicates 2.9 ± 2.2 Myr [6]). However, the acapulcoite age is slightly older than Hf-W ages reported for H5 and H6 chondrites (6.0 ± 0.9 Myr and 9.6 ± 1.0 Myr [3]) that were not melted during thermal overprint.

Assuming an internal heat source for these parent bodies, this marked age difference in peak temperatures most likely reflects a higher ²⁶Al content in the acapulcoite parent body compared to the H-chondrite parent body. The apparent age cluster for solidification of the most ancient differentiated meteorites of around 4–5 Myr most likely marks a minimum age required for ²⁶Al being the driving force for asteroid differentiation. If thermal peaks were reached at a later time, as for example in the H-chondrite parent body, internal heating was insufficient to trigger melting and efficient metal-silicate separation. The younger Hf-W isochron for winonaites (14.5 ± 2.8 Myr [1]), on the other hand, clearly highlights the role of impacts as a driving force for parent body differentiation and metamorphism later than 5 Myr.

References: [1] Schulz T. et al. 2007. [2] Burkhardt C. et al. 2007. [3] Kleine T. et al. 2008. [4] Markowski A. et al. 2007. [5] Kleine T. et al. 2004. [6] Schulz T. et al. 2006.

5009

NOBLE GASES IN TWO SHERGOTTITES AND A NAKHLITE FROM ANTARCTICA: Y-000027, Y-000097, AND Y-000593

S. P. Schwenzer^{1, 2}, S. Herrmann², and U. Ott². ¹Lunar and Planetary Institute, USRA, 3600 Bay Area Boulevard, Houston, TX 77058, USA. E-mail: schwenzer@lpi.usra.edu. ²Max-Planck-Institut für Chemie, J.-J. Becher Weg 27, 55128 Mainz, Germany.

Introduction: Three Martian meteorites from Antarctica have been investigated for noble gases: the shergottites Y-000027 and Y-000097, and the nakhlite Y-000593. The results are currently prepared for publication [1].

Experimental: For each meteorite a pair of rim and interior samples was obtained. These were measured in four temperature steps: 500, 1000, 1400, and 1800 °C. For experimental details, see [2].

Results: The amount of ⁴He in the four shergottite samples ranges between 33.8 and 39.4×10^{-8} ccSTP/g. ²²Ne is on the order of 14×10^{-8} ccSTP/g. The nakhlite contains $\sim 800 \times 10^{-8}$ ccSTP/g and $\sim 26 \times 10^{-8}$ ccSTP/g of ⁴He and ²²Ne, respectively. The heavy noble gases show large differences between the rim and interior samples, with the rim having 1.5–38, and 1.4–20 times as much ⁸⁴Kr and ¹³²Xe compared to the corresponding interior.

Discussion and Conclusions: *Helium Loss:* The ⁴He/³He ratio of the two shergottites is ~5, which indicates essentially complete loss of radiogenic ⁴He [3], as can be expected given their high shock pressure [4]. Hints for solar cosmic ray contributions to the neon budget can be seen in three of the four shergottite samples, and also, interestingly, the nakhlite Y-000593 (rim).

Cosmic Ray Exposure Ages: For calculating exposure ages we use the average chemical composition for shergottites from [5] and for the nakhlite from [6]. Y-000027 and Y-000097 are probably paired [4] and $T_{(3+21+38)}$ of this shergottite is 3.68 Ma, in good agreement with cosmic ray exposure ages for other Iherzolitic shergottites (e.g., [6]). For Y-000593 we obtain an age $T_{(3+21)} = 11.86 \pm 0.27$ Ma, which is in good agreement with the exposure ages of the other nakhlites [7].

Terrestrial Contamination and Martian Components: The enrichment of heavy noble gases in the rim samples indicates severe contamination by air. From the ¹²⁹Xe/¹³²Xe and ⁸⁴Kr/¹³²Xe relationship, it is evident that the incorporation mechanism caused elemental fractionation between Kr and Xe and that in the Y-000027/97 and Y-000593 (rim) samples any Martian signature is, with few exceptions, completely masked. However, the Y-000593 interior sample shows the shift to the left that is characteristic for fractionated Martian atmosphere in the nakhlites. In all but one sample a Martian atmospheric component can be seen in the 1400 °C step. No further disentangling of Martian components is possible without measuring mineral separates, however.

Acknowledgements: We thank the Antarctic Meteorite Research Center, National Institute for Polar Research, Japan, in particular Dr. K. Misawa, for providing the samples.

References: [1] Schwenzer et al. Forthcoming. Noble gases in two shergottites and a nakhlite from Antarctica: Y-000027, Y-000097, and Y-000593. *Polar Science*. [2] Schwenzer et al. 2007. *Meteoritics & Planetary Science* 42:387–412. [3] Schwenzer S. P. et al. 2004. *Meteoritics & Planetary Science* 39:A96. [4] Mikouchi T. and Kurihara T. 2007. *Meteoritics & Planetary Science* 42:A107. [5] Shirai and Ebihara. 2008. *Polar Science*. [6] Eugster et al. 1997. *Geochimica et Cosmochimica Acta* 61: 2749–2757. [7] Treiman A. H. 2005. *Chemie der Erde* 65:203–270.

5059

Fe²⁺ DISORDER STUDY IN PYROXENE FROM THE SHERGOTTI METEORITE BY MÖSSBAUER SPECTROSCOPY

R. B. Scorzelli¹, P. Munayco¹, and M. E. Varela². ¹Centro Brasileiro de Pesquisas Físicas (CBPF/MCT), Rua Xavier Sigaud 150, 22290-180 Rio de Janeiro, Brazil. E-mail: scorza@cbpf.br. ²Complejo Astronómico El Leoncito (CASLEO), Av. España 1512 Sur, CP J5402DSP San Juan, Argentina.

Introduction: The Shergotty SNC achondrite is believed to originate from Mars [1]. It consists mainly of pyroxenes (augite and pigeonite) and maskelynite with minor (~2%) ilmenite and titanomagnetite [2]. It also contains dense varieties of SiO₂. Nevertheless, there is no agreement on the p-T conditions of neither these phases nor the rock itself [2–4]. Here we report on our preliminary results of a Mössbauer study of the Shergotty pyroxenes to constrain these conditions.

Results: The average composition of the Shergotty pyroxene determined by electron microprobe analysis is SiO₂ 54(49.7), Al₂O₃ 0.74(0.66), TiO₂ 0.08(0.4), Cr₂O₃ 0.43(0.1), FeO 16.9(31.1), MnO 0.53(0.78), MgO 21.8(11), CaO 6.11(6.64), Na₂O 0.07(0.09), for core and rim, respectively [5].

The Mössbauer spectra of Shergotty meteorite shows Fe²⁺ in two different crystallographic sites, M₁ and M₂, in pyroxene. One intense inner doublet due to Fe²⁺ at M₂ site and a second one less intense due to Fe²⁺ at the M₁ site, whose relative areas are A₂(M₂) = 77% and A₁(M₁) = 23%. The resolution of the M₁ and M₂ doublets increases with decreasing temperature as a result of the differential dependence of the quadrupole splitting on temperature. Using the normalized Mössbauer relative areas of the doublets at 50 K, the Fe²⁺ fractions at the M₁ and M₂ sites are found to be 0.35 and 0.65, respectively. By means of the relative areas (A₁ and A₂) we determine the population of Fe²⁺ in M₁ and M₂ crystallographic sites. The Fe²⁺ occupancies at M₁ and M₂ in two nonequivalent sites are given by X_{Fe}(M₁) = 2yA₁/(A₁ + A₂) and X_{Fe}(M₂) = 2yA₂/(A₁ + A₂), being A₁ and A₂ the Mössbauer relative areas and y = Fe/(Fe + Al + Mg + Ca). Considering the disordering reaction due to intracrystalline Mg²⁺ and Fe²⁺ exchange among the nonequivalent M₁ and M₂ sites, the site population of Fe²⁺ and Mg²⁺ can be related to the disordering coefficient *p*, defined by $p = X_1(1 - X_2)/X_2(1 - X_1)$ where X₁ = X_{Fe}(M₁) and X₂ = X_{Fe}(M₂). Taking into account the chemical composition data, our results yields disordering parameters *p* = 0.21 and *p* = 0.08 for core and rim composition, respectively. This experimental result compared with *p* values obtained from pressure experiments under controlled conditions [6] may indicate that the pigeonite of the Shergotty meteorite exhibits a cation distribution corresponding to a closure temperature of at least 1000 °C for the core and lower ones for the rim. More detailed experiments are in progress in order to better estimate the p-T conditions.

References: [1] Nyquist et al. 2000. *Space Science Reviews* 96:105–164. [2] Stöffler et al. 1986. *Geochimica et Cosmochimica Acta* 50:889–903. [3] Chen M. and El Goresy A. 2000. *Earth and Planetary Science Letters* 179:489–502. [4] El Goresy et al. 2000. *Science* 288:1632–1634. [5] Smith J. V. and Hervig R. L. 1979. *Meteoritics* 14:121–142. [6] Dundon R. W. and Hafner S. S. 1971. *Science* 174:581–582.

5284

METEORITE PARENT BODIES: WHAT CAN THEY TELL US ABOUT THE FORMATION AND EVOLUTION OF THE ASTEROID BELT?

Edward R. D. Scott. Hawai'i Institute of Geophysics and Planetology. University of Hawai'i. Honolulu, HI 96822, USA. E-mail: escott@hawaii.edu.

Groups of related meteorites provide clues to the numbers and sizes of the meteorite parent bodies and their thermal and impact histories. Combining this information with astronomical and spacecraft observations of the current asteroids and with results from dynamical models allows us to understand better how the asteroids formed and evolved.

Many meteorite and asteroid properties appear consistent with a primordial asteroid belt that was only a few times more massive than the existing belt and was gradually ground down over 4.5 Gyr. For example, the onion-shell model for H chondrites and the survival of Vesta's basaltic surface imply that parent bodies were relatively undisturbed while they were heated and cooled. Most differentiated bodies were relatively small—only 20–200 km across—assuming that iron meteorites cooled inside intact differentiated asteroids.

By contrast, the standard model for accreting planets leads naturally to a situation where the initial mass of the asteroid belt was 10^{3–4} times the current mass and included Moon-to-Mars sized protoplanets. Such a model can explain the mass depletion of the belt, the inclined orbits of asteroids, the mixing of diverse types of asteroids, and their size distribution. Protoplanets would have excited the orbits of planetesimals leading to a period of intense collisional evolution until Jupiter reached its current mass and rapidly ejected all but a few lucky survivors, which were decimated during the Late Heavy Bombardment. In this model, the demolition of meteorite parent bodies would have peaked during ²⁶Al heating and subsequent cooling, and to a lesser extent during the LHB. In addition, differentiated asteroids and meteorites may have formed from impact debris generated by protoplanetary collisions.

Meteorites with thermal histories or other properties that appear to require a more massive asteroid belt with an early period of intense bombardment include both chondrites and differentiated meteorites. Protoplanetary collisions have been invoked to form CB chondrites from an impact plume and to allow group IVA irons to cool at diverse rates in a 300 km metallic body. Ureilites formed in a 200 km body that was catastrophically disrupted so that rocks at 1100 °C cooled in days. Group IAB and IIE irons are best explained by impact disruption of partly molten bodies to mix chondritic and achondritic clasts and silicate melt with molten metal. Pallasites probably formed in impacts that disrupted differentiated bodies making offspring composed of olivine mantle fragments and molten metallic Fe,Ni from cores. Mesosiderites formed in an impact that scrambled molten Fe,Ni from a core with basalt and other igneous rocks making a 300 km ball of breccia.

Major unsolved problems for the more massive asteroid belt model include the following: How can we understand H chondrite thermal histories and Vesta's intact crust? Why did planetesimal accretion last for 5 Myr? Did protoplanets form throughout the asteroid belt? How did protoplanetary debris accrete in the disk if protoplanets prevented nearby planetesimals from accreting?

5237

PRIMITIVE MATERIALS ON ASTEROIDS

D. W. G. Sears, K. Gietzen, D. Ostrowski, C. Lacy, and V. Chevrier. Arkansas Center for Space and Planetary Sciences, University of Arkansas, Fayetteville, Arkansas 72701, USA. E-mail: dsears@uark.edu.

Introduction: The linkage between asteroids and meteorites is critical if we are to fully understand the origin and evolution of the primitive materials of the solar system [1]. Usually, astronomical spectra are obtained and meteorite matches are sought. We are reversing this, and searching for what we perceive to be likely primitive materials among the asteroid spectra, emphasizing NEA [2–4]. We are focusing on type 3 ordinary chondrites and terrestrial phyllosilicates, not relying on the rare C chondrite observed falls as a point of comparison because of selection effects of the atmosphere. To add to the database of published spectra, we also run our own program of IRTF observations.

Type 3 (Unequilibrated) Ordinary Chondrites (UOC): To date we have located IR spectra of six UOC, run the MGM spectral analysis program [5, 6] and plotted the data on the Gaffey plot [7]. Few if any of the UOC plot in the ordinary chondrite fields of the Gaffey plot, but when analyzed by MGM all have absorption dips at $\sim 2 \mu\text{m}$ normally associated with calcic pyroxene. This band is almost certainly due to monoclinic pyroxene a major phase in UOC [2, 3]. The question thus arises whether any of the asteroids for which calcic pyroxene has been reported are actually the source objects for UOC. The discovery of asteroids whose surfaces are uniformly covered with UOC material would suggest that those objects are internally heated monoliths, with equilibrated ordinary chondrites coming from the interiors during fragmentation. The presence of UOC material on one side of the asteroid would indicate fragmentation, whereas patchy occurrences of UOC material, only observable with spacecraft resolution, would indicate rubble piles.

Phyllosilicates: While some authors have focused on finding bands of hydrated minerals or water on asteroids [8, 9], others have used continuum slope as a basis for comparison [10]. We find that the slope of the continuum of phyllosilicate IR spectra depends on composition and structure, and does not overlap with similar data for the C asteroids unless the phyllosilicates are heated in the laboratory to temperatures $\sim 900^\circ\text{C}$ [4]. This suggests that the surfaces of C asteroids are covered with hydrated phyllosilicates, presumably dehydrated by the heat of micrometeorite impact. We are optimistic that further analysis will make it possible to constrain the nature of the phyllosilicates and the degree of heating.

References: [1] Wetherill G. and Chapman C. 1988. In *Meteorites and the early solar system*. Tucson, Arizona: The University of Arizona Press. p. 35. [2] Gietzen K. and Lacy C. 2007. 38th LPSC. [3] Gietzen K. et al. 2008. 39th LPSC. [4] Ostrowski D. et al. 2008. 39th LPSC. [5] Sunshine J. M. and Pieters C. M. 1993. *Journal of Geophysical Research* 98:9075. [6] Sunshine J. M. and Pieters C. M. 1998. *Journal of Geophysical Research* 103:13,675. [7] Gaffey M. J. et al. 1993. *Icarus* 106:573. [8] Vilas F. and Gaffey M. J. 1989. *Science* 246:790–792. [9] Jones T. D. et al. 1990. *Icarus* 88:172–192.

5241

THERMOLUMINESCENCE AS A TECHNIQUE FOR DETERMINING THE NATURE AND HISTORY OF SMALL PARTICLES

D. W. G. Sears, F. Sedaghatpour, and J. Craig. Arkansas Center for Space and Planetary Sciences, University of Arkansas, Fayetteville, Arkansas 72701, USA. E-mail: dsears@uark.edu.

Introduction: Thermoluminescence (TL) and closely related cathodoluminescence (CL) provide unique information on thermal and radiation history of extraterrestrial samples and the nature and composition of certain key minerals and phases in these materials [1]. The techniques have been particularly useful in addressing the metamorphic history of little-metamorphosed chondrites [2] and surveying the geologically recent history of Antarctic meteorites [3]. For several years we have been considering the value of these techniques in exploring the nature and history of small particles, such as Stardust particles and IDPs, and here summarize results for 50–100 μm fragments of Semarkona matrix and 100–160 μm micrometeorites [4–7].

Semarkona Matrix: We analyzed eight fragments, characterized them with SEM and EDX, and measured their natural and induced TL using methods we have frequently described. We detected induced TL signals from all these samples, but the characteristics (TL peak temperature and width) were unlike those of UOCs where the phosphor is feldspar. CL suggests that the major luminescence phase in the Semarkona matrix is forsterite. The present data showed similarities to terrestrial forsterites from igneous and metamorphic locations, but sufficient differences to suggest that they were formed by a different mechanism, perhaps vapor deposition. We suggest that vapor deposited forsterite is an important component of primitive materials.

Micrometeorites: We obtained seven micrometeorites from Cecile Engstrand. Three of these objects show measurable induced TL and the shape of the TL curves resembled those of CO and certain CV chondrites, and unlike ordinary chondrites. Four of these objects showed no measurable TL, and in this sense resemble CI and most CM chondrites. These data would suggest that micrometeorites are related to the C chondrite classes, but to date we have not detected any that appear to be ordinary chondrites. Of course, this is in stark contrast to observed meteorite falls where ordinary chondrites dominate and C chondrites are rare.

Concluding Remarks: The results suggest that TL and CL can provide information for these small particles similar to that obtained for several decades on macroscopic samples.

References: [1] Sears D. W. G. 1988. *Nuclear Tracks and Radiation Measurements* 14:5–17. [2] Sears D.W. G. et al. 1980. *Nature* 287:791–795. [3] Benoit P. H. et al. 1992. *Journal of Geophysical Research* 97:4629–4647. [4] Craig J. et al. 2007. Abstract #1095. 38th LPSC. [5] Sears D. et al. 2007. Abstract #1055. 38th LPSC. [6] Craig J. and Sears D. W. G. 2008. Abstract #1081. 39th LPSC. [7] Sedaghatpour et al. 2008. Abstract #1161. 39th LPSC.

5021

CHEMISTRY AND MICROSTRUCTURE OF COS FROM ACER 094 CARBONACEOUS CHONDRITE

Y. Seto¹, N. Sakamoto², K. Fujino¹, and H. Yurimoto^{1,2}. ¹Department of Natural History Sciences, Hokkaido University, Sapporo 060-0810, Japan. E-mail: seto@mail.sci.hokudai.ac.jp. ²Isotope Imaging Laboratory, Creative Research Initiative "Sousei," Hokkaido University, Sapporo 001-0021, Japan.

Introduction: Recently, the isotopically anomalous ($\delta^{17,18}\text{OSMOW} \sim +180\%$) material has been discovered in the ungrouped carbonaceous chondrite Acfer 094 [1]. This material is mainly composed of Fe, Ni, O, and S. Fe and Ni contents are complementary to each other, keeping an O/S atom ratio of about 4 [1]. The material is referred to as cosmic symplectite (COS) because one of the COS grains consists of the symplectically intergrown magnetite and pentlandite [2]. However, the sample observed in [2] has relatively high Ni content, and low Ni samples are yet to be examined. Here, we report mineral characterization of both high- and low-Ni COS grains using synchrotron radiation X-ray diffraction analysis (SR-XRD) and transmission electron microscopy (TEM).

Experiments: Samples for SR-XRD and TEM were cut out from a polished thin section of Acfer 094 by a focused ion beam (FIB) technique using SMI3050TB system of SII NanoTechnology. SR-XRD measurements were carried out in the BL10XU beam line at SPring-8, Japan. Microstructural observations and electron diffraction analyses were undertaken using a conventional TEM (JEOL JEM-2010) equipped with a LaB₆ cathode and an EDS system (Thermo Electron Noran system SIX) of the Mineralogy Laboratory of Hokkaido University. Elemental maps were performed with a scanning TEM (HITACHI HD2000) and an EDS system (EDAX Genesis) of the Open Facility of Hokkaido University.

Results and Discussion: The SR-XRD and TEM studies show following clear differences or similarities between the two samples; (1) The high-Ni COS grain consists of magnetite + pentlandite, while the low-Ni one consists of magnetite + pyrrhotite (+minor pentlandite). (2) The high-Ni one is an aggregate of wormy grains (100~300 nm), which are an assemblage of magnetite-pentlandite showing a symplectitic texture in tens of nm scale. On the other hand, the low-Ni one is an aggregate consisting of idiomorphic magnetite (~100 nm) and pyrrhotite (~50 nm) grains. (3) Electron diffraction analyses indicate the magnetite in the high Ni COS grain has a 3-fold superstructure, while the magnetite in the low Ni COS does not have any superstructure. (4) No electron diffraction pattern from pentlandite in the both samples has been observed, although XRD patterns from pentlandite have been identified.

We infer that the COS grains were formed by sulfurization and oxidization of metal grains. The chemical and microstructural differences are probably reflected in the texture and the chemistry of precursor materials before the oxidization.

References: [1] Sakamoto N. et al. 2007. *Science* 317:231–233. [2] Seto et al. 2008. *Geochimica et Cosmochimica Acta*, doi:10.1016/j.gca.2008.03.010.

5317

SHOCK VEINS IN L6 CHONDRITES AND CONSTRAINTS ON THE IMPACT HISTORY OF THE L6 PARENT BODY

T. G. Sharp¹, Z. Xie², and P. S. De Carli². ¹School of Earth and Space Exploration, Arizona State University, Tempe, AZ 85287, USA. E-mail: tom.sharp@asu.edu. ²Nanjing University, Nanjing, China. E-mail: zhidongx@nju.edu.cn. ³SRI International, 333 Ravenwood Avenue, Menlo Park, CA 94025, USA. E-mail: paul.decarli@sri.com.

Introduction: High-pressure minerals that occur in and adjacent to shock-induced melt veins in chondrites provide constraints on the pressures and temperatures of shock metamorphism in these samples [1–3]. The duration of the shock pulse in such samples can be constrained by either using silicate-transformation kinetics [4–6] or by modeling melt vein cooling [1, 7, 8]. Impact velocities and impactor sizes can be calculated from pressure and duration data using simple planar-shock-wave approximations [8] or by hydrodynamic calculations [9]. In this study we use hydrodynamic calculations to explore possible impact conditions and sample locations on the L6 parent body for the highly shocked L6 chondrite RC106 [10].

Results: The melt vein in RC106 is 1.3 mm to 4 mm wide with a crystallization assemblage consisting of majorite garnet plus magnesiowüstite. There are two important features of this assemblage: 1) the mineralogy is constant throughout the veins, implying that melt-vein crystallization occurred under near isobaric conditions between 18 and 25 GPa; and 2) the vein contains a textural transition from large equant majorite garnets (up to 30 μm wide) in the vein center to finely dendritic majorite near the melt-vein edge. These textures are consistent with rapid cooling of the vein margin by conduction to a relatively cool host rock. Melt-vein cooling was modeled by assuming a planar melt vein at an initial temperature of 2500 K, surrounded by the solid host rock at 400 K. Using thermal conductivity values of 10 and 3 W/m², the center of a 1.3 mm melt vein would quench to the solidus in 165 and 550 ms, respectively.

To model possible impact scenarios, we assume a spherical L-chondritic impactor striking a much larger L-chondritic body. By placing pressure gauges throughout the model, we can investigate the pressure-time history of any position in the parent body. Assuming a porous surface regolith on the parent body, a 4km/s impact with a 10 km chondritic object can produce an RC106-like shock pulse for a sample at 8 km depth in the L-chondrite parent body.

References: [1] Xie Z. et al. 2006. *Geochimica et Cosmochimica Acta* 70:504–515. [2] Chen M. et al. 1996. *Science* 271:1570–1573. [3] Xie Z. and Sharp T. G. 2004. *Meteoritics & Planetary Science* 39:2043–2054. [4] Ohtani E. et al. 2004. *Earth and Planetary Science Letters* 227:505–515. [5] Chen et al. 2004. *Proceedings of the National Academy of Sciences* 101: 15,033–15,037. [6] Xie Z. and Sharp T. G. 2007. *Earth and Planetary Science Letters* 254:433–445. [7] Langenhorst F. and Poirier J. P. 2000. *Earth and Planetary Science Letters* 184:37–55. [8] Sharp T. and De Carli P. S. 2006. *Meteorites and the early solar system II*. pp. 653–677. [9] De Carli P. S. et al. 2007. AGU abstract. [10] Aramovich C. 2003. M.S. thesis, Arizona State University.

5248

CONSTRAINTS ON THE MAGMATISM OF MARS INFERRED FROM CHEMICAL COMPOSITIONS AND RADIOGENIC ISOTOPIC COMPOSITIONS OF SHERGOTTITES

N. Shirai¹ and M. Ebihara. Department of Chemistry, Graduate School of Science, Tokyo Metropolitan University, Hachioji, Tokyo 192-0397, Japan. ¹Present address: National High Magnetic Laboratory and Department of Geological Sciences, Florida State University, Tallahassee, FL 32310, USA. E-mail: shirai@magnet.fsu.edu.

Introduction: A wide range of Zr/Hf ratios was previously reported among shergottites [1, 2]. Based on chemical compositions for shergottites and assembled partition coefficients for Zr and Hf for several phases, Shirai and Ebihara [2] concluded that clinopyroxene and majorite are responsible for the fractionation of Zr and Hf in shergottites. Shirai and Ebihara [2] suggested that Mars and the Moon must have experienced different magmatism. However, the timing of the fractionation of Zr and Hf in shergottites is still not established.

Recently, improved analytical techniques represented by MC-ICP-MS and TIMS increased our knowledge concerning the time scale of the core formation and early differentiation on Mars [e.g., 3]. Foley et al. [3] reported that the silicate differentiation which formed the shergottites's mantle source occurred 4.525 Ga. In this study, we conducted a chemical study of shergottites and combined chemical compositions with isotopic compositions to elucidate the timing of the fractionation of Zr and Hf in shergottites.

Analytical Procedures: NWA 856 (basaltic shergottite), Y-000097 (lherzolitic shergottite) and NWA 1068 (olivine-phyric shergottite) were analyzed for bulk major, minor, and trace element compositions by using three nuclear analytical methods (PGA, INAA, and IPAA).

Results and Discussions: Zr/Hf ratio of NWA 856 (36.6 ± 1.4) is chondritic and is in agreement with that for basaltic shergottites represented by Shergotty and Zagami. Some olivine-phyric shergottites (EETA79001A, DaG 476, SaU 005, and Y-980459) were reported to have subchondritic Zr/Hf ratios [1, 2], while the olivine-phyric shergottite NWA 1068 has a chondritic Zr/Hf ratio (39.0 ± 2.1). Zr/Hf ratio of Y-000097 is subchondritic (26.5 ± 1.8) and consistent with those for other lherzolitic shergottites and olivine-phyric shergottites (EETA79001A, DaG 476, SaU 005, and Y-980459). Three shergottites (NWA 856, NWA 1068, and Y-000097) analyzed in this study fall on a positive line in the plot of Zr abundances versus Zr/Hf ratios.

Shergottites were reported to have a large variation of $\epsilon^{142}\text{Nd}$ [3]. Zr/Hf ratios are found to decrease with increasing of $\epsilon^{142}\text{Nd}$ among shergottites, indicating that the fractionation of Zr and Hf and Sm and Nd in shergottites occurred contemporaneously and during early silicate differentiation. It was previously suggested that shergottites were formed by different degrees of mixing of components derived from depleted and enriched parent magmas, implying that the correlation trend between Zr/Hf ratios and $\epsilon^{142}\text{Nd}$ presents a mixing line. Lherzolitic shergottites and olivine-phyric shergottites (EETA79001A) do not fall on the correlation line of Zr/Hf ratios and $\epsilon^{142}\text{Nd}$. Lherzolitic shergottites and EETA79001A must have experienced the different petrogenesis from that for the other shergottites.

References: [1] Münker C. et al. 2003. *Science* 301:84–87. [2] Shirai N. and Ebihara M. 2006. Abstract #1917. 37th LPSC. [3] Foley C. N. et al. 2005. *Geochimica et Cosmochimica Acta* 69:4557–4571.

5294

MODERATELY SIDEROPHILE ELEMENT ABUNDANCES IN ANGRITES

N. Shirai¹, M. Humayun¹, and K. Righter². ¹National High Magnetic Field Laboratory and Department of Geological Sciences, Florida State University, Tallahassee, FL 32310, USA. E-mail: shirai@magnet.fsu.edu. ²NASA Johnson Space Center, 2101 NASA Parkway, Houston, TX 77058, USA.

Introduction: Angrites are an enigmatic group of achondrites that constitute the largest group of basalts not affiliated with the Moon, Mars, or Vesta (HEDs). It has been proposed that angrites are associated with Mercury [1]. Chemically, angrites are exceptionally refractory element-enriched (e.g., Al, Ca) and volatile element-depleted (e.g., Na and K) achondrites [2]. Highly volatile siderophile and chalcophile elements (Zn, Ge, and Se) may be less depleted than alkalis and Ga, taken to imply a fractionation of plagiophile elements [2]. Chemical similarities between angrites and Group IVB iron meteorites led to a proposed link where Group IVBs may be the core of the APB [3]. An alternative approach to exploring this link is through application of metal-silicate partition coefficients to moderately siderophile element (MSE) abundances in the silicate portions of the APB [4]. This approach is limited by the dearth of MSE data for angrites (e.g., Mo, Ge).

The recent increase in angrite numbers (12) has greatly increased our knowledge of the compositional diversity of the angrite parent body (APB). In this study, we report new Ga, Ge, Mo, Sb, and W abundances for angrites by laser ablation ICP-MS in order to place constraints on core formation of APB.

Analytical Methodology: A 1 mm² raster (<50 μm depth) was performed on a representative area of a polished potted butt of D'Orbigny, UNM 1115, by laser ablation ICP-MS. A New Wave UP213 system was coupled to an Element, operated in medium resolution ($R = 4000$) to resolve molecular isobaric interferences, particularly ArSi^+ on $^{69}\text{Ga}^+$. The peaks ^{23}Na , ^{25}Mg , ^{27}Al , ^{29}Si , ^{44}Ca , ^{45}Sc , ^{48}Ti , ^{51}V , ^{52}Cr , ^{55}Mn , ^{56}Fe , ^{59}Co , ^{58}Ni , ^{69}Ga , ^{73}Ge , ^{74}Ge , ^{95}Mo , ^{97}Mo , ^{121}Sb , ^{123}Sb , ^{139}La , ^{144}Nd , ^{182}W , and ^{193}Ir were monitored. Correct isotope ratios were obtained on Mo and Sb peaks, but ^{73}Ge showed an interference and was not used further. Elemental abundances were obtained using relative sensitivity factors obtained from reference values for MPI-DING glasses: ML3-B, T1, StHs 6/80, and ATHO, and values for NIST SRM 612, with the exception of Ir.

Results and Discussion: The abundances of Ga, Mo, Sb, and W were readily recovered from the raster, while an upper limit was obtained for Ge (15 ppb). The Ga abundance (0.37 ppm) agreed well with the literature value [5] for bulk D'Orbigny (0.37 ppm), while Sb (55 ppb), W (360 ppb), and Ir (<5 ppb) were higher than literature values [5, 6]. Discrepancies of Sb and W abundances between our data and literature values are due to sample heterogeneity. New data were obtained for Mo (250 ppb), with a $\text{Mo/Nd} = 0.027$. The $(\text{Sb/Nd})_{\text{CI}} = 0.016$ for the APB is similar to that for the Earth (0.023 ± 0.010) [7, 8]. The $(\text{W/Mo})_{\text{CI}} = 14$ for the APB based on D'Orbigny is different from that of the EPB, implying that the two parent bodies (APB and EPB) may have had different core formation conditions.

References: [1] Irving A. J. et al. 2007. American Geophysical Union, FM 2005, #P51A-0898. [2] Warren P. H. et al. 1995. *Antarctic Meteorite Research* 20:261–264. [3] Campbell A. J. and Humayun M. 2005. *Geochimica et Cosmochimica Acta* 69:4733–4744. [4] Righter K. 2008. Abstract #1936. 39th LPSC. [5] Kurat G. et al. 2004. *Geochimica et Cosmochimica Acta* 68:1901–1921. [6] Mittlefehldt D. W. et al. 2002. *Meteoritics & Planetary Science* 37:345–369. [7] Jochum K. P. and Hoffman A. W. 1997. *Chemical Geology* 139:39–49. [8] Hoffman A. W. 1988. *Earth and Planetary Science Letters* 90:297–314.

5131

APPLICATIONS OF KAGUYA'S TERRAIN CAMERA IMAGES TO PROMOTION OF SCIENTIFIC EDUCATION AND GEOLOGICAL RESEARCHES

Motomaro Shirao¹, Junichi Haruyama², Hiroshi Takeda³, Makiko Ohtake², Tsuneo Matsunaga⁴, and LISM working group. ¹1-3-11 Nishi-Asakusa, Taito-ku, Tokyo 111-0035, Japan. E-mail: motomaro@ga2.so-net.ne.jp. ²Inst. of Space and Astronautical Sci., Japan Aerospace Exploration Agency, Japan. ³Department of Earth and Planetary Science, University of Tokyo, Hongo, Tokyo 113-0033, Japan. ⁴Center for Global Environmental Research, National Institute for Environmental Studies, Japan.

Introduction: On September 14, 2007, the Japanese Moon explorer Kaguya (Selene) was successfully launched [1, 2]. The Terrain Camera (TC) of Kaguya is a push-broom stereoscopic imager with forward-looking and aft-looking optical heads with slant angles of ± 15 degrees from the nadir vector [1, 2]. The spatial resolution of TC is 10 m/pixel from the Kaguya nominal altitude of 100 km. The TC will provide (1) global/local high-contrast mosaic maps and (2) digital terrain models (DTMs) for the Moon's entirety with a relative height resolution of a few tens of meters or better and ultimately a DEM with absolute height information.

Results and Discussion: The nominal swath of the TC is 35 km, and the interval between Kaguya's adjacent orbits is 33 km at an altitude of 100 km. Consequently, the TC adjacent strip images will have extended overlaps with the same solar angle conditions, which will facilitate the production of large 3-D mosaic images. These images are enable us to observe any point of lunar surface at a preferable altitude, direction, and magnification. Figure 1 shows an example of 3-D bird's-eye view images of the Apollo 17 landing site. A similar image of Hadley rill and the Apennine Mountains, which was not possible to see from the Apollo 15 mission, has been constructed by the same routine. We also produced a video-movie by stacking successive 3-D images of a slight different viewpoint for the crater Tycho along the crater walls, and the Alpine Valley.

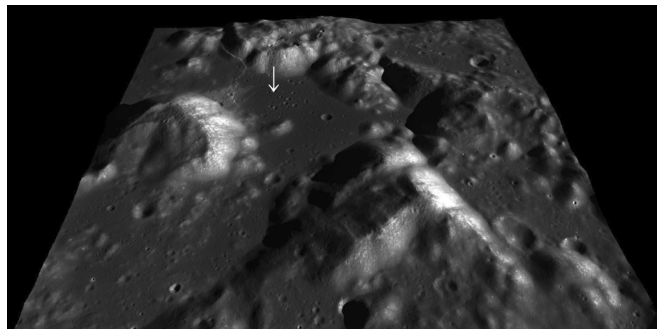


Fig. 1. 3-D image of Apollo 17 landing site (arrow) in the valley of Taurus-Littrow, produced by Kaguya's TC images. View from South. Image width is 35 km.

These TC 3-D images and video-movies, together with Kaguya's high-definition TV images [3], is expected to be utilized for education of planetary geology, to find geologically interesting sites for lunar researchers, as well as for public outreach.

References: [1] Haruyama J. et al. 2008. *Earth, Planets and Space* 60: 242–255. [2] Haruyama J. et al. 2008. Abstract #1308. 39th LPSC. [3] Honda R. et al. 2008. Abstract #1876. 39th LPSC.

5114

OBSERVATION AND ANALYSIS OF MARTIAN METEORITE Y-000593: EVIDENCE OF BIOSIGNATURES

L. M. Spencer¹, D. S. McKay², E. K. Gibson², K. L. Thomas-Keprta¹, S. J. Wentworth¹, and S. J. Clemett¹. ¹ESC Group, Mail Code JE23, NASA-JSC, Houston, TX 77058, USA. ²NASA Johnson Space Center, Houston, TX 77058, USA.

Introduction: Yamato-000593 is a meteorite discovered in Antarctica by JARE in 2000 and identified as a Martian nakhlite [1, 2]. Previously, Fisk et al. [5] suggested tunnels and galleries, along with secondary clay and carbonate phases, discovered in both oceanic basalts and the Nakhla meteorite are likely the result of biogenic activity. Here we report the first in-depth analysis of secondary alteration features in Y-000593, suggesting the presence of carbonate phases and pre-terrestrial iddingsite clay associated with tunnels and galleries similar to those previously studied in Nakhla and oceanic basalts. No evidence of terrestrial contamination has yet been found in Y-000593. It is known that the iddingsite in Nakhla formed under low-temperature, aqueous weathering conditions [3]; consequently, the presence of this mineral as well as carbonate in Y-000593 may be further evidence supporting a past history of warmer and wetter climate on Mars [4].

Results: Optical and FE-SEM analysis of a polished thin section revealed iddingsite-filled impact microfractures. Within grains of olivine and veins of high-silica glass, we document 1–4 μm tunnels and galleries that extend outward from fractures and that are quite similar to those in Nakhla [3–5]. EDX analyses of these alteration features also reveal carbonate phases with high Mn and Ca abundances. Iddingsite and carbonate phases are both closely associated with the tunnel and gallery features.

Discussion: Alteration in Y-000593 appears similar in size and distribution to tunnels and galleries previously observed in Nakhla as well as oceanic basalts containing live DNA [5]. EDX compositions of alteration products in both Martian meteorites are consistent with phases observed in oceanic basalts and attributed to biotic weathering.

References: [1] Meyer C. 2003. *Mars Meteorite Compendium*, XXII-1–XXII-5. [2] Imae N. 2002. 33rd LPSC. [3] Gooding et al. 1991. *Meteoritics* 26:135–143. [4] Wentworth et al. 2005. *Icarus* 174:382–395. [5] Fisk et al. 2006. *Astrobiology* 6:48–68.

5106

RESEARCH ON EXTRATERRESTRIAL SAMPLES IN LARGE PUBLIC INSTITUTIONS I: CHALLENGES TO LAB INTEGRITY AND SOLUTIONS

G. Srinivasan. Department of Geology, University of Toronto, ON M5S 3B1, Canada. E-mail: sri@geology.utoronto.ca.

Introduction: Research on extraterrestrial samples offer fundamental clues to the origin and evolution of the solar system. In recent years the increased awareness of planetary science and exploration is resulting in major efforts to build research groups at intra- and inter-institutional levels. Studies involving “rocks from space” are embedded in departments of geology, which introduces its own challenges and benefits. In my endeavor to set up an extraterrestrial research lab, I faced several challenges in setting up the infrastructure involving clean lab conditions and in minimizing the potential hazard of contamination from terrestrial samples, a nightmare for a Principal Investigator of a laboratory in its nascent stages of establishment.

A typical geochemical laboratory dealing with chemical and isotopic analyses of rocks, sample preparation requires 1) rock crushing and preparation; 2) chemical dissolution in inorganic acids; 3) elution of elements using ion exchange columns; and 4) analyses (e.g., TIMS, ICPMS). The reliability and quality of measurements is dependent on tracking and minimizing “laboratory blanks” and eliminating potential sources of contamination of sample or the analytical tools and reagents. Laboratory blank is an integral part of analytical environment which can be monitored, quantified, and factored in assessing the limitations of the measurement. On the other hand, “contamination” has a negative connotation and evokes images of an uncontrolled environment. In a laboratory analyzing a mixed bag of samples (terrestrial and extraterrestrial samples) and training undergraduate and graduate students, some basic precautions by all stakeholders can help to significantly minimize the potential of contamination. For example, all participants in such laboratory must adhere to the principle that access to various subsections of a composite laboratory is based upon need and not merely guaranteed by association. The PI and the senior research staff must constantly strive to eliminate the risk of contamination during sample preparation. However, no amount of care and precaution can mitigate the risk associated with uncontrolled access to laboratory by personnel not associated with the research. In the following I assess the risk associated with such access.

Case Study: While studying Fe-Mn nodule for Nd isotopic analyses extra precautions were taken by crushing the sample in an environment removed from meteorite crushing and preparation. Fe-Mn nodules with a Nd concentration of ~80 ppm and $\epsilon^{143}\text{Nd}$ of ~-12 in some cases can easily alter the composition and chondrites which have a Nd concentration ~1 ppm and $\epsilon^{143}\text{Nd}$ of ~0. To answer the question of how contamination from continental rocks (Fe-Mn nodule as a proxy for continental rocks) is needed to shift the $\epsilon^{143}\text{Nd}$ of chondrites by a magnitude comparable to the targeted external precision of 20 ppm, I carried out a simple mass balance calculation for a 100 mg sample with the above mentioned composition and concentration for Nd. 20 micrograms of Fe-Mn nodule powder as contaminant can cause shift of 20 ppm in the observed value of chondrite. This amount is close to the detection limit of my precision balance! A researcher who works in a traditional rock-crushing room with continental rocks can easily sabotage and ruin high-quality measurements on chondrites if he/she accesses the extraterrestrial lab without proper precautions.

5211

CONSTRAINTS ON EARLY EVOLUTION OF SOLAR NEBULA FROM ^{26}Al ABUNDANCE IN EFREMOVKA CAIsG. Srinivasan¹ and M. Chaussidon². ¹Department of Geology, University of Toronto, Toronto, ON M5S 3B1, Canada. E-mail: sri@geology.utoronto.ca. ²CRPG-CNRA, BP 20, 54501 Vandoeuvre-les-Nancy, France. E-mail: chocho@crpg.cnrs-nancy.fr.

Introduction: In a comprehensive review of available Mg data for CAIs, MacPherson et al. (1995) [1] concluded that the initial $^{26}\text{Al}/^{27}\text{Al}$ ratio at the time of solar system formation was $\sim 4.5 \times 10^{-5}$. The available data at that time was primarily obtained by small geometry ion microprobe using mono-collection and by current standards of measurement technique, precision was subject to large uncertainties. Recent high-precision multi-collector ICPMS data of CAI Al-Mg composition (bulk and mineral) by [2–4] suggests a higher initial $^{26}\text{Al}/^{27}\text{Al}$ ratio of $\sim 5.85 \times 10^{-5}$ at the time of CAI formation. Data from others [5, 6] suggest a lower value for initial $^{26}\text{Al}/^{27}\text{Al}$ $\sim 5.2 \times 10^{-5}$ to 4.9×10^{-5} . Are the differences in initial $^{26}\text{Al}/^{27}\text{Al}$ between laboratories real or are they merely a product of inter-laboratory measurement bias? We have used the large geometry ion microprobe Cameca ims 1270 in CRPG in Faraday Cups multi-collection mode to address this question. The large geometry ion microprobe with superior transmission in multi-collection in Faraday Cups enables measurement of higher signal strength thereby improving counting statistics and precision.

Al-Mg Measurements: We have reanalyzed the data of CAIs [7] E65 (type B1) [8] and E66 (type A) and carried out new measurements of E36 from CV3 chondrite Efremovka for ^{26}Al studies. The reanalyses of the data is mandated by precise recalibration of the Al/Mg ion yields for mineral phases with widely varying Al/Mg ratios. The Mg isotopic studies were carried out with a primary ion beam of ~50 nano-amperes and ^{24}Mg ion signal $\sim 10^7$ – 10^8 cps. Terrestrial reference sample yield extremely precise values; for example, San Carlos Olivine $\delta^{26}\text{Mg} = 0.003 \pm 0.024\%$ (n = 27); spinel, $\delta^{26}\text{Mg} = 0.002 \pm 0.041\%$ (n = 9). For E66 Al-Mg isochron initial $^{26}\text{Al}/^{27}\text{Al} = (4.57 \pm 0.17) \times 10^{-5}$ ($2\sigma_m$) and initial $\delta^{26}\text{Mg} = 0.02 \pm 0.24\%$. In E65, the melilite-spinel Al-Mg evolution diagram gives an initial $^{26}\text{Al}/^{27}\text{Al} = (4.29 \pm 0.47) \times 10^{-5}$ ($2\sigma_m$) and $\delta^{26}\text{Mg} = -0.09 \pm 0.19\%$ and E36 $^{26}\text{Al}/^{27}\text{Al}$ value = $(4.40 \pm 0.32) \times 10^{-5}$ and $\delta^{26}\text{Mg} = -0.09 \pm 0.19\%$. The initial ^{26}Al abundance in the 3 Efremovka CAIs overlap with in errors and are lower than the value of 4.9×10^{-5} reported for Allende [5] and the value of 5.85×10^{-5} reported by [3]. Supracanonical observations of ^{26}Al abundance [2–4] cannot be ruled out from the above Efremovka CAI mineral isochron data. These mineral isochrons record ^{26}Al abundance after thermal processing following separation from reservoir. The highest value for ^{26}Al in E66 is lower than either of whole-rock values [2–4 or 5–6] and suggests that this CAI achieved its closure within ~66,000 years (for canonical ^{26}Al abundance) or ~270,000 years for supracanonical values. The Efremovka CAIs achieved closure of Al-Mg system within a short time (<20,000 years) interval of each other. The Al-Mg closure of Efremovka CAIs was completed within class I stage of premain sequence stars [9].

References: [1] MacPherson et al. 1995. *Meteoritics* 30:365. [2] Young et al. 2005. *Science* 308:223. [3] Thrane et al. 2006. *The Astrophysical Journal* 646:L159. [4] Tonui et al. 2008. Abstract #1380. 39th LPSC. [5] MacPherson et al. 2007. Abstract #1378. 38th LPSC. [6] Jacobsen et al. Forthcoming. *Earth and Planetary Science Letters*. [7] Srinivasan et al. 2007. [8] Goswami et al. 1994. *Geochimica et Cosmochimica Acta* 58:431. [9] Wood J. 2004. *Geochimica et Cosmochimica Acta* 68:4007.

5105

DETERMINING THE ELEMENTAL AND ISOTOPIC MAKEUP OF COSMIC DUST FROM RESIDUES IN IMPACT CRATERS: PREPARATION FOR THE ISPE

F. J. Stadermann and C. Floss. Laboratory for Space Sciences, Physics Department, Washington University, 1 Brookings Drive, Saint Louis, MO 63130, USA. E-mail: fjs@wuphys.wustl.edu.

Introduction: The Stardust mission used both aerogel tiles and Al foils to gather dust from the coma of comet Wild 2. Although hypervelocity impacts in solid metal targets are generally highly disruptive, the residues were found to preserve significant portions of the original projectile material [1, 2]. Analyses of crater residues led to the identification of several surviving presolar grains among the cometary samples [3–5]. A second collector on the Stardust spacecraft was used to capture possible contemporary interstellar dust traversing the solar system. The study of these interstellar samples is analytically highly challenging and the upcoming preliminary examination (ISPE) will initially consist only of nondestructive surveys [6]. Previously, we have used the Auger spectrometer and the NanoSIMS for the elemental and isotopic characterization of cometary dust residues at high spatial resolution [4, 5, 7]. We have now tested various analytical approaches for the ISPE.

Details: The interstellar collector foils will not only have many fewer and smaller impact craters than the cometary ones, but the amount of residue per crater will also be significantly lower than in the cometary collection. This is due to the larger ratio of crater diameter to projectile diameter at the higher impact velocities that are expected for the interstellar grains. To partially simulate the conditions expected on the interstellar collector, we performed NanoSIMS isotopic and Auger elemental measurements of impact debris on a selection of the smallest cometary craters and on samples from LDEF experiments in low Earth orbit, where impact velocities were generally higher. This will allow us to test the suitability of high resolution Auger spectroscopy for the nondestructive elemental characterization of smaller and/or thinner residue deposits than previously studied. We also search for signatures of presolar grains in the residues to evaluate their survival characteristics under different impact conditions.

Results and Discussion: The Stardust measurements focused on the heavily cratered foil C2010W, and the LDEF samples were from capture cell experiment A0187-2 and Au craters A0187-1 [8]. We analyzed residues in craters as small as 200 nm and found that Auger spectroscopy was in all cases able to determine clear elemental signatures of the projectile residue and in many cases could even detect compositional heterogeneities among the debris. The Auger measurements were able to “see through” the unavoidable minute layer of surface contaminants without requiring any sputter cleaning. Although NanoSIMS isotopic measurements are not planned for the ISPE, we found that we would achieve sufficient precision to detect presolar isotopic signatures in the residues, if such material is present.

References: [1] Hörz F. et al. 2006. *Science* 314:1716–1719. [2] Kearsley A. T. et al. 2008. *Meteoritics & Planetary Science* 43:41–73. [3] McKeegan K. D. et al. 2006. *Science* 314:1724–1728. [4] Stadermann F. J. et al. 2008. *Meteoritics & Planetary Science* 43:299–313. [5] Stadermann F. J. and Floss C. 2008. Abstract #1889. 39th LPSC. [6] Westphal A. J. et al. 2008. Abstract #1855. 39th LPSC. [7] Stadermann F. J. et al. 2007. Abstract #1334. 38th LPSC. [8] Stadermann F. J. et al. 1994. *LDEF—69 months in space*. pp. 461–473.

5188

CHEMICAL AND MINERALOGICAL PROPERTIES OF COMETARY SAMPLES CAPTURED BY STARDUST

T. Stephan¹ and C. H. van der Bogert². ¹University of Chicago, Department of the Geophysical Sciences, 5734 South Ellis Avenue, Chicago, IL 60637, USA. E-mail: tstephan@uchicago.edu. ²Institut für Planetologie, Wilhelm-Klemm-Str. 10, 48149 Münster, Germany.

Introduction: Dust particles from comet Wild 2 were collected by the Stardust mission and returned to Earth in 2006 [1]. Low-density silica aerogel was used as primary capture medium to gently decelerate impacting dust particles in an effort to preserve them as intactly as possible. However, at a sampling velocity of 6.1 km/s, most particles fragmented and most cometary material was heavily altered. Understanding the effects of aerogel capture on Wild 2 dust is a prerequisite to relate the properties of the material collected by Stardust to their cometary origin.

Samples and Analytical Techniques: Time-of-flight secondary ion mass spectrometry (TOF-SIMS) and transmission electron microscopy (TEM) were used to study fragments of cometary matter extracted from tracks in Stardust aerogel [2–4].

Sections of nine cometary fragments from five different tracks have been studied by TOF-SIMS so far. Four samples are so-called terminal particles, while the remaining five fragments were extracted from the walls in the aerogel along the tracks. Samples—terminal particles as well as track wall material—from two other tracks are presently under investigation.

Results: TOF-SIMS results show that all Wild 2 fragments extracted from the walls along tracks are dominated by Si, with Si/Mg ratios between 40 and 64, but have CI-like abundances of major and minor elements relative to Mg. TEM measurements revealed that during the capture process the cometary material melted and mixed with aerogel that also partially melted. These samples consist of silica-rich glass with varying Fe, Mg, and Si contents and small FeNi and FeS spherules.

Two of the four terminal particles in this study survived the capture process with less alteration. Their Si/Mg ratios of 1.2 and 1.0, respectively, are close to CI (0.93). They have thin coatings of compressed and melted aerogel with some adhered material similar to the capture-melted fragments. However, both samples were primarily single- to coarse-grained crystalline mineral phases (enstatite) in contrast to the mixed glasses in track walls.

However, not all terminal particles survived the impact into aerogel intact. The other two terminal particles in this study showed melting and mixing with aerogel (Si/Mg ratios of 20 and 70, respectively) like all fragments from along the tracks.

Conclusions: The results suggest that Wild 2 particles, prior to their encounter with Stardust aerogel, consisted of a mixture of single and multi-mineralic grains, embedded in a fine-grained, porous matrix, which is probably similar to chondritic porous interplanetary dust particles [5]. During impact into the aerogel, the matrix was stripped from the larger mineral grains, melted and mixed with aerogel, and deposited along the track walls. The more compact mineral grains survived as terminal particles.

References: [1] Brownlee D. E. et al. 2003. *Journal of Geophysical Research* 108:E8111. [2] Stephan T. et al. 2008. *Meteoritics & Planetary Science* 43(1/2). [3] Stephan T. and van der Bogert C. H. 2008. Abstract #1508. 39th LPSC. [4] Van der Bogert C. H. and Stephan T. 2008. Abstract #1732. 39th LPSC. [5] Van der Bogert C. H. et al. 2008. Abstract #8257. *Asteroids, Comets, Meteors 2008*.

5259

MICROCRACK POROSITY IN BEAVER CREEK AND MENOW, HIGH-POROSITY ORDINARY CHONDRITESM. M. Strait¹ and G. J. Consolmagno SJ². ¹Alma College, Alma MI 48801, USA. E-mail: straitm@alma.edu. ²Specola Vaticana, Vatican City State.

Introduction: Porosity of meteorites gives us insight into the origin and evolution of the fabric of materials in the solar system. We have been evaluating meteorite porosity for a number of years using both helium pycnometry [1] and a computerized point-counting system [2]. Most ordinary chondrites fall into a surprisingly narrow range of porosity values. And both measurement methods give comparable values for the porosity of ordinary chondrites, with the bulk of the porosity apparently in the microcracks that are visible using SEM imaging as well as accessible to the He for the pycnometry measurements.

By contrast, carbonaceous chondrites exhibit a major discrepancy between the results generated by the two methods [2, 3]. Pycnometry values for the carbonaceous chondrites are as much as an order of magnitude larger than those made by point-counting or using fluids like water or carbon tetrachloride to determine bulk and grain volumes. Even when adjusting for visible holes and cracks in the fabric of the thin section, which might be attributed to thin section preparation effects, the porosity measurements do not agree. The visual appearance of the sample in the SEM is very compact with minimal microcracking and these images do not reveal where the porosity measured with pycnometry is located.

Two Exceptional Ordinary Chondrites: In this study we look at two H4 ordinary chondrites that appear to have high porosity, Beaver Creek (shock level S3) and Menow (shock level S1). Using pycnometry and beads, the porosity of Beaver Creek is $15.3 \pm 2.2\%$ [4]; the measured porosity of Menow is $13.2 \pm 2.6\%$ [4] but when corrected for weathering, Menow's model porosity is $18.6 \pm 0.8\%$ [1]. In a visual examination of their thin sections, there is a fair amount of porosity in the form of holes and cracks in the fabric in both samples. The porosity measured with point-counting of the SEM images is 11.8% (3.7% to 25.7%) for Beaver Creek and 6.9% (2.7% to 14.6%) for Menow. Both these measurements are within the normal range observed in the ordinary chondrites. The discrepancy between hand sample and point counting porosities is less extreme than that observed for carbonaceous chondrites, but nonetheless points to the presence of porosity in meteoritic materials that is accessible to He, but not visually observable at the scale we are using to image these samples. It may be a sampling bias in the case of the images chosen for the point-counting, but may also be due to the same problems observed in the carbonaceous chondrites.

Discussion: We had found [1] that the porosity of low shock (S1 and S2) meteorites can range from typical (5–10%) ordinary chondrite values, to more than 20% porosity, approaching the range of some carbonaceous chondrites. Menow represents this group of meteorites. Beaver Creek, at shock S3, is a unique high porosity outlier for moderate shock ordinary chondrites. For carbonaceous chondrites, it is argued [2] that the high porosity seen is at a scale too large to be visible in thin section, and due to incomplete compaction and lithification. This may also be true here, but further work is necessary to confirm the location of the porosity that is not visually observed.

References: [1] Consolmagno G. J. et al. 2008. *Chemie der Erde* 68:1–29. [2] Strait M. M. and Consolmagno G. J. 2002. *Meteoritics & Planetary Science* 37:A137. [3] Consolmagno G. J. et al. 2008. This issue. [4] Wilkison S. L. et al. 2003. *Meteoritics & Planetary Science* 38:1533–1546.

5201

TRANSMISSION ELECTRON MICROSCOPY OF IN SITU PRESOLAR SILICATES IN ALLAN HILLS 77307R. M. Stroud¹, A. N. Nguyen², C. M. O'D. Alexander², L. R. Nittler², and F. J. Stadermann³. ¹Code 6366, Naval Research Laboratory, Washington, D.C. 20375, USA. E-mail: rhonda.stroud@nrl.navy.mil. ²Department of Terrestrial Magnetism, Carnegie Institution of Washington, Washington, D.C. 20015, USA. ³Laboratory for Space Sciences, Washington University, St. Louis, MO 63130, USA.

Introduction: Presolar grains are dust grains that condensed in the outflows from stars that predate the Sun. They exhibit isotopic signatures that deviate so far from solar values that they can only be explained as the results of nucleosynthesis in stars. Silicates are the most abundant unequivocally presolar grain phase, with concentrations exceeding 100 ppm in some anhydrous interplanetary dust particles [1] and primitive meteorites, e.g., ALHA77307 [2, 3]. Previous coordinated secondary ion mass spectrometry (SIMS) and scanning Auger electron spectroscopy studies of ALHA77307 have identified over 100 individual presolar silicate grains, with a wide range of compositions, e.g., Fe-rich, Ca-Al-rich, pure SiO₂ [2]. In order to better understand the structure and composition of the silicate grains, and the relationship to the surrounding matrix material, we have begun focused ion beam-enabled in situ transmission electron microscopy studies.

Methods: The presolar silicate grains were identified in a thin section of ALHA77307 using the Carnegie NanoSIMS 50L. Elemental maps of the grains and surrounding areas were obtained with the PHI 700 Auger Spectrometer at Washington University. Details of these measurements were reported previously [2]. Sections of two of the grains were extracted in situ using focused ion beam (FIB) lift-out with the FEI Nova 600 FIB-SEM at the Naval Research Laboratory (NRL). Structural and elemental analysis of the section was performed using the NRL JEOL 2200FS transmission electron microscope (TEM).

Results and Discussion: Grain 166a has an oxygen isotope composition of $\delta^{17}\text{O} +680\%$ and $\delta^{18}\text{O} -220\%$. Auger measurements suggest that it is an ~700 nm silicate with a Ca-Al-rich core and a Mg-rich rim. From cross-sectional scanning TEM-based energy dispersive spectrometry mapping, it is apparent that the Mg-rich material is adjacent to but does not surround the Ca-Al-rich grain. Variation of the Si, Ca, and Al intensity inside the grain suggests that it is either an inhomogeneous glass or a polycrystalline aggregate. The lack of metal and sulfides rules out the possibility of a GEMS identity. Diffraction analysis and high-resolution TEM of the grain is planned, pending further FIB thinning of the section. Grain 65a has an oxygen isotope composition of $\delta^{17}\text{O} +1225\%$ and $\delta^{18}\text{O} +385\%$. The Auger composition measurements show it to be a Ca-rich silicate surrounded by Fe-rich silicates. Cross-sectional STEM analysis revealed that despite the ~600 nm grain diameter at the surface, the grain extended only ~20 nm below the section surface after SIMS measurements. The TEM data from these two grains underscores the complexity of presolar grain microstructures and the potential pitfalls of extrapolating to 3-D from surface imaging.

References: [1] Floss C. et al. 2006. *Geochimica et Cosmochimica Acta* 70:2371–2399. [2] Nguyen A. N. et al. Abstract #2142. 39th LPSC. [3] Nguyen A. N. et al. 2007. *The Astrophysical Journal* 656:1223–1240.

5029

SODIUM-METASOMATISM IN CAIs AND MATRIX IN THE NINGQIANG CARBONACEOUS CHONDRITE

M. Sugita and K. Tomeoka. Department of Earth and Planetary Sciences, Faculty of Science, Kobe University, Nada, Kobe 657-8501, Japan. E-mail: 026d860n@stu.kobe-u.ac.jp.

Introduction: Ningqiang has been described as an anomalous CV3 chondrite containing low abundances of CAIs (~1.0 vol%) and refractory lithophile elements [1]. In order to find a clue to the anomalous characteristics and possibly unique formation history of Ningqiang, we performed a detailed mineralogical and petrological investigation of this meteorite. We found evidence suggesting that Ningqiang has gone through a significant degree of Na metasomatism.

Results: *CAIs:* We found 64 inclusions in the four thin sections (~820 mm² total area) that range in size from 80–1250 μm. The modal abundance of the CAIs is ~0.9 vol%, which is much lower than the mean (5.1 vol%) for the CV3 chondrites. The CAIs include coarse-grained melilite-rich type (28%), fine-grained melilite-spinel-rich type (25%), and fine-grained spinel-pyroxene-rich type (34%). 33 (52%) of the CAIs contain various amounts of Na-rich nepheline, which commonly occurs as porous aggregates of fine grains. Nepheline has been mainly formed by replacing melilite. We found three relatively large inclusions (190–510 μm in size) consisting entirely of fine-grained melilite, spinel, and nepheline. In addition, numerous smaller inclusions (<80 μm), most of which contain nepheline, are scattered in the matrix.

Matrix: The matrix consists mainly of fine grains of Fe-rich olivine, resembling the CV3 matrices. However, it has unusual characteristics. The matrix consists of an intermixture of two distinct regions (10–100 μm in size): one consists mainly of fine grains (<1 μm in size) of relatively Fe-poor olivine (Fa₅₀), and the other consists mainly of coarser grains (2–20 μm) of relatively Fe-rich olivine (Fa₅₃). In the former Fe-poor regions, fine-grained nepheline occurs pervasively, whereas in the latter Fe-rich regions, nepheline is rare but fine-grained Fe sulfide and magnetite occur abundantly. The bulk composition of the matrix is similar to that of CV3 matrix for most elements except that Na and Al are significantly higher (3.2 and 1.7 by factor, respectively).

Discussion: A major fraction of the CAIs has experienced various degrees of nephelinization. We suggest that the nephelinization occurred under a hydrothermal condition on the meteorite parent body [2]. In that process, CAIs became fine-grained and porous, and during brecciation, they were disaggregated and mixed into matrix.

We interpret that the matrix of Ningqiang formed by mixing of materials derived from two different reservoirs in the meteorite parent body. In the Fe-poor reservoir, nephelinization occurred, whereas in the Fe-rich reservoir, nephelinization did not occur but concentration of Fe sulfide and magnetite occurred. The nepheline in the CAIs presumably formed in the Fe-poor reservoir. These imply that the Ningqiang parent body has undergone a heterogeneous distribution of its alteration condition and intermixing of the materials from different locations.

References: [1] Rubin A. E. et al. 1988. *Meteoritics* 23:13–23. [2] Tomeoka K. and Itoh D. 2004. *Meteoritics & Planetary Science* 39:1359–1373.

5070

AN IGNEOUS CLAST WITH BOTH GRAPHITE-BEARING AND GRAPHITE-FREE LITHOLOGIES IN THE NORTHWEST AFRICA 801 CR2 CHONDRITE

N. Sugiura¹, S. Takehana¹, H. Hiyagon¹, and N. T. Kita². ¹Department Earth Planet. Sci., University of Tokyo, Japan. E-mail: sugiura@eps.s.u-tokyo.ac.jp. ²University of Wisconsin–Madison, USA.

Introduction: Clasts of igneous texture containing graphite laths were found on two polished sections (#2 and #6) of NWA 801. Such achondritic material is rare. We intend to find out if it is related to ureilites. The electron microscopic observation and the REE abundances are reported here.

Results: One clast (on #2) is about 3 × 1.5 mm and another (on #6) is 1 × 0.7 mm in size, respectively. The latter is texturally homogeneous and contains graphite (up to 25 μm long). The former consists of two lithologies: graphite-bearing and graphite-free lithologies. The graphite-free lithology (GFL) occupies the central part of the clast and the graphite-bearing lithology (GBL) is found at both ends of the clast. Mineralogy of GBL on both polished sections is similar, suggesting that they are different sections of one clast. Therefore, the following description is mainly based on the observation of the clast on the polished section #2.

GBL mainly consists of olivine with minor amounts of Ca-poor pyroxene (Mg#~24) and Ca (Na, Cr)-rich pyroxene. Trace amounts of phosphate, sulfide, metal, and graphite are present. GFL mainly consists of olivine with minor amounts of Ca (Na,Cr)-rich pyroxene and potassium-rich devitrified mesostasis. Trace amounts of phosphate, sulfide, and metal are present. The olivine compositions in both lithologies are similar (Fa~32), suggesting equilibration after these lithologies were put together. In contrast to ureilites, reduction of olivine rim is not observed. A typical grain size of olivine in GBL is ~20 μm. It is slightly larger in GFL. It is to be noted that the grain sizes of graphite and olivine in the clast are much smaller than those in ureilites.

REE abundance patterns in phosphates in both lithologies are similar and LREE-enriched (~100 × CI at La). Based on the modal abundances of phosphates, the bulk REE abundances in both lithologies were estimated to be <0.1 × CI at La. (Ca-rich pyroxene does not contribute significantly to the bulk REE abundance.) In contrast to REE, incompatible elements like potassium and phosphorous are considerably enriched in GFL. They are not particularly enriched in GBL.

Discussion: LREE-enriched patterns confirm igneous origin of the clast. However, the absolute abundances of REE lower than those in CI suggest its complicated igneous history. Abundances of incompatible trace elements (K and P) suggest that GFL and GBL were igneously fractionated from each other. The graphite-bearing lithology which is not enriched in incompatible trace elements, may, similar to ureilites, represent mantle of a parent body.

The high Fa number suggests that smelting did not occur extensively in the GBL. However, the presence of GFL testifies to extensive loss of graphite by smelting, if both GFL and GFL were derived from the same source material. Fully self-consistent history of this achondritic material is yet to be constructed.

5035

ORGANIC AND MINERAL TRANSFORMATIONS DURING EXPERIMENTAL AQUEOUS ALTERATION OF CARBONACEOUS CHONDRITE NINGQIANG

A. Suzuki¹, Y. Yamamoto², S. Nakashima¹, and T. Nakamura³. ¹Department of Earth and Space Science, Faculty of Science, Osaka University, Machikaneyama, Toyonaka, Osaka 560-0043, Japan. E-mail: akiko.s@ess.sci.osaka-u.ac.jp. ²Environmental Science Center, University of Tokyo, Hongo, Bunkyo-ku, Tokyo 113-0033, Japan. ³Department of Earth and Planetary Science, Faculty of Science, Kyushu University, Hakozaki, Fukuoka 812-8581, Japan.

Introduction: Carbonaceous materials in primitive meteorites have been generally influenced by aqueous alteration. The organics have been suggested to be closely associated with clay minerals, which were produced by aqueous alteration [1]. Therefore, in this study, we investigate the transformation of carbonaceous materials in an anhydrous carbonaceous chondrite during experimental hydrothermal reactions and compare the results to naturally altered carbonaceous chondrites such as Murchison and so on.

Materials and Method: The starting material, Ningqiang, is classified to CV3- [2, 3] or CK3-anomalous [e.g., 4] type. This chondrite consists entirely of anhydrous minerals and it has been suggested that it had not experienced extensive aqueous alteration in its parent body. We prepared bulk Ningqiang powders (μm in size) weighing 600 mg and 50 g neutral liquid water. Samples were loaded into a gold tube and were kept at 200 °C in an autoclave for reacting with water vapor. After 0.5, 1, 2, 5, 10, and 20 days, 100 mg of the sample was recovered and the rest of the sample was kept soaked [see details in 5]. Natural and altered samples were analyzed by infrared (IR) and Raman spectroscopy for characterizing carbonaceous materials and mineral phases.

Results and Discussion: IR spectra of all natural and experimentally altered samples showed the peaks of Si-O at 880 and 1010 cm^{-1} , OH at 3400 and 3250 cm^{-1} , and aliphatic hydrocarbon at 2960 and 2925 cm^{-1} . Peak heights of both CH_2 and CH_3 increased first from 0 to 0.5 days, then decreased from 0.5 to 10 days and increased again from 10 to 20 days. During 20 days hydrothermal alteration, the first Si-O peak at 880 cm^{-1} decreased but the second Si-O peak at 1010 cm^{-1} increased. The OH peak heights became higher in samples of 10 and 20 days alteration. These IR results clearly indicate that the transformation of anhydrous minerals to hydrous phyllosilicates took place in association with some modification of aliphatic organic moieties.

Raman spectra of all natural and experimentally altered samples indicate the presence of D and G bands of carbonaceous materials. For the 20 days hydrothermal treatment, the G band position shifted to the lower wavenumber region and its FWHM became wider, indicating that the maturity of graphitic materials decreased during hydrothermal alteration. With increasing degree of experimental aqueous alteration, the maturation degree of carbonaceous materials is lowered. This confirms the tendency observed in carbonaceous materials in carbonaceous chondrites that experienced alteration in space.

References: [1] Pearson V. K. et al. 2002. *Meteoritics & Planetary Science* 37:1829–1833. [2] Rubin A. E. et al. 1988. *Meteoritics* 23:13–23. [3] Koeberl C. et al. 1987. 18th LPSC. pp. 499–500. [4] Kallemeyn G. W. 1996. 27th LPSC. pp. 635–636. [5] Yamamoto Y. et al. 2008. *Meteoritics & Planetary Science* 43. This issue.

5045

⁴⁰Ar-³⁹Ar STUDIES OF HEAVILY SHOCKED YAMATO CHONDRITES

T. D. Swindle¹ and M. Kimura². ¹Lunar and Planetary Laboratory, The University of Arizona, Tucson, AZ, USA. E-mail: tswindle@u.arizona.edu. ²Faculty of Science, Ibaraki University, Mito, Japan.

We have begun a ⁴⁰Ar-³⁹Ar study of heavily shocked Yamato chondrites, both to build the data base on the chronology of impact events in the Main Asteroid Belt and to better understand the histories of these specific meteorites. Here we report on a study of Yamato-75100 (Y-75100), a heavily shocked (S6) H6 with shock veins containing a variety of high-pressure minerals, including Ca-rich majorite [1]. We have analyzed four samples of the host chondrite and two samples of vein materials.

All of the samples exhibit low apparent ages at low extraction temperatures (as low as 1500–2000 Ma), with apparent age increasing with increasing extraction temperature. Five of the six samples exhibit what resembles a plateau at intermediate temperatures, followed by lower apparent ages (presumably the result of recoil during irradiation) at the highest temperatures. If most or all of these gave the same answer, one would think that answer would be the age of some major event in the meteorite's history, but they do not. Actually, the two vein samples agree at about 4420 Ma, and three of the four host samples agree at about 4300 Ma (the fourth doesn't have anything that qualifies as a plateau). However, those two numbers disagree with each other, and the samples all come from the same meteorite. Our interpretation is:

- There was a thermal event, probably a shock, no earlier than ~1500–2000 Ma ago (the lowest apparent ages) that caused partial resetting of the K-Ar system in this meteorite. If it was the vein-forming event, the rapid cooling of the vein [1] must have prevented total resetting.
- The most recent event before that was probably no more recent than 4420 Ma (the plateau age in the veins), and could have been earlier. This could be the formation or metamorphism on the parent body. Alternatively, if this was the shock event that produced the veins, it must have happened during the accretionary phase of the Solar System. Although most chondritic impact melts record more recent events, there are a few others that survive from the accretionary era. The H chondrites Portales Valley [2] and Ourique [3] record impacts from this era, as do a few L chondrites, including Sahara 98222 [4].
- In the most recent event, the host material lost slightly more Ar than the veins did. This seems to be in contrast with the chemistry results of [5], which suggested that if there was any difference, the veins might be depleted in the most thermally labile elements. However, if the most recent event that affected the Ar was not the shock that created the veins [6], the more recent event might not have been strong enough to cause much loss of Zn or Ag anywhere, but there could have been more loss of those in the vein during the vein-producing shock event.

References: [1] Tomioka N. and Kimura M. 2003. *Earth and Planetary Science Letters* 208:271–278. [2] Garrison D. H. and Bogard D. D. 2001. Abstract #1137. 32nd LPSC. [3] Kring D. A. et al. 2000. Abstract #1688. 31st LPSC. [4] Ozawa S. et al. 2008. *Meteoritics & Planetary Science* 43. This issue. [5] Friedrich J. M. et al. 2007. *Meteoritics & Planetary Science* 42: A52. [6] Kunz J. et al. 1997. *Meteoritics & Planetary Science* 32:647–670.

5270

NON-EQUILIBRIUM CONDENSATION IN THE Mg-Si-O SYSTEM: AN EXPERIMENTAL STUDY

S. Tachibana, H. Nagahara, K. Ozawa, and S. Tamada. Department of Earth and Planetary Science, University of Tokyo, 7-3-1 Hongo, Tokyo 113-0033, Japan. E-mail: tachi@eps.s.u-tokyo.ac.jp.

Introduction: Magnesian silicates are major constituents of dust particles in protoplanetary disks and circumstellar environments. Their sizes, shapes, compositions, and the crystalline/amorphous ratio reflect their formation histories, and thus understanding of formation processes of magnesian crystalline/amorphous silicates leads to estimation of physical and chemical conditions in dust-forming environments. Condensation of magnesian silicate dust particles is one of the most crucial processes for dust-formation, and several experimental studies have been done under plausible low-pressure conditions [e.g., 1, 2]. However, quantitative discussion on kinetic processes, such as dependences on partial pressures of condensing gas species and supersaturation ratio, was not made in previous studies due to experimental difficulties. In this study, we carried out condensation experiments in the Mg-Si-O system using infrared vacuum furnace, where partial pressures of condensing gas and supersaturation ratios could be estimated, and discuss non-equilibrium condensation behaviors of magnesian silicates.

Experiments: A single crystal of forsterite was heated at ~1850 K by focusing infrared lights from halogen lamps. Gaseous Mg, SiO, and O evaporated from forsterite were condensed on a substrate of molybdenum plate, put at various distances from forsterite to control condensation temperatures from 1145–480 °C. The total pressure in the silica glass vacuum chamber was ~10⁻⁵ Pa, and the experimental duration ranged from 24 to 72 hours. Condensates were observed with FE-SEM, and their chemical compositions and crystallinities were determined by EDS and EBSD.

Results and Discussion: Condensation did not occur at >1310 K, Si condensed as molybdenum silicide at ~1130 K, and amorphous magnesian silicates condensed at <840 K. Condensates in the present study are different from those formed in the Mg-Fe-Si-O system [1] and in the Mg-Si-O-H system at a total pressure of 1.4 Pa [2]. Very little condensates were found in [2] at the total pressure of 0.14 Pa and lower, which is consistent with the present study. Partial pressures of Mg and SiO above the molybdenum substrate were estimated to be much larger than equilibrium vapor pressures of forsterite, MgO, and SiO₂, indicating that such mineral phases could be condensed in the present experimental conditions. However, such phases, all of which require encounter of different gas species on the substrate for heterogeneous nucleation, did not condense in this study. SiO condensed as silicide probably due to reduction on the substrate, which required no other gas species. Amorphous magnesian silicates condensed at lower temperatures, which could be because condensation of relatively-volatile SiO was allowed with lowering temperatures, and Mg began to condense once amorphous SiO (or SiO₂) formed. These condensation behaviors could be due to smaller incoming fluxes of Mg, SiO, and O onto the substrate than those in previous studies with condensation of crystalline silicates. Condensation experiments under more-oxidizing conditions will also be reported at the meeting.

References: [1] Nagahara H. et al. 1988. *Nature* 331:516. [2] Tsuchiyama A. 1998. *Mineral J* 20:50–89.

5043

FINE-GRAINED CHONDRULE RIMS IN THE TAGISH LAKE CHONDRITE: EVIDENCE FOR PARENT-BODY PROCESSES

A. Takayama and K. Tomeoka. Department of Earth and Planetary Sciences, Faculty of Science, Kobe University, Nada, Kobe 657-8501, Japan. E-mail: akiko-13@stu.kobe-u.ac.jp.

Introduction: Most chondrules and coarse-grained aggregates in the Tagish Lake carbonaceous chondrite are surrounded by fine-grained rims [1, 2]. Previous workers [2] suggested that the rims in Tagish Lake were formed by accretion of dust in the solar nebula, and subsequently after accretion, they experienced aqueous alteration on the meteorite parent body. Here we present the results of our mineralogical and petrological study of fine-grained rims surrounding chondrules and coarse-grained aggregates in Tagish Lake.

Results and Discussion: We found 87 chondrules, 12 olivine-rich aggregates, and two CAIs in ~114 μm² area of two thin sections. These coarse-grained components are embedded in the matrix consisting mainly of phyllosilicates. 95% of the coarse-grained components are surrounded by fine-grained rims ranging in thickness from 2–220 μm. The rims consist mainly of phyllosilicates similar to those in the surrounding matrix but have a distinctly smoother appearance and slightly more Mg-poor compositions. ~50% of the rims exhibit a double-layer feature, consisting of Mg-rich/Fe-poor inner layer and Mg-poor/Fe-rich outer layer. Single-layered rims and the inner layers of the double-layered rims are similar in texture and mineralogy. ~80% of all the rims contain characteristic round-shaped phyllosilicate-rich objects, typically along the core-rim boundary, which are identical to the pseudomorphs in their interior chondrules. The rims commonly have radial cracks running from the core-rim boundary toward the rim-matrix boundary.

We found evidence suggesting that the chondrules with the rims have gone through a fragmentation process. The chondrules commonly partly lack rims. There are abundant clasts (90–480 μm in size) that resemble the chondrule rims in texture and mineralogy. Nine of the 55 clasts studied contain two to three chondrules, and their matrices have cracks emanating from the chondrule surfaces; the cracks resemble impact fractures observed in the matrix of the experimentally shocked Murchison CM chondrite [3]. These observations suggest that the individual chondrules with the rims are actually clasts that were produced during brecciation; the process is similar to that proposed for the chondrule rims in Vigarano [4].

We conclude that the single-layered rims and the inner layers of the double-layered rims were formed, at least partially, by replacing their interior chondrules during aqueous alteration on the parent body. Following fragmentation caused by shock impacts on the parent body, the chondrules with the rims were probably transported and then re-incorporated into the present host matrix. The outer layers of the double-layered rims, especially those with cracks, appear to be remnants of the interchondrule matrix of the material from the former location.

References: [1] Zolensky M. E. et al. 2002. *Meteoritics & Planetary Science* 37:737–761. [2] Greshake A. et al. 2005. *Meteoritics & Planetary Science* 40:1413–1431. [3] Tomeoka K. et al. 1999. *Geochimica et Cosmochimica Acta* 63:3683–3703. [4] Tomeoka K. and Tanimura I. 2000. *Geochimica et Cosmochimica Acta* 64:1971–1988.

5187

TWO OLIVINE-RICH UREILITES AMONG NINE NEW NORTHWEST AFRICA UREILITES AND THEIR PROPOSED ORIGIN

H. Takeda¹ and A. Yamaguchi². ¹Department of Earth and Planet. Sci., University of Tokyo, Hongo, Tokyo 113-0033, Japan. E-mail: takeda.hiroshi@it-chiba.ac.jp. (Chiba Inst. of Tech.). ²National Inst. of Polar Res., Tokyo 173-8515, Japan.

Introduction: Discoveries of Antarctic samples have almost tripled the number of known ureilites by 1991 [1]. Now more ureilites have been recovered from hot deserts, and 74 ureilites from Northwest Africa (NWA) were recorded among 241 total ureilite samples [2]. Augite (Aug)- or orthopyroxene (Opx)-bearing ureilites found first in Antarctica fall outside the original definition of ureilites [3]. We described nine ureilites from NWA, including an Opx-Aug ureilite, NWA 2236 with Mg-rich olivine [4], and two olivine-rich ureilites, NWA 4520 [2] and NWA 3222 [2]. We reexamine the formation mechanism of ureilites on the basis of these findings.

Samples: The PTSs of nine samples (NWA 2234, 2236, 3221, 3222, 3223, 4508, 4519, 4520, 4507) were studied by an optical microscope and EPMA at NIPR and Ocean Res. Inst. (ORI) of University of Tokyo.

Results: Brief descriptions of nine NWA ureilites are given in the Meteoritical Bulletin [2, 4, 5]. In this abstract, we report some features not known in other ureilites.

Chemical Variations of Minerals: The chemical trends of pyroxenes are within the known range of ureilites, except for NWA 2236 (Fo 97) with small Opx grains (Fs_{3.0}Wo_{4.8}) and diopside grains (Fs₂Wo₃₈). The variation of olivines in the NWA 3221 polymict ureilite (Fo74–90) cover the entire ranges of core compositions of the other ureilites (NWA 3222: Fo87–89; 4508: Fo83–86; 4519: Fo83–80; 4520: Fo79–82; 3223: Fo77–80).

Olivine-Rich Ureilites: NWA 4520 contains olivine only, observed in two PTSs made 2 cm apart. One PTS shows a typical ureilite texture with carbonaceous veins. A large part of the other PTS consists of large olivine crystals up to 3.2 × 2.7 mm in size, with thin grain boundaries essentially without opaque materials. Small olivine grains (0.2 × 0.1 mm) with carbonaceous veins are present around the large olivine part. NWA 3222 consists of angular fragments of olivine and poikilitically encloses small rounded to oval Opx (Fs_{11.2}Wo_{4.8}) and Aug (Fs₇Wo₃₇) grains.

Discussion: We proposed a model that ureilites are residues of disequilibrium partial melting of a carbon-rich CV-like body, and grain-coarsening at high temperatures. The NWA 4520 olivine ureilite is similar to magmatic inclusion found in DaG 319 [7], but the presence of a region with carbon veins in NWA 4520 suggests that grain-coarsening of olivine with little liquid is an important process for the formation of such ureilites.

References: [1] Takeda H. 1991. *Geochimica et Cosmochimica Acta* 55:35–47. [2] Connolly H. C. Jr. et al. 2007. The Meteoritical Bulletin, no. 92. *Meteoritics & Planetary Science* 42:1647–1694. [3] Takeda H. et al. 1989. *Meteoritics* 24:73–81. [4] Russell S. S. et al. 2004. The Meteoritical Bulletin, no. 88. *Meteoritics & Planetary Science* 39:A215–A272. [5] Connolly H. C. Jr. et al. 2007. The Meteoritical Bulletin, no. 91. *Meteoritics & Planetary Science* 42:413–466. [6] Ikeda Y. and Prinz M. 2001. *Meteoritics & Planetary Science* 36:481–499.

5080

CHONDRULES AND PHOTOPHORESIS—OLD FRIENDS MEET AGAIN!

J. Teiser¹, G. Wurm¹, H. Haack², A. Bischoff¹, and J. Roszjar¹. ¹Institute für Planetologie, University of Münster, Wilhelm-Klemm-Str. 10, D-48149 Münster, Germany. E-mail: j.teiser@uni-muenster.de. ²Geological Museum, Øster Voldgade 5-7, 1350 Copenhagen K, Denmark.

Introduction: Results from studies on cometary and meteoritical materials show that high temperature minerals and CAIs are not only found in the hot inner regions of the Solar System but also in regions where the temperatures are not expected to be high enough to form these constituents. To explain these observations photophoresis has been proposed [1, 2]. Photophoresis is also important for chondrules which might be transported and size sorted by the effect [1].

Experimental Aspects: To verify and quantify photophoretic transport models, we performed microgravity experiments at the drop tower in Bremen and measured the photophoretic force on chondrules, dustmantled chondrules and dust agglomerates. We used chondrules from the meteorite Bjurböle with sizes from ~0.3 mm to ~2.5 mm. The chondrules were released to be free floating in a vacuum chamber at low pressure and then illuminated with a light beam of a focused halogen lamp reaching an intensity of 25 kW/m². The chondrules were observed by two video cameras aligned perpendicular to each other and perpendicular to the light beam. For calibration and to neglect thermophoresis due to temperature gradients within the vacuum chamber, we performed the same measurements with steel and glass spheres.

Preliminary Results: For mm-size, cleaned chondrules (without matrix material attached) the photophoretic acceleration is about 10⁻³ m/s² at ~10 Pa gas pressure and ~25 kW/m² irradiance. For chondrules mantled with dust, the linear acceleration is about one order of magnitude larger than for cleaned chondrules. In this work not only the linear acceleration was determined, but (weg) also the influence of photophoresis on the rotation of the particles could be studied. Due to deviations from the perfect spherical shape an analogue effect to the YORP effect (Yarkowski-O'Keefe-Radzievskii-Paddack) could also be observed. Exposed to the light the rotation of the chondrules changed and at least some chondrules were spinning up.

Conclusions: Photophoresis is one of the most important forces in the solar nebula. Although it is important, its influence on chondrules has not been studied until now. We present the first measurements of the photophoretic force on chondrules. Rotation is not a general obstacle to photophoresis as has been argued before but rotation will be determined by photophoresis. In further studies we will carry out a more detailed analysis of the data and supposedly correlate the results to the influence of mineralogical composition for different chondrules.

References: [1] Wurm G. and Krauss O. 2006. *Icarus* 180:487–495. [2] Krauss O., Wurm G., Mousis O., Petit J.-M., Horner J., and Alibert Y. 2007. *Astronomy and Astrophysics* 462:977–987.

5199

CHRONOLOGY OF LUNAR BASALTIC METEORITES BASED ON THE IN SITU U-Pb DATING

K. Terada¹, H. Hidaka¹, and Y. Sano². ¹Department of Earth and Planetary Systems Science, Hiroshima University, Higashi-Hiroshima 739-8526, Japan. E-mail: terada@sci.hiroshima-u.ac.jp. ²Center for Advanced Marine Research, Ocean Research Institute, The University of Tokyo, Nakano-ku 164-8639, Japan.

Introduction: Recent discoveries of lunar meteorites in the hot deserts and Antarctic ice field have provided great impetus to lunar science. These meteorites provide potentially new insights into the petrologic history of unexplored regions of the Moon. Although chronological studies of lunar meteorites had been difficult because of their complex textures, recent in situ U-Pb dating method has been successfully applied to brecciated meteorites and has enabled us to unravel the lunar evolution [1–7].

Results and Discussion: In spite that the basaltic meteorites are possibly derived from unexplored regions of the Moon, crystallization ages obtained from the most of basaltic meteorites indicate the later magmatic activity, spanning from 3.9 to 2.9 Ga, similar to those of the Apollo and Luna collection [8]. These results are also consistent with activity of “visible” mare basalts on the Moon inferred from the “relative chronology” based on recent remote-sensing studies [9], leading to the previously proposed hypothesis that mare volcanism occurred mainly after the late heavy bombardment that ended at ~3.9 Ga. However, each age distribution of low-Ti and very-low-Ti (VLT) basalts in lunar meteorites is quite different from those of collected samples [10].

One remarkable exception, Kalahari 009 shows the oldest age of 4.35 Ga [6] and the shortest exposure age of 220 yr [11], concluding that VLT-type cryptomaria had been formed prior to the late heavy bombardment, as inferred from the remote-sensing data of excavated mare basalts on the Moon [12–14]. The ancient age and geochemical features [15] of Kalahari 009 appear compatible with the “active” mechanism model, and maybe a manifestation of a pre-Imbrium basin-forming event on the Moon [6].

References: [1] Anand M. et al. 2003. *Geochimica et Cosmochimica Acta* 67:3499–3518. [2] Terada K. et al. 2005. *Geophysical Research Letters* 32, doi:10.1029/2005GL023909. [3] Anand M. et al. 2006. *Geochimica et Cosmochimica Acta* 70:246–264. [4] Terada K. et al. 2006. Abstract #5129. *Meteoritics & Planetary Science* 41:A173. [5] Terada K. et al. 2007. *Earth and Planetary Science Letters* 77–84. [6] Terada K. et al. 2007. *Nature* 450: 849–852. [7] Terada K. et al. Forthcoming. *Earth and Planetary Science Letters*. [8] Nyquist L. E. et al. 2001. In *The century of space science*. pp. 1325–1376. [9] Heisinger H. et al. 2008. Abstract #1269. 39th LPSC. [10] Terada K. et al. 2008. Abstract #1681. 39th LPSC. [11] Nishiizumi et al. 2005. Abstract #5270. *Meteoritics & Planetary Science* 40:A113. [12] Giguere T. A. et al. 2003. *Journal of Geological Research* 108:4.1–4.14. [13] Hawke B. R. et al. 2005. *Journal of Geological Research* 110, doi:10.1029/2004JE002383. [14] Hawke B. R. et al. 2005. Abstract #1642. 36th LPSC. [15] Schulz et al. 2007. Abstract #5151. *Meteoritics & Planetary Science* 42: A137.

5218

IRON ISOTOPE COMPOSITION OF ZONED CARBONATES FROM ALH 84001

K. J. Theis, I. Lyon, R. Burgess, and G. Turner. School of Earth, Atmospheric, and Environmental Sciences, University of Manchester, Manchester M13 9PL, UK. E-mail: karen.j.theis@postgrad.manchester.ac.uk.

Introduction: ALH 84001, the ~4 Ga coarse grained Martian orthopyroxene meteorite, contains an inner crushed zone with zoned carbonate rosettes [1, 2]. These carbonates formed during the early “wet and warm” period of Mars by secondary fluid processes. Some authors have suggested high-temperature hydrothermal precipitation and others have supported a low-temperature formation. The aim of this study is to constrain the temperature of formation by analyzing the iron isotope composition relative to bulk Martian silicates [3].

Sample Preparation: The zoned carbonates were gently scraped from the surface of an internal, pristine fragment of ALH 84001,287 using a tungsten carbide microdrill bit. The carbonate was then dissolved in 2% HNO₃ acid for 1 hour before being filtered ready for analysis.

Mass Spectrometry: Analysis was carried out on the Nu Instruments multicollector inductively coupled plasma mass spectrometer operated in pseudo-high-resolution using the standard/sample bracketing method relative to the IRMM014 iron isotope standard. Measurements were taken on the iron “shoulder” [4] for high precision.

Matrix Effects: The sample was not purified by anion chromatography prior to analysis to reduce the risk of fractionation occurring in the chromatographic column. Instead, matrix-matching was used whereby the Ca and Mg of the sample were accurately measured and the standard spiked accordingly. There was no matrix effect on the iron isotope composition and the precision was the same as a pure Fe solution ($\delta^{56}\text{Fe} \pm 0.02\%$ at 2σ).

Results: The chemical composition of the sample was determined to be Mg 34%, Ca 30%, and Fe 36%, which is similar to compositions reported in previous studies [5, 6] for the “rosettes.” The iron isotope composition relative to IRMM014 is $\delta^{56}\text{Fe} = -0.62 \pm 0.11\%$ and $\delta^{57}\text{Fe} = -0.83 \pm 0.15\%$.

Discussion: By plotting the reduced partition coefficients for silicate-carbonate fractionation, based on the data in [7], then the isotopic fractionation between the bulk Martian silicate and the carbonates ($\Delta^{56}\text{Fe} = 0.6\%$) can be used to determine a temperature of carbonate precipitation. Assuming that the carbonates were derived from the same iron reservoir as the silicates then this work supports a low temperature formation at around $-10 \text{ }^\circ\text{C} \pm 30 \text{ }^\circ\text{C}$.

Acknowledgements: STFC for funding for KJT, NASA for provision of sample, The University of Manchester for SRIF funding for MC-ICP-MS. Thanks also to D. Blagburn, C. Davies, B. Clementson, and H. Williams for their technical advice and help.

References: [1] Mittlefehldt D. W. 1994. *Meteoritics & Planetary Science* 29:214–221. [2] Harvey R. P. and McSween H. Y. Jr. 1996. *Nature* 382:49–51. [3] Poitrasson F. et al. 2004. *Earth and Planetary Science Letters* 223:253–266. [4] Weyer S. and Schwieters J. B. 2003. *International Journal of Mass Spectrometry* 226:355–368. [5] Saxton J. M. et al. 1998. *Earth and Planetary Science Letters* 160:811–822. [6] Holland G. et al. 2005. *Geochimica et Cosmochimica Acta* 69:1359–1369. [7] Polyakov V. B. and Mineev S. D. 2000. *Geochimica et Cosmochimica Acta* 64:849–865.

5212

REASSESSMENT OF THE “LIFE ON MARS” HYPOTHESIS

K. L. Thomas-Keptra¹, S. J. Clemett¹, D. S. McKay², E. K. Gibson², S. J. Wentworth¹, and FEI Corporation³. ¹ESCG-NASA, Houston, TX USA. ²NASA-Johnson Space Center, USA. ³FEI Company, Hillsboro, OR, USA.

Introduction: The Mars meteorite ALH 84001 is a sample of the ancient Martian surface with a crystallization age of 4.5 Ga. Internal cracks and fissures within this meteorite preserve evidence of early Martian hydrothermal activity in the form of carbonate-magnetite assemblages, with disk-like appearance, that are dated at 3.9 Ga. The mechanism(s) by which these carbonate disks formed, and in particular the origin of the embedded nanocrystal magnetites, has been a subject of considerable debate ever since the suggestion that biological processes could, in part, be responsible [1]. Subsequently, a number of alternative purely “inorganic mechanisms” have been advocated which all invoke the partial thermal decomposition of sideritic carbonate ($3\text{FeCO}_3 \rightleftharpoons \text{Fe}_3\text{O}_4 + 2\text{CO}_2 + \text{CO}$) as the origin of the nanophase magnetite. The primary difference between these “inorganic mechanisms” lies in the time scale of the decomposition event, ranging from a gradual thermal pulse (“slow bake”), in the Martian subsurface [2] to the nearly instantaneous heating and rapid radiative cooling (“fast bake”), associated with the ejection of the meteorite from the Martian regolith [3].

Results and Discussion: We have investigated the viability of these “inorganic mechanisms” through a combination of experimental and theoretical modeling studies, in concert with new TEM observations of ALH 84001 carbonate extracted in situ using focused ion-beam techniques. In our experimental studies, samples of the natural carbonate Roxbury siderite, which is compositionally similar to the most Fe-rich component of the ALH 84001 carbonate disks, were subject to thermally decomposed over a range of heating regimes. Detailed TEM characterization of samples before and after heating demonstrated that irrespective of the heating rates, which differing by over ten orders of magnitude, the product of thermal decomposition always was always a mixed [Mg,Mn]-ferrite. These findings, which are supported by both kinetic thermodynamic equilibrium modeling studies, are not similar to the chemically pure magnetites characteristic of ALH 84001 carbonate. TEM/EDX analysis of the FIB extracted thin sections has provided the most comprehensive description of ALH 84001 carbonates to date. Our new observations indicate that at least a significant fraction of magnetites in ALH 84001 carbonate, by virtue of either composition or spatial location within the carbonate disk could not be the product of thermal decomposition. These include the presence of chemically pure magnetites embedded in carbonate containing little to no detectable iron and impure magnetites with minor amount of Cr, an element which is unable to substitute into the trigonal (R-3c) carbonate structure. Perhaps the most interesting finding, enabled by the ability to examine large area thin sections of carbonate in which both spatial and structural integrity have been maintained, is the presence of textural and chemical evidence for episodic exposure of the ALH 84001 carbonate disks to fluids after formation. Based on our results we argue that a thermal decomposition model for the origin of magnetites in ALH 84001 is incorrect.

References: [1] McKay et al. 1996. *Science* 273:924–930. [2] Treiman. 2003. *Astrobiology* 3:369. [3] Brearley. 1998. Abstract #1451. 29th LPSC.

5039

INDICATORS OF MULTIPLE PARENT-BODY PROCESSES: CHONDRULES AND FINE-GRAINED RIMS IN THE MOKOIA CV3 CHONDRITE

K. Tomeoka and I. Ohnishi. Department of Earth and Planetary Sciences, Faculty of Science, Kobe University, Nada, Kobe 657-8501, Japan. E-mail: tomeoka@kobe-u.ac.jp.

Introduction: Fine-grained rims surrounding chondrules in chondrites are widely believed to have formed by direct accretion of dust onto the surfaces of chondrules in the solar nebula [e.g., 1, 2]. However, some authors suggested that they were formed by parent-body processes [e.g., 3]. Here we present the results of our mineralogical and petrological investigation of chondrules and fine-grained rims in the Mokoia CV3 chondrite. Mokoia is one of the rare CV3 chondrites that contain abundant hydrous phyllosilicates [4].

Results: We studied a total of 112 chondrules >400 μm in diameter, in $\sim 272 \text{ mm}^2$ area of six thin sections, of which 86 (77%) were enclosed by fine-grained rims. 63 of the rims (73%) consist mainly of olivine and phyllosilicates, and the remainder 23 (27%) consist mainly of olivine. In this paper, we focus on the former type of rims.

All the chondrules contain <5–30 vol% of phyllosilicates, which are mostly saponite and minor amounts of phlogopite. Saponite has been formed by replacing enstatite, and phlogopite has been formed by replacing anorthite. Olivine and diopside remain unaltered. The degree of alteration differs in a wide range among the chondrules. In some chondrules, phyllosilicates constitute $80 \times 60 \mu\text{m}$ in area.

The rims range in thickness from 20–300 μm , and most of them partly enclose their interior chondrules. The rims consist mainly of fine grains of olivine (<1–10 μm in size) and saponite, resembling the host matrix except that the rims contain higher amounts of saponite. The relative volume proportion of olivine and saponite differs in a wide range among the rims, and has a tendency to decrease with the increasing degree of alteration within the interior chondrule. The rims commonly have a characteristic vein-like feature, consisting of Fe-rich olivine, magnetite, and Fe-Ni sulfide. The veins emanate from the chondrule/rim interface and terminate at the rim/matrix interface.

Discussion: Both the chondrules with and without rims show abundant evidence of extensive aqueous alteration. In contrast, the matrix surrounding them largely remains unaltered [4]. These observations suggest that the chondrules with and without rims have not experienced aqueous alteration in the present setting. We suggest that they are actually clasts transported from a precursor material during brecciation on the meteorite parent body, and the rims are fragmented remnants of an interchondrule matrix of the precursor material. The precursor material was probably located in a more extensively aqueously altered portion than the location where the present meteorite was. These observations and interpretations are consistent with the results reported from the study of the chondrules and their rims in the Vigarano CV3 chondrite [3].

References: [1] Metzler K. et al. 1992. *Geochimica et Cosmochimica Acta* 56:2873–2897. [2] Hua X. et al. 1996. *Geochimica et Cosmochimica Acta* 60:4265–4274. [3] Tomeoka K. and Tanimura I. 2000. *Geochimica et Cosmochimica Acta* 64:1971–1988. [4] Tomeoka K. and Buseck P. R. 1990. *Geochimica et Cosmochimica Acta* 54:1745–1754.

5048

OXIDATION OF SYNTHETIC AND METEORITIC Fe-RICH OLIVINE BY HEATING IN AIR

N. Tomioka^{1,2}, A. Morlok^{1,3}, C. Koike⁴, and M. M. Grady⁵. ¹Department of Earth and Planetary Sciences, Kobe University, Japan. ²PML, ISEI, Okayama University, Japan. E-mail: nao@misasa.okayama-u.ac.jp. ³CRPG-CNRS, France. ⁴Department of Earth and Space Sciences, Osaka University, Japan. ⁵PSSRI, The Open University, UK.

In situ mid-infrared transmission measurements of matrices from the Vigarano and Ningqiang carbonaceous CV chondrites heated up to 572 °C in air were conducted by a FTIR spectroscopy. The FTIR spectra of the matrices mainly showed olivine features. With increasing temperature, the spectra did not show significant spectral changes except band shift to higher wavelength up to 477 °C. However, at 572 °C, the spectra showed a splitting of ~11 micron band and the relative intensity of ~10 micron to ~11 micron largely increased. We also examined recovered samples of synthetic Fe-rich olivine (Fo₄₇) heated at 600 °C in air. The mid-infrared spectra of the olivine showed similar spectral changes to those of meteoritic samples.

In TEM observation, Vigarano and Ningqiang samples after cooling are mainly consists of olivine and pyroxene and lesser amount of Si-rich glass, kamacite, and hematite. Selected area electron diffraction (SAED) patterns of a part of olivine grains in both samples showed streaking along c^*_{ol} axis suggesting stacking disorder on (001) plane. SAED patterns of some olivine grains in Ningqiang showed diffraction spots correspond to those of magnetite. The interlayered olivine and magnetite exhibited the following crystallographic orientation: (100)_{ol}//(111)_{mg} and (001)_{ol}//(101)_{mg}. Many of grains in Vigarano and Ningqiang showed diffraction patterns different from the interlayered olivine and magnetite. The SAED pattern of the grains showed extra spots along c^*_{ol} direction in addition to streaking along c^*_{ol} . These extra spots correspond to a superstructure of three-fold periodicity along c_{ol} . This superstructure is known as laihunite-3M which has an olivine structure with a composition of Fe²⁺_{2-3x}Fe³⁺_{2x}SiO₄ [1, 2].

The synthetic Fe-rich olivine before heating does not have any defect structures. However, heated Fe-rich olivine commonly has stacking disorder and laihunite lamellae on (001)_{ol} as well as olivine in heated Ningqiang. Therefore, the changes in mid-infrared spectra of the matrices of Vigarano and Ningqiang would not have been caused by chemical reactions among their constituent minerals or partial melting, but would mainly caused by oxidation of iron in olivine. These FTIR features could be reference data for search for laihunite on the Martian surface and in partially oxidized meteorites or asteroidal surfaces.

References: [1] Kiramura M. et al. 1984. *American Mineralogist* 69: 154–160. [2] Shen B. et al. 1986. *American Mineralogist* 71:1455–1460.

5286

STUDYING THE OXYGEN AND CARBON ISOTOPE CHARACTERISTICS OF CARBONATE ANALOGUES TO ALH 84001

T. Tomkinson, J. Wade, H. Busemann, I. A. Franchi, A. Hagermann, I. P. Wright, S. Wolters, and M. M. Grady. PSSRI, The Open University, Walton Hall, Milton Keynes MK7 6AA, UK. E-mail: t.o.r.tomkinson@open.ac.uk.

Introduction: Martian meteorites provide an insight into the lithosphere, atmosphere, and, potentially, the hydrosphere of Mars. It is hence important that these samples are studied to help us determine the environment in which they were produced. Water reacts with soluble salts on Mars; temperature changes then allow precipitation of evaporites such as anhydrite, gypsum, and carbonates. Primary silicates are also altered, by hydration, eventually leading to formation of hydroxides and clay minerals. Owing to the igneous origins of the meteorites, formation of secondary alteration products is particularly intriguing because of their fluvial origins. Carbonates are an important part of Martian meteorite studies with their potential insights into Martian atmospheric and crustal interactions [1] and the possibility of associated organic molecules [2]. In particular, the meteorite ALH 84001, which as well as having the highest abundance of carbonates in any Martian meteorite (~1%) [3], was reported as containing fossilized Martian bacteria [4].

We intend to investigate the paragenesis of carbonates on Mars through synthesis of carbonates under a range of environmental conditions appropriate for the surface of Mars (low temperature, low pressure CO₂ atmosphere, very low water/rock ratio, etc). Carbonate “rosettes” analogous to those observed in ALH 84001 have been produced [5, 6]; we will follow this technique for precipitating carbonates, and then characterize zoning in the carbonates by XRD, SEM, and Cameca NanoSIMS 50L. The $\delta^{13}\text{C}$ values of carbonates in Martian meteorites are ¹³C-enriched and variable (+27 to +64‰) compared with terrestrial formations [1]. The $\delta^{13}\text{C}$ values from synthesized complex analogue carbonates have not yet been measured. The $\delta^{18}\text{O}$ isotopic composition of ALH 84001 carbonates also has a large variation (~21‰), from $\delta^{18}\text{O} \sim +22\%$ Mg-rich rims to isolated ankerite $\delta^{18}\text{O} \sim +1\%$ [8]. This range in $\delta^{18}\text{O}$ values requires significant change in composition and/or fluid temperature during formation. By synthesizing carbonates under a range of potential Martian environments, it should be possible to determine the most favorable formation conditions and help explain the ~37‰ and ~21‰ variations in $\delta^{13}\text{C}$ and $\delta^{18}\text{O}$, respectively. In addition, this will aid our understanding of how the CO₂-carbonate carbon isotope fractionation factor varies with composition and temperature.

With Phoenix landing this year and MSL launching in 2009, there is the potential to receive further data on carbon isotopes from the Martian atmosphere and regolith. Insights gained from this study will assist interpretation of results from these missions.

References: [1] Grady M. M. et al. 2007. Abstract #1826. 38th LPSC. [2] Wright I. P. et al. 1989. *Nature* 340:220–222. [3] McKay D. S. et al. 1996. *Science*. [4] Romanek C. S. 1994. *Nature* 372:655–657. [5] Golden D. C. et al. 2000. Abstract #1799. 31st LPSC. [6] Golden D. C. et al. 2000. *Meteoritics & Planetary Science* 35:457–465. [7] Saxton J. M. et al. 1998. *Earth and Planetary Science Letters* 160:811–822. [8] Niles P. B. et al. 2007. Abstract #2157. 38th LPSC. [9] Niles P. B. et al. 2005. *Geochimica et Cosmochimica Acta* 69:2931–2944.

5301

Hf-W THERMOCHRONOMETRY OF THE ACAPULCOITE-LODRANITE PARENT BODY

M. Touboul¹, T. Kleine¹, B. Bourdon¹, J. A. van Orman², C. Maden¹, J. Zipfel³, A. J. Irving⁴, and T. E. Bunch⁵. ¹Institute for Isotope Geochemistry and Mineral Resources, ETH Zürich, Switzerland. E-mail: touboul@erdw.ethz.ch. ²Department of Geological Sciences, Case Western Reserve University, Cleveland, OH, USA. ³Forschungsinstitut und Naturmuseum Senckenberg, Frankfurt am Main, Germany. ⁴Department of Earth and Space Sciences, University of Washington, Seattle, WA, USA. ⁵Department of Geology, Northern Arizona University, Flagstaff, AZ, USA.

Key issues in the formation and early evolution of meteorite parent bodies are the time scales of accretion, differentiation and cooling. The ¹⁸²Hf-¹⁸²W system is a powerful tool to obtain such age constraints and has been used to date the differentiation of iron meteorite parent bodies [1] and to constrain the thermal evolution of the H chondrite parent body [2]. Whereas heating of the iron meteorite parent bodies was sufficient to cause global differentiation, ordinary chondrite parent bodies did not ever melt. In contrast, acapulcoites and lodranites were partly melted, yet their parent body did not differentiate. To constrain the parameters that control the thermal evolution of the acapulcoite-lodranite parent body, we applied the Hf-W chronometer to several acapulcoites and lodranites.

Metal and silicate fractions from acapulcoites define an isochron, whose slope corresponds to an age of 5.1 ± 0.8 Ma after CAI formation. Likewise, a metal-silicate isochron for lodranites corresponds to an age of 5.7 ± 1.0 Ma. Relative to the Pb-Pb ages for angrites D'Orbigny and Sahara 99555 [3], these relative ages correspond to "absolute" Hf-W ages of 4563.5 ± 0.7 Ma for acapulcoites and 4563.0 ± 0.9 Ma for lodranites. These ages are older than Pb-Pb ages for Acapulco phosphates [4], which reflects the relatively high closure temperature of the Hf-W system. The Hf-W closure temperatures were estimated from numerical simulations of W diffusion in high-Ca pyroxenes (the major host of radiogenic ¹⁸²W) [2] and are ~ 975 °C for acapulcoites and ~ 1050 °C for lodranites, significantly higher than the Pb-Pb closure temperature of ~ 550 °C for Acapulco phosphates [5]. The Hf-W and Pb-Pb constraints correspond to a cooling rate of ~ 65 °C/Ma and indicate that acapulcoites/lodranites, in spite of higher peak temperatures, cooled much faster than H6 chondrites. Thermal modelling of spherical asteroids heated by ²⁶Al decay indicate that the thermal history of acapulcoites/lodranites appears most consistent with a parent body of 30–40 km radius that accreted instantaneously at ~ 2 Ma after CAI formation. Compared to a thermal model for the H chondrite parent body [2], the acapulcoite/lodranite parent body accreted earlier (which is consistent with its higher peak temperature) and is smaller (which is consistent with the faster cooling of its interior).

References: [1] Kleine T. et al. 2005. *Geochimica et Cosmochimica Acta* 69:5805–5818. [2] Kleine T. et al. 2008. *Earth and Planetary Science Letters* 270:106–118. [3] Amelin Y. 2008. *Geochimica et Cosmochimica Acta* 72:221–232. [4] Göpel C. et al. 1992. *Meteoritics* 27:226. [5] Zipfel J. et al. 1995. *Geochimica et Cosmochimica Acta* 59:3607–3627.

5336

THREE-DIMENSIONAL MORPHOLOGIES AND ELEMENTAL DISTRIBUTIONS OF STARDUST IMPACT TRACKS

A. Tsuchiyama¹, Y. Iida¹, T. Kadono², T. Nakamura³, K. Sakamoto³, T. Nakano⁴, K. Uesugi⁵, and M. E. Zolensky⁶. ¹Department of Earth and Space Science, Graduate School of Science, Osaka University, Toyonaka 560-0043, Japan. E-mail: akira@ess.sci.osaka-u.ac.jp. ²Institute of Laser Engineering, Osaka University, Suita 565-0871, Japan. ³Department of Earth and Planetary Science, Faculty of Science, Kyushu University, Hakozaki, Fukuoka 812-8581, Japan. ⁴Geological Survey of Japan, Advanced Industrial Science and Technology, Tsukuba 305-8567, Japan. ⁵Synchrotron Radiation Research Institute, SPring-8, Sayo, Hyogo 679-5198, Japan. ⁶KT NASA Johnson Space Center Houston, TX 77058, USA.

Introduction: Impact tracks formed by cometary dust capture in silica aerogel collectors in the Stardust mission [1] have a variety of shapes, showing diversity of the cometary dust [2]. We have investigated 3-D structures and elemental compositions of eight impact tracks using synchrotron radiation X-ray analyses (microtomography and XRF) [3]. In this study, additional three tracks were investigated by the same analytical method.

Experiments: In addition to the previous tracks (type-A [2]: T46 (Gobou), T68 (Skyrocket), T96 (Ichiro), T97, T98 (Heiji), T99 (Spiral-B), T100 (Spiral-A) and type-C [2]: T67 (Namekuji)), one type-A tracks (T66) and two type-B/C tracks (T65, T140) were examined. Keystones having the impact tracks were imaged at beamline BL47XU or BL20B2 of SPring-8, Japan, using projection microtomography [4] at 8–10 keV with the voxel (pixel in 3-D) size of 0.21, 0.50, 1.05, or 2.74 μm depending on the track sizes. Distributions of elemental mass (mainly Fe) along the tracks were obtained by XRF at 15 keV with a basaltic glass standard.

Results and Discussion: Track cavities including radial cracks, condensed aerogels, and captured grains including terminal grains were recognized three-dimensionally. The quantitative size parameters of the tracks, such as length, width, and volume, were obtained based on the voxel size. By assuming cylindrical symmetry of the tracks (track diameter as a function of the depth) the entrance hole sizes were determined precisely. The sizes of the original cometary dust impactors were also estimated from the total Fe contents of the tracks (i.e., Fe contents of the impactors) by assuming the Fe content of CI and densities (1 g/cm³ for fine aggregate and 3 g/cm³ for crystalline grains). They were compared with the entrance hole size, and deviation from the Fe content of CI was discussed.

The quantitative track shapes shows that some bulbous portions are more or less present as well as thin trackseven in type A (carrot-like) tracks. Distributions of the Fe mass along the tracks were compared with the track shapes. Fe is enriched in bulbous portions and some of large captured grains. In bulbous portions, Fe is distributed unevenly toward the deeper parts, suggesting movement of disaggregated fine particles during the capture.

References: [1] Brownlee D. et al. 2006. *Science* 314:1711. [2] Hörz F. et al. 2006. *Science* 314:1716. [3] Tsuchiyama A. et al. 2008. 39th LPSC. [4] Uesugi K. et al. 2003. *Journal de Physique. IV France* 104:45.

5172

ISOTOPE VARIATION AT NANOMOLAR CARBONATE IN THE MURCHISON METEORITE

Shin Tsutsui and Hiroshi Naraoka. Department of Earth and Planetary Sciences, Kyushu University, Japan. E-mail: stsutsui@geo.kyushu-u.ac.jp.

Introduction: Carbonate occurs in carbonaceous chondrites by up to ~0.3 wt% of the whole-rock sample with the ^{13}C -enriched composition (~+24–+80‰ relative to PDB: [1]). The carbonate has been supposed to be formed as a secondary product through aqueous alteration from other carbon-bearing materials on the meteorite parent bodies. The C-bearing precursors have been unclear, although the ^{13}C -enriched species of organic matter as well as minor “exotic” components such as presolar graphite and SiC grains could play an important role for the $\delta^{13}\text{C}$ distribution [2]. For example, ^{13}C -enriched component has been generated by hydrous pyrolysis of macromolecular insoluble organic matter (IOM) [3]. The $\delta^{13}\text{C}$ variation in a single meteorite is relatively small compared to that for all classes of carbonaceous chondrites probably due to the different degree of aqueous alteration of the meteorites. However, $\delta^{13}\text{C}$ of the Murchison carbonate still ranges widely from +31.6 to +41.9‰ [1]. Because organic matter and presolar grains distribute heterogeneously in a meteorite, the detailed spatial examination can provide additional insights into processes of carbonate formation as well as aqueous alteration. As we have recently developed carbon and oxygen isotope analysis at nanomolar level CO_2 , the isotope distribution is examined with relevance to its textures.

Sample and Analytical Procedures: The Murchison meteorite (CM2) is used in this study. In the preliminary examination, 0.2–2.3 mg samples of Murchison are treated with 100% phosphoric acid in an evacuated and sealed glass tube to give CO_2 . The cryogenically purified CO_2 is analyzed by gas chromatography/isotope ratio mass spectrometry. For carbon isotope, analytical accuracy ($\pm 0.3\%$) and precision ($\pm 0.3\%$) have been established for a few nanomolar CO_2 .

Results and Discussion: The CO_2 content in this study ranges from 15 to 89 ppm with the $\delta^{13}\text{C}$ value of +23.4 to +42.9‰. The $\delta^{13}\text{C}$ range of this study is consistent with that of previous report (+31.6 to +41.9‰) [1], showing a little wider variation. Because the meteorite amount used in this study (0.2–2.3 mg) is smaller than that used by previous study (19.5–52.9 mg) [1], this wider isotope range could be attributable to heterogeneity of carbonate. If the carbonate is a secondary product via aqueous alteration, this ~20‰ variation within a single meteorite specimen suggests that not only the precursor materials are present heterogeneously but also the aqueous activity is locally limited. Further investigations of small-scale isotopic variation with respect to meteorite textures promise better understanding for formation processes and origins of carbonate in meteorites.

References: [1] Grady M. M. et al. 1988. *Geochimica et Cosmochimica Acta* 52:2855. [2] Grady M. M. and Wright I. P. 2003. *Space Science Review* 106:231. [3] Oba Y. and Naraoka H. Forthcoming. *Meteoritics & Planetary Science*.

5225

NEUTRON EXPOSURE ON THE LUNAR SURFACE BASED ON ^{235}U FISSION IN ZIRCON

Grenville Turner. SEAES, University of Manchester, Manchester M13 9PL, UK. E-mail: grenville.turner@manchester.ac.uk.

Neutron capture by stable isotopes with large cross sections (e.g., ^{149}Sm , ^{155}Gd , and ^{157}Gd) has been used in combination with in situ measurements of the neutron flux [1] to study the evolution of the lunar regolith, so-called “neutron stratigraphy” [2]. These procedures determine the time integrated neutron exposure, $\int \phi(t).dt$, of a sample but provide no direct indication of when that exposure occurred. ^{235}U differs from Sm and Gd as a target in that its abundance was much higher in the past, a factor of 64, 4 billion years ago and fissionogenic xenon production is determined instead by, $\int \phi(t).exp(\lambda t).dt$. For a sample experiencing a single stage irradiation with uniform flux, ϕ , between times t_1 and t_2 these expressions become, respectively, $\phi.(t_1 - t_2)$ and $\phi/\lambda.(exp(\lambda t_1) - exp(\lambda t_2))$. Measurement of $^{150}\text{Sm}/^{149}\text{Sm}$ and $^{134}\text{Xe}_{\text{nef}}/\text{U}$ in the same zircon sample would permit a determination of the ratio, $A = (exp(\lambda t_1) - exp(\lambda t_2))/(t_1 - t_2)$. For a brief irradiation, where $t_1 \sim t_2 = t$, this simplifies to: $t = 1/\lambda. \ln(A/\lambda)$.

Neutron fission of ^{235}U in lunar regolith samples has previously been used in conjunction with cosmogenic noble gases to demonstrate pre-exposure of lunar soils and to determine the time dependence of $^{40}\text{Ar}/^{36}\text{Ar}$ in “solar wind” implanted argon [3]. These measurements were based on ^{136}Xe production in “bulk” samples of mineral concentrates on account of the generally low abundance of uranium. The use of the resonance ionization mass spectrometer, RELAX [4], to measure the individual xenon contributions, from spontaneous fission of ^{238}U and ^{244}Pu and neutron-induced fission of ^{235}U , in single terrestrial zircons has recently been demonstrated [5, 6]. This analysis is possible because of the high concentration of uranium, ~200 ppm, the very small corrections for trapped xenon, and the high sensitivity of RELAX. The neutron fluences employed in [6] were comparable to those in the lunar surface and suggest that the technique might be usefully adapted to study neutron exposure on the Moon. Zircons of sufficient size to carry out xenon analyses appear to be present in sufficient numbers in the lunar sample collection [7]. U abundance may be estimated from ^{134}Xe from spontaneous fission of ^{238}U and a knowledge of the U-Pb age of the zircon.

Possible applications include: studies of the surface residence history of ancient highland regolith breccias and regolith formation during the time of the late heavy bombardment; regolith dating of lunar meteorite breccias; a quantitative investigation of the recent suggestion that lunar soil breccias, from the Earth-facing lunar surface, may contain terrestrial atmosphere entrained within the solar wind during times of low or zero magnetic field. The procedures described should also lead independently to improved estimates of the lunar Pu/U ratio, which was the original motivation.

References: [1] Burnett D. S. and Woolum D. S. 1974. *Proceedings, 5th LSC*, pp. 2061–2074. [2] Curtis D. B. and Wasserburg G. J. 1975. *The Moon* 13:185–227. [3] Eugster O. et al. 2001. *Meteoritics & Planetary Science* 36:1097–1115. [4] Crowther S. A. et al. 2008. *Journal of Analytical Atomic Spectrometry*, doi:10.1039/B802899K. [5] Turner G. et al. 2004. *Science* 306:89–91. [6] Turner G. et al. 2007. *Earth and Planetary Science Letters* 261:491–499. [7] McKeegan K., personal communication.

5014

HEATING EXPERIMENT FOR THE EJECTION OF IRON GLOBULES FROM MELTED CHONDRULES

M. Uesugi, M. Oka, K. Saiki, and A. Tsuchiyama. Department of Earth and Space Science, Graduate School of Science, Osaka University 1-1 Machikaneyama-cho, Toyonaka-shi, Osaka, Japan. E-mail: uesugi@astroboy.ess.sci.osaka-u.ac.jp.

Introduction: Chondrules have relatively lower contents of siderophile elements than other elements compared to the solar elemental abundance [e.g., 1]. The origin of this feature is still unknown and has been in debate [2]. Recently, Uesugi et al. [3, 4] showed that iron globules were ejected from inside to outside of melted chondrules due to surface tension force, if they could reach the surface during chondrule formation, based on the calculation of kinetic stability. If the energy dissipation of viscosity during the ejection was large, the iron globules would lose their energy of motion, and would be trapped on the surface of the melted chondrule.

We investigated the metal-silicate separation process by heating experiment. Results of our experiment show that the ejection would be an important process for the origin of the chemical composition of chondrules.

Method: A mixture of reagent grade oxides was used as a starting material in the present experiments. We used CaCO_3 , K_2CO_3 , and Na_2CO_3 instead of CaO , K_2O , and Na_2O . Bulk composition of the sample is solar elemental abundance [5]. The iron was included as FeO in the sample. The sample was compacted into 20 mg pellets with 2 mm radius and 1 mm height, and fixed on the Pt wire. The sample and Pt wire were covered with carbon capsule. Furnace was filled by H_2 atmosphere with 4 torr pressure in the experiment. The liquidus temperature of this composition is 1900 K, and we heated the samples to this temperature. The duration of heating was 5 min, and both heating and cooling rate were 100 K/min. The heated samples were observed by X-ray CT at Osaka university, with pixel size 11 μm .

Results and Discussion: There are no metallic-iron globules on the surface of the melted silicate. The globules distribute inside the melted silicate or on the surface of outer carbon capsule. This tendency is consistent with the result of calculations of stability [3], and indicates that the dissipation of energy due to the viscosity during the passage of the surface would be considerably small compared to the kinetic energy of motion of iron globules. The results also indicate the possibility either metallic-iron globule is kinetically unstable on the surface of melted silicate, or reduction from FeO occurs not on the surface but inside the melted silicate material. Though more investigations are needed for the origin of iron globules in natural chondrules and precise kinetics of their ejection, the results of our experiment show the possibility that the iron-silicate separation effectively occurred during chondrule formation.

References: [1] Osborn T. et al. 1973. *Geochimica et Cosmochimica Acta* 38:1359–1378. [2] Grossman J. N. and Wasson J. T. 1985. *Geochimica et Cosmochimica Acta* 49:925–939. [3] Uesugi M., Sekiya M., and Nakamura T. Forthcoming. *Meteoritics & Planetary Science*. [4] Uesugi M. et al. 2006. *Meteoritics & Planetary Science* 41:A5172. [5] Anders E. and Grevesse N. 1989. *Geochimica et Cosmochimica Acta* 53:197–214.

5121

NON-DESTRUCTIVE OBSERVATION OF STRUCTURE OF COMPOUND CHONDRULES BY X-RAY CT

M. Uesugi¹, K. Uesugi², and M. Oka¹. ¹Department of Earth and Space Science, Graduate School of Science, Osaka University, 1-1 Machikaneyama-cho, Toyonaka-shi, Osaka, Japan. E-mail: uesugi@astroboy.ess.sci.osaka-u.ac.jp. ²Japan Synchrotron Radiation Research Institute (JASRI) 1-1-1 Kouto, Sayo-cho, Sayo-gun, Hyogo, Japan.

Introduction: The configuration of compound chondrules clearly shows that chondrules have different degree of melting at the time of chondrule formation [1, 2]. Previous study showed that nearly 50% of secondary chondrules, which lost their spherical shape due to the sticking, have higher liquidus temperature than primaries, which retain their spherical shape.

This feature indicates the inhomogeneity of temperature of chondrules during the heating event. If constituent chondrules in compound have different radius, they would have different cooling rate after the heating, and would have different temperature at the time of collision. We developed a method for high-quality three-dimensional imaging of meteorite using synchrotron radiation X-ray CT, and observed compound chondrules inside several meteorites.

Experiment: The experiment was performed at BL20B2 of Spring-8, with X-ray energy 25–30 keV and pixel size 2.74 μm . Samples were cut into ϕ 4–5 mm chip and fixed on the rotation stage of X-ray CT. We observed 3 chips of Y-790448 (LL3), a chip of Allende (CV3), and a chip of Y-791717 (CO3).

Results and Discussions: The average radius ratio of a secondary chondrule to a primary chondrule is smaller than unity. This result shows that primary chondrules would experience slower cooling than the secondaries, so they would have higher temperature than secondaries at the time of collisions. Moreover, some primary chondrules have higher bulk X-ray linear absorption coefficient (LAC). It might indicate that the primaries have higher bulk Fe contents than secondaries, and then the primaries have lower liquidus temperature than the secondaries. The structure is inconsistent, if they were formed in a single heating event.

These results might indicate that the primary and secondary chondrules formed in different heating events.

References: [1] Wasson J. T. et al. 1995. *Geochimica et Cosmochimica Acta* 59:1847–1869. [2] Akaki T. and Nakamura T. 2006. *The Astrophysical Journal* 31:101–102.

5192

THE EFFECT OF IMPACT ON PARAMAGNETIC DEFECTS IN QUARTZ

T. Usami, S. Toyoda, K. Noritake, and K. Ninagawa. Okayama University of Science, Japan. E-mail: s06rd01@physics.dap.ous.ac.jp.

Introduction: The impact is one of the major processes in the formation of the solar system as well as those which the earth has experienced from outer space in its history. The relics of such impacts are sometimes found in the crystal features as planar deformation features (PDFs). However, when the impact was not strong enough to make such features, the debate whether the crater-like geomorphic feature was made by an impact or not would be very tough. In the present paper, we would like to propose that electron spin resonance (ESR) signals in quartz could be such an indicator to detect impact phenomena.

Experiments: A slice of natural quartz crystal used in the present experiments was taken from Naegi quartz crystal in Naegi, Nakatsugawa city, Gifu Prefecture, Japan. This crystal was sliced in about 5 mm thickness and irradiated to a gamma ray dose of 2.5 Gy. Four column samples (diameter of 5 mm, height of 5 mm) were then taken from the slice. Shock experiments were performed with the two-stage light gas gun at JAXA (Japan Aerospace Exploration Agency). The velocities of the bullets were 1.85, 3.26, 3.33, and 3.76 km/s. The shocked sample became powder by the impact. Gamma ray doses from 0.1 kGy to 2.0 kGy were subsequently given again to the shocked sample. ESR measurements were made for those samples. Al and Ti-Li centers were measured at liquid nitrogen temperature and Ge and heat treated E_1' centers were measured at room temperature. After all ESR measurements, qualitative X-ray diffraction analysis was performed.

Results: The signals of Al, Ti-Li, Ge, and heat-treated E_1' centers were observed by the ESR measurements after the first gamma ray irradiation. The signals of all those centers completely vanished after the shock experiments even with the lowest velocity. All the signals did not recover even after the second irradiation after the impact. These experimental results indicate that impact shock not only erases the ESR signals but also destroys the "seed" of the signals while the samples were proven still to be quartz by the qualitative X-ray diffraction analysis. ESR signals could be used as indicators of impact for quartz crystals in the shock range that no crystallographic changes are observed.

5052

PETROGENESIS OF GEOCHEMICALLY ENRICHED IHERZOLITIC SHERGOTTITES RBT 04261 AND RBT 04262

T. Usui¹, M. E. Sanborn², M. Wadhwa², and H. Y. McSween Jr.¹
¹Department of Earth and Planetary Sciences, University of Tennessee, Knoxville, TN 37996-1410, USA. E-mail: tusui@utk.edu. ²SESE, Arizona State University, Tempe, AZ 85287-1404, USA.

Introduction: Shergottites sampled two distinct geochemical reservoirs that produce correlations in their magmatic oxidation states, oxygen and radiogenic isotope compositions, and trace element abundances. However, these reservoirs do not correlate with mineralogical and major element compositions. Basaltic and olivine-phyric shergottites individually sampled both geochemically enriched and depleted reservoirs, whereas lherzolitic shergottites are known only to have sampled the depleted one. Here we show that recently discovered shergottites RBT 04261 and RBT 04262 are the first examples of lherzolitic shergottites originating from the geochemically enriched reservoir based on petrographic observations and rare earth element (REE) compositions of minerals.

Results and Discussions: RBT 04261 and RBT 04262, which were initially identified as olivine-phyric shergottites, are actually lherzolitic shergottites [1]. Both meteorites exhibit similar textures and mineral compositions, suggesting that they should be paired. Each consists of two distinct textures: poikilitic and non-poikilitic. The poikilitic areas are composed of pyroxene oikocrysts enclosing olivine grains; all pyroxene oikocrysts have pigeonite cores mantled by augite. The non-poikilitic areas are composed of olivine, pyroxene, plagioclase (maskelynite), and minor amounts of merrillite, chromite, and Ti-magnetite. Olivines and pyroxenes show the lowest Mg# (~58 for olivine and ~62 for pyroxene), and plagioclase is the poorest in An component (~4) among the lherzolitic shergottites. Moreover, the modal abundances of maskelynite in these two meteorites (20.2 vol% for RBT 04261 and 15.9 vol% for RBT 04262) are distinctly higher than any other lherzolitic shergottites, although further investigation will be required to determine if the studied thin sections are representative.

The REE budgets of RBT 04261 and RBT 04262 are dominated by merrillite (La ~ 190 × Cl). The slightly LREE-enriched pattern of this mineral ($[La/Yb]_{Cl} \sim 1.6$) is similar to that of merrillite in the geochemically enriched basaltic shergottites Shergotty and Zagami, and unlike the LREE-depleted pattern of merrillite in the other lherzolitic shergottites [2]. REE patterns of both high- and low-Ca pyroxenes are also similar to those in Shergotty and Zagami. The calculated REE patterns of melts in equilibrium with the pyroxenes are parallel to that of RBT 04262 whole-rock [3] as well as other geochemically enriched basaltic shergottites.

Conclusions: These petrographic and geochemical observations suggest that RBT 04261 and RBT 04262 represent the most evolved magma among the lherzolitic shergottites and that this magma originated from the geochemically enriched reservoir. Despite having separate launch ages (and sites), all three shergottite types sampled both the depleted and enriched reservoirs.

References: [1] Mikouchi T. et al. 2008. Abstract #2403. 39th LPSC. [2] Sanborn M. E. et al. 2008. Abstract #912. 18th Goldschmidt Conference. [3] Anand M. et al. 2008. Abstract #2173. 39th LPSC.

5065

WEATHERING PATTERNS OF ORDINARY CHONDRITES FROM DIFFERENT LOCATIONS IN THE ATACAMA DESERT (CHILE)

E. M. Valenzuela¹, M. D. Leclerc², P. Munayco³, R. B. Scorzelli³, A. J. T. Jull², P. Rochette⁴, J. Gattacceca⁴, C. Suavet⁴, M. Denise⁵, and D. Morata¹.
¹Dep. de Geología, Universidad de Chile, Plaza Ercilla 803, Santiago, Chile. E-mail: edvalenz@cec.uchile.cl. ²NSF-Arizona AMS Laboratory, The University of Arizona, Tucson, USA. ³Centro Brasileiro de Pesquisas Físicas (CBPF/MCT), RJ, Brazil. ⁴CEREGE CNRS Université Aix-Marseille, France. ⁵MNHN Paris, France.

Introduction: Over the last years an interdisciplinary exhaustive study has been done with meteorite samples from the Atacama Desert (northern Chile), one of the oldest and driest desert of the world [1], in an attempt to understand the weathering processes acting on these primitive materials, the conditions of the accumulation surfaces that have preserved them, and compare these results with studies done with ordinary chondrites (OCs) from other hot desert areas [2–5] that have shown important relations between their terrestrial ages and the weathering stage of their primary mineralogy.

Samples and Past Studies: The samples correspond to 34 OCs of the three chemical groups (H, L, and LL) and 1 carbonaceous chondrite (first CO discovered on this desert), 15 of them found in 3 recent expeditions. Their characterization was done using different approaches as magnetic and density measurements [6], Mössbauer spectroscopy (MS) and XRD [7–9], ¹⁴C terrestrial ages [10] and chemical analyses.

Accumulation Surfaces Conditions: The meteorite recovery surfaces are located in areas of the Atacama Desert with slightly different climatic conditions: a) one in the coastal domain (Pampa-La Yesera), with some moisture coming from the Pacific Ocean, and b) other areas spread through the central part of the desert (mainly San Juan and other single areas), with precipitation rates less than 2 mm/year, if any.

Oxidation-Terrestrial Age Distributions: New data from low-temperature MS [9] and ¹⁴C terrestrial ages [10] allowed the reconstruction of the oxidation-terrestrial age distributions for the different populations of Atacama OCs, that show a fluctuating oxidation pattern over time, with at least 3 peaks of high oxidation for San Juan area and at least 4 for the coastal domain, that are not all coincident between sites, reflecting differences in the humid-arid cycle of the Atacama, as pointed by [2] for other deserts. H chondrites are more highly weathered than L-LL chondrites for a given terrestrial age, in both sites. We will discuss the possible explanations of these behaviors in terms of the different parameters that affect weathering at the Atacama.

Acknowledgements: This study is supported by CNRS-CONICYT (France-Chile), CBPF-MCT (Brazil), and CONICYT-BHIRF Ph.D. grant for M. Valenzuela.

References: [1] Dunai et al. 2005. *Geology* 33:321. [2] Bland P. A. et al. 1998. *Geochimica et Cosmochimica Acta* 62:3169. [3] Bland P. A. et al. 2000. *Quaternary Research* 53:131. [4] Jull A. J. T. 2006. In *Meteorites in the early solar system II*, p. 889. [5] Al-Kathiri A. et al. 2005. *Meteoritics & Planetary Science* 40:1215. [6] Valenzuela E. M. et al. 2006a. Abstract #9013. Desert Meteorite Workshop. [7] Valenzuela et al. E. M. 2006b. Abstract #5203. *Meteoritics & Planetary Science* 41:A179. [8] Valenzuela E. M. et al. 2007. Abstract #5099. *Meteoritics & Planetary Science* 42:A152. [9] Munayco P. et al. 2008. This issue. [10] Leclerc M. et al. 2008. This issue.

5084

MICROMETEORITES IN THE 400–1100 μm SIZE RANGE FROM THE TRANSANTARCTIC MOUNTAINS

M. van Ginneken¹, L. Folco¹, and P. Rochette². ¹Museo Nazionale dell'Antartide, Università di Siena, Italy. E-mail: vanginneken@unisi.it. ²CEREGE, Université Aix-Marseille III, France.

Introduction: We report the discovery of hundreds of unmelted micrometeorites in the 400–1100 μm size range from the Transantarctic Mountains. This extraordinary collection of extraterrestrial matter was found together with thousands of smaller micrometeorites and cosmic spherules within the micrometeorite traps discovered on the tops of Frontier Mountain and Miller Butte (Victoria Land) during the Italian 2003 and 2006 PNRA expeditions [1]. These traps consists of joints and weathering pits of million year old, flat, glacially eroded granitic surfaces [2, 3] filled with fine-grained bedrock detritus. These are extraordinary structures for the collection of fallout material from the last million years, as recently testified by Australasian microtektites found therein [4].

Samples and Methods: Hundreds of micrometeorites were magnetically extracted from 11.5 kg of detritus in the 400–2000 μm size range. Over 130 unmelted particles in the 400–1100 μm size range were studied using a SEM-EDS to gain information about size, morphology, structure, and surface mineralogy. So far, six particles have been mounted in epoxy, sectioned and polished for SEM-EDS petrographic study and EMP analyses.

Physical Characteristics: About 30% of the studied particles are fresh and show rounded to subrounded shapes. Some of these show angular sides and are likely fragments of larger particles. Fresh micrometeorites exhibit a magnetite-rich, scoriaceous crust. One particle shows unusual spherulitic structure [5]. The remaining particles are partially to totally covered by Fe-oxides and/or sulfate-rich encrustations due to terrestrial weathering. The variable degree of weathering attests to the different terrestrial residence times of particles.

Petrography: The six sectioned particles are coarse-grained micrometeorites with chondritic structure and mineralogy. Four particles contain readily delineated chondrules typical of low petrographic types, whereas two others exhibit granoblastic textures typical of high petrographic types. Olivine and low-Ca pyroxene compositions are in the Fa₁₈-Fs₁₇ to Fa₂₆-Fs₂₂ range, indicating H and L chondritic chemical classes. The six particles represent at least two lithologies, with four non-equilibrated H4 particles, and two equilibrated L6 particles. The fusion crust observed in some sections shows a magnetic rim typical of unmelted and scoriaceous micrometeorites.

Conclusions: The presumed age of the micrometeorite traps and the size fraction studied here are unique. Their ongoing study will therefore provide new insight into the flux of micrometeorites to Earth over the recent geological past. The ordinary chondritic composition of some of the particles studied so far is an outstanding discovery, which shows for the first time that at least part of the extraterrestrial micrometeorite flux to Earth in the 400–1100 μm size range is related to ordinary chondritic material.

Acknowledgements: This work was supported by PNRA and by the EU-funded ORIGINS project.

References: [1] Folco L. et al. 2006. *Meteoritics & Planetary Science* 41:343–353. [2] Welten et al. Forthcoming. *Earth and Planetary Science Letters*. [3] Van der Wateren et al. 1999. *GPC* 23:145–172. [4] Folco L. et al. 2008. *Geology* 36:291–294. [5] Van Ginneken M. et al. 2008. *Meteoritics & Planetary Science*. This issue.

5087

AN UNUSUAL PARTICLE FROM THE TRANSANTACTIC MOUNTAIN MICROMETEORITE COLLECTION LIKELY RELATED TO THE ~480 KA COSMIC DUST LAYER IN THE EPICA DOME-C AND DOME FUJI ICE CORES

M. van Ginneken¹, L. Folco¹, P. Rochette², and N. Perchiazzi³. ¹Museo Nazionale dell'Antartide, Siena, Italy. E-mail: vanginneken@unisi.it. ²CEREGE, Université Aix-Marseille III, France. ³DST, Pisa, Italy.

We provide the preliminary mineralogical description of an unusual particle from the Transantarctic Mountain micrometeorite collection [1].

Method: The particle (#20c.25) was magnetically extracted from a sample of detritus collected from a joint of the million-year-old, glacially eroded top surface of Miller Butte in Victoria during the 2006 PNRA expedition [1]. SEM-EDS analysis of the particle provided preliminary information on its size, morphology, and composition. The particle is presently mounted in a glass capillary tube for synchrotron X-ray diffraction analysis at the BM8 GILDA beam-line of the European Synchrotron Radiation Facility in Grenoble, France. Analyses will be run mid-May, and data will be presented at the meeting.

Physical Characteristics and Petrography: The particle is ~700 μm in size and mainly consists of a porous aggregate of spherules from <1 to 50 μm in diameter. Its hemispheric shape is probably the result of fragmentation of a particle that was originally spherical. The base of the hemisphere shows rounded hollows up to 300 μm in diameter that are likely crack-open vesicles. The constituting spherules are dominated by Fe-oxide dendrites set in a silicate matrix that are similar to the rare (<1% [2]) G-type cosmic spherules. A 50 μm silica-rich crystal and a 200 μm silica- and alumina-rich crystal both appear to be embedded in the spherulitic aggregate. Their nature as well as that of the material which holds the spherules together will possibly be determined by the planned synchrotron X-ray diffraction analyses. The SEM-EDS bulk composition of the particle is broadly chondritic, although slightly enriched in Al, Ti, and K and depleted in Mg and S relative to the CI-chondrite composition.

Conclusions: Similar spherulitic aggregates ~20 μm in size (and/or disaggregated spherules) have only been found previously in one of the two extraterrestrial dust-rich layers in the Dome Fuji and EPICA Dome C East Antarctic ice sheet cores, namely the 2833 m and 2788 m deep layers with a model age of 481 ± 6 ka [3, 4]. We therefore argue that the relatively large aggregate found at Miller Butte is the best representative sample of the parent lithology of the extraterrestrial dust found in the Dome-F and Dome-C cores now available for study. Furthermore, the unique characteristics of the above aggregates, along with their compatible age (the micrometeorite trap in which particle #20c.25 was found is >0.8 Ma old, [5]), strongly suggests that they are paired, thereby documenting a continental-scale distribution of the extraterrestrial debris associated with a major, possibly global, meteoritic event ~480 ago. This remarkable finding further confirms [1, 5] the great scientific value of the Transantarctic Mountain micrometeorite collection.

Acknowledgements: This work was supported by the PNRA and by the EU-funded ORIGINS project.

References: [1] Van Ginneken M. et al. 2008. *Meteoritics & Planetary Science*. This issue. [2] Genge M. et al. Forthcoming. *Meteoritics & Planetary Science*. [3] Narcisi B. et al. 2007. *Geophysical Research Letters* 34:L15502. [4] Misawa K. et al. 2008. Abstract #1690. 39th LPSC. [5] Folco L. et al. 2008. *Geology* 36:291–294.

5331

KAMACITE ASSEMBLAGES IN EH3 METEORITES

D. van Niekerk, G. Huss, and K. Keil. Hawai'i Institute of Geophysics and Planetology, University of Hawai'i at Manoa, Honolulu, HI, 96822, USA. E-mail: dionysos@higp.hawaii.edu.

Introduction: Metallic objects in EH3 chondrites remain poorly characterized, with the exception of Y-691 [1–3] and Qingzhen [2]. Y-691 is considered to be one of the most pristine EH3 chondrites based on its high content of presolar silicates [4]. Its diverse population of opaque mineral nodules was classified as massive or concentric with respect to the intergrowth of constituent sulfides, kamacite, or silicates [3]. Massive kamacite has been suggested to have precipitated from a melt [3] or condensed from a gas [1, 3], whereas concentric kamacite cores apparently precipitated from a melt but the rims condensed from a gas [3]. Various silicate inclusions are thought to be products of solid-gas reactions, disaggregation of chondrules, fractional condensation [3], or oxidation of metal during changes in nebula $f\text{O}_2$ [1]. We are systematically studying the opaque assemblages in polished thin sections of 12 EH3s by optical- and electron microscopy, and electron microprobe.

Results: Kamacite-bearing objects in all the EH3s may be similarly classified as concentric or massive, as in Y-691. Perryite and schreibersite are ubiquitous in kamacite. Schreibersite may occur as large inclusions irrespective of location in the host, while perryite is frequently found in thin zones around the edges of kamacite. The kamacite is always unzoned in Ni, Si, P, and Co regardless of inclusions or intergrowths. Silicate inclusions are present in kamacite-bearing objects in all the meteorites studied and include enstatite, albite, and sometimes dominantly a silica mineral. These inclusions are not euhedral like the ones found in the majority of the EL3s [5]. The EH3 inclusions are smaller, graphic or irregular in shape, and are isolated in the metal or connected via thin veins to the exterior of the objects. The veins could possibly indicate incomplete equilibration during thermal reprocessing. The lack of Si-zonation in the metal surrounding the silica phase suggests that secondary oxidation of Si in metal did not produce the inclusions. In MET 01018 fine euhedral silicates sometimes protrude into kamacite objects from the surrounds, while large globules of enstatite protrude into, and are isolated within, kamacite. This suggests a parent body origin for such objects. Sulfides occur both intergrown with, and isolated from, kamacite. Although troilite is always present, sulfide mineralogy varies between EH3s—for example, MET 01018 has oldhamite as its main accessory sulfide, while others (e.g., GRO 95517, Y-792959) have no oldhamite but are dominated by daubreelite. Surprisingly, niningerite (ubiquitous with equilibrated EHs) is not always present in EH3s.

The observed textural and sulfide-mineralogical heterogeneity between EH3s possibly reflect variable parent body processing superimposed on minor bulk chemical differences. It is possible that opaque mineral assemblages record parent body thermal processing, thus indicating that EH3's are not pristine—a point consistent with conclusions of [4] for Y-691.

References: [1] Kimura M. 1988. *Proceedings of the NIPR Symposium on Antarctic Meteorites* 1:51–64. [2] El Goresy A. et al. 1988. *Proceedings of the NIPR Symposium on Antarctic Meteorites* 1:65–101. [3] Ikeda Y. 1989. *Proceedings of the NIPR Symposium of Antarctic Meteorites* 2:109–146. [4] Ebata S. et al. 2006. Abstract #1619. 37th LPSC. [5] Van Niekerk D. and Keil K. 2008. Abstract #2296. 39th LPSC.

5115

GLASSES IN MICROMETEORITES

M. E. Varela¹ and G. Kurat². ¹CASLEO, Av. España 1512 Sur, San Juan, Argentina. E-mail: evarela@casleo.gov.ar. ²Department of Lithospheric Sciences, University of Vienna, Althanstrasse 14, 1090 Vienna, Austria.

Introduction: Micrometeorites (MMs) are by far the most common extraterrestrial matter collected by the Earth that constitutes a class of its own with relationships to CM chondrites [1] and comets [2]. Recently, extensive studies of glasses in meteorites were rewarding and lead to the formulation of a new model of the formation of chondritic constituents and also non-chondritic meteoritic rocks [3–5]. As no such data existed for MMs, we started a study to fill this gap. Here we give a preliminary report on the results obtained on MMs collected from the Antarctic ice near Cap Prudhomme.

Samples and Results: MMs labeled 10M, M92-6b, AM9, and M1-M7 (NHM, Vienna) are of the crystalline MM type as define by [1]. All of them are mainly (e.g., Mc7 and AM9) or exclusively (e.g., 10M and M92-6b) composed of euhedral to subhedral olivine in clear mesostasis glass. Glass inclusions in olivine are also composed of clear glass and a shrinkage bubble and range in size from 5 to 10 μm . The primary glass inclusions of the 10M and M92-6b MMs are hosted by olivines containing 16.6 and 28.5 wt% FeO and 0.03 and 0.36 wt% CaO, respectively.

Discussion: Glasses in the studied MMs have high contents of FeO and MgO as compared to clear inclusion glasses in olivines and mesostasis of carbonaceous and ordinary chondrites constituents (FeO and MgO contents in CC and OC are <4 and <7 wt%, respectively, e.g., [3, 4]). However, the contents of both elements match those observed in experimentally heated glasses from Allende [6] suggesting that glasses in MMs have suffered a thermal event, which is no surprise. In addition, the texture of MMs, as well as the similar chemical composition of inclusion and mesostasis glasses with respect to olivine-incompatible elements, indicates that these glasses are not pristine. The samples investigated by us very likely are the product of MM melting during atmospheric entry—as are the olivines associated with them. Variations in the local redox conditions experienced by individual MMs could explain variable losses of Fe from the melt from which the new olivines grew as well as non-equilibrium Cr and Ca distributions between glasses and olivines [e.g., 7].

References: [1] Kurat et al. 1994. *Geochimica et Cosmochimica Acta* 58:3879–3904. [2] Maurette. 2006. Berlin: Springer Verlag. 330 p. [3] Varela et al. 2005. *Icarus* 178:553–569. [4] Engler et al. 2007. *Icarus* 192:248–286. [5] Varela and Kurat. Forthcoming. *Icarus*. [6] Varela. Forthcoming. *Geochimica et Cosmochimica Acta*. [7] Green. 1994. *Chemical Geology* 117: 1–36.

5179

HIGH-PRECISION ²⁶Al-²⁶Mg SYSTEMATICS OF TYPE I AND TYPE II CHONDRULES FROM SEMARKONA (LL3.0)

J. Villeneuve¹, M. Chaussidon¹, and G. Libourel^{1, 2}. ¹CRPG-Nancy Université-INSU/CNRS, UPR2300, BP 20, 54501 Vandoeuvre-lès-Nancy, France. ²ENSG-Nancy Université, 54500 Vandoeuvre-lès-Nancy, France. Email: johanv@crpg.cnrs-nancy.fr.

The ²⁶Al-²⁶Mg system, because of the short half life of ²⁶Al (0.73 Myr), is a potential chronometer of early solar system evolution, provided that the level of homogeneity of ²⁶Al in the accretion disk can be quantified precisely. One key process in this early evolution is chondrule formation. Earlier studies of ²⁶Al in chondrules [1, 2] suggested that they formed ≈ 2 Myr after Ca-Al-rich inclusions (CAIs) considering an initial ²⁶Al/²⁷Al ratio in CAIs of $5.23(\pm 0.13) \times 10^{-5}$ [3] or of $5.85(\pm 0.05) \times 10^{-5}$ [4]. However, the precision of existing data is not sufficient to be able to resolve possible time differences between different chondrules or different chondrule types (e.g., reduced-type I and oxidized-type II) and the data set may be biased toward chondrules having glassy mesostases with extremely high Al/Mg ratio.

High-precision analyses of the ²⁶Al-²⁶Mg system were developed with the CRPG Cameca IMS 1270 ion microprobe in order to be able to measure radiogenic ²⁶Mg excesses in “normal” chondrules’s glasses with low ²⁷Al/²⁴Mg atomic ratios (less than 10). The simultaneous measurement of ²⁴Mg, ²⁵Mg, ²⁶Mg, and ²⁷Al in multi-collection mode on Faraday’s cups allows the ²⁶Mg excesses and the ²⁷Al/²⁴Mg ratios to be measured with a precision (± 2 sigma) of 0.05–0.2% and 7%, respectively.

Chondrules from the Semarkona LL3.0 chondrite were studied because the very low degree of parent body thermal metamorphism registered by Semarkona is favorable to a good preservation of the Al-Mg isotopic system in chondrules since their formation. Among the 20 “normal” Semarkona type I and type II chondrules (with low Al/Mg ratios) selected by SEM and analyzed, 8 showed well-resolved ²⁶Mg excesses, with inferred initial ²⁶Al/²⁷Al ratios ranging from $(1.40 \pm 0.39) \times 10^{-5}$ to $(0.60 \pm 0.21) \times 10^{-5}$.

The ²⁶Al/²⁷Al ratios obtained in this study for Semarkona chondrules are in agreement with previous data [1, 2, 5]. In the hypothesis of a homogeneous ²⁶Al distribution in the accretion disk, they would confirm the suggestion that chondrules formation began at least 1.5 Myr after CAIs. These preliminary results suggest a very short duration for chondrule formation of less than 0.9 Myr. However, lower initial ²⁶Al/²⁷Al ratios from 3×10^{-6} to 6×10^{-6} have also been reported in Semarkona and Bishunpur [2, 6]. These data would argue for an extended duration of chondrule formation, unless the ²⁶Al-²⁶Mg was partially reset by parent body metamorphism or alteration. In opposition to data from CO chondrules [7, 8], our preliminary results show no significant formation age difference between Semarkona type I and type II chondrules, suggesting that an oxidized and a reduced environment for chondrules formation coexisted in the protosolar nebula.

References: [1] Kita N. et al. 2000. *Geochimica et Cosmochimica Acta* 64:3913. [2] Mostéfaoui S. et al. 2002. *Meteoritics & Planetary Science* 37: 421. [3] Thrane K. et al. 2006. *The Astrophysical Journal* 644:L159. [4] Jacobsen B. et al. Forthcoming. *Earth and Planetary Science Letters*. [5] Rudraswami N. G. and Goswami J. N. 2007. *Earth and Planetary Science Letters* 257:231. [6] McKeegan K. et al. 2000. Abstract #2009. 31st LPSC. [7] Kunihiro T. et al. 2004. *Geochimica et Cosmochimica Acta* 68:2947. [8] Kurahashi E. et al. 2007. Abstract #4027. Workshop on the Chronology of MESS.

5071

CO-GENETIC FLUID+MELT JETS IN THE POPIGAI LECHATÉLIERITES: A MULTI-STAGE ORIGIN

S. A. Vishnevsky, N. A. Gibsher, and N. A. Palchik. Inst. of Geol. & Mineral., Novosibirsk, 630090, Russia. E-mail: svish@uiggm.nsc.ru.

Introduction: Water plays an important role at all stages of the impact cratering, what can be shown on the Popigai examples: impact anatexis of target gneisses [1], origin of suevite+tagamite mega-mixtures [2] impact fluidites [3], high-pressure H₂O inclusions [4], etc. The lechatelierites (Ls) with several fluid+melt injections from outside are the further example of so kind. Below, the petrography and the microprobe data on the Ls are presented; ion probe studies of their volatiles are in progress.

The Glass Petrography: Ls are collected from the Daldyn type suevites [5] as splash-form particles and fragments 3 to 5 cm in size; sometimes, they contain blocks of the diaplectic quartz glasses (DQGs). Both the Ls and DQGs are fresh and clear. Flowing bands of melt + fluid jets penetrate the L particles from outside. Some jets (type I and II glasses) are colorless or pale yellowish, show the traces of partial homogenization with the host L, and are highly saturated with fluid inclusions. Other jets (type III glasses) are brown-yellowish low-porous bands clearly separated from the host L but show turbulent and swirled traces of dynamic interaction on the contact without mixing. Type I and II glasses contain cogenetic gas, gas+liquid and entirely liquid at 20 °C low-salt H₂O inclusions [4]; type III glasses have gas bubbles only.

Geochemistry of the Glasses: All data are of average, in wt%. Ls + DQGs contain poor impurities (12 analyses): SiO₂ 98.91; other main petrogenic oxides, MPOs, 0.19; a loss of analyses, LA, 0.90. Type I glasses are high-silica, with a clear K-Na specificity (8 analyses): SiO₂ 96.88; other MPOs 1.47, including Na₂O + K₂O 0.53; Al₂O₃ 0.33; LA 1.65. Type II glasses are also high-silica (14 analyses, SiO₂ 93.99), but show increase in MPOs (3.67), including Na₂O 0.35; K₂O 0.71; Al₂O₃ 1.49; FeO 0.42; MgO 0.31; CaO 0.25; TiO₂ 0.11; LA 2.34. Type III glasses are equal to usual Popigai tagamites in terms of bulk geochemistry (10 analyses): SiO₂ 63.58; Al₂O₃ 15.72; Na₂O 1.75; K₂O 2.56; FeO 6.84; MgO 3.71; CaO 2.92; TiO₂ 0.56; MnO 0.09; LA 2.27.

Discussion and Conclusions: Type I and II glasses are the earlier hot and mobile volatile-rich jets, having a lot of H₂O inclusions and increased LA comparing to the same of the lost L (1.65 and 2.34 versus 0.90, correspondingly). Type I glasses are the result of unlimited mixing between silica and the products derived from K-Na feldspars; a less of Al₂O₃ (K₂O + Na₂O/Al₂O₃ ~ 1.6) can suppose the earlier impact anatexis in their origin, with mobilization of SiO₂, K₂O, Na₂O, and H₂O versus Al₂O₃ and other MPOs, like it is known in the Popigai [1]. Type II glasses are the result of unlimited mixing between silica and mixed melts derived from the “wet” target gneisses. Type III glasses are the result of dynamic interaction between silica and mixed glasses derived from usual target gneisses. So, the Ls have complex multi-stage origin and various sources for type I, II and III glasses quenched in suevites.

Acknowledgements: This study was supported by RFBR grant #08-05-00468.

References: [1] Vishnevsky S. and Pospelova L. 1986. *Meteoritic matter and Earth*. Novosibirsk: Nauka Press. pp. 117–131. In Russian. [2] Vishnevsky S. 2003. Abstract #4024. 3rd International Conference on Large Meteorite Impacts. [3] Vishnevsky S. et al. 2006. *Russian Geology and Geophysics* 47:711–730. [4] Vishnevsky S. and Gibsher N. 2008. Abstract #1043. 39th LPSC. [5] Vishnevsky S. and Montanari A. 1999. *Geological Society of America Special Paper* #339. pp. 19–59.

5266

EXPOSURE AGES OF IAB IRONS: IMPLICATIONS FOR THE FORMATION AND COLLISIONAL HISTORY OF THE IAB PARENT BODY

N. Vogel and I. Leya. Institute of Physics, University of Berne, Switzerland. E-mail: nvogel@space.unibe.ch.

Introduction: Following a study to unravel the formation history of the IAB parent body by Ar-Ar thermochronology [1], we now investigate its later collisional history and try to answer the question about potential irradiation of IAB silicates prior to their mixing with liquid metal. We therefore determined ³He, ²¹Ne, and ³⁸Ar exposure ages for the metal phases and silicate inclusions of Caddo County, Landes, and Ocotillo using a new set of model calculations, which are consistent for iron and stony meteorites [2] and thus allow a direct comparison of metal and silicate ages.

Methods: We analyzed He, Ne, and Ar in metal samples and olivine separates from adjacent silicate inclusions. The chemical compositions of the samples were determined by SEM and electron microprobe. We calculated for all samples endmember exposure ages assuming irradiation in a pure iron meteorite matrix on the one hand and in ordinary chondrite matrix on the other. The IAB bulk chemistry and thus the “true” exposure ages lie in between those endmembers. Minimum preatmospheric radii were estimated using the recovered weights of the meteorites and measured ⁴He/²¹Ne in metal samples. These radii are at least ~20 cm for Caddo and Landes, and at least ~30 cm for Ocotillo.

Results and Discussion: Exposure ages determined from ³He, ²¹Ne, and ³⁸Ar in metal agree excellently and are ~2 Ma for Caddo County, ~200 Ma for Landes, and ~600 Ma for Ocotillo. Substantial production rate variations due to variations in shielding are only expected for Ocotillo.

³He exposure ages for Caddo County olivines are slightly higher than the metal ages, while metal and olivine ²¹Ne ages are in good agreement. In contrast, ³He and ²¹Ne exposure ages for Landes and Ocotillo olivines are significantly lower than the respective metal ages. Thus, loss of cosmogenic He and Ne from olivine is probably an issue for these samples. ³⁸Ar exposure ages for olivines from all three meteorites are significantly higher than the respective metal ages. This is attributed to contamination of the olivine separates used for noble gas analysis with clinopyroxene adding a significant amount of Ca to the samples. However, also uncertainties in the ³⁸Ar production rates from Ca cannot be excluded.

Conclusions and Outlook: (1) Consistent ³He, ²¹Ne, and ³⁸Ar exposure ages were obtained for IAB metal. (2) Most exposure ages determined for IAB silicates suffer from noble gas loss and/or the fact that sample chemistry and noble gas analyses are—unlike for cosmogenic radionuclides—not determined on the same aliquot. (3) The three investigated meteorites have very different exposure ages and thus were ejected from the IAB parent body in different collisional events. The last of these collisions must have occurred only few Ma ago. (4) Due to the extremely low exposure age of Caddo County, a significant pre-irradiation of its silicates compared to the metal phase should easily be detectable, but can be excluded based on our data.

We anticipate to present noble gas exposure ages for several further IAB irons at the conference.

References: [1] Vogel N. and Renne P. R. 2008. *Geochimica et Cosmochimica Acta* 72:1231–1255. [2] Ammon K. and Leya I. Forthcoming. *Meteoritics & Planetary Science*.

5054

ATYPICAL MAGNESIUM ABUNDANCES IN OXYGEN-RICH STARDUST: NANOSIMS AND AUGER ANALYSES

C. Vollmer¹, F. J. Stadermann², C. Floss², P. Hoppe¹, and F. E. Brenker³.
¹Max Planck Institute for Chemistry, 55020 Mainz, Germany. ²Laboratory for Space Sciences, Washington University, St. Louis, MO 63130, USA.
³Geoscience Institute/Mineralogy, JWG-University, 60054 Frankfurt, Germany.

Introduction: Astronomical observations indicate that silicates are the major dust component of O-rich red giant stars. The Mg/Si and Mg/Fe abundance ratios in these circumstellar shells are of particular interest, as they strongly influence the types of dust to condense [1]. These data can be tested on Earth by high precision laboratory analyses of presolar silicates found within primitive Solar System materials [2]. Auger spectroscopy is a powerful tool to study the chemistry of these stardust grains on a <30 nm scale. It has been used to analyze rare presolar grain types [3] and also allows characterization of composite phases [4]. Here we report on results from combined NanoSIMS/Auger measurements on O-rich stardust from the Acfer 094 meteorite.

Methods: Presolar silicates/oxides were identified by NanoSIMS O isotope mapping at the MPI for Chemistry [5]. Auger analyses of selected grains were performed with the St. Louis Scanning Auger Nanoprobe using a 10 kV/ 0.3-1 nA beam.

Results and Discussion: Four of 29 analyzed grains belong to Group II ($^{18}\text{O}/^{16}\text{O} < 1 \times 10^{-3}$), indicative of lower-than-solar metallicity or cool bottom processing in red giant stars. Two of these are Al oxides with low Mg contents (Al_2O_3 or hibonite) and one is a highly Si-enriched glass, possibly SiO_2 . Recent studies by NanoSIMS/TEM also revealed two presolar silicates with low $^{18}\text{O}/^{16}\text{O}$ ratios and low Mg contents [6, 7]. Astrophysical observations indicate that stars of very low metallicities ($<0.01 \times$ solar) have low Mg/Si ratios [1], which may thus be alternative stellar sources of the grains described here. However, the $^{18}\text{O}/^{16}\text{O}$ ratios of the grains are still too high to support this scenario, and it is questionable whether dust grains can form under such low metallicity conditions at all. One grain of particular interest has an unusually high Mg abundance and O/Si ratio (58.7% O, 31.9% Mg, 9.4% Si), and is not compatible with any standard silicate. Two presolar grains of similar composition have been detected recently in the CR chondrites QUE 99177 and MET 00426 [8, unpublished data]. These chemically similar phases therefore represent a new type of Mg-rich stardust, although their isotope characteristics (two Group I grains of different $^{17}\text{O}/^{16}\text{O}$ ratios, one Group IV grain) point to unrelated origins. Under non-equilibrium conditions MgO is expected to condense around stars with low mass loss rates ($<4 \times 10^{-6} M_{\odot} \text{ a}^{-1}$) and $\text{Mg/Si} > 2$ [1, 9]. The grains's compositions are clearly not compatible with pure MgO, but our discoveries emphasize that condensation of highly MgO enriched dust as predicted by theory [9] is possible in circumstellar shells. The MgO-rich grain from Acfer 094 also exhibits a rim of Fe-rich oxide, which is clearly also anomalous in oxygen. If this rim condensed at lower temperatures onto the Mg-rich grain, this supports the non-equilibrium formation scenario [e.g., 3].

References: [1] Ferrarotti A. S. and Gail H.-P. 2001. *Astronomy and Astrophysics* 371:133. [2] Hoppe P. and Vollmer C. 2008. AIP Conference Proceedings 1001, p. 254. [3] Floss C. et al. 2008. *The Astrophysical Journal* 672:1266. [4] Vollmer C. et al. 2007. *Meteoritics & Planetary Science* 69: 5107. [5] Vollmer C. et al. 2007. *The Astrophysical Journal* 666:L49. [6] Nguyen A. N. et al. 2007. *The Astrophysical Journal* 656:1223. [7] Vollmer C. et al. 2007. Abstract #1262. 38th LPSC. [8] Floss C. and Stadermann F. 2008. Abstract #1280. 39th LPSC. [9] Ferrarotti A. S. and Gail H.-P. 2003. *Astronomy and Astrophysics* 398:1029.

5004

NUMERICAL SIMULATIONS OF PLANETESIMAL-FORMING GRAVITATIONAL INSTABILITY IN A PROTOPLANETARY DISK USING A THIN DUST LAYER MODEL

S. Wakita and M. Sekiya. Department of Earth and Planetary Sciences, Kyushu University, Fukuoka 812-8581, Japan. E-mail: shigeru@geo.kyushu-u.ac.jp.

Introduction: There are two major models for the planetesimal formation: one is the growth of dust aggregates through mutual sticking by nongravitational forces [1] and another is the gravitational instability (GI) of the dust layer in a protoplanetary disk [2–4]. Previous two-dimensional numerical simulations of the GI [5] investigated the process that the dust layer fragments into rings circling the central star, based on assumption that the dust layer is axisymmetric with respect to the rotation axis. However, three-dimensional simulations including the azimuthal direction are needed to obtain a planetesimal size distribution. For the first step of this aim, we study numerically the growth of GI including motion in the azimuthal direction and estimate an initial planetesimal size.

Model: We construct a two-dimensional thin disk model of the dust layer, in which coordinates in the radial and azimuthal directions on the midplane are taken as independent variables. A computational region is a local square with the length of each side being 80,000 km at 1 AU. Assuming the dust and gas couple firmly by the mutual friction, we neglect the relative velocity between the dust and gas parallel to the disk plane, i.e., groups of the dust can be treated as a fluid. In addition, we take account of the dust settling by using an analytic solution of dust spatial density growth. The radius and the material density of the dust are assumed to 0.03 m and 3000 kg/m³, respectively.

Results: We find that the GI grows nonaxisymmetrically independent of initial dust spatial density. Consequently, the trailing waves break into a number of dense clumps, which may result in planetesimals of the order of 10¹⁶ kg. If the planetesimals are spherical, their diameter would be on the order of 10 km. These results are comparable with the values estimated previously assuming an axisymmetric mode grows first [2–4].

References: [1] Weidenschilling S. J. and Cuzzi J. N. 1993. In *Protostars and planets III*. pp. 1031–1060. [2] Safronov V. S. 1969. In *Evolution of the protoplanetary cloud and formation of the Earth and the planets*. [3] Goldreich P. and Ward W. R. 1973. *The Astrophysical Journal* 183:1051–1061. [4] Sekiya M. 1983. *Progress of Theoretical Physics* 69: 1116–1130. [5] Yamoto F. and Sekiya M. 2006. *The Astrophysical Journal* 646:L155–L158.

5146

COMPARISON OF Mg ISOTOPE COMPOSITIONS BETWEEN BULK METEORITES AND MAFIC-ULTRAMAFIC ROCKS FROM TERRESTRIAL MANTLE

G. Wang¹, Y. Lin², and D. Wang. ¹Key Laboratory of Isotope Geochronology and Geochemistry, Guangzhou Institute of Geochemistry, CAS, Guangzhou, China. E-mail: guiqinwang@gig.ac.cn. ²Key Laboratory of the Earth's Deep Interior, Institute of Geology and Geophysics, CAS, Beijing, China.

Introduction: It is still few and inconsistent for the published Mg-isotope data of terrestrial and extraterrestrial samples [1–3]. In addition, whether terrestrial materials show Mg isotopic characteristics similar to chondrites or non-chondrites has been disputed [2, 3]. Here we present Mg isotopic data of sixteen peridotites (including mineral separates), ten basalts and picrites derived from the mantle, and four bulk meteorites analyzed by MC-ICPMS. Based on the new data, this study attempts to better understand Mg isotopic variation and fractionation in solar nebula and earth mantle.

Results and Discussions: Mg isotopic compositions of 3 chondrites, i.e., Allende (CV3), Ningqiang (ungrouped C3), and Jilin (H5), are rather homogeneous, with $\delta^{26}\text{Mg}$ (relative to DSM3) between 0.04‰ and 0.06‰ and $\delta^{25}\text{Mg}$ between 0.01‰ and 0.03‰. The bulk sample of GRV 99027, a Martian lherzolite little contaminated by the crust of Mars [4, 5], has the same Mg isotopic composition as the chondrites, with $\delta^{26}\text{Mg}$ of $0.04 \pm 0.02\%$ and $\delta^{25}\text{Mg}$ of $0.00 \pm 0.02\%$. The uniform data of the various chemical groups of chondrites and the Martian meteorite indicate that the solar nebula has a rather homogeneous Mg isotopic composition, similar to iron isotopes [6].

The similar Mg isotopic composition of the Martian lherzolite with those of chondrites suggest little fractionation of Mg isotopes during formation of GRV 99027. In contrast, terrestrial mafic and ultramafic rocks that probably derived from the mantle display significant variation of $\delta^{26}\text{Mg}$ from -0.52% to 0.19% , suggestive of heterogeneous compositions of Mg isotopes of the terrestrial mantle. These variations may not be due to simple partial melting and/or fractional crystallization, because mineral separates (including olivine, clinopyroxene, and orthopyroxene) of the peridotites show no fractionation of Mg isotopes.

It is also noted that most of the terrestrial ultramafic rocks analyzed in this work are depleted in heavier isotopes of Mg relative to chondrites. In addition, a loess samples, which may represent the mean crust of the Earth, have $\delta^{26}\text{Mg}$ of -0.41% . To account for mass balance, heavier Mg isotope-enriched components are required if the Earth has a bulk composition of chondrites.

Acknowledgements: The Martian meteorite was supplied by the Polar Research Institute of China. This study was supported by the Knowledge Innovation Program (kzcx2-yw-110 and GIGCX-07-19) of the Chinese Academy of Sciences.

References: [1] Pearson N. J. et al. 2006. *Chemical Geology* 226:115–133. [2] Wiechert U. and Halliday A. N. 2007. *Earth and Planetary Science Letters* 256:360–371. [3] Teng F.-Z. et al. 2007. *Earth and Planetary Science Letters* 261: 84–92. [4] Lin Y. et al. 2005. *Meteoritics & Planetary Science* 40:1599–1619. [5] Lin Y. et al. Forthcoming. *Meteoritics & Planetary Science*. [6] Zhu X. K. et al. 2001. *Nature* 412:311–313.

5123

PETROGRAPHIC STUDY OF NINGQIANG SODALITE

Y. Wang and W. Hsu. Laboratory for Astrochemistry and Planetary Sciences, Purple Mountain Observatory, Nanjing 210008, China. E-mail: y_wang@pmo.ac.cn.

Introduction: Sodalite ($\text{Na}_8\text{Al}_6\text{Si}_6\text{O}_{24}\text{Cl}_2$) is a rare halogen-rich silicate mineral. It occurs widely in various chondrites. Recently, sodalite grains in CAIs and chondrules of carbonaceous chondrites were found to exhibit potential ^{36}S excesses, suggesting the presence of short-lived ^{36}Cl in the early solar system [1, 2]. Sodalite is not a primary phase, but a secondary alteration product. It is therefore important to know under what conditions and environment sodalite formed. Here we report a petrographic study of sodalite in the Ningqiang chondrite.

Results and Discussion: The overall abundance of sodalite is very low ($\ll 1$ vol%) in Ningqiang. Sodalite grains are very small (sub- μm up to $10 \mu\text{m}$) and subhedral to anhedral in shape. They are widely present in chondritic components, such as CAIs, chondrules, AOAs, dark inclusions, and matrix. Sodalite usually occurs interstitially between primary silicate phases (olivine and pyroxene) and coexists with other secondary phases such as nepheline, hedenbergite, and fayalitic olivine. Sodalite in silicate aggregates occurs around diopside grains. In matrix, sodalite usually intergrows with fayalitic olivine grains. Individual sodalite grains are rare in the matrix.

Sodalite was probably formed by alkali-halogen metasomatism of anorthite and anorthite-normative glasses in chondritic components [3, 4]. There is a long-standing debate on whether alteration processes occurred in the solar nebula or on asteroidal bodies [3, 4]. Our petrographic observation of sodalite occurrence in Ningqiang supports a nebular environment. The abundance of sodalite is relatively lower in Ningqiang matrix than in other chondritic components. For example, there is a fine-grained dark inclusion (DI), which is composed of fine grained ($5\text{--}20 \mu\text{m}$) sodalite, nepheline, diopside, fayalitic olivine, and some mesostases. Sodalite and nepheline are subhedral to anhedral and account for 25 vol%. Diopside (30 vol%) is porous, and fayalitic olivine (10 vol%) appears as long platy crystal. The rest is sub- μm matrix-like materials (35 vol%). DI is distinct from surrounding matrix. The mean grain size of DI is coarser than that of matrix. The abundance of sodalite is significantly higher in DI (10 vol%) than its surrounding matrix ($\ll 1$ vol%). This sharp contrast indicates that the environment for sodalite formation is not an asteroidal body, but most likely the solar nebula before accretion. Matrix is mainly composed of fine mineral grains with high porosity and permeability. If sodalite formed by secondary alteration processes in an asteroidal environment, matrix should be more susceptible to alteration than other chondritic components, and thereby contains more sodalite grains.

Our petrographic observation is consistent with oxygen isotopic characteristics of Ningqiang sodalite, which fall along the CCAM line on the three oxygen isotope diagram [5], indicating sodalite formation in a nebular environment.

References: [1] Lin Y. et al. 2005. *Proceedings of the National Academy of Sciences* 102:1306–1311. [2] Hsu W. et al. 2006. *The Astrophysical Journal* 640:525–529. [3] Kimura M. and Ikeda Y. 1995. *Proceedings of the NIPR Symposium on Antarctic Meteorites* 8:123–138. [4] Krot et al. 1995. *Meteoritics* 30:748–775. [5] Guan Y. et al. 2005. Abstract #2027. 26th LPSC.

5335

SIDEROPHILE AND OTHER ELEMENT DISTRIBUTIONS AMONG HED-METEORITIC BRECCIAS

Paul H. Warren and Heinz Huber. Institute of Geophysics and Planetary Physics, University of California, Los Angeles, CA 90095-1567, USA. E-mail: pwarren@ucla.edu.

We have used neutron activation analysis (mainly INAA, but in a few cases also RNAA) to measure the bulk compositions of some 83 separate HED meteorites; the vast majority of which are manifestly brecciated. The emphasis in this study has been to determine siderophile elements, especially Ni and Ir, along with numerous other elements to give context to the siderophile data. The HED parent asteroid experienced cratering and megaregolith/regolith development analogous to the processes that pervasively altered the chemistry and structure of the upper crust of the Moon. These two bodies differ in size by at least a factor of 200 (in mass), and impact velocities are much smaller (by a factor of ~3) in the asteroid belt [1]. However, based on our new data as well as literature data, the statistical mean and variance of breccia siderophile concentrations are roughly similar for the two bodies (taking the highlands as representative of the Moon).

Besides constraining the bombardment history of the parent body, siderophile data can help to elucidate pairing and classification; in particular, a siderophile measurement can be an excellent test of the monomict hypothesis for brecciated samples (the lack of overall compositional-petrologic diversity among eucrites makes spotting polymict breccias difficult). For example, Igdi is classified as a monomict breccia, but our two separate analyses both show enrichments in Ni (31–59 µg/g) and Ir (2.2–2.4 ng/g).

We find a marginally significant tendency for breccias classified as howardites to be enriched in Ni and Ir relative to those classified as polymict eucrites. But the HED data show great scatter, and some aspects of the scatter are surprising and enigmatic. For example, FRO 97045 is a polymict breccia that reportedly contains glass spheroids [2]. By analogy with the Moon, glass spheroids are a sure indication of at least a minor component of regolithic derivation. Yet this breccia's siderophile levels (11 µg/g Ni, <1.4 ng/g Ir) are remarkably low, by lunar or HED polymict-breccia standards. Hughes 004 is classified as a howardite, yet our data from two separately acquired chip allocations show siderophile levels very similar to FRO 97045. This is puzzling, because our other data (e.g., Mg = 84–85 mg/g, V = 100–124 µg/g) confirm the howardite classification.

References: [1] Farinella P. and Davis D. R. *Icarus* 97:111–123. [2] The Meteorological Bulletin, no. 84. *Meteoritics & Planetary Science*.

5064

KREEP: A KEY, AND STILL ENIGMATIC, ASPECT OF THE MOON'S GLOBAL DIFFERENTIATION

Paul H. Warren¹ and Dianne J. Taylor². ¹Institute of Geophysics, UCLA, Los Angeles, CA, USA. E-mail: pwarren@ucla.edu. ²Department of Earth and Space Sciences, University of California, Los Angeles, CA 90095-1567, USA.

KREEP, the main repository of lunar incompatible elements, is known more as a chemical component thoroughly disseminated in polymict impactites than as a common variety of pristine igneous rock. Yet the Lunar Prospector mission showed that in a global sense KREEP (as exemplified by Th [1]) is not widely disseminated. About 52% of the Moon's regolith Th is confined within the Procellarum KREEP Terrain (PKT), an oval centered at ~20°N, 30°W, and comprising ~15% of the global surface. Despite a partial veneering by moderate-Th mare basalt, the PKT's average surface Th (5 µg/g) is 6× the average (0.83 µg/g) for the other 85% of the lunar surface [2].

The greatest unresolved issue concerning KREEP is its vertical distribution within the PKT. Many of the highest-Th areas are within a few hundred km of Imbrium, locales where the megaregolith is rich in Imbrium ejecta. But the PKT's center is hundreds of km south of Imbrium's. Wilhelms [3] argued for a mostly Imbrium provenance for the Fra Mauro Formation, exemplary south-PKT sampled by Apollo 14. Cratering physics [4] indicates the local upper megaregolith should consist of ~32% primary Imbrium ejecta plus two-thirds older debris churned by the primary ejecta. The churned component could be smaller if the primary-ejecta size distribution was unconventionally small. But for various reasons (e.g., analogy with Ap-16), the proportion of primary-Imbrium matter is probably neither <<25% nor >>50%. Yet this large Imbrium component is enigmatically hard to identify. The most distinctive large subset among the non-regolithic Ap-14 breccias is a group of clast-poor impact melts [5] with only moderate (by PKT standards) levels of KREEP. A N-to-S trajectory for the Imbrium impact is almost 90° from the direction inferred by [3]. An ultrahigh KREEP content for Imbrium ejecta is also not favored by the evident lack [6] of a Th anomaly linkable to the Imbrium antipode. Direct constraints on the vertical distribution of KREEP within the PKT come from young craters as "natural drills." PKT craters up to 55 km in *d* (e.g., Aristillus) typically show as Th highs. However, the deepest sampling, at Copernicus (*d* ~ 95 km, "drill sample" depth of order 5 km), is an obvious Th *low* [1]. Contrary to conventional assumptions, modeling of the density evolution of the last residual melt of the magma ocean suggests that urKREEP should have promptly and fairly efficiently concentrated near the surface, especially in an Ap-14-like region of relatively mafic-noritic crust.

The timing of the isolation of KREEP from the expiring magma ocean is another key issue that has not yet been resolved. Although coupled Sm-Nd [7] studies indicate it took >200 Ma after solar system formation for this process to occur, both the Hf-W (>60 Ma [8]) and the Lu-Hf (50–100 Ma [9]) chronometers imply a shorter time scale for primary silicate differentiation of the Moon and closure of the urKREEP reservoir.

References: [1] Lawrence D. J. et al. 2007. *Geophysical Research Letters*. [2] Warren P. H. 2005. *Meteoritics & Planetary Science* 40:477. [3] Wilhelms D. E. 1987. *The geologic history of the Moon*. [4] Haskin L. A. et al. 2003. *Meteoritics & Planetary Science* 38:13. [5] McKay G. A. et al. 1978. *Proceedings, 9th LPSC*. p. 661. [6] Garrick-Bethel I. and Zuber M. T. 2005. *Geophysical Research Letters* 32. [7] Rankenburg K. et al. 2006. *Science* 312:1369. [8] Touboul M. et al. 2007. *Nature* 450:1206. [9] Taylor D. T. et al. 2007. Abstract #2130. 38th LPSC.

5323

IMPACT MELTING AND ^{182}W ANOMALIES IN MAGMATIC IRON METEORITES

John T. Wasson. University of California, Los Angeles, CA 90095-1567, USA. E-mail: jtwasson@ucla.edu.

Introduction: Asteroidal impact processes produced large-scale metallic melts that migrated from the original formation site and engulfed relatively unaltered silicates. The classic example is the Portales Valley meteorite in which melt sheets having thicknesses of several cm are in contact with silicates that have retained metal and troilite (some S also seems to have moved through the gas phase). The very limited ranges in Ir fractionation observed in main-group IAB irons seems best explained by "crystal-settling" (from a large, $>1 \text{ km}^3$ melt) rather than by fractional crystallization responsible for large ranges in the magmatic groups (IIAB, IIIAB, IVA). The metal in IABs engulfed silicates some of which retained chondritic compositions including FeS and planetary rare gas. Slow heating by an internal heat source such as ^{26}Al would have caused early loss of FeS-rich and albite-rich melts and major outgassing of rare-gas hosts. Wasson et al. [1] argued that if, as indicated by the O-isotopic composition, the IVA irons formed from an L-LL chondritic precursor, impact melting offered a plausible mechanism to explain both the loss of the volatile metals Ga and Ge and the reduction of FeO to lower the Ni content of the metal. Although some researchers doubt that asteroidal impacts (mean impact velocity 5 km/s, 20% $>7 \text{ km/s}$) can produce large-scale (kilometer-scale) melts, the high porosity inherited from the first planetesimals would have greatly increased the efficiency of melt production.

Impact-Shock versus ^{26}Al Heating: Internal heating by ^{26}Al decay is temporally and spatially very different from impact heating. Heating by ^{26}Al is a very slow process producing the highest temperatures at the center of the asteroid; about 10^6 years are necessary to provide enough sensible and latent heat to increase the temperature from 1400 K where silicate melting begins to 1600 K, when large-scale melting leads to phase separation (core formation and/or basalt extrusion). A problem with an ^{26}Al model specific to the IVA iron meteorites is that separation of a basaltic magma would occur long before low-S metal melted at $\sim 1770 \text{ K}$.

^{182}W in an Impact-Heated Asteroid: A recent study by Burkhardt et al. [2] revealed $\epsilon^{182}\text{W}$ values (with no cosmogenic contribution) in magmatic iron meteorites (IVA Gibeon and IIAB Negrillos) that are marginally lower than the initial solar-system value obtained by analyzing refractory inclusions from CV3 chondrite Allende. Because nebular Hf is expected to be concentrated in chondrule mesostasis and clinopyroxene, much of the radiogenic ^{182}W was probably inside chondrules at the time of impact heating of the IVA asteroid. Rapid formation of a metallic melt and migration to the center of the asteroid can thus account for low amounts of radiogenic ^{182}W in the metal. The W isotopic composition then provides only a lower limit for the time of the impact. Because one would expect minor contamination by radiogenic W, the solar-system initial $\epsilon^{182}\text{W}$ was somewhat lower than that measured by [2] in these two irons.

References: [1] Wasson J. T., Matsunami Y., and Rubin A. E. 2006. *Geochimica et Cosmochimica Acta* 70:3149. [2] Burkhardt C., Kleine T., Bourdon B., Palme H., Zipfel J., Friedrich J., and Ebel D. Forthcoming. *Geochimica et Cosmochimica Acta*.

5112

COMPOSITION OF MATRIX IN C3.0 ACFER 094

John T. Wasson and Alan E. Rubin. University of California, Los Angeles, CA 90095-1567, USA. E-mail: jtwasson@ucla.edu.

Introduction and Experimental: The origin of the nebular fine fraction is a matter of contention. Some have proposed that it largely preserves the record of presolar materials [1], others that it is almost entirely the product of evaporation and recondensation in the solar nebula [2]. These end models lead to different predictions: uniform compositions for presolar fines, variable compositions for recycled fines.

The ACFer 094 ungrouped C3.0 chondrite appears to have largely avoided aqueous alteration and thermal metamorphism. It has volatile abundances similar to those in CM chondrites [3] but our recent analysis [4] showed a highly fractionated K/Na ratio (0.8, $10\times$ lower than mean CM-CO-CV). Evidence that it is especially primitive is the presence of anomalous ^{17}O -rich isotopic compositions [5].

We used a $3 \mu\text{m}$ electron microprobe beam to determine concentrations of 10 elements in 10 49-point grids, each $\sim 50 \mu\text{m}$ on a side. An advantage of this approach compared to broad-beam analysis is that we could develop criteria for eliminating anomalous points (e.g., those with excessive amounts of a mineral phase or low totals). The fraction of discarded points was 26%. Duplicate grid analyses on different days on the LAP 02342 CR chondrite showed excellent reproducibility.

Results and Discussion: Of special importance is S, the most volatile element in our set. We measured 29.5 mg/g S in the matrix; this is $1.33\times$ the bulk value of Dreibus et al. [3].

As observed in LAP 02342, compositions vary among grid areas; points that cluster on one diagram are resolved on other diagrams. On the K-Al diagram (Fig. 1), 3 grids are fully resolved from all other grids; the remainder overlap 1 other grid (2 points), 2 grids (1 point), or 3 grids (4 points). The cluster of 4 points (right-center in Fig. 1) resolve into 2 clusters on a Na-Al diagram; one of these has a unique composition on a S-Fe diagram.

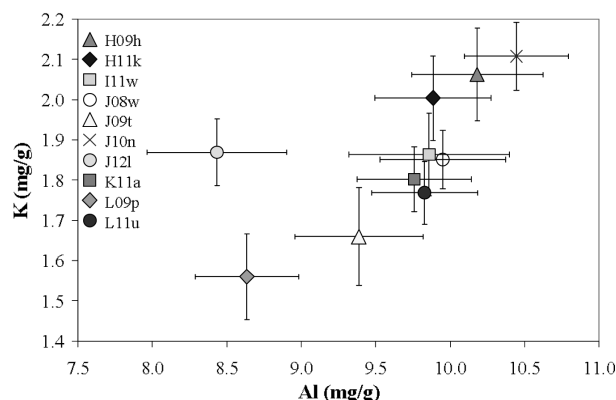


Fig. 1.

The simplest model to explain these variations is that the fine nebular fraction preserves a clumpiness in the distribution of phases vaporized or lost as mesostasis spray during chondrule forming events. We suggest that low-degree ($\sim 10\%$) melting of chondrule precursors created structures that survive nebular processing prior to agglomeration. That the same features are shared by ACFer and LAP implies that the processes were widespread.

References: [1] Alexander C. 2005. *Meteoritics & Planetary Science* 40:943. [2] Wasson J. Forthcoming. *Icarus*. [3] Dreibus et al. 1995. *Meteoritics* 30:439. [4] Rubin et al. *Geochimica et Cosmochimica Acta* 71: 2361. [5] Sakamoto et al. 2007. *Science* 317:231.

5125

METAL-RICH OLIVINE AGGREGATES IN THE RENAZZO CR CHONDRITE

M. K. Weisberg^{1, 2}, D. S. Ebel², H. C. Connolly Jr.^{1, 2}, N. T. Kita³, T. Ushikubo³, and J. W. Valley³. ¹Department Phys. Sci., Kingsborough College, City University New York, Brooklyn, NY 11235, USA. E-mail: mweisberg@kbcc.cuny.edu. ²Department Earth Planet. Sci., American Museum Natural History, New York, NY 10024, USA. ³Department Geology and Geophys., University Wisconsin–Madison, WI 53706, USA.

Introduction: Amoeboid olivine aggregates (AOA) are irregular-shaped, fine-grained aggregates of olivine (Ol) and refractory assemblages (anorthite, Ca-pyroxene, spinel, perovskite) [1–4]. AOA in CRs are particularly intriguing because some contain low-Fe, Mn-enriched (LIME) Ol similar to that in IDPs and Comets [5, 6] and some are metal-rich. AOA phases are ¹⁶O-rich consistent with a primitive origin, and formation from the same ¹⁶O-rich reservoir as CAIs [7]. Refractory minerals in CR AOA have ²⁶Mg excesses indicating ²⁶Al values as high as in CAIs suggesting they formed contemporaneously [7]. Here we report on 3 metal-rich AOA in Renazzo.

Results: We discovered three unusually metal-rich AOA in two small (cm-size) slabs of Renazzo using X-ray tomography. Slabs were cut to expose and polish surfaces for SEM, EMP, LA-ICPMS (trace element), and SIMS (O isotope) analysis. The AOA have highly irregular shapes and contain remarkable (50 μm size) metal blebs surrounded by thin coatings of fine Ol (Fig. 1) and central Ca-,Al-rich assemblages of Ca-pyroxene, anorthite and/or MgAl spinel with tiny (μm-size) perovskite. Metal is up to 15 vol%. The Ol in two AOAs has (wt%) 0.6–1.8 FeO, 0.1–0.3 MnO, and 0.02–0.3 Cr₂O₃. The other AOA (a2) has a high abundance of LIME Ol with 0.3–2.2 FeO, 0.1–0.6 MnO, and 0.1–0.4 Cr₂O₃; some has Fe/Mn ratios of 1. Metal has 5–7% Ni with solar Ni:Co. We are currently measuring O isotopes in Ol and trace elements in metal.

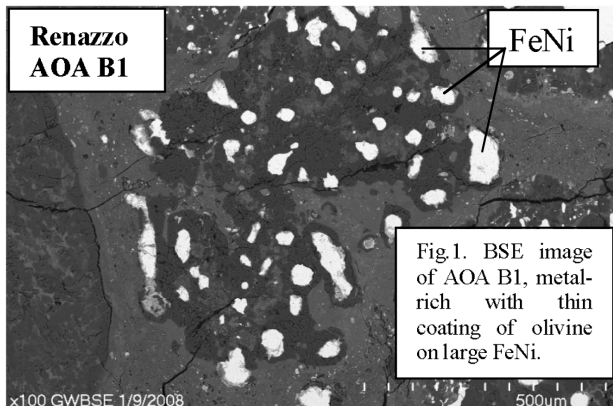


Fig. 1.

Discussion: These unusual AOA show minimal melting and are consistent with being aggregates of condensates. The metal was either captured by Ol, the Ol nucleated onto the metal or the metal formed by reduction of Fe from silicate. The latter hypothesis is unlikely and would require that the silicate was initially Fe (and Ni)-rich. Thus, the metal may be a primitive component incorporated into the inclusions.

References: [1] Grossman L. and Steele I. M. 1976. *Geochimica et Cosmochimica Acta* 40:149–155. [2] Aleon J. et al. 2002. *Meteoritics & Planetary Science* 37:1729–1755. [3] Weisberg M. K. et al. 2004. *Meteoritics & Planetary Science* 39:1741–1753. [4] Krot A. N. et al. 2004. *Chemie der Erde* 64:185–239. [5] Klöck W. et al. 1989. *Nature* 339:126–128. [6] Zolensky M. E. et al. 2006. *Science* 314:1735–1739. [7] Weisberg M. K. et al. 2007. Abstract #1588. 38th LPSC.

5290

COSMOGENIC RADIONUCLIDES IN PAIRED DIOGENITES FROM LAPAZ ICEFIELD, ANTARCTICA

K. C. Welten¹, M. W. Caffee², and J. Masarik³. ¹Space Sciences Laboratory, University of California, Berkeley, CA 94720–7450, USA. ²PRIME Laboratory, Purdue University, West Lafayette, IN 47907, USA. ³Nuclear Physics Department, Comenius University, Bratislava, Slovakia.

Introduction: Diogenites are the least abundant members of the HED achondrite clan. To date, only 11 diogenite falls have been reported, while more than 160 finds are known, including 122 from Antarctica and 44 from hot deserts; many of the Antarctic specimens belong to a few large showers, such as the Yamato (A) and (B) diogenites, which include ~70 specimens. Between 1991 and 2004, the ANSMET program recovered fourteen diogenites from a single location, LaPaz (LAP) icefield, of which at least 10 are believed to be paired. Noble gases and radionuclides have previously been reported for LAP 91900, indicating a CRE age of ~18 Myr [1], a pre-atmospheric radius of ~30 cm and a terrestrial age <30 kyr [2]. We now report cosmogenic ¹⁰Be, ²⁶Al, and ³⁶Cl in seven LAP diogenites to verify pairing and to study variations in radionuclide concentrations as a function of depth in a medium-sized object. Measured concentrations are compared with calculated depth profiles of ¹⁰Be, ²⁶Al, and ³⁶Cl obtained using the LCS model [2, 3].

Results and Discussion: The LAP diogenites show moderate to large variations in ³⁶Cl (25%), ¹⁰Be (40%), and ²⁶Al (80%). These variations are not due to compositional effects, because the 7 LAP diogenites are remarkably homogeneous (Table 1). The large variations in ²⁶Al are consistent with calculated depth profiles for objects of 30–45 cm in radius [2], assuming that LAP 02216, 03781, and 04844 were near the surface of the meteoroid (D < 5 cm), while LAP 91900, 03630, and 04839 came from the interior portion (D > 20 cm). Based on a constant ³⁶Cl production rate of 23 dpm/kg[Fe] (and small contributions from Ti, Cr, and Mn), we derived elemental ³⁶Cl production rates of ~160 to ~300 dpm/kg[Ca] for the LAP samples, which are also in excellent agreement with model calculations [3]. The excellent correlation between P(³⁶Cl)_{Ca} and P(²⁶Al) can be used to calculate ³⁶Cl production rates for howardites and eucrites, where ³⁶Cl production is dominated by spallation from Ca. These production rates will improve terrestrial age determinations for Antarctic and non-Antarctic achondrite finds.

Table 1. Concentrations of major elements (in wt%) and cosmogenic radionuclides (in dpm/kg) in LaPaz Icefield diogenites.

LAP	Mg	Al	Ca	Fe	¹⁰ Be	²⁶ Al	³⁶ Cl
91900	15.8	0.35	0.83	11.6	24.1 ± 0.5	78.5 ± 1.2	5.1 ± 0.2
02216	17.5	0.41	0.78	11.6	19.6 ± 0.4	53.6 ± 1.2	4.2 ± 0.1
03569	16.8	0.54	0.83	13.1	22.3 ± 0.9	63.8 ± 1.6	4.8 ± 0.1
03630	14.4	0.36	0.86	11.6	25.5 ± 0.8	77.7 ± 2.0	5.3 ± 0.1
03781	15.7	0.38	0.83	12.6	20.0 ± 0.4	52.1 ± 1.5	–
04839	15.6	0.34	0.88	11.9	26.6 ± 0.5	82.4 ± 2.3	–
04844	15.5	0.35	0.86	12.4	19.2 ± 0.4	46.3 ± 1.2	4.3 ± 0.1

References: [1] Welten K. C. et al. 1997. *Meteoritics & Planetary Science* 32:891–902. [2] Welten K. C. et al. 2007. *Nuclear Instruments and Methods in Physics Research B* 259:653–662. [3] Masarik J. and Reedy R. C. 1994. *Geochimica et Cosmochimica Acta* 58:5307–5317.

5305

STARDUST INTERSTELLAR PRELIMINARY EXAMINATION—FIRST RESULTS

A. J. Westphal¹, C. Allen², S. Bajt²⁷, R. Bastien², H. A. Bechtel¹⁸, P. Bleuet²², J. Borg³, F. Brenker⁴, J. Bridges⁵, D. E. Brownlee⁶, A. L. Butterworth¹, M. Burchell²¹, M. Burghammer²², B. Clark²⁶, P. Cloetens²², G. Cody¹³, T. Ferroir²⁷, C. Floss⁷, G. Flynn⁸, D. Frank¹, Z. Gainsforth¹, E. Grün⁹, P. Hoppe¹⁰, A. Kearsley¹¹, N. Kelley¹, L. Lemelle²⁷, H. Leroux¹², L. R. Nittler¹³, R. Lettieri¹, B. Mendez¹, W. Marchant¹, S. A. Sandford¹⁴, T. See², A. Simionovici¹⁵, F. Stadermann⁷, Z. Sternovsky²³, R. M. Stroud¹⁶, J. Susini²², S. Sutton²⁴, P. Tsou¹⁷, A. Tsuchiyama²⁰, T. Tyliczszak¹⁸, B. Vekemans²⁵, L. Vincze²⁵, J. Warren², M. E. Zolensky², and >23,000 Stardust@home dusters¹⁹. ¹Space Sciences Laboratory, UC Berkeley, CA, USA. E-mail: westphal@ssl.berkeley.edu. ²NASA Johnson Space Center, USA. ³IAS Orsay, France. ⁴Universität Frankfurt am Main, Germany. ⁵University of Leicester, UK. ⁶University of Washington, USA. ⁷Washington University, St. Louis, USA. ⁸SUNY Plattsburgh, USA. ⁹Max-Planck-Institut für Kernphysik, Germany. ¹⁰Max-Planck-Institut für Chemie, Germany. ¹¹The Natural History Museum, London, UK. ¹²Université des Sciences et Technologies de Lille, France. ¹³Carnegie Institution of Washington, USA. ¹⁴Ames Research Center, USA. ¹⁵Observatoire des Sciences de l'Univers de Grenoble, France. ¹⁶Naval Research Laboratory, USA. ¹⁷Jet Propulsion Laboratory, USA. ¹⁸Advanced Light Source, LBNL, USA. ¹⁹Worldwide. ²⁰Osaka University, Japan. ²¹University of Kent, UK. ²²ESRF, Grenoble, France. ²³University of Colorado, Boulder, CO, USA. ²⁴Advanced Photon Source, ANL. ²⁵University of Ghent, Belgium. ²⁶Lockheed-Martin Corporation, USA. ²⁷DESY. ²⁸ENS Lyon, France.

The Stardust spacecraft exposed an aerogel and aluminum foil collector to the interstellar dust stream for a total of 195 days before its encounter with comet P81/Wild2. We report the first results of the Stardust Interstellar Preliminary Examination. This is a formidable task because of the large collecting area (~1000 cm²), the small expected statistics (a few dozen particles), the diminutive size of the captured particles (<1 μm), the challenging nature of the collecting media, and the requirement that only minimally destructive techniques be used. We have close coupling between state of the art techniques and these challenging samples. The first analyses have been performed using aerogel keystones and picokeystones [1] extracted directly from the Stardust Interstellar Collector in order to preserve trajectory information. In the first analyses we have focused on contamination and beam damage assessment, and on the composition of high-angle tracks that we considered to be likely secondary ejecta from impacts of meteoroids on the spacecraft. These tracks were discovered by a consortium of >23,000 “citizen scientists” worldwide using the Stardust@home virtual microscope tools. We have confirmed this identification of secondary ejecta by the identification of Ce and Zn in these particles, but also detected evidence for extraterrestrial material from the original impactors in the form of Fe, Ni, and Mg. FTIR and STXM analyses give quantitative upper limits on extraterrestrial organics, and have allowed for the quantitative evaluation of beam damage and carbon deposition during analyses. We have also identified alumina as a contaminant in the aerogel. No measurements have yet been made on the Al foil collectors.

References: [1] Westphal A. J. et al. 2004. *Meteoritics & Planetary Science* 39:1375.

5081

CHONDRULES, CAIs, AND DUST IN PROTOPLANETARY DISKS IN THE FRAMEWORK OF PHOTOPHORETIC FORCES

G. Wurm¹, H. Haack², J. Teiser¹, A. Bischoff¹, and J. Roszjar¹. ¹Institut für Planetologie, University of Münster, Wilhelm-Klemm-Str. 10, D-48149 Münster, Germany. E-mail: gwurm@uni-muenster.de. ²Geological Museum, Øster Voldgade 5-7, 1350 Copenhagen K, Denmark.

Introduction: Transport processes are fundamental to the early Solar System. In recent years it was proposed that photophoresis can be an important component in moving chondrules, CAIs, and dust over long and short range distances [1–3]. We relate first values from laboratory experiments to formerly assumed properties of chondrules and dust aggregates with respect to photophoresis.

Experiment and Estimate: The basic quantity in photophoretic transport models is the photophoretic force on particles itself. As many particle parameters enter (optical properties, thermal properties, and surface properties) only estimates could be given so far for dust aggregates and chondrules. In a first set of experiments we quantified photophoretic forces under microgravity at the drop tower in Bremen [4]. We used bare and dust mantled chondrules from the Bjurböle meteorite and mm-sized SiC dust aggregates.

The Photophoretic Picture: Chondrules, mantled chondrules, and dust aggregates represent a sequence in the strength of photophoretic forces for a given light source from low to strong, respectively [4]. Due to this variation in photophoretic strength, the different particle categories are transported differently in protoplanetary disks, radially and vertically. We will discuss some of the consequences. (1) Dust aggregates are transported to the surface of protoplanetary disks [5]. (2) In energetic events CAIs are transported over the surface of the disk from the inner system to several AU [5]. (3) All particles are strongly concentrated at dense inner disk edges [2, 3]. (4) Chondrules and mantled chondrules move to the asteroid belt region in late stage disk evolution [1]. (5) Photophoresis sorts particles according to size and other properties [1]. (6) Photophoresis transports dust particles to several tens of AU in late stage disk evolution [2].

References: [1] Wurm G. and Krauss O. 2006. *Icarus* 180:487–495. [2] Krauss O. et al. 2007. *Astronomy and Astrophysics* 462:977–987. [3] Haack H. and Wurm G. 2007. Abstract #5157. *Meteoritics & Planetary Science* 42:A62. [4] Teiser et al. 2008. This issue. [5] Haack H. and Wurm G. 2008. This issue.

5049

NATURAL OCCURRENCE OF A NEW MINERAL WITH AN OLIVINE STRUCTURE AND PYROXENE COMPOSITION IN THE SHOCK-INDUCED MELT VEINS OF TENHAM L6 CHONDRITE

Zhidong Xie, Thomas G. Sharp, Kurt Leinenweber, and Paul S. DeCarli.

Here we report a new mineral with an olivine structure and a pyroxene composition, which occurs in shock-induced melt veins of the Tenham L6 chondrite. This new phase was identified with transmission electron microscopy (TEM) using SAED and EDS. It occurs in clusters of acicular crystals in a glassy matrix within shock melt veins. The crystals have a distinctive curvature and aspect ratios up to 25, with width ranging from 5 nm to 20 nm and length up to 500 nm. EDS analyses provides relative cation abundances that are consistent with a pyroxene stoichiometry: $\text{Na}_{0.06}\text{Ca}_{0.02}\text{Mg}_{0.71}\text{Fe}_{0.20}\text{Al}_{0.11}\text{Si}_{0.94}\text{O}_3$. These compositions are similar to that of majorite garnet from the vein center and to that of the vitrified perovskite from the vein edge. Single-crystal and polycrystalline SAED patterns are consistent with the olivine structure and space group (Pbnm). The refined cell parameters for this orthorhombic structure are: $a = 4.782 \text{ \AA}$, $b = 10.119 \text{ \AA}$, and $c = 5.946 \text{ \AA}$. The new olivine-structured phase crystallized either at the rapidly quenched margins of large veins or within thin, $<30 \mu\text{m}$ melt veins. Our hypothesis is that the extremely rapid quench in these samples led to significant under-cooling of the melt to temperatures below the metastable melting curve of olivine. This allowed the rapid crystallization of the new phase with high-entropy compositional features and unusual morphologies.

Our diffraction and EDS data pose a problem of how to accommodate a pyroxene-like composition in an olivine structure. If we write an olivine chemical formula based on an enstatite composition ($\text{Mg}_{1.33}\text{Si}_{0.33}\Delta_{0.33}\text{SiO}_4$), the olivine structure requires 0.33 formula units of Si^{4+} in octahedral sites and 0.33 formula units of octahedral vacancies (Δ). If we do the same with our EDS data from new phase ($\text{Na}_{0.06}\text{Ca}_{0.04}\text{Mg}_{1.01}\text{Fe}_{0.29}\text{Al}_{0.10}\text{Si}_{0.24}$) $_{1.74}\Delta_{0.26}\text{Si}_{1.00}\text{O}_4$, the olivine structure requires about 0.25 formula units of Si^{4+} in octahedral M1 sites, about 0.25 formula units of vacant M sites (Δ), and 0.10 formula units of Na^+ and Ca^{2+} in M2 octahedral sites.

Our observations demonstrate that the olivine structure can accommodate a pyroxene-like composition with vacancies, Na^+ , Ca^{2+} , and excess Si^{4+} in octahedral sites at high-pressure and temperature. These defects may also be found in olivine from high pressure liquidus quench experiments. However, such quench products may not have been adequately characterized. If non-stoichiometry and excess silica occur in equilibrated olivines, one might expect them to also occur in hot regions of the deep upper mantle. We suggest that it would be useful to investigate the stability of this phase via ab initio calculations and high-pressure experiments.

5220

AROMATIC MACROMOLECULAR VARIATIONS OF INSOLUBLE ORGANIC MATTER FROM METAMORPHOSED CM2 OBSERVED IN SOFT X-RAY ABSORPTION ENERGY SHIFTS

H. Yabuta¹, G. D. Cody², C. M. O'D. Alexander³, and A. L. D. Kilcoyne⁴.

¹Department of Earth and Space Science, Osaka University, Japan.

²Geophysical Laboratory, Carnegie Institution of Washington, USA.

³Department of Terrestrial Magnetism, Carnegie Institution of Washington, USA.

⁴Advanced Light Source, LBNL, USA. E-mail: hyabuta@ess.sci.osaka-u.ac.jp.

Introduction: Metamorphosed CM2 chondrites experienced unique and diverse secondary processes. The complex histories of the individual meteorites are reflected in the elemental and isotopic variations of their insoluble organic matter (IOM) [1, 2]. On the other hand, solid state ¹³C NMR spectra of the IOM have shown no clear differences between them in the relative abundance or chemical shift of the dominant aromatic peak [3, 4]. Also, the weak exciton intensity (291.1 eV) in the carbon X-ray absorption near edge spectroscopy (C-XANES) spectra of their IOM are not as useful as those of type 3 chondrite IOM for evaluating the thermal histories [4, 5]. To try to better characterize changes in IOM structure associated with the secondary processes, this study has taken a close look at the lower photon energy range in C-XANES spectra of IOM from the metamorphosed CM2.

Experimental: The meteorite samples used in this study include: 5 kinds of metamorphosed CM2s (LEW 85311, Yamato- [Y-] 793321, Y-86720, PCA 91008, and WIS 91600), an unheated CM2 (Murchison), CI (Orgueil), and Tagish Lake. The IOM were prepared by demineralization of the bulk meteorites using a CsF-HF solution. The IOM was embedded into sulfur, microtomed to ~100 nm thickness, and was analyzed by XANES combined with scanning transmission X-ray microscopy (STXM).

Results and Discussion: Small but discernable energy shifts in the 285–287 eV range of the normalized C-XANES spectra are seen for the IOM from the 5 metamorphosed CM2s, while similar C-XANES spectral patterns without energy shifts are seen for the unheated CM, CI, and Tagish Lake IOM. The energy (eV) of the peak for C1s $\rightarrow \pi^*_{\text{C=C}}$ transition assigned to aromatic carbon is 285.1 for Murchison, 285.2 for LEW 85311, 285.3 for Y-793321 and WIS91600, 285.6 for Y-86720 and PCA 91008, respectively. Energy calibration using CO₂ absorption features and constant energy for the C1s (C=O) $\rightarrow \pi^*_{\text{C=O}}$ transition for all meteoritic IOM demonstrate that the energy shifts are not due to instrumental drift during the analyses. Similar behavior is reported for the specific chemical structure of a variety of aromatic polymers [6]. The energy shifts are not clearly correlated with the H/C ratio of IOM, but could be related to inductive effects of various side groups and/or hetero atoms (N, O) substitution in aromatic rings. In fact, the peaks for C1s $\rightarrow \pi^*_{\text{C=C}}$ for most of the metamorphosed CM2s are broader than those for the unheated CM and CI, which appears to indicate greater complexity in their aromatic structures as a result of the range of secondary processes they experienced.

References: [1] Alexander C. M. O'D. et al. 2007. *Geochimica et Cosmochimica Acta* 71:4380–4403. [2] Naraoka H. and Oba Y. 2007. Abstract #5096. *Meteoritics & Planetary Science* 42:A116. [3] Yabuta H. et al. 2005. *Meteoritics & Planetary Science* 40. pp. 779–787. [4] Yabuta H. et al. 2008. Abstract #2273. 39th LPSC. [5] Cody G. D. et al. Forthcoming. *Earth and Planetary Science Letters*. [6] Dhez et al. 2003. *Journal of Electron Spectroscopy and Related Phenomena* 128:85–96.

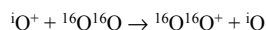
5205

SOME CONSIDERATIONS REGARDING OXYGEN COMPOSITION IN THE LUNAR SOIL

A. Yamada¹, Y. Hiraki², T. Seta³, K. Seki², Y. Kasai³, and M. Ozima¹.
¹Department of Earth and Planetary Science, University of Tokyo, Tokyo 113-0033, Japan. E-mail: yamada@eps.s.u-tokyo.ac.jp. ²University of Nagoya, Nagoya, Japan. ³National Institute of Information and Communications Technology (NICT), Tokyo, Japan.

Introduction: From the analyses of the Geotail Mission, Seki et al. [1] suggested that about 10% of O⁺ ions escaping from the terrestrial upper atmosphere encountered the lunar surface, which may be discernible if their isotopic composition were distinct from oxygen implanted on lunar soils by SW [2]. If confirmed, the existence of terrestrial oxygen would impose unparalleled means to trace the evolution of biotic oxygen atmosphere in the Earth through lunar soil studies. Here, we examined possible oxygen isotopic fractionation in the upper atmosphere above 100 km.

Methods: Current information on the isotopic composition of O either by measurements (e.g., [3]) or theoretical calculation is limited to <100 km, and is not useful in accessing the isotopic characteristics of oxygen ions, of which escaping must start above 100 km. We made 1-D numerical photochemical model on the isotopic composition of O⁺ including oxygen and nitrogen chemistry with ion, neutral, and electron processes in the altitude 100–800 km. In order to examine the isotopic composition of O⁺ (which includes ¹⁶O, ¹⁷O, ¹⁸O) at >100 km, we solved 60 sets of photochemical reaction equations including oxygen isotopes for 21 molecular species, atoms, ions, and electrons. Here, we considered the following three major reactions:



reaction rates are k_i , where $i = 16, 17, 18$.

Since reaction rates are not known, we examined the dependence of the isotopic composition of O⁺ on relative magnitude of reaction rates k_{17}/k_{16} and k_{18}/k_{16} on the above reactions. Although the basic scheme of our calculation is standard and similar to those by previous workers [e.g., 4], our calculation is the first attempt in examining the isotopic composition of O⁺ in high altitude (>100 km).

Results and Conclusions: We found that O⁺ number density overwhelms that of O₂⁺ above ~300 km, being consistent with the observation that Earth escaping ions are essentially O⁺.

Around 300 km where O⁺ number density reaches maximum, $\Delta^{17}\text{O}$ values show >20‰, provided that the reaction rates in the reactions for k_{17} and k_{18} are smaller by 10% than that of k_{16} . We are currently investigating to see if this much difference in reaction rate is theoretically feasible.

References: [1] Seki K. et al. 2001. *Science* 291:1939–1941. [2] Ozima M. et al. 2007. 38th LPSC. pp. 1129–1130. [3] Boering K. A. et al. 2004. *Geophysical Research Letters* 31:L03109. [4] Lyons J. R. 2001. *Geophysical Research Letters* 28:3231–3234.

5210

NANOSTRUCTURAL CHARACTERIZATION OF THE ALLENDE CV CHONDRITE AND L CHONDRITE USING POSITRONIUM TIME OF FLIGHT SPECTROSCOPY: THE HISTORY OF CHONDRITE PARENT BODY FORMATION

Akinori Yamada¹, Hiroyuki K. M. Tanaka^{2,3}, Yusuke Yamauchi⁴, Toshikazu Kurihara⁵, and Naoji Sugiura¹. ¹Department of Earth and Planetary Science, University of Tokyo, 7-3-1 Hongo, Bunkyo-ku, Tokyo 113-0033, Japan. E-mail: yamada@eps.s.u-tokyo.ac.jp. ²Earthquake Research Institute, the University of Tokyo, 1-1-1 Yayoi, Bunkyo-ku, Tokyo 113-0032, Japan. ³Atomic Physics Laboratory, RIKEN, 2-1 Hirosawa, Wako-shi, Saitama 351-0198, Japan. ⁴International Center for Materials Nanoarchitectonics (MANA), National Institute for Materials Science (NIMS), 1-1 Namiki, Tsukuba-shi, Ibaraki 305-0044, Japan. ⁵Slow Positron Facility, Institute of Materials Science Structure Science (IMSS), High Energy Accelerator Research Organization (KEK), 1-1 Oho, Tsukuba-shi, Ibaraki 305-0801, Japan.

Chondrites are classified according to magnitude of thermal metamorphism due to petrologic and mineralogical distinctions. From the shapes of the mineral grains in chondrites, one can infer whether or not the chondrites have been metamorphosed by thermal or pressure shocks. In this study, we investigated the nanostructural characteristics by depth-profiled positron spectroscopy with an aid of nitrogen absorption-desorption measurements, and compared between two different types of chondrites with or without chondrules that retain their original shape.

Nitrogen adsorption-desorption measurements were conducted on samples exploited from Allende (carbonaceous chondrite, CV3) and Yamato-74362 (ordinary chondrite, L6). The porosity was calculated by BJH method [1] and the specific surface area by BET method [2]. The observed pore size distribution is unimodal which comprises interparticle mesoporosity of 5 nm in diameter. The specific surface area is 12–16 m²/g that is larger than non-porous glass but smaller than typical mesoporous silica. There are two possibilities to explain the origin of those openings on the analogy to the mesostructure of mesoporous silica: (a) nanocluster coagulation and growth and (b) the vapor of a part of meteorites make holes.

Based on this information, we performed depth profiled positronium time of flight (Ps-TOF) spectroscopy, which serves to provide the accessibility of mesochannels [3, 4]. Such mesochannels form a passage allowing positronium atoms to diffuse and escape into vacuum. Ps-TOF measures the time between when Ps was generated in the mesoporous silica and when Ps escaped from the surface of the film. The results give a detailed picture of the structure and connectivity for different depths and different mesopore systems. An advantage of this technique is that contrary to the other SEM or TEM technique, we can dynamically obtain the accessibility of the pore system by tracking Ps atoms that diffuse out of the sample. Our goal is to understand the nanostructure of chondrites and to reveal the history of chondrite parent body formation.

Additional Information: If you have any questions, please send an e-mail message to H. K. M. Tanaka (ht@riken.jp).

References: [1] Brunauer S. et al. 1938. *Journal of the American Chemical Society* 60:309. [2] Barrett E. P. et al. *Journal of the American Chemical Society* 73:373. [3] Tanaka H. K. M. et al. 2005. *Physical Review B* 72:193408. [4] Tanaka H. K. M. et al. 2008. *Advanced Materials*.

5280

SUBSURFACE GEOLOGY OF MARE SERENITATIS AND SURROUND REGIONS OF THE MOON AS REVEALED BY THE LUNAR RADAR SOUNDER ONBOARD KAGUYA (SELENE)

A. Yamaji¹, Y. Yamaguchi², S. Oshigami², T. Ono³, A. Kumamoto³, H. Nakagawa³, T. Kobayashi⁴, and Y. Kasahara⁵. ¹Division of Earth and Planetary Sciences, Kyoto University, Kyoto 606-8502, Japan. E-mail: yamaji@kueps.kyoto-u.ac.jp. ²Department of Earth and Environmental Studies, Nagoya University, Nagoya 464-8601, Japan. ³Department of Geophysics, Tohoku University, Sendai 980-8578, Japan. ⁴Korea Institute of Geology and Mineral Resources, Daejeon 305-350, Korea. ⁵Information Media Center, Kanazawa University, Kanazawa 920-1192, Japan.

Introduction: Subsurface geology of the Serenitatis and its surrounding regions of the Moon was investigated by the Lunar Radar Sounder (LRS) onboard the Kaguya (Selene) spacecraft. LRS is capable of surveying to depths of several kilometers with a range resolution of <100 m and a footprint of several tens of kilometers. Mare Serenitatis, a circular Nectarian basin with a diameter of ~600 km, is a typical mascon basin with thick mare deposits and the topographic features thought to be the results of mascon tectonics [e.g., 1].

Results: Despite of simple data processing applied to data from each shot, LRS revealed subsurface stratifications. Numerous horizontal and subhorizontal interfaces were found under the mare. Most of their reflections were faint, but there were prominent ones as well.

We compared our results with those by Peeples et al. [2] who reported subsurface layering in the southern part of the region using the Apollo Radar Sounder Experiment (ALSE) data. LRS detected prominent reflectors at a depth of a few hundred meters below the mare surface in the area. Some of those were identified at the same or similar depths along neighboring tracks. From the ALSE data along the parallel at 20° N, two interfaces were depicted by previous researchers [2], but they have been not verified by LRS. Prominent reflectors evidenced by LRS in the southern Serenitatis were significantly shallower than them.

Mare ridges were largely tectonic in origin [2, 3]—there were folded or faulted strata found under the ridges in our data. Faults themselves were not imaged but ambiguously inferred by the discontinuity of reflectors.

Subhorizontal reflectors were found under highlands around Serenitatis. Signals from those reflectors were weak, but their apparent dip angles and/or inclinations were similar to each other under different tracks. Such coherence indicates the confidence of their existence. Strata under the northern highlands from Montes Caucasus to Lacus Somniorum showed basin-ward gentle tilting.

References: [1] Solomon S. C. and Head J. W. 1979. *Journal of Geophysical Research* 84:1667–1682. [2] Peeples W., Sill W., May T., Ward S., Phillips R., Jourdan R., Abbott E., and Killpack T. 1978. *Journal of Geophysical Research* 83:3459–3468. [3] Maxwell T. A., El-Baz F., and Ward S. H. 1975. *Geological Society of America Bulletin* 86:1273–1278.

5256

SPECTROSCOPIC STUDY OF NEARSIDE HIGHLAND BY REMOTE SENSING DATA AND APOLLO 16 ROCK SAMPLES

A. Yamamoto¹, T. Arai², M. Miyamoto³, and H. Takeda³. ¹Remote Sensing Technology Center of Japan, Japan. E-mail: aya@restec.or.jp. ²Antarctic Meteorite Research Center, National Institute of Polar Research, Japan. ³Department Earth and Planetary Science, the University of Tokyo, Japan.

Introduction: To understand lunar remote sensing data such as Clementine and Kaguya (Selene), studies of reflectance spectral data of returned Apollo samples are helpful as a substitute for the ground truth tour. In this study, we discussed the diversity of reflectance spectra of the nearside lunar highland, based on the spectral data of various types of Apollo 16 rock samples and remote sensing data of Apollo 16 landing site.

Methods: Bidirectional reflectance spectra from 0.3–2.5 μm were measured using a UV-visible-near IR spectrophotometer of the University of Tokyo. Rock chips and powdered samples were used for the spectral measurement and Halon powder was used for the standard. Composite absorption features in the spectra and calculated band parameters of orbital remote sensing sensors were discussed, instead of decomposing into individual absorption bands. For the remote sensing data analysis, images of Clementine UV-VIS camera were used. Mineralogical analyses were done by JEOL 8200 Electron Microprobe at National Institute of Polar Research.

Result and Discussions: Five Apollo 16 rock samples with different texture, modal abundance, and mineral composition were selected. Differences in rock textures are due to the extent of shock effect. In the sense of modal abundance and mineral composition, these five roughly represent compositional diversity and textural range of rock types in Apollo 16 site [1]. Remote-sensing data of the nearside highland around Apollo 16 site might be explained by the combination of spectral signature of the five samples to variable extent.

Composite absorption band positions around 1 and 2 μm of those samples shows consistent correlation with mineralogical diversity. Since 60025/60019 and 67016/67235/67667 were respectively located within a single pixel (100–300 m) of the Clementine onboard UV-VIS camera images, it was difficult to detect the systematic spectral difference of the rock samples from the imaging analysis result. With the orbital spectral data with a higher spacial resolution of several 10 meters (KAGUYA or future spacecraft instruments), spectral data of the each sampling site of 60### and 67### might reveal the spectral discrepancy due to the above compositional and textural varieties of the samples. There are some possible band combinations for detecting those spectral discrepancy using laboratory data.

References: [1] Korotev R. L. 1997. *Meteoritics & Planetary Science* 32:447–478. [2] Nozette et al. 1994. *Science* 266:1835–1839.

5162

MINERALOGICAL AND NOBLE GAS COMPOSITIONAL CHANGES IN THE NINGQIANG CARBONACEOUS CHONDRITE DURING EXPERIMENTAL AQUEOUS ALTERATION WITH WATER VAPOR

Y. Yamamoto^{1,2}, T. Nakamura³, T. Noguchi⁴, and K. Nagao¹. ¹Laboratory for Earthquake Chemistry, University of Tokyo, Japan. ²Environmental Science Center, University of Tokyo, Japan. E-mail: y-yamam@esc.u-tokyo.ac.jp. ³Department of Earth and Planetary Sciences, Kyushu University, Japan. ⁴College of Science, Ibaraki University, Japan.

Introduction: Carbonaceous chondrites that experienced aqueous alteration in their parent bodies might have changed its mineralogy and noble gas compositions. In the previous work [1], we performed experimental aqueous alteration with a water/rock ratio much higher than that expected in hydrous asteroids because it facilitates the reaction of aqueous alteration in a limited experimental duration. In this work, in order to simulate the condition close to the environment of hydrous asteroids, experimental aqueous alteration was performed to see reactions of anhydrous carbonaceous chondrite Ningqiang with water vapor. Bulk Ningqiang powder (μm in size) weighing 600 mg was loaded into gold tube and kept at 200 °C in an autoclave with 50 g liquid water. The sample powder and liquid water were placed separately to make reactions the sample and water vapor. After 0.5, 1, 2, 5, 10, and 20 days, 100 mg of the sample was recovered and the rest was kept being soaked for another days. Mineralogy and noble gases signatures of altered Ningqiang were characterized and the results were compared with those obtained in our previous work done with larger amounts of liquid water [1].

Results and Discussion: Mineralogical differences were hardly observed between liquid-water experiment and water-vapor one. In both experiments silicates and iron sulfide were decomposed and serpentine and hematite were formed. In contrast to the mineralogical changes, noble gas compositional changes differ between the two experiments. Primordial components such as Q and Ar-rich gases were more retained in the sample reacted with water vapor than those reacted with liquid water. During the alteration with water vapor, 86% and 8% of Q and Ar-rich gases, respectively, were retained in 20-day sample, whereas lesser portions of Q (28%) and Ar-rich (2%) gases were remained during the alteration with liquid water. The elemental ratio in the altered sample suggests that noble gases lost during water-vapor experiment were dominated by Ar-rich gas. The $^{36}\text{Ar}/^{132}\text{Xe}$ ratio of the released gas was 350, which is higher than that during liquid-water experiment (254). These ratios were in the range of Ar-rich gas in enstatite chondrites [2] and ureilites [3]. The higher $^{36}\text{Ar}/^{132}\text{Xe}$ ratio in the noble gases lost during the water-vapor experiment indicates that there was higher portion of Ar-rich gas in the noble gases lost during water-vapor alteration than those in lost noble gases during liquid-water one. These results suggest that selective loss of Ar-rich gas occurred during aqueous alteration with water vapor.

References: [1] Yamamoto Y. et al. 2005. 29th NIPR Symposium on Antarctic Meteorites. pp. 98–99. [2] Crabb J. and Anders E. 1981. *Geochimica et Cosmochimica Acta* 45:2443–2464. [3] Wacker J. F. 1986. *Geochimica et Cosmochimica Acta* 50:633–642.

5137

MINERALOGY AND SIZE DISTRIBUTION OF LARGE MICROMETEORITES RECOVERED FROM THE BLUE ICE FIELD AT CAPE TOTTUKI IN ANTARCTICA

Y. Yamauchi¹, T. Nakamura¹, M. Doi², and T. Nakamoto². ¹Department of Earth and Planetary Sciences, Graduate School of Sciences, Kyushu University, 6-10-1 Hakozaki, Fukuoka 812-8581, Japan. E-mail: yu-yama@geo.kyushu-u.ac.jp. ²Earth and Planetary Sciences, Tokyo Institute of Technology, 2-12-1, Ookayama, Meguro-ku, Tokyo 152-8550, Japan.

Antarctic micrometeorites (AMMs) used in this study were recovered from the blue ice field at Cape Tottuki in Antarctica [1]. Fine particles were separated into size fractions of 25–40, 40–100, 100–238, and >238 μm , and those used in this study were taken from the size range of 100–238 μm . 2046 particles of AMM candidates were hand-picked under an optical microscope. These include Antarctic moraine glacial sand as well as AMMs. Among them, 903 particles were identified as AMMs based on surface chemical composition using a SEM/EDS. Based on the degree of melting, AMMs are divided into three groups: spherules, scoriaceous, and unmelted. Then, three-dimensional shapes of most of AMMs including 530 spherules, 230 scoriaceous, and 77 unmelted AMMs were measured using an optical microscope, in order to obtain size distribution of AMMs in 100–238 μm fraction. The largest population is observed at size range from 125 to 140 μm . At smaller sizes, the population steeply decreases, probably because irregularly shaped AMMs with one >100 μm but two <100 μm dimensions went through the 100 μm sieve. At size range larger than 140 μm , the total population gradually decreases but the ratio of spherules to scoriaceous + unmelted AMMs increases with increasing size. This suggests that larger particles are subject to higher intensity of heating on atmospheric entry.

The bulk mineralogy of 19 unmelted AMMs was determined by synchrotron X-ray diffraction (S-XRD) using Gandolfi camera. Then they were polished and analyzed for major element abundances using an electron probe micro-analyzer. No phyllosilicate-rich samples were detected by S-XRD. Most samples consist of olivine, low-Ca pyroxene, magnetite, and minor magnesiowüstite and sulfides. Close inspection using an electron microscope revealed common occurrence of fibrous textures characteristic of phyllosilicates. Therefore, a majority of unmelted AMMs studied is decomposed products of hydrous micrometeoroids. Based on major element abundances, the AMMs are similar to CM, CI, and Tagish Lake carbonaceous chondrites. The similarity to hydrous carbonaceous chondrites is already known [e.g., 2] and this study confirms that the mineralogy of 100–238 μm AMMs is similar to that of smaller AMMs. One unmelted AMMs has mineralogy distinct from any hydrous carbonaceous chondrites and previously known AMMs. Therefore, it is a new type AMM.

References: [1] Yada T. and Kojima H. 2000. *Antarctic Meteorite Research* 13:9–18. [2] Kurat G. et al. 1994. *Geochimica et Cosmochimica Acta* 58:3879–3904.

5169

LUNAR IMPACT FLASHES BY GEMINID METEOROIDS IN 2007

M. Yanagisawa¹, H. Ikegami¹, M. Ishida², H. Karasaki³, J. Takahashi⁴, K. Kinoshita⁴, and K. Ohnishi⁵. ¹University Electro-Communications, Tokyo 182-8585, Japan. E-mail: yanagi@ice.ucc.ac.jp. ²Moriyama-shi, Shiga 524-0104, Japan. ³Nerima-ku, Tokyo 176-0002, Japan. ⁴Kobe University, Department of Earth and Planetary Sciences, Kobe 657-8501, Japan. ⁵Nagano National College of Technology, Nagano 381-8550, Japan.

Introduction: High-velocity impacts of large meteoric particles (meteoroids) onto the lunar surface generate optical flashes (lunar impact flashes). The frequency of bright flashes is usually low, i.e., once in several tens of hours for seventh in brightness magnitude. The flashes are thus difficult to observe. However, the impact velocities of meteoroids are several tens of km/s, and we can study the hypervelocity impact phenomena the velocity of which is not available in laboratory impact experiments, by means of Lunar Impact Flash observations. Further, we may be able to know the composition of meteoroid and lunar material by their spectroscopic studies in future.

The flashes have been confirmed by video observations for the Leonid [1–3] and Perseid [4] meteoric activities. Though the flashes have been reported during the Geminid activities [e.g., 5], none had been confirmed by independent observers separated far enough from each other to discard the possibility of satellite glints. Here, we report the first confirmed observation of Geminid lunar impact flashes.

Observations: During the Geminid activity on December 15, 2007, observers in Japan confirmed four lunar flashes (B, C, D, E) by small telescopes with apertures of about 20 cm in diameter. A flash (A) was also recorded with two independent video cameras attached to a 45 cm telescope in an observatory. Brightness magnitude (mag.) and duration are summarized in Table 1.

They must be caused by the impacts of Geminid meteoroids. The velocity vector is then known for them (33 km/s). Assuming that the optical energy is 0.2% of the kinetic energy of meteoroid, masses of meteoroids are estimated. They are listed in Table 1 with the impact angles measured from lunar local horizon.

Table 1. Geminids lunar impact flashes on December 15, 2007.

Flash	Time (UT)	Mag.	Duration (s)	Mass (kg)	Impact angle
A	8:28:18	9	0.033	0.1	51
B	8:54:25	6	0.017	2	57
C	8:55:26	5	0.32	3	42
D	9:13:36	7	0.05	0.8	79
E	10:08:10	5	0.32	5	47

Discussion: It is interesting to note that Flash B appeared only in a half-frame of video (1/60 s), while the others were followed by after-glows (long duration). The contrast may be due to the difference in physical properties of target (lunar surface) and/or projectile (meteoroid).

References: [1] Dunham D. W. et al. 2000. Abstract #1547. 31st LPSC. [2] Ortiz J. L. et al. 2000. *Nature* 405:921–923. [3] Yanagisawa M. and Kisaichi N. 2002. *Icarus* 159:31–38. [4] Yanagisawa M. et al. 2006. *Icarus* 182:489–495. [5] Suggs R. M. *Earth, Moon and Planets*, doi:10.1007/s11038-007-9184-0.

5067

TISHOMINGO IRON METEORITE: A UNIQUE MICROSTRUCTURE AND THERMAL HISTORY

J. Yang¹, J. I. Goldstein¹, J. R. Michael², P. G. Kotula², A. Grimberg³, and I. Leya³. ¹Department of Mechanical and Industrial Engineering, University of Massachusetts, Amherst, MA 01003, USA. E-mail: jiyang@ecs.umass.edu. ²Materials Characterization Department, Sandia National Laboratories, Albuquerque, NM 87185, USA. ³Physikalisches Institut, Universität Bern, CH-3012 Bern, Switzerland.

Introduction: Most metal in irons, stony irons, and chondrites contains a region of martensite (α_2) at $< \sim 28$ wt% Ni and a cloudy zone (spinodal) microstructure at $> \sim 28$ wt% Ni in the em-shaped Ni profile in taenite [1]. The cooling rates of these meteorites are from ~ 1 to 10,000 °C/Myr. Tishomingo contains 32.5 wt% Ni and is composed of 80 vol% martensite and 20 vol% taenite [2, 3]. The presence of martensite and the lack of a spinodal structure make Tishomingo unique. In order to understand how this unique meteorite formed we determined its microstructure and chemistry using SEM, AEM, and EBSD, and its cosmic ray exposure (CRE) age by measuring the noble gases.

Results: SEM and EBSD data show that residual taenite is single crystal fcc, but martensite is composed of both fcc and bcc phases which have a Kurdzumov-Sachs (K-S) or Nishiyama-Wasserman (N-W) orientation relationship. Some of the fcc phases in martensite have a similar crystallographic orientation to the residual-original fcc taenite, but some do not. Some of the bcc phases in martensite have K-S or N-W orientation relationship with residual-original fcc taenite. However, some bcc phases are not directly associated to the original taenite. AEM results from TEM thin foils obtained by focused ion beam (FIB) shows that in the martensite region the Ni content changes from ~ 4 wt% to ~ 55 wt%. The AEM data confirm that martensite contains bcc α and fcc γ phases [2, 3].

Noble gas measurements show that Tishomingo was exposed to space as a meteoroid with a pre-atmospheric radius of 20–40 cm for a remarkably short time of about ~ 30 –70 Myr.

Discussion: Tishomingo is a large taenite single crystal. To produce such a structure, the cooling rate during solidification at around 1450 °C was slow. The solidification process would require that the meteorite was buried deeply inside its parent body. The fact that martensite forms rather than a spinodal structure indicates that Tishomingo cooled so fast at 250 °C that spinodal decomposition did not take place. Therefore, it is probable that after solidification, the parent body broke up before the temperature reached ~ 250 °C. This break up may have happened as early as a few hundreds to a few millions of years after solidification. Tishomingo relocated very close to the surface of a second generation parent body, but farther than 1 meter below the body's surface. A recent break-up event took place at least ~ 30 –70 Myr ago (no information about the terrestrial age) and Tishomingo became a meter-sized meteoroid.

The EBSD and AEM data suggest that, after martensite formed, Tishomingo experienced a rapid reheating probably by impact which converted some of the newly formed bcc martensite to fcc. Subsequent cooling/annealing results in the formation of bcc α and fcc γ in residual martensite.

References: [1] Zhang J. et al. 1991. *Geochimica et Cosmochimica Acta* 57:3725–3735. [2] Buchwald V. F. 1975. *Handbook of iron meteorites*. UC Press. [3] Ives L. K. et al. 1978. *Geochimica et Cosmochimica Acta* 42: 1051–1066.

5145

CONDITIONS FOR COMPOUND CHONDRULE FORMATION

S. Yasuda¹ and T. Nakamoto². ¹Pure and Applied Sciences, University of Tsukuba, Japan. E-mail: yasuda@geo.titech.ac.jp. ²Earth and Planetary Sciences, Tokyo Institute of Technology, Japan.

Introduction: Chondrules are spherical-shaped silicate particles that are one of the main components of chondritic meteorites. They are thought to have been formed by heating (melting) events in the early solar nebula. There are compound chondrules, which are two or more chondrules fused together, in the various kinds of chondrites. Some compound chondrules seem to be formed by collisions of two independent particles during heating events. Although some researchers noticed collision probability of particles so far [1, 2], they seldom noticed the collision conditions. If two melting particles experience the high-speed or grazing collision, they cannot coalesce. Or if the viscosities of both components are too low, they cannot keep their shape and will fuse together by surface tension and we cannot observe them as compound chondrules. Thus we are necessary to consider the collision conditions to compare the various formation models for compound chondrules with the observational results. In this study, we numerically simulated the collision of two silicate drops by using the three-dimensional hydrodynamics code and examined the collision conditions for compound chondrule formation.

Condition for Coalescence: Firstly, we examined “condition for coalescence” for various parameters: the collision velocity, the collision angle, the size ratio of drops, and viscosities of drops. We can categorize the results of drops’s collisions into three groups: “stretching separation,” which occurred when the collision angle is large, “fission,” which occurred when the collision velocity is large, and “coalescence.” If the drops have relatively lower viscosities (1 poise), our results agree well with water and organic matter drops’s collision experiments [3, 4]. In this case, the maximum velocity for coalescence (u_{\max}) is about 5 m/s. In the larger viscosity case, because the viscous dissipation becomes effective, the region of coalescence is expanded to larger collision velocity and collision angle. For example, when the viscous coefficients are 10 poise and 100 poise, u_{\max} is about 15 m/s and 50 m/s, respectively. In addition, we found that the boundary of coalescence—stretching separation and coalescence—fission can be expressed by comparing the kinetic energy, surface energy, viscous dissipation, and rotational energy. Then we can obtain the condition for coalescence for various parameters.

Condition for Keeping Their Shape: If we add “condition for keeping their shape” to these results, we will be able to obtain the collision conditions for the compound chondrules formation. In order to keep their shape, the deformation time scale has to be longer than the cooling time scale. We can examine the deformation time scale using our numerical simulations. For example, when the drops has lower viscosity (1 poise), this time scale is $\sim 10^{-4}$ s. Moreover, we found that this time scale is approximately proportional to the viscosity of drops.

It is necessary for compound chondrules formation to satisfy both conditions and we should consider them when we compare the formation models with the observational results.

References: [1] Sekiya M. and Nakamura T. 1996. *Proceedings of the NIPR Symposium on Antarctic Meteorites* 9:208–217. [2] Miura H., Yasuda S., and Nakamoto T. 2008. *Icarus* 194:811–821. [3] Ashgriz N. and Poo J. Y. 1990. *Journal of Fluid Mechanics* 221:183–204. [4] Qian J. and Law C. K. 1997. *Journal of Fluid Mechanics* 331:59–80.

5285

MINERALOGICAL AND Pb-ISOTOPIC STUDY OF AN ALLENDE CAI

M. Yoshitake¹ and K. Yamashita². ¹Antarct. Meteorite Res. Center, National Inst. of Polar Res., 1-9-10 Kaga, Itabashi, Tokyo 173-8515, Japan. E-mail: yoshitake.miwa@nipr.ac.jp. ²Institute for Study of the Earth’s Interior, Okayama University, Yamada 827 Misasa, Tottori 682-0193, Japan.

Introduction: Calcium-aluminum-rich inclusions (CAIs) consist of high temperature minerals in the solar nebula. CAIs show the oldest age in the Solar System [1]. In addition, there are report that difference minerals in a CAI show difference formation age [2]. On the other hand, chondrules have no evidence of live-²⁶Al [3] and evidence of live-²⁶Al [4]. In order to reveal the formation time interval between CAIs, chondrules, and each mineral, it is need the high-precision chronometer. There are some reports about Pb-Pb age of CAIs and chondrules [1, 5]. However there are not many systematically studies of mineralogical and isotopic about CAIs. We applied new sample preparation method to link mineralogical and petrological studies to the absolute age. This is preliminary report.

Sample Preparation: CAI (KA01) was picked up from chip of Allende meteorite. This chip was cut into two thin sections and three chips. The thin sections were coated with a 30 nm thick carbon film for analyzing of electron microscopy.

The fragment of CAI was carved out from the one of chips. In order to analyses for Pb-isotopes, this fragment was grinded to powder as two fractions. These powders (13.78 mg and 16.51 mg) were applied 6 steps and 10 steps chemical treatment using HCl, HNO₃, and HF. After dissolution of each fraction, Pb was separated by through column containing ~ 50 μ l of anionite AG50W x8 for analyzing using TIMS at Kobe University. We applied isotope dilution method using ²⁰³Pb spike by NIST. We prepared total 16 blanks at the same time.

After column chemistry, we collected the residue. We observed the residue by FESEM-EDS at Hokkaido University.

Results and Discussion: Major minerals of KA01 were melilite and spinel. These minerals are probably primary phase. It is surround by spinel and fassaite rim. Anorthite and grossular occur near the rim and crack. Hedenbergite is rare. It is block in shape and occurs in the crack. These minerals seem to be secondary phases. Perovskite grains are in melilite grand-mass. These textures and their mineral assemblage indicate that KA01 is type A CAI. ²⁰⁷Pb/²⁰⁶Pb ratios in this CAI are from 0.61625 to 0.62932. ²⁰⁶Pb/²⁰⁴Pb ratios are from 28.33 to 415.05. These date are not plotted single isochron. Pb-isotopic compositions of each fraction slightly differed. We observed minerals in several residues. First step of residue consist of spinel grains and Al-rich material. Last step residue is almost Al-rich material. There are no silicate minerals in the residues.

These results indicate followed possibility. (1) Each mineral or each fraction have different Pb-isotopic composition. (2) Mass fractionation occurred during chemical treatment. (3) There are multiple sources of Pb-isotopes. Further investigation into details is required.

References: [1] Amelin Y. et al. 2002. *Science* 297:1678–1683. [2] Yoshitake M. and Yurimoto H. 2006. Abstract #90604. 19th General Meeting of the International Mineralogical Association. [3] MacPherson G. J. et al. 1995. *Meteoritics* 30:365–386. [4] Bizzarro et al. 2004. *Science* 431:275–278. [5] Krot A. N. et al. 2005. *Nature* 436:989–992.

5122

MINERALOGICAL AND RAMAN SPECTROSCOPIC STUDIES OF NORTHWESTERN AFRICA 2977 LUNAR METEORITE

Aicheng Zhang and Weibiao Hsu. Purple Mountain Observatory, Nanjing 210008, China. E-mail: aczhang@pmo.ac.cn.

Introduction: Northwest Africa (NWA) 2977 is a newly found lunar cumulate olivine gabbro. It is composed of olivine, low-Ca and high-Ca pyroxenes, and plagioclase with some minor phases [1]. Olivine and pyroxenes commonly exhibit radiation fractures, and plagioclase is partially converted to maskelynite, indicating a shock history. Here, we report mineralogical and Raman spectroscopic studies of this meteorite.

Results and Discussion: One polished thick section of NWA 2977 was studied using a scanning electron microscope (SEM), an electron microprobe (EMP), and a Raman microprobe (RMP). Modal abundances of the section are 40 vol% olivine (Fo₆₈), 50 vol% pyroxene (low-Ca: Wo_{2.5-20.5}En_{58.3-70.8}Fs_{21.0-28.9}, high-Ca: Wo_{32.3-44.6}En_{38.7-51.9}Fs_{12.8-17.1}), 7 vol% plagioclase (An_{80.1-93.5}Ab_{5.4-12.9}Or_{0.9-7.5}), 0.5 vol% oxide (Ti,Al-rich chromite, ilmenite, and baddeleyite) and sulfide, 0.2 vol% phosphate (apatite and whitlockite), and 0.1 vol% K-feldspar. NWA 2977 shows a cumulate texture of euhedral olivine and pyroxene grains. Plagioclase usually occurs interstitially between olivine and pyroxenes along with other minor phases (e.g., apatite, whitlockite, ilmenite, K,Ba-rich feldspar, and baddeleyite). Some olivine grains contain melt inclusions, but pyroxene grains do not. The melt inclusions are partially or completely crystallized and contain various mineral assemblages. Mineral assemblages in some melt inclusions are similar to those interstitial materials. Other inclusions contain Si,Al-glasses or pyroxene, K-rich glass (5.08 wt% K₂O), and Ca-rich glass (11.65 wt% CaO). The average Fe-Mn ratios of olivine and pyroxene are 99 and 52, respectively, consistent with previous results [1].

Two thin melt veins and some irregular melt pockets are observed in the section. In this study, a 25 μm wide melt vein and some large grains of olivine, pyroxene, and Ti,Al-rich chromite are analyzed with a Raman microprobe. Raman spectra of minerals within and adjacent to the vein exhibit low-pressure characteristics. One large Ti,Al-rich chromite grain (170 μm) shows two sets of light lamellae (<2 μm wide) on its BSE image. EMPA results show no compositional difference between the chromite host and lamellae. The Raman spectrum of the chromite host has a broad band centered at 669 cm⁻¹ and a relatively weak band centered at 507 cm⁻¹; whereas that of the lamellae shows a broad band at 669 cm⁻¹ and two relatively sharp bands at 400 cm⁻¹ and 287 cm⁻¹. The 400 cm⁻¹ band can be attributed to spinel, but the nature of 287 cm⁻¹ band is unclear. These Raman peaks are different from those of pure chromite and its high-pressure polymorphs in ordinary chondrite [2, 3]. The Raman spectra suggest that the lamellae could be assemblage of chromite, spinel, and other oxides, which are decomposition products of Ti,Al-rich chromite under high pressure. A detailed analysis is in progress.

Acknowledgements: The sample used in this study was generously provided by Mike Farmer.

References: [1] Bunch T. E. et al. 2006. Abstract #1375. 36th LPSC. [2] Chen M. et al. 2003. *Geochimica et Cosmochimica Acta* 67:3937–3942. [3] Zhang A. C. et al. 2006. *European Journal of Mineralogy* 18:719–726.

5159

A LARGE FRACTION OF INTERSTELLAR DUST WITH SOLAR ISOTOPIC COMPOSITIONS. Zhukovska¹, H.-P. Gail¹, and M. Tieloff². ¹Zentrum für Astronomie, Ruprecht-Karls-Universität Heidelberg, Albert-Überle-Str. 2, D-69120 Heidelberg, Germany. ²Mineralogisches Institut, Ruprecht-Karls-Universität Heidelberg, Im Neuenheimer Feld 236, D-69120 Heidelberg, Germany. E-mail: trieloff@min.uni-heidelberg.de.

Introduction: Meteorites contain circumstellar dust with strong isotopic anomalies that reflect the nucleosynthesis of the host stars where they condensed in the stellar outflow [1]. The abundance of isotopically anomalous circumstellar grains is low, generally <1 permil [1], and commonly ascribed to processing in the protoplanetary disc of the early solar system which erased isotope anomalies by mixing, intragrain diffusion, evaporation, and condensation. In contrary, for the outer disk of the early solar nebula where comets formed, considerably higher abundances of surviving stardust were expected [2]. However, among comet Wild 2 particles returned by the Stardust mission only one circumstellar dust grain was identified up to now [2]. Although few cometary particles rich in refractory Ca, Al, or of forsterite composition could be the result of radial mixing processes from the inner to the outer early solar system, the high fraction of isotopically normal (solar) cometary matter seems surprising, the more as some isotopically normal particles like GEMS were long considered as primary candidates for interstellar grains.

Model: We present a model based on our previously published calculations [3] of condensation of stardust (SiC, carbon dust, silicates, iron) in AGB star outflows and supernovae, that account for variations of elemental abundances, mass loss rates, stellar atmospheric temperature, density profiles, and outflow velocities during AGB evolution. In order to appropriately model interstellar dust abundance resulting from various star populations at the time of solar system formation, we furthermore modelled the galactic chemical evolution at the solar circle, as the abundance of the different stardust species will significantly vary with increasing metallicity. We also added a model component that describes grain processing in the interstellar medium and accounts for (i) cycling of matter between stars and interstellar matter on time scales of 2500 Ma, (ii) grain destruction by supernova shocks resulting in average lifetimes of stardust grains of 400–600 Ma, and (iii)—in order to explain the high condensation degree in the diffuse interstellar medium—condensation processes in cold, dense molecular clouds.

Results: An important result is that molecular cloud grown silicates are about 200 times more abundant than stardust silicates, implying that 5000 ppm is the maximum stardust abundance expected for a comet consisting entirely of interstellar material. This value is close to the initial estimate by Messenger et al. [4], but other IDPs (from possibly other cometary sources) display a lower abundance, down to 500 ppm which would mean that 90% of this matter experienced processing in the solar nebula disc.

References: [1] Nittler L. R. 2003. *Earth and Planetary Science Letters* 209:259. [2] McKeegan K. D. et al. 2006. *Science* 314:1724. [3] Zhukovska S., Gail H.-P., and Tieloff M. 2008. *Astronomy and Astrophysics* 479:453. [4] Messenger S. et al. 2003. *Science* 300:105.

5265

PIECES OF KUIPER BELT BODIES IN METEORITES

M. E. Zolensky¹, M. Gounelle², G. Briani², W. Bottke³, E. Young⁴, K. Dyl⁴, and M. K. Weisberg⁵. ¹NASA Johnson Space Center, Houston, TX 77058, USA. E-mail: michael.e.zolensky@nasa.gov. ²Muséum National d'Histoire Naturelle, Paris, France. ³Southwest Research Institute, Boulder, CO 80302, USA. ⁴Institute of Geophysics and Planetary Physics, UCLA, Los Angeles, CA 90095, USA. ⁵Kingsborough Community College, Brooklyn, NY 11235, USA.

Implications of the Nice Model: The Nice model [1–3] describes a scenario whereby the Jovian planets experienced a violent reshuffling event ~3:9 Ga. Jupiter and Saturn crossed a mutual mean motion resonance, existing small body reservoirs were depleted or eliminated, and new reservoirs were created in particular locations [1–6]. One problem with the Nice model is that it predicts that transported Kuiper Belt objects (KBOs) (resembling D class asteroids) should predominate in the outer asteroid belt, whereas only about 10% of the outer main asteroid belt actually look like D-class objects. However, Bottke et al. [7] argue that more than 90% of the objects captured in the outer main belt could have been eliminated by impacts if they had been weakly indurated objects. These disrupted objects should have left behind pieces in the ancient regoliths of other, presumably stronger asteroids [8]. Thus, a derived prediction of the Nice model is that ancient regolith samples (regolith-bearing meteorites) should contain fragments of collisionally destroyed Kuiper belt objects.

Xenoliths in Meteorites: We have previously searched through regolith-bearing meteorites to locate and characterize the most common types of meteorite xenoliths. At that time these materials were generally called C1- or C2-clasts, or “dark inclusions” in the literature, and were reported in many types of meteorites. We concluded that these clasts were most commonly similar to CM2 and CR2 chondrites [9–11], but that significant differences exist (which we will discuss in the presentation), and that in fact similarities to unmelted Antarctic meteorites were more apparent [8, 12, 13]. Note that we draw a critical distinction between these xenolithic clasts and cognate clasts (often called “dark inclusions”) such as the metamorphosed CV clasts in CV3s [14] and pure matrix clasts such as those found in Sharps and Vigarano [11]. We are examining clasts in 13 HEDs, 21 ordinary chondrites, 1 aubrite, 15 carbonaceous chondrites, and Kaidun. Recent advances in technology now permit us to measure bulk O isotopic and majors though trace elements of sub-mm-sized discrete clasts. Our new investigation will therefore serve to establish relationships of these clasts (if any) to established meteorites groups, micrometeorites, IDPs, or Wild 2 materials.

References: [1] Tsiganis et al. 2005. *Nature* 435:459–461. [2] Morbidelli et al. 2005. *Nature* 435:462–465. [3] Gomes et al. 2005. *Nature* 435:466. [4] Levison et al. Forthcoming. *Icarus*. [5] Nesvorný et al. 2007. *The Astrophysical Journal* 133:1962–1976. [6] Strom et al. 2005. *Science* 309:1847–1950. [7] Bottke et al. 2008. Abstract #1447. 39th LPSC. [8] Gounelle et al. 2008. In *The Solar System beyond Neptune*. Tucson, Arizona: The University of Arizona Press. 525 p. [9] Buchanan et al. 1993. *Meteoritics* 28:659–682. [10] Zolensky et al. 1993. *Meteoritics* 27:596–604. [11] Zolensky et al. 1996. 27th LPSC. pp. 1507–1508. [12] Gounelle et al. 2005. *Geochimica et Cosmochimica Acta* 69:3431–3443. [13] Gounelle et al. 2003. *Geochimica et Cosmochimica Acta* 67:507–527. [14] Krot et al. 1995. *Meteoritics* 30:748–775.

5261

AQUEOUS ALTERATION OF CM2 CHONDRITES EVALUATED WITH KINETIC MODELS

M. Yu. Zolotov¹ and M. V. Mironenko². ¹School of Earth and Space Exploration, Arizona State University, Tempe, AZ 85287, USA. E-mail: zolotov@asu.edu. ²Vernadsky Institute, Russian Academy of Sciences, Moscow 119991, Russia.

Introduction: CM2 carbonaceous chondrites reveal early stages of low-temperature aqueous alteration in a parent asteroid [e.g., 1–3]. Secondary phyllosilicates (cronstedtite, serpentine), some magnetite, and tochilinite in fine-grained matrices and chondrule rims imply hydration and oxidation of primary olivine, enstatite, and kamacite. Secondary mineralogy also indicates special and temporal variations in solution pH [4]. Here we model sequences of mineral dissolution and precipitation, chemical evolution of solution, and time scales of early alteration in a parent body of CM chondrites.

Model: We perform kinetic-equilibrium modeling in closed Fe-Mg-Si-O-H solution-solids-gas systems. At each time step, the numerical model considers pH-dependent rates of mineral dissolution and calculates chemical equilibrium in solution, which affects secondary precipitation [cf. 5]. A procedure is developed to calculate pH- and PH_2 -dependent rate of metal oxidation via reaction $3Fe^0 + 4H_2O(l) \rightarrow Fe_3O_4 + 4H_2$ (gas and solute) (1). In addition to kinetic and thermodynamic data, input parameters include initial mineralogy (forsterite, enstatite, Fe^0 metal) and solution composition, surface area (e.g., grain sizes), water/rock ratio (W/R , 0.1–10), temperature (T , 0–25 °C), and pressure ($P \approx PH_2$). Escape versus accumulation scenarios are considered for H_2 . The output includes amounts and compositions of gas, solution, and primary and secondary solids.

Results: Modeling shows faster alteration of the metal compared to silicates ($Fe^0 > \text{enstatite} > \text{forsterite}$). Correspondingly, a low Mg/Fe ratio in early solutions leads to formation of Fe-serpentine in association with magnetite. Although cronstedtite is expected to form from H_2 -, Mg-less, low- T solutions, it does not form in the models. At later stages, increasing supply of Mg and SiO_2 from dissolving silicates leads to deposition of increasingly Mg-rich serpentine. Once metal is oxidized, serpentine with Mg/Fe + Mg ratio >70 becomes dominant. Magnetite dissolves partially and Fe (including Fe^{2+} reduced from Fe^{3+}) goes to serpentine. Higher PH_2 values slow Fe^0 oxidation. Lower volume of free space leads to faster increase in P . However, at typical asteroidal $P < \sim 102$ bar, accumulation of H_2 cannot suppress Fe^0 oxidation via Equation 1 unless $H_2O(l)$ is consumed earlier, as observed in runs with low W/R ratios. At 0 °C, major alteration of 1 μm grains occurs by 10^2 – 10^4 yr, but it is faster for smaller sizes and higher T . Solution pH increases rapidly (in 1–10 yr) and is about 10 to 11 thereafter.

Conclusions: The results allow estimates of sequence and timing of aqueous alteration and are roughly consistent with observations. The lack of cronstedtite in modeled assemblages may reflect a tentative nature of used thermodynamic data [6].

References: [1] McSween H. Y. Jr. 1987. *Geochimica et Cosmochimica Acta* 51:2469–2477. [2] Zolensky M. E. et al. 1993. *Geochimica et Cosmochimica Acta* 57:3123–3148. [3] Bland P. A. et al. 2004. *Meteoritics & Planetary Science* 39:3–16. [4] Brearley A. J. 2006. Abstract #2074. 37th LPSC. [5] Zolotov M. Yu. and Mironenko M. V. 2007. *Journal of Geophysical Research* 112:E07006. [6] Wolery T. J. and Jove-Colon C. F. 2004. *Qualification of thermodynamic data*. Bechtel SAIC Company.

5173

LIGHT SCATTERING BY HIGHLY ABSORBING IRREGULARLY SHAPED PARTICLES

E. Zubko^{1,2}, H. Kimura³, Yu. Shkuratov², K. Muinonen⁴, T. Yamamoto³, and G. Videen⁵. ¹Tohoku University, Japan. E-mail: zubko@caos-a.geophys.tohoku.ac.jp. ²Kharkov National University, Ukraine. ³Hokkaido University, Japan. ⁴University of Helsinki, Finland. ⁵Army Research Laboratory AMSRL-CI-EM, USA.

Introduction: Organic material is an abundant component of cosmic dust. Optical properties of the organic material strongly depend on the dose of UV radiation and ion bombardment. For instance, at wavelength of $\lambda = 0.5 \mu\text{m}$, the processing of organic material in a form expected in the diffuse interstellar medium yields $m = 1.57 + 0.14i$ [1]. Heavier processing changes the refractive index to $m = 1.86 + 0.45i$. Thus, the organic material is transient between dielectric and conductor ones. Using our own implementation of the discrete dipole approximation (DDA) [see, e.g., 2], we study light scattering by irregularly shaped particles composed of such a material.

Model of Particles: We generate irregularly shaped model particles by damaging a perfect sphere with the following simple algorithm. The spherical volume is filled with a regular cubic lattice that is considered as the initial matrix of the irregular particles. All cubic cells forming this initial matrix are divided into two groups: cells belonging to the surface layer and cells internal to the surface layer. Among the surface dipoles we choose randomly 100 cells that are considered as seed cells of empty space. In the set of internal dipoles, we randomly choose 21 and 20 seed cells of material and empty space, respectively. Each cell distinct from the seed cells is marked with the same optical properties as that of the nearest seed cell. Images of particles generated in this way can be found in [2].

We consider particles at four size parameters $x = 5, 10, 20,$ and 30 ($x = 2\pi r/\lambda$, r is the radius of initial matrix, λ is the wavelength). In the first case, the radius of initial matrix is 16 cells, in the second case it is 32 cells, and in the two last cases it is 64 cells. The real part of refractive index m has been fixed at 1.5. Excluding the case of $x = 30$, the imaginary part is varied from 0 to 1.3. For the largest particles the convergence of calculations cannot be reached at $\text{Im}(m) = 0$. For all particle sizes, a large imaginary part of the refractive index did not cause problems with the convergence.

Results: We have found that at all particle sizes the degree of positive polarization changes with $\text{Im}(m)$ non-monotonically. For low absorptions, the degree increases together with the absorption until some maximal value. Further increasing $\text{Im}(m)$ results in a decrease of the degree. The inflection occurs at $\text{Im}(m)$ varying from 1 ($x = 5$) to 0.5 ($x = 30$); at that the linear polarization degree is as high as 70–80%. When $\text{Im}(m) > 0.5$, the angular profile of linear polarization becomes bimodal and further increasing $\text{Im}(m)$ makes this effect more explicit. This feature is the most pronounced in the case of the smallest particles as increasing particle size tends to wash it away. Note, a similar bimodal profile of polarization curve was found in laboratory measurements of hematite particles [3].

References: [1] Jenniskens P. 1993. *Astronomy and Astrophysics* 274: 653–661. [2] Zubko E. et al. 2006. *Journal of Quantitative Spectroscopy and Radiative Transfer* 101:416–434. [3] Muñoz O. et al. 2006. *Astronomy and Astrophysics* 446:525–535.